Université de Paris

Bio Sorbonne Paris Cité 562

Lyssavirus, épidémiologie et neuropathologie

Départment de Santé Globale

Institut Pasteur

Role of glial cells during rabies virus infection

Lena Franziska FEIGE

Thèse de Doctorat Infectiologie

Dirigée par Hervé BOURHY

Date de soutenance : 03-12-2021

Membres du jury:

Christine GOFFINET, Professeur, Charité - Universitätsmedizin Berlin, Rapporteur

Karl-Klaus CONZELMANN, Professeur, LMU Munich, Rapporteur

Carole ESCARTIN, Chargé de recherche, Université Paris-Saclay, Examinateur

Anastasia KOMAROVA, Chargé de recherche, Institut Pasteur, Examinateur

Arpiar SAUNDERS, PhD, Oregon Health and Science University, Examinateur

Pierre-Emmanuel CECCALDI, Université de Paris, Examinateur

Jean-Pierre PERON, Professeur, University of São Paolo, Examinateur

Hervé BOURHY, Professeur, Université de Paris, Directeur de thèse

‘The best research you can do is talk to people’

~ Terry Pratchett

‘Change is the law of life and those who look only to the past or present are certain to miss the future’

~ John F. Kennedy

In hope of a drastic change in science where collaboration outweighs competition.

Abstract

In recent years, human populations are more and more threatened by newly emerging viruses such as the Ebola virus or Sars-Cov-2. Despite and maybe partly due to the increasing awareness for newly emerging viral threats, little awareness remains for those which are known to affect the human mankind already for millennia: rabies is one of the deadliest zoonotic diseases affecting humans, still causing 60.000 deaths annually, most of them in Africa and Asia. Rabies is caused by rabies virus (RABV), genus *Lyssavirus*, family *Rhabdoviridae*, which induces an acute and fatal form of encephalomyelitis in humans if left untreated.

RABV tropism, or the specificity of RABV to infect a particular cell type is crucial in determining the success of virus replication, viral spread, and host survival. Although RABV is classically believed to replicate mainly in neurons, RABV was recently reported to successfully infect glial cells *in vivo* particularly astrocytes and Schwann cells, depending on the viral strain and infection route used. Nowadays, we do not completely understand all the factors which shape RABV tropism and why glial cells are unable to clear RABV from the infected brain.

The goal of this PhD project is to investigate cellular susceptibilities of human CNS cell types and their cell type-specific immune responses upon RABV infection *in vitro*. Therefore, the PhD object implied the following objectives:

The main objective implied the investigation of cellular tropism and immune responses of CNS cell types by using two RABV strains: i) the highly virulent strain Tha which was constructed via reverse genetics from a field RABV strain isolated from the brain of a rabid Thai patient and ii) a less virulent Tha2P-4M which bears the same genetic background except for mutations introduced in viral phospho- and matrix proteins hindering Th2P-4M to escape the host innate immune response. In detail, viral tropism and immune responses were investigated by quantifying gene expression and protein levels, immunofluorescence, and single-cell sequencing approaches.

The second objective implied quantification of gene expression of a panel of inflammatory genes in human brains of rabid patients to obtain a detailed overview of the inflammatory reaction happening in the human brain.

Keywords: Astrocytes, microglia, rabies virus, innate immunity

Résumé

Ces dernières années, les populations humaines sont de plus en plus menacées par des virus émergents comme le virus Ebola ou le Sars-Cov-2. Malgré et peut-être en partie à cause de la prise de conscience des nouvelles menaces virales émergentes, celles qui sont connues pour affecter l'humanité depuis des millénaires, reçoivent peu d'attention. C'est le cas de la rage qui affecterait l'humanité depuis au moins 4000 ans et qui reste une maladie négligée représentant un fardeau particulièrement élevé pour les pays à faible revenu. Il s'agit de l'une des zoonoses les plus mortelles affectant l'homme, causant environ 60 000 décès par an, la plupart d'entre eux en Afrique (36,4%) et en Asie (59,6%). La rage est causée majoritairement par le virus de la rage (RABV), appartenant à la famille des *Rhabdoviridae* et au genre *Lyssavirus*, qui présente une distribution mondiale. Le RABV est responsable d'une infection enzootique chez une grande variété de carnivores sauvages, notamment le renard, les ratons laveurs, les mouffettes et les mangoustes. Bien que le RABV possède un vaste réservoir viral, les chiens représentent le principal hôte primaire et vecteur de transmission du RABV, à l'homme (responsable d'environ 99 % des cas humains). Le RABV est donc le membre le plus important du genre *Lyssavirus* du point de vue de la santé publique. La transmission se produit lors d'une morsure, d'égratignures, de léchage de plaies ou de projection de matériel infectieux sur une muqueuse. Ensuite, le RABV se réplique localement et pénètre dans le système nerveux périphérique (SNP) via la jonction neuromusculaire. Le RABV se déplace ensuite de manière rétrograde par propagation transsynaptique entre les nerfs périphériques jusqu'au système nerveux central (SNC). Une fois le SNC atteint, la rage entraîne une encéphalomyélite mortelle chez les personnes non vaccinées et les symptômes commencent à se développer. Étant donné qu'un traitement efficace fait toujours défaut, la rage est mortelle à 100% hormis quelques rares exceptions.

La famille des *Rhabdoviridae* comprend 20 genres et 144 espèces de virus avec des génomes à ARN simple brin de sens négatif (10-16 kb). Presque tous codent pour les mêmes cinq protéines, à savoir, la nucléoprotéine (protéine N), la phosphoprotéine (protéine P), la protéine de matrice (protéine M), la glycoprotéine (protéine G) et la polymérase L (protéine L). Parmi la famille des *Rhabdoviridae*, le genre *Lyssavirus* comprend des virus qui présentent la caractéristique de n'être pas transmis par des arthropodes vecteurs mais directement via effraction cutanée. Le tropisme du RABV, ou la spécificité du RABV pour infecter un certain type cellulaire, est crucial pour déterminer le succès de la réplication et de la propagation virale, ainsi que la survie de l'hôte. Bien que classiquement défini comme neurotrope, il a été récemment rapporté que le RABV, selon la souche virale et la voie d'infection utilisées, infectait

aussi avec succès les cellules gliales *in vivo*, en particulier les astrocytes et les cellules de Schwann. Cependant, nous ne comprenons pas complètement à ce jour les facteurs déterminant le tropisme du RABV et pourquoi les cellules gliales sont incapables d'éliminer le RABV du cerveau infecté.

L'objectif général de ce projet de thèse est d'étudier la susceptibilité des différents types de cellules du SNC chez l'homme ainsi que leurs réponses immunitaires spécifiques lors d'une infection par le RABV *in vitro*. Il se décompose en deux objectifs spécifiques suivants.

Le premier impliquait l'étude du tropisme cellulaire et des réponses immunitaires des différents types de cellules du SNC en utilisant deux souches RABV : i) le virus Tha, un isolat provenant de Thailande et ii) Th2P-4M moins virulent qui porte le même bagage génétique que Tha à l'exception des mutations introduites dans les protéines P et M empêchant Th2P-4M d'échapper à la réponse immunitaire innée de l'hôte. Le tropisme viral et les réponses immunitaires ont été étudiés en détail, en quantifiant les niveaux de transcription des gènes et les niveaux d'expression des protéines par des approches de séquençage de cellule unique et par immunofluorescence.

Enfin, le deuxième objectif impliquait la quantification de la transcription d'un panel de gènes impliqués dans l'inflammation dans des biopsies cérébrales provenant de patients enragés afin d'obtenir un aperçu détaillé de la réaction inflammatoire se produisant dans le cerveau humain en phase terminale d'infection.

En infectant différents types de cellules neurales avec les virus Tha et Th2P-4M, je fournis la preuve que les facteurs intrinsèques au virus, en particulier les fonctions accessoires des protéines virales P et M, ainsi que les réponses immunitaires spécifiques des différents types de cellule déterminent le tropisme du RABV *in vitro*. De manière plus détaillée, je montre que des facteurs dépendants des cellules déterminent le tropisme du RABV: la simple présence de cellules gliales dans les co-cultures ainsi que le transfert de surnageant provenant de cellules gliales influencent ce tropisme. De plus, la présence de cellules SVGp12 de type astrocytaire et de cellules HMC3 de type microglial limite la réplication de Tha dans des neurones (SK-N-SH), suggérant que la communication entre types cellulaires induite par la glie joue un rôle important dans l'inhibition de la propagation virale dans les cellules neuronales. Les mécanismes sous-jacents possibles comprennent une signalisation médiée par les cellules gliales directement via des contacts de cellule à cellule ou via la sécrétion de protéines inflammatoires. Cette activation modulerait la transcription de gènes impliqués dans l'inflammation et la production des protéines inflammatoires spécifiques des différents types cellulaires et induirait des cascades de signalisation secondaire dans les cellules environnantes. Ceci suggère que le tropisme spécifique du RABV vis-à-vis des neurones est

en partie façonné par leur absence de réponse antivirale contrairement aux cellules gliales. Fait encore plus intéressant, j'ai montré que la souche RABV Tha infecte les neurones et les astrocytes humains mais n'est pas capable d'infecter la microglie dérivée de cellules souches *in vitro*. En outre, en utilisant des approches de séquençage de cellule unique, j'ai fourni la preuve que Tha perturbe les voies de signalisation du SNC. En conséquence, Tha n'a pas besoin d'infecter tous les types de cellules du SNC pour moduler leurs profils de transcription, mais l'interférence virale avec les voies de signalisation intercellulaire est suffisante pour moduler les réponses cellulaires des cellules neuronales infectées ou non.

Dans le cadre de mon deuxième objectif, j'ai comparé le profil transcriptomique des cerveaux des souris infectées expérimentalement avec celui des biopsies cérébrales provenant de patients décédés de la rage. Contrairement au cerveau murin, les cerveaux humains naturellement infectés montrent peu d'inflammation lors de l'infection par le RABV. Plus précisément, sur les 33 gènes étudiés, 20 sont exprimés de manière différentielle (par rapport aux contrôles) dans le cortex et le tronc cérébral/cervelet des souris, alors qu'un seul gène est exprimé de manière différentielle dans le tronc cérébral/cervelet humain de patients cambodgiens enragés, à savoir le *Chemokine C-X-C Motif Ligand 16* (CXCL16). Plus précisément, nous montrons une régulation positive significative de *CXCL16* dans le cerveau murin et une régulation négative significative de *CXCL16* dans des biopsies de patients enragés morts au Cambodge. L'étude de l'expression de *CXCL16 in vitro* révèle que le RABV Tha régule négativement l'expression de *CXCL16* dans les lignées cellulaires neuronales, astrocytaires et microgliales humaines stimulées par l'IFN-α, tandis que *CXCL16* est induit dans les astrocytes murins stimulés par l'IFN-α. Dans l'ensemble, nos données fournissent les preuves d'une expression de *CXCL16* spécifique de l'espèce pendant l'infection par le RABV.

Le premier axe de mes recherches a permis de montrer que Tha perturbe spécifiquement la signalisation du SNC, modulant les réponses de chaque type cellulaire de manière spécifique et indépendante de l'infection virale. Étant donné que le RABV ne provoque pas d'inflammation évidente dans le SNC, les réponses inflammatoires dans le SNC pourraient être limitées par un mécanisme d'interférence se propageant par le biais de communication intercellulaire. Ensuite, j'ai démontré l'existence de différences plus profondes entre les réponses immunitaires innées des cellules du SNC dérivées de cellules souches et celles des lignées cellulaires. Étant donné que la modulation de la réponse immunitaire innée était moins importante dans les modèles issus de lignées cellulaires, ces derniers pourraient être inappropriés pour étudier les interactions cellulaires complexes s'établissant dans le contexte du SNC infecté par le virus. Nous avons donc développé un modèle de SNC humain *ex vivo* dérivé de cellules souches qui, certes ne reflète pas totalement la complexité du SNC, mais semble, entre nos mains, approprié pour étudier les interactions hôte-pathogène dans un

contexte plus physiologique par rapport aux modèles de lignées cellulaires classiques. En conséquence, les recherches pour étudier les interactions spécifiques de chaque type de cellule du SNC avec le RABV devraient préférentiellement utiliser des modèles dérivés de cellules souches.

L'analyse du transcriptome lors de l'infection par le RBV *in vivo* a apporté d'autres éclairages. En particulier, l'identification de la modulation spécifique de l'expression de *CXCL16* dans le cerveau humain infecté par RABV augmente nos connaissances sur la pathogenèse de la rage. CXCL16 est une chimiokine transmembranaire qui est clivée par des métalloprotéases et libérée à partir de la microglie ou des astrocytes, agissant par conséquent comme un agent chimiotactique pour les cellules T, les cellules NK ou les précurseurs gliaux.

L'encéphalomyélite induite par le RABV présente une régulation négative de l'expression de *CXCL16* au stade final de la maladie. Par conséquent, nous émettons l'hypothèse qu'une expression réduite de CXCL16 pourrait inhiber le recrutement de cellules exprimant CXCR6/Bonzo dans le SNC, permettant finalement au RABV de se répliquer sans mécanisme de clairance virale. Cela correspond à l'image globale de la pathogenèse de la rage, à savoir une inflammation et une apoptose limitées dans le cerveau humain malgré la fatalité de la maladie. En dehors de l'interaction avec les cellules exprimant CXCR6/Bonzo, CXCL16 est aussi connu pour moduler la neurotransmission. Dans l'hippocampe murin, CXCL16 s'est avéré exercer une activité modulatrice sur les synapses excitatrices et inhibitrices. Cependant, le mécanisme exact par lequel RABV régule spécifiquement à la baisse l'expression de *CXCL16* et comment cette baisse d'expression pourrait potentiellement affecter la neurotransmission, restent à déterminer.

Le travail effectué dans cette thèse a éclairé le rôle des cellules gliales au cours de l'infection par le RABV. Bien que les mécanismes immunitaires innés au cours de la pathogenèse du RABV soient couramment étudiés dans les cultures neuronales, de vastes avancées technologiques ces dernières années nous ont permis d'étudier les agents pathogènes dans des systèmes *ex vivo* plus complexes. Le processus de culture et de séquençage que j'ai mis en place au cours de ma thèse peut être utilisé pour étudier des maladies neurologiques complexes *in vitro*, sans avoir besoin de sacrifier des animaux pour des expériences d'infection. Bien que le protocole proposé soit encore long, laborieux et coûteux, les approches de séquençage de cellule unique appliquées aux cultures mixtes de cellules humaines du SNC conduisent à la génération d'ensembles de données gigantesques dont l'analyse aidera à émettre des hypothèses de recherche sur le rôle du dialogue inter-cellulaire. Ces analyses devraient être collaboratives pour être à la hauteur des défis rencontrés. Ce type d'approche pourraient notamment être utilisés pour évaluer i) le rôle des

différents types cellulaires dans l'homéostasie au sein du SNC, ii) le rôle des types cellulaires du SNC pendant la maladie, et iii) les interférences potentielles de signaux entre les différents types cellulaires.

Mots clés: Astrocytes, microglie, virus de la rage, immunité innée

Table of Contents

Abbreviations ..... **i**

List of figures ..... **iii**

1. Introduction **1**

1.1. Neglected: known for millennia and still a silent killer 1

1.2. The diverse phylogenetic group of lyssaviruses 3

1.3. How does RABV look like? 6

1.4. Transmission and propagation strategies of RABV 10

1.5. The horrifying clinical picture of rabies 12

1.6. Taking a glimpse at the molecular pathogenesis of rabies 14

1.7. Innate immune mechanisms shaping CNS homeostasis 18

1.8. So little and yet so smart 19

1.9. Re-defining RABV tropism: Neuron-specific tropism or not? 21

1.10. Cellular players in innate immunity 23

1.11. Project outline and objectives 27

2. Results **29**

2.1 Glial biology in herpes and rabies virus induced encephalitis (#Article 1) 29

2.2 Cell type-specific insights into RABV tropism (Article #2) 79

2.3 RABV modulates intercellular CNS signalling (Article #3) 108

2.4 Identification of CXCL16 as a new viral target (Article #4) 134

3. Discussion **168**

3.1. Studying the role of glial cells during RABV infection *in vitro* 169

3.2. And what is happening in naturally infected humans? 179

4. Concluding remarks **183**

4.1. Challenges and perspectives 183

4.2. Closing remarks 184

Acknowledgements **185**

Appendices **186**

4.3. Lessons from Sars-Cov-2 (Article #5) 186

4.4. RABomics (Article #6) 201

Literature **241**

Abbreviations

ABLV	Australian bat lyssavirus
ARAV	Aravan lyssavirus
BBLV	Bokeloh bat lyssavirus
CCL5	C-C Motif Chemokine Ligand 5
CNS	Central nervous system
CNSC	Complete neural stem cell
CVS	Challenge virus standard
CXCL10	Chemokine (C-X-C Motif) Ligand 10
CXCL16	Chemokine (C-X-C Motif) Ligand 16
DALYs	Disability-adjusted life years
DAMPS	Danger-associated molecular patterns
DEGs	Differentially expressed genes
DRN	Dorsal raphe nucleus
dsRNA	Double-stranded RNA
DUVV	Duvenhague virus
ER	Endoplasmic reticulum
FBS	Fetal bovine serum
FFU	Fluorescent forming units
EBLV-1	European bat lyssavirus 1
EBLV-2	European bat lyssavirus 2
G-protein	Glycoprotein
GBLV	Gannoruwa bat lyssavirus
GFAP	Glial fibrillary acidic protein
GLAST-1	GLutamate ASpartate Transporter *1*
GTPases	Guanosine triphosphatases
hiMacs	Human induced macrophage-like cells
HIV	Human immunodeficiency virus
hNSC	human neural stem cell
HSV	Herpes simplex virus
IBA-1	Ionized calcium-binding adapter molecule 1
IDO1	Indoleamine 2,3-Dioxygenase 1
IFIT	IFN-induced protein with tetratricopeptide repeats
IFITM	IFN-induced transmembrane protein
IFN	Interferon
IKOV	Ikoma lyssavirus
iPSC	Induced pluripotent stem cells
IRKV	Irkut lyssavirus
ISGs	IFN-stimulated genes
JAK	Janus kinase
JEV	Japanese encephalitis virus
KHUV	Khujand lyssavirus
L-protein	Polymerase L
LBV	Lagos bat lyssavirus

LLEBV	Lleida bat lyssavirus
M-protein	Matrix protein
MAPK	Mitogen-activated protein kinase
MAVS	Mitochondrial anti-viral signalling protein
mGluR2	Metabotropic glutamate receptor subtype 2
MOI	Multiplicity of infection
MOKV	Mokola virus
MRCA	Most recent common ancestor
MRI	Magnetic resonance imaging
N-protein	Nucleoprotein
nAChR	Nicotinic acetylcholine receptor
NCAM	Neural cell adhesion molecule
NF-κB	Nuclear factor kappa-light-chain-enhancer of activated B-cells
NLRP3	NOD-, LRR- and pyrin domain-containing protein 3
NOD-like receptors	Nucleotide-binding oligomerization domain-like receptors
ORF	Open reading frame
P-protein	Phosphoprotein
PAMPs	Pathogen-associated molecular pattern
PINK1	PTEN-induced kinase 1
PRKN	Parkin RBR E3 Ubiquitin Protein Ligase
hiAstroocytes	Human neural stem cell-derived astrocytes
PEP	Post-exposure prophylaxis
PMA	4-β-phorbol 12-myristate 13-acetate
hiNeurons	Human neural stem cell-derived neurons
PNS	Peripheral nervous system
hiMicros	human induced pluripotent stem cell-derived microglia-like cells
PRRS	Pattern recognition receptors
p75NTR	p75 neurotropin receptor
qPCR	Quantitative polymerase chain reaction
RABV	Rabies virus
RIG-I	Retinoic acid-inducible gene I (RIG-I)
RLR	Retinoic acid-inducible gene I (RIG-I) like helicase
RNP	Ribonucleoprotein
Sc RNA-Seq	Single cell RNA sequencing
SCs	Schwann cells
SHIBV	Shimoni bat virus
Socs	Suppressor of cytokine signalling
STAT	Signal Transducers and Activators of Transcription
TLR	Toll-like receptor
TUNEL	Terminal deoxynucleotidyltransferase-mediated DNA nick-end labelling
TUBB3	β(III)tubulin
VGCC	Voltage-gated calcium channel
WCBV	West Caucasian bat virus
WNV	West Nile virus
wt	Wildtype

List of figures

Introduction (chapter 1)

Figure 1 Global burden of human loss due to canine rabies.
Figure 2 Phylogenetic tree of the lyssavirus genus based on the complete N-protein gene sequence
Figure 3 RABV structure
Figure 4 RABV life cycle
Figure 5 RABV propagation and spread.
Figure 6 Molecular mechanisms underlying RABV-mediated immune evasion
Figure 7 Representative overview illustrating the interplay between CNS cell types in the RABV-infected CNS.

Article #1 (chapter 2.1.2)

Figure 1 Infection routes of neurotropic viruses.
Figure 2 Comparative histopathology of RABV and HSV-1 infection in the murine brain.
Figure 3 Cellular tropism of RABV and HSV in the CNS and PNS.
Figure 4 Hypothesis of cell-specific innate immune responses of CNS cell types upon RABV and HSV infection.

Article #2 (chapter 2.2.2)

Figure 1 Tha-eGFP and Th2P-4M-eGFP preferentially replicate and spread in human SK-N-SH compared to astrocyte-like (SVGp12) and microglia-like (HMC3) cell lines *in vitro*.
Figure 2 Astrocyte-like SVGp12 and microglia-like HMC3 protect SK-N-SH from Tha-eGFP infection *in vitro*.
Figure 3 Whereas hiNeurons and hiAstrocytes are highly susceptible towards Tha-eGFP and Th2P-4M-eGFP infection, hiMicros are resistant to Tha-eGFP or Th2P-4M-eGFP infection *in vitro*.
Figure 4 The virulent RABV strain Tha is highly adapted to evade the neural innate immune system.
Figure 5 Astrocytes, astrocyte-like SVGp12 and microglia-like cells exhibit a cell-specific induction of protein expression upon Tha and Th2P-4M infection.
Figure 6 Neither IL-1β, IL-6 nor LIF protect human hiNeurons or hiAstrocytes from Tha-eGFP or Th2P-4M-eGFP infection *in vitro*.

Article #3 (chapter 2.3.2)

Figure 1 Human stem cell-derived CNS cell types revealed distinct transcriptome profiles and different susceptibilities towards Tha and Th2P-4M infection *in vitro*.
Figure 2 Tha differentially regulates immune responses, intracellular and transmembrane transport, and mitochondrial functions in distinct CNS cell types *in vitro*.
Figure 3 Tha similarly modulates the cytoskeleton, immune responses, and pathways implicated in neural function of infected and non-infected bystander hiNeurons and hiAstrocytes.

Article #4 (chapter 2.4.2)

Figure 1 Inflammatory transcription profile of murine CX and BSC upon RABV strain Tha infection at day 8 post-infection.
Figure 2 Clinical presentation of Cambodian rabid patients from group 1 (n=10).
Figure 3 Human and murine transcription profiles upon RABV infection.
Figure 4 CXCL16 gene expression in human and murine brains and CNS cell types during RABV infection.
Figure 5 CXCL16 interaction network.

Discussion

Figure 1 Cell type-specific signalling pathways modulated during Tha infection.

1. Introduction

1.1. Neglected: known for millennia and still a silent killer

Rabies is a viral zoonosis which still results in approximately 60.000 human deaths and over 3.7 million disability-adjusted life years (DALYs) worldwide due to fatal encephalomyelitis (1). Rabies is caused by viruses belonging to the *Rhabdoviridae* family (*Lyssavirus* genus) among which rabies virus (RABV) is the only significant pathogen affecting humans. Due to the global distribution of RABV (1) and its long history of study (2), RABV is the most prominent member of the *Lyssavirus* genus. Regarding human populations, rabies is an ancient disease which is reported to affect humankind for the last 4000 years (3). Still, and despite being known for millennia (3), rabies remains a neglected disease which presents a particular high burden to low-income countries (1). RABV is enzootic in a variety of wildlife carnivora including fox, racoons, skunks, and mongoose. Although RABV has a wide viral reservoir including all warm-blooded animals, dogs represent the main reservoir and vector for RABV transmission contributing to 99% of all human cases (4,5). Transmission occurs upon a bite, scratches, or licking of wounds, subsequently introducing virus containing-saliva from the rabid animal into the open wound (4). Upon the bite, RABV replicates locally in the wound and enters the peripheral nervous system (PNS) via the neuromuscular junction (6–8). From there, RABV travels retrogradely and by trans-synaptic spread between peripheral nerves to the central nervous system (CNS) (9,10). Once inside the CNS, rabies leads to fatal encephalomyelitis in unvaccinated individuals and symptoms start developing. Given that an effective treatment is still missing, rabies is almost 100% fatal (11,12).

Overall, the history of rabies is also a history of inequality and economic wealth: most of the RABV-related deaths still appear in Africa (36.4%) and Asia (59.6%) (Figure 1) (1,13,14). Strikingly, estimates of rabies cases tend to be strongly underreported since death is inevitable following the onset of clinical symptoms. Particularly in Africa and Asia, it is predicted that only 3% of human rabies deaths are reported by local health authorities (14). As a result, most of rabies cases never reach health facilities and fail to be recognized after diagnosis. On top of that, misdiagnosis of neurological symptoms presents a common problem, especially in malaria endemic regions (15). Despite the lack of an effective treatment (16) and problems diagnosing rabies (15), however, onset of RABV-induced fatal encephalitis can be prevented

via prompt administration of post-exposure prophylaxis (PEP) (17). The history of PEP remains one of the scarce rays of hope in rabies history: Louis Pasteur introduced rabies vaccination in the late 1880s (2), opening the way to pre- and PEP protocols we are using nowadays (18,19). Although vaccination was a breakthrough in eliminating rabies (2), it remains unavailable for the vast majority of people living in endemic regions emphasizing once again the inequality in fighting rabies (1). Worldwide, it is estimated that over 20 million people receive PEP annually (20). However, taking a closer look at PEP administration in Dakar (Senegal) revealed that only 54.5% of all individuals who originally sought PEP in 2013-2014 completed the full vaccination schedule. Factors leading to the premature discontinuation of the PEP schedule included vaccine costs and affordability, as well as the missing knowledge on status of biting animal (21). Hence, large vaccination campaigns and effective treatments for rabies are urgently needed.

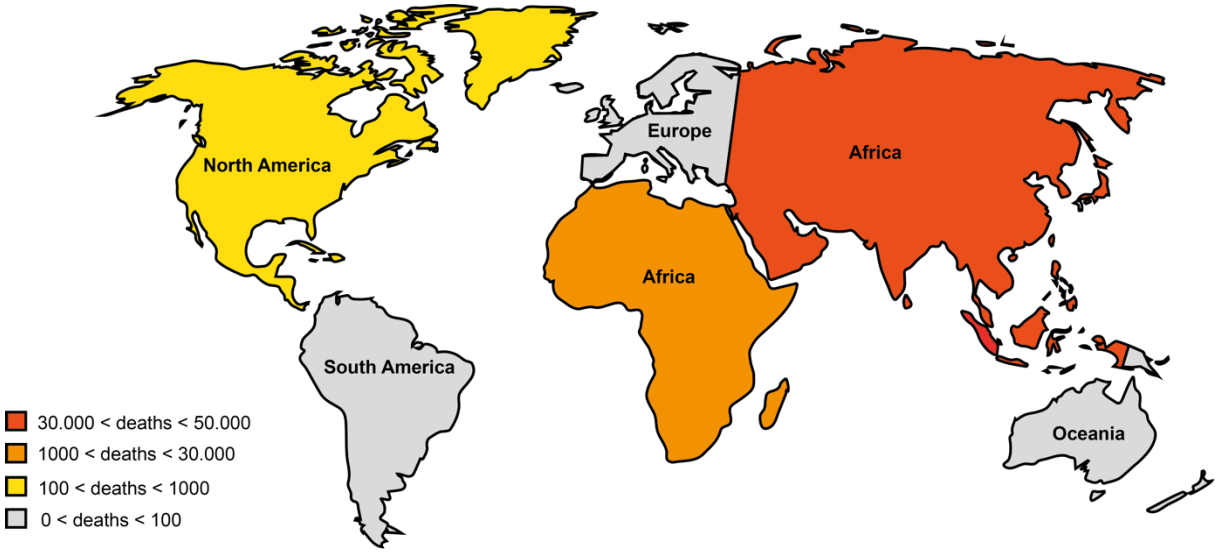

Figure 1 | Global burden of human loss due to canine rabies. Although largely neglected, rabies remains an important infectious disease in Africa and Asia. Disparities between countries are mainly due to affordability and accessibility to PEP treatment, and the risk of exposure to rabid dogs. Numbers represent absolute numbers disregarding the population size. Data for figure generation were taken from Hampson *et al.*, Knobel *et al.*, and the WHO (1,13,14)).

Overall speaking, India accounts for 35 % of total human rabies deaths, representing most of the total numbers compared to other countries. Considering relative numbers, the estimated per-person death rate was the highest in countries of sub-Saharan Africa (1,22). Despite the presence of global attempts, control schemes, and dog vaccination campaigns, over 95% of the RABV-induced deaths occur in Africa and Asia, where canine rabies is still enzootic (11). Lowering RABV-induced human deaths can only be controlled by mass vaccination of animal reservoirs such as dogs (23). Despite the fact that most industrialized countries successfully eliminated RABV from the host reservoir, rabies remains a serious public health problem in

most of the developing countries (24). On top of the global burden due to human loss, the overall economic costs were estimated as 8.6 billion US dollar due to due to productivity losses from premature deaths, lost income, and direct costs for PEP (1). Taken together, Hampson and colleagues provided evidence that the global burden due to canine rabies is substantial (1). Thus, more effort should target long-term mass dog vaccination and searching for a proper treatment to control rabies.

1.2. The diverse phylogenetic group of lyssaviruses

Rabies is caused by viruses belonging to the order *Mononegavirales*, the *Rhabdoviridea* family, and the *Lyssavirus* genus. The *Rhabdoviridea* family comprises a group of diverse RNA viruses which have a large host reservoir including vertebrates, invertebrates, and plants. The *Rhabdoviridea* family includes 20 genera and 144 virus species with negative-sense, single-stranded RNA genomes (10-16 kb). Almost all code for the five structural proteins, namely the glycoprotein (G-protein), matrix protein (M protein), nucleoprotein (N-protein), phosphoprotein (P-protein), and the polymerase L (L-protein) (25). Apart from this rhabdovirus-typical structure some genera among the *Rhabdoviridea* family contain additional genome sequences: Viruses belonging to the *Ephemerovirus* genus contain additional open reading frames (ORFs) between genes coding for G-protein and polymerase L, encoding an additional G-protein and other structural proteins (26–29). Likewise, the *Novirhabdovirus* genus contains an additional ORF between G-protein and the polymerase L gene encoding a non-structural protein (30).

The *Rhabdoviridea* family presents an ecologically diverse group of viruses, infecting vertebrates, invertebrates, birds, reptiles, and fish. Most rhabdovirus genera (*Vesiculovirus*, *Ephemerovirus*, *Tibrovirus*, *Hapavirus*, *Curiovirus*, *Sri-puvirusand*, *Ledantevirus*) are transmitted by arthropods and infect plants, mammals, or fishes. Some of them are associated with livestock diseases and some are directly causing disease in humans.

In the past, studies of phylogenetic relationships among the *Rhabdoviridae* family were mainly based on structural properties of the viral genome, biological properties such as transmission routes and host range, as well as serological reactions. Currently, sequencing presents the main basis to define taxonomic relationships. Bourhy and colleagues investigated the phylogenetic relationship among 56 rhabdoviruses via sequence comparison of the block III of the polymerase L gene (31). This sequence is conserved among RNA-dependent RNA polymerases since it is essential for polymerase function (32,33). Mutations in this region abolish polymerase activity, making it a useful tool to explore evolutionary relationships among rhabdoviruses (34). This study mainly, although not entirely, re-produced the main groupings

and taxa of the *Rhabdoviridae* evolutionary tree (31). The mammalian rhabdoviruses belonging to the *Lyssavirus* genus, the fish rhabdoviruses belonging to the *Novirhabdovirus* genus, and the plant rhabdoviruses belonging to *Cytorhabdovirus* and *Nuclearhabdovirus* genera were easily distinguishable and fell into distinct clades. Although *Vesiculovirus* and *Ephemerovirus* genera clustered into monophyletic groups, those clusters were much less supported. The taxonomic tree revealed a major splitting point between viruses which infect fish (*Novorhabdovirus*), plant rhabdoviruses (*Cytorhabdovirus* and *Nucleorrhabdovirus*), and rhabdoviruses which infect mammals, lizards, and dipterans (referred to as *Dimarhabdovirus*). Thus, rhabdovirus clustering could have been strongly influenced by the host physiology and the mode of transmission (31). Further, Walker and colleagues performed a maximum-likelihood phylogenetic tree of 100 rhabdovirus L protein sequences, clustering into 17 well-supported monophyletic groups. In detail, eight clades corresponded to already established genera (*Lyssavirus*, *Vesiculovirus*, *Perhabdovirus*, *Sigmavirus*, *Ephemerovirus*, *Tibrovirus*, *Tupavirus* and *Sprivivirus),* whereas seven new genera were assigned (*Almendravirus*, *Bahiavirus*, *Curiovirus*, *Hapavirus*, *Ledantevirus*, *Sawgravirus* and *Sripuvirus*) (35).

Among the *Rhabdoviridae* family, the *Lyssavirus* genus presents a distinct monophyletic group based on sequence similarity of the complete N-protein gene sequence. This relatively recent genus comprises unique viruses which are not transmitted by arthropod vectors but directly via bites, scratches, and contaminated mucous membranes. This group encompasses 16 distinct *Lyssavirus* species, negative-stranded RNA viruses which cause acute progressive fatal encephalomyelitis. Viruses belonging to the *Lyssavirus* genus are distributed worldwide, except Antarctica and several isolated islands (36). Different viral genotypes have been assigned to the *Lyssavirus* genus based on sequence similarity of the N-protein gene (37,38). Hayman and colleagues aligned the N-protein gene sequences of 153 virus representatives of the 16 *Lyssavirus* species to develop a phylogenetic tree which incorporated relevant geographical and temporal data (Figure 2).

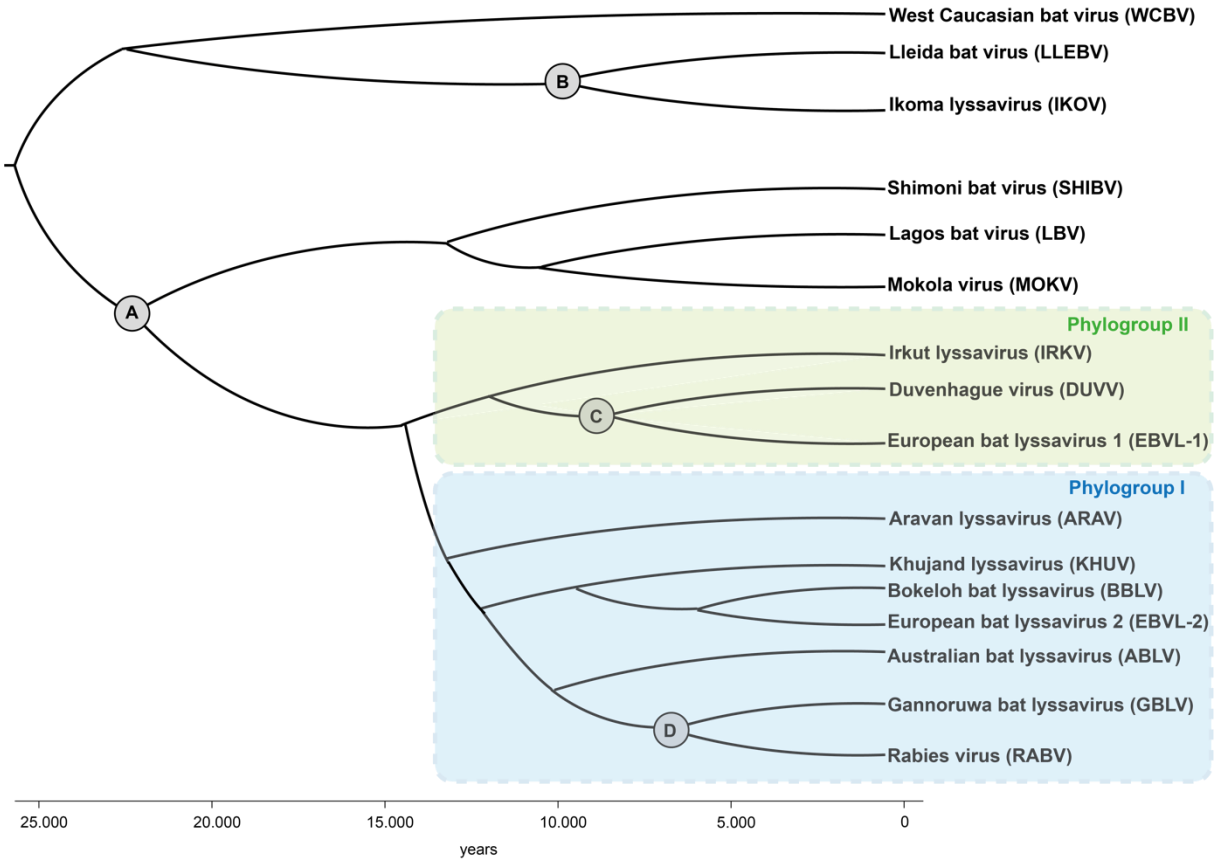

Figure 2 | Phylogenetic tree of the *Lyssavirus* genus based on the complete sequence of the N-protein gene. The phylogenetic tree was taken and modified from Hayman *et al.* (39). Phylogroups I and II were added according to the 10th report of the *International Committee on the Taxonomy of Viruses* (36).

Their data reinforced the palearctic origin of lyssaviruses (39) thereby confronting the '*Out of Africa*' hypothesis. From the Palearctic region, Hayman and colleagues suggested three independent transmission events to the African region. From there, lyssaviruses spread to the East to Australasia and the Americas. Although the uncertainty of the time to the most recent common ancestor (MRCA) is large, the event is believed to have taken place tens of thousands of years ago. Around 20.820 years ago (node A), the branching event which lead to the emergence of the Palearctic (SHIBV, LBV, MOKV) and Afrotropical region (IRKV, DUVV, EBLV-1, EBLV-2, ARAV, KHUV, BBLV, ABLV, GBLV, RABV) clades took place. The MRCA of LLEBV and IKOV lived 9.676 years ago (node B) and the MRCA of DUVV and EBLV-1 approximately 9.048 years ago (node C). The MRCA of the oldest RABV analyzed in their dataset dated back 3.726 years ago (node D). Despite the high diversity of lyssaviruses in Africa, their results suggested the spread of lyssaviruses from the Palearctic to the African region leading to the emergence of three phylogroups (39). According to the 10th report of the International Committee on the Taxonomy of Viruses, the *Lyssavirus* genus is subdivided into two phylogroups based on their antigenic properties and phylogenetic relationships.

Phylogroup III, which Hayman and colleagues assigned to the most divergent lyssaviruses WCBV, LLEBV, and IKOV is not officially recognized as an independent phylogroup (36,40).

Antibodies targeting the ribonucleoprotein (RNP) cross-react between all members of the *Lyssavirus* genus (41). Glycoprotein antigens are relatively similar within phylogroups (> 75%) but not between phylogroups (< 65%). Consequently, rabies vaccines and immunoglobulins protect against phylogroup I lyssaviruses but not phylogroup II lyssaviruses (40,42–45).

Most probably, RABV evolved from bat-associated progenitors (46). It is believed that host-switching events lead to the variety of RABV lineages known nowadays with each lineage harboring multiple variants (47). The most widespread lineage is found in dogs and several wildlife populations (fox, skunks, racoons, jackals) in Europe, Asia, Africa, and the Americas (48). In the Americas, RABV persist in bat populations, causing harm to humans in North America and livestock diseases in South America (49).

1.3. How does RABV look like?

So what do we know so far about rabies virus morphology? RABV is a bullet-shaped enveloped viral particle with a 12 kb non-segmented, negative-stranded viral genome in the order 3'-N-P-M-G-L-5' (Figure 3). Viral replication takes place in the cytoplasm, leading to the transcription of the viral genome into five polyadenylated monocistronic messenger species. Overall, all RABV transcripts code for proteins which are essential for RABV replication cycle (50).

1.3.1. Structural features of the RABV genome

RABV is structured in an internal helical-shaped protein core named nucleocapsid and an outer lipid envelope of cellular origin containing trimeric G-protein spikes. The nucleocapsid contains the RNP comprising the single-stranded viral genome, the N-protein, the RNA-dependent polymerase L, and the viral P-protein (Figure 3).

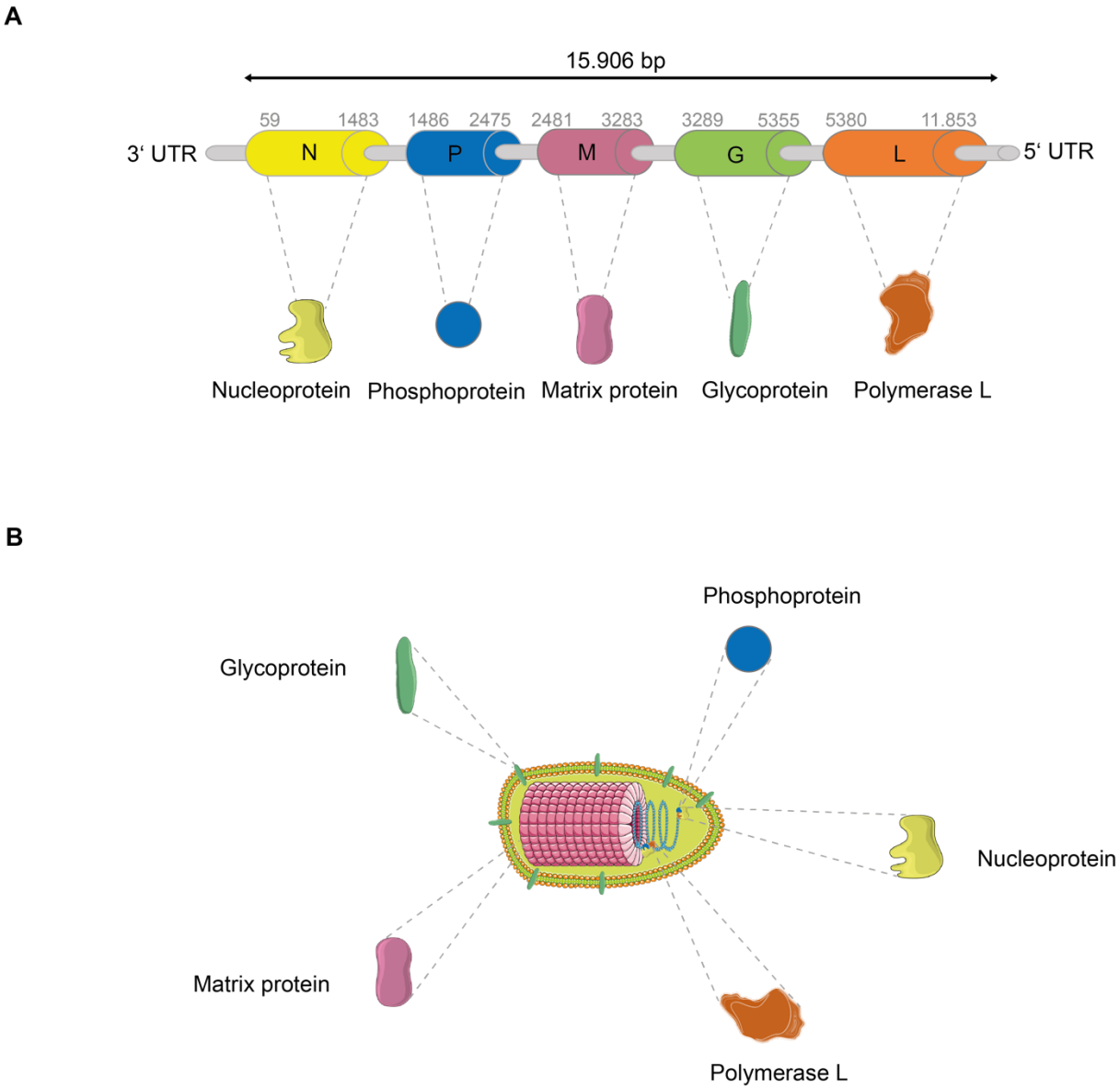

Figure 3 | Schematic presentation of RABV genomic organization and morphology. (A) Genomic organization of the rabies lyssavirus species. Rabies viral particles are encoded by a negative-stranded viral genome which encodes the five genes N, P, M, G, and L. **(B)** Schematic presentation of the RABV particle. Rabies virus is a bullet-shaped virus containing trimeric G-protein spikes on the lipid membrane, and a layer of viral M protein located beneath the membrane. Below the envelope, viral P-protein, N-protein and polymerase L build the helical-shaped protein core named nucleocapsid (51). N = N-protein gene; P = P-protein gene; M = M-protein gene; G = G-protein gene; L = polymerase L gene.

The enzymatic-active RNA polymerase L transcribes and replicates the viral RNA with the help of its cofactor, the P-protein (36). Inside the virus, the helically-coiled RNP structure protects the viral genome via tight embedding, making it highly insensitive to nuclease activity (52). Inside the cytoplasm, the RNP complex is uncoiled and filamentous to enable replication and transcription. The outer level comprises a lipid bilayer with glycoprotein spikes which are interacting with the RNP via the M protein (36). All five viral genes (N-protein, P-protein, M protein, G-protein, and polymerase L) encode structural proteins of RABV.

Each of the structural protein coding regions are bordered by internal nucleotide consensus sequences, termed leader sequences at 3' end and trailer sequences at the 5' end. Leader and trailer sequences harbor start and stop signals for viral transcription. Those initiation and termination signals indicate the viral RNA-polymerase where to start transcription and where to end transcription adding a poly-adenylation signal (53,54). Only viral P-protein and G-protein genes of several RABV vaccine strains harbor two consecutive stop signals which are used to produce shorter or longer mRNAs (55–57). In addition to the intergenic regions, the genome is bordered by an external 3' polymerization promoter and a 5' encapsidation promoter. The polymerization promoter signals the polymerase complex where to initiate transcription and replication whereas the encapsidation promoter indicates the N-protein to initiate encapsidation (53).

1.3.2. Functional features of the RABV genome

Virus among the *rhabdovirus* family present a generalized virus life cycle (Figure 4) (58). Firstly, virions enter the cell via adsorptive endocytosis without the requirement of active metabolic processes (59). Secondly, the viral envelope fuses with the endosomal membrane at an acidic pH (60–62). In neurons, RABV uptake is mainly observed at the axon terminals of cultured hippocampal neurons (63). Recently, Piccinotti and colleagues showed that RABV internalization is predominantly mediated via clathrin-mediated endocytosis via incomplete coated pits. In detail, complete internalization requires the help of the actin cytoskeleton (64). Further studies identified dynamin being crucial for RABV uptake in distal neurites (62). Dynamin belongs to the family of large guanosine triphosphatases (GTPases) and mediates vesicle formation during clathrin-mediated endocytosis (65). Apart from non-specific clathrin-mediated RABV uptake, the presence of some receptors is known to accelerate RABV uptake: The viral G-protein is known to bind to the nicotinic acetylcholine receptor (nAChR) (66), neuronal cell adhesion molecule (NCAM) (67), low-affinity p75 neurotropin receptor (p75NTR) (68), and the metabotropic glutamate receptor subtype 2 (mGluR2) (69). None of the above-mentioned receptors, however, is known to be essential *in vitro*. *In vitro* studies revealed differences in the speed of viral uptake and spread between bat-derived RABV and a RABV vaccine strain, suggesting the use of receptors strongly depends on the viral strain (70). Still, more research is needed to elucidate the role of different RABV receptors, their strain-specificity, the need of co-receptors, and the involvement in infection and spread. After receptor- (66–69) or clathrin-mediated endocytosis (64), the low pH within the endosomal transport vesicles induces a conformational change of the viral G-protein inducing the fusion of viral and cellular membranes (71). As a result, the viral RNP complex is released into the cellular cytoplasm. The RNP complex comprises all necessary elements to successfully mediate transcription and replication (72). Both processes start at the 3' end and progress

towards the 5’ end of the viral genome (73). Prior to the occurrence of viral replication, the viral RNA polymerase mediates transcription resulting in the synthesis of monocistronic transcripts (54,74). Firstly, a non-capped non-polyadenylated leader RNA is produced which is transformed into five capped and polyadenylated mRNAs coding for the five structural proteins. Transcriptional efficiency is decreasing from 3’ towards the 5’ end suggesting that gene expression strongly depends on its genomic location. Replication results in the generation of a positive-stranded genome that serves as a template to generate the negative-stranded genome for RABV progeny virions. Thus, the RNP complex can act as a transcriptase or a replicase. The proportion of transcription/replication depends on the concentration of viral N-protein. In the initial phase of infection, limited amounts of viral N-protein result in the release of a 5’ leader RNA. This leader RNA uncouples the encapsidation promoter from the generation of mRNAs. As a result, synthesized mRNAs are transcribed and translated, decreasing the viral replication rate. When enough viral N-protein is being present, the viral RNP complex turns into a replicase. Consequently, the leader sequence gets coupled with newly generated positive-stranded viral RNA, enabling viral encapsidation (58,75).

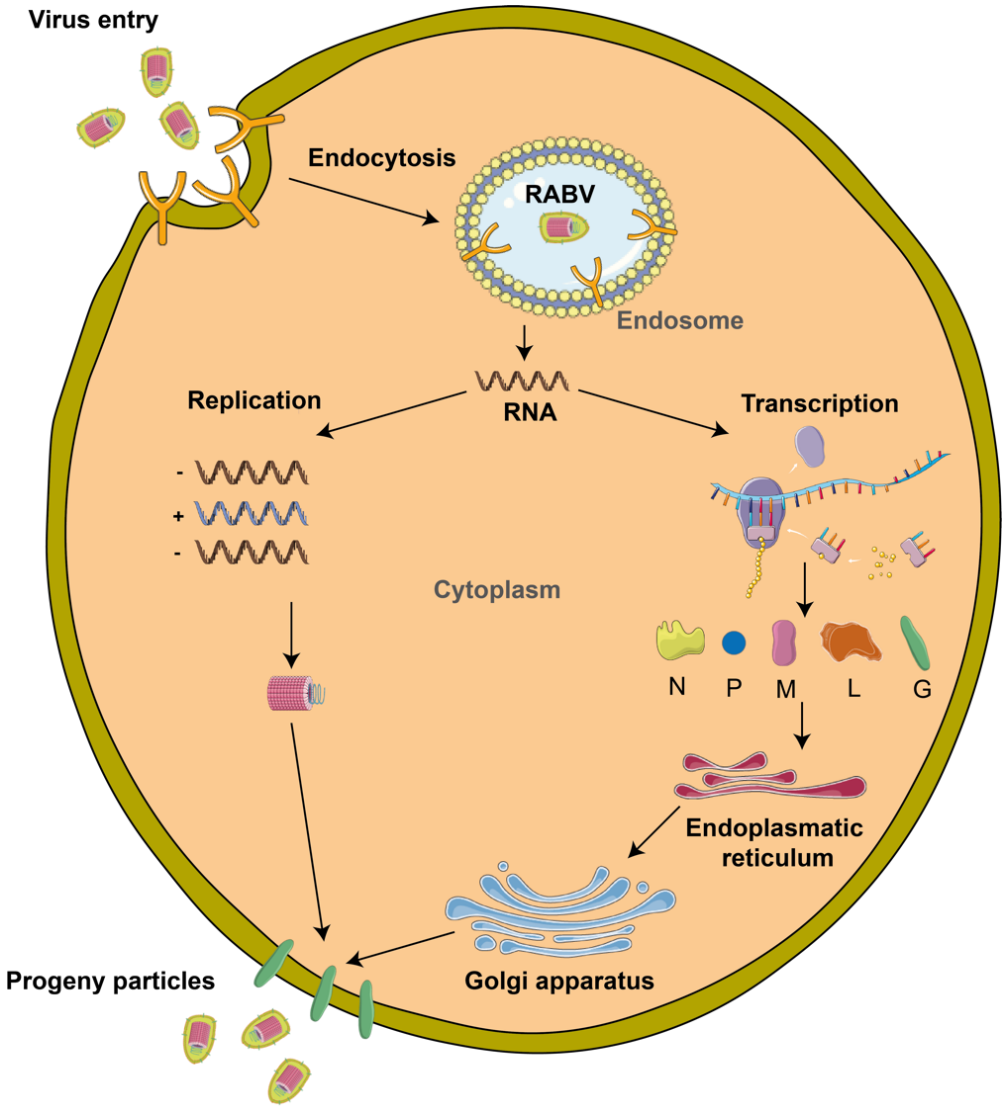

Figure 4 | Schematic presentation of the life cycle of RABV. After receptor-mediated endocytosis of RABV, G-protein-mediated fusion of viral membrane and endosomal membrane triggers the release of RABV into the cytoplasm. Transcription and translation of RABV occurs in the cytoplasm leading to the assembly of new virions in the cellular cytoplasm. Virions bud from the plasma membranes leading to the release of RABV particles at the end of the cycle (8,58). N = N-protein gene; P = P-protein gene; M = M-protein gene; G = G-protein gene; L = polymerase L gene.

1.4. Transmission and propagation strategies of RABV

Neurotropic RABV spreads from the infected entry tissue first to the PNS and subsequently to the CNS (Figure 5). In detail, the most efficient way of rabies transmission presents the exposure of broken skin to saliva from an infected animal (76). Classically, dog bites are the main source for RABV transmission to humans but even unrecognized superficial skin lesions might be the source of RABV infection (77). Other less efficient transmission routes include organ transplantation (78–81), inhalation of aerosolised RABV (82–85), as well as contamination of open wounds or mucous membranes with infected tissue (86). In the main transmission way, RABV is introduced into deeper tissue layers and replicates locally at the

entry site upon a bite (76). Differences in tropism and replication between different RABV strains in epithelial cells and fibroblasts site suggest that genetic differences between viruses account for viral tropism and replication potential at the entry site (6).

In detail, RABV is taken up by receptor-mediated endocytosis, from which the nicotinic acetylcholine receptor (NAchR) is expressed on the postsynaptic membrane of muscle cells, whereas the other receptors, neural cell adhesion molecule (NCAM) (67), p75 neurotrophin receptor (p75NTR) (68), and metabotropic glutamate receptor 2 (mGluR2) (69), represent *bona fide* neuronal surface receptor molecules (66,87). Expression of nAchR on the muscle membrane might be important for infection of muscle cells and subsequent infection of connected motor neurons via the neuromuscular junction (87). Viral uptake into unmyelinated terminals of sensory or motor nerves is mediated via receptor-mediated entry. Virions are embedded into endosomal transport vesicles and retrogradely transported along microtubules (10,88–91). In the neural soma, RNPs are released into the cytoplasm and a primary round of transcription occurs (62). Production of viral proteins results in the formation of viral inclusion bodies where a secondary transcription round takes place (92). Transcription results in the generation of newly synthesized RNPs which are consequently transported to the post-synaptic membrane. At the post-synaptic membrane, virions are assembled and bud through the post-synaptic neural membrane, giving the virions their outer lipid envelope. Released RABV particles are released to the neural cleft and taken up via receptor-mediated endocytosis at the pre-synaptic membrane (93).

The virions eventually reach the brain via G-protein-dependent transsynaptic transmission to next-order neurons. In the brain, RABV first infects the motor neurons which innervate the viral site of entry. Although the exact propagation of RABV in the CNS is still unknown (76,94), *post-mortem* examinations of human rabies patients showed that brainstem and spinal cord were preferential sites of virus entry (95). Despite the clinical diversity of furious and paralytic rabies forms, magnetic resonance imaging studies showed the involvement of brainstem, hippocampus, and hypothalamus in both forms (96). After viral propagation to the brain, RABV spreads to the salivary glands where virions are secreted into the saliva. Although RABV secretion into the saliva closes the transmission cycle, humans are likely to present a dead-end host for RABV infection (47).

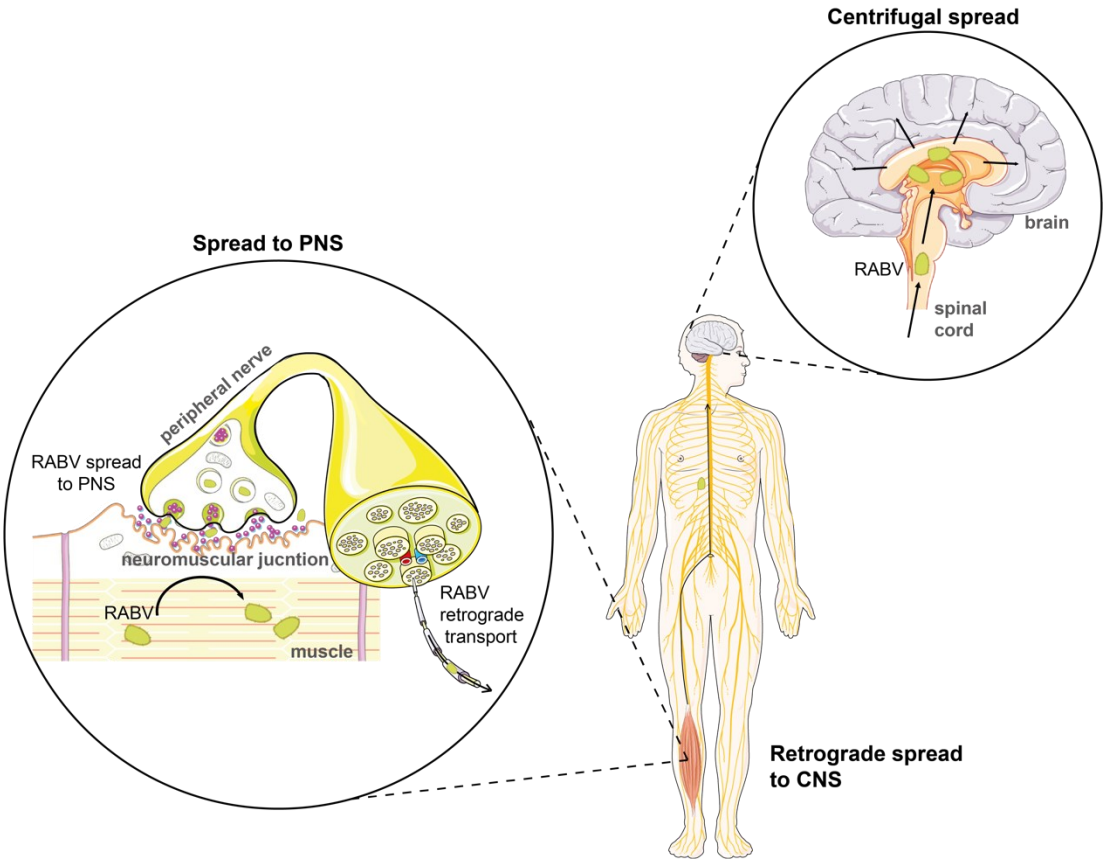

Figure 5 | RABV propagation and spread. RABV locally replicates in the wound before it spreads to the PNS via the neuromuscular junction. Once inside the PNS, RABV travels in a retrograde fashion along neuronal microtubules prior to CNS infection. After RABV arrives in the CNS, the virus distributes in the brain via centrifugal spread. Like this, RABV reaches the salivary glands to ensure transmission to other hosts to complete the RABV life cycle (8).

1.5. The horrifying clinical picture of rabies

Clinical features of rabies are generally divided into the incubation period (20-90 days), the prodromal stage (2-10 days), and the acute neurological phase (2-7 days) which is followed by coma (0-14 days) and ultimately death. Within this classification, the acute neurological phase can be re-divided into two distinct clinical syndromes: The classic form, encompassing encephalitic/furious and paralytic rabies, and the non-classic form. In the classic form of rabies limbic symptoms dominate whereas paralysis of lower motor neurons dominates in the non-classic form (97).

The incubation period is most commonly between 1-2 months, although in some cases the onset of symptoms appeared after less than seven days to more than 6 years. Unusually long incubation periods of several years have been found in immigrants who migrated from Asia to the United States (98). On the contrary, especially short incubation periods have been

observed in cases where RABV was directly inoculated into the nervous tissue via brachia-plexus injury from dog bites (Hemachudha and Phuapradit, 1997).

The incubation period ends when RABV virions enter the dorsal root ganglia causing neuropathic pain and fever. At this prodromal stage, symptoms are vague and non-specific, and most patients will die within two weeks. However, most people describe local symptoms or neuropathic pain earlier during the course of infection: Around a third of dog-transmitted human rabies cases and 75% of bat-transmitted human rabies cases experienced a burning sensation, numbness, itching, or pruritus at the bite site (100).

After the prodromal stage, the acute neurological phase starts presenting in clear signs of nervous system dysfunction. In the acute neurological phase, the classic form of rabies presents signs of nervous system dysfunction whereas non-classic forms of rabies do not present this distinct characteristic. As a result, non-classic rabies resembles encephalitis forms caused by other viral species such as enterovirus-71 (101), Nipah virus (102), or Japanese encephalitis virus (103). Around two third of the classic rabies cases present the furious form while the rest presents the paralytic form. Clinical data from 115 rabies patients revealed shorter survival periods for patients contracting the furious form (5.7 days) compared to the paralytic form (11 days). All patients contracting furious rabies form presented fluctuating consciousness, inspiratory spasms, hydro- or aerophobia, and signs of autonomic dysfunction (99). One of the first symptoms in furious rabies are hyperactivity provoked by thirst, anxiety, light, and many other stimuli. Within the next 24 hours, patients present fluctuating consciousness, inspiratory spasms, and signs of autonomic dysfunction. Mentally, patients alternate between normal periods and periods of progressive depression. Upon the appearance of those cardinal signs, patient's consciousness gradually worsens until patients fall into coma. Comatose patients present flaccid limb weakness, a manifestation which is often leads to a misdiagnosis with paralytic rabies (104). Paralytic rabies lacks major cardinal signs completely or signs appear late, often resulting in misdiagnosis. Symptoms which might appear during the disease course include phobic spasms, inspiratory spasms, and facial diparesis. Cardinal features of paralytic rabies include motor weakness of all limbs and respiratory muscles as initial manifestations. Most likely, peripheral nerve dysfunction causes the motor weakness in paralytic patients (105). Moreover, segmental demyelination of peripheral nerves was observed in *post-mortem* studies of human patients. Chopra and colleagues suggested that a protein of RABV might be cross-reacting with myelin leading to primary demyelination of peripheral nerves (106).

In the final phase of the disease, inspiratory spasms and tachycardias is in some cases followed by supraventricular and ventricular arrhythmia. A reduction of the ejection fraction

leads to hypotension. This might result from viral-induced myocarditis. In almost all cases, patients fall into coma before circulatory insufficiency manifests. In around half of the patients, hematemesis is observed several hours before death (100).

Dissemination of RABV in the CNS is accompanied by the occurrence of pathological changes in the brain, such as neuronal necrosis and perivascular cuffing (97,107). Eventually, rabid patients die due to circulatory insufficiency, cardiac arrest, or respiratory failure. Still, the exact mechanisms underlying RABV-induced death are still not completely understood.

1.6. Taking a glimpse at the molecular pathogenesis of rabies

Despite severe clinical manifestations in RABV patients, macroscopic and histopathological changes in the CNS of infected patients appear quite mild and non-specific (95,108,109). Only approximately 50% of paralytic rabies patients show pleocytosis and elevation of protein levels above 40 mg/cl (106). Due to the lack of studies investigating human infections we are far from understanding the link between the RABV infection pattern in the CNS and clinical symptomatology. Additionally, examining *post-mortem* human brains provides only a snapshot of the final stage of the disease without linking RABV spread to its clinical manifestations.

In general, both rabies forms show signs and symptoms indicating firstly a derangement of peripheral nerves or anterior horn cells in the spinal cord and secondly the impairment of cerebral functions. In human rabies, however, magnetic resonance imaging (MRI) fails to explain this clinical diversity (96). Hyperintense lesions on MRI scans appear due to increased water content disregarding its cause. Consequently, MRI scans of rabies patient cannot distinguish between inflammation, demyelination, edema, or axonal loss rendering it impossible to correlate pathophysiological lesions with clinical disability (110). Similarly, RABV antigen distribution in brainstem and spinal cord does not correlate with clinical presentation of rabies patients. Most of the patients showed a high number of antigen-containing neurons in brainstem and spinal cord whereas only a small amount of RABV antigen was found in hippocampi and hippo thalami. Eight days after the onset of clinical symptoms, RABV antigen are being found in the whole neuroaxis. Signs of inflammation are usually observed in the brain stem and/or spinal cord. Inflamed tissues presented perivascular and parenchymal infiltration with mononuclear cells. Neuronal degeneration is rarely observed throughout the infected CNS (95).

1.6.1. Electrophysiological studies

Electrophysiologic studies showed evidence that peripheral nerve dysfunction contributes to the observed weakness in paralytic rabies patients. Paralytic patients presented multifocal demyelination, sensory neuropathy, reduction of conduction velocities, as well as loss of motor and sensory amplitudes. Additionally, paralytic rabies patients presented more intense inflammation of spinal nerve roots compared to furious rabies patients. In contrast, furious rabies patients showed chromatolysis of anterior horn cells suggesting that different sites of neural involvement are responsible for the clinical differentiation into two rabies forms (105).

1.6.2. Histopathological studies

Histopathological studies observed segmental demyelination remyelination of peripheral nerves in paralytic patients strengthening the link between peripheral nerve dysfunction and paralysis (106). In contrast, demyelination was absent in furious rabies patients (111). The most striking observation of Chopra and colleagues was severe inflammation of the spinal cord. Inflammation most emphasized on anterior horns, especially the lumbar and lower dorsal segments, with decreasing inflammation at higher levels. Inflamed tissues displayed infiltrating lymphocytes and proliferating microglia. In the brain, inflammation was mostly located in the medulla (106). Often rabies patients display cerebral edema and congestion of leptomeningeal and parenchymal blood vessels might occur (111,112). Brain herniation, subarachnoid, or parenchymal hemorrhage, however, are not features of rabies encephalitis (113). Histopathological features observed in the brain of rabies patients include mononuclear cell infiltration of leptomeninges and neuronophagia (114), perivascular cuffing and microglial activation (106,115) with the formation of *Babes nodules*[1] (116). Still, those features are not unique features of rabies but rather common features of a variety of other viral encephalitis (117). Yet, eosinophilic cytoplasmic viral inclusions mainly found in neurons, named Negri bodies, are unique to rabies (92,118). Commonly, inflammatory cell infiltration of the leptomeninges is observed in *post-mortem* examinations of human rabies patients although the degree of inflammation varies enormously (109,111,114). Infiltrating cells include mainly lymphocytes and monocytes, however, neutrophils can predominate when inflammation is severe as observed in fulminant childhood cases (109,111). Babes was the first who described microscopic accumulations of cells surrounding degenerated neurons, the so-called *Babes nodules*. Later, Dupont and Earle observed them in 42% of their cases. In many cases activated microglia were found in the medulla and exhibited a rod-like morphology (114). While examining a patient who died 17 days after the onset of encephalitic rabies, Iwasaki and

[1] pericellular inflammatory islets of rabies and predominantly composed of activated monocytes and microglia, in the literature commonly referred to as *Babes nodules* (116)

colleagues showed that 50 – 70% of perivascular mononuclear cells were $CD3^+$ T helper cells. Nevertheless, another rabies virus patient who survived for 9 days displayed no inflammation despite the presence of numerous Negri bodies (119,120).

Neuronophagia[2], is a common feature of rabies, however, its extent varies enormously between rabies patients. Among their 49 fatal rabies cases, Dupont and Earle observed neuronophagia in 57% (114). Within these microscopic patterns, neurons exhibit a shrunken morphology with a condensed cytoplasm and pyknotic nuclei (109). Some paralytic rabies patients revealed extensive neuronal degeneration and loss in anterior and posterior horns of the spinal cord (106). Other cases showed occasional chromatolysis of neurons, characterized by cytological swelling of the neural soma (115). In contrast to humans, rodents experimentally infected with RABV street virus display intact neurons showing little pathological alterations at the level of their organelles. Yet, infecting rodents with fixed virus variants using artificial inoculation methods like intracerebral inoculation leads to extensive inflammation in the CNS. Frequently, animals exhibit widespread neuronal injury, cell death, and intracellular edema (121,122).

Although it is still not understood yet, which role apoptotic cell death plays in rabies pathogenesis, current data suggest that apoptosis is not a main process involved in human rabies (123). By investigating the CNS of 10 human rabies cases, Junkatrul *et al.* showed that neurons throughout the neuroaxis showed apoptotic features in contrast to neurons in the spinal cord (124). Still, apart from cytochrome-c immunoreactivity and terminal deoxynucleotidyltransferase-mediated DNA nick-end labelling (TUNEL), morphological features of apoptosis were not investigating leaving the role of apoptosis in natural rabies infection debatable. Adult and immature mice which were intracerebrally inoculated with the challenge virus standard (CVS) strain or fixed RABV strains or revealed prominent signs of neuronal apoptosis (123,125–128). Peripheral inoculation of fruit-eating bat species *Artibeus jamaicensis* with rabies CVS strain did not reveal signs of apoptosis (129). Intracerebrally inoculating bats with street RABV strains showed little or no $TUNEL^+$ neurons (126,130) except for one study (131). Although current data suggests that the molecular pathophysiology of rabies strongly depends on the virus strain, its host, as well as host factors, we still do not understand the molecular pathways underlying rabies clinical presentation. Baloul and Lafon proposed that RABV induces a '*subversive neuroinvasive strategy'* helping RABV to preserve an intact neuronal network thereby guaranteeing the transmission to the next host. According

[2] accumulation of activated macrophages and microglia which are phagocytosing degenerated neurons

to this strategy, RABV avoids neuronal apoptosis, permitting RABV dissemination and ensuring its excretion into the host saliva (132).

1.6.3. Transcriptome studies

To better understand rabies pathogenesis, numerous transcriptome studies have been performed *in vivo* (133–139) and *in vitro* (140–142) to gain an insight of the underlying signalling pathways shaping rabies pathogenesis. While comparing transcriptome profiles of wt RABV infection (silver-haired bat RABV, abbreviated SHBRV) and lab-attenuated RABV infection (B2C) in infected mouse brains using an Affymetrix array, Wang *et al.* revealed that attenuated RABV activates whereas pathogenic RABV rather evades the host immune response (133). In detail, genes coding for interferon regulatory proteins, the 2′-5′-oligoadenylate synthetase or myxovirus proteins were highly induced in B2C infection but not in SHBRV infection. Further, Zhang and colleagues compared infection of the lab-attenuated RABV strain HEP-Flury with the virulent RABV strain CVS-11 (135). After intranasal inoculation, infected mice exhibited subtle clinical signs and recovered whereas CVS-11 infection was fatal. Comparing RNA-Seq profiles of both viruses, various genes involved in MHC class II-mediated antigen presentation were induced to a higher extent during HEP-Flury infection compared to CVS-11 infection. As a result, Zhang *at al.* hypothesised that MHC class II signalling is crucial to clear attenuated RABV from the infected CNS (135). Additionally, Jamalkandi *et al.* identified important signalling pathways implied in rabies pathogenesis (138). Using a data-driven approach from systems biology, they meta-analysed whole-transcriptome microarray datasets of mice (CNS) infected with the CVS-11 strain. The analysis of signalling pathways revealed that RABV modulates pathways implied in controlling immunity, cell cycle and survival, viral replication and folding, as well as synapse regulation (138). Apart from classical transcriptome studies focusing on the differential expression of total RNAs or mRNAs, recent publications provided evidence that wt RABV differentially modulates lncRNA (136,139) and circRNA expression (137). Although the role of lncRNAs and circRNAs in RABV is still elusive, it is speculated that modulation of lncRNAs and circRNAs interferes with host immune responses (136,137), immune evasion and neuronal injury (139), as well as cell plasticity and synapse function (137).

Apart from *in vivo* studies, *in vitro* transcriptome studies were performed to elucidate the signalling pathways of the distinct CNS cell types during RABV infection (140–142). Recently, Huang and colleagues conducted the first single cell RNA sequencing (sc RNA-Seq) experiment investigating transcriptional responses of mouse dorsal raphe nucleus (DRN) upon axonal infection of dorsal raphe serotonergic neurons (141). Following intracranial injection of glycoprotein-deleted rabies virus (SADΔG B19 strain), sc RNA-Seq was conducted on the

DRN at 7 days post-injection. Pathway analysis provided evidence that the SADΔG B19 strain downregulated metabolic processes and neurotransmission. Further, diverse infiltrating leukocyte populations were found in the DRN following infection. Further, type I and II IFN responses were orchestrated from infiltrating $CD4^+$ T cells and microglia (141).

Although both, *in vivo* and *in vitro* transcriptome studies provided evidence for underlying signalling pathways shaping rabies pathogenesis (133–142), the exact mechanisms of immune circumvent and why humans are unable to clear RABV from the infected CNS are poorly understood. Consequently, the lack of knowledge deciphering the distinct signalling pathways between the diverse cell types of the CNS upon RABV infection urges further research.

1.7. Innate immune mechanisms shaping CNS homeostasis

To protect our body from foreign invaders, the innate immune system displays the first defensive shield against pathogenic invasions. Unlike being unspecific, as originally assumed, it can differentiate between self and foreign structures. On a molecular level, germline-encoded pattern-recognition receptors (PRRs) recognize structural components of the invaders, so called pathogen-associated molecular patterns (PAMPs) or secreted components referred to as danger-associated molecular patterns (DAMPs) (143). PAMPS of RNA viruses are double-stranded RNA (dsRNA) or uncapped RNA containing a 5’ triphosphate, products that usually appear during viral replication or transcription (144). Each PRR reacts with a specific PAMP or DAMP, inducing a distinct signalling pathway which leads to the establishment of an immune response. In detail, PRRs are divided into different groups such as toll-like receptors (TLRs), retinoic acid-inducible gene I (RIG-I) like helicases (RLRs) or nucleotide-binding oligomerization domain-like receptors (NOD-like receptors) (143). For instance, during viral replication viral RNA products often stimulate cytoplasmic RLRs (145). Different receptor types are constitutively expressed in mammalians whereas receptors differ in their cellular location. Moreover, cells differentiate in their expression level of PRRs and their cell-specific receptor reservoir (146,147).

The neural network of the CNS is protected by resident glial cells which are classically divided into astrocytes, oligodendrocytes, and microglia. Inside the CNS, astrocytes are the most abundant type of glial cells and important players in monitoring brain development as well as modulating synaptic activity (148). Oligodendrocytes are the myelin-producing cells of the CNS, insulating neuronal axons thereby enabling the rapid transmission of axon potentials (149,150). Microglia, a rather small population of the human CNS, are macrophage-like cells derived from primitive myeloid progenitors in the yolk sac (151). Microglia are the counterpart

of macrophages in the periphery and play pivotal roles in immunosurveillance of the CNS (152). Interaction between neurons and glial cells is critical for CNS immunity: Under physiological conditions, the constitutive expression of off signals prevents the activation of glial cells, suppressing inflammation in the healthy CNS (153–156). Initiation of neuronal death modulates the expression of those inhibitory molecules leading to the abrogation of glial expression and the induction of inflammation (154,157,158).

1.8. So little and yet so smart

Like many other viruses, RABV expresses proteins which directly interfere with the interferon (IFN) signalling pathway. RABV seems to have evolved a neuro-protective capacity which enables viral replication in neurons without inducing an excessive activation of glial cells. Maintenance of an integer and healthy neural network is one of the key features of RABV infection and spread. A variety of available data revealed accessory immune evasive functions of viral P-protein, N-protein, and M protein (Figure 6) (159).

1.8.1. Phosphoprotein

The P-protein is present in all viruses of the *Mononegavirales* order. Yet, no or little similarity has been found between P-protein gene sequences from different Mononegavirales families or within members of the Rhabdoviridae family (160). Still, sequence data suggest a modular organization of viral P-protein gene explaining the flexibility of viral P-protein: The P-protein is essential for viral replication but fulfils many other functions by interacting with host proteins (161–164). Regarding accessory functions, RABV P-protein is the best studied protein of RABV (165–168). By translocating the P-protein gene to a promoter-distal gene position, Brzózka and colleagues showed that RABV expressing low levels of P-protein failed to successfully prevent the induction of IFNs (169). Adjacently, the Conzelmann group showed that P-protein inhibits IRF3/IRF7 phosphorylation via TBK1 (170,171). Subsequently, it was shown that P-protein interacts with Signal Transducers and Activators of Transcription (STAT) 1 and STAT2 hindering their nuclear translocation in response to type-I and type-II IFNs (172,173). Recently, it was also shown that the P-protein inhibits IL-6 dependent signalling via STAT1-mediated interaction with STAT3 (174,175). Apart from full length P-protein which interacts with the polymerase L (referred to as P-protein or P1), RABV P-protein gene expresses four N-terminal truncated isoforms, P2 – P5. Since P2 – P5 lack the N-terminal binding sequence it is suggested that they perform alternative functions in IFN antagonism (165). P1/P2 efficiently exploit the cellular trafficking machinery: P1/P2-associated STATs are excluded from the nucleus (164,172–174,176–178). P3 locates at microtubules enabling the

cytoplasmic arrest of P3-associated STATs and modulates DNA binding of STAT1 (179,180). In a nutshell, viral P-protein shows efficient shutdown of the antiviral response via its IFN and IL-6 signalling antagonism.

1.8.2. Matrix protein

Viral M protein targets RelAp43, a member of the nuclear factor 'kappa-light-chain-enhancer' of activated B-cells (NF-κB) family subsequently inhibiting the NF-κB pathway (181). This interaction is crucial for expression of IFN-β, TNF-α, IL-8, and CXCL2, emphasizing its role in the suppression of the host innate immune response (181). Further studies revealed that the M protein interaction with RelAp43, ABIN2, and TPL2 perturbs the RelAp43-p105-ABIN2-TPL2 complex which is crucial for the control of IFN-β, TNF-α, and CXCL2 (182). Recently, it was shown that the M protein cooperates with viral P-protein: Upon type-I IFN stimulation, the M protein interacts with pSTAT1 thereby strengthening the capacity of viral P-protein to interact with pSTAT1 and to restraint it in the cytoplasm (183). Thus, viral M protein is involved in NF-κB, JAK (Janus kinases) and STAT antagonism.

1.8.3. Nucleoprotein

RABV N-protein also seems to have IFN antagonistic functions by interacting with intracellular sensors such as RIG-I (184–186). Masatani and colleagues showed that the N-protein of the pathogenic RABV Nishigahara strain evades the activation of RLR RIG-I thereby suppressing the expression of IFNs and chemokines such as C-C Motif Chemokine Ligand 5 (*CCL5*) and C-X-C Motif Chemokine Ligand 10 (*CXCL10*) (186). Analysis of the N-protein sequence revealed that amino acids at position 273 and 394 were responsible for evasion from RIG-I-mediated antiviral responses (185,186). In contrast to viral P-protein (187), N-protein mediated evasion from the host immune responses acts upstream of TBK1/IRF3 at the level of viral sensors (186).

1.8.4. Polymerase

The large protein L of RABV is a multifunctional RNA polymerase with remarkable homology to the L protein of VSV. Based on the strong homology, it is assumed that the viral L protein of RABV catalyzes similar processes, such as 5′-capping, cap methylation, and 3′-polyadenylation (188). Generally, uncapped RNA molecules are rapidly detected as ‘non-self’ resulting in degradation of RNA structures and the production of IFNs. Further, RNA capping modulates RNA stability, splicing, and translation (189). Thus, although little is known so far about the underlying mechanisms of polymerase L-mediated RNA capping (190), it can be suggested that the L-protein hinders innate immune detection by inducing post-transcriptional modifications into viral RNA structures. Still, more research is needed to understand the exact function of how the viral L-protein escapes TLR and RLR recognition.

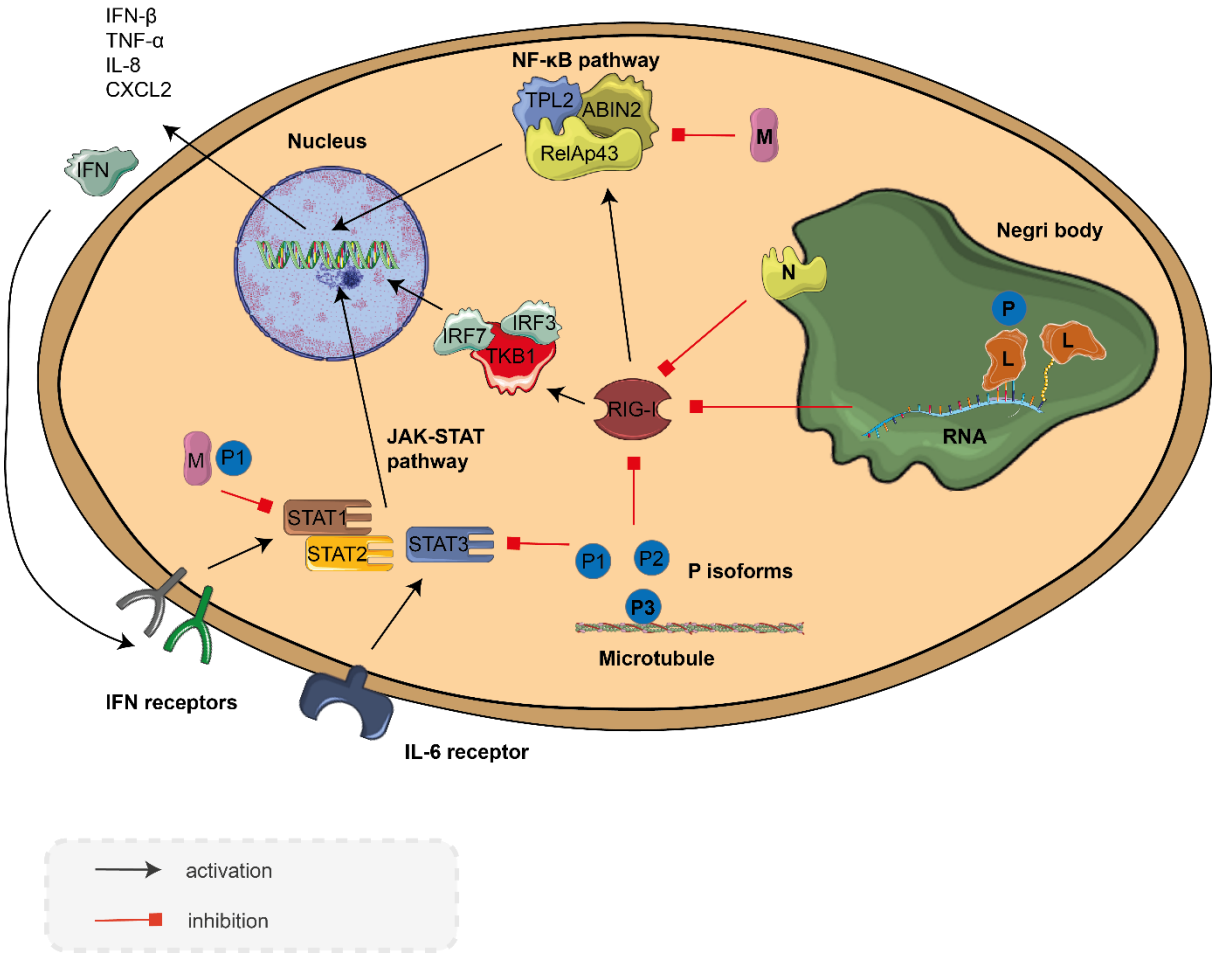

Figure 6 | Molecular mechanisms underlying RABV-mediated immune evasion. RABV efficiently suppresses the innate immune response of the host via accessory functions of viral N-protein, P-protein, M-protein, and L-protein. Whereas the N-protein acts on the level of cellular receptors (RIG-I) (186), P- and M proteins target the downstream signalling pathways: Viral P-protein shows a profound STAT antagonism (172–175) as well as inhibition of IRF3/IRF7 phosphorylation downstream of RIG-I activation (170,171). Additionally, the viral M protein shows STAT antagonism (183) as well as suppression of the NF-κB pathway (181,182). Viral N-protein mediates capping of viral RNA structures (190), suggesting interference with recognition from TLRs and RLRs. Figure is taken and modified from Ito *at al.* (159).

1.9. Re-defining RABV tropism: Neuron-specific tropism or not?

As mentioned earlier, RABV is classically referred to as neurotropic (191,192). In short, that means nothing more than that RABV infection and replication is preferentially seen in the nervous system. In detail, however, RABV is originally believed a neuron-specific pathogen and was consequently used as a transneuronal tracer (9). Nevertheless, recent data provide

evidence of infection of other cells of the nervous system *in vivo* (193,194), particularly astrocytes and Schwann cells, questioning a neuron-specific tropism.

The RABV replication cycle starts with the viral G-protein binding to different RABV receptors thereby enabling RABV entry to the cell: whereas NCAM (67), p75NTR (68), and mGluR2 (69) represent *bona fide* neuronal surface receptor molecules, NAchR (66) is expressed on muscle cells and may support RABV amplification prior to neuron infection through moto-neuronal endplates. The fact that RABV receptor expression in mice and humans does not positively correlate with cellular susceptibility to RABV infection (66,195) suggests that receptor usage alone is not determining the strong neuron-specific tropism of RABV. Recent single-cell sequencing data of human brains provide evidence that p75NTR, mGluR2, and NAchR expression is relatively low in the human brain, whereas NCAM is robustly expressed. In detail, NCAM was predominantly found on neuronal cells, but shown to be also highly expressed on oligodendrocytes and certain astrocyte subsets. In contrast to cells of ectodermal origin, microglia show low or no expression of NCAM in the human brain (196). Considering the remarkable tropism of field RABV strains for non-neuronal cells in comparison to less virulent laboratory-attenuated strains (194) and the broad distribution of RABV receptors in the CNS (87,196), evidence is accumulating that RABV neuron-specific tropism may not exclusively be a result of neuron-specific receptor expression. Apart from the concentration of RABV cell entry receptors (87), preferential infection of neurons by RABV is shaped by several additional factors: intraneuronal long distance virus transport processes at the virus entry site and after replication and specific trans-synaptic spread between neurons (197–200).

Apart from receptor usage and cytoskeletal specificities, cell type-specific inhibition of virus replication in non-neuronal cells might play a crucial role in RABV neuron-specific tropism. Generally, it is believed that vertebrates are incapable of tolerating the death of non-renewable cell types, such as neurons, as a strategy to control virus infection (201–203). It is suggested that neurons lack robust innate immune signalling pathways, particularly robust IFN signalling pathways, to minimize harm (204). There are evidence reporting that neurons rather activate the autophagy pathway, including several distinct forms of lysosomal degradation, to restrict RABV replication (205). Likewise, a lower protective antiviral immune response in neurons as compared to other susceptible cell types might result in the preferential infection of neurons (206). In contrast to neuronal cells, entry to non-neuronal cell types induces immediate and strong innate immune responses (207,208) in a virus strain dependent manner (194) which might result in the abortion of viral infection. Although little is known about the underlying mechanisms defining RABV tropism, it is hypothesised neurotropic strategy of RABV might present a viral adaption mechanism avoiding the detection of the viral invader by the host

(206). Apart from cell-intrinsic effects, paracrine effects through cytokine release by abortively or productively infected non-neuronal cells like astrocytes or Schwann cells surrounding neurons (193,194) may also determine the susceptibility and survival of neurons and other cell types that can be easily infected *in vitro* (209). Still, more research is needed to link cellular susceptibility to the pathogenicity of the viral strains.

In short, more and more reports relativize the concept of an almost exclusive infection of neurons (193,194,210–212). Therefore, the concept of an almost exclusive infection of neurons must be relativized.

1.10. Cellular players in innate immunity

Inside the CNS, the neuronal network is protected from pathogens via resident glial cells (213). The role of glial cells during RABV infection is controversially discussed. In contrast to the strong neuron-specific tropism observed *in vivo*, a broad range of cell types including glial cells can be infected *in vitro* (171–173). Although RABV is classically demonstrating a highly neuron-specific tropism *in vivo*, recent publications revealed that glial cells, especially astrocytes and Schwann cells, can be heavily infected *in vivo* (167,169,174,175). Even though several other cell types, except for neurons, are susceptible towards RABV infection, induced immune responses upon infection differ tremendously (Figure 7). Still, little is known about the role of glial cells during RABV infection although the impact of glial cells in the RABV-infected CNS remains a significant question of interest.

1.10.1. Neurons

RABV strongly infects neurons *in vitro* (191) and *in vivo* (9,197,198,214). Upon CVS challenge, human TLR3$^+$ neuronal NT2-N cells strongly induce the upregulate the expression of IFN-β, chemokines, and cytokines (215). Additionally, CVS infection of human neuroblastoma cells leads to the localization of TLR3 into spherical perinuclear structures (216), which are referred to as Negri bodies (NBs) and represent active replicates sites for RABV (92,217). Together with enhanced TLR3 expression in cerebral cortical tissues in rabies patients (218), it seems that RABV inactivates the physiological function of TLR3 as a viral sensor and exploits TLR3 functions for the spatial arrangement of RABV-induced NBs to support viral replication (216,217). Additionally, TLR3 was shown to mediate neuronal apoptosis (219), suggesting that RABV-mediated sequestration of TLR3 might allow RABV to escape TLR3-mediated apoptosis. Apart from TLR3, wt RABV induces autophagy in neuroblastoma cells *in vitro* which can in turn decrease apoptosis (205). Overall, RABV-

mediated inhibition of apoptosis and inflammation ensures the integrity of the neuronal network subsequently enabling RABV transport throughout the CNS (132). Although neurons have an intrinsic machinery to sense viral infection (205,215), it is believed that neural immune responses to viral infections are limited in comparison to surrounding glial cells (201–204).

1.10.2. Astrocytes

Like neurons, scientific evidence show that RABV successfully infects astrocytes *in vitro* and *in vivo* (194,207,208). *In vivo* infection, however, might result in abortive infection due to the strong induction of type-I IFNs upon infection with attenuated RABV (207). I*n vitro* studies revealed that attenuated RABV synthesizes more double-stranded RNA (dsRNA) compared to wildtype (wt) RABV. As a result, dsRNA is recognized by RLRs such as RIG-I and melanoma differentiation-associated protein 5 (Mda5). Subsequently, activation of RLRs results in the activation of dsRNA-dependent mitochondrial antiviral signalling protein (MAVS) by attenuated RABV which is supposedly suppressed during wildtype RABV infection. Subsequently, MAVS triggers the expression of IFN-stimulated genes (ISGs) thereby inhibiting RABV replication and spread in astrocytes. Induction of inflammatory cytokines (TNF-α, IL-6, IL-1β, IFN-γ, IL-17, and VEGF) by astrocytes affects BBB permeability subsequently strongly influencing the disease outcome (208). Other *in vitro* studies confirmed infection of astrocytes but did not observe differences between lab-attenuated and street viruses (220). A comparison of different recombinant field and lab-attenuated strains in infected mice highlighted the productive infection of astrocytes in the CNS in mice intramuscularly infected with highly virulent field RABV. In contrast, lab-attenuated RABV or vaccine strains revealed no or only abortive infection of astrocytes (194).

In general, astrocytes have a higher basal expression level of ISGs rendering them less susceptible towards viral infections (221). Upon attenuated RABV infection, astrocytes induce the expression of IFN-β via RLR and TLR signal transduction pathways, presenting the principal producers of IFN-β in the virus infected CNS (207). Similarly, astrocytes have been shown to be the key producers of IFN-β for other neurotropic infections suggesting a pivotal role for astrocytes in the viral infected CNS (222,223). Interestingly, pathogenic field RABV strongly modulated miRNA expression of infected mice. Targets included TGFβ, JAK2, suppressor of cytokine signalling (Socs2), and Socs4 (224). The JAK2/STAT3 signal transduction pathway is well known to play a crucial role in astrocyte reactivity upon multiple pathological conditions (225). Pathological RABV might evade JAK2/STAT3 signalling leading to the productive replication of RABV in astrocytes. Thus, immune evasive functions of RABV proteins might be able to suppress astrocytic innate immune responses enabling pathogenic RABV to replicate and spread in astrocytes.

1.10.3. Microglia

Apart from astrocytes or oligodendrocytes, human microglia were shown to be susceptible to the culture-adapted RABV ERA strain i*n vitro* (209). *In vivo*, ramified microglia of infected mice infected with a virulent RABV strain were shown to stain positive for RABV antigens. Yet, it is not clear if RABV successfully infects microglia or if microglia are rather phagocytosing degenerated infected neurons (226). Although it remains a matter of debate if RABV is actively replicating inside microglial cells, there are several reports which show that microglia are activated during RABV infection (140,183,227). Zhao *et al* showed by infecting the murine microglia cell line BV-2 with the lethal RABV CVS-11 strain that RABV induces the expression of ISGs (Isg15, Isg20, OASL1, OASL2, IFIT2, IRF7 and Ifi203), chemokine genes (CCL5, CXCL10 and CCRL2) and pro-inflammatory genes (IL-6) (140). Moreover, studying RABV infection of macrophages, the microglial counterpart of the periphery, revealed that chemokine expression was under the control of the ERK1/2 signalling cascade. In detail, endocytosis of inactivated RABV particles or infectious viruses lead to the induction of the chemokines via the ERK1/2 signalling pathway. Yet, RAW264 murine macrophages showed an extremely low susceptibility to RABV infection (228). In a following publication, Nakamichi and colleagues demonstrated that RABV can successfully infect Ra2 murine microglia *in vitro* and express viral proteins whereas genome synthesis and production of progeny viruses is vastly impaired. Infection with the highly neurovirulent CVS-11 strain resulted in upregulation of CXCL10 and CCL5 via induction of MAPK and NF-κB signalling pathways (229). Next to astrocytes, microglia present an important source of IFN-β during RABV infection *in vivo* (207).

1.10.4. Oligodendrocytes

Compared to astrocytes, oligodendrocytes present a rather small population of glial cells (230). Unlike astrocytes, little is known about the role of oligodendrocytes during RABV infection. Studying monosynaptic viral RABV tracers demonstrated occasional infection of oligodendrocytes (231,232). The functional counterpart of oligodendrocytes in the CNS are myelinating Schwann cells (SCs) in the peripheral nervous system (PNS) (233). Despite the fact that electron microscopy pictures demonstrated virion accumulation between axons and membranes of SCs, as well as nodes of Ranvier (122,234,235), SCs were long considered as unsusceptible towards lyssavirus infection (236). Recently, using a three-dimensional immunofluorescence imaging approach for high-volume tissue imaging revealed the detection of RABV-infected SCs in mice intramuscular and intracranial infected with field RABV (237). Consequently, Potratz and Zaeck suggested a model in which infection of peripheral SCs

suppresses glial-mediated innate immune responses and delays antiviral signalling in field RABV infections (193).

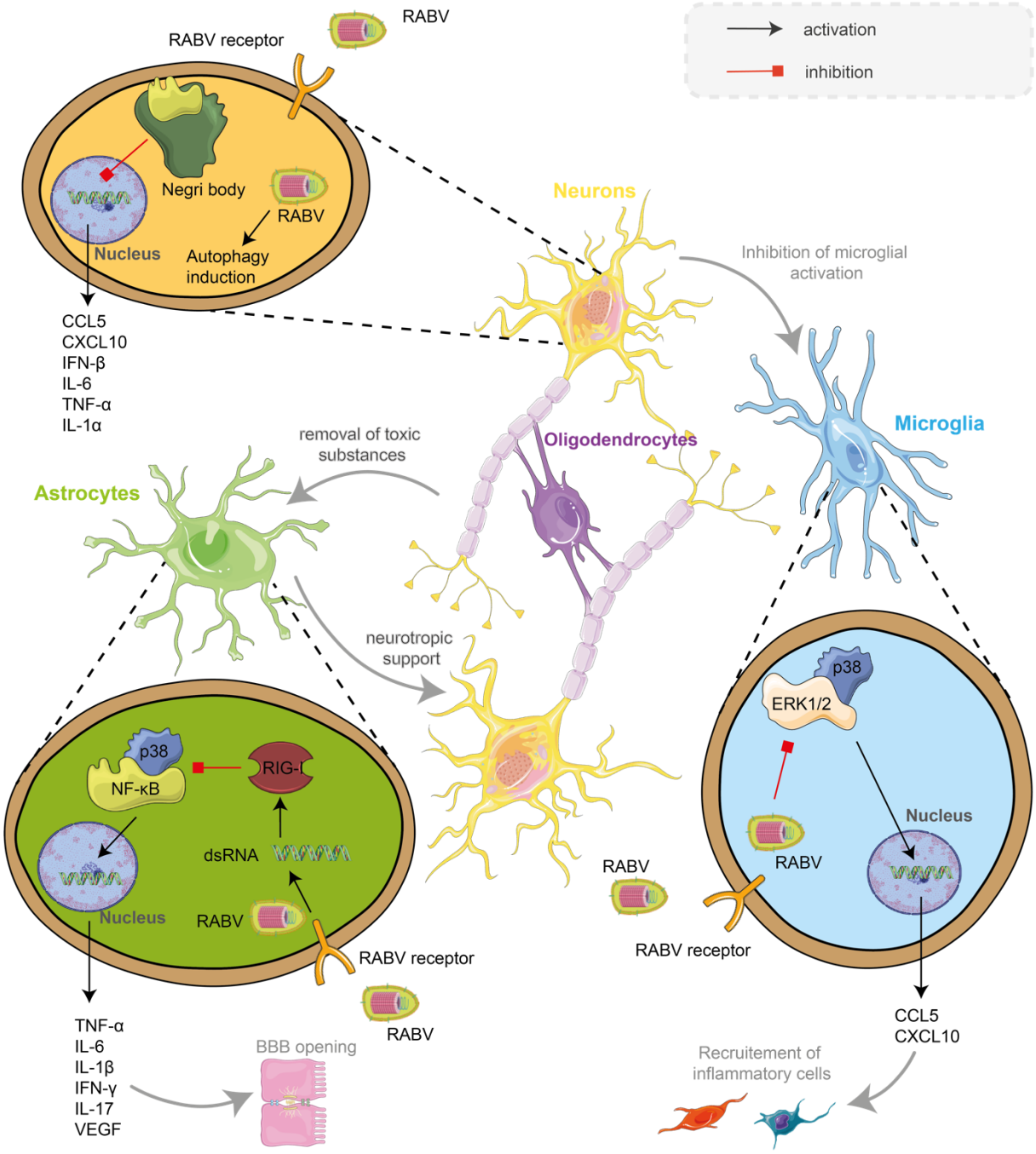

Figure 7 | Representative overview illustrating the inflammatory immune responses of CNS cell types upon RABV infection. RABV seems to limit inflammatory reactions initiated by neurons and neuronal apoptosis via the formation of viral production and inclusion bodies, so-called Negri bodies (NB). Functions of viral sensory, such as TLR3, are sequestered and exploited for the arrangement and functions of NBs (216,238). Like neurons, astrocytes are also permissive to RABV infection (194). It is suggested that wildtype RABV produces less dsRNA compared to attenuated strains, thus limiting sensing of RABV via RIG-I. Viral evasion of RIG-I-mediated NF-κB signalling pathway inhibits the expression of type I IFNs, pro-inflammatory interleukins, and growth factors thereby limiting blood-brain barrier (BBB) opening (208). Microglia sense RABV via the ERK1/2-p38 signalling pathway resulting in the secretion of the chemokines CCL5 and CXCL10 (229).

1.11. Project outline and objectives

Recently, the strict neuron-specific tropism of RABV has been questioned (193,194) and more research is needed to understand the roles of glial cell in the infected CNS. Previous data gave evidence that conserved resides in viral P-protein and M protein evade JAK-STAT and NF-κB signalling pathways (164,175,178,181,239). Still, gene expression studies of ISGs depend enormously on the investigated cell type and the used RABV strain thus do not present a reliable and universally applicable mechanism. Consequently, this research project targets to main objectives:

The first objective aimed at understanding the susceptibilities and immune responses of human glial cells in RABV pathogenesis *in vitro*. By introducing site-directed mutations into conserved residues of viral P-protein (W265G, M287V) and M protein (R77K, D100A, A104S, M110L) which were previously described to interfere with JAK-STAT and NF-κB pathways (164,175,178,181,239), we aimed to study their accessory roles in immune evasion in the different CNS cell types. Downstream analysis investigated cell specific immune responses of glial cells as well as the contribution of P- and M-proteins in counteracting the establishment of an antiviral response. More particularly, we used molecular cloning and high content screening to determine cellular susceptibilities. Further, we used gene expression quantification methods (quantitative PCR), protein quantification methods (Drop Array), and sc RNA-Seq approaches (10x) to determine cell type-specific immune responses to RABV.

The second objective was to determine the inflammatory transcriptome profile observed in the human brain of rabid patients. Although RABV is believed to cause only limited inflammation in the brain (8,206), most of the data that provide evidence are coming from cell culture (181,186,187,239,240) or animal experiments (133,241). Yet, a transcriptome analysis of *post-mortem* human brains from rabid patients is still missing. Therefore, we investigated the expression of a panel of inflammatory genes known to be involved in rabies pathogenesis in Tha-infected mice and compared the expression to *post-mortem* human brains of rabid patients from Cambodia. This project was conducted with the help of the Institute Pasteur of Cambodia which gave us the unique opportunity to get firsthand access to brain biopsies from rabid patients.

Objective 1: Studying RABV tropism *in vitro*

- Can we observe RABV neuron-specific tropism *in vitro*?
  - Are all CNS cell types susceptible towards RABV infection?
  - Can glial cells protect neurons from RABV infection?
  - Do CNS cell lines behave like stem cell-derived CNS cell types?
  - Do Tha and Th2P-4M show a similar viral tropism?
- Which immune responses induce the different CNS cell types upon RABV infection?
  - How do monocultures respond to RABV infection in terms of gene expression?
  - How do monocultures respond to RABV infection in terms of protein expression?
  - How do co-cultures respond to RABV infection in terms of gene expression?

Objective 2: Investigating the human inflammatory transcriptome profile during natural RABV infection

- Do murine and human RABV-infected brains show similarities in their inflammatory transcriptome profile?
- How can we explain similar or different host responses?

2. Results

2.1 Glial biology in herpes and rabies virus induced encephalitis (#Article 1)

2.1.1 The Big Bang of glial cells

During my PhD thesis, I contributed to a review that describes the roles of glial cells in viral encephalitis, particularly their roles in herpes- and rabies virus-induced encephalitis. Apart from summarizing the state-of-the art of innate immune signalling of glial cells, it urges researchers to take a closer look at the role of glial cells since glial cells remain poorly studied cells in neurotropic CNS infections.

Glial cells, more particularly astrocytes, microglia, and oligodendrocytes, constitute a large fraction of the mammalian brain which contributes between 33% and 66% of the total brain mass depending on the mammalian species (242,243). Nevertheless, and maybe since they were originally considered as simple glue for neurons (244), their physiological and pathological conditions remain to a certain extent unresolved (245). Distinct cell populations in the human brain are very heterogenous and mediate diverse and distinct cellular functions. Although neurons are key players in the transmission of electrical signals, recent data gave evidence that neurons are impaired in IFN signalling, the major pathway involved in antiviral signalling (204). In contrast, glial cells are known to be strong IFN inducers and to play major roles in viral clearance (207,246,247). However, and since most neurotropic viruses reveal a strong tropism for neurons in contrast to glial cells, neurotropic viral infections tend to be primarily studied in neuronal cells. As a result, little is known about the role of astrocytes or microglia in neurotropic infections.

Around 100 years ago, Pío del Río Hortega discovered oligodendrocytes and microglia (248,249) marking the Big Bang of glial biology. Although tremendous work has been performed in the field of glial biology (244), the underlying pathways determining differences between glial cell types and neurons regarding viral tropism and viral clearance remain to be exploited. In the future, modern technologies achieved by recent technological breakthroughs

will allow to answer more questions asked by glio-scientists, particularly helping to assess glial contribution to brain homeostasis or disease (250).

The review named '*Innate immune signalling and role of glial cells in herpes virus and rabies virus induced encephalitis'* sheds light to what is known so far about the susceptibilities of glial cells in herpes simplex virus (HSV) and RABV infection. Further, it elucidates the capabilities of neurons, astrocytes, and microglia in mounting innate immune responses against herpes and rabies virus infections. The following review article presents a draft which is currently in revision in the *Journal of Neuroscience Research*.

2.1.2 Article #1 *(in revision)*

Innate immune signalling and role of glial cells in herpes simplex virus and rabies virus-induced encephalitis

Lena Feige[1, 2], Luca M. Zaeck[3], Julia Sehl[4], Stefan Finke[3], Hervé Bourhy[1, *]

Author affiliations:

[1] Institut Pasteur, Lyssavirus Epidemiology and Neuropathology, 28 rue du docteur Roux, 75015 Paris, France

[2] University Paris Diderot, Sorbonne Paris Cité (SPCBio), Université de Paris, Sorbonne Paris Cité, Paris, France

[3] Friedrich-Loeffler-Institut (FLI), Federal Institute of Animal Health, Institute of Molecular Virology and Cell Biology, Südufer 10, 17493 Greifswald-Insel Riems, Germany

[4] Friedrich-Loeffler-Institut (FLI), Federal Institute of Animal Health, Department of Experimental Animal Facilities and Biorisk Management, Südufer 10, 17493 Greifswald-Insel Riems, Germany

Correspondence to: Hervé Bourhy

Full address: Institut Pasteur, Lyssavirus Epidemiology and Neuropathology, 28 rue du docteur Roux, 75015 Paris, France

E-mail: herve.bourhy@pasteur.fr

Abbreviations: AP-1 = activator protein 1; AQP4 = aquaporin 4; BBB = blood-brain barrier; cGAMP = cyclic guanosine monophosphate-adenosine monophosphate; cGAS = cGAMP synthase; CNS = central nervous system; COSR = coyote street RABV; CVS = challenge virus standard; DAI = DNA-dependent activator of IFN-regulatory factors; DCs = dendritic cells; ECs = endothelial cells; ERK = extracellular signal-regulated kinases; g = (HSV) Glycoprotein; G-protein = (RABV) Glycoprotein; HSE = HSV encephalitis; HSV = herpes simplex virus; HVEM = herpesvirus entry mediator; IFIT = interferon induced proteins with tetratricopeptide repeats; IFNAR = interferon receptor, IFN = interferons; ISG = interferon-stimulated genes; LAT = latency-associated transcript; LBNSE-GM-CSF = RABV expressing granulocyte-macrophage colony-stimulating factor; M protein = matrix protein; MAPK = mitogen-activated protein kinases; MAVS = mitochondrial antiviral signalling protein; MDA5 = melanoma differentiation-associated protein 5; mGluR2 = metabotropic glutamate receptor subtype 2; miRNA = microRNA; MMP = matrix metalloproteinases; MYH9 = myosin heavy chain 9; NAchR = nicotinic acetylcholine receptor; NBs = Negri bodies; NCAM = = neuronal cell adhesion molecule; NK = natural killer; N-protein = nucleoprotein; PILRA = paired immunoglobulin-like type 2 receptor α; PKR = protein kinase R; PNS = peripheral nervous system; PRRs = pattern recognition receptors; p75NTR = low-affinity nerve growth factor receptor; P-protein = phosphoprotein; RABV = rabies virus; RIG-I = retinoic acid-inducible gene I; RLRs = retinoic acid-inducible gene I like helicases; ROS = reactive oxygen species; SCs = schwann cells;

SHBRV = silver-haired bat variant of RABV; STING = stimulator of interferon genes; TG = trigeminal ganglion; TLRs = toll-like receptor; TNFRSF14 = TNF receptor superfamily member 14; VSV = vesicular stomatitis virus; wt = wildtype

Acknowledgements

We would like to thank Jean-Marc Cavaillon for his scientific advice, especially his expertise concerning the molecular pathways underlying innate immunity. We highly appreciate the support from Soren Riis Paludan and Line Reinert from Aarhus University, Denmark, who kindly provided tissue sections from HSV-1 infected mice. Figures were created with BioRender.com.

Abstract

The environment of the central nervous system (CNS) represents a double-edged sword in the context of viral infections. On one hand, the infectious route for viral pathogens is restricted via neuroprotective barriers, while on the other hand viruses benefit from the immunologically quiescent neural environment after CNS entry. Both herpes simplex virus (HSV) and rabies virus (RABV) bypass the neuroprotective blood-brain barrier (BBB) and successfully enter the CNS parenchyma via nerve endings. Despite the differences in the molecular nature of both viruses, each virus uses retrograde transport along peripheral nerves to reach the human CNS. Once inside the CNS parenchyma, HSV infection results in severe acute inflammation, necrosis and haemorrhaging, while RABV preserves the intact neuronal network by inhibiting apoptosis and limiting inflammation. During RABV neuroinvasion, surveilling-glial cells fail to generate a sufficient type I interferon (IFN) response, enabling RABV to replicate undetected, ultimately leading to its fatal outcome. To date, we do not fully understand the molecular mechanisms underlying activation or suppression of the host inflammatory responses of surveilling glial cells, presenting important pathways shaping viral pathogenesis and clinical outcome in viral encephalitis. Here, we compare innate immune responses of glial cells in the RABV- and HSV-infected CNS highlighting different viral strategies of neuroprotection or neuroinflammation in the context of viral encephalitis.

Keywords: Astrocytes; microglia; viral encephalomyelitis; herpes simplex virus, rabies virus

Main points

- Neurons do not exhibit strong immune responses to RABV or HSV-1 infection and rather require autophagy to restrict viral replication
- Despite profound clinical differences between RABV- and HSV-induced encephalitis, astrocytes and microglia were shown to be a critical component of the innate immune response to RABV and HSV infection
- Assessing the role of glial cells during neurotropic virus infection could help to close important knowledge gaps and reveal new promising targets for treatment options, which are currently missing

1. Viral infection routes to enter the central nervous system

1.1 General considerations

In contrast to other tissues, the micromilieu of the central nervous system (CNS) tightly controls brain immunity by different and unique immunomodulatory properties: the presence of tightly controlled physical barriers, the lack of a classical lymphatic drainage system, the presence of functional lymphatic vessels (Louveau et al., 2015), the relative deficiency of constitutive MHC expression, and the immunomodulatory properties regulated via the expression of immunosuppressive proteins (Forrester, McMenamin, & Dando, 2018). In the context of infection, access of pathogens to the CNS is limited by the blood-brain barrier (BBB), comprising a tightly connected endothelium and the glia limitans lining the CNS parenchyma (Daneman & Prat, 2015). If a pathogen gains access to the CNS, resident cells mount innate immune responses which lead to the recruitment of adaptive immune cells from the periphery. Under physiological conditions, immune responses in the CNS are limited to protect vulnerable and non-renewable cells such as neurons. Blood-borne viral pathogens, however, evolved three different mechanisms to cross the neuroprotective BBB (Figure 1): (i) transcellular entry (West Nile virus, Zika virus, Japanese encephalitis virus), (ii) paracellular entry (Marburg virus, dengue virus, Ebola virus), and (iii) the so- called ‘trojan horse entry’ in which the virus enters the CNS via circulating immune cells (HIV, Japanese encephalitis virus, measles virus, canine distemper virus) (Spindler & Hsu, 2012). In contrast to paracellular transport, transcellular transport usually does not depend on the disruption of junction proteins, actin cytoskeleton, or the basal lamina (Spindler & Hsu, 2012). It is further sub-divided into (i) free and passive diffusion limited to lipophilic substances, (ii) carrier-mediated transport, and (iii) vesicle-mediated transport (De Bock et al., 2016). In contrast, direct entry mechanisms (RABV, HSV, poliovirus, henipavirus) aim to bypass the neuroprotective barriers and enter the CNS via infection of nerve endings and long distance transport of viral particles within the neuronal network (Figure 1) (Forrester et al., 2018). The exact mechanism how viral pathogens such as RABV and HSV, both causing lethal encephalitis in humans, efficiently infect the CNS and how host immune responses contribute or counteract efficient neuroinvasion remains a question of significant interest.

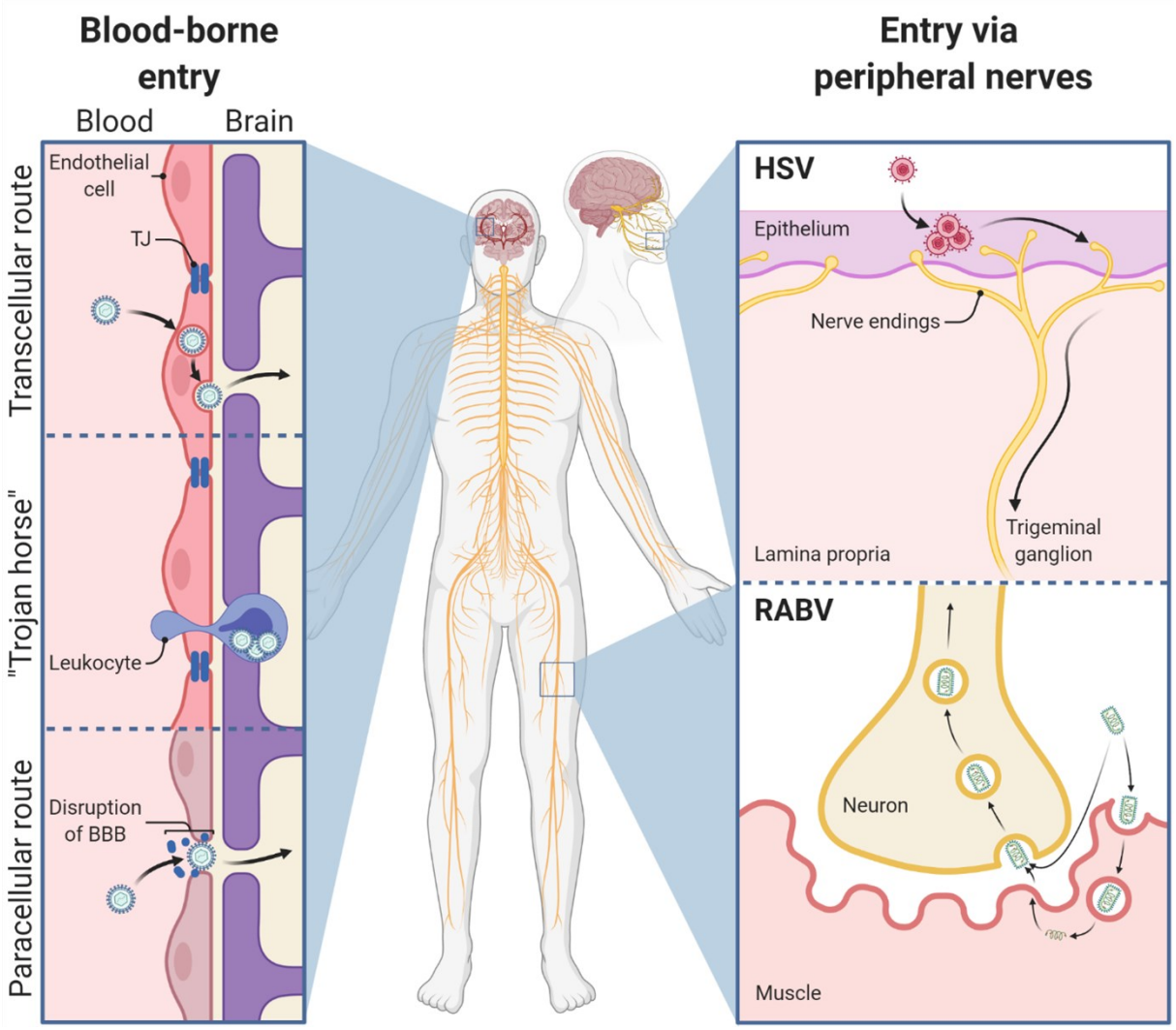

Figure 1 | Infection routes of neurotropic viruses. Pathogens can enter the CNS via two distinct routes, the blood (left) or the nervous system (right). Entry via the bloodstream is mediated by crossing the BBB (left) or the blood-cerebrospinal fluid barrier (not illustrated here). Mechanisms to cross the BBB include the transcellular, 'trojan horse', or paracellular routes (Forrester et al., 2018). Transcellular transport describes the transport of viruses by a direct diffusion pathway across the endothelial monolayer (De Bock et al., 2016). The 'trojan horse' route refers to viruses, which infect peripheral cells and enter the CNS parenchyma via paracellular or transcellular means. Paracellular entry of viruses is associated with the disruption of the BBB preferably via alterations in the phosphorylation status of tight junction proteins, the disruption of the actin cytoskeleton, or the disruption of the basal lamina (Spindler & Hsu, 2012). In contrast to this, RABV and HSV bypass the neuro-protective barriers and enter the CNS via retrograde transport along peripheral nerves (right). Upon the bite of an infected rabid animal, RABV enters the broken skin and infects peripheral nerves at the motor endplate of neuromuscular junctions or other innervated tissues. After receptor-mediated entry, RABV is retrogradely transported in endosomal transport vesicles to higher order neurons until the virus reaches the CNS (Fooks et al., 2017). HSV enters the termini of sensory neurons, which innervate the exposed skin. It is then retrogradely transported to autonomic nerve terminals of neurons in the trigeminal ganglion (TG), in which viral DNA remains in a latency phase. After reactivation, HSV can reach the brain via anterograde transport (Smith, 2012).

Rabies, one of the oldest and most fatal diseases described in humans (Baer, 1975), is still responsible for approximately 60.000 human deaths per year (Fooks et al., 2014). About 50% of fatal cases occur in children, which causes about 3.7 million disability-adjusted life years

(Hampson et al., 2015). The causative agent of rabies is the rabies virus (RABV), a bullet-shaped negative-sense single-stranded RNA rhabdovirus belonging to the family of Mononegavirales. RABV is mostly (> 99%) transmitted to humans upon the bite of a rabid dog (Fooks et al., 2017). Thereafter, canine RABV variants replicate locally in striated muscle cells and spread to the peripheral nervous system (PNS) via the neuromuscular junction (Murphy & Bauer, 1974; Watson, Tignor, & Smith, 1981). Compared to coyote street RABV (COSR), the silver-haired bat variant of RABV (SHBRV) showed a more effective local replication in epithelial cells and fibroblasts, two cellular components of the dermis (Morimoto et al., 1996). Thus, differences in RABV strains seem to define RABV tropism and replication potential at the entry site. Once inside the PNS, RABV is transported by motor neurons in the retrograde direction (Ugolini, 2011). Dependent on the site of infection, it may also use sensory and autonomic neurons to reach the CNS (Begeman et al., 2017). Inoculation of the planar footpad of adult mice with RABV leads to capture of viral particles by dorsal root ganglia and their transport to the spinal cord and later the brain (Velandia-Romero, Castellanos, & Martínez-Gutiérrez, 2013). Unlike necrotizing HSV encephalitis (HSE), RABV preserves an intact neuronal network until the final stage of the disease by inhibiting apoptosis and limiting inflammation within the CNS, two crucial factors ensuring RABV transmission (Alan C. Jackson & Fu, 2013). Around a week after the onset of symptoms, major histopathological lesions are still absent in the RABV-infected CNS. Clinical onset of the disease develops only after RABV is widely disseminated in the CNS. Neurons which are infected with RABV for several days, do not exhibit cytopathic changes and remain metabolically viable *in vivo* (Graf, Gerrits, Yatim-Dhiba, & Ugolini, 2002; Morcuende, Delgado-García, Ugolini, Delgado-Garcia, & Ugolini, 2002; Tang, Rampin, Giuliano, & Ugolini, 1999; Ugolini, 2010; Ugolini et al., 2006). In mice, the development of severe clinical disease occurs along with protein expression changes in ion homeostasis as well as docking and fusion of synaptic vesicles to the presynaptic membranes (Dhingra, Li, Liu, & Fu, 2007), which is hypothesised to be responsible for the defective neurotransmission recognised in rabies (Fu & Jackson, 2005). In humans, rabies manifests in two clinical forms: furious rabies and paralytic rabies (Hemachudha, 1994). In both forms, RABV induced dysfunction of the local dorsal root ganglia causes pain, paresthesia, or pruritus. After the prodrome, encephalitic patients show hypersalivation and periods of agitation alternating with lucidity, hydrophobia, and difficulty to swallow, ultimately leading to death. The paralytic form leads to an early onset of muscle weakness followed by a longer time between disease onset and death, or coma compared to the encephalitic form. Following onset of symptoms, rabies is almost invariably fatal (Hemachudha et al., 2013). In contrast to humans, several RABV-exposed mammal species produce RABV-neutralizing antibodies that clear RABV prior to CNS invasion (Almeida et al., 2005; Benavides et al., 2020; Obregón-Morales et al., 2017). As a result, subclinical or mitigated infections show mild or no symptoms. These nonlethal RABV infections have been shown or suggested for bats (Almeida et al., 2005; F. R. Jackson et al., 2008; Obregón-Morales et al., 2017; Turmelle, Jackson, Green, McCracken, & Rupprecht, 2010), cattle (Benavides et al., 2020), wild canids (Gnanadurai et al., 2013; Manickama, Basheer, & Jayakumar, 2008; Rocha, de Oliveira, Heinemann, & Gonçalves, 2017), and non-human primates (Kotait et al., 2019; Machado et al., 2012; Rocha et al., 2017). Although pre- and post-exposure vaccinations against rabies are available (O'Brien & Nolan, 2019; WHO, 2018), no treatment exists thus far, which shows a high therapeutic efficiency. In 2004, a young and unvaccinated patient from Wisconsin survived rabies (Willoughby et al., 2005). The therapeutic approach used, more specifically the induction of a therapeutic coma and the use of N-methyl D-aspartate receptor antagonist therapy, is since then known as the Milwaukee protocol (Willoughby et al., 2005). Despite its relentless promotion, there are at least 31 documented failures using the Milwaukee protocol, raising concerns about its efficiency (Zeiler & Jackson, 2016). Therefore, improving our

understanding of the interplay between RABV and the host immune system may result in improved medical management of rabid patients.

Like RABV, herpes simplex virus (HSV) invades the CNS by bypassing the BBB via retrograde transport along nerves. HSV-1 is a double-stranded DNA virus belonging to the highly neurotropic alphaherpesviruses. It is assumed that after initial replication in epithelial cells, HSV enters sensory nerve endings and establishes life-long latency in peripheral sensory ganglia such as the TG. Unlike RABV, alphaherpesviruses rarely spread to the CNS of immunocompetent hosts. Nevertheless, HSE does not occur more frequently in immunocompromised than in immunocompetent hosts, since it is believed that both, virus-mediated and indirect immune-mediated mechanisms contribute to the observed CNS damages (R. Whitley & Kimberlin, 2005). In contrast to immunocompetent patients, however, immunosuppressed patients might more likely show atypical or aggressive infections (Price, Chernik, Horta-Barbosa, & Posner, 1973). In sporadic cases, spread to the CNS can result from primary herpetic infection, reinfection by a second herpesvirus or reactivation of latent HSV (R. Whitley, Lakeman, Nahmias, & Roizman, 1982). After CNS invasion, HSV-1 causes necrotizing meningoencephalitis (Gnann & Whitley, 2017). In this point, HSV-1 clearly differs from RABV, since HSV-1 infection leads to a fulminant inflammatory response while this does not occur with RABV. HSE, which is the most common form of sporadically occurring fatal encephalitis in humans worldwide, is mainly caused by HSV-1, with HSV-2 representing less than 10% of the cases which are mostly affecting neonates. The neonatal form of HSE involves the periventricular white matter, mainly spares temporal and frontal lobes (Leonard et al., 2000), and is rarely haemorrhagic (Leonard et al., 2000; Vossough, Zimmerman, Bilaniuk, & Schwartz, 2008). In contrast, reactivation of HSV in the trigeminal sensory ganglion of older children and adolescents can lead to virus dissemination in temporal and frontal lobes (Baskin & Hedlund, 2007). To date, the mechanisms leading to CNS access and strong temporo-frontal lobe tropism of HSV-1 are not fully understood. Unlike, rabies, HSE caused by HSV-1 shows a bimodal age distribution and occurs either in children or adolescents younger than 20 years, or in adults over 50 years (Bradshaw & Venkatesan, 2016). Although the pathogenesis of neonatal HSE is not well understood, it has been hypothesised that different routes of virus entry to the brain may account for different localizations of virus dissemination observed in HSE. In infants, HSV may spread hematogenously across the immature BBB (Leonard et al., 2000). In adults, however, HSV-1 most likely enters the CNS via the trigeminal or olfactory route. After nonspecific clinical signs, HSE patients develop neurological deficits as well as characteristic behavioral and personality changes such as disorientation, speech disturbances, and focal or diffuse neurological signs such as seizures or hemiparesis (Steiner & Benninger, 2018; R. J. Whitley & Gnann, 2002). A prospective clinical study in 2007 showed that the high mortality of HSE of 70% can be reduced to 5 % using acyclovir therapy (J P Stahl, Mailles, & De Broucker, 2012). However, surviving people suffer from severe neuropsychological long-term sequelae, including mainly cognitive dysfunctions (Jean Paul Stahl & Mailles, 2019).

1.2 Which factors support RABV and HSV replication in the nervous system?

RABV enters the cell via the interaction of the RABV glycoprotein (G-protein) with RABV entry receptors, triggering clathrin-mediated endocytosis of RABV particles (Etessami et al., 2000; Le Blanc et al., 2005; S. Piccinotti, Kirchhausen, & Whelan, 2013). One reason for a favoured infection of neuronal tissues might be the higher expression levels of RABV entry receptors on neurons and postsynaptic membranes of muscle cells in the neuromuscular junction (Monique Lafon, 2005). Although the presence of RABV receptors might not be sufficient for productive infection of non-neuronal cells due to inhibition by respective antiviral responses of the target cells, presence of a specific receptor represents a prerequisite of infection. After viral entry into

the cell, RABV G-protein induces fusion of the viral envelope with the endosomal membranes liberating the viral nucleocapsid into the cytoplasm. In detail, viral G-protein is a class III membrane fusion protein, which undergoes a conformational change in the acidic environment of the endosome (Baquero, Albertini, & Gaudin, 2015; Y Gaudin, Tuffereau, Segretain, Knossow, & Flamand, 1991; Le Blanc et al., 2005). Like HSV, after entry at presynaptic axon membranes, RABV particles are transported in a retrograde fashion along microtubules (Bauer et al., 2014; Gluska et al., 2014; Klingen, Conzelmann, & Finke, 2008). Although the viral phosphoprotein (P-protein) was shown to interact with a light chain of the dynein motor complex (Jacob, Badrane, Ceccaldi, & Tordo, 2000; Raux, Flamand, & Blondel, 2000), axonal transport of RABV to the CNS is independent of this interaction (Mebatsion, 2001). More specifically, the binding domain of viral P-protein seems to rather have a crucial role in RABV primary transcription than intracellular transport of RABV (Bauer, Nolden, Nemitz, Perlson, & Finke, 2015). For long distance axonal transport, enveloped RABV virions are transported within internalized endosomes (Gluska et al., 2014; Klingen et al., 2008). Upon arrival in the neuronal cell body, the viral polymerase L initiates transcription by taking the ribonucleoprotein complex as the template (Bauer et al., 2015). Once a certain threshold of viral nucleoprotein (N-protein) is synthesized, viral replication is initiated, leading the production of a full-length, positive-sense RNA antigenome (Abraham & Banerjee, 1976; Finke, Mueller-Waldeck, & Conzelmann, 2003; P. Liu, Yang, Wu, & Fu, 2004). This intermediate serves as the template for the full-length negative-sense genome. The G-protein is inserted into the plasma membrane (Mebatsion, Konig, & Conzelmann, 1996; Okumura & Harty, 2011). Connection of the viral ribonucleoprotein with G-protein comprising membranes triggers membrane envelopment. Subsequently, the matrix protein (M-protein) mediates RABV budding (Mebatsion, Weiland, & Conzelmann, 1999) for transmission to next order neurons. It is thought that RABV buds from the synapse to start another round of infection in next order neurons (Ugolini, 2011). Consequently, RABV uses trans-synaptic spread to reach the CNS. The brain area in which the infection starts depends on the innervation site of the infected motor neurons. From the brain, RABV centrifugally spreads to salivary glands and several extra-neural organs (Fooks et al., 2017; A C Jackson et al., 1999; Jogai, Radotra, & Banerjee, 2002). In contrast to HSV (Gnann & Whitley, 2017), RABV does not persist in the nervous system and ultimately leads to the death of the host (Hemachudha et al., 2013).

Unlike spreading via the neuromuscular junction, HSV-1 must overcome the barrier between epithelial cells and free-ending nerve fibers from the PNS. After initial replication, neuroinvasion of HSV-1 is mediated via the herpesviral conserved deubiquitinase domain of the tegument protein pUL36 (Huffmaster, Sollars, Richards, Pickard, & Smith, 2015; Lee et al., 2009). Sensory neurons are readily infected, but if deeper layers of the epithelium are affected, also efferent as well as autonomic nerve fibers can be infected. Following fusion-mediated entry in neurons at axonal nerve endings, virus capsids and their inner tegument layer are released into the cell (Aggarwal et al., 2012; Luxton et al., 2005), which is in contrast to the clathrin-mediated and receptor-dependent endocytosis of RABV (S. Piccinotti et al., 2013; Silvia Piccinotti & Whelan, 2016). Comparable to intra-endosomal RABV particles, HSV-1 nucleocapsids are then retrogradely transported along microtubules, which is mainly mediated by the viral proteins pUL36 and pUL37 (Antinone & Smith, 2010; Luxton et al., 2005) together with the cellular dynein motor complex (Twelvetrees et al., 2016). Once in the cell body, virions dock at nuclear pores and deliver viral DNA into the neuronal nucleus (Wolfstein et al., 2006). Following primary infection, latency is established in infected neurons where progression of productive infection and subsequent cell death is blocked (Koyuncu, MacGibeny, & Enquist, 2018). During latency, the production of viral proteins is abrogated due to inactive viral transcriptional activator UL48, while instead latency-associated transcript (LAT), a non-protein coding RNA, is synthesized. LAT inhibits apoptosis of the infected cell and mediates

maintenance of the latent state (Nicoll, Proenca, & Efstathiou, 2012). After reactivation in sensory ganglia, newly formed viral particles are anterogradely transported back to the periphery, where initial infection has originally started. Alternatively, the virus spreads to higher-order neurons via anterograde microtubule-based transport using cellular kinesin motor proteins. Transport back to the periphery leads to the development of HSV lesions (herpes labialis or cold sores), whereas invasion of second order neurons and transport to the CNS is associated with severe disease (Smith, 2012).

2. The role of glial cells in maintaining CNS homeostasis

Inside the CNS, the neuronal network is protected from pathogens via resident glial cells, which can be divided to oligodendrocytes, astrocytes, and microglia. Oligodendrocytes are myelin-producing cells of the brain, which insulate neuronal axons and thereby facilitate rapid propagation of axon potentials (Kuhn, Gritti, Crooks, & Dombrowski, 2019; Philips & Rothstein, 2017). Schwann cells (SCs) represent the counterparts of oligodendrocytes in the PNS, responsible of forming myelin sheaths around peripheral neurons. In comparison, satellite cells which are closely related to SCs, ensheath the cell bodies of sensory neurons located in trigeminal and dorsal root ganglia, and share similarities with astrocytes (George, Ahrens, & Lambert, 2018; Rajasekhar, Poole, & Veldhuis, 2017). Astrocytes are the most abundant cell type in the CNS and play an essential role in the initiation of viral defence in a type I interferon (IFN)-dependent mechanism. They monitor brain development and function, especially by controlling potassium levels, removing toxic substances, and modulating synaptic activity (Soung & Klein, 2018). In contrast, microglia represent a rather small and unique myeloid cell population which derive from primitive myeloid progenitors from the yolk sac (Ginhoux et al., 2010). They are the CNS-resident macrophages and largely contribute to immunosurveillance in the brain (Z. Chen, Zhong, & Li, 2019; Metchnikoff, Mesnil, & Weinberg, 1902). Under physiological conditions, the homeostatic brain microenvironment constitutively expresses ‘off’ signals which prevent astrocytic and microglial activation. Those microglia-astrocyte-neuron interactions are critical for CNS innate immunity (Carty, Reinert, Paludan, & Bowie, 2014). In detail, neurons constitutively express surface molecules or secrete molecules which inhibit microglial activity. For example, healthy neurons express CD200 to keep CD200R+ microglia in a quiescent state (Broderick et al., 2002; Hoek et al., 2000; Yi et al., 2012; S. Zhang et al., 2011). In the case of neuronal death or injury, the expression of those inhibitory molecules is modulated, leading to the abrogation of microglial and astrocytic suppression (Broderick et al., 2002; Hoek et al., 2000; Pabon, Bachstetter, Hudson, Gemma, & Bickford, 2011). Damaged or stressed neurons activate astrocytes and microglia via the release of cytokines (IFN-γ, IL-6) and chemokines (CX3CL1, CCL2). In response, glial cells sense neuronal damage via cell-specific receptors and produce an array of cytokines (IL-1, IL-6, IL-12, TNF, CCL2, CCL4, CCL5, CCL7, CXCL10) depending on the specific pathogen. This results in upregulation of MHC I and II proteins on the microglial cell surface and increased expression of adhesion molecules on endothelial cells (ECs) (Griffin, 2003; Malone, Stohlman, Ramakrishna, Macklin, & Bergmann, 2008). Apart from neurons, numerous other players, such as peripheral immune cells and peripherally produced molecules can induce glial activation (Sriram, 2011).

Infecting mice with a wildtype (wt) bat RABV revealed upregulation of microglial-specific CD200R in the virus-infected CNS, suggesting that RABV influences neuron-microglia signalling (Appolinário et al., 2016). In HSE, microglia were shown to sense HSV-1 through the cyclic guanosine monophosphate-adenosine monophosphate (cGAMP) synthase/stimulator of interferon genes (cGAS/STING) pathway, initiating the production of type I IFN and immune-priming of neighbouring cells (Reinert et al., 2016). Apart from microglia, astrocytes are the main producers of IFN-β in the RABV-infected brain (Pfefferkorn et al., 2016). Similarly, astrocytic secretion of IFN-β was shown in other viral CNS infections

such as vesicular stomatitis virus (VSV) and La crosse virus, suggesting that astrocytes are important immune modulators triggering viral clearance in the infected CNS (Detje et al., 2015; Kallfass et al., 2012).

Since morphological changes in the CNS of rabies patients (Adle-Biassette et al., 1996) and infected animals appear mild despite its fatal outcome (Gnanadurai et al., 2015; Miao et al., 2017), it is believed that neuronal dysfunction is responsible for RABV-induced death (Fu & Jackson, 2005). The ability of RABV to antagonize an early IFN response enables the virus to limit apoptosis and inflammation in the CNS (Baloul & Lafon, 2003; Krzysztof Brzózka, Finke, & Brzo, 2005; Prehaud, Lay, Dietzschold, & Lafon, 2003). Consequently, the innate immune system fails to prime an adaptive immune response in time to clear the virus from the infected CNS. Unlike rabies, HSV infection initiates a fulminant inflammatory cascade, recruiting innate immune cells and activating adaptive immune mechanisms to the infected CNS area (Figure 2).

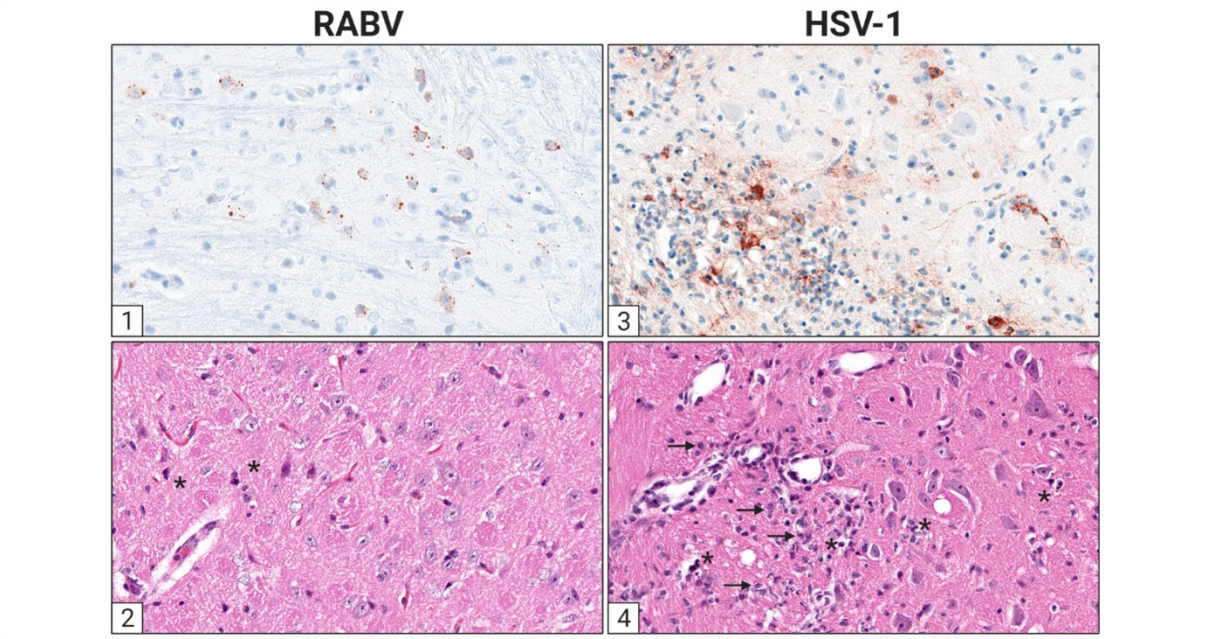

Figure 2 | Comparative histopathology of RABV and HSV-1 infection in the murine brain. (1) Multiple RABV infected brain stem neurons, immunohistochemistry, ABC method. (2) Consecutive section of RABV infected brain stem showing a small number of necrotic neurons (asterisk). Inflammatory cells are absent, haematoxylin eosin. (3) Detection of HSV-1 antigen in multiple neurons and glial cells, immunohistochemistry, ABC method. (4) In contrast to RABV, HSV-1 infection induces a marked inflammatory response mainly consisting of infiltrating histiocytes and lymphocytes (arrow). Infected cells are necrotic (asterisk), haematoxylin eosin.

Although we are far from understanding the exact molecular pathways underlying neuron-glia interactions in the virus-infected CNS, RABV and HSV both modulate gene expression of signalling molecules which are important for neuron-glia communication, thereby interfering with CNS homeostasis. Taken together, the outcome of viral infection depends on two main factors: the pathogenicity of the virus and the triggered antiviral response. The latter is mainly mediated by glial cells in the CNS. Both viral pathogenicity and host immune response modulate one another, and their synergistic effects can result in adverse outcomes, either due to a highly pathogenic virus or an inadequate immune response. At the end stage of the disease, RABV leads to an invariably fatal encephalomyelitis by evading the immune response of glial cells, subsequently enabling RABV to extensively replicate in the CNS. In contrast, HSV

mediates death by inducing necrotizing inflammation in the CNS, a process that is aggravated by an excessive immune response.

3. The cellular infection pattern of RABV and HSV in the nervous system

As elaborated earlier, RABV and HSV are classically referred to as neurotropic viruses since both preferentially spread to the nervous system (Steiner, Kennedy, & Pachner, 2007; Ugolini, 2011). Whereas most of the research succeeded in linking immune evasive mechanisms of RABV to distinct viral proteins (Bernhard Dietzschold, Li, Faber, & Schnell, 2008; Ito, Moseley, & Sugiyama, 2016), it is less understood how they influence the strong neuron-specific tropism of RABV or why in some cases glial cell infection can be detected (Iwasaki & Clark, 1975; Alan C Jackson, Phelan, & Rossiter, 2000; Potratz, Zaeck, Christen, et al., 2020; Potratz, Zaeck, Weigel, et al., 2020; Sung, Hayano, Mastri, & Okagaki, 1976). Deciphering the requirements for a strict neuron-specific tropism or broader host cell multi-tropism in the nervous system and discovering cell-specific responses restricting viral replication is of utmost importance to understand viral pathogenesis and antiviral host mechanisms.

3.1 Viral entry

Regarding viral tropism, a broad range of cell types, including neuroglia, can be infected *in vitro* by both street and laboratory-attenuated RABV (Potratz, Zaeck, Christen, et al., 2020; Prosniak et al., 2003; Ray, Power, Lynch, Ewalt, & Lodmell, 1997; Sugamata et al., 1992), contrasting the pronounced neuron-specific tropism *in vivo*. It is suggested that RABV neuron-specific tropism represents a viral adaptation mechanism to avoid immune detection by the host (M Lafon, 2008). Different RABV receptors bind the viral G-protein, of which neuronal cell adhesion molecule (NCAM) (Thoulouze et al., 1998), low-affinity nerve growth factor receptor (p75NTR) (Tuffereau, Bénéjean, Blondel, Kieffer, & Flamand, 1998), or metabotropic glutamate receptor subtype 2 (mGluR2) (J. Wang et al., 2018) represent bona fide neuronal surface receptor molecules, whereas nicotinic acetylcholine receptor (NAchR) (Lentz, Burrage, Smith, Crick, & Tignor, 1982) is expressed in muscle cells and may support RABV amplification prior to neuron infection through moto-neuronal endplates. However, RABV receptor expression in mice and humans (Y. Zhang et al., 2014, 2016) does not positively correlate with cellular susceptibility to RABV infection, implying that receptor usage alone is not determining the strong neuron-specific tropism of RABV. Recent single-cell sequencing data of human brains revealed that expression of p75NTR, mGluR2, and NAchR is relatively low in the human brain, whereas NCAM is highly expressed in the human brain. More specifically, NCAM was predominantly found on neuronal cells, but shown to be also highly expressed on oligodendrocytes and certain astrocyte subsets. In contrast, microglia showed low or no expression of NCAM in the human brain (Hawrylycz et al., 2012).

A major factor determining tissue and cell-specific permissivity to HSV infection is the cellular receptor mediating entry of the virus. For HSV-1 cellular entry, different glycoproteins (glycoprotein (g)D, gB, gH, and gL) are required to bind to specific cellular receptors. Initially, gB and gH attach to cell-surface heparan sulfate proteoglycans, which are present in various cells, including neurons. Next, gD binds to cell surface receptors nectin-1 (also referred to as poliovirus receptor-like protein 1) or TNF receptor superfamily member 14 (TNFRSF14), also known as herpesvirus entry mediator (HVEM), which mediates the activation of the gH/gL complex and subsequently transformation of gB into a fusogenic state (Campadelli-Fiume, Cocchi, Menotti, & Lopez, 2000). For successful fusion of the viral envelope with the cell membrane, a gB receptor such as paired immunoglobulin-like type 2 receptor α (PILRA), another paired-type receptor with homology to PILRA, myelin-associated glycoprotein, and myosin heavy chain 9 (MYH9, also known as NMMHC-IIA) is required (Campadelli-Fiume et al., 2000). The gD receptor nectin-1 is a member of the immunoglobulin superfamily and

present at cellular adherens and tight junctions involved in cell-cell adhesion of epithelial and ECs (Takahashi et al., 1999). Most likely, nectin-1 presents the most important receptor for HSV-1 infection of epithelial and neuronal cells (Campadelli-Fiume et al., 2000; Kopp et al., 2009). Although HVEM is widely expressed in the liver, kidney, lung as well as in T and B lymphocytes, leukocytes, epithelial cells, fibroblasts, and neurons on which it controls diverse pro-inflammatory and inhibitory signalling pathways (Steinberg, Cheung, & Ware, 2011; Tiwari et al., 2005), it seems to be largely irrelevant for the course of HSE since the patterns of HSV replication in the brain of wt and HVEM knockout mice were indistinguishable (Kopp et al., 2009). The distribution of HSV-1 receptors has been examined in the human (Tiwari et al., 2005) and murine brain (Guzman, Oh, Shukla, Engelhard, & Valyi-Nagy, 2006). Specifically, nectin-1, TNFRFS14, and MYH9 were increasingly expressed in the human hippocampus and it has been shown for nectin-1 in the murine hippocampus to be the underlying cause for the higher susceptibility of this brain area to HSV-1 infection. Abundant nectin-1 levels were also found in sensory, sympathetic, and parasympathetic nerves (Haarr, Shukla, Rodahl, Dal Canto, & Spear, 2001). Immunohistochemical studies on nectin-1 expression in neuronal and non-neuronal cells of the human nervous tissue revealed that neurons of the basal ganglia, cerebral cortex, diencephalon, brainstem, spinal cord, and peripheral dorsal root and trigeminal ganglia are highly positive. Further, ependymal cells, choroid plexus epithelial cells and vascular endothelium showed strong nectin-1 expression. Variable, but still positive immunoreactivity was present in oligodendrocytes, astrocytes, pericytes, SCs, and satellite cells, demonstrating potential target cells for HSV-1 (Guzman et al., 2006).

In a nutshell, multiple receptors are known to be responsible for the cellular uptake of RABV and HSV. Like RABV, not all the cells expressing the viral entry receptors get predominantly and productively infected by HSV, suggesting that more factors shape HSV tropism.

3.2 RABV tropism

Considering the remarkable tropism of field RABV strains for non-neuronal cells in comparison to less virulent laboratory strains (Potratz, Zaeck, Christen, et al., 2020) as well as the broad distribution of the potential RABV receptors in the central and peripheral nervous systems (Hawrylycz et al., 2012; Monique Lafon, 2005), evidence is accumulating that RABV neuron-specific tropism may not exclusively be a result of specific receptor expression by neurons. More likely, a lower protective immune response in neurons as compared to other susceptible cell types may result in productive infection. In contrast, entry in non-neuronal cell types seems to result in abortive infection due to immediate and strong innate immune responses (Pfefferkorn et al., 2016; Tian et al., 2018) in a virus strain dependent manner (Potratz, Zaeck, Christen, et al., 2020). Considering reports about *in vivo* infection of non-neuronal cells by field RABV (Balachandran & Charlton, 1994; Charlton & Casey, 1979; Charlton, Nadin-Davis, Casey, & Wandeler, 1997; Potratz, Zaeck, Christen, et al., 2020; Potratz, Zaeck, Weigel, et al., 2020), the concept of an almost exclusive infection of neurons has to be relativized. In summary, RABV host cell tropism and *in vivo* spread is due to multiple factors: the presence of RABV cell entry receptors on their plasma membrane, intraneuronal long distance virus transport processes at both virus entry and after replication, specific trans-synaptic spread between neurons, and the neuronal metabolism which actively supports RABV replication. Paracrine effects through cytokine release by abortively or productively infected non-neuronal cells like astrocytes or SCs surrounding neurons (Potratz, Zaeck, Christen, et al., 2020; Potratz, Zaeck, Weigel, et al., 2020) may also determine the susceptibility and survival of neurons and other cell types that can be easily infected *in vitro* (Ray et al., 1997).

3.2.1 Astrocytes

Besides receptor usage, negative regulation by cell type-specific inhibition of virus replication in non-neuronal cells might play a decisive role in viral tropism of neurotropic pathogens. *In vivo*, abortive infection of astrocytes with RABV SAD carrying the G protein of the more neurotropic challenge virus standard (CVS) strain has been suggested to be the result of type I IFN induction (Pfefferkorn et al., 2016). *In vitro*, this correlates with the activation of double-stranded (ds) RNA-dependent mitochondrial antiviral signalling protein (MAVS), whereas wt RABV is able to infect astrocytes without exhibiting MAVS activation by laboratory-adapted RABV (Tian et al., 2018). Other studies using *in vitro* neuron or astrocyte cultures confirmed astrocyte infection by RABV *in vitro*, without remarking discernible differences between lab-attenuated and street RABV (Potratz, Zaeck, Christen, et al., 2020; Ray et al., 1997; Tsiang, Koulakoff, Bizzini, & Berwald-Netter, 1983). A broad quantitative comparison of different recombinant field and lab-attenuated strains in infected mice, however, highlighted infection of astrocytes in the CNS after intramuscular infection only with highly virulent field RABV. In addition, no astrocyte infection was detected after infection with lab-attenuated or vaccine strains (Potratz, Zaeck, Christen, et al., 2020). Abundant expression of the RABV P-protein, a major IFN antagonist of RABV in astrocytes (K. Brzózka, Finke, & Conzelmann, 2006; Krzysztof Brzózka et al., 2005; Ito et al., 2010; Moseley et al., 2009; Rieder et al., 2011; Vidy, Chelbi-Alix, & Blondel, 2005; Vidy, El Bougrini, Chelbi-Alix, & Blondel, 2007), suggests that inhibition or delay of innate immune responses in astrocytes may be a hallmark of pathogenic field RABV pathogenesis. Accordingly, non-abortive infection of astrocytes by pathogenic field RABV may critically influence the CNS microenvironment, including for example a failure to permeabilize the BBB upon infection, which has been linked to contribute to lethal disease progression as outlined earlier. In summary, RABV infection of immune and neuron-regulatory astroglia strongly depends on the viral strain and RABV pathogenesis may depend on the ability to abortively or productively infect these cell types in the brain.

3.2.2 Microglia

While activation of microglia has been observed during RABV infection *in vitro* and *in vivo* (Bertoune et al., 2017; S. Q. Liu, Gao, Xie, Wang, & Zhu, 2020; S. Q. Liu, Xie, Gao, Wang, & Zhu, 2020; Sonthonnax et al., 2019; Zhao et al., 2013), the detection of viral antigen in infected microglia *in vivo* was assumed to be the result of microglial phagocytosis of infected neurons (Sugamata et al., 1992). Ray and colleagued provide evidence that human microglia are susceptible to RABV infection *in vitro* (Ray et al., 1997). Recently, the susceptibility of human induced pluripotent stem cell-derived microglia-like cells *in vitro* has been questioned (Feige et al., 2021). Thus, more research is necessary to assess if microglia productively support RABV infection.

3.2.3 Oligodendrocytes

Like microglia, oligodendrocytes represent another comparatively small population of glial cells (Valério-Gomes, Guimarães, Szczupak, & Lent, 2018). In contrast, oligodendrocytes are highly vulnerable to cytotoxic by-products such as ROS, high iron content, high glutamate concentrations, as well as high ATP concentrations (Kuhn et al., 2019). Yet, little is known about the role of oligodendrocytes during RABV infection. Recent advances with monosynaptic viral RABV tracers demonstrated occasional oligodendrocyte infection (Osanai et al., 2017; Valério-Gomes et al., 2018).

3.2.4 Schwann cells

Whereas awareness about the role of CNS neuroglia in RABV pathogenesis has increased in the last years, a contribution of peripheral neuroglia such as SCs may have not been considered adequately. SCs are highly immunocompetent and exert key functions in immune regulation by antigen presentation, pathogen detection, and cytokine production (Gold, Archelos, & Hartung, 1999; Ydens et al., 2013). Although release and virion accumulation between axonal and SCs membranes as well as nodes of Ranvier has been demonstrated by electron microscopy, until recently, SCs were considered unsusceptible to lyssavirus infection (Charlton, Casey, Wandeler, & Nadin-Davis, 1995; Jenson, Rabin, Bentinck, & Melnick, 1969). A recent three-dimensional immunofluorescence imaging approach for high-volume tissue imaging (Zaeck, Potratz, Freuling, Müller, & Finke, 2019), however, enabled the detection of RABV-infected SCs in peripheral nerves after field RABV infection of mice via the natural (intramuscular) and an artificial (intracranial) inoculation route. Accordingly, a model was suggested, in which the infection of peripheral SCs suppresses glia-mediated innate immunity and delays antiviral responses to field virus infections (Potratz, Zaeck, Weigel, et al., 2020).

3.3 HSV tropism

Herpesviruses are pantropic, causing lytic infection in various tissues and cell types *in vitro*. In humans, herpes labialis is caused by HSV-1 infecting epithelial cells of the oro-labial mucosa, followed by virus uptake and transport from closely adjacent axons of sensory nerve endings to ganglia of the PNS. Further, HSV-1 is able to infect the corneal or genital mucosal epithelium causing herpes genitalis or herpes keratitis, respectively (R. Whitley & Baines, 2018). Once in the PNS, HSV-1 establishes life-long latency within sensory as well as autonomic peripheral ganglia of the head and spinal cord. It can be periodically reactivated by various stimuli (Obara et al., 1997; Richter, Dias, Gilbert, & Atherton, 2009).

HSV-1 tropism to the frontal and temporal lobe has been discussed given the respective invasion route and synaptical connections by which the virus may reach the brain, the olfactory and trigeminal nerve (Davis & Johnson, 1979). Thus, direct connections from the PNS to the CNS facilitate invasion towards the brain across synapse-linked neurons. However, detailed research is still needed on that point, especially why HSV-1 maintains the devastating potential to reach into the CNS in rare cases, but otherwise resides latently in peripheral ganglia (Johnson & Mims, 1968). Moreover, it is not yet clear whether HSV-1 reaches the CNS directly after primary infection, which leads to encephalitis, or whether this happens after reactivation of the virus in latent infected tissue (Gnann & Whitley, 2017). This is in contrast to rabies, which is always virulent and invariably fatal, when entering the nervous system (R. J. Whitley & Gnann, 2002).

3.3.1 Astrocytes

Apart from neurons, glial cells have been shown to be permissive to HSV-1 infection (Esiri, 1982; Kennedy, Clements, & Brown, 1983). Lokensgard and colleagues reported that astrocytes are highly susceptible to productive HSV-1 infection and fail to produce cytokines upon infection (Esiri, 1982; Kennedy et al., 1983). Other studies, however, reported the upregulation of pathogen recognition receptors, DNA/RNA sensors, INFs, and IFN-stimulated genes (ISGs) in astrocytes upon HSV-1 infection (Y D Bansode, Chattopadhyay, & Saha, 2019; Yashvant D Bansode, Chattopadhyay, & Saha, 2020; Z. Liu et al., 2013). Upon *in vitro* and *in vivo* infection, astrocytes respond to infection with hypertrophy as well as rounding and syncytia formation (Fiacco, Agulhon, & McCarthy, 2009; Gumenyuk et al., 2018; Hensel et al., 2019).

3.3.2 Microglia

In microglia, HSV-1 infection does not result in productive viral replication, but instead in the production of significant amounts of pro-inflammatory cytokines (Aravalli, Hu, Rowen, Palmquist, & Lokensgard, 2005). In HSV-1 infected brains, microglia are present around cell bodies and dendrites of neurons before mature viral particles are detectable (Fekete et al., 2018).

3.3.3 Oligodendrocytes

Apart from astrocytes, human oligodendrocytes have been shown to be variably permissive to HSV-1 infection *in vitro* (Bello-Morales, Fedetz, Alcina, Tabares, & Lopez-Guerrero, 2005; Kastrukoff & Kim, 2002). However, in HSV-1 infected mice, HSV-1 antigen-positive oligodendrocytes were found in the spinal trigeminal tract (Ugolini, Kuypers, & Simmons, 1987). In line with this, the occurrence of demyelinating lesions in rodents supports the susceptibility of oligodendrocytes to HSV-1 infection (Boukhvalova et al., 2019).

3.3.4 Schwann cells

It has been shown that murine SCs can be infected after intraocular inoculation, but produce no viral progeny, whereas direct inoculation into the sciatic nerve led to productive HSV-1 infection (Townsend & Collins, 1986). In another study, infection of SCs has been demonstrated only at late time points after infection, confirming the notion that (i) those cells are not the primary target of HSV-1 and (ii) do not play a role in retrograde transport upon neuroinvasion. Thus, it is very likely that SCs become infected via productive infection of the neuronal cell body, the subsequent escape of HSV-1 along axons, and the emergence into associated SCs along the nerve tract (Shimeld, Efstathiou, & Hill, 2001). Similar to SCs, the infection of satellite cells seems to be abortive since only empty capsids have been detected by electron microscopy of chicken dorsal root ganglia (Hill & Field, 1973). In line with this, very limited infection was reported in satellite cells from mouse and human dorsal root ganglia (Wilkinson, Leaver, Simmons, & Pereira, 1999; Zerboni et al., 2013).

Taken together, RABV (field strains) and HSV-1 productively infect neurons and astrocytes *in vivo*, while microglia and oligodendroglia are less or not at all susceptible to infection. Infection of SCs has been observed for field RABV and HSV infection, but the role of infected SCs in viral encephalitis remains poorly understood. On the one hand, the strain-specificity of the virus and, on the other hand, receptor expression and cell-specific immune responses of the cellular host determine cellular tropism and infection outcome. Although it is suggested that RABV and HSV bear a neuron-specific tropism, cellular tropism might be much wider than initially believed (Figure 3).

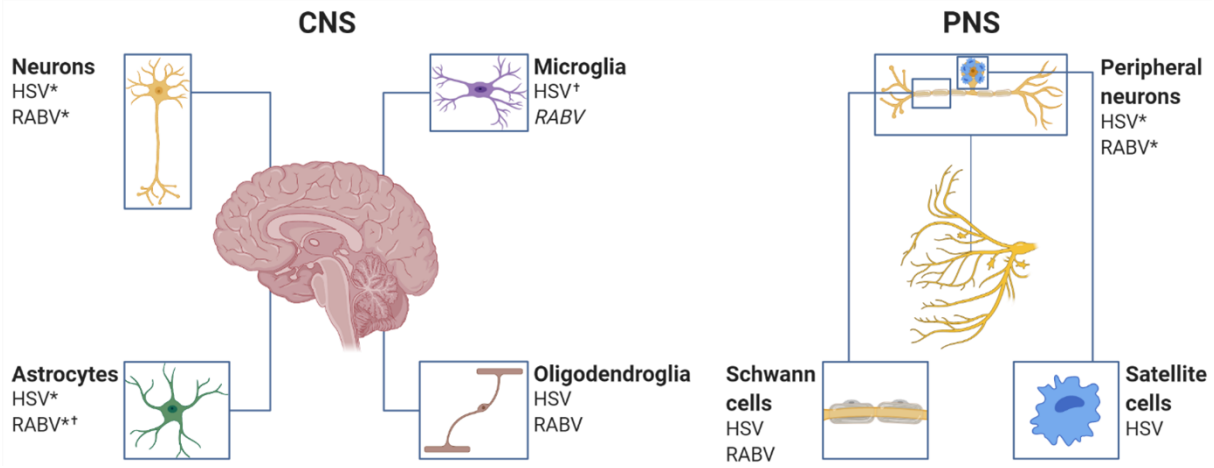

Figure 3 | Cellular tropism of RABV and HSV in the CNS and PNS. Both RABV and HSV infect a variety of cells in the CNS (left) and PNS (right) in both abortive (†) and non-abortive (*) manners. For RABV, a strain-specific ability of pathogenic RABV to non-abortively infect murine astrocytes *in vivo* has been suggested (Potratz, Zaeck, Christen, et al., 2020). If neither has been demonstrated thus far or productive infection can vary, no indicator has been assigned. For RABV, positive viral antigen staining was demonstrated to occur in neurons, astrocytes, and oligodendrocytes of *post-mortem* human brain tissues (Suja, Mahadevan, Madhusudana, & Shankar, 2011), whereas infection of SCs have thus far only been shown in a mouse animal model (Potratz, Zaeck, Weigel, et al., 2020). So far, fetal human microglia only stained positive for RABV antigen *in vitro* (italics) (Ray et al., 1997), however, the susceptibility of human induced pluripotent stem cell-derived microglia-like cells has been questioned recently (Feige et al., 2021). In *post-mortem* human brain tissues, neurons, astrocytes, and oligodendrocytes stained positive for HSV antigens (Esiri, 1982), whereas infected SCs have only been demonstrated in a mouse animal model (Townsend & Collins, 1986). Microglia are supposedly not permissive to HSV infection (Fekete et al., 2018; Lokensgard et al., 2001).

4. The role of the blood-brain barrier in HSV and RABV infections

Blood vessels vascularizing the CNS deliver oxygen and nutrients to the nervous tissue, analogous to blood vessel functions in peripheral organs. Apart from this, however, the BBB possesses unique properties allowing the precise control of molecule and cell movements between the blood and the brain. Physiological barrier properties are mediated by ECs, which are tightly regulated by vascular, immune, and neural cells. The main function of the BBB is the protection of neural tissue from toxins and pathogens (Daneman & Prat, 2015). Conversely, however, alterations of BBB functions endanger CNS homeostasis and are implied in numerous neurological diseases such ascerebral ischemia, brain trauma, brain tumours, and brain infections (Rosenberg, 2012).

4.1 Rabies virus

Infection of nerve endings and retrograde axonal transport enables RABV to bypass the neuroprotective BBB, which normally restricts viral entry (Schnell, McGettigan, Wirblich, & Papaneri, 2009). Subsequently, RABV benefits from the immunologically quiescent neural environment of the CNS (Pape, Tamouza, Leboyer, & Zipp, 2019). More importantly, viral protein-mediated sequestration of the immune response, especially its antagonism against the early IFN response, enables RABV to successfully replicate inside the CNS (Ito et al., 2016; T. Scott & Nel, 2016). RABV-mediated sequestration of the host immune response hinders the opening of the BBB leading to lethal RABV infection (Phares, Kean, Mikheeva, & Hooper,

2006; A. Roy & Hooper, 2007; Anirban Roy, Phares, Koprowski, & Hooper, 2007). Accordingly, Roy and colleagues showed that mice infected with the lethal SHBRV develop a fully functional immune response in the periphery, while immune cells are unable to migrate to the infected CNS (Anirban Roy & Hooper, 2008). As a consequence of deficits to increase the BBB permeability in the cerebellum, immune effectors cells and associated virus-neutralizing antibodies cannot reach the CNS for RABV clearance (Gnanadurai et al., 2015; Hooper, Roy, Barkhouse, Li, & Kean, 2011; Miao et al., 2017). However, the exact mechanisms linking RABV-mediated sequestration of the host immune response and the failure to open the BBB remain to be elucidated.

Even though an effective therapy for rabies is still missing, studies reported the survival of a few RABV patients with acute illness (Alvarez et al., 1994; Hattwick, Weis, Stechschulte, Baer, & Gregg, 1972; W. T. Hu, Willoughby, Dhonau, & Mack, 2007; Madhusudana, Nagaraj, Uday, Ratnavalli, & Kumar, 2002; Porras et al., 1976). One of the main findings associated with non-lethal RABV infection was the presence of virus-neutralizing antibodies in serum or CSF of RABV survivors (Centers for Disease Control and Prevention (CDC), 2004, 2012). In mice, crossing of virus-neutralizing antibodies through an increased permeable BBB protects against lethal RABV infection (B Dietzschold et al., 1992; Phares et al., 2006). By comparing mice with different genetic backgrounds, Roy and Hooper showed that the opening of the BBB is of utmost importance in the clearance of RABV from the infected CNS (A. Roy & Hooper, 2007). Accordingly, SJL mice known to develop more extensive CNS inflammation due to the increased recruitment of infiltrating IL-10 producing CD4+ cells than other mice (Rowell & Griffin, 1999; Singh et al., 2005) more often survive wt bat RABV infection compared to other mouse strains (Lodmell & Ewalt, 1985; H. Wang et al., 2011). In contrast 129/SvEv mice succumb to infection with SHBRV due to the failure of opening the BBB (Anirban Roy et al., 2007). To increase BBB permeability, SJL mice were immunized with myelin basic protein to induce experimental allergic encephalomyelitis prior to SHBRV infection. Immunized and infected mice showed higher survival rates compared to non-immunized and infected mice. Vice versa, mice with reduced BBB permeability after treatment with the steroid hormone dehydroepiandrosterone presented higher morbidity, pointing out that the infiltration of immune effector cells across the BBB is critical to survive RABV infection (A. Roy & Hooper, 2007). Emphasizing the importance of immune response-stimulating agents, intracerebral administration of recombinant RABV expressing granulocyte-macrophage colony-stimulating factor (LBNSE-GM-CSF) protected more mice from developing rabies compared to administration of UV-inactivated LBNSE-GM-CSF. LBNSE-GM-CSF infection led to significantly higher levels of chemokine and cytokine expression and more infiltrating immune cells in the CNS than UV-inactivated LBNSE-GM-CSF. Also direct administration of immune response-stimulating agents to the CNS enhanced BBB permeability and infiltration of immune cells, consequently preventing the development of rabies (A. Roy & Hooper, 2007). Overall, the failure of opening the BBB during RABV infection enables the virus to successfully replicate in the tightly controlled immunosuppressive micromilieu of the CNS. Clearance of RABV from the CNS requires RABV-specific immunity, such as the presence of circulating virus-neutralizing antibodies, and the enhancement of BBB permeability to allow immune effectors to access the CNS. Concomitant peripheral and intracerebroventricular administration of the two potent neutralizing monoclonal antibodies RVC20/RVC58 directed against the viral G-protein cured symptomatic rabid mice (de Melo et al., 2020; Hellert et al., 2020). Antibody-based therapeutic approaches remain a promising treatment to treat neurological symptoms and cure symptomatic rabies.

4.2 Herpes simplex virus

In contrast to rabies, the disruption of the BBB is a crucial pathological mechanism in the development of HSE, which has been recently reviewed in detail (H. Liu, Qiu, He, Lei, & Lu, 2019). Brain damage is mediated by lytic infection of neurons and glial cells as well as by neuroinflammatory processes (Lundberg et al., 2008). Toll-like receptor (TLR)-dependent recognition of HSV-1 by neurons and glia leads to the initial production of cytokines such as type I IFN, IL-6, IL-1β, IFN-γ and TNF consequently resulting in the disruption of the BBB (Mancini & Vidal, 2018). Consequently, immune cells are recruited to the brain parenchyma resulting in an enhanced inflammatory response towards HSV-1 infection and increased neuronal damage. *In vivo*, CD4+ or CD8+ T cells and macrophages are present in perivascular infiltrates close to HSV-infected cells in the murine brain stem (Chan, Javanovic, & Lukic, 1989). In addition, vasogenic edema and haemorrhage may occur (H. Liu et al., 2019). In general, leukocyte entry into the CNS is regulated by several factors, including the expression of adhesion molecules (PECAM, CD99, VE-cadherin and JAM-A,-B and -C) (Muller, 2002), expression of matrix metalloproteinases (MMPs) (Brundula, Rewcastle, Metz, Bernard, & Yong, 2002; Yong, Power, & Edwards, 2001), as well as endothelial expression of cytokines (CCL2, CCL5) and chemokines (CXCL10, CXCL8) (Subileau et al., 2009). Briefly, HSV-1 affects the structure and function of the BBB, probably via inflammatory-induced activation (Kim, Bang, Lee, & Lee, 2000) and direct infection of ECs (Brankin, Hart, Cosby, Fabry, & Allen, 1995; Sobel, Mitchell, & Fondren, 1990). More specifically, HSV-1-induced increase of ICAM-1 expression on ECs mediates an increased interaction between ECs and circulating leukocytes, and subsequently leads to infiltration of immune cells into the brain parenchyma (Brankin et al., 1995; Kim et al., 2000). Very recently, it could be demonstrated that HSV-1 alters the Golgi structure in ECs of the BBB and thus reduces integrity of the same (He et al., 2020). Further, MMPs which are thought to cleave tight junction proteins of the BBB, are significantly upregulated in HSV-1-infected humans and mice. High levels of MMP2 and MMP9 have been shown to play a pivotal role in BBB damage in HSE (Zhou, Lu, Guo, & Mei, 2010) and other brain infections such as West Nile Virus encephalitis (P. Wang et al., 2008). Reactive oxygen species (ROS), which are increasingly produced by microglia in HSE, are both beneficial and disadvantageous. On the one hand, they prevent further spread of the pathogen, on the other hand they degrade tight junction proteins and thus increase the permeability of the BBB (S. Hu, Sheng, Schachtele, & Lokensgard, 2011). However, how HSE-associated ROS alters tight junction integrity urges further research. CCL2, a major chemokine in CNS inflammation, also plays an essential role in the regulation of the BBB permeability, endothelial dysfunction and increased leukocyte recruitment (Roberts et al., 2012). Different molecular pathways include reorganization of the actin cytoskeleton of ECs mediated through the interaction between CCL2 and its receptor CCR2 (Stamatovic, Keep, Kunkel, & Andjelkovic, 2003) or disruption of adherens junctions by Src kinase-dependent phosphorylation of β-catenin (Roberts et al., 2012). Dysfunction of the BBB can also be caused by astrocyte disturbances as HSV-1 can infect not only neurons, but also glial cells such as astrocytes. HSV-1 has been reported to increase the expression of aquaporin 4 (AQP4) on astrocytes, which regulates water transport across the BBB (Jung et al., 1994). An increase of AQP4 leads to water influx into astrocytes and the basement membrane, indirectly leading to the disruption of the BBB (Papadopoulos & Verkman, 2013). In addition, this mechanism leads to intracellular or extracellular brain edema, which is associated with a high mortality in HSE patients (Safain, Roguski, Kryzanski, & Weller, 2015). Furthermore, HSV-1 infection of astrocytes leads to apoptosis through the interaction between the virus and mitochondria, resulting in the destruction of the BBB (H. Liu et al., 2019). Whether reactive astrocytes are beneficial in HSE remains under debate. In an HSE mouse model for chronic inflammation, it was demonstrated that astrogliosis occurs acutely and chronically after infection, and is associated with a

persistent inflammatory, potentially harmful reaction (Armien et al., 2010). In contrast, reactive astrocytes are able to release vascular protective factors which promote repair of the BBB thereby decreasing the expression of endothelial surface receptors and leukocyte infiltration (Michinaga & Koyama, 2019). In summary, HSV-1 infection of the brain, in contrast to RABV infection, leads to compromised BBB function and subsequently to a fulminant immune response, whose neuroprotective versus neurodestructive properties have yet to be defined.

5. Differences in cell-type specific innate immune responses between RABV and HSV infection in the CNS

The innate immune system represents the first line of defence against viral invaders. Germline-encoded pattern recognition receptors (PRRs), such as TLRs and retinoic acid-inducible gene I (RIG-I) like helicases (RLRs), sense evolutionary conserved pathogen-associated molecular patterns and danger-associated molecular patterns (Takeuchi & Akira, 2010). All major glial cells, more specifically astrocytes, microglia, oligodendrocytes, and SCs, as well as neurons express a different repertoire of TLRs. In detail, TLR2 and TLR9 are expressed by microglia and astrocytes, whereas TLR3 is found in microglia, astrocytes, oligodendrocytes, and neurons (Y D Bansode et al., 2019; Guo et al., 2015; Zhou et al., 2009). Further, the RLR RIG-I and melanoma differentiation-associated protein 5 (MDA5) are present in microglia, astrocytes, and neurons (Furr & Marriott, 2012). Generally, viral recognition via PRRs leads to an early IFN response, which restricts viral growth. Another essential function of the innate immune system is to prime and initiate an adaptive immune response (Katz, Guedes, Fernandes, & dos Ramos Silva, 2017). Compared to glial cells, it is thought that neurons may lack robust innate immune signalling to avoid damage to this largely irreplaceable and non-renewable cell population (Yordy, Iijima, Huttner, Leib, & Iwasaki, 2012). Overall, distinct cell-specific innate immune responses towards viral infection may account for viral tropism and pathophysiological findings such as a rather quiescent versus fulminant inflammatory response (Figure 4).

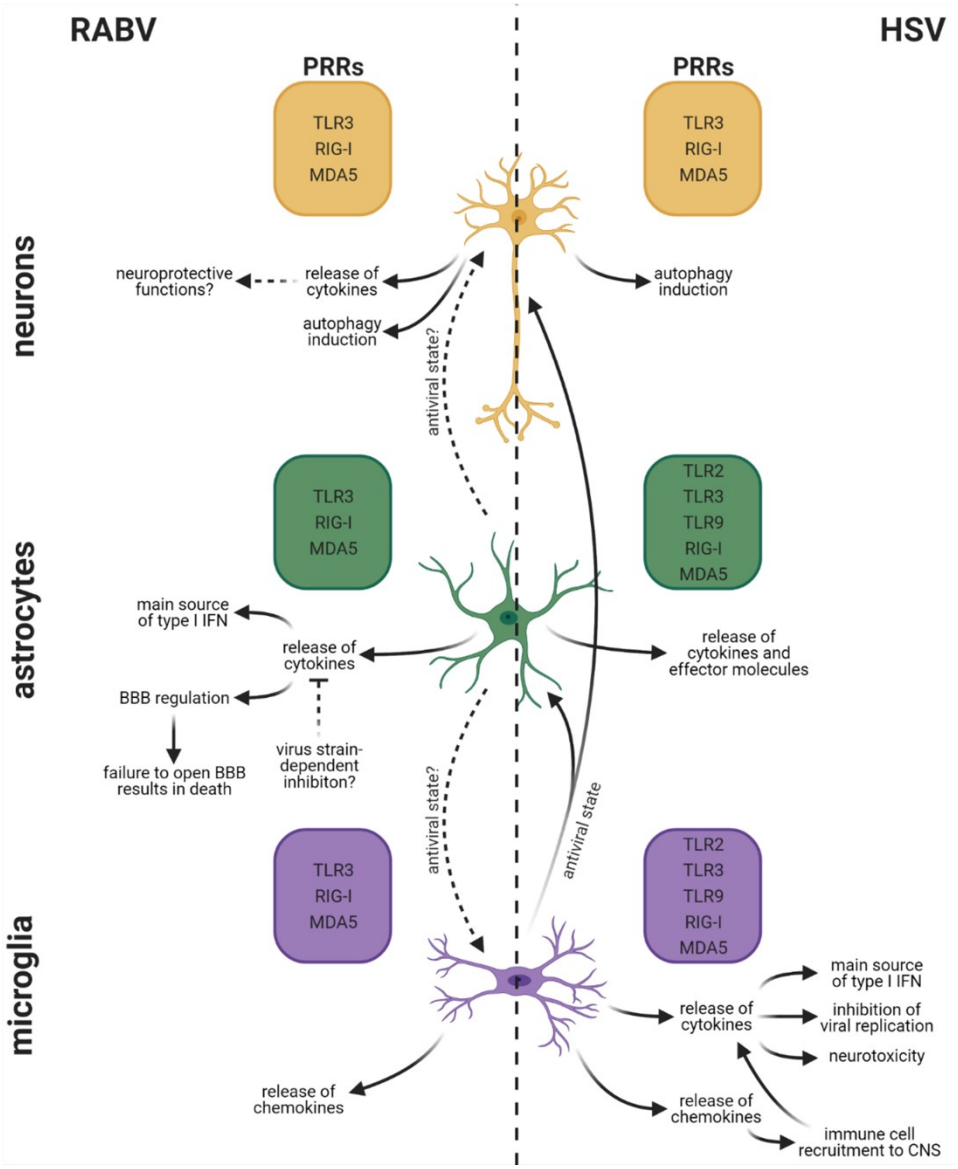

Figure 4 | Hypothesis of cell-specific innate immune responses of CNS cell types upon RABV and HSV infection. Neurons (yellow), astrocytes (green), and microglia (purple) are productively or non-productively infected by HSV and RABV (figure 3). Infection is sensed via a cell-specific set of PRRs, which trigger downstream signalling pathways and lead to the induction of an innate immune response (Takeuchi & Akira, 2010). Whereas certain PRRs are associated with RABV and HSV infection, neurons do not exhibit evident immune responses upon viral infection. It is suggested that neurons lack robust innate immune signalling to minimize harm and rather require autophagy to restrict RABV (Peng et al., 2016) and HSV (Yakoub & Shukla, 2015; Yordy et al., 2012) replication. In contrast, astrocytes and microglia respond to RABV and HSV infection via production of cytokines and chemokines (Cagnin et al., 2001; Conrady et al., 2010; Fujii et al., 1999; Lokensgard et al., 2001; Nakamichi et al., 2005; Pfefferkorn et al., 2016; Reinert et al., 2012; Tian et al., 2018). While for HSV, microglia are the main source of type I IFN in the CNS and result in pronounced immune cell infiltration (Reinert et al., 2016), astrocytes comprise the primary type I IFN producers for RABV (Pfefferkorn et al., 2016). Dashed arrows indicate putative or suggested effects.

5.1 Rabies virus

RABV is immediately recognized by the innate immune system after the virus is exposed to the skin or muscle by bites or scratches. Innate PRRs sense RABV at first in the periphery and afterwards the CNS (Li, Faber, Dietzschold, & Hooper, 2011). Intracellularly, RABV is recognized via MDA5 and RIG-I (Faul et al., 2010; Pfefferkorn et al., 2016; Tian et al., 2018), TLR3 (Alan C. Jackson, Rossiter, & Lafon, 2006; Ménager et al., 2009; Prehaud et al., 2005), or TLR7 (R. Liu, Wang, Yang, Khan, & Zhu, 2016; Luo et al., 2019, 2020), consequently leading to the activation of the NF-κB (nuclear factor 'kappa-light-chain-enhancer' of activated B-cells) pathway and the secretion of type I IFNs (Katz et al., 2017).

After cellular recognition of RABV by the innate immune system, macrophages play crucial roles in the uptake of pathogens via specialized endocytic mechanisms (Mercer & Greber, 2013). Lytle and colleagues observed that after rabies immunization, macrophages accumulate at the entry site (Lytle, Shen, & McGettigan, 2015) probably due to the chemokine-mediated recruitment of circulating monocytes. Like macrophages, dendritic cells (DCs) also efficiently ingest circulating pathogens and display antigens to prime adaptive immune responses (Mercer & Greber, 2013). Infection with lab-attenuated RABV leads to the RIG-I-dependent activation of DCs and subsequent production of type I IFNs (Faul et al., 2010; Hornung et al., 2006). In contrast, binding and entry into DCs by wt RABV was severely blocked and infection does not efficiently induce DC activation (Yang et al., 2015). Despite the inability of DCs to activate T cells during wt RABV infection, activated CD69+ T cells can be found in the draining lymph nodes and peripheral blood of infected mice, independent of the virulence of the RABV strain (M Lafon, 2005; A. Roy & Hooper, 2007).

Once the virus enters the CNS, RABV triggers innate immune responses of neurons (Prehaud et al., 2005), astrocytes (Pfefferkorn et al., 2016; Tian et al., 2018), and microglia (Nakamichi et al., 2005; Pfefferkorn et al., 2016) which mount primary IFN responses (activation of NF-κB) and secondary IFN responses (activation of Janus kinase-signal transducers and activators of transcription (JAK-STAT)), inducing the production of ISGs such as cytokines and chemokines (Katz et al., 2017). However, the extent of immune responses triggered strongly depends on the cell type (Pfefferkorn et al., 2016) and the viral strain used (Gnanadurai et al., 2015; Potratz, Zaeck, Christen, et al., 2020; Sui et al., 2021; Tian et al., 2018). Cytokines and chemokines are crucial to recruit peripheral immune cells to the CNS, since both favour changes in BBB permeability which in turn regulates the contact between circulating immune cells and the neural tissue (Griffin, 2003). Since wt RABV stimulates little or no inflammatory response, recruitment of peripheral cells to the CNS is limited (Anirban Roy & Hooper, 2008; Anirban Roy et al., 2007).

5.1.1 Neurons

TLR3 is involved in RABV pathogenesis (Ménager et al., 2009, 2008) and is expressed by glial cells and neurons (Soung & Klein, 2018). Upon RABV infection, human neuronal NT2-N cells upregulate TLR3 expression *in vitro* after challenge with the RABV strain CVS, possibly due to sensing of viral dsRNA. TLR3, subcellularly located in endosomes, senses endocytosed dsRNA (Matsumoto, Oshiumi, & Seya, 2011). In a human neuroblastoma cell line, CVS infection led to localization of TLR3 in spherical perinuclear structures (Ménager et al., 2009), which are also called Negri bodies (NBs), and which represent active RABV replication sites (Yves Gaudin et al., 2017; Lahaye et al., 2009). Together with enhanced TLR3 expression in cerebral cortical tissues in rabies patients (Alan C. Jackson et al., 2006), this led to the hypothesis that RABV inactivates the physiological function of TLR3 as a viral sensor and exploits the protein to help the spatial arrangement of RABV-induced NBs to support viral replication (Yves Gaudin et al., 2017; Ménager et al., 2009). Additionally, taking into account

that TLR3 can mediate neuronal apoptosis (Salaun, Coste, Rissoan, Lebecque, & Renno, 2006), sequestration of TLR3 might allow RABV to escape TLR-mediated apoptosis. Further, Peng and colleagues provide evidence that wt RABV induces autophagy which can in turn decrease apoptosis in neuroblastoma cells *in vitro* (Peng et al., 2016). During RABV neuroinvasion, RABV limits apoptosis and inflammation to ensure the integrity of the neuronal network subsequently enabling RABV transport throughout the CNS (Baloul & Lafon, 2003). Following CVS infection, human neuronal NT2-N cells strongly upregulate expression of IFN-β, CCL5, CXCL10, IL-6, TNF-α, and IL-1α (Prehaud et al., 2005). There is increasing evidence stating that IFN-β (Plioplys & Massimini, 1995), CCL5 (Meucci et al., 1998), and IL-6 (Hirota, Kiyama, Kishimoto, & Taga, 1996; Pizzi et al., 2004) also harbor neuroprotective functions. Despite the onset of rabies-induced neurological signs and symptoms, histological lesions stay relatively mild in the RABV-infected CNS (Iwasaki Y, 2002). Although apoptosis is limited, neurons exhibit marked beading and fragmentation of dendrites and axons, as well as swollen mitochondria in perikarya and proximal dendrites in the CVS-infected murine cerebral cortex (C. A. Scott, Rossiter, Andrew, & Jackson, 2008). Both, structural changes of neurons (C. A. Scott et al., 2008) and neuronal dysfunction (Fu & Jackson, 2005) are assumed to explain the fatal outcome of rabies rather than neuronal death.

5.1.2 Astrocytes

Dependent on the virus strain, astrocytes can support RABV infection *in vitro* and *in vivo* (Potratz, Zaeck, Christen, et al., 2020). In general, astrocytes have higher expression levels of ISGs, rendering them less susceptible towards viral infections than other cell types (Lindqvist et al., 2016). There is growing evidence that inflammatory upregulation of TLR3 expression in human astrocytes results in neuroprotection (Bsibsi et al., 2006). However, the role of TLR3-mediated signalling in astrocytes during RABV infection is still unknown. Besides TLRs, RLRs represent another group of PRRs, which sense RABV (Pfefferkorn et al., 2016) and consequently trigger antiviral responses via activation of NF-κB and JAK-STAT pathways (Rehwinkel & Gack, 2020). RLRs MDA5 and RIG-I are cytoplasmic viral sensors, which recognize viral replication via recognition of dsRNA resulting in IPS-1 (IFN-β promoter stimulator-1)-mediated IRF3 activation (Hornung et al., 2006). In astrocytes, lab-attenuated RABV produces higher levels of dsRNA compared to wt RABV. As a result, lab-attenuated RABV induces MDA5/RIG-I-mediated activation of IPS-1/p38/NF-κB to a higher degree than wt RABV. Consequent production of ISGs and inflammatory cytokines leads to the clearance of lab-attenuated RABV from astrocytes. In contrast, wt RABV non-abortively infects astrocytes through the evasion of the MDA5/RIG-I-sensory pathway (Tian et al., 2018). Primary murine astrocytes respond with the expression of IL-6 and TNF-α to VSV infection, a rhabdovirus which closely resembles RABV. In contrast, heat-inactivated VSV robustly lowered astrocyte-mediated cytokine expression, viral replication, and sensing of viral RNA by RLRs (Chauhan et al., 2010). Overall, RLRs may play a crucial role for RABV sensing and initiating cytokine production in infected astrocytes, however, more experimental data are needed to confirm this hypothesis. *In vivo*, astrocytes induce IFN-β production via RLR and TLR signalling transduction pathways, representing the main source of IFN-β in the virus infected brain (Pfefferkorn et al., 2016). For other neurotropic virus infections, astrocytes have also been implicated as the main type I IFN producers in the CNS (Detje et al., 2015; Kallfass et al., 2012). Moreover, lab-attenuated RABV induces the expression of a variety of inflammatory cytokines (TNF-α, IL-6, IL-1β, IFN-γ, IL-17, and VEGF) in astrocytes, which in turn regulate BBB permeability (Tian et al., 2018). Generally, astrocytes are also known as innate immune neuroglia releasing a variety of neurotrophins as well as pro- and anti-inflammatory mediators (e.g., TGF-β, IL-1β, IL-6, CXCL10, CXCL12), enabling the communication with neighboring cells and recruiting adaptive immune cells to the CNS (Griffin, 2003). Interestingly, it was

shown that pathogenic field RABV infection strongly modulates microRNA (miRNA) expression in the brains of infected mice. Predicted targets of RABV-modulated miRNAs involved the TGF-β signalling pathway (Zhao et al., 2012), which is strongly associated with astrocyte scar formation (Diniz, Matias, Siqueira, Stipursky, & Gomes, 2019). Other targets of RABV-modulated miRNAs included the JAK-STAT signalling pathway, especially JAK2, suppressor of cytokine signalling (Socs3), and Socs4 (Zhao et al., 2012). It is well known, that the JAK2-STAT3 pathway plays a central role in astrocyte reactivity upon multiple pathological conditions (Ceyzériat, Abjean, Carrillo-de Sauvage, Ben Haim, & Escartin, 2016), making them a possible target of RABV-modulated miRNAs.

5.1.3 Microglia

Besides immunologically active astrocytes, microglia respond to infection via expression of ISGs, chemokines, and proinflammatory cytokines (Lytle et al., 2015). In detail, macrophage-mediated endocytosis of RABV-inactivated and infectious virions activates the ERK1/2 signalling pathways, ultimately leading to chemokine expression (Nakamichi, Inoue, Takasaki, Morimoto, & Kurane, 2004). Chemokine secretion mediates leukocyte recruitment into the CNS in a multistep process (Michlmayr et al., 2014). Not only RNA levels of CXCL10 and CCL5 in RABV-infected murine microglial cells Ra2 were approximately 3000-fold higher compared to mock-infected cells but also protein levels increased steeply, reaching a plateau phase at 20 hours post-infection. Furthermore, expression of CCL5 and CXCL10 was modulated upon RABV replication since UV-inactivated virions did not trigger chemokine expression (Nakamichi et al., 2005). Emphasizing the importance of the mitogen-activated protein kinases (MAPK) subfamilies p38, c-Jun N-terminal kinases (JNK), and extracellular signal-regulated kinases (ERK) 1/2 in the establishment of an antiviral response against RABV (Besson et al., 2019; Nakamichi et al., 2004), Nakamichi and colleagues discovered that RABV triggers phosphorylation of MAPK signal transduction pathways in murine microglia, possibly triggering chemokine secretion (Nakamichi et al., 2005). Interestingly, activation of p38 and ERK1/2 signal transduction pathways stimulates CXCL10 expression, whereas CCL5 expression is positively regulated by p38 and negatively regulated by ERK1/2. Particularly p38 is required for the NF-κB-mediated expression of CXCL10 and CCL5 (Nakamichi et al., 2005), chemokines known to act as proinflammatory mediators during viral encephalitis (Bhowmick et al., 2007; C.-J. Chen, Chen, Chen, Liao, & Raung, 2004; Kalita, Srivastava, Mishra, Basu, & Misra, 2010; McKimmie & Michlmayr, 2014). Apart from the secretion of cytokines and chemokines, microglia also produce important amounts of type I IFN during RABV infection (Pfefferkorn et al., 2016).

5.2 Herpes simplex virus

HSV-1 infection is controlled by both the innate and adaptive immune system and is initially recognized by TLR2, TLR3, and TLR9 (Ma & He, 2014). While HSV glycoproteins are sensed by TLR2 on the cell surface, viral DNA is detected by endosomal TLR9 followed by activation of cGAS and the adaptor protein STING. Besides TLRs, RLRs including RIG-I and MDA5 are described to detect HSV-1 RNA in the cytoplasm of infected cells, leading to activation of the IPS-1 adaptor, NF-κB, activator protein 1 (AP-1) and IFN regulatory factor (IRF) such as IRF3 and IRF7. These molecules act as transcription factors, which result in the production of pro-inflammatory cytokines and type I IFN (Mogensen, 2009), triggering the initial response towards HSV-1 infection (Perry, Chen, Zheng, Tang, & Cheng, 2005). IFN-α and IFN-β signal through the interaction with interferon receptors (IFNAR) 1 and 2, resulting in subsequent activation of the JAK-STAT signalling pathway (Nan, Wu, & Zhang, 2017). In the CNS, HSV-1 is mainly recognized by microglia and astrocytes.

The immune response in HSE has been described as a ‘double-edged sword’. It is crucial to control viral replication early after infection, as otherwise an uncontrolled immune response can lead to excessive reactions that can be fatal for the host (Piret & Boivin, 2015). The first-line viral defence is mediated by the TLR2 receptor driving the expression of various interleukins, type I IFN and TNF-α (Y. Wang et al., 2019). However, since mice lacking TLR2 revealed higher survival rates after HSV-1 infection than the wt strain, the TLR2-mediated response can have detrimental effects on the outcome of HSE (Kurt-Jones et al., 2004). In contrast to TLR2, TLR9 does not play a major role in the fight against HSV-1 (J. P. Wang et al., 2012), but rather functions simultaneously with TLR2 by recruiting natural killer (NK) cells to the CNS (Kato et al., 2006; Sorensen et al., 2008). For control of HSV-1 replication and the production of type I and II IFNs in the brain, TLR3-mediated sensing of HSV-1 has been described as most important (Menasria et al., 2013). Unlike HSV-1, wt RABV successfully evades TLR3 signalling thereby inhibiting the induction of IFN (Ménager et al., 2009; Nikolic et al., 2017).

5.2.1 Neurons

Neurons are highly susceptible to HSV infection. Lafaille and colleagues provide strong evidence that neuronal induction of IFN-β and/or IFN-γ is highly dependent on UNC-93B, which is associated with TLR-mediated responses (Lafaille et al., 2012). Further, UNC-93B-deficient human neurons exhibited impaired IFN-β and IFN-γ responses to HSV-1 infection and were more susceptible towards HSV-1 infection (Lafaille et al., 2012). Although secretion of IFNs impairs HSV-1 replication in iPSC-derived human neurons (Lafaille et al., 2012), type I IFN treatment failed to completely block HSV-1 replication in murine neurons (Yordy et al., 2012). Similar to RABV, autophagy, not IFN signalling, is suggested to be the dominant antiviral strategy employed by neurons to control HSV infection (Yakoub & Shukla, 2015; Yordy et al., 2012). Using an *in vitro* system of purified TG neurons from adult mice grown in compartmentalized chambers, Rosato and colleagues showed that the administration of IFN-β at either the soma or axon is capable of restricting HSV-1 replication. Moreover, they showed that non-neuronal IFN signalling is insufficient to control HSV-1 dissemination and mortality *in vivo*, whereas neuronal IFN signalling alone is necessary to control HSV-1 replication, disease, and survival (Rosato & Leib, 2015). Recently, studies highlighted the importance of the neuronal differentiation state and subtype on antiviral signalling capabilities (Cho et al., 2013; Farmer, Altschaefl, O’Shea, & Miller, 2013; Schultz, Vernon, & Griffin, 2015). Thus, different models and differentiation states might explain differences observed in the role of the neuronal type I IFN response. Taken together, neurons might restrict HSV replication via the induction of autophagy (Yakoub & Shukla, 2015; Yordy et al., 2012) and type I IFNs (Lafaille et al., 2012; Rosato & Leib, 2015).

5.2.2 Astrocytes

Astrocytes have not been intensively studied in HSV-1 brain infection. Recently, the expression of TLRs in response to HSV-1 infection in astrocytes has been investigated in more detail (Y D Bansode et al., 2019). Mainly TLR2, TLR6, TLR7, TLR8, and TLR9, as well as DNA-dependent activator of IFN-regulatory factors (DAI), cGAS and MDA5 are upregulated by astrocytes while IFI204, which senses nuclear DNA, is downregulated implicating a potential viral immune evasion strategy. Upon infection, astrocytes react with the production of type I and II IFNs, which in turn activate the JAK-STAT pathway. Especially STAT4 expression is increased, which may stimulate the pro-inflammatory IL-12 cascade. In addition, different ISGs have been identified, which elicit antiviral properties in response to HSV-1 infection of astrocytes such as RNase L, PKR (protein kinase R), IFIT (interferon induced proteins with tetratricopeptide repeats) and viperin. In contrast to microglia, astrocytes do not produce any

neurotoxic substances (Lokensgard, Cheeran, Hu, Gekker, & Peterson, 2002). Moreover, TLR3 expression in astrocytes is necessary to respond towards neurotropic HSV-2 infection with the induction of IFN-β production, possibly preventing viral spread (Reinert et al., 2012).

5.2.3 Microglia

Cytokines produced by glial cells play a crucial role in the activation of glia in the CNS itself and in the attraction of immune cells such as DCs, NK cells and lymphocytes towards the brain (Conrady, Drevets, & Carr, 2010). Specifically, human microglia produce high amounts of CCL5, CXCL10, TNF-α, IL-1β as well as lower amounts of IL-6, IL-8, CCL3, CCL4 and CCL2 in a TLR3-dependent manner (Lokensgard et al., 2001). Similar to astrocytes in RABV pathogenesis, microglia are the main source of type I IFN in HSE (Reinert et al., 2016). Those glial cell-produced factors reveal variable antiviral properties *in vitro*. Whereas TNF-α drastically limits viral replication in astrocytes, IL-1β decreases viral replication comparably little. In neurons, however, TNF-α and IL-1β have no effect on viral replication, whereas CXCL10 drastically decreases HSV-1 replication (Lokensgard et al., 2001). For HSV-1 it could be shown that microglia transfer its antiviral response to neurons and astrocytes (Reinert et al., 2016). Through the expression of IFN-α, microglia upregulate specific TLRs such as TLR3, TLR4, and TLR7 on DCs, NK cells, and lymphocytes, and thus increase the production of IFN and cytokines (Conrady et al., 2010). Specifically, CCL5, CCL2, and CXCL10 recruit peripheral immune cells to the infected brain (Cédile, Wlodarczyk, & Owens, 2017; Ransohoff et al., 1993; Robichon, Patel, Connor, & La Flamme, 2020), of which CXCL10 in particular has been shown to attract lymphocytes towards HSV-1 infection (Lokensgard et al., 2001). Microglial IFN-β further mediates the production of IL-10, a known immunosuppressor which can prevent severe inflammation (Broad, Kirby, Jones, Applied, & Transplantation Research, 2007), and IL-6 which protects against neuronal loss (Chucair-Elliott et al., 2014). Cytokines and chemokines primarily originating from microglia also comprise neurotoxic activity as it has been reported for TNF-α and IL-1β (Lokensgard et al., 2001). HSV-1-infected microglial cells have been shown to produce ROS, leading to higher amounts of inducible nitric oxide synthase and cytotoxic nitric oxide, which are responsible for brain damage (Fujii, Akaike, & Maeda, 1999). Microglia-mediated immune responses can also have detrimental long-term consequences. Chronic HSV-1 infection leads to persistent activation of microglia (Cagnin et al., 2001), resulting into prolonged upregulation of ISGs, reinforcing chronic inflammation and neuronal damage (Marques, Hu, Sheng, & Lokensgard, 2006).

6. Future directions

Even though the CNS remains a highly vulnerable tissue for a few specialized viral diseases such as rabies and HSE, little is known about the role of glial cells during neuroinvasive infections. Deciphering the underlying mechanisms of highly distinct viral growth characteristics between different CNS cell types may unravel factors that limit viral replication.

Up to today, neurotropic RABV is often studied in animal models and neuronal cell types using lab-attenuated viruses. Therefore, data is scarce about the role of non-neuronal CNS cell types during viral encephalomyelitis in humans. Like for rabies, the roles of astrocytes, oligodendrocytes, and microglia during HSE are still not fully understood. Studying HSV or RABV in neuronal monocultures does not reflect the diversity of the CNS. More importantly, the crosstalk between neurons, astrocytes, oligodendrocytes, and microglia is crucial to ensure CNS homeostasis and to protect the infected CNS from pathological conditions. More sophisticated models, which reflect the human brain in a physiological context are needed to understand the interaction of HSV and RABV with cell-specific signalling pathways. Thus, determining the molecular mechanisms defining cellular susceptibility of neurotropic HSV and RABV remains crucial to discover new and promising therapeutic targets.

7. Declarations

7.1 Conflicts of interests

The authors declare that they have no competing interests.

7.2 Funding

Lena Feige was supported by the Pasteur - Paris University (PPU) International PhD Program. FLI work was supported by an intramural collaborative research grant at the Friedrich-Loeffler-Institute (Ri-0372) to S.F.

7.3 Authorship

LF, LMZ, and JS wrote the manuscript. JS performed the histopathology. LMZ generated the figures. All authors read and approved the final manuscript.

7.4 Data sharing and data accessibility

Data sharing is not applicable to this article as no datasets were generated or analysed during the current study.

8. References

Abraham, G., & Banerjee, A. K. (1976). Sequential transcription of the genes of vesicular stomatitis virus. Proceedings of the National Academy of Sciences of the United States of America, 73(5), 1504–1508. https://doi.org/10.1073/pnas.73.5.1504

Adle-Biassette, H., Bourhy, H., Gisselbrecht, M., Chrétien, F., Wingertsmann, L., Baudrimont, M., … F, G. (1996). Rabies encephalitis in a patient with AIDS: a clinicopathological study. Acta Neuropathologica, 92(4), 415–420. https://doi.org/10.1007/s004010050538

Aggarwal, A., Miranda-Saksena, M., Boadle, R. A., Kelly, B. J., Diefenbach, R. J., Alam, W., & Cunningham, A. L. (2012). Ultrastructural Visualization of Individual Tegument Protein Dissociation during Entry of Herpes Simplex Virus 1 into Human and Rat Dorsal Root Ganglion Neurons. Journal of Virology, 86(11), 6123–6137. https://doi.org/10.1128/jvi.07016-11

Almeida, M. F., Martorelli, L. F. A., Aires, C. C., Sallum, P. C., Durigon, E. L., & Massad, E. (2005). Experimental rabies infection in haematophagous bats Desmodus rotundus. Epidemiology and Infection, 133(3), 523–527. https://doi.org/10.1017/s0950268804003656

Alvarez, L., Fajardo, R., Lopez, E., Pedroza, R., Hemachudha, T., Kamolvarin, N., … Baer, G. M. (1994). Partial recovery from rabies in a nine-year-old boy. The Pediatric Infectious Disease Journal, 13(12), 1154–1155. https://doi.org/10.1097/00006454-199412000-00020

Antinone, S. E., & Smith, G. A. (2010). Retrograde axon transport of herpes simplex virus and pseudorabies virus: a live-cell comparative analysis. J Virol, 84(3), 1504–1512. https://doi.org/10.1128/JVI.02029-09

Appolinário, C. M., Allendorf, S. D., Peres, M. G., Ribeiro, B. D., Fonseca, C. R., Vicente, A. F., … Jane, M. (2016). Profile of cytokines and chemokines triggered by wild-type strains of rabies virus in mice. American Journal of Tropical Medicine and Hygiene, 94(2), 378–383. https://doi.org/10.4269/ajtmh.15-0361

Aravalli, R. N., Hu, S., Rowen, T. N., Palmquist, J. M., & Lokensgard, J. R. (2005). TLR2-mediated proinflammatory cytokine and chemokine production by microglial cells in response

to herpes simplex virus. Journal of Immunology, 175(7), 4189–4193. https://doi.org/10.4049/jimmunol.175.7.4189

Armien, A. G., Hu, S., Little, M. R., Robinson, N., Lokensgard, J. R., Low, W. C., & Cheeran, M. C. (2010). Chronic cortical and subcortical pathology with associated neurological deficits ensuing experimental herpes encephalitis. Brain Pathol, 20(4), 738–750. https://doi.org/10.1111/j.1750-3639.2009.00354.x

Baer, G. M. (1975). The Natural History of Rabies. In CRC Press. New York: Academic Press. https://doi.org/10.1016/0168-1702(91)90006-H

Balachandran, A., & Charlton, K. (1994). Experimental rabies infection of non-nervous tissues in skunks (Mephitis mephitis) and foxes (Vulpes vulpes). Veterinary Pathology, 31(1), 93–102. https://doi.org/10.1177/030098589403100112

Baloul, L., & Lafon, M. (2003). Apoptosis and rabies virus neuroinvasion. Biochimie, 85(8), 777–788. https://doi.org/10.1016/S0300-9084(03)00137-8

Bansode, Y D, Chattopadhyay, D., & Saha, B. (2019). Innate immune response in astrocytes infected with herpes simplex virus 1. Arch Virol, 164(5), 1433–1439. https://doi.org/10.1007/s00705-019-04197-x

Bansode, Yashvant D, Chattopadhyay, D., & Saha, B. (2020). Transcriptomic Analysis of Interferon Response in Toll-Like Receptor 2 Ligand-Treated and Herpes Simplex Virus 1-Infected Neurons and Astrocytes. Viral Immunology. https://doi.org/10.1089/vim.2020.0238

Baquero, E., Albertini, A. A. V, & Gaudin, Y. (2015). Recent mechanistic and structural insights on class III viral fusion glycoproteins. Current Opinion in Structural Biology, 33, 52–60. https://doi.org/10.1016/j.sbi.2015.07.011

Baskin, H. J., & Hedlund, G. (2007). Neuroimaging of herpesvirus infections in children. Pediatr Radiol, 37(10), 949–963. https://doi.org/10.1007/s00247-007-0506-1

Bauer, A., Nolden, T., Nemitz, S., Perlson, E., & Finke, S. (2015). A Dynein Light Chain 1 Binding Motif in Rabies Virus Polymerase L Protein Plays a Role in Microtubule Reorganization and Viral Primary Transcription. Journal of Virology, 89(18), 9591–9600. https://doi.org/10.1128/JVI.01298-15

Bauer, A., Nolden, T., Schröter, J., Römer-Oberdörfer, A., Gluska, S., Perlson, E., & Finke, S. (2014). Anterograde glycoprotein-dependent transport of newly generated rabies virus in dorsal root ganglion neurons. Journal of Virology, 88(24), 14172–14183. https://doi.org/10.1128/JVI.02254-14

Begeman, L., GeurtsvanKessel, C., Finke, S., Freuling, C. M., Koopmans, M., Müller, T., … Kuiken, T. (2017). Comparative pathogenesis of rabies in bats and carnivores, and implications for spillover to humans. The Lancet Infectious Diseases, 18(4), e147–e159. https://doi.org/10.1016/S1473-3099(17)30574-1

Bello-Morales, R., Fedetz, M., Alcina, A., Tabares, E., & Lopez-Guerrero, J. A. (2005). High susceptibility of a human oligodendroglial cell line to herpes simplex type 1 infection. J Neurovirol, 11(2), 190–198. https://doi.org/10.1080/13550280590924179

Benavides, J. A., Velasco-Villa, A., Godino, L. C., Satheshkumar, P. S., Nino, R., Rojas-Paniagua, E., … Streicker, D. G. (2020). Abortive vampire bat rabies infections in Peruvian peridomestic livestock. PLoS Neglected Tropical Diseases, 14(6), e0008194. https://doi.org/10.1371/journal.pntd.0008194

Bertoune, M., Nickl, B., Krieger, T., Wohlers, L., Bonaterra, G. A., Dietzschold, B., … Bette, M. (2017). The phenotype of the RABV glycoprotein determines cellular and global virus load in the brain and is decisive for the pace of the disease. Virology, 511, 82–94. https://doi.org/10.1016/j.virol.2017.08.019

Besson, B., Kim, S., Kim, T., Ko, Y., Lee, S., Larrous, F., … Bourhy, H. (2019). Kinome-Wide RNA Interference Screening Identifies Mitogen-Activated Protein Kinases and Phosphatidylinositol Metabolism as Key Factors for Rabies Virus Infection. MSphere, 4(3). https://doi.org/10.1128/mSphere.00047-19

Bhowmick, S., Duseja, R., Das, S., Appaiahgiri, M. B., Vrati, S., & Basu, A. (2007). Induction of IP-10 (CXCL10) in astrocytes following Japanese encephalitis. Neuroscience Letters, 414(1), 45–50. https://doi.org/10.1016/j.neulet.2006.11.070

Boukhvalova, M. S., Mortensen, E., Mbaye, A., Lopez, D., Kastrukoff, L., & Blanco, J. C. G. (2019). Herpes Simplex Virus 1 Induces Brain Inflammation and Multifocal Demyelination in the Cotton Rat Sigmodon hispidus. J Virol, 94(1). https://doi.org/10.1128/JVI.01161-19

Bradshaw, M. J., & Venkatesan, A. (2016). Herpes Simplex Virus-1 Encephalitis in Adults: Pathophysiology, Diagnosis, and Management. Neurotherapeutics, 13(3), 493–508. https://doi.org/10.1007/s13311-016-0433-7

Brankin, B., Hart, M. N., Cosby, S. L., Fabry, Z., & Allen, I. V. (1995). Adhesion molecule expression and lymphocyte adhesion to cerebral endothelium: effects of measles virus and herpes simplex 1 virus. J Neuroimmunol, 56(1), 1–8. https://doi.org/10.1016/0165-5728(94)00110-a

Broad, A., Kirby, J. A., Jones, D. E., Applied, I., & Transplantation Research, G. (2007). Toll-like receptor interactions: tolerance of MyD88-dependent cytokines but enhancement of MyD88-independent interferon-beta production. Immunology, 120(1), 103–111. https://doi.org/10.1111/j.1365-2567.2006.02485.x

Broderick, C., Hoek, R. M., Forrester, J. V, Liversidge, J., Sedgwick, J. D., & Dick, A. D. (2002). Constitutive retinal CD200 expression regulates resident microglia and activation state of inflammatory cells during experimental autoimmune uveoretinitis. The American Journal of Pathology, 161(5), 1669–1677. https://doi.org/10.1016/S0002-9440(10)64444-6

Brundula, V., Rewcastle, N. B., Metz, L. M., Bernard, C. C., & Yong, V. W. (2002). Targeting leukocyte MMPs and transmigration: minocycline as a potential therapy for multiple sclerosis. Brain : A Journal of Neurology, 125(Pt 6), 1297–1308. https://doi.org/10.1093/brain/awf133

Brzózka, K., Finke, S., & Conzelmann, K.-K. (2006). Inhibition of Interferon Signaling by Rabies Virus Phosphoprotein P: Activation-Dependent Binding of STAT1 and STAT2. Journal of Virology, 80(6), 2675–2683. https://doi.org/10.1128/JVI.80.6.2675-2683.2006

Brzózka, Krzysztof, Finke, S., & Brzo, K. (2005). Identification of the Rabies Virus Alpha / Beta Interferon Antagonist : Phosphoprotein P Interferes with Phosphorylation of Interferon Regulatory Factor 3 Identification of the Rabies Virus Alpha / Beta Interferon Antagonist : Phosphoprotein P Interferes. Journal, 79(12), 7673–7681. https://doi.org/10.1128/JVI.79.12.7673

Bsibsi, M., Persoon-Deen, C., Verwer, R. W. H., Meeuwsen, S., Ravid, R., & Van Noort, J. M. (2006). Toll-like receptor 3 on adult human astrocytes triggers production of neuroprotective mediators. Glia, 53(7), 688–695. https://doi.org/10.1002/glia.20328

Cagnin, A., Myers, R., Gunn, R. N., Lawrence, A. D., Stevens, T., Kreutzberg, G. W., … Banati, R. B. (2001). In vivo visualization of activated glia by [11C] (R)-PK11195-PET following herpes encephalitis reveals projected neuronal damage beyond the primary focal lesion. Brain, 124(Pt 10), 2014–2027. https://doi.org/10.1093/brain/124.10.2014

Campadelli-Fiume, G., Cocchi, F., Menotti, L., & Lopez, M. (2000). The novel receptors that mediate the entry of herpes simplex viruses and animal alphaherpesviruses into cells. Rev Med Virol, 10(5), 305–319. https://doi.org/10.1002/1099-1654(200009/10)10:5<305::aid-rmv286>3.0.co;2-t

Carty, M., Reinert, L., Paludan, S. R., & Bowie, A. G. (2014). Innate antiviral signalling in the central nervous system. Trends in Immunology, 35(2), 79–87. https://doi.org/10.1016/j.it.2013.10.012

Cédile, O., Wlodarczyk, A., & Owens, T. (2017). CCL2 recruits T cells into the brain in a CCR2-independent manner. APMIS : Acta Pathologica, Microbiologica, et Immunologica Scandinavica, 125(11), 945–956. https://doi.org/10.1111/apm.12740

Centers for Disease Control and Prevention (CDC). (2004). Recovery of a patient from clinical rabies--Wisconsin, 2004. MMWR. Morbidity and Mortality Weekly Report, 53(50), 1171–1173. Retrieved from https://pubmed.ncbi.nlm.nih.gov/15614231/

Centers for Disease Control and Prevention (CDC). (2012). Recovery of a patient from clinical rabies--California, 2011. MMWR. Morbidity and Mortality Weekly Report, 61(4), 61–65. Retrieved from https://pubmed.ncbi.nlm.nih.gov/22298301/

Ceyzériat, K., Abjean, L., Carrillo-de Sauvage, M. A., Ben Haim, L., & Escartin, C. (2016). The complex STATes of astrocyte reactivity: How are they controlled by the JAK-STAT3 pathway? Neuroscience, 330, 205–218. https://doi.org/10.1016/j.neuroscience.2016.05.043

Chan, W. L., Javanovic, T., & Lukic, M. L. (1989). Infiltration of immune T cells in the brain of mice with herpes simplex virus-induced encephalitis. Journal of Neuroimmunology, 23(3), 195–201. https://doi.org/10.1016/0165-5728(89)90051-9

Charlton, K. M., & Casey, G. A. (1979). Experimental rabies in skunks: immunofluorescence light and electron microscopic studies. Laboratory Investigation; a Journal of Technical Methods and Pathology, 41(1), 36–44.

Charlton, K. M., Casey, G. A., Wandeler, A. I., & Nadin-Davis, S. (1995). Early events in rabies virus infection of the central nervous system in skunks (Mephitis mephitis). Acta Neuropathologica, 91(1), 89–98. https://doi.org/10.1007/s004010050397

Charlton, K. M., Nadin-Davis, S., Casey, G. A., & Wandeler, A. I. (1997). The long incubation period in rabies: delayed progression of infection in muscle at the site of exposure. Acta Neuropathologica, 94(1), 73–77. https://doi.org/10.1007/s004010050674

Chauhan, V. S., Furr, S. R., Sterka David G., J. G., Nelson, D. A., Moerdyk-Schauwecker, M., Marriott, I., & Grdzelishvili, V. Z. (2010). Vesicular stomatitis virus infects resident cells of the central nervous system and induces replication-dependent inflammatory responses. Virology, 400(2), 187–196. https://doi.org/10.1016/j.virol.2010.01.025

Chen, C.-J., Chen, J.-H., Chen, S.-Y., Liao, S.-L., & Raung, S.-L. (2004). Upregulation of RANTES Gene Expression in Neuroglia by Japanese Encephalitis Virus Infection. Journal of Virology, 78(22), 12107–12119. https://doi.org/10.1128/jvi.78.22.12107-12119.2004

Chen, Z., Zhong, D., & Li, G. (2019). The role of microglia in viral encephalitis: a review. J Neuroinflammation, 16(1), 76. https://doi.org/10.1186/s12974-019-1443-2

Cho, H., Proll, S. C., Szretter, K. J., Katze, M. G., Gale, M., & Diamond, M. S. (2013). Differential innate immune response programs in neuronal subtypes determine susceptibility to infection in the brain by positive-stranded RNA viruses. Nature Medicine, 19(4), 458–464. https://doi.org/10.1038/nm.3108

Chucair-Elliott, A. J., Conrady, C., Zheng, M., Kroll, C. M., Lane, T. E., & Carr, D. J. (2014). Microglia-induced IL-6 protects against neuronal loss following HSV-1 infection of neural progenitor cells. Glia, 62(9), 1418–1434. https://doi.org/10.1002/glia.22689

Conrady, C. D., Drevets, D. A., & Carr, D. J. (2010). Herpes simplex type I (HSV-1) infection of the nervous system: is an immune response a good thing? J Neuroimmunol, 220(1–2), 1–9. https://doi.org/10.1016/j.jneuroim.2009.09.013

Daneman, R., & Prat, A. (2015). The blood–brain barrier. Cold Spring Harbor Perspectives in Biology, 7(1). https://doi.org/10.1101/cshperspect.a020412

Davis, L. E., & Johnson, R. T. (1979). An explanation for the localization of herpes simplex encephalitis? Ann Neurol, 5(1), 2–5. https://doi.org/10.1002/ana.410050103

De Bock, M., Van Haver, V., Vandenbroucke, R. E., Decrock, E., Wang, N., & Leybaert, L. (2016). Into rather unexplored terrain-transcellular transport across the blood-brain barrier. Glia, 64(7), 1097–1123. https://doi.org/10.1002/glia.22960

de Melo, G. D., Sonthonnax, F., Lepousez, G., Jouvion, G., Minola, A., Zatta, F., … Bourhy, H. (2020). A combination of two human monoclonal antibodies cures symptomatic rabies. EMBO Molecular Medicine, 12(11), 1–10. https://doi.org/10.15252/emmm.202012628

Detje, C. N., Lienenklaus, S., Chhatbar, C., Spanier, J., Prajeeth, C. K., Soldner, C., … Kalinke, U. (2015). Upon intranasal vesicular stomatitis virus infection, astrocytes in the olfactory bulb are important interferon Beta producers that protect from lethal encephalitis. Journal of Virology, 89(5), 2731–2738. https://doi.org/10.1128/JVI.02044-14

Dhingra, V., Li, X., Liu, Y., & Fu, Z. F. (2007). Proteomic profiling reveals that rabies virus infection results in differential expression of host proteins involved in ion homeostasis and synaptic physiology in the central nervous system. Journal of NeuroVirology, 13(2), 107–117. https://doi.org/10.1080/13550280601178226

Dietzschold, B, Kao, M., Zheng, Y. M., Chen, Z. Y., Maul, G., Fu, Z. F., … Koprowski, H. (1992). Delineation of putative mechanisms involved in antibody-mediated clearance of rabies virus from the central nervous system. Proceedings of the National Academy of Sciences of the United States of America, 89(15), 7252–7256. https://doi.org/10.1073/pnas.89.15.7252

Dietzschold, Bernhard, Li, J., Faber, M., & Schnell, M. (2008). Concepts in the pathogenesis of rabies. Future Virology, 3(5), 481–490. https://doi.org/10.2217/17460794.3.5.481

Diniz, L. P., Matias, I., Siqueira, M., Stipursky, J., & Gomes, F. C. A. (2019, July 1). Astrocytes and the TGF-β1 Pathway in the Healthy and Diseased Brain: a Double-Edged Sword. Molecular Neurobiology, Vol. 56, pp. 4653–4679. Humana Press Inc. https://doi.org/10.1007/s12035-018-1396-y

Esiri, M. M. (1982). Herpes-Simplex Encephalitis - an Immunohistological Study of the Distribution of Viral-Antigen within the Brain. Journal of the Neurological Sciences, 54(2), 209–226. https://doi.org/Doi 10.1016/0022-510x(82)90183-6

Etessami, R., Conzelmann, K.-K., Fadai-Ghotbi, B., Natelson, B., Tsiang, H., & Ceccaldi, P.-E. (2000). Spread and pathogenic characteristics of a G-deficient rabies virus recombinant: an in vitro and in vivo study. The Journal of General Virology, 81(Pt 9), 2147–2153. https://doi.org/10.1099/0022-1317-81-9-2147

Farmer, J. R., Altschaefl, K. M., O'Shea, K. S., & Miller, D. J. (2013). Activation of the Type I Interferon Pathway Is Enhanced in Response to Human Neuronal Differentiation. PLoS ONE, 8(3). https://doi.org/10.1371/journal.pone.0058813

Faul, E. J., Wanjalla, C. N., Suthar, M. S., Gale, M., Wirblich, C., & Schnell, M. J. (2010). Rabies Virus Infection Induces Type I Interferon Production in an IPS-1 Dependent Manner While Dendritic Cell Activation Relies on IFNAR Signaling. PLoS Pathogens, 6(7), e1001016. https://doi.org/10.1371/journal.ppat.1001016

Feige, L., Kozaki, T., Dias de Melo, G., Guillemot, V., Larrous, F., Ginhoux, F., & Bourhy, H. (2021). Cell-type specific innate immune responses shape rabies virus tropism. Manuscript Submitted for Publication. https://doi.org/https://doi.org/10.1101/2021.07.26.453802

Fekete, R., Cserep, C., Lenart, N., Toth, K., Orsolits, B., Martinecz, B., … Denes, A. (2018). Microglia control the spread of neurotropic virus infection via P2Y12 signalling and recruit monocytes through P2Y12-independent mechanisms. Acta Neuropathol, 136(3), 461–482. https://doi.org/10.1007/s00401-018-1885-0

Fiacco, T. A., Agulhon, C., & McCarthy, K. D. (2009). Sorting Out Astrocyte Physiology from Pharmacology. Annual Review of Pharmacology and Toxicology, 49(1), 151–174. https://doi.org/10.1146/annurev.pharmtox.011008.145602

Finke, S., Mueller-Waldeck, R., & Conzelmann, K. K. (2003). Rabies virus matrix protein regulates the balance of virus transcription and replication. Journal of General Virology, 84(6), 1613–1621. https://doi.org/10.1099/vir.0.19128-0

Fooks, A. R., Banyard, A. C., Horton, D. L., Johnson, N., Mcelhinney, L. M., & Jackson, A. C. (2014). Current status of rabies and prospects for elimination. The Lancet, 384(9951), 1389–1399. https://doi.org/10.1016/S0140-6736(13)62707-5

Fooks, A. R., Cliquet, F., Finke, S., Freuling, C., Hemachudha, T., Mani, R. S., … Banyard, A. C. (2017). Rabies. Nature Reviews Disease Primers, 3, 17091. https://doi.org/10.1038/nrdp.2017.91

Forrester, J. V., McMenamin, P. G., & Dando, S. J. (2018). CNS infection and immune privilege. Nature Reviews Neuroscience, 19(11), 655–671. https://doi.org/10.1038/s41583-018-0070-8

Fu, Z. F., & Jackson, A. C. (2005). Neuronal dysfunction and death in rabies virus infection. Journal of NeuroVirology, 11(1), 101–106. https://doi.org/10.1080/13550280590900445

Fujii, S., Akaike, T., & Maeda, H. (1999). Role of nitric oxide in pathogenesis of herpes simplex virus encephalitis in rats. Virology, 256(2), 203–212. https://doi.org/10.1006/viro.1999.9610

Furr, S. R., & Marriott, I. (2012). Viral CNS infections: Role of glial pattern recognition receptors in neuroinflammation. Frontiers in Microbiology, 3(JUN), 1–12. https://doi.org/10.3389/fmicb.2012.00201

Gaudin, Y, Tuffereau, C., Segretain, D., Knossow, M., & Flamand, A. (1991). Reversible conformational changes and fusion activity of rabies virus glycoprotein. Journal of Virology, 65(9), 4853–4859. Retrieved from http://www.ncbi.nlm.nih.gov/pubmed/1870204

Gaudin, Yves, Bars, R. Le, Lama, Z., Scrima, N., Lagaudrière-gesbert, C., & Blondel, D. (2017). Negri bodies are viral factories with properties of liquid organelles. Nature Communications, 5(8), 1–12. https://doi.org/10.1038/s41467-017-00102-9

George, D., Ahrens, P., & Lambert, S. (2018). Satellite glial cells represent a population of developmentally arrested Schwann cells. Glia, 66(7), 1496–1506. https://doi.org/10.1002/glia.23320

Ginhoux, F., Greter, M., Leboeuf, M., Nandi, S., See, P., Gokhan, S., … Merad, M. (2010). Fate mapping analysis reveals that adult microglia derive from primitive macrophages. Science (New York, N.Y.), 330(6005), 841–845. https://doi.org/10.1126/science.1194637

Gluska, S., Zahavi, E. E., Chein, M., Gradus, T., Bauer, A., Finke, S., & Perlson, E. (2014). Rabies Virus Hijacks and Accelerates the p75NTR Retrograde Axonal Transport Machinery. PLoS Pathogens, 10(8), e1004348. https://doi.org/10.1371/journal.ppat.1004348

Gnanadurai, C. W., Yang, Y., Huang, Y., Li, Z., Leyson, C. M., Cooper, T. L., … Fu, Z. F. (2015). Differential host immune responses after infection with wild-type or lab-attenuated rabies viruses in dogs. PLoS Neglected Tropical Diseases, 9(8), 1–15. https://doi.org/10.1371/journal.pntd.0004023

Gnanadurai, C. W., Zhou, M., He, W., Leyson, C. M., Huang, C.-T., Salyards, G., … Fu, Z. F. (2013). Presence of virus neutralizing antibodies in cerebral spinal fluid correlates with non-lethal rabies in dogs. PLoS Neglected Tropical Diseases, 7(9), e2375. https://doi.org/10.1371/journal.pntd.0002375

Gnann, J., & Whitley, R. (2017). Herpes Simplex Encephalitis: an Update. Current Infectious Disease Reports, 19(3), 13. https://doi.org/10.1007/s11908-017-0568-7

Gold, R., Archelos, J. J., & Hartung, H. P. (1999). Mechanisms of immune regulation in the peripheral nervous system. Brain Pathology (Zurich, Switzerland), 9(2), 343–360. https://doi.org/10.1111/j.1750-3639.1999.tb00231.x

Graf, W., Gerrits, N., Yatim-Dhiba, N., & Ugolini, G. (2002). Mapping the oculomotor system: the power of transneuronal labelling with rabies virus. The European Journal of Neuroscience, 15(9), 1557–1562. https://doi.org/10.1046/j.1460-9568.2002.01994.x

Griffin, D. E. (2003). Immune responses to RNA-virus infections of the CNS. Nature Reviews Immunology, 3(6), 493–502. https://doi.org/10.1038/nri1105

Gumenyuk, A. V, Tykhomyrov, A. A., Savosko, S. I., Guzyk, M. M., Rybalko, S. L., Ryzha, A. O., & Chaikovsky, Y. B. (2018). State of Astrocytes in the Mice Brain under Conditions of Herpes Viral Infection and Modeled Stroke. Neurophysiology, 50(5), 326–331. https://doi.org/10.1007/s11062-019-09757-0

Guo, Y. J., Luo, T., Wu, F., Mei, Y. W., Peng, J., Liu, H., … Zhao, L. (2015). Involvement of TLR2 and TLR9 in the anti-inflammatory effects of chlorogenic acid in HSV-1-infected microglia. Life Sci, 127, 12–18. https://doi.org/10.1016/j.lfs.2015.01.036

Guzman, G., Oh, S., Shukla, D., Engelhard, H. H., & Valyi-Nagy, T. (2006). Expression of entry receptor nectin-1 of herpes simplex virus 1 and/or herpes simplex virus 2 in normal and neoplastic human nervous system tissues. Acta Virol, 50(1), 59–66. Retrieved from https://www.ncbi.nlm.nih.gov/pubmed/16599187

Haarr, L., Shukla, D., Rodahl, E., Dal Canto, M. C., & Spear, P. G. (2001). Transcription from the gene encoding the herpesvirus entry receptor nectin-1 (HveC) in nervous tissue of adult mouse. Virology, 287(2), 301–309. https://doi.org/10.1006/viro.2001.1041

Hampson, K., Coudeville, L., Lembo, T., Sambo, M., Kieffer, A., Attlan, M., … Dushoff, J. (2015). Estimating the Global Burden of Endemic Canine Rabies. PLoS Neglected Tropical Diseases, 9(4), 1–20. https://doi.org/10.1371/journal.pntd.0003709

Hattwick, M. A., Weis, T. T., Stechschulte, C. J., Baer, G. M., & Gregg, M. B. (1972). Recovery from rabies. A case report. Annals of Internal Medicine, 76(6), 931–942. https://doi.org/10.7326/0003-4819-76-6-931

Hawrylycz, M. J., Lein, E. S., Guillozet-Bongaarts, A. L., Shen, E. H., Ng, L., Miller, J. A., … Jones, A. R. (2012). An anatomically comprehensive atlas of the adult human brain transcriptome. Nature, 489(7416), 391–399. https://doi.org/10.1038/nature11405

He, Q., Liu, H., Huang, C., Wang, R., Luo, M., & Lu, W. (2020). Herpes Simplex Virus 1-Induced Blood-Brain Barrier Damage Involves Apoptosis Associated With GM130-Mediated Golgi Stress. Front Mol Neurosci, 13, 1–16. https://doi.org/10.3389/fnmol.2020.00002

Hellert, J., Buchrieser, J., Larrous, F., Minola, A., de Melo, G. D., Soriaga, L., … Rey, F. A. (2020). Structure of the prefusion-locking broadly neutralizing antibody RVC20 bound to the rabies virus glycoprotein. Nature Communications, 11(1), 596. https://doi.org/10.1038/s41467-020-14398-7

Hemachudha, T. (1994). Human rabies: clinical aspects, pathogenesis, and potential therapy. Current Topics in Microbiology and Immunology, 187, 121–143. https://doi.org/10.1007/978-3-642-78490-3_7

Hemachudha, T., Ugolini, G., Wacharapluesadee, S., Sungkarat, W., Shuangshoti, S., & Laothamatas, J. (2013). Human rabies: neuropathogenesis, diagnosis, and management. The Lancet Neurology, 12(5), 498–513. https://doi.org/10.1016/S1474-4422(13)70038-3

Hensel, N., Raker, V., Forthmann, B., Detering, N. T., Kubinski, S., Buch, A., … Claus, P. (2019). HSV-1 triggers paracrine fibroblast growth factor response from cortical brain cells via immediate-early protein ICP0. J Neuroinflammation, 16(1), 248. https://doi.org/10.1186/s12974-019-1647-5

Hill, T. J., & Field, H. J. (1973). The interaction of herpes simplex virus with cultures of peripheral nervous tissue: an electron microscopic study. J Gen Virol, 21(1), 123–133. https://doi.org/10.1099/0022-1317-21-1-123

Hirota, H., Kiyama, H., Kishimoto, T., & Taga, T. (1996). Accelerated nerve regeneration in mice by upregulated expression of interleukin (IL) 6 and IL-6 receptor after trauma. Journal of Experimental Medicine, 183(6), 2627–2634. https://doi.org/10.1084/jem.183.6.2627

Hoek, R. M., Ruuls, S. R., Murphy, C. A., Wright, G. J., Goddard, R., Zurawski, S. M., … Sedgwick, J. D. (2000). Down-regulation of the macrophage lineage through interaction with OX2 (CD200). Science (New York, N.Y.), 290(5497), 1768–1771. https://doi.org/10.1126/science.290.5497.1768

Hooper, D. C., Roy, A., Barkhouse, D. A., Li, J., & Kean, R. B. (2011). Rabies Virus Clearance from the Central Nervous System. In Advances in Virus Research (1st ed., Vol. 79). Elsevier Inc. https://doi.org/10.1016/B978-0-12-387040-7.00004-4

Hornung, V., Ellegast, J., Kim, S., Brzózka, K., Jung, A., Kato, H., … Hartmann, G. (2006). 5'-Triphosphate RNA is the ligand for RIG-I. Science (New York, N.Y.), 314(5801), 994–997. https://doi.org/10.1126/science.1132505

Hu, S., Sheng, W. S., Schachtele, S. J., & Lokensgard, J. R. (2011). Reactive oxygen species drive herpes simplex virus (HSV)-1-induced proinflammatory cytokine production by murine microglia. J Neuroinflammation, 8, 123. https://doi.org/10.1186/1742-2094-8-123

Hu, W. T., Willoughby, R. E. J., Dhonau, H., & Mack, K. J. (2007, August). Long-term follow-up after treatment of rabies by induction of coma. The New England Journal of Medicine, Vol. 357, pp. 945–946. United States. https://doi.org/10.1056/NEJMc062479

Huffmaster, N. J., Sollars, P. J., Richards, A. L., Pickard, G. E., & Smith, G. A. (2015). Dynamic ubiquitination drives herpesvirus neuroinvasion. Proc Natl Acad Sci U S A, 112(41), 12818–12823. https://doi.org/10.1073/pnas.1512559112

Ito, N., Moseley, G. W., Blondel, D., Shimizu, K., Rowe, C. L., Ito, Y., … Sugiyama, M. (2010). Role of interferon antagonist activity of rabies virus phosphoprotein in viral pathogenicity. Journal of Virology, 84(13), 6699–6710. https://doi.org/10.1128/JVI.00011-10

Ito, N., Moseley, G. W., & Sugiyama, M. (2016). The importance of immune evasion in the pathogenesis of rabies virus. Vet. Med. Sci., 7(116), 1089–1098. https://doi.org/10.1292/jvms.16-0092

Iwasaki, Y., & Clark, H. F. (1975). Cell to cell transmission of virus in the central nervous system. II. Experimental rabies in mouse. Laboratory Investigation; a Journal of Technical Methods and Pathology, 33(4), 391–399.

Iwasaki Y, T. M. (2002). Pathology. In Rabies (pp. 283–306).

Jackson, A C, Ye, H., Phelan, C. C., Ridaura-Sanz, C., Zheng, Q., Li, Z., … Lopez-Corella, E. (1999). Extraneural organ involvement in human rabies. Laboratory Investigation; a Journal of Technical Methods and Pathology, 79(8), 945–951.

Jackson, Alan C., & Fu, Z. F. (2013). Pathogenesis. In Rabies (Third Edit). Elsevier Inc. https://doi.org/10.1016/B978-0-12-396547-9.00008-0

Jackson, Alan C., Rossiter, J. P., & Lafon, M. (2006). Expression of Toll-like receptor 3 in the human cerebellar cortex in rabies, herpes simplex encephalitis, and other neurological diseases. Journal of NeuroVirology, 12(3), 229–234. https://doi.org/10.1080/13550280600848399

Jackson, Alan C, Phelan, C. C., & Rossiter, J. P. (2000). Infection of Bergmann glia in the cerebellum of a skunk experimentally infected with street rabies virus. Canadian Journal of Veterinary Research, 64, 226–228.

Jackson, F. R., Turmelle, A. S., Farino, D. M., Franka, R., McCracken, G. F., & Rupprecht, C. E. (2008). Experimental rabies virus infection of big brown bats (Eptesicus fuscus). Journal of Wildlife Diseases, 44(3), 612–621. https://doi.org/10.7589/0090-3558-44.3.612

Jacob, Y., Badrane, H., Ceccaldi, P. E., & Tordo, N. (2000). Cytoplasmic dynein LC8 interacts with lyssavirus phosphoprotein. Journal of Virology, 74(21), 10217–10222. https://doi.org/10.1128/jvi.74.21.10217-10222.2000

Jenson, A. B., Rabin, E. R., Bentinck, D. C., & Melnick, J. L. (1969). Rabies virus neuronitis. Journal of Virology, 3(2), 265–269. https://doi.org/10.1128/JVI.3.2.265-269.1969

Jogai, S., Radotra, B. D., & Banerjee, A. K. (2002). Rabies viral antigen in extracranial organs: a post-mortem study. Neuropathology and Applied Neurobiology, 28(4), 334–338. https://doi.org/10.1046/j.1365-2990.2002.00400.x

Johnson, R. T., & Mims, C. A. (1968). Pathogenesis of viral infections of the nervous system. N Engl J Med, 278(1), 23-30 contd. https://doi.org/10.1056/NEJM196801042780106

Jung, J. S., Bhat, R. V, Preston, G. M., Guggino, W. B., Baraban, J. M., & Agre, P. (1994). Molecular characterization of an aquaporin cDNA from brain: candidate osmoreceptor and regulator of water balance. Proc Natl Acad Sci U S A, 91(26), 13052–13056. https://doi.org/10.1073/pnas.91.26.13052

Kalita, J., Srivastava, R., Mishra, M. K., Basu, A., & Misra, U. K. (2010). Cytokines and chemokines in viral encephalitis: A clinicoradiological correlation. Neuroscience Letters, 473(1), 48–51. https://doi.org/10.1016/j.neulet.2010.02.017

Kallfass, C., Ackerman, A., Lienenklaus, S., Weiss, S., Heimrich, B., & Staeheli, P. (2012). Visualizing production of beta interferon by astrocytes and microglia in brain of La Crosse virus-infected mice. Journal of Virology, 86(20), 11223–11230. https://doi.org/10.1128/JVI.01093-12

Kastrukoff, L. F., & Kim, S. U. (2002). Oligodendrocytes from human donors differ in resistance to herpes simplex virus 1 (HSV-1). Glia, 38(1), 87–92. https://doi.org/10.1002/glia.10043

Kato, H., Takeuchi, O., Sato, S., Yoneyama, M., Yamamoto, M., Matsui, K., … Akira, S. (2006). Differential roles of MDA5 and RIG-I helicases in the recognition of RNA viruses. Nature, 441(7089), 101–105. https://doi.org/10.1038/nature04734

Katz, I. S. S., Guedes, F., Fernandes, E. R., & dos Ramos Silva, S. (2017). Immunological aspects of rabies: a literature review. Archives of Virology, 162(11), 3251–3268. https://doi.org/10.1007/s00705-017-3484-0

Kennedy, P. G., Clements, G. B., & Brown, S. M. (1983). Differential susceptibility of human neural cell types in culture to infection with herpes simplex virus. Brain, 106 (Pt 1), 101–119. https://doi.org/10.1093/brain/106.1.101

Kim, Y. C., Bang, D., Lee, S., & Lee, K. H. (2000). The effect of herpesvirus infection on the expression of cell adhesion molecules on cultured human dermal microvascular endothelial cells. Journal of Dermatological Science, 24(1), 38–47. https://doi.org/10.1016/S0923-1811(00)00080-3

Klingen, Y., Conzelmann, K.-K., & Finke, S. (2008). Double-Labeled Rabies Virus: Live Tracking of Enveloped Virus Transport. Journal of Virology, 82(1), 237–245. https://doi.org/10.1128/JVI.01342-07

Kopp, S. J., Banisadr, G., Glajch, K., Maurer, U. E., Grunewald, K., Miller, R. J., … Spear, P. G. (2009). Infection of neurons and encephalitis after intracranial inoculation of herpes simplex virus requires the entry receptor nectin-1. Proc Natl Acad Sci U S A, 106(42), 17916–17920. https://doi.org/10.1073/pnas.0908892106

Kotait, I., Oliveira, R. de N., Carrieri, M. L., Castilho, J. G., Macedo, C. I., Pereira, P. M. C., … Rupprecht, C. E. (2019). Non-human primates as a reservoir for rabies virus in Brazil. Zoonoses and Public Health, 66(1), 47–59. https://doi.org/10.1111/zph.12527

Koyuncu, O. O., MacGibeny, M. A., & Enquist, L. W. (2018). Latent versus productive infection: the alpha herpesvirus switch. Future Virology, 13(6), 431–443. https://doi.org/10.2217/fvl-2018-0023

Kuhn, S., Gritti, L., Crooks, D., & Dombrowski, Y. (2019). Oligodendrocytes in Development, Myelin Generation and Beyond. Cells, 8(11). https://doi.org/10.3390/cells8111424

Kurt-Jones, E. A., Chan, M., Zhou, S., Wang, J., Reed, G., Bronson, R., … Finberg, R. W. (2004). Herpes simplex virus 1 interaction with Toll-like receptor 2 contributes to lethal encephalitis. Proc Natl Acad Sci U S A, 101(5), 1315–1320. https://doi.org/10.1073/pnas.0308057100

Lafaille, F. G., Pessach, I. M., Zhang, S. Y., Ciancanelli, M. J., Herman, M., Abhyankar, A., … Notarangelo, L. D. (2012). Impaired intrinsic immunity to HSV-1 in human iPSC-derived TLR3-deficient CNS cells. Nature, 491(7426), 769–773. https://doi.org/10.1038/nature11583

Lafon, M. (2005). Modulation of the immune response in the nervous system by rabies virus. Current Topics in Microbiology and Immunology, 289, 239–258. https://doi.org/10.1007/3-540-27320-4

Lafon, M. (2008). Immune evasion, a critical strategy for rabies virus. Developments in Biologicals, 131, 413–419.

Lafon, Monique. (2005). Rabies virus receptors. Journal of Neurovirology, 11(1), 82–87. https://doi.org/10.1080/13550280590900427

Lahaye, X., Vidy, A., Pomier, C., Obiang, L., Harper, F., Gaudin, Y., & Blondel, D. (2009). Functional Characterization of Negri Bodies (NBs) in Rabies Virus-Infected Cells: Evidence that NBs Are Sites of Viral Transcription and Replication. Journal of Virology, 83(16), 7948–7958. https://doi.org/10.1128/JVI.00554-09

Le Blanc, I., Luyet, P.-P., Pons, V., Ferguson, C., Emans, N., Petiot, A., … Gruenberg, J. (2005). Endosome-to-cytosol transport of viral nucleocapsids. Nature Cell Biology, 7(7), 653–664. https://doi.org/10.1038/ncb1269

Lee, J. I., Sollars, P. J., Baver, S. B., Pickard, G. E., Leelawong, M., & Smith, G. A. (2009). A herpesvirus encoded deubiquitinase is a novel neuroinvasive determinant. PLoS Pathog, 5(4), e1000387. https://doi.org/10.1371/journal.ppat.1000387

Lentz, T. L., Burrage, T. G., Smith, A. L., Crick, J., & Tignor, G. H. (1982). Is the acetylcholine receptor a rabies virus receptor? Science (New York, N.Y.), 215(4529), 182–184. Retrieved from http://www.ncbi.nlm.nih.gov/pubmed/7053569

Leonard, J. R., Moran, C. J., Cross, D. W. T., Wippold, F. J., Schlesinger, Y., & Storch, G. A. (2000). MR imaging of herpes simplex type I encephalitis in infants and young children: A separate pattern of findings. American Journal of Roentgenology, 174(6), 1651–1655. https://doi.org/10.2214/ajr.174.6.1741651

Li, J., Faber, M., Dietzschold, B., & Hooper, D. C. (2011). The Role of Toll-Like Receptors in the Induction of Immune Responses During Rabies Virus Infection. In Advances in Virus Research (1st ed., Vol. 79). Elsevier Inc. https://doi.org/10.1016/B978-0-12-387040-7.00007-X

Lindqvist, R., Mundt, F., Gilthorpe, J. D., Wölfel, S., Gekara, N. O., Kröger, A., & Överby, A. K. (2016). Fast type I interferon response protects astrocytes from flavivirus infection and virus-

induced cytopathic effects. Journal of Neuroinflammation, 13(1), 1–15. https://doi.org/10.1186/s12974-016-0748-7

Liu, H., Qiu, K., He, Q., Lei, Q., & Lu, W. (2019). Mechanisms of Blood-Brain Barrier Disruption in Herpes Simplex Encephalitis. J Neuroimmune Pharmacol, 14(2), 157–172. https://doi.org/10.1007/s11481-018-9821-6

Liu, P., Yang, J., Wu, X., & Fu, Z. F. (2004). Interactions amongst rabies virus nucleoprotein, phosphoprotein and genomic RNA in virus-infected and transfected cells. The Journal of General Virology, 85(Pt 12), 3725–3734. https://doi.org/10.1099/vir.0.80325-0

Liu, R., Wang, J., Yang, Y., Khan, I., & Zhu, N. (2016). Rabies virus lipopeptide conjugated to a TLR7 agonist improves the magnitude and quality of the Th1-biased humoral immune response in mice. Virology, 497, 102–110. https://doi.org/10.1016/j.virol.2016.06.019

Liu, S. Q., Gao, X., Xie, Y., Wang, Q., & Zhu, W. Y. (2020). Rabies viruses of different virulence regulates inflammatory responses both in vivo and in vitro via MAPK and NF-κB pathway. Molecular Immunology, 125, 70–82. https://doi.org/10.1016/j.molimm.2020.06.011

Liu, S. Q., Xie, Y., Gao, X., Wang, Q., & Zhu, W. Y. (2020). Inflammatory response and MAPK and NF-κB pathway activation induced by natural street rabies virus infection in the brain tissues of dogs and humans. Virology Journal, 17(1), 157. https://doi.org/10.1186/s12985-020-01429-4

Liu, Z., Guan, Y., Sun, X., Shi, L., Liang, R., Lv, X., & Xin, W. (2013). HSV-1 activates NF-kappaB in mouse astrocytes and increases TNF-alpha and IL-6 expression via Toll-like receptor 3. Neurological Research, 35(7), 755–762. https://doi.org/10.1179/016164113X13703372991516

Lodmell, D. L., & Ewalt, L. C. (1985). Pathogenesis of street rabies virus infections in resistant and susceptible strains of mice. Journal of Virology, 55(3), 788–795. https://doi.org/10.1128/JVI.55.3.788-795.1985

Lokensgard, J. R., Cheeran, M. C., Hu, S., Gekker, G., & Peterson, P. K. (2002). Glial cell responses to herpesvirus infections: role in defense and immunopathogenesis. J Infect Dis, 186 Suppl, S171-9. https://doi.org/10.1086/344272

Lokensgard, J. R., Hu, S., Sheng, W., vanOijen, M., Cox, D., Cheeran, M. C.-J. J., … Peterson, P. K. (2001). Robust expression of TNF- , IL-1 , RANTES, and IP-10 by human microglial cells during nonproductive infection with herpes simplex virus. Journal of NeuroVirology, 7(3), 208–219. https://doi.org/10.1080/13550280152403254

Louveau, A., Smirnov, I., Keyes, T. J., Eccles, J. D., Rouhani, S. J., Peske, J. D., … Kipnis, J. (2015). Structural and functional features of central nervous system lymphatic vessels. Nature, 523(7560), 337–341. https://doi.org/10.1038/nature14432

Lundberg, P., Ramakrishna, C., Brown, J., Tyszka, J. M., Hamamura, M., Hinton, D. R., … Cantin, E. M. (2008). The immune response to herpes simplex virus type 1 infection in susceptible mice is a major cause of central nervous system pathology resulting in fatal encephalitis. Journal of Virology, 82(14), 7078–7088. https://doi.org/10.1128/JVI.00619-08

Luo, Z., Li, Y., Zhou, M., Lv, L., Wu, Q., Chen, C., … Zhao, L. (2019). Toll-like receptor 7 enhances rabies virus-induced humoral immunity by facilitating the formation of germinal centers. Frontiers in Immunology, 10(MAR). https://doi.org/10.3389/fimmu.2019.00429

Luo, Z., Lv, L., Li, Y., Sui, B., Wu, Q., Zhang, Y., … Zhao, L. (2020). Dual Role of Toll-Like Receptor 7 in the Pathogenesis of Rabies Virus in a Mouse Model. Journal of Virology, 94(9). https://doi.org/10.1128/jvi.00111-20

Luxton, G. W., Haverlock, S., Coller, K. E., Antinone, S. E., Pincetic, A., & Smith, G. A. (2005). Targeting of herpesvirus capsid transport in axons is coupled to association with specific sets of tegument proteins. Proc Natl Acad Sci U S A, 102(16), 5832–5837. https://doi.org/10.1073/pnas.0500803102

Lytle, A. G., Shen, S., & McGettigan, J. P. (2015). Lymph Node but Not Intradermal Injection Site Macrophages Are Critical for Germinal Center Formation and Antibody Responses to Rabies Vaccination. Journal of Virology, 89(5), 2842–2848. https://doi.org/10.1128/jvi.03409-14

Ma, Y., & He, B. (2014). Recognition of herpes simplex viruses: toll-like receptors and beyond. J Mol Biol, 426(6), 1133–1147. https://doi.org/10.1016/j.jmb.2013.11.012

Machado, G. P., Antunes, J. M. A. de P., Uieda, W., Biondo, A. W., Cruvinel, T. M. de A., Kataoka, A. P., … Megid, J. (2012). Exposure to rabies virus in a population of free-ranging capuchin monkeys (Cebus apella nigritus) in a fragmented, environmentally protected area in southeastern Brazil. Primates; Journal of Primatology, 53(3), 227–231. https://doi.org/10.1007/s10329-012-0306-6

Madhusudana, S. N., Nagaraj, D., Uday, M., Ratnavalli, E., & Kumar, M. V. (2002, March). Partial recovery from rabies in a six-year-old girl. International Journal of Infectious Diseases : IJID : Official Publication of the International Society for Infectious Diseases, Vol. 6, pp. 85–86. Canada. https://doi.org/10.1016/s1201-9712(02)90144-x

Malone, K. E., Stohlman, S. A., Ramakrishna, C., Macklin, W., & Bergmann, C. C. (2008). Induction of class I antigen processing components in oligodendroglia and microglia during viral encephalomyelitis. Glia, 56(4), 426–435. https://doi.org/10.1002/glia.20625

Mancini, M., & Vidal, S. M. (2018). Insights into the pathogenesis of herpes simplex encephalitis from mouse models. Mammalian Genome : Official Journal of the International Mammalian Genome Society, 29(7–8), 425–445. https://doi.org/10.1007/s00335-018-9772-5

Manickama, R., Basheer, M. D., & Jayakumar, R. (2008). Post-exposure prophylaxis (PEP) of rabies-infected Indian street dogs. Vaccine, 26(51), 6564–6568. https://doi.org/10.1016/j.vaccine.2008.09.053

Marques, C. P., Hu, S., Sheng, W., & Lokensgard, J. R. (2006). Microglial cells initiate vigorous yet non-protective immune responses during HSV-1 brain infection. Virus Res, 121(1), 1–10. https://doi.org/10.1016/j.virusres.2006.03.009

Matsumoto, M., Oshiumi, H., & Seya, T. (2011, March). Antiviral responses induced by the TLR3 pathway. Reviews in Medical Virology, Vol. 21, pp. 67–77. https://doi.org/10.1002/rmv.680

McKimmie, C., & Michlmayr, D. (2014). Role of CXCL10 in central nervous system inflammation. International Journal of Interferon, Cytokine and Mediator Research, 6(1), 1. https://doi.org/10.2147/IJICMR.S35953

Mebatsion, T. (2001). Extensive attenuation of rabies virus by simultaneously modifying the dynein light chain binding site in the P protein and replacing Arg333 in the G protein. Journal of Virology, 75(23), 11496–11502. https://doi.org/10.1128/JVI.75.23.11496-11502.2001

Mebatsion, T., Konig, M., & Conzelmann, K. K. (1996). Budding of rabies virus particles in the absence of the spike glycoprotein. Cell, 84(6), 941–951. https://doi.org/10.1016/s0092-8674(00)81072-7

Mebatsion, T., Weiland, F., & Conzelmann, K. K. (1999). Matrix protein of rabies virus is responsible for the assembly and budding of bullet-shaped particles and interacts with the transmembrane spike glycoprotein G. Journal of Virology, 73(1), 242–250. Retrieved from http://www.ncbi.nlm.nih.gov/pubmed/9847327

Ménager, P., Roux, P., Mégret, F., Bourgeois, J.-P., Le Sourd, A.-M., Danckaert, A., … Lafon, M. (2009). Toll-like receptor 3 (TLR3) plays a major role in the formation of rabies virus Negri Bodies. PLoS Pathogens, 5(2), e1000315. https://doi.org/10.1371/journal.ppat.1000315

Ménager, P., Roux, P., Mégret, F., Préhaud, C., Bourgeois, J.-P., Le Sourd, A.-M., … Lafon, M. (2008). TLR3 is a key component of rabies virus induced Negri bodies. BMC Proceedings, 2(S1), 3. https://doi.org/10.1186/1753-6561-2-s1-p41

Menasria, R., Boivin, N., Lebel, M., Piret, J., Gosselin, J., & Boivin, G. (2013). Both TRIF and IPS-1 Adaptor Proteins Contribute to the Cerebral Innate Immune Response against Herpes Simplex Virus 1 Infection. Journal of Virology, 87(13), 7301–7308. https://doi.org/10.1128/Jvi.00591-13

Mercer, J., & Greber, U. F. (2013, August 1). Virus interactions with endocytic pathways in macrophages and dendritic cells. Trends in Microbiology, Vol. 21, pp. 380–388. Elsevier. https://doi.org/10.1016/j.tim.2013.06.001

Metchnikoff, E., Mesnil, & Weinberg. (1902). Etudes biologiques sur la vieillesse : II. Recherches sur la vieillesse des perroquets. In Ann. Inst. Pasteur (Vol. 13).

Meucci, O., Fatatis, A., Simen, A. A., Bushell, T. J., Gray, P. W., & Miller, R. J. (1998). Chemokines regulate hippocampal neuronal signaling and gp120 neurotoxicity. Proceedings of the National Academy of Sciences of the United States of America, 95(24), 14500–14505. https://doi.org/10.1073/pnas.95.24.14500

Miao, F.-M., Zhang, S.-F., Wang, S.-C., Liu, Y., Zhang, F., & Hu, R.-L. (2017). Comparison of immune responses to attenuated rabies virus and street virus in mouse brain. Archives of Virology, 162(1), 247–257. https://doi.org/10.1007/s00705-016-3081-7

Michinaga, S., & Koyama, Y. (2019). Dual Roles of Astrocyte-Derived Factors in Regulation of Blood-Brain Barrier Function after Brain Damage. Int J Mol Sci, 20(3), 571. https://doi.org/10.3390/ijms20030571

Michlmayr, D., McKimmie, C. S., Pingen, M., Haxton, B., Mansfield, K., Johnson, N., … Graham, G. J. (2014). Defining the Chemokine Basis for Leukocyte Recruitment during Viral Encephalitis. Journal of Virology, 88(17), 9553–9567. https://doi.org/10.1128/jvi.03421-13

Mogensen, T. H. (2009). Pathogen recognition and inflammatory signaling in innate immune defenses. Clinical Microbiology Reviews, 22(2), 240–273. https://doi.org/10.1128/CMR.00046-08

Morcuende, S., Delgado-García, J. M., Ugolini, G., Delgado-Garcia, J.-M., & Ugolini, G. (2002). Neuronal premotor networks involved in eyelid responses: retrograde transneuronal tracing with rabies virus from the orbicularis oculi muscle in the rat. The Journal of Neuroscience : The Official Journal of the Society for Neuroscience, 22(20), 8808–8818. https://doi.org/10.1523/JNEUROSCI.22-20-08808.2002

Morimoto, K., Patel, M., Corisdeo, S., Hooper, D. C., Fu, Z. F., Rupprecht, C. E., … Dietzschold, B. (1996). Characterization of a unique variant of bat rabies virus responsible for newly emerging human cases in North America. Proceedings of the National Academy of Sciences of the United States of America, 93(11), 5653–5658. Retrieved from http://www.ncbi.nlm.nih.gov/pubmed/8643632

Moseley, G. W., Lahaye, X., Roth, D. M., Oksayan, S., Filmer, R. P., Rowe, C. L., … Jans, D. A. (2009). Dual modes of rabies P-protein association with microtubules: a novel strategy to suppress the antiviral response. Journal of Cell Science, 122(Pt 20), 3652–3662. https://doi.org/10.1242/jcs.045542

Muller, W. A. (2002). Leukocyte-endothelial cell interactions in the inflammatory response. Laboratory Investigation; a Journal of Technical Methods and Pathology, 82(5), 521–533. https://doi.org/10.1038/labinvest.3780446

Murphy, F. A., & Bauer, S. P. (1974). Early street rabies virus infection in striated muscle and later progression to the central nervous system. Intervirology, 3(4), 256–268. https://doi.org/10.1159/000149762

Nakamichi, K., Inoue, S., Takasaki, T., Morimoto, K., & Kurane, I. (2004). Rabies Virus Stimulates Nitric Oxide Production and CXC Chemokine Ligand 10 Expression in Macrophages through Activation of Extracellular Signal-Regulated Kinases 1 and 2. Journal of Virology, 78(17), 9376–9388. https://doi.org/10.1128/JVI.78.17.9376

Nakamichi, K., Saiki, M., Sawada, M., Takayama-Ito, M., Yamamuro, Y., Morimoto, K., & Kurane, I. (2005). Rabies Virus-Induced Activation of Mitogen-Activated Protein Kinase and NF- B Signaling Pathways Regulates Expression of CXC and CC Chemokine Ligands in Microglia. Journal of Virology, 79(18), 11801–11812. https://doi.org/10.1128/jvi.79.18.11801-11812.2005

Nan, Y., Wu, C., & Zhang, Y.-J. (2017). Interplay between Janus Kinase/Signal Transducer and Activator of Transcription Signaling Activated by Type I Interferons and Viral Antagonism. Frontiers in Immunology, 8, 1758. https://doi.org/10.3389/fimmu.2017.01758

Nicoll, M. P., Proenca, J. T., & Efstathiou, S. (2012). The molecular basis of herpes simplex virus latency. FEMS Microbiol Rev, 36(3), 684–705. https://doi.org/10.1111/j.1574-6976.2011.00320.x

Nikolic, J., Le Bars, R., Lama, Z., Scrima, N., Lagaudrière-Gesbert, C., Gaudin, Y., & Blondel, D. (2017). Negri bodies are viral factories with properties of liquid organelles. Nature Communications, 8(1). https://doi.org/10.1038/s41467-017-00102-9

O'Brien, K. L., & Nolan, T. (2019, October 3). The WHO position on rabies immunization – 2018 updates. Vaccine, Vol. 37, pp. A85–A87. Elsevier Ltd. https://doi.org/10.1016/j.vaccine.2018.10.014

Obara, Y., Furuta, Y., Takasu, T., Suzuki, S., Suzuki, H., Matsukawa, S., … Nagashima, K. (1997). Distribution of herpes simplex virus types 1 and 2 genomes in human spinal ganglia studied by PCR and in situ hybridization. J Med Virol, 52(2), 136–142. Retrieved from https://www.ncbi.nlm.nih.gov/pubmed/9179758

Obregón-Morales, C., Aguilar-Setién, Á., Perea Martínez, L., Galvez-Romero, G., Martínez-Martínez, F. O., & Aréchiga-Ceballos, N. (2017). Experimental infection of Artibeus intermedius with a vampire bat rabies virus. Comparative Immunology, Microbiology and Infectious Diseases, 52, 43–47. https://doi.org/10.1016/j.cimid.2017.05.008

Okumura, A., & Harty, R. N. (2011). Rabies virus assembly and budding. Advances in Virus Research, 79, 23–32. https://doi.org/10.1016/B978-0-12-387040-7.00002-0

Osanai, Y., Shimizu, T., Mori, T., Yoshimura, Y., Hatanaka, N., Nambu, A., … Ikenaka, K. (2017). Rabies virus-mediated oligodendrocyte labeling reveals a single oligodendrocyte myelinates axons from distinct brain regions. Glia, 65(1), 93–105. https://doi.org/10.1002/glia.23076

Pabon, M. M., Bachstetter, A. D., Hudson, C. E., Gemma, C., & Bickford, P. C. (2011). CX3CL1 reduces neurotoxicity and microglial activation in a rat model of Parkinson's disease. Journal of Neuroinflammation, 8, 9. https://doi.org/10.1186/1742-2094-8-9

Papadopoulos, M. C., & Verkman, A. S. (2013). Aquaporin water channels in the nervous system. Nat Rev Neurosci, 14(4), 265–277. https://doi.org/10.1038/nrn3468

Pape, K., Tamouza, R., Leboyer, M., & Zipp, F. (2019). Immunoneuropsychiatry — novel perspectives on brain disorders. Nature Reviews Neurology, 15(6), 317–328. https://doi.org/10.1038/s41582-019-0174-4

Peng, J., Zhu, S., Hu, L., Ye, P., Wang, Y., Tian, Q., … Guo, X. (2016). Wild-type rabies virus induces autophagy in human and mouse neuroblastoma cell lines. Autophagy, 12(10), 1704–1720. https://doi.org/10.1080/15548627.2016.1196315

Perry, A. K., Chen, G., Zheng, D., Tang, H., & Cheng, G. (2005). The host type I interferon response to viral and bacterial infections. Cell Res, 15(6), 407–422. https://doi.org/10.1038/sj.cr.7290309

Pfefferkorn, C., Kallfass, C., Lienenklaus, S., Spanier, J., Kalinke, U., Rieder, M., … Staeheli, P. (2016). Abortively Infected Astrocytes Appear To Represent the Main Source of Interferon Beta in the Virus-Infected Brain. Journal of Virology, 90(4), 2031–2038. https://doi.org/10.1128/JVI.02979-15

Phares, T. W., Kean, R. B., Mikheeva, T., & Hooper, D. C. (2006). Regional Differences in Blood-Brain Barrier Permeability Changes and Inflammation in the Apathogenic Clearance of Virus from the Central Nervous System. The Journal of Immunology, 176(12), 7666–7675. https://doi.org/10.4049/jimmunol.176.12.7666

Philips, T., & Rothstein, J. D. (2017). Oligodendroglia: metabolic supporters of neurons. J Clin Invest, 127(9), 3271–3280. https://doi.org/10.1172/JCI90610

Piccinotti, S., Kirchhausen, T., & Whelan, S. P. J. (2013). Uptake of Rabies Virus into Epithelial Cells by Clathrin-Mediated Endocytosis Depends upon Actin. Journal of Virology, 87(21), 11637–11647. https://doi.org/10.1128/jvi.01648-13

Piccinotti, Silvia, & Whelan, S. P. J. (2016). Rabies Internalizes into Primary Peripheral Neurons via Clathrin Coated Pits and Requires Fusion at the Cell Body. PLOS Pathogens, 12(7), e1005753. https://doi.org/10.1371/journal.ppat.1005753

Piret, J., & Boivin, G. (2015). Innate immune response during herpes simplex virus encephalitis and development of immunomodulatory strategies. Rev Med Virol, 25(5), 300–319. https://doi.org/10.1002/rmv.1848

Pizzi, M., Sarnico, I., Boroni, F., Benarese, M., Dreano, M., Garotta, G., … Spano, P. (2004). Prevention of neuron and oligodendrocyte degeneration by interleukin-6 (IL-6) and IL-6 receptor/IL-6 fusion protein in organotypic hippocampal slices. Molecular and Cellular Neuroscience, 25(2), 301–311. https://doi.org/10.1016/j.mcn.2003.10.022

Plioplys, A. V, & Massimini, N. (1995). Alpha/Beta Interferon Is a Neuronal Growth Factor. Neuroimmunomodulation, 2(1), 31–35. https://doi.org/10.1159/000096838

Porras, C., Barboza, J. J., Fuenzalida, E., Adaros, H. L., Oviedo, A. M., & Furst, J. (1976). Recovery from rabies in man. Annals of Internal Medicine, 85(1), 44–48. https://doi.org/10.7326/0003-4819-85-1-44

Potratz, M., Zaeck, L., Christen, M., Kamp, V., Klein, A., Freuling, C. M., … Finke, S. (2020). Astrocyte Infection during Rabies Encephalitis Depends on the Virus Strain and Infection Route as Demonstrated by Novel Quantitative 3D Analysis of Cell Tropism. Cells, 9(January), 1–25. https://doi.org/10.20944/preprints202001.0160.v1

Potratz, M., Zaeck, L. M., Weigel, C., Klein, A., Freuling, C. M., Müller, T., & Finke, S. (2020). Neuroglia infection by rabies virus after anterograde virus spread in peripheral neurons. Acta Neuropathologica Communications, 8(1), 199. https://doi.org/10.1186/s40478-020-01074-6

Prehaud, C., Lay, S., Dietzschold, B., & Lafon, M. (2003). Glycoprotein of nonpathogenic rabies viruses is a key determinant of human cell apoptosis. Journal of Virology, 77(19), 10537–10547. https://doi.org/10.1128/JVI.77.19.10537

Prehaud, C., Mégret, F., Lafage, M., Lafon, M., Préhaud, C., Mégret, F., … Lafon, M. (2005). Virus infection switches TLR-3-positive human neurons to become strong producers of beta interferon. Journal of Virology, 79(20), 12893–12904. https://doi.org/10.1128/JVI.79.20.12893

Price, R., Chernik, N. L., Horta-Barbosa, L., & Posner, J. B. (1973). Herpes simplex encephalitis in an anergic patient. The American Journal of Medicine, 54(2), 222–228. https://doi.org/10.1016/0002-9343(73)90226-x

Prosniak, M., Zborek, A., Scott, G. S., Roy, A., Phares, T. W., Koprowski, H., & Hooper, D. C. (2003). Differential expression of growth factors at the cellular level in virus-infected brain. Proceedings of the National Academy of Sciences of the United States of America, 100(11), 6765–6770. https://doi.org/10.1073/pnas.0430999100

Rajasekhar, P., Poole, D. P., & Veldhuis, N. A. (2017). Chapter Four - Role of Nonneuronal TRPV4 Signaling in Inflammatory Processes. In D. P. Geraghty & L. D. Rash (Eds.), Advances in Pharmacology (Vol. 79, pp. 117–139). Academic Press. https://doi.org/https://doi.org/10.1016/bs.apha.2017.03.002

Ransohoff, R. M., Hamilton, T. A., Tani, M., Stoler, M. H., Shick, H. E., Major, J. A., … Tuohy, V. K. (1993). Astrocyte expression of mRNA encoding cytokines IP-10 and JE/MCP-1 in experimental autoimmune encephalomyelitis. FASEB Journal : Official Publication of the Federation of American Societies for Experimental Biology, 7(6), 592–600. https://doi.org/10.1096/fasebj.7.6.8472896

Raux, H., Flamand, A., & Blondel, D. (2000). Interaction of the Rabies Virus P Protein with the LC8 Dynein Light Chain. Journal of Virology, 74(21), 10212–10216. https://doi.org/10.1128/jvi.74.21.10212-10216.2000

Ray, N. B., Power, C., Lynch, W. P. P., Ewalt, L. C. C., & Lodmell, D. L. L. (1997). Rabies viruses infect primary cultures of murine, feline, and human microglia and astrocytes. Archives of Virology, 142(5), 1011–1019. https://doi.org/10.1007/s007050050136

Rehwinkel, J., & Gack, M. U. (2020, September 1). RIG-I-like receptors: their regulation and roles in RNA sensing. Nature Reviews Immunology, Vol. 20, pp. 537–551. Nature Research. https://doi.org/10.1038/s41577-020-0288-3

Reinert, L. S., Harder, L., Holm, C. K., Iversen, M. B., Horan, K. A., Dagnæs-Hansen, F., … Paludan, S. R. (2012). TLR3 deficiency renders astrocytes permissive to herpes simplex virus infection and facilitates establishment of CNS infection in mice. Journal of Clinical Investigation, 122(4), 1368–1376. https://doi.org/10.1172/JCI60893

Reinert, L. S., Lopušná, K., Winther, H., Sun, C., Thomsen, M. K., Nandakumar, R., … Paludan, S. R. (2016). Sensing of HSV-1 by the cGAS-STING pathway in microglia orchestrates antiviral defence in the CNS. Nature Communications, 7. https://doi.org/10.1038/ncomms13348

Richter, E. R., Dias, J. K., Gilbert, J. E., & Atherton, S. S. (2009). Distribution of herpes simplex virus type 1 and varicella zoster virus in ganglia of the human head and neck. J Infect Dis, 200(12), 1901–1906. https://doi.org/10.1086/648474

Rieder, M., Brzozka, K., Pfaller, C. K., Cox, J. H., Stitz, L., & Conzelmann, K. (2011). Genetic Dissection of Interferon-Antagonistic Functions of Rabies Virus Phosphoprotein: Inhibition of Interferon Regulatory Factor 3 Activation Is Important for Pathogenicity. Journal of Virology, 85(2), 842–852. https://doi.org/10.1128/JVI.01427-10

Roberts, T. K., Eugenin, E. A., Lopez, L., Romero, I. A., Weksler, B. B., Couraud, P. O., & Berman, J. W. (2012). CCL2 disrupts the adherens junction: Implications for neuroinflammation. Laboratory Investigation, 92(8), 1213–1233. https://doi.org/10.1038/labinvest.2012.80

Robichon, K., Patel, V., Connor, B., & La Flamme, A. C. (2020). Clozapine reduces infiltration into the CNS by targeting migration in experimental autoimmune encephalomyelitis. Journal of Neuroinflammation, Vol. 17, p. 53. School of Biological Sciences, Victoria University of Wellington, Wellington, New Zealand. https://doi.org/10.1186/s12974-020-01733-4

Rocha, S. M., de Oliveira, S. V, Heinemann, M. B., & Gonçalves, V. S. P. (2017). Epidemiological Profile of Wild Rabies in Brazil (2002-2012). Transboundary and Emerging Diseases, 64(2), 624–633. https://doi.org/10.1111/tbed.12428

Rosato, P. C., & Leib, D. A. (2015). Neuronal Interferon Signaling Is Required for Protection against Herpes Simplex Virus Replication and Pathogenesis. PLoS Pathogens, 11(7). https://doi.org/10.1371/journal.ppat.1005028

Rosenberg, G. A. (2012). Neurological diseases in relation to the blood-brain barrier. Journal of Cerebral Blood Flow and Metabolism, 32(7), 1139–1151. https://doi.org/10.1038/jcbfm.2011.197

Rowell, J. F., & Griffin, D. E. (1999). The inflammatory response to nonfatal Sindbis virus infection of the nervous system is more severe in SJL than in BALB/c mice and is associated with low levels of IL-4 mRNA and high levels of IL-10-producing CD4+ T cells. Journal of Immunology (Baltimore, Md. : 1950), 162(3), 1624–1632.

Roy, A., & Hooper, D. C. (2007). Lethal Silver-Haired Bat Rabies Virus Infection Can Be Prevented by Opening the Blood-Brain Barrier. Journal of Virology, 81(15), 7993–7998. https://doi.org/10.1128/JVI.00710-07

Roy, Anirban, & Hooper, D. C. (2008). Immune evasion by rabies viruses through the maintenance of blood-brain barrier integrity. Journal of NeuroVirology, 14(5), 401–411. https://doi.org/10.1080/13550280802235924

Roy, Anirban, Phares, T. W., Koprowski, H., & Hooper, D. C. (2007). Failure to open the blood-brain barrier and deliver immune effectors to central nervous system tissues leads to the lethal outcome of silver-haired bat rabies virus infection. Journal of Virology, 81(3), 1110–1118. https://doi.org/10.1128/JVI.01964-06

Safain, M. G., Roguski, M., Kryzanski, J. T., & Weller, S. J. (2015). A review of the combined medical and surgical management in patients with herpes simplex encephalitis. Clin Neurol Neurosurg, 128, 10–16. https://doi.org/10.1016/j.clineuro.2014.10.015

Salaun, B., Coste, I., Rissoan, M.-C., Lebecque, S. J., & Renno, T. (2006). TLR3 Can Directly Trigger Apoptosis in Human Cancer Cells. The Journal of Immunology, 176(8), 4894–4901. https://doi.org/10.4049/jimmunol.176.8.4894

Schnell, M. J., McGettigan, J. P., Wirblich, C., & Papaneri, A. (2009). The cell biology of rabies virus: using stealth to reach the brain. Nature Reviews Microbiology, 8, 51–61. https://doi.org/10.1038/nrmicro2260

Schultz, K. L. W., Vernon, P. S., & Griffin, D. E. (2015). Differentiation of Neurons Restricts Arbovirus Replication and Increases Expression of the Alpha Isoform of IRF-7. Journal of Virology, 89(1), 48–60. https://doi.org/10.1128/jvi.02394-14

Scott, C. A., Rossiter, J. P., Andrew, R. D., & Jackson, A. C. (2008). Structural Abnormalities in Neurons Are Sufficient To Explain the Clinical Disease and Fatal Outcome of Experimental Rabies in Yellow Fluorescent Protein-Expressing Transgenic Mice. Journal of Virology, 82(1), 513–521. https://doi.org/10.1128/JVI.01677-07

Scott, T., & Nel, L. (2016). Subversion of the Immune Response by Rabies Virus. Viruses, 8(8), 231. https://doi.org/10.3390/v8080231

Shimeld, C., Efstathiou, S., & Hill, T. (2001). Tracking the spread of a lacZ-tagged herpes simplex virus type 1 between the eye and the nervous system of the mouse: comparison of primary and recurrent infection. J Virol, 75(11), 5252–5262. https://doi.org/10.1128/JVI.75.11.5252-5262.2001

Singh, A. K., Yang, J.-Q., Parekh, V. V, Wei, J., Wang, C.-R., Joyce, S., … Van Kaer, L. (2005). The natural killer T cell ligand alpha-galactosylceramide prevents or promotes pristane-induced lupus in mice. European Journal of Immunology, 35(4), 1143–1154. https://doi.org/10.1002/eji.200425861

Smith, G. (2012). Herpesvirus transport to the nervous system and back again. Annu Rev Microbiol, 66, 153–176. https://doi.org/10.1146/annurev-micro-092611-150051

Sobel, R. A., Mitchell, M. E., & Fondren, G. (1990). Intercellular adhesion molecule-1 (ICAM-1) in cellular immune reactions in the human central nervous system. American Journal of Pathology, 136(6), 1309–1316. Retrieved from https://www.ncbi.nlm.nih.gov/pmc/articles/pmid/1972610/?tool=EBI

Sonthonnax, F., Besson, B. B., Bonnaud, E., Jouvion, G., Merino, D., Larrous, F., & Bourhy, H. (2019). Lyssavirus matrix protein cooperates with phosphoprotein to modulate the Jak-Stat pathway. Scientific Reports, 9(1), 1–13. https://doi.org/10.1038/s41598-019-48507-4

Sorensen, L. N., Reinert, L. S., Malmgaard, L., Bartholdy, C., Thomsen, A. R., & Paludan, S. R. (2008). TLR2 and TLR9 synergistically control herpes simplex virus infection in the brain. J Immunol, 181(12), 8604–8612. https://doi.org/10.4049/jimmunol.181.12.8604

Soung, A., & Klein, R. S. (2018). Viral Encephalitis and Neurologic Diseases: Focus on Astrocytes. Trends in Molecular Medicine, 24(11), 950–962. https://doi.org/10.1016/j.molmed.2018.09.001

Spindler, K. R., & Hsu, T.-H. (2012). Viral disruption of the blood-brain barrier. Trends in Microbiology, 20(6), 282–290. https://doi.org/10.1016/j.tim.2012.03.009

Sriram, S. (2011, October 28). Role of glial cells in innate immunity and their role in CNS demyelination. Journal of Neuroimmunology, Vol. 239, pp. 13–20. Elsevier. https://doi.org/10.1016/j.jneuroim.2011.08.012

Stahl, J P, Mailles, A., & De Broucker, T. (2012). Herpes simplex encephalitis and management of acyclovir in encephalitis patients in France. Epidemiology and Infection, 140(2), 372–381. https://doi.org/10.1017/S0950268811000483

Stahl, Jean Paul, & Mailles, A. (2019). Herpes simplex virus encephalitis update. Current Opinion in Infectious Diseases, 32(3), 239–243. Retrieved from https://journals.lww.com/co-infectiousdiseases/Fulltext/2019/06000/Herpes_simplex_virus_encephalitis_update.11.aspx

Stamatovic, S. M., Keep, R. F., Kunkel, S. L., & Andjelkovic, A. V. (2003). Potential role of MCP-1 in endothelial cell tight junction “opening”: signaling via Rho and Rho kinase. J Cell Sci, 116(Pt 22), 4615–4628. https://doi.org/10.1242/jcs.00755

Steinberg, M. W., Cheung, T. C., & Ware, C. F. (2011). The signaling networks of the herpesvirus entry mediator (TNFRSF14) in immune regulation. Immunol Rev, 244(1), 169–187. https://doi.org/10.1111/j.1600-065X.2011.01064.x

Steiner, I., & Benninger, F. (2018). Manifestations of Herpes Virus Infections in the Nervous System. Neurologic Clinics, 36(4), 725–738. https://doi.org/10.1016/j.ncl.2018.06.005

Steiner, I., Kennedy, P. G., & Pachner, A. R. (2007, November 1). The neurotropic herpes viruses: herpes simplex and varicella-zoster. Lancet Neurology, Vol. 6, pp. 1015–1028. Elsevier. https://doi.org/10.1016/S1474-4422(07)70267-3

Subileau, E. A., Rezaie, P., Davies, H. A., Colyer, F. M., Greenwood, J., Male, D. K., & Romero, I. A. (2009). Expression of Chemokines and Their Receptors by Human Brain Endothelium: Implications for Multiple Sclerosis. Journal of Neuropathology & Experimental Neurology, 68(3), 227–240. https://doi.org/10.1097/NEN.0b013e318197eca7

Sugamata, M., Miyazawa, M., Mori, S., Spangrude, G. J., Ewalt, L. C., & Lodmell, D. L. (1992). Paralysis of street rabies virus-infected mice is dependent on T lymphocytes. Journal of Virology, 66(2), 1252–1260.

Sui, B., Chen, D., Liu, W., Tian, B., Lv, L., Pei, J., … Zhao, L. (2021). Comparison of lncRNA and mRNA expression in mouse brains infected by a wild-type and a lab-attenuated Rabies lyssavirus. The Journal of General Virology, 102(3). https://doi.org/10.1099/jgv.0.001538

Suja, M. S., Mahadevan, A., Madhusudana, S. N., & Shankar, S. K. (2011). Role of Apoptosis in Rabies Viral Encephalitis: A Comparative Study in Mice, Canine, and Human Brain with a Review of Literature. Pathology Research International, 2011, 1–13. https://doi.org/10.4061/2011/374286

Sung, J. H., Hayano, M., Mastri, A. R., & Okagaki, T. (1976). A case of human rabies and ultrastructure of the Negri body. Journal of Neuropathology and Experimental Neurology, 35(5), 541–559. https://doi.org/10.1097/00005072-197609000-00006

Takahashi, K., Nakanishi, H., Miyahara, M., Mandai, K., Satoh, K., Satoh, A., … Takai, Y. (1999). Nectin/PRR: an immunoglobulin-like cell adhesion molecule recruited to cadherin-based adherens junctions through interaction with Afadin, a PDZ domain-containing protein. J Cell Biol, 145(3), 539–549. https://doi.org/10.1083/jcb.145.3.539

Takeuchi, O., & Akira, S. (2010). Pattern Recognition Receptors and Inflammation. Cell, 140(6), 805–820. https://doi.org/10.1016/j.cell.2010.01.022

Tang, Y., Rampin, O., Giuliano, F., & Ugolini, G. (1999). Spinal and brain circuits to motoneurons of the bulbospongiosus muscle: Retrograde transneuronal tracing with rabies virus. The Journal of Comparative Neurology, 414(2), 167–192. https://doi.org/10.1002/(SICI)1096-9861(19991115)414:2<167::AID-CNE3>3.0.CO;2-P

Thoulouze, M. I., Lafage, M., Schachner, M., Hartmann, U., Cremer, H., & Lafon, M. (1998). The neural cell adhesion molecule is a receptor for rabies virus. Journal of Virology, 72(9), 7181–7190. Retrieved from http://www.ncbi.nlm.nih.gov/pubmed/9696812

Tian, B., Zhou, M., Yang, Y., Yu, L., Luo, Z., Tian, D., … Zhao, L. (2018). Lab-attenuated rabies virus causes abortive infection and induces cytokine expression in astrocytes by activating mitochondrial antiviral-signaling protein signaling pathway. Frontiers in Immunology, 8(JAN), 1–17. https://doi.org/10.3389/fimmu.2017.02011

Tiwari, V., Clement, C., Scanlan, P. M., Kowlessur, D., Yue, B. Y., & Shukla, D. (2005). A role for herpesvirus entry mediator as the receptor for herpes simplex virus 1 entry into primary human trabecular meshwork cells. J Virol, 79(20), 13173–13179. https://doi.org/10.1128/JVI.79.20.13173-13179.2005

Townsend, J. J., & Collins, P. K. (1986). Peripheral nervous system demyelination with herpes simplex virus. J Neuropathol Exp Neurol, 45(4), 419–425. https://doi.org/10.1097/00005072-198607000-00004

Tsiang, H., Koulakoff, A., Bizzini, B., & Berwald-Netter, Y. (1983). Neurotropism of rabies virus. An in vitro study. Journal of Neuropathology and Experimental Neurology, 42(4), 439–452. Retrieved from http://www.ncbi.nlm.nih.gov/pubmed/6864237

Tuffereau, C., Bénéjean, J., Blondel, D., Kieffer, B., & Flamand, A. (1998). Low-affinity nerve-growth factor receptor (P75NTR) can serve as a receptor for rabies virus. The EMBO Journal, 17(24), 7250–7259. https://doi.org/10.1093/emboj/17.24.7250

Turmelle, A. S., Jackson, F. R., Green, D., McCracken, G. F., & Rupprecht, C. E. (2010). Host immunity to repeated rabies virus infection in big brown bats. The Journal of General Virology, 91(Pt 9), 2360–2366. https://doi.org/10.1099/vir.0.020073-0

Twelvetrees, A. E., Pernigo, S., Sanger, A., Guedes-Dias, P., Schiavo, G., Steiner, R. A., … Holzbaur, E. L. (2016). The Dynamic Localization of Cytoplasmic Dynein in Neurons Is Driven by Kinesin-1. Neuron, 90(5), 1000–1015. https://doi.org/10.1016/j.neuron.2016.04.046

Ugolini, G. (2010). Advances in viral transneuronal tracing. Journal of Neuroscience Methods, 194(1), 2–20. https://doi.org/10.1016/j.jneumeth.2009.12.001

Ugolini, G. (2011). Rabies virus as a transneuronal tracer of neuronal connections. Advances in Virus Research, 79, 165–202. https://doi.org/10.1016/B978-0-12-387040-7.00010-X

Ugolini, G., Klam, F., Dans, M. D., Dubayle, D., Brandi, A. M., Büttner-Ennever, J., & Graf, W. (2006). Horizontal eye movement networks in primates as revealed by retrograde transneuronal transfer of rabies virus: Differences in monosynaptic input to “slow” and “fast”

abducens motoneurons. Journal of Comparative Neurology, 498(6), 762–785. https://doi.org/10.1002/cne.21092

Ugolini, G., Kuypers, H. G., & Simmons, A. (1987). Retrograde transneuronal transfer of herpes simplex virus type 1 (HSV 1) from motoneurones. Brain Res, 422(2), 242–256. https://doi.org/10.1016/0006-8993(87)90931-0

Valério-Gomes, B., Guimarães, D. M., Szczupak, D., & Lent, R. (2018). The Absolute Number of Oligodendrocytes in the Adult Mouse Brain. Frontiers in Neuroanatomy, 12, 90. https://doi.org/10.3389/fnana.2018.00090

Velandia-Romero, M. L., Castellanos, J. E., & Martínez-Gutiérrez, M. (2013). In vivo differential susceptibility of sensory neurons to rabies virus infection. Journal of Neurovirology, 19, 367–375. https://doi.org/10.1007/s13365-013-0179-5

Vidy, A., Chelbi-Alix, M., & Blondel, D. (2005). Rabies Virus P Protein Interacts with STAT1 and Inhibits Interferon Signal Transduction Pathways. Journal of Virology, 79(22), 14411–14420. https://doi.org/10.1128/JVI.79.22.14411-14420.2005

Vidy, A., El Bougrini, J., Chelbi-Alix, M. K., & Blondel, D. (2007). The Nucleocytoplasmic Rabies Virus P Protein Counteracts Interferon Signaling by Inhibiting both Nuclear Accumulation and DNA Binding of STAT1. Journal of Virology, 81(8), 4255–4263. https://doi.org/10.1128/JVI.01930-06

Vossough, A., Zimmerman, R. A., Bilaniuk, L. T., & Schwartz, E. M. (2008). Imaging findings of neonatal herpes simplex virus type 2 encephalitis. Neuroradiology, 50(4), 355–366. https://doi.org/10.1007/s00234-007-0349-3

Wang, H., Zhang, G., Wen, Y., Yang, S., Xia, X., & Fu, Z. F. (2011). Intracerebral Administration of Recombinant Rabies Virus Expressing GM-CSF Prevents the Development of Rabies after Infection with Street Virus. PLoS ONE, 6(9), e25414. https://doi.org/10.1371/journal.pone.0025414

Wang, J. P., Bowen, G. N., Zhou, S., Cerny, A., Zacharia, A., Knipe, D. M., … Kurt-Jones, E. A. (2012). Role of specific innate immune responses in herpes simplex virus infection of the central nervous system. J Virol, 86(4), 2273–2281. https://doi.org/10.1128/JVI.06010-11

Wang, J., Wang, Z., Liu, R., Shuai, L., Wang, X., Luo, J., … Bu, Z. (2018). Metabotropic glutamate receptor subtype 2 is a cellular receptor for rabies virus. 2, 1–21.

Wang, P., Dai, J., Bai, F., Kong, K. F., Wong, S. J., Montgomery, R. R., … Fikrig, E. (2008). Matrix metalloproteinase 9 facilitates West Nile virus entry into the brain. J Virol, 82(18), 8978–8985. https://doi.org/10.1128/JVI.00314-08

Wang, Y., Jia, J., Wang, Y., Li, F., Song, X., Qin, S., … Wang, Y. (2019). Roles of HSV-1 infection-induced microglial immune responses in CNS diseases: friends or foes? Crit Rev Microbiol, 45(5–6), 581–594. https://doi.org/10.1080/1040841X.2019.1660615

Watson, H. D., Tignor, G. H., & Smith, A. L. (1981). Entry of rabies virus into the peripheral nerves of mice. The Journal of General Virology, 56(Pt 2), 372–382. https://doi.org/10.1099/0022-1317-56-2-371

Whitley, R., & Baines, J. (2018). Clinical management of herpes simplex virus infections: past, present, and future. F1000Res, 7. https://doi.org/10.12688/f1000research.16157.1

Whitley, R. J., & Gnann, J. W. (2002). Viral encephalitis: familiar infections and emerging pathogens. Lancet, 359(9305), 507–513. https://doi.org/10.1016/S0140-6736(02)07681-X

Whitley, R., & Kimberlin, D. W. (2005). Herpes simplex: Encephalitis children and adolescents. Seminars in Pediatric Infectious Diseases, 16(1 SPEC.ISS.), 17–23. https://doi.org/10.1053/j.spid.2004.09.007

Whitley, R., Lakeman, A. D., Nahmias, A., & Roizman, B. (1982). DNA Restriction-Enzyme Analysis of Herpes Simplex Virus Isolates Obtained from Patients with Encephalitis. New England Journal of Medicine, 307(17), 1060–1062. https://doi.org/10.1056/nejm198210213071706

WHO. (2018). Weekly epidemiological record, vol 93, 16. Retrieved from http://www.who.int/wer

Wilkinson, R., Leaver, C., Simmons, A., & Pereira, R. A. (1999). Restricted replication of herpes simplex virus in satellite glial cell cultures clonally derived from adult mice. J Neurovirol, 5(4), 384–391. https://doi.org/10.3109/13550289909029479

Willoughby, R. E. J., Tieves, K. S., Hoffman, G. M., Ghanayem, N. S., Amlie-Lefond, C. M., Schwabe, M. J., … Rupprecht, C. E. (2005). Survival after treatment of rabies with induction of coma. The New England Journal of Medicine, 352(24), 2508–2514. https://doi.org/10.1056/NEJMoa050382

Wolfstein, A., Nagel, C. H., Radtke, K., Dohner, K., Allan, V. J., & Sodeik, B. (2006). The inner tegument promotes herpes simplex virus capsid motility along microtubules in vitro. Traffic, 7(2), 227–237. https://doi.org/10.1111/j.1600-0854.2005.00379.x

Yakoub, A. M., & Shukla, D. (2015). Autophagy stimulation abrogates herpes simplex virus-1 infection. Scientific Reports, 5(1), 1–7. https://doi.org/10.1038/srep09730

Yang, Y., Huang, Y., Gnanadurai, C. W., Cao, S., Liu, X., Cui, M., & Fu, Z. F. (2015). The Inability of Wild-Type Rabies Virus To Activate Dendritic Cells Is Dependent on the Glycoprotein and Correlates with Its Low Level of the De Novo -Synthesized Leader RNA . Journal of Virology, 89(4), 2157–2169. https://doi.org/10.1128/jvi.02092-14

Ydens, E., Lornet, G., Smits, V., Goethals, S., Timmerman, V., & Janssens, S. (2013). The neuroinflammatory role of Schwann cells in disease. Neurobiology of Disease, 55, 95–103. https://doi.org/10.1016/j.nbd.2013.03.005

Yi, M. H., Zhang, E., Kang, J. W., Shin, Y. N., Byun, J. Y., Oh, S. H., … Kim, D. W. (2012). Expression of CD200 in alternative activation of microglia following an excitotoxic lesion in the mouse hippocampus. Brain Research, 1481, 90–96. https://doi.org/10.1016/j.brainres.2012.08.053

Yong, V. W., Power, C., & Edwards, D. R. (2001). Metalloproteinases in biology and pathology of the nervous system. Nature Reviews Neuroscience, 2(7), 502–511. https://doi.org/10.1038/35081571

Yordy, B., Iijima, N., Huttner, A., Leib, D., & Iwasaki, A. (2012). A neuron-specific role for autophagy in antiviral defense against herpes simplex virus. Cell Host and Microbe, 12(3), 334–345. https://doi.org/10.1016/j.chom.2012.07.013

Zaeck, L., Potratz, M., Freuling, C. M., Müller, T., & Finke, S. (2019). High-Resolution 3D Imaging of Rabies Virus Infection in Solvent-Cleared Brain Tissue. JoVE, (146), e59402. https://doi.org/doi:10.3791/59402

Zeiler, F. A., & Jackson, A. C. (2016). Critical Appraisal of the Milwaukee Protocol for Rabies: This Failed Approach Should Be Abandoned. The Canadian Journal of Neurological Sciences. Le Journal Canadien Des Sciences Neurologiques, 43(1), 44–51. https://doi.org/10.1017/cjn.2015.331

Zerboni, L., Che, X., Reichelt, M., Qiao, Y., Gu, H., & Arvin, A. (2013). Herpes simplex virus 1 tropism for human sensory ganglion neurons in the severe combined immunodeficiency mouse model of neuropathogenesis. J Virol, 87(5), 2791–2802. https://doi.org/10.1128/JVI.01375-12

Zhang, S., Wang, X. J., Tian, L. P., Pan, J., Lu, G. Q., Zhang, Y. J., … Chen, S. Di. (2011). CD200-CD200R dysfunction exacerbates microglial activation and dopaminergic neurodegeneration in a rat model of Parkinson's disease. Journal of Neuroinflammation, 8(1), 154. https://doi.org/10.1186/1742-2094-8-154

Zhang, Y., Chen, K., Sloan, S. A., Bennett, M. L., Scholze, A. R., O'Keeffe, S., … Wu, J. Q. (2014). An RNA-sequencing transcriptome and splicing database of glia, neurons, and vascular cells of the cerebral cortex. Journal of Neuroscience, 34(36), 11929–11947. https://doi.org/10.1523/JNEUROSCI.1860-14.2014

Zhang, Y., Sloan, S. A. A., Clarke, L. E. E., Caneda, C., Plaza, C. A. A., Blumenthal, P. D. D., … Barres, B. A. A. (2016). Purification and Characterization of Progenitor and Mature Human Astrocytes Reveals Transcriptional and Functional Differences with Mouse. Neuron, 89(1), 37–53. https://doi.org/10.1016/j.neuron.2015.11.013

Zhao, P., Yang, Y., Feng, H., Zhao, L., Qin, J., Zhang, T., … Xia, X. (2013). Global gene expression changes in BV2 microglial cell line during rabies virus infection. Infection, Genetics and Evolution, 20, 257–269. https://doi.org/10.1016/j.meegid.2013.09.016

Zhao, P., Zhao, L., Zhang, K., Feng, H., Wang, H., Wang, T., … Xia, X. (2012). Infection with street strain rabies virus induces modulation of the microRNA profile of the mouse brain. Virology Journal, 9(1), 1. https://doi.org/10.1186/1743-422X-9-159

Zhou, Y., Lu, Z. N., Guo, Y. J., & Mei, Y. W. (2010). Favorable effects of MMP-9 knockdown in murine herpes simplex encephalitis using small interfering RNA. Neurol Res, 32(8), 801–809. https://doi.org/10.1179/016164110X12644252260556

Zhou, Y., Ye, L., Wan, Q., Zhou, L., Wang, X., Li, J., … Ho, W. (2009). Activation of Toll-like receptors inhibits herpes simplex virus-1 infection of human neuronal cells. J Neurosci Res, 87(13), 2916–2925. https://doi.org/10.1002/jnr.22110

2.2 Cell type-specific insights into RABV tropism (Article #2)

2.2.1 Yin and yang of RABV biology: neuron-specific tropism or not?

This chapter focusses on RABV tropism. As mentioned above, RABV is classically believed to present a neuron-specific tropism (191). Depending on the RABV strain, a broad tropism can be observed *in vitro* whereas *in vivo*, classically speaking, RABV preferably infects and replicates in neurons (9,251). Nevertheless, recent data provide evidence that the neuron-specific tropism of RABV is less profound than originally believed (193,194).

In 1983, one of the first well known studies performed on RABV tropism was conducted by Tsiang and colleagues. They investigated the relative susceptibility of murine neuroblastoma and glial cells to fixed rabies virus CVS infection via immunofluorescence or virus titration. Titration revealed that murine neuroblastoma cells produced the highest viral titers which steadily increased over time. In contrast, glial cells produced the lowest viral titers which remained constant over time. Staining of the nucleocapsid antigen showed that differentiated neuroblastoma cells, in contrast to undifferentiated ones, were more likely to stain positive for the nucleocapsid antigen. Further, immunofluorescence revealed that 90 – 100% of neurons had viral inclusion bodies whereas less than 1% of astrocytes showed viral inclusion bodies in murine brain cell cultures (191).

Fourteen years later, Ray and colleagues investigated the susceptibility of RABV again, this time comparing susceptibilities of murine, feline, and human glial cells. In detail, Ray and colleagues explored susceptibilities of cells originating from different species to the tissue culture-adapted ERA strain, the mouse brain-adapted SRV strain, and unpassaged street virus isolates from brain homogenates originating from skunk or sheep. Immunofluorescent staining and titration of cellular supernatants revealed that human fetal astrocytes and adult microglia were susceptible to SRV and ERA strains. Further, human fetal astrocytes were susceptible to unpassaged street virus isolates from skunks and sheep (209).

In recent years, imaging technologies and tracing techniques advanced quickly allowing the visualization of the entire functional neuronal network (199). Particularly the fixed CVS-11 strain, presents a specific transneural tracer since this virus moves preferably retrogradely, propagates exclusively between connected neurons, and does not cause neuronal degeneration (197,200,252–254). Nevertheless it has become increasingly clear that RABV tropism highly depends on the viral strain and infection route used (194). In this context, Potratz and colleagues pointed out that field RABV strains led to non-neglectable astrocyte infection frequencies (8-27%) independent of the infection route used (194). Recently, more data

provided evidence that infection of glial cells, particularly Schwann cells, appears *in vivo* (193), questioning the strict neuron-specific tropism of RABV. Thus, my first objective focussed on investigating RABV tropism *in vitro* using more sophisticated quantitative imaging technologies, namely high content screening. Further, I tried to correlate cellular immune responses with cellular susceptibilities by quantifying gene and protein expression levels of different human CNS cell types.

In this research article named '*Cell type-specific innate immune responses shape RABV tropism'*, I provide evidence that viral-intrinsic factors, particularly accessory functions of viral P- and M-proteins, as well as cell type specific immune responses determine RABV tropism *in vitro*. In detail, it suggests that RABV neuron-specific tropism is partly shaped by the deficiency of neurons to mount a strong antiviral response in contrast to glial cell types. The following research article presents a draft which is currently submitted to the journal *Viruses.*

More information about the research article can be found here:

https://www.dropbox.com/sh/j4j0vf9ybxkqdii/AADehANudcNeReRSoB_GNIqHa?dl=0

2.2.2 Article #2 *(submitted)*

Cell type-specific innate immune responses shape rabies virus tropism in neural cells

Lena Feige[1], Tatsuya Kozaki[2], Guilherme Dias de Melo[1], Vincent Guillemot[3], Florence Larrous[1], Florent Ginhoux[2,4,5], Hervé Bourhy[1,*]

[1] Institut Pasteur, Université de Paris, Lyssavirus Epidemiology and Neuropathology, F75015, Paris, France.

[2] Singapore Immunology Network, Agency for Science, Technology and Research, 8A Biomedical Grove, Immunos Building, Level 3, Singapore 138648, Singapore.

[3] Hub de Bioinformatique et Biostatistique – Département Biologie Computationnelle, Institut Pasteur, Paris, France.

[4] Shanghai Institute of Immunology, Shanghai JiaoTong University School of Medicine, 280 South Chongqing Road, Shanghai 200025, China.

[5] Translational Immunology Institute, SingHealth Duke-NUS Academic Medical Center, 20 College Road, Discovery Tower Level 8, Singapore 169856, Singapore.

Correspondence to: herve.bourhy@pasteur.fr

Keywords: Rabies, astrocytes, microglia, neurons, viral tropism, immune evasion

Abstract

Rabies is caused by neurotropic rabies virus (RABV), contributing to 60.000 human deaths annually. Even though rabies leads to major public health concerns worldwide, we still do not fully understand factors determining RABV tropism and why glial cells are unable to clear RABV from the infected brain. Here, we compare susceptibilities and immune responses of CNS cell types towards infection with two RABV strains, Tha and its attenuated variant Th2P-4M mutated on phospho- (P-protein) and matrix protein (M-protein). We demonstrate that RABV replicates in human stem cell-derived neurons and astrocytes but fails to infect human iPSC-derived microglia. Further, astrocytes and microglial cells protect neurons from RABV infection via a filtrable and transferable agent. Additionally, we observed major differences in transcription profiles and quantification of intracellular protein levels between antiviral immune responses mediated by neurons, astrocytes (*IFNB1*, *CCL5*, *CXCL10*, IL1B, IL6, LIF), and microglia (*CCL5*, *CXCL10*, *ISG15*, *MX1*, IL6) upon Tha infection. Further, we show that P- and M-proteins of Tha mediate evasion of NF-κB- and JAK-STAT-controlled antiviral host responses in neuronal cell types, thereby partly shaping RABV tropism. Overall, our study provides novel insights into RABV neurotropism, especially the importance of viral P- and M-proteins in defining cellular susceptibilities.

Abbreviations

CI_{95} = 95% confidence interval; CNS = central nervous system; CNSC = complete neural stem cell; DAMPS = danger-associated molecular patterns; eGFP = enhanced green fluorescent protein; G-protein = glycoprotein; GLAST-1 = Glutamate Aspartate Transporter 1; hiMacs = human induced pluripotent stem cells-derived macrophage-like cells; hiMicros = human induced pluripotent stem cell-derived microglia-like cells; hNSC = human neural stem cells; IBA1 = Ionized calcium-binding adaptor molecule; IFNAR = IFN alpha and beta receptor subunit; IFN-β = interferon beta; IL-1β = interleukin 1 beta; IL-6R = interleukin 6 receptor; iPSC = induced pluripotent stem cells; IRF-3 = interferon regulatory factor 3; ISGs = interferon-stimulated genes; JAK = janus kinase; L-protein = RNA-polymerase; LIF = leukemia inhibitory factor; M-protein = matrix protein; mGluR2 = metabotropic glutamate receptor subtype 2; MOI = multiplicity of infection; nAChR = nicotinic acetylcholine receptor; NCAM = neuronal cell adhesion molecule; NDM = neural differentiation medium; NF-κB = nuclear factor kappa-light-chain-enhancer of activated B cells; NOD-like receptors = nucleotide-binding oligomerization domain-like receptors; N-protein = nucleoprotein; PAMPS = pathogen-associated molecular patterns; hiAstrocytes = human induced NSC-derived astrocytes; hiNeurons = human induced NSC-derived neurons; P-protein = phosphoprotein; RABV = rabies virus; RIG-I = retinoic acid-inducible gene I; RLRs = retinoic acid-inducible gene I-like helicases; PRRs = pattern recognition receptors; p75NTR = low-affinity p75 neurotropin receptor; STAT = signal transducer and activator of transcription, TLRs = toll-like receptors; TUBB3 = Class III Beta-Tubulin

1. Introduction

Rabies is caused by RABV, a negative-sense single-stranded RNA virus belonging to the family of *Mononegavirales* [11]. RABV belongs to the genus Lyssavirus, family *Rhabdoviridae*, and presents a negative stranded RNA virus of 12 kb length: the viral genome encodes nucleoprotein (N-protein), phosphoprotein (P-protein), matrix protein (M-protein), glycoprotein (G-protein), and the RNA-dependent RNA-polymerase (L-protein). RABV, classically believed to bear a neuron-specific tropism, reaches the CNS via retrograde transport along the neural network where it establishes fatal encephalomyelitis in mammals, including humans [12,13]. Once inside the CNS, RABV successfully hides inside the neural network from glial surveillance [14]. Up to date, we do not fully understand the exact mechanisms underlying viral-mediated immune evasion of glial cells.

Viral tropism refers to the ability of a virus to productively infect a certain cell type. Primary infection can be productive, leading to the production of progeny viruses, or abortive, blocking the production of progeny viruses and thereby viral spread. Cellular tropism relies on two major determinants, the expression of entry receptors which enables virus entry and the cellular immune response which allows or restricts productive viral replication [15]. The innate immune system therefore represents the first line of defence against viral invaders. It senses viruses via germline-encoded pattern recognition receptors (PRRs) including toll-like receptors (TLRs), retinoic acid-inducible gene I (RIG-I) like helicases (RLRs) and nucleotide-binding oligomerization domain-like receptors (NOD-like receptors). TLR3 and RLRs in the host cells recognize virus-derived RNAs, leading to the activation of transcription factors, more specifically interferon regulatory factor 3 (IRF-3) and nuclear factor κB (NF-κB), which establish antiviral responses via the production of type I IFNs and proinflammatory cytokines [16]. Subsequently, type I IFNs bind type I IFN receptors (IFNAR) and activate the Janus kinase

(JAK) and signal transducer and activator of transcription protein 1 (STAT1) signalling pathway, elevating the expression of interferon-stimulated genes (ISGs) with antiviral activity.

RABV uses several receptors to enter cells via clathrin-mediated endocytosis [17–19]: nicotinic acetylcholine receptor (nAChR) [1], neuronal cell adhesion molecule (NCAM) [2], low-affinity p75 neurotropin receptor (p75NTR) [3], and metabotropic glutamate receptor subtype 2 (mGluR2) [4]. However, those broadly expressed receptors are not essential for RABV entry *per se* [20] but lead to an acceleration of RABV infection [6]. In contrast to its profound neuron-specific tropism *in vivo* [21,22], most cell types are susceptible to RABV infection *in vitro* [23–25]. Whereas most of the research is focussing on the discovery of RABV receptors [1–4] and their interaction with the RABV G-protein [20], less research focusses on how cellular host immune responses shape RABV tropism and how distinct neural immune responses in the CNS could collectively lead to the establishment of an antiviral response. Recently, several publications reported infection of different glial cells *in vivo*, particularly astrocytes [26,27] and Schwann cells [9], depending on the viral strain and the infection route used [8]. Nevertheless, we are far from understanding the molecular pathways underlying susceptibility to RABV infection although it is crucial in determining infection outcome.

Here, we investigated cellular immune responses and susceptibilities of different CNS cell types towards infection with two canine RABV strains (Tha and Th2P-4M) *in vitro*. Tha is a cell culture-adapted virus isolate [28] which shares the same genetic background with Th2P-4M, except for mutations introduced into P- (W265G, M287V) and M-proteins (R77K, D100A, A104S, M110L), consequently inhibiting viral evasion of NF-κB and STAT pathways [10,29–31]. We provide evidence that virulent Tha and less virulent Th2P-4M successfully replicate in hiNeurons and hiAstrocytes but not in hiMicros. Surprisingly, Th2P-4M presents a more pronounced neuron-specific tropism in hNSC-derived CNS cultures compared to Tha, suggesting that immune-modulatory functions of viral P- and M-proteins are determining RABV tropism. Whereas successful infection might highly depend on the concentration of RABV receptors on the cellular surface, we suggest that cell type-specific innate immune responses are critical for the success of RABV replication and spread in the distinct CNS cell types. Hence, our study emphasizes the need to study RABV in relevant CNS culture models to understand the underlying pathways shaping RABV tropism as well as to elucidate the role of glial cells in the RABV-infected brain.

2. Materials and methods

2.1 Viruses

Thailand virus, referred to as 8764THA (Genbank No. EU293111) is a field strain of RABV isolated from the brain of a Thai patient who died of rabies after being bitten by a rabid dog (EVAg collection, Ref-SKU: 014V-02106) [28]. This virus was further adapted to cell culture on BSR cells (a BHK-21 clone, kindly provided by Monique Lafon, Institute Pasteur, Paris) [32], consequently called 8743THA (Genbank No. EU293121) [28] and in this manuscript referred to as Tha. Sequence comparison between the cell culture-adapted RABV strain 8743THA (GenBank No. EU293121) and the original field isolate 8764THA (GenBank No. EU293111) demonstrated 98.56% identity (52 mutations) and 99.36% similarity between concatenated protein sequences. The recombinant Th2P-4M virus harbours the same genetic background as Tha apart from bearing two mutations in the viral P-protein (W265G, M287V) and four mutations in the viral M-protein (R77K, D100A, A104S, M110L) which were previously described [10,33,34]. To monitor viral infection, recombinant viral Tha-eGFP and Th2P-4M-eGFP constructs were used which were generated by cloning sequences of eGFP (recovered from pEGFP-C1 plasmid, Promega) into the genetic sequence of Tha [35] and Th2P-4M,

respectively. Viral strains were sequenced before used for infection experiments. Viral titers were determined by virus titration on BSR cells, more specifically via staining of the viral nucleoprotein (5100, Sigma-Aldrich). Further, the impact of introduced mutations into viral P- and M-proteins was shown to have no impact on viral replication (S1 Fig).

2.2 Cell culture and infection

The human neuroblastoma cell line SK-N-SH (ATCC® HTB-11™), the human astrocyte-like cell line SVGp12 (ATCC® CRL8621™), and the human microglial cell line HMC3 (ATCC® CRL-3304™) were cultured in Dulbecco's Modified Eagle Medium (10566016, Invitrogen) supplemented with 10% heat-inactivated fetal bovine serum (FCS, S182H-500, Eurobio) at 37°C and 5% CO_2.

Human neuronal progenitor cells (EnStem-A™ SCC003, Millipore) were cultured on plates previously coated with geltrex (A1413201, Invitrogen) in complete neural stem cell (CNSC) medium containing Knock-out D-MEM/F-12 (A1370801, Thermo Fisher), 2 mM Glutamax (35050038, Thermo Fisher), 2% StemPro Neural Supplement (A1050801, Thermo Fisher), 20 ng/mL FGF (PHG0026, Thermo Fisher), and 20 ng/mL EGF (PHG0311, Thermo Fisher) for amplification purpose at 37°C and 5% CO_2.

Human fetal pAstrocytes (N7805100, Thermo Fisher) were cultured on geltrex-coated plates (A1413201, Thermo Fisher) in complete astrocyte medium containing D-MEM (10566016, Thermo Fisher), 2% fetal bovine serum (S182H-500, Eurobio) and N-2 Supplement (17502048, Thermo Fisher) at 37°C and 5% CO_2.

Human iPSCs (XCL-1, IP-001-1V, XCell Science) were cultured on Matrigel-coated plates (354277, Corning) in mTeSR1 medium (85850, STEMCELL Technology). The medium was changed daily.

Upon 80% confluency, cells were used for infection experiments. The cell medium was aspirated, and cells were washed once with PBS (10010023, Thermo Scientific) prior to infection. Adjacently, Tha and Th2P-4M were diluted in culture medium according to the appropriate multiplicity of infection (MOI). Cells were incubated with viral suspension for two hours at 37°C and 5% CO_2. After two hours, the viral suspension was removed, and the appropriate culture medium was added. Twenty-four hours post infection, cells were treated with 2500 U/mL of IFN-α (I4401-100KU, Sigma-Aldrich) and incubated for 24 hours at 37°C and 5% CO_2 prior to cell lysis.

2.3 Differentiation of hNSC to hiNeurons

To induce neural differentiation, EnStem-A cells were cultured at a density of $5x10^4$ cells/cm^2 on plates previously coated with geltrex (A1413302, Thermo Fisher) according to the manufacturer's instructions. One day after seeding, CNSC was changed to neural differentiation medium (NDM) consisting of neurobasal medium (10880022, Thermo Fisher), B-27 Serum Free Supplement (17504044, Thermo Fisher), 2 mM GlutaMAX (35050038, Thermo Fisher), CultureOne Supplement (A33202-01, Thermo Fisher), and 200 μM ascorbid acid (A4403, Sigma-Aldrich). After 21 days of differentiation, differentiated neurons were used for downstream experiments.

2.4 Differentiation of hiPSCs to hiMacs

Human induced macrophage-like cells (hiMacs) were generated from iPSCs (IP-001-1V, XCell Science) according to a published method described by Takata et al. [36]. In short, 5 ng/mL BMP-4 (314-BP-050, R&D Systems), 50 ng/mL VEGF (293-VE-500, R&D Systems), 2 μM CHIR99021 (4423, TOCRIS) induced mesoderm specification of human XCL-1 iPSC colonies

and hemangioblast-like cell formation [37]. Replacement of CHIR99021 by 20 ng/mL FGF-2 (223-FB-500, R&D Systems), followed by maintenance in 15 ng/mL VEGF and 5 ng/mL FGF-2 induced differentiation into the hematopoietic lineage according to a modified protocol from Grigoriadis et al. [38]. Wnt signalling was inhibited and hematopoietic stem cells were matured by incubation with 50 ng/ml SCF (255-SC-01M), 10 ng/mL FGF-2, 20 ng/mL IL-3 (203-IL-050, R&D Systems), 10 ng/mL IL-6 (206-IL-050, R&D Systems), 10 ng/mL VEGF and 30 ng/mL DKK-1(5439-DK-500) for 6 days and with 50 ng/mL SCF, 10 ng/mL FGF-2, 20 ng/mL IL-3 and 10 ng/mL IL-6 for 4 days. To promote terminal differentiation of hiMacs, cells were cultured with 50 ng/mL CSF-1 (216-MC-01M, R&D Systems) for 14 days [39–41].

2.5 Differentiation of hiMacs to hiMicros

After hiMac generation, hiMacs were positively selected by fluorescence-activated cell sorting (FACS, MoFlo Astrios, Beckman Coulter) using CD45-BV605 (304042, Biolegend, 1:300), CD11b-BV421 (301324, Biolegend, 1:300), CD14-FITC (982502, Biolegend, 1:300), CD163-APC (333610, Biolegend, 1:300) and CX3CR1-PE (341604, Biolegend, 1:300). FACS-sorted cells were co-cultured with 70 – 80% confluent three-weeks old (day 0 = induction of neural induction) hiNeurons for three weeks. After three weeks of co-culture, cells were used for imaging. To obtain a pure culture of hiMicros for downstream qPCR analysis, FACS-sorted hiMacs were co-cultured for three weeks on 24-well-plates in inserts (353495, Falcon, pore size 0.4 μm) with confluent three-weeks old hiNeurons. During co-culture, 50 ng/mL recombinant human CSF-1 (216-MC-010, R & D Systems) and 50 ng/mL human IL-34 (5265-IL-010, R & D Systems) were added every third day to the culture medium.

2.6 Transfer of conditioned medium

Cell lines (SK-N-SH, HMC3, SVGp12) were seeded in 6-well-plates at a density of $1x10^5$ cells/cm^2. Twenty-four hours after seeding, cells were infected with Tha or Th2P-4M at a MOI of 5. After two hours, the viral suspension was removed, and 1 mL of culture medium was added per well. SK-N-SH cells were seeded into 96-well-plates (655086, Greiner Bio) at a density of $1.8x10^4$ cells/cm^2. After 24 hours, SK-N-SH previously seeded in 96-well-plates (655086, Greiner Bio) were infected with Tha-eGFP or Th2P-4M-eGFP at a MOI of 0.5. After two hours the viral suspension was removed and replaced via 100 μL of the supernatant taken from previously infected cells (SK-N-SH, HMC3, SVGp12, at 24 hours post-infection) filtered through a 100 kilodalton membrane (28-9322-58, Dutcher). After 24 hours, the medium was removed, and cells were treated with 2500 U/mL of IFN-α (I4401-100KU, Sigma-Aldrich). Cells were imaged at 48 hours post-infection using the Opera PhenixTM High Content Screening System (Perkin Elmer).

2.7 Treatment of hiNeurons with human recombinant IL-1β, IL-6, and LIF

Human NSC were seeded at a density of $15.6x10^4$ cells/cm^2 into 96-well-plates (655086, Greiner Bio) and differentiated to hiNeurons as described above. Twenty-one days after differentiation, hiNeurons were infected with Tha-eGFP or Th2P-4M-eGFP at a MOI of 0.5. Two hours after infection, the viral suspension was removed and replaced via 100 μL of NDM or NDM supplemented with 100 ng/mL of recombinant human IL-1β (200-01B, Peprotech), IL-6 (200-06, Peprotech), or LIF (300-05, Peprotech). Cells were imaged at 48 hours post-infection using the Opera PhenixTM High Content Screening System (Perkin Elmer).

2.8 Opera PhenixTM High Content Screening Assay

Cell lines were seeded at a density of $1.8x10^4$ cells/cm^2. In the case of co-cultures, different cell lines were seeded in equal quantities within wells. Twenty-four hours after seeding, cells were infected with Tha-eGFP and Th2P-4M-eGFP. Twenty-four hours post-infection, cells

were treated with 2500 U/mL of IFN-α (I4401-100KU, Sigma-Aldrich) and incubated for 24 hours at 37°C and 5% CO_2 prior to fixation. Cells were fixed using 4% PFA (Alfa Aesar, J61984) for 15 minutes at room temperature, washed with PBS (10010023, Thermo Scientific) and permeabilized using 0.5% triton X-100 (648463, Millipore) for 10 minutes. Cells were stained with primary and secondary antibodies listed in S1 Table according to the manufacturer's instructions. Apoptotic cells were quantified by the *In situ* cell death detection kit (12156792910, Roche) according to the manufacturer's instructions. Dead cells were detected with the ReadyProbes® Cell Viability Imaging Kit (R37610, Thermo Fisher). Images were acquired via the Opera PhenixTM High Content Screening System (Perkin Elmer) using the parameters mentioned in S2 Table.

2.9 RNA isolation and cDNA synthesis

Total RNA was isolated by the following procedure: EzDNase (11766051, Thermo Fisher) was used to eliminate genomic DNA. Adjacently, 500 ng or 1 μg of purified RNA was converted into first-strand cDNA using the SuperScript™ VILO™ IV enzyme (11756050, Thermo Scientific) according to the manufacturer's instructions. For real-time qPCR experiments, cDNA was diluted 1/50 or 1/100, respectively.

2.10 Quantitative PCR

Quantitative PCR, based on the detection of the SYBR Green dye, was performed by using 2.5 μL of the synthesized and diluted cDNA in the presence of 5 μL QuantiTect SYBR Green (204143, Qiagen) and 1 mM specific primers (S3 Table) in a final volume of 10 μL. Oligonucleotides were used for PCR at a concentration of 10 pmol/μL. All the samples were measured in triplicates. Gene expression levels were normalized to the endogenous expression of the housekeeping gene 18S (Eurofins) and the respective non-infected cells (mock). Quantitative PCR was performed on the 7500 Real-Time PCR System (Applied Biosystem, 7500 Software v2.3) using the following: initial denaturation step (1x repetition, 10 min, 95°C), amplification step (40 repetitions, 15 sec at 95°C, 1 min at 60°C), and melting curve determination step (1x repetition, 15 sec at 95°C, 1 min at 60°C, 15 sec at 95°C, 15 sec at 60°C). Gene expression was normalized to expression of housekeeping gene *18S* (ΔCT) and the difference in gene expression was calculated as the difference between infected and non-infected samples (ΔΔCT) [42].

2.11 Protein quantification

Cells were seeded at a density of $1x10^5$ cells/cm^2 and infected with Tha or Th2P-4M at a MOI of 5. Forty-eight hours post-infection, cells were lysed using ProcartaplexTM cell lysis buffer (EPX-99999-000, Thermo Scientific) according to the manufacturer's instructions to quantify protein expression in the cellular cytoplasm. Intracellular protein concentrations of human IFN-β, IFN-γ, IL-1β, IL-6, IL-15, CXCL10, LIF, CCL5, and TNF-α were quantified using a 9-plex Procartaplex assay (PPX-09, Thermo Scientific). In short, DropArray 96-well-plates (96-CC-BD-05, Curiox) were blocked using 1% BSA for 30 min. After blocking, 20 μL of cell lysate was added per well. According to the protocol, plates were stepwise incubated with 5 μL detection antibody, 10 μL streptavidin-PE, and 10 μL reading buffer per well before being read by the Luminex 200™ instrument (Thermo Scientific).

2.12 Statistical analysis

Percentages and means ± standard deviation (SD) were calculated with Prism 9 (Version 9) and R (version 4.0.4). Standard deviation and statistical significance were only calculated when three independent experiments were conducted. Multiple comparisons of data were performed using either the GraphPad Prism software (Version 9), or the lme4 package within

R (version 4.1.1) with the test being indicated in the figure legend. If multiple comparisons were performed, significance thresholds were lowered to account for multiple testing. Principal component analysis and hierarchical clustering on gene expression values was performed using R (version 4.0.4). Heatmaps represent normalized gene expression values that were clustered after centering gene expression values on their mean. Figures were generated using Adobe Illustrator (CC 2019).

The analysis of the proportion of $eGFP^+$ cells in co-cultures (mixed in equal ratios) performed in Fig S2 was based on the comparison of confidence intervals in each co-culture to a linear combination (with equal weights because the mixture ratios are the same) of the corresponding monocultures. More precisely, the first step of this analysis is the computation of the expected (from monocultures) confidence intervals on the percentages of $eGFP^+$ cells for co-cultures (1) and triple cultures (2).

(1) CI_{95} (expected) = 0.5 x CI_{95} (cell type A) + 0.5 x CI_{95} (cell type B)

(2) CI_{95} (expected) = 0.33 x CI_{95} (cell type A) + 0.33 x CI_{95} (cell type B) + 0.33 x CI_{95} (cell type C)

The second step is to compute an observed confidence interval on the actual values measured in the co-cultures. Finally, If the observed confidence intervals overlapped with the expected confidence intervals, we concluded that the proportion of $eGFP^+$ cells in co-cultures was not a consequence of an interaction between culture cell-types.

3. Results

3.1 Astrocytic and microglial cell lines show a lower susceptibility to Tha and Th2P-4M infection compared to SK-N-SH

Using reverse genetics, we introduced six mutations in conserved residues of the lyssavirus P-protein [34,43] and M-protein [33,44,45] of the pathogenic dog RABV Tha to diminish RABV pathogenicity (Fig 1A) [10]. Upon infection with the two fluorescent RABV strains, Tha-eGFP and Th2P-4M-eGFP respectively, eGFP was expressed in all different CNS cell lines indicating successful infection of SK-N-SH, astrocyte-like SVGp12, and microglia-like HMC3 cells *in vitro* (Fig 1B). Quantification of eGFP expression via fluorescence microscopy revealed that, in average, 78.9% of SK-N-SH expressed eGFP whereas significantly less astrocyte-like SVGp12 (21.3%) and microglial-like HMC3 (25.4%) expressed eGFP upon Tha-eGFP infection at a MOI of 0.5 (adjusted p-value<0.000016, Fig 1C). Similarly, Th2P-4M-eGFP induced eGFP expression in significantly less astrocyte-like SVGp12 (17.6%) and microglial-like HMC3 (21.8%) compared to infected SK-N-SH (64.3%, adjusted p-value<0.000016, Fig 1C). Comparing the proportions of infected cells between Tha-eGFP and Th2P-4M-eGFP did not reveal a significant difference between viral strains. Taken together, Tha-eGFP and Th2P-4M-eGFP exhibited a profound neuron-specific tropism *in vitro* (Fig 1C).

Adding exogenous IFN-α artificially activates the JAK-STAT pathway resulting in the expression of ISGs and antiviral proteins. IFN-α treatment reduced infection in all conditions, although some conditions reached no statistical significance towards non-treated cells (Fig 1C-D). After IFN-α treatment, Tha and Th2P-4M-eGFP both exhibited a decreased tropism for SK-N-SH cells although a statistical difference to non-treated SK-N-SH (Fig 1C) was only observed during Th2P-4M-eGFP infection (adjusted p-value<0.0083) and not during Tha-eGFP infection (Fig 1D). In detail, exogenous IFN-α lowered Tha-eGFP infection of SK-N-SH from 78.9% to 63.5% and Th2P-4M-eGFP infection was reduced from 64.3% to 30.2% (adjusted p-

value<0.0083, Fig 1C and 1D). The same effect, was observed for IFN-α-treated SVGp12 infected with Tha-eGFP (9.7%) and Th2P-4M-eGFP (8.4%, adjusted p-value<0.0083). In contrast, $eGFP^+$ HMC3 decreased only slightly during Tha-eGFP (19.8%) and Th2P-4M-eGFP infection (14.5%) upon IFN-α treatment (Fig 1D) compared to non-treated HMC3 (Fig 1C). Thus, conserved residues in viral P-protein and M-protein of Tha-eGFP seem to be crucial to evade the IFN-α-induced antiviral responses of neuronal cells but less important in the case of microglial cells.

Further, viral growth of Tha and Th2P-4M was assessed in SK-N-SH, SVGp12, and HMC3. Although no differences were observed between the distinct CNS cell types for neither Tha nor Th2P-4M at 12-, 24-, and 36-hours post-infection, SK-N-SH produced significantly more infectious progeny particles compared to SVGp12 and HMC3 at 48 hours post-infection (S1 Fig).

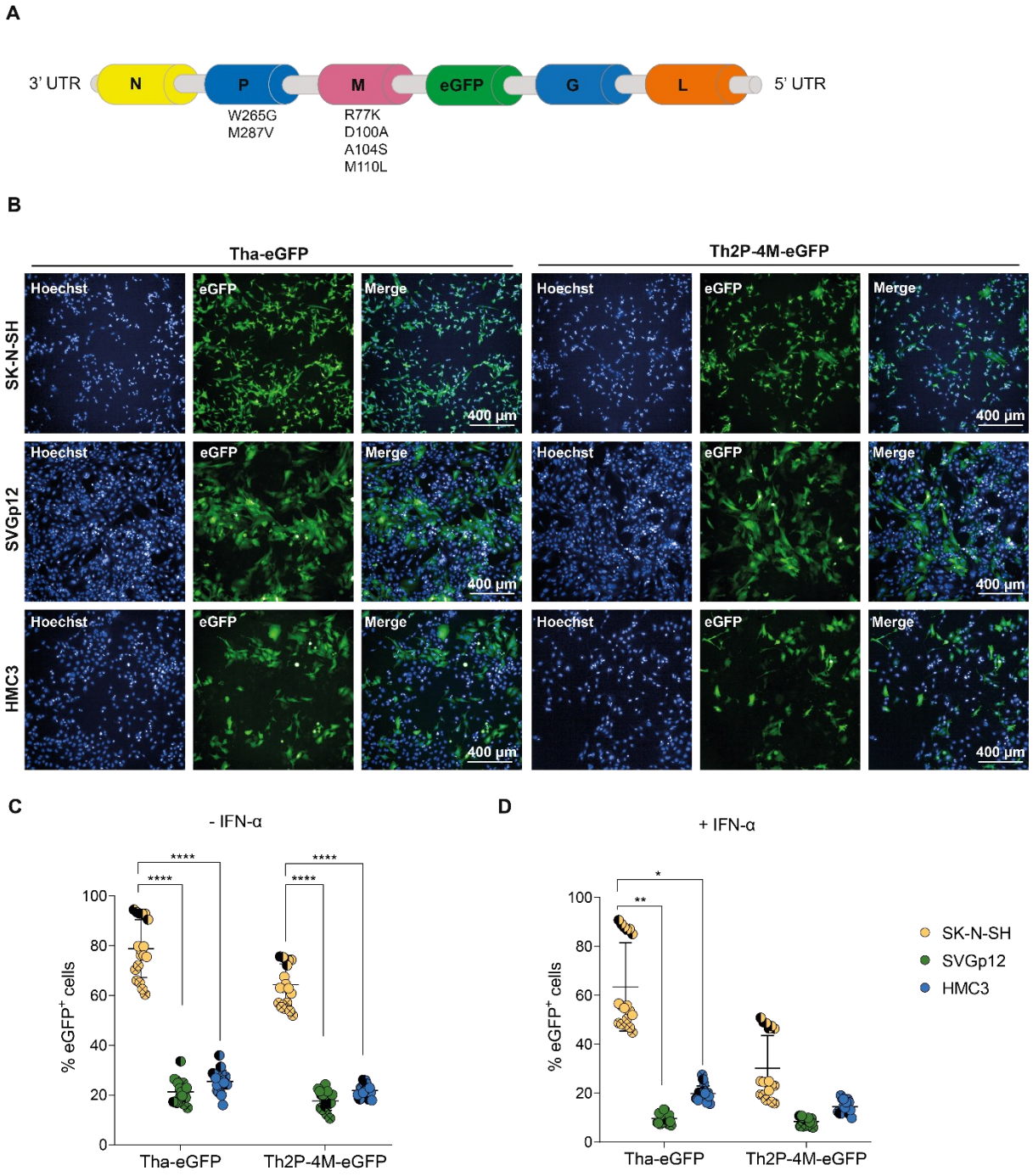

Fig 1. Tha-eGFP and Th2P-4M-eGFP preferentially replicate and spread in human SK-N-SH compared to astrocyte-like (SVGp12) and microglia-like (HMC3) cell lines *in vitro*. (A) Schematic overview of the genomic organization of Tha-eGFP and Th2P-4M-eGFP. Tha-eGFP and Th2P-4M-eGFP harbour the same genetic background except for two mutations introduced in viral P-protein (W265G, M287V) and four mutations introduced in the M protein (R77K, D100A, A104S, M110L) [10,33,34]. For imaging purposes, the eGFP sequence was introduced after the M protein gene sequence as described previously [35]. (B) Representative immunofluorescence pictures of SK-N-SH, SVGp12, and HMC3 cells upon infection with Tha-eGFP and Th2P-4M-eGFP. (C) Quantification of eGFP⁺ cells in human CNS monocultures upon Tha-eGFP or Th2P-4M-eGFP infection. (D) Quantification of eGFP⁺ cells in human CNS monocultures upon Tha-eGFP or Th2P-4M-eGFP infection and subsequent IFN-α treatment at 24 hours post-infection. (B-D) Cells were infected with Tha-eGFP or Th2P-4M-eGFP (MOI 0.5) and imaged at 48 hours post-infection. All experiments were performed three times (n=3) independently. (C-D) Each dot represents imaging of one well of a 96-well-plate

(approx. $8x10^3$ cells/well). Bars show mean ± SD. Different colours present different biological conditions and different symbol shapes indicate the three technical replicates performed. The percentages of $eGFP^+$ cells were analyzed using a mixed model with the replication factor as a random effect, followed by multiple comparisons corrected by Tukey's method (**** adjusted p-value<0.000016, *** adjusted p-value<0.00016, ** adjusted p-value<0.0016, * adjusted p-value<0.0083). If no p-value is indicated, no significant difference was observed. eGFP = Enhanced Green Fluorescent Protein.

3.2 Glial cell lines constitutively protect SK-N-SH from Tha infection

Since CNS monocultures do not reflect the complexity of the CNS, we investigated if glial cells limit RABV infection in RABV-infected CNS co-culture models. Therefore, we compared the percentage of infection of SK-N-SH monocultures to co-cultures of SK-N-SH and astrocyte-like cells (SK-N-SH + SVGp12), co-cultures of SK-N-SH and microglia-like cells (SK-N-SH + HMC3) and co-cultures of SK-N-SH, astrocyte- and microglia-like cells (SK-N-SH + SVGp12 + HMC3, Fig 2A). For all experiments, cells were mixed in equal ratios (1:1 for co-cultures, 1:1:1 for triple cultures). During Tha-eGFP and Th2P-4M-eGFP infection, the presence of SVGp12, HMC3, or both cell types in co-cultures significantly reduced the proportion of total $eGFP^+$ cells (adjusted p-value<0.000016) compared to SK-N-SH monocultures (Fig 2A). Since previous results suggested a reduced percentage of $eGFP^+$ cells due to the lower susceptibilities of SVGp12 and HMC3 cells (Fig 1), we assessed if this effect was purely due to the presence of less susceptible glial cells or if there was an additive effect, potentially mediated by cellular crosstalk (S2 Fig). This mathematical comparison revealed that the presence of glial cells lowered the percentage of $eGFP^+$ cells in Tha-eGFP-infected co-cultures not more than expected beforehand from lower susceptibilities observed in Tha-eGFP-infected glial monocultures even if a tendency is observed (Fig 1C, S2 Fig). In contrast, the presence of glial cells (SVGp12, HMC3, or SVGp12 and HMC3) in Th2P-4M-eGFP-infected co-cultures significantly reduced the percentage of $eGFP^+$ cells more than expected beforehand from lower susceptibilities observed in glial monocultures (Fig 2A, S2 Fig). Therefore, our data suggest that at least Th2P-4M-eGFP induces the secretion of antiviral proteins which leads to a crosstalk between SK-N-SH, astrocyte-like SVGp12, and microglia-like HMC3 and in turn enhances restriction of viral replication compared to the wildtype infection.

In the next experimental set-up, instead of simply determining the proportion of $eGFP^+$ cells, the proportion of $TUBB3^+$ $eGFP^+$ cells was determined, which corresponds to the percentage of infected SK-N-SH present in the co-cultures (Fig 2B). This experiment is expected to give more precise results than the previous analysis (Fig 2A, S2 Fig). In that case, cells of glial origin, SVGp12, HMC3, or SVGp12 and HMC3 together, significantly reduced infection of Class III Beta-Tubulin ($TUBB3^+$) SK-N-SH during both Tha-eGFP (adjusted p-value<0.000016, Fig 2B) and Th2P-4M-eGFP infection (adjusted p-value<0.000016, Fig 2B).

Further, we investigated if glial-mediated restriction of SK-N-SH infection is mediated via the secretion of glial-derived proteins to the supernatant. Therefore, we transferred the medium of non-infected or homotypic infected SK-N-SH, SVGp12 or HMC3 cells after viral particle-removal, to freshly infected SK-N-SH cells to assess if conditioned medium reduces the percentage of $eGFP^+$ SK-N-SH compared to the transfer of fresh cell culture medium (Fig 2C-E).

During both Tha-eGFP and Th2P-4M-eGFP infection of SK-N-SH, adding exogenous IFN-α significantly restricted viral infection and was therefore used as a positive control (adjusted p-value<0.0016, Fig 2C-E). Transfer of conditioned medium originating from non-infected SK-N-SH or any of the RABV-infected SK-N-SH to respective RABV-infected SK-N-SH cells did not

lower the percentage of eGFP⁺ SK-N-SH significantly (Fig 2C). This suggests that in our experimental set-up, there is no crosstalk occurring between RABV-infected SK-N-SH. In contrast, we observed a constitutive effect of SVGp12 and HMC3 independent of homotypic infection: transfer of non-infected or Tha-eGFP-infected SVGp12 (adjusted p-value<0.0083, Fig 2D) or HMC3 (adjusted p-value<0.000016, Fig 2E) significantly reduced the percentage of eGFP⁺ SK-N-SH in Tha-eGFP infected cultures. Overall, and in contrast to SK-N-SH, non-infected and Tha-infected SVGp12 and HMC3 constitutively protect SK-N-SH from Tha-eGFP infection via the secretion of glial-derived proteins (Fig 2C-E).

These constitutive effects, however, were not observed during Th2P-4M-eGFP infection: in Th2P-4M-eGFP infection, transfer of supernatant originating from non-infected or infected SVGp12 (Fig 2D) or HMC3 (Fig 2E) had no effect on the proportion of eGFP⁺ SK-N-SH except for the transfer of supernatant originating from Th2P-4M-eGFP-infected HMC3 which significantly reduced the proportion of eGFP⁺ SK-N-SH (adjusted p-value<0.0083, Fig 2E). This means that Th2P-4M-eGFP induces a cell type-specific effect in HMC3 which lowered the proportion of eGFP⁺ SK-N-SH (Fig 2E) which was not observed with transfers of supernatants of of infected SK-N-SH (Fig 2C) or SVGp12 (Fig 2D).

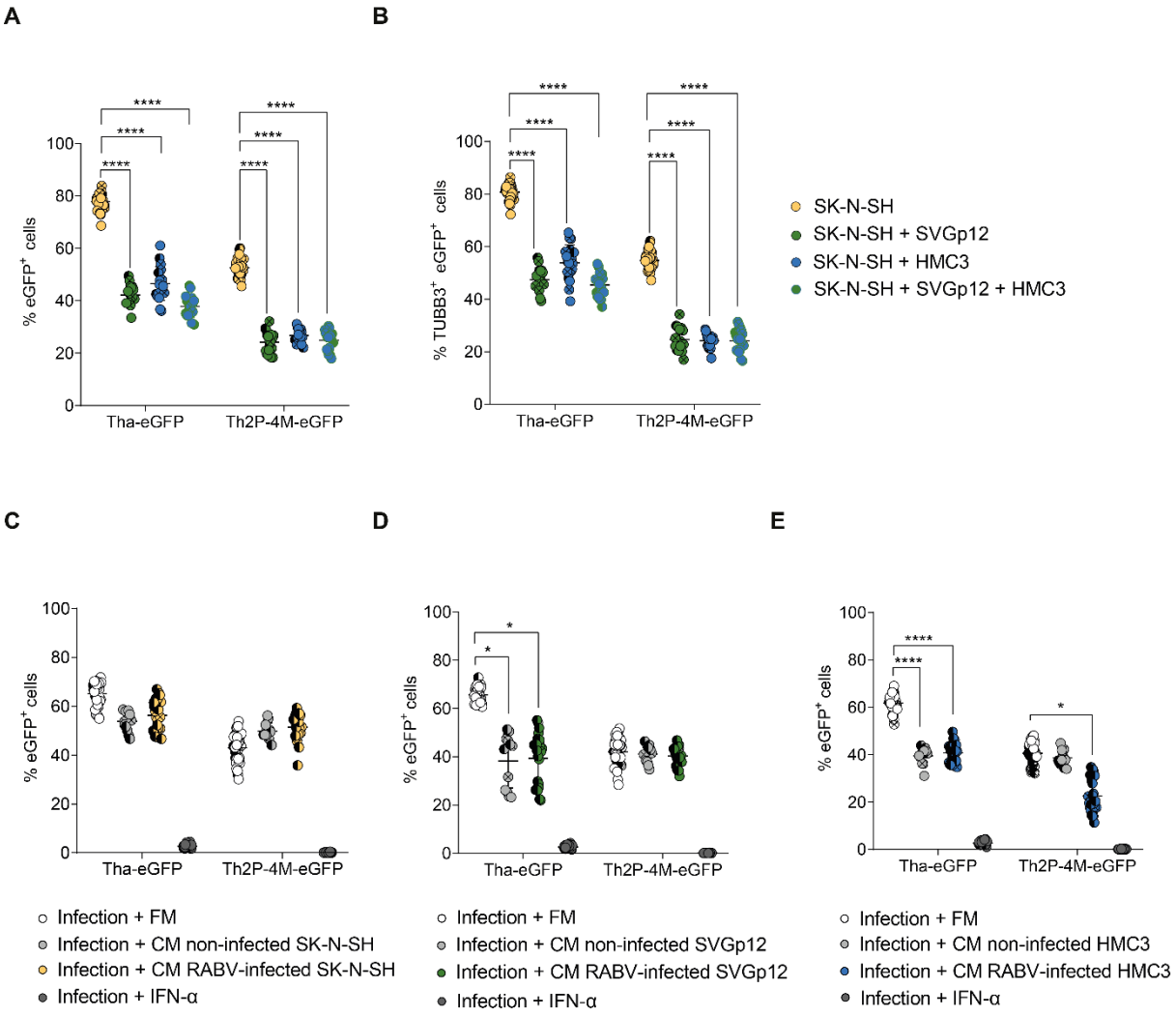

Fig 2. Astrocyte-like SVGp12 and microglia-like HMC3 constitutively protect SK-N-SH from Tha-eGFP infection *in vitro*. (A) Quantification of eGFP⁺ cells in mono- and co-cultures. (B) Quantification of TUBB3⁺ eGFP⁺ cells in mono- and co-cultures. (A – B) Mono- or co-cultures were infected with Tha-eGFP or Th2P-4M-eGFP (MOI 0.5) and imaged at 48 hours post-infection using the OPERA Phenix®

High Content Screening System (Perkin Elmer). (C-E) Quantification of eGFP$^+$ cells in SK-N-SH monocultures. After infection with Tha-eGFP or Th2P-4M-eGFP (MOI 0.5), SK-N-SH cells were incubated with the filtered fresh medium (FM) or filtered conditioned medium (CM) from non-infected or homotypic infected (MOI 5, 24 hours post-infection) SK-N-SH (C), SVGp12 (D), or HMC3 (E). In detail, Tha-eGFP-infected cells were only treated with supernatants from cells previously infected with Tha-eGFP. Correspondingly, Th2P-4M-eGFP-infected cells were only treated with supernatants from cells previously infected with Th2P-4M-eGFP. Cells were imaged at 48 hours post-infection. (A – E) All experiments were performed three times (n=3) independently. Each dot represents imaging of one well of a 96-well-plate (approx. $8x10^3$ cells/well). Bars show mean ± SD. Different colours present different biological conditions and different symbol shapes indicate the three technical replicates performed. The percentages of eGFP$^+$ cells or eGFP$^+$ TUBB3$^+$ cells were analysed using a mixed model with the replication factor as a random effect, followed by multiple comparisons corrected by Tukey's method (**** adjusted p-value<0.000016, *** adjusted p-value<0.00016, ** adjusted p-value<0.0016, * adjusted p-value<0.0083). (C-E) Comparisons between all conditions and infection + IFN-α treatment were significant (** adjusted p-value<0.0016) but not indicated in the figure. For the remaining comparisons, it applies that if no p-value is indicated, no significant difference was observed.

3.3 RABV infects human NSC-derived hiNeurons and hiAstrocytes but fails to infect hiMicros *in vitro*

After investigating the role of astrocyte-like and microglia-like cells in restricting RABV infection, we investigated the role of human stem cell-derived glial cells on RABV infection. First, we differentiated hNSC into hiNeurons and hiAstrocytes and iPSC into hiMicros according to a published protocol [36]. After differentiation, cellular fate was validated by immunofluorescence (Fig 3A), qPCR, or FACS (S3 Fig). As a matter of fact, differentiation of hNSC to hiNeurons resulted in a culture containing in average 85.6 % hiNeurons (CI_{95} 84.3-86%, S4 Table) but also not negligible proportions of hiAstrocytes (CI_{95} 14-15.7%, S4 Table). Hence, our experimental set-up did not allow us to fully reproduce previously obtained results from CNS cell line models (Fig 2) in a primary CNS model since we were unable to obtain pure monocultures of hiNeurons or hiAstrocyes separately. To obtain hiMicros, we differentiated iPSC-derived hiMacs for three consecutive weeks with hiNeurons and hiAstrocytes co-cultures. Prior to infection, cultures revealed in average 71.0% hiNeurons, 18.4% hiAstrocytes, and 10.6% hiMicros (S5 Table). Consequently, we investigated viral tropism in co-cultures containing hiNeurons and hiAstrocytes and co-cultures containing hiNeurons, hiAstrocytes, and hiMicros (Fig 3B-C).

Upon infection, Tha-eGFP and Th2P-4M-eGFP successfully replicated in TUBB3$^+$ hiNeurons and GLAST-1$^+$ hiAstrocytes but failed to infect IBA1$^+$ hiMicros (Fig 3A). In accordance with CNS cell line models, both viral strains showed a neurotropic behaviour in hiNeurons and hiAstrocytes co-cultures (Fig 3B-C). However, the neuron-specific tropism was more profound during Th2P-4M-eGFP (Fig 3C) infection compared to Tha-eGFP infection (Fig 3B). In this experimental set up, we were not able to quantify the protective effect of astrocytes on the infectivity of neurones as done with cell line models (Fig 2).

However, we wanted to compare the influence of hiMicros on RABV tropism. Adding hiMicros to hiNeurons and hiAstrocytes co-cultures did not limit RABV infection of hiNeurons (Fig 3B-C), suggesting that microglial cells did not provide any additional protective effects to neurones when they are already co-cultured with astrocytes, as previously observed in the cell line co-culture model (Fig 2B).

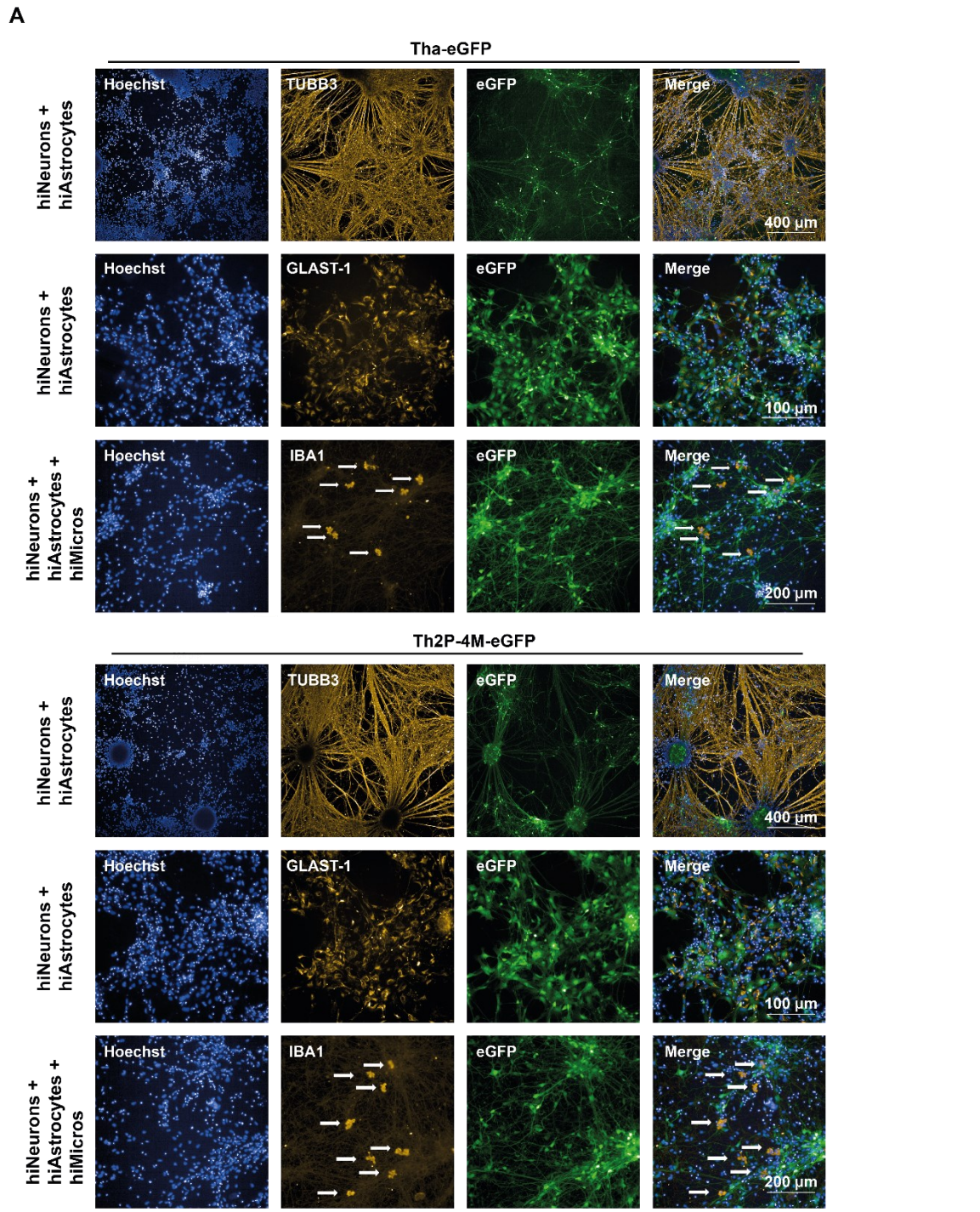
A
Tha-eGFP
Th2P-4M-eGFP
hiNeurons + hiAstrocytes
hiNeurons + hiAstrocytes + hiMicros
Hoechst
TUBB3
GLAST-1
IBA1
eGFP
Merge
400 µm
100 µm
200 µm
B
Tha-eGFP
C
Th2P-4M-eGFP
% eGFP⁺ cells
0
20
40
60
80
100
****
hiNeurons
hiAstrocytes
hiNeurons + hiAstrocytes
hiNeurons + hiAstrocytes + hiMicros

Fig 3. Whereas hiNeurons and hiAstrocytes are highly susceptible towards Tha-eGFP and Th2P-4M-eGFP infection, hiMicros are resistant to Tha-eGFP or Th2P-4M-eGFP infection *in vitro*. (A) Representative immunofluorescence pictures of hiNeurons, hiAstrocytes, and hiMicros upon infection with Tha-eGFP and Th2P-4M-eGFP. Cells were stained in cultures consisting of hiNeurons, hiAstrocytes, and hiMicros (S5 Table). IBA1$^+$ hiMicros are indicated with a flash. (B) Quantification of eGFP$^+$ cells in Tha-eGFP-infected co-cultures consisting of hiNeurons and hiAstrocytes or in triple cultures consisting of hiNeurons, hiAstrocytes, and hiMicros. Prior to infection, cultures consisted of hiNeurons (85.6%) and hiAstrocytes (14.4%, S4 Table). (C) Quantification of eGFP$^+$ cells in Th2P-4M-eGFP-infected co-cultures consisting of hiNeurons and hiAstrocytes or in triple cultures consisting of hiNeurons, hiAstrocytes, and hiMicros. Prior to infection, cultures consisted of hiNeurons (71.0%), hiAstrocytes (18.4%), and hiMicros (10.6%, S5 Table). (A-C) Cells were infected with Tha-eGFP or Th2P-4M-eGFP (MOI 0.5) and imaged at 48 hours post-infection. All experiments were performed three times (n=3) independently. (B-C) Every dot represents imaging of one well of a 96-well-plate (approx. $1x10^4$ cells/well). Bars show mean ± SD. Different colours present different biological conditions and different symbol shapes indicate the three technical replicates performed. The percentages of eGFP$^+$ cells were analyzed using a mixed model with the replication factor as a random effect, followed by multiple comparisons corrected by Tukey's method (**** adjusted p-value<0.000025). If no p-value is indicated, no significant difference was observed. eGFP = Enhanced Green Fluorescent Protein; GLAST-1 = Glutamate Aspartate Transporter-1; IBA1 = Ionized calcium-binding adaptor molecule 1; TUBB3 = Class III Beta-Tubulin.

3.4 Tha induces little innate immune gene expression in cells of neuronal origin whereas glial cells strongly respond to Tha infection

To further investigate the roles of neural cells in inducing cell type-specific immune responses, different CNS cell types were cultured in monocultures and the expression of a panel of selected innate immunity genes (*TLR3, TLR7, IFIH1, DDX58, DHX58, IRF7, IFNB1, CCL5, CXCL10, ISG15, MX1, IL1B, IL6, LIF*) was quantified via qPCR.

Comparing basal expression levels of innate immunity genes between CNS cell types by qPCR revealed that hiMicros present a strong basal expression of RLRs (*IFIH1, DDX58, DHX58*) *TLR3*, adaptor molecules (*IRF7*), chemokines (*CCL5*) and antiviral proteins (*MX1*). In contrast, fetal pAstrocytes revealed a strong expression of the RLR *DDX58* (encoding RIG-I) and SK-N-SH showed a strong expression of *TLR3*, although this was not observed in hiNeurons (S4A Fig). Upon IFN-α treatment, astrocytes, astrocyte-like cells, microglia-like, and SK-N-SH cells strongly amplified the inflammatory response via the expression of *TLR3, IFIH1, DDX58, DHX58, IRF7, ISG15,* and *MX1*. In contrast, hiNeurons showed little response to IFN-α stimulation. In detail, *DDX58, ISG15*, and *MX1* were the only genes that were modestly modulated by IFN-α in hiNeurons (S4B Fig). Additionally, we also noticed a strong and specific amplification of *CXCL10* in fetal pAstrocytes upon IFN-α treatment.

In the next step, we quantified the expression of innate immunity genes upon Tha and Th2P-4M infection via qPCR (Fig 4A and 4B). We used a high level of MOI (MOI 5) to ensure that all cell types would have a comparable level of infection, regardless of their susceptibility to infection. First, Th2P-4M induced a stronger innate immune response compared to Tha. Despite the induction of strong immune responses, neither Tha nor Th2P-4M strongly induced cell death or apoptosis in SK-N-SH, astrocyte-like, or microglia-like cells (S5 Fig). Secondly, fetal pAstrocytes and hiMicros strongly induced the expression of innate immunity genes upon Tha and Th2P-4M infection which was not observed in respective astrocyte-like (SVGp12) and microglia-like (HMC3) cell lines. Lastly, little differences were observed between CNS cell lines (SK-N-SH, SVGp12, and HMC3), whereas profound differences were observed in the innate immune response of hiNeurons, fetal pAstrocytes, and hiMicros (S6 and S7 Fig). Upon Tha

and Th2P-4M infection, fetal pAstrocytes strongly induced the expression of *IFIH1, CCL5*, and *CXCL10* whereas hiMicros strongly upregulated expression of CXCL10 and genes coding for antiviral proteins *ISG15* and *MX1* (Fig 4A). This further illustrates the differences between primary CNS cells and cell lines and the interest to base our conclusions on the most-relevant model, the primary CNS cells.

Subsequently, we stimulated cells with IFN-α at 24 hours post-infection to artificially activate the JAK-STAT pathway. Expression of innate immunity genes was quantified at 48 hours post-infection to test if Tha or Th2P-4M can inhibit the IFN-α-induced inflammatory response (Fig 4B). First, we assessed expression of *IFNAR1* and *IFNAR2* in the distinct CNS cell types (S8 Fig) to better understand the distinct cellular responses towards IFN-α treatment. Overall, *IFNAR1* expression was higher and more homogenous among the distinct CNS cell types compared to *IFNAR2* expression. In detail, hiMicros showed a slightly higher *IFNAR1* expression compared to hiNeurons or pAstrocytes (S8A Fig). Regarding *IFNAR2* expression, profound differences were observed among distinct cell types: Microglia-like cells (hiMicros and HMC3) showed the strongest expression of *IFNAR2*, followed by astrocytes (pAstrocytes and SVGp12) and neurons (hiNeurons and SK-N-SH, S8B Fig).

Regarding the expression of ISGs, profound differences were observed without IFN-α treatment (Fig 4A). Strikingly, cell type-specific differences were less profound after IFN-α stimulation (Fig 4B, S6 and S7 Fig) despite the strong differences in *IFNAR2* expression among the distinct CNS cell types (S8 Fig). Despite IFN-α treatment, virulent Tha suppressed the expression of innate immunity genes compared to less virulent Th2P-4M. In detail, IFN-α-treated fetal pAstrocytes strongly expressed *TLR7, IFNB1, CCL5, IL1B,* and IL6 upon Tha infection. IFN-α-treated microglia-like HMC3 upregulated *IFNB1, CCL5, CXCL10*, and IL6 upon Tha infection (Fig 4B). In contrast to Th2P-4M, Tha strongly downregulated the expression of *TLR3*, RLRs (*IFIH1, DDX58, DHX58*) and the antiviral proteins *MX1* and *ISG15* in IFN-α-treated cells of neuronal origin (SK-N-SH and hiNeurons) as well as expression of RLRs (*IFIH1, DDX58, DHX58*) and *ISG15* in microglia-like HMC3.

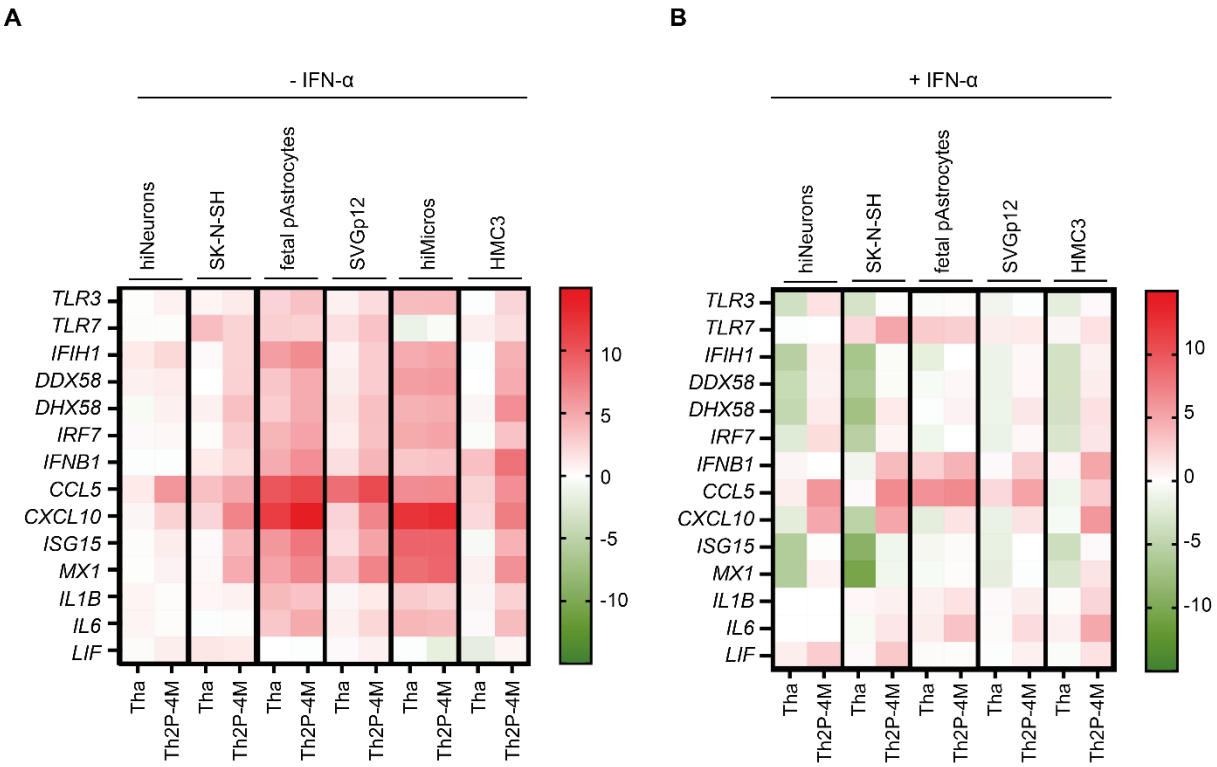

Fig 4. Tha is highly adapted to evade the neural innate immune system. (A) Expression of innate immune genes upon Tha and Th2P-4M infection. (B) Expression of innate immune genes upon Tha and Th2P-4M infection with subsequent IFN-α treatment at 24 hours post-infection. (A-B) Cells were infected with Tha or Th2P-4M (MOI 5) and gene expression was quantified at 48 hours post-infection via qPCR. To obtain hiNeurons, hNSC were differentiated for 21 days resulting in cultures which contained 85.6% hiNeurons (S4 Table). hiMacs were differentiated to hiMicros by co-culturing them for three consecutive weeks in inserts with hiNeurons (see Material and Methods). All experiments were performed three times (n=3) independently. Heatmaps present gene expression (ΔΔCT) which was normalized to the expression of the reference gene 18S and the respective mock-infected (A) or IFN-α-treated mock (B). Colour scaling presents differences observed in gene expression (ΔΔCT) between infected and respective non-infected controls.

Overall, we show that Tha induces little innate immune responses in cells of neuronal origin (SK-N-SH and hiNeurons), whereas glial cells (fetal pAstrocytes and hiMicros) strongly respond to Tha infection (Fig 4, S6 and S7 Fig).

3.5 Glial expression of IL-1β, IL-6, or LIF does not protect hiNeurons or hiAstrocytes from RABV infection

To see if cell-specific immune responses can be observed by quantifying protein expression levels of infected cells, we quantified intracellular proteins corresponding to genes which were identified in our previous transcriptomic analysis (IFN-β, IL-1β, IL-6, CXCL10, LIF, CCL5; Fig 4), and a few additional proteins (IFN-γ, IL-15, TNF-α; Fig 5). Intracellular protein concentrations revealed the induction of cell type-specific immune responses upon RABV infection: both neuronal cell types investigated, SK-N-SH and hiNeurons, did not induce any of the beforementioned proteins upon Tha or Th2P-4M infection but constitutively expressed modest levels of TNF-α (Fig 5A-B). In contrast, Tha and Th2P-4M infection induced expression of IL-1β and LIF in astrocyte-like SVGp12 although observed differences were not significant (Fig 5C). Pure cultures of fetal pAstrocytes did not induce the expression of any of the abovementioned proteins upon neither Tha nor Th2P-4M infection but constitutively expressed modest levels of LIF and TNF- α (Fig 5D). Microglia-like HMC3 induced expression of IL-6 upon Tha and Th2P-4M infection. Further HMC3 constitutively expressed moderate levels of LIF and TNF-α (Fig 5E).

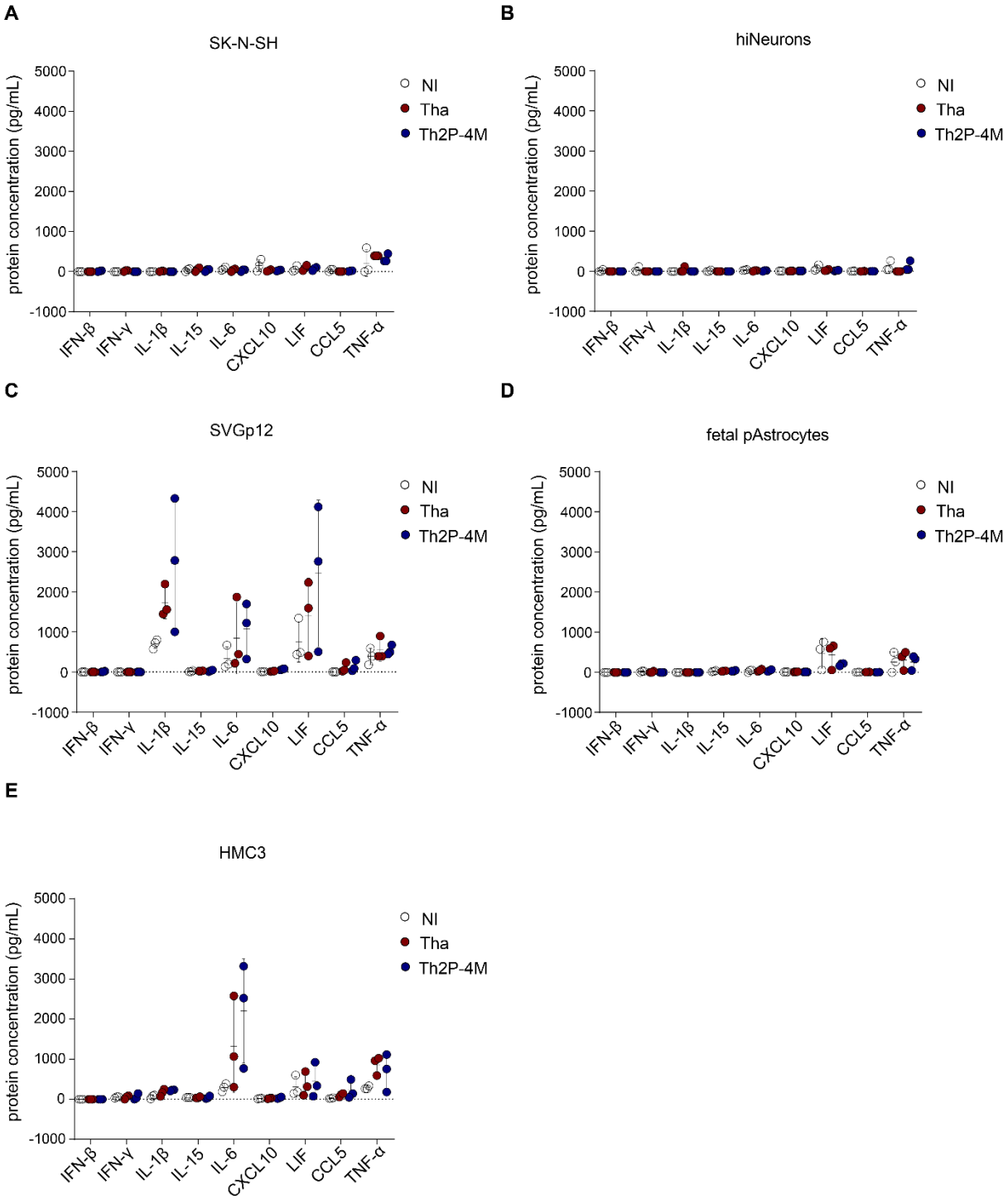

Fig 5. Glial cells induce the expression of IL-1β, IL-6, and LIF upon Tha and Th2P-4M infection. (A) Intracellular protein concentrations of SK-N-SH cells upon Tha or Th2P-4M infection. (B) Intracellular protein concentrations of hiNeurons upon Tha or Th2P-4M infection. (C) Intracellular protein concentrations of astrocyte-like SVGp12 cells upon Tha or Th2P-4M infection. (D) Intracellular protein concentrations of fetal pAstrocytes upon Tha or Th2P-4M infection. (E) Intracellular protein concentrations of microglia-like HMC3 cells upon Tha or Th2P-4M infection. (A-E) Cells were infected with Tha or Th2P-4M (MOI 5) and intracellular protein concentration was quantified at 48 hours post-infection using the DropArray system (Curiox). All experiments were performed three times (n=3) independently. All bars show mean ± SD with a one-way ANOVA analysis. To correct for multiple testing, the p-value was corrected accordingly (* adjusted p-value<0.0055). If no p-value is indicated, no significant difference was observed.

Since Tha and Th2P-4M induce the production of IL-1β, IL-6, and LIF in glial cells, we wanted to investigate if these cytokines can restrict RABV replication in hiNeurons or hiAstrocytes via the induction of secondary signalling pathways. Therefore, hiNeurons and hiAstrocytes were infected with Tha-eGFP or Th2P-4M-eGFP and treated with human recombinant IL-1β, IL-6, or LIF two hours after infection. Forty-eight hours post-infection, the proportion of $eGFP^+$ hiNeurons and hiAstrocytes was quantified by fluorescence microscopy (Fig S9).

Fluorescence imaging revealed that neither IL-1β (Fig S9A-B), IL-6 (Fig S9C-D), nor LIF (Fig S9E-F) significantly modulated the percentage of $eGFP^+$ hiNeurons or hiAstrocytes at 48 hours post-infection. Further, neither IL-1β, IL-6, nor LIF lowered the percentage of dead cells in Tha-eGFP-infected or Th2P-4M-infected hNSC-derived CNS cultures (S10 Fig). Therefore, we can conclude that there is no additional effect of exogenous IL-1β, IL-6 or LIF to the constitutive modulation exerted by astrocytes on the percentage of $eGFP^+$ hiNeurons.

4. Discussion

Here, we report that cell-dependent factors determine RABV tropism: the simple presence of glial cells in co-cultures as well as the transfer of supernatant from glial cells influences Tha tropism (Fig 2). Additionally, the presence of astrocyte-like SVGp12 and microglia-like HMC3 restrict Tha-eGFP replication in SK-N-SH (Fig 2), suggesting a role in glial-induced communication in inhibiting viral spread in the CNS. Possible underlying mechanisms comprise glial-mediated signalling directly via cell-to-cell contacts or via the secretion of inflammatory proteins (Fig 2 and 3), the induction of inflammatory genes (Fig 4) as well as the induction of cell type-specific inflammatory proteins (Fig 5) which can induce secondary signalling cascades in surrounding cells.

Although differentially expressed mRNAs generally present a useful tool to predict protein expression due to their good correlation [46], for unknown reasons, discrepancies were observed between gene expression obtained from qPCR (Fig. 4) and protein expression in the cytoplasm (Fig.5) upon Tha and Th2P-4M infection (e.g. *IFNB1*, LIF, *CXCL10*). This could be explained by several factors impacting this correlation, such as RNA secondary structures, presence of regulatory proteins and regulatory small RNAs, codon bias, and differences in ribosomal density [47].

Overall, we show that cell type-specific immune responses of distinct CNS cells partly shape RABV tropism *in vitro*. This has already been shown for poliovirus, where the type I IFN system induces the expression of ISGs particularly PKR and OAS in atropic tissues [48]. Further, the IFN system dictates viral tropism for VSV [49], West Nile Virus [50], and neurotropic coronavirus [51]. As a result, mice lacking functional type I responses lead to highly systematic infections instead of sub-clinical localized infections [15].

A comparative transcriptomic analysis between Tha- and Th2P-4M-infected cells focusing on innate immune gene expression implied in RABV pathogenesis revealed that Tha specifically evades neuronal immune responses via P- and M-protein-mediated evasion of NF-κB and JAK-STAT pathways (Fig 4). Although antiviral signalling via IFNs was originally considered as a universal mechanism to control viral infections, recent evidence suggests that neurons lack robust innate immune signalling pathways to minimize the detrimental effects of viral infection to this non-renewable cell population [52,53]. Further, the neuronal capacity to respond to IFN stimulation seems limited given the low gene expression of *IFNAR1* and *IFNAR2* compared to cells of glial origin (S8 Fig). In contrast to neuronal impairment to respond to Tha infection via IFN induction, we show that glial cells induce strong innate immune responses upon Tha and Th2P-4M infection (Fig 4 and 5). Consequently, we suggest that the pronounced neuron-specific tropism of Th2P-4M results from its limited or delayed capacity to

evade strong immune responses, thus restricting cellular tropism to cell types that are more defective in IFN signalling, such as cells of neuronal origin [53]. Overall, we provide evidence that RABV neuron-specific tropism relies on more than simply the structure of the RABV G-protein [17,54] or the expression of RABV surface receptors [6], but accessory functions of viral P- and M-proteins in viral-mediated immune evasion.

Additionally, we report that Tha-eGFP and Th2P-4M-eGFP infect hiNeurons and hiAstrocytes, whereas hiMicros are not susceptible towards Tha-eGFP nor Th2P-4M-eGFP infection *in vitro* (Fig 3). Although Ray and colleagues previously reported that the tissue culture-adapted ERA strain and mouse-adapted bat SRV strain successfully replicate in primary adult human microglia *in vitro* [24], we suggest that the different nature of RABV strains, their culture adaptation, or insufficient cell purification might account for different susceptibilities towards RABV infection observed between these studies. Consequently, our results question the capability of canine RABV strains to successfully enter and replicate in human microglia (Fig 3A). Microscopic analysis of post-mortem human brain tissues of rabid patients revealed enhanced activation of microglia which surrounded degenerated neurons [55] which are referred to as Babes nodules [56] and observed in other viral encephalitides and infectious disorders [57]. Given that microglia phagocyte degenerated neurons and thereby take up RABV components [55], viral transcripts that are detected in microglia [58] do not necessarily mean that microglia actively support RABV infection. Nevertheless, more research is needed to elucidate the susceptibility and function of microglia in human rabies infection, particularly by using more sophisticated models which reflect the complexity of the human CNS.

In detail, we identified the upregulation of IFN-inducible genes with antiviral responses (*CXCL10, ISG15, MX1*) in hiMicros as well as an increase in IL-6 protein expression in microglial-like cells upon Tha and Th2P-4M infection. Microglia are already known to induce *CXCL10* [59,60] and *ISG15* [58,60,61] expression during viral infection. Generally, activated microglia are well-known to release pro-inflammatory cytokines in pathological conditions such as IL-6, resulting in cytotoxicity, immune activation, neuronal excitotoxicity, and apoptosis [62]. Here, we show that IL-6 does not directly restrict RABV replication in hiNeurons or hiAstrocytes (Fig 6), nor reduce the percentage of dead cells in Tha-eGFP- or Th2P-4M-infected co-cultures (S9 Fig). Despite the lack of IL-6-mediated antiviral or anti-apoptotic activity in our model, IL-6 might potentially modulate other biological processes in the CNS, such as microglia and T-cell activation, BBB permeability [63], or synaptic function [64]. Targeting the highly dynamic activation of microglia state is believed to be a new therapeutic avenue for several neuropathologies [65], including parkinson's disease [66], depression disorders [67], and acute traumatic brain injury [68]. Although neuronal dysfunction rather than disease-associated microglia is believed to cause the fatal outcome of rabies encephalomyelitis [69], targeting the molecular signature of microglia might support RABV clearance from the infected brain.

Like microglia, astrocytes strongly induce the transcription of cytokines and adaptor molecules (*IFIH1, TLR7, IFNB1, CCL5, CXCL10*, IL1B, LIF) upon Tha and Th2P-4M infection *in vitro*. We assume that astrocytes sense Tha via RLRs (*IFIH1, DDX58, DHX58*) and TLRs (*TLR3, TLR7*) in turn inducing the expression of type I IFNs (*IFNB1*), chemokines (*CCL5, CXCL10*), and interleukins (IL1B). Both, IFN-β and IL-1β are known to increase BBB permeability, to activate monocytes, microglia, and astrocytes, and to induce the production of neuroprotective mediators [70]. Further, astrocytic expression of CCL5 and CXCL10 chemokines induces the recruitment of monocytes, macrophages, dendritic cells, T and B lymphocytes, neutrophils, and regulates microglial activity as well as astrocyte survival [70]. Taken together, we hypothesise that astrocytes sense Tha via RLRs and TLRs, triggering the expression of chemokines and interleukins which in turn increase BBB permeability, induce the recruitment and activation of inflammatory and glial cells. Previously, it has been shown that murine

astrocytes strongly respond towards infection with a recombinant RABV carrying the G protein of the CVS strain (SAD-G_{CVS}) via RLR- and TLRs-induced expression of IFN-β *in vivo*. As a consequence, the IFN response aborts RABV infection of astrocytes [26]. In contrast to attenuated RABV strains, a recent quantitative analysis of astrocyte tropism *in vivo* revealed a strong tropism for astrocytes by RABV field strains (8 - 27%). In accordance with these data, we showed that the culture-adapted field isolate Tha presents a profound astrocyte tropism *in vitro* (CI_{95} 20.7-31.6%, Fig 3C) despite the induction of a strong astrocyte-mediated immune response upon infection (Fig 4 and 5). Nevertheless, considering the mild and non-specific histopathological changes in the CNS of rabies patients [71] as well as viral-mediated inhibition of the BBB opening [72,73], astrocyte-mediated immune responses fail to induce the opening of the BBB and subsequently clear RABV from the infected CNS. Understanding why the astrocyte-induced inflammatory response does not result in the abortion of astrocyte infection in our model might help understanding why astrocytes fail to induce secondary effects such as the opening of the BBB during natural human rabies infection. Thus, more research is necessary to understand the consequences of astrocyte-mediated antiviral responses on RABV replication.

Apart from astrocyte-mediated IFN and interleukin expression, we show that Tha and Th2P-4M induce LIF protein expression in astrocyte-like cells. LIF is a neurotrophic factor known to be released by astrocytes supporting neuronal survival, differentiation, function, and regeneration, as well as oligodendrocyte survival [70]. Recently, it was shown LIF expression in astrocytes is among the most differentially regulated genes upon Zika virus infection [74]. In our model, LIF did neither actively restrict RABV replication in hNSC-derived CNS cultures (Fig 6), nor increase cell viability infected CNS cultures *in vitro* (S9 Fig). Although the role of astrocytic LIF expression during RABV infection is not well understood, LIF might be considered as a marker for the induction of several pathways rather than a direct effector to RABV infection. Still, the exact mechanism of RABV interference with LIF signalling remains a question of significant interest. The fact that the antiviral activity of LIF [75,76], IL-1β [77], and IL-6 [78,79] has been described previously in different *in vitro* and *in vivo* models for various human pathogens, urges further research to understand the pleiotropic nature of these interleukins during viral infections, particularly regarding RABV infection.

5. Conclusion

Overall, our results point out that innate immune responses of CNS cell types towards RABV infection *in vitro* strongly vary according to the CNS cell type investigated. Whereas neurons lack major antiviral signalling pathways to restrict Tha infection, astrocytes and microglia mount strong immune responses towards Tha infection *in vitro* and modulate the susceptibility of neurons towards RABV infection via a filtrable and transferable agent. Nevertheless, we need to admit that gene and protein expression levels were measured in monocultures which do not reflect the complexity of the CNS. Cellular interactions strongly influence immune responses during physiological and pathological states [80], consequently limiting the validity of our study to extrapolate data directly to the human CNS. Thus, more sophisticated models such as suitable human *ex-vivo* CNS models and single cell approaches are needed to elucidate the underlying cell type-specific differences in mounting innate immune responses upon RABV infection. Apart from the role of glial cells in restricting RABV replication, we show that RABV tropism strongly depends on the role of accessory functions of viral P- and M-proteins in viral-mediated immune evasion possibly via interference with NF-κB and JAK-STAT pathways. At last, we conclude that more research is needed to understand the underlying pathways defining RABV tropism and cell type-specific immune responses. Further, the analysis of distinct cellular responses in the CNS, particularly the characterization of transcriptome profiles

of different neural cell types, would help to understand the intimate interplay of the different CNS cell types during RABV infection and its implications in RABV tropism.

6. Funding

Lena Feige was supported by the Pasteur - Paris University (PPU) International PhD Program.

7. Acknowledgements

Image acquisition with the Opera Phenix® Plus High Content Screening System (Perkin Elmer) and data analysis via the Columbus software (Perkin Elmer) were conducted with the help of Anne Danckaert and Nathalie Aulner of UTechS Photonic BioImaging (PBI) core at Institut Pasteur Paris. PBI, a member of the national infrastructure France-BioImaging supported by the French National Research Agency (ANR-10-INBS-04), kindly acknowledges the financial support of the Région Ile-de France (program DIM1Health) and the Institut Pasteur.

8. Authors' contributions

Conceptualization, Hervé Bourhy; Data curation, Lena Feige and Tatsuya Kozaki; Formal analysis, Lena Feige and Vincent Guillemot; Funding acquisition, Hervé Bourhy; Methodology, Tatsuya Kozaki and Florent Ginhoux; Project administration, Lena Feige; Resources, Florent Ginhoux; Software, Vincent Guillemot; Supervision, Guilherme Dias de Melo, Florence Larrous, Florent Ginhoux and Hervé Bourhy; Writing – original draft, Lena Feige; Writing – review & editing, Tatsuya Kozaki, Guilherme Dias de Melo, Vincent Guillemot, Florence Larrous, Florent Ginhoux and Hervé Bourhy.

9. Institutional Review Board Statement

Not applicable

10. Informed Consent Statement

Not applicable

11. Data Availability Statement

The data presented in this study are available in additional files 1 – 3 supplied by the authors.

12. Conflicts of Interest

The authors declare no conflict of interest.

13. References

1. Lentz, T.L.; Burrage, T.G.; Smith, A.L.; Crick, J.; Tignor, G.H. Is the acetylcholine receptor a rabies virus receptor? Science 1982, 215, 182–4.

2. Thoulouze, M.I.; Lafage, M.; Schachner, M.; Hartmann, U.; Cremer, H.; Lafon, M. The neural cell adhesion molecule is a receptor for rabies virus. J. Virol. 1998, 72, 7181–90.

3. Tuffereau, C.; Bénéjean, J.; Blondel, D.; Kieffer, B.; Flamand, A. Low-affinity nerve-growth factor receptor (P75NTR) can serve as a receptor for rabies virus. EMBO J. 1998, 17, 7250–9, doi:10.1093/emboj/17.24.7250.

4. Wang, J.; Wang, Z.; Liu, R.; Shuai, L.; Wang, X.; Luo, J.; Wang, C.; Chen, W.; Wang, X.; Ge, J.; et al. Metabotropic glutamate receptor subtype 2 is a cellular receptor for rabies virus. 2018, 2, 1–21.

5. Tuffereau, C.; Schmidt, K.; Langevin, C.; Lafay, F.; Dechant, G.; Koltzenburg, M. The rabies virus glycoprotein receptor p75NTR is not essential for rabies virus infection. J. Virol. 2007, 81, 13622–13630, doi:10.1128/JVI.02368-06.

6. Lafon, M. Rabies virus receptors. J. Neurovirol. 2005, 11, 82–87, doi:10.1080/13550280590900427.

7. Tsiang, H.; Koulakoff, A.; Bizzini, B.; Berwald-Netter, Y. Neurotropism of rabies virus. An in vitro study. J. Neuropathol. Exp. Neurol. 1983, 42, 439–52.

8. Potratz, M.; Zaeck, L.; Christen, M.; Kamp, V.; Klein, A.; Freuling, C.M.; Müller, T.; Finke, S. Astrocyte Infection during Rabies Encephalitis Depends on the Virus Strain and Infection Route as Demonstrated by Novel Quantitative 3D Analysis of Cell Tropism. Cells 2020, 9, 1–25, doi:10.20944/preprints202001.0160.v1.

9. Potratz, M.; Zaeck, L.M.; Weigel, C.; Klein, A.; Freuling, C.M.; Müller, T.; Finke, S. Neuroglia infection by rabies virus after anterograde virus spread in peripheral neurons. Acta Neuropathol. Commun. 2020, 8, 199, doi:10.1186/s40478-020-01074-6.

10. Sonthonnax, F.; Besson, B.B.; Bonnaud, E.; Jouvion, G.; Merino, D.; Larrous, F.; Bourhy, H. Lyssavirus matrix protein cooperates with phosphoprotein to modulate the Jak-Stat pathway. Sci. Rep. 2019, 9, 1–13, doi:10.1038/s41598-019-48507-4.

11. Fooks, A.R.; Banyard, A.C.; Horton, D.L.; Johnson, N.; Mcelhinney, L.M.; Jackson, A.C. Current status of rabies and prospects for elimination. Lancet 2014, 384, 1389–1399, doi:10.1016/S0140-6736(13)62707-5.

12. Fooks, A.R.; Cliquet, F.; Finke, S.; Freuling, C.; Hemachudha, T.; Mani, R.S.; Müller, T.; Nadin-Davis, S.; Picard-Meyer, E.; Wilde, H.; et al. Rabies. Nat. Rev. Dis. Prim. 2017, 3, 17091, doi:10.1038/nrdp.2017.91.

13. Ugolini, G. Rabies virus as a transneuronal tracer of neuronal connections. Adv. Virus Res. 2011, 79, 165–202, doi:10.1016/B978-0-12-387040-7.00010-X.

14. Lafon, M. Evasive Strategies in Rabies Virus Infection; 1st ed.; Elsevier Inc., 2011; Vol. 79; ISBN 9780123870407.

15. McFadden, G.; Mohamed, M.R.; Rahman, M.M.; Bartee, E. Cytokine determinants of viral tropism. Nat. Rev. Immunol. 2009, 9, 645–655.

16. Akira, S.; Uematsu, S.; Takeuchi, O. Pathogen recognition and innate immunity. Cell 2006, 124, 783–801, doi:10.1016/j.cell.2006.02.015.

17. Etessami, R.; Conzelmann, K.-K.; Fadai-Ghotbi, B.; Natelson, B.; Tsiang, H.; Ceccaldi, P.-E. Spread and pathogenic characteristics of a G-deficient rabies virus recombinant: an in vitro and in vivo study. J. Gen. Virol. 2000, 81, 2147–2153, doi:10.1099/0022-1317-81-9-2147.

18. Le Blanc, I.; Luyet, P.-P.; Pons, V.; Ferguson, C.; Emans, N.; Petiot, A.; Mayran, N.; Demaurex, N.; Fauré, J.; Sadoul, R.; et al. Endosome-to-cytosol transport of viral nucleocapsids. Nat. Cell Biol. 2005, 7, 653–664, doi:10.1038/ncb1269.

19. Piccinotti, S.; Kirchhausen, T.; Whelan, S.P.J. Uptake of Rabies Virus into Epithelial Cells by Clathrin-Mediated Endocytosis Depends upon Actin. J. Virol. 2013, 87, 11637–11647, doi:10.1128/jvi.01648-13.

20. Dietzschold, B.; Wiktor, T.J.; Trojanowski, J.Q.; Macfarlan, R.I.; Wunner, W.H.; Torres-Anjel, M.J.; Koprowski, H. Differences in cell-to-cell spread of pathogenic and apathogenic rabies virus in vivo and in vitro. J. Virol. 1985, 56, 12–18, doi:10.1128/jvi.56.1.12-18.1985.

21. Wickersham, I.R.; Finke, S.; Conzelmann, K.K.; Callaway, E.M. Retrograde neuronal tracing with a deletion-mutant rabies virus. Nat. Methods 2007, 4, 47–49, doi:10.1038/nmeth999.

22. Wickersham, I.R.; Lyon, D.C.; Barnard, R.J.O.; Mori, T.; Finke, S.; Conzelmann, K.K.; Young, J.A.T.; Callaway, E.M. Monosynaptic Restriction of Transsynaptic Tracing from Single, Genetically Targeted Neurons. Neuron 2007, 53, 639–647, doi:10.1016/j.neuron.2007.01.033.

23. Prosniak, M.; Zborek, A.; Scott, G.S.; Roy, A.; Phares, T.W.; Koprowski, H.; Hooper, D.C. Differential expression of growth factors at the cellular level in virus-infected brain. Proc. Natl. Acad. Sci. U. S. A. 2003, 100, 6765–6770, doi:10.1073/pnas.0430999100.

24. Ray, N.B.; Power, C.; Lynch, W.P.P.; Ewalt, L.C.C.; Lodmell, D.L.L. Rabies viruses infect primary cultures of murine, feline, and human microglia and astrocytes. Arch. Virol. 1997, 142, 1011–1019, doi:10.1007/s007050050136.

25. Sugamata, M.; Miyazawa, M.; Mori, S.; Spangrude, G.J.; Ewalt, L.C.; Lodmell, D.L. Paralysis of street rabies virus-infected mice is dependent on T lymphocytes. J. Virol. 1992, 66, 1252–1260.

26. Pfefferkorn, C.; Kallfass, C.; Lienenklaus, S.; Spanier, J.; Kalinke, U.; Rieder, M.; Conzelmann, K.-K.; Michiels, T.; Staeheli, P. Abortively Infected Astrocytes Appear To Represent the Main Source of Interferon Beta in the Virus-Infected Brain. J. Virol. 2016, 90, 2031–2038, doi:10.1128/JVI.02979-15.

27. Zaeck, L.; Potratz, M.; Freuling, C.M.; Müller, T.; Finke, S. High-Resolution 3D Imaging of Rabies Virus Infection in Solvent-Cleared Brain Tissue. JoVE 2019, e59402, doi:doi:10.3791/59402.

28. Delmas, O.; Holmes, E.C.; Talbi, C.; Larrous, F.; Dacheux, L.; Bouchier, C.; Bourhy, H. Genomic diversity and evolution of the lyssaviruses. PLoS One 2008, 3, 1–6, doi:10.1371/journal.pone.0002057.

29. Vidy, A.; Chelbi-Alix, M.; Blondel, D. Rabies Virus P Protein Interacts with STAT1 and Inhibits Interferon Signal Transduction Pathways. J. Virol. 2005, 79, 14411–14420, doi:10.1128/JVI.79.22.14411-14420.2005.

30. Vidy, A.; El Bougrini, J.; Chelbi-Alix, M.K.; Blondel, D. The Nucleocytoplasmic Rabies Virus P Protein Counteracts Interferon Signaling by Inhibiting both Nuclear Accumulation and DNA Binding of STAT1. J. Virol. 2007, 81, 4255–4263, doi:10.1128/JVI.01930-06.

31. Hossain, M.A.; Larrous, F.; Rawlinson, S.M.; Zhan, J.; Sethi, A.; Ibrahim, Y.; Aloi, M.; Lieu, K.G.; Mok, Y.F.; Griffin, M.D.W.; et al. Structural Elucidation of Viral Antagonism of Innate Immunity at the STAT1 Interface. Cell Rep. 2019, 29, 1934-1945.e8, doi:10.1016/j.celrep.2019.10.020.

32. Sato, M.; Maeda, N.; Yoshida, H.; Urade, M.; Saito, S.; Miyazaki, T.; Shibata, T.; Watanabe, M. Plaque formation of herpes virus hominis type 2 and rubella virus in variants isolated from the colonies of BHK21/WI-2 cells formed in soft agar. Arch. Virol. 1977, 53, 269–273, doi:10.1007/BF01314672.

33. Ben Khalifa, Y.; Luco, S.; Besson, B.; Sonthonnax, F.; Archambaud, M.; Grimes, J.M.; Larrous, F.; Bourhy, H. The matrix protein of rabies virus binds to RelAp43 to modulate NF-κB-dependent gene expression related to innate immunity. Sci. Rep. 2016, 6, 39420, doi:10.1038/srep39420.

34. Wiltzer, L.; Okada, K.; Yamaoka, S.; Larrous, F.; Kuusisto, H.V.; Sugiyama, M.; Blondel, D.; Bourhy, H.; Jans, D.A.; Ito, N.; et al. Interaction of Rabies Virus P-Protein With STAT Proteins is Critical to Lethal Rabies Disease. J. Infect. Dis. 2014, 209, 1744–53, doi:10.1093/infdis/jit829.

35. Besson, B.; Kim, S.; Kim, T.; Ko, Y.; Lee, S.; Larrous, F.; Song, J.; Shum, D.; Grailhe, R.; Bourhy, H. Kinome-Wide RNA Interference Screening Identifies Mitogen-Activated Protein Kinases and Phosphatidylinositol Metabolism as Key Factors for Rabies Virus Infection. mSphere 2019, 4, doi:10.1128/mSphere.00047-19.

36. Takata, K.; Kozaki, T.; Lee, C.Z.W.; Thion, M.S.; Otsuka, M.; Lim, S.; Utami, K.H.; Fidan, K.; Park, D.S.; Malleret, B.; et al. Induced-Pluripotent-Stem-Cell-Derived Primitive Macrophages Provide a Platform for Modeling Tissue-Resident Macrophage Differentiation and Function. Immunity 2017, 47, 183-198.e6, doi:10.1016/j.immuni.2017.06.017.

37. Kanke, K.; Masaki, H.; Saito, T.; Komiyama, Y.; Hojo, H.; Nakauchi, H.; Lichtler, A.C.; Takato, T.; Chung, U.-I.; Ohba, S. Stepwise differentiation of pluripotent stem cells into osteoblasts using four small molecules under serum-free and feeder-free conditions. Stem cell reports 2014, 2, 751–760, doi:10.1016/j.stemcr.2014.04.016.

38. Grigoriadis, A.E.; Kennedy, M.; Bozec, A.; Brunton, F.; Stenbeck, G.; Park, I.-H.; Wagner, E.F.; Keller, G.M. Directed differentiation of hematopoietic precursors and functional osteoclasts from human ES and iPS cells. Blood 2010, 115, 2769–2776, doi:10.1182/blood-2009-07-234690.

39. Sturgeon, C.M.; Ditadi, A.; Awong, G.; Kennedy, M.; Keller, G. Wnt signaling controls the specification of definitive and primitive hematopoiesis from human pluripotent stem cells. Nat. Biotechnol. 2014, 32, 554–561, doi:10.1038/nbt.2915.

40. Ackermann, M.; Liebhaber, S.; Klusmann, J.-H.; Lachmann, N. Lost in translation: pluripotent stem cell-derived hematopoiesis. EMBO Mol. Med. 2015, 7, 1388–1402, doi:10.15252/emmm.201505301.

41. Chomarat, P.; Banchereau, J.; Davoust, J.; Palucka, A.K. IL-6 switches the differentiation of monocytes from dendritic cells to macrophages. Nat. Immunol. 2000, 1, 510–514, doi:10.1038/82763.

42. Pfaffl, M.W. A new mathematical model for relative quantification in real-time RT-PCR. Nucleic Acids Res. 2001, 29, e45, doi:10.1093/nar/29.9.e45.

43. Wiltzer, L.; Larrous, F.; Oksayan, S.; Ito, N.; Marsh, G. a.; Wang, L.F.; Blondel, D.; Bourhy, H.; Jans, D. a.; Moseley, G.W. Conservation of a Unique Mechanism of Immune Evasion across the Lyssavirus Genus. J. Virol. 2012, 86, 10194–10199, doi:10.1128/JVI.01249-12.

44. Besson, B.; Sonthonnax, F.; Duchateau, M.; Ben Khalifa, Y.; Larrous, F.; Eun, H.; Hourdel, V.; Matondo, M.; Chamot-Rooke, J.; Grailhe, R.; et al. Regulation of NF-κB by the p105-ABIN2-TPL2 complex and RelAp43 during rabies virus infection. PLoS Pathog. 2017, 13, e1006697, doi:10.1371/journal.ppat.1006697.

45. Luco, S.; Delmas, O.; Vidalain, P.-O.O.; Tangy, F.; Weil, R.; Bourhy, H. RelAp43, a Member of the NF-κB Family Involved in Innate Immune Response against Lyssavirus Infection. PLoS Pathog. 2012, 8, e1003060, doi:10.1371/journal.ppat.1003060.

46. Koussounadis, A.; Langdon, S.P.; Um, I.H.; Harrison, D.J.; Smith, V.A. Relationship between differentially expressed mRNA and mRNA-protein correlations in a xenograft model system. Sci. Rep. 2015, 5, 10775, doi:10.1038/srep10775.

47. Maier, T.; Güell, M.; Serrano, L. Correlation of mRNA and protein in complex biological samples. FEBS Lett. 2009, 583, 3966–3973, doi:https://doi.org/10.1016/j.febslet.2009.10.036.

48. Ida-Hosonuma, M.; Iwasaki, T.; Yoshikawa, T.; Nagata, N.; Sato, Y.; Sata, T.; Yoneyama, M.; Fujita, T.; Taya, C.; Yonekawa, H.; et al. The alpha/beta interferon response controls tissue tropism and pathogenicity of poliovirus. J. Virol. 2005, 79, 4460–4469, doi:10.1128/JVI.79.7.4460-4469.2005.

49. Steinhoff, U.; Müller, U.; Schertler, A.; Hengartner, H.; Aguet, M.; Zinkernagel, R.M. Antiviral protection by vesicular stomatitis virus-specific antibodies in alpha/beta interferon receptor-deficient mice. J. Virol. 1995, 69, 2153–2158, doi:10.1128/JVI.69.4.2153-2158.1995.

50. Samuel, M.A.; Diamond, M.S. Alpha/beta interferon protects against lethal West Nile virus infection by restricting cellular tropism and enhancing neuronal survival. J. Virol. 2005, 79, 13350–13361, doi:10.1128/JVI.79.21.13350-13361.2005.

51. Ireland, D.D.C.; Stohlman, S.A.; Hinton, D.R.; Atkinson, R.; Bergmann, C.C. Type I interferons are essential in controlling neurotropic coronavirus infection irrespective of functional CD8 T cells. J. Virol. 2008, 82, 300–310, doi:10.1128/JVI.01794-07.

52. Griffin, D.E. Recovery from viral encephalomyelitis: Immune-mediated noncytolytic virus clearance from neurons. Immunol. Res. 2010, 47, 123–133.

53. Yordy, B.; Iijima, N.; Huttner, A.; Leib, D.; Iwasaki, A. A neuron-specific role for autophagy in antiviral defense against herpes simplex virus. Cell Host Microbe 2012, 12, 334–345, doi:10.1016/j.chom.2012.07.013.

54. Mebatsion, T.; Konig, M.; Conzelmann, K.K. Budding of rabies virus particles in the absence of the spike glycoprotein. Cell 1996, 84, 941–951, doi:10.1016/s0092-8674(00)81072-7.

55. Liu, S.Q.; Xie, Y.; Gao, X.; Wang, Q.; Zhu, W.Y. Inflammatory response and MAPK and NF-κB pathway activation induced by natural street rabies virus infection in the brain tissues of dogs and humans. Virol. J. 2020, 17, 157, doi:10.1186/s12985-020-01429-4.

56. Babes V.M. Sur certains caractères des lésions histologiques de la rage. In Annales de L'Institut Pasteur; 1892; pp. 209–223.

57. Love, S.; Wiley, C. Viral diseases. In Greenfield's Neuropathology (7th edition); 2002; pp. 1–105.

58. Huang, K.W.; Sabatini, B.L. Single-Cell Analysis of Neuroinflammatory Responses Following Intracranial Injection of G-Deleted Rabies Viruses. Front. Cell. Neurosci. 2020, 14, doi:10.3389/fncel.2020.00065.

59. Nakamichi, K.; Saiki, M.; Sawada, M.; Takayama-Ito, M.; Yamamuro, Y.; Morimoto, K.; Kurane, I. Rabies Virus-Induced Activation of Mitogen-Activated Protein Kinase and NF- B

Signaling Pathways Regulates Expression of CXC and CC Chemokine Ligands in Microglia. J. Virol. 2005, 79, 11801–11812, doi:10.1128/jvi.79.18.11801-11812.2005.

60. Zhao, P.; Yang, Y.; Feng, H.; Zhao, L.; Qin, J.; Zhang, T.; Wang, H.; Yang, S.; Xia, X. Global gene expression changes in BV2 microglial cell line during rabies virus infection. Infect. Genet. Evol. 2013, 20, 257–269, doi:10.1016/j.meegid.2013.09.016.

61. Zhao, P.; Jiang, T.; Zhong, Z.; Zhao, L.; Yang, S.; Xia, X. Inhibition of rabies virus replication by interferon-stimulated gene 15 and its activating enzyme UBA7. Infect. Genet. Evol. 2017, 56, 44–53, doi:10.1016/j.meegid.2017.10.016.

62. Smith, J.A.; Das, A.; Ray, S.K.; Banik, N.L. Role of pro-inflammatory cytokines released from microglia in neurodegenerative diseases. Brain Res. Bull. 2012, 87, 10–20.

63. Rothaug, M.; Becker-Pauly, C.; Rose-John, S. The role of interleukin-6 signaling in nervous tissue. Biochim. Biophys. Acta - Mol. Cell Res. 2016, 1863, 1218–1227.

64. Gruol, D.L. IL-6 regulation of synaptic function in the CNS. Neuropharmacology 2015, 96, 42–54, doi:10.1016/j.neuropharm.2014.10.023.

65. O, F.; T, I.; T, Y. Microglia as therapeutic target in central nervous system disorders. J. Pharmacol. Sci. 2020, 144, 102–118, doi:10.1016/J.JPHS.2020.07.004.

66. Subramaniam, S.R.; Federoff, H.J. Targeting Microglial Activation States as a Therapeutic Avenue in Parkinson's Disease. Front. Aging Neurosci. 2017, 9, 176, doi:10.3389/FNAGI.2017.00176.

67. Zhang, L.; Zhang, J.; You, Z. Switching of the Microglial Activation Phenotype Is a Possible Treatment for Depression Disorder. Front. Cell. Neurosci. 2018, 12, 306, doi:10.3389/FNCEL.2018.00306.

68. CC, C.; MT, L.; CP, C. Microglial activation as a compelling target for treating acute traumatic brain injury. Curr. Med. Chem. 2015, 22, 759–770, doi:10.2174/0929867321666141106124657.

69. Fu, Z.F.; Jackson, A.C. Neuronal dysfunction and death in rabies virus infection. J. Neurovirol. 2005, 11, 101–106, doi:10.1080/13550280590900445.

70. Farina, C.; Aloisi, F.; Meinl, E. Astrocytes are active players in cerebral innate immunity. Trends Immunol. 2007, 28, 138–145.

71. Hemachudha, T.; Ugolini, G.; Wacharapluesadee, S.; Sungkarat, W.; Shuangshoti, S.; Laothamatas, J. Human rabies: neuropathogenesis, diagnosis, and management. Lancet Neurol. 2013, 12, 498–513, doi:10.1016/S1474-4422(13)70038-3.

72. Roy, A.; Phares, T.W.; Koprowski, H.; Hooper, D.C. Failure to open the blood-brain barrier and deliver immune effectors to central nervous system tissues leads to the lethal outcome of silver-haired bat rabies virus infection. J. Virol. 2007, 81, 1110–8, doi:10.1128/JVI.01964-06.

73. Phares, T.W.; Kean, R.B.; Mikheeva, T.; Hooper, D.C. Regional Differences in Blood-Brain Barrier Permeability Changes and Inflammation in the Apathogenic Clearance of Virus from the Central Nervous System. J. Immunol. 2006, 176, 7666–7675, doi:10.4049/jimmunol.176.12.7666.

74. Shereen, M.A.; Bashir, N.; Su, R.; Liu, F.; Wu, K.; Luo, Z.; Wu, J. Zika virus dysregulates the expression of astrocytic genes involved in neurodevelopment. PLoS Negl. Trop. Dis. 2021, 15, e0009362, doi:10.1371/journal.pntd.0009362.

75. Yeh, J.X.; Schultz, K.L.W.; Calvert, V.; Petricoin, E.F.; Griffin, D.E. The NF-κB/leukemia inhibitory factor/STAT3 signaling pathway in antibody-mediated suppression of Sindbis virus replication in neurons. Proc. Natl. Acad. Sci. U. S. A. 2020, 117, 29035–29045, doi:10.1073/pnas.2016691117.

76. Patterson, B.K.; Behbahani, H.; Kabat, W.J.; Sullivan, Y.; O'Gorman, M.R.; Landay, A.; Flener, Z.; Khan, N.; Yogev, R.; Andersson, J. Leukemia inhibitory factor inhibits HIV-1 replication and is upregulated in placentae from nontransmitting women. J. Clin. Invest. 2001, 107, 287–294, doi:10.1172/JCI11481.

77. Aarreberg, L.D.; Wilkins, C.; Ramos, H.J.; Green, R.; Davis, M.A.; Chow, K.; Gale, M.J. Interleukin-1β Signaling in Dendritic Cells Induces Antiviral Interferon Responses. MBio 2018, 9, doi:10.1128/mBio.00342-18.

78. Kuo, T.-M.; Hu, C.-P.; Chen, Y.-L.; Hong, M.-H.; Jeng, K.-S.; Liang, C.-C.T.; Chen, M.-L.; Chang, C. HBV replication is significantly reduced by IL-6. J. Biomed. Sci. 2009, 16, 41, doi:10.1186/1423-0127-16-41.

79. Luo, J.; Zhang, B.; Wu, Y.; Tian, Q.; Mo, M.; Long, T.; Mei, M.; Fan, R.; Lyu, Z.; Jiang, H.; et al. Recombinant rabies virus expressing interleukin-6 enhances the immune response in mouse brain. Arch. Virol. 2018, 163, 1889–1895, doi:10.1007/s00705-018-3808-8.

80. Armingol, E.; Officer, A.; Harismendy, O.; Lewis, N.E. Deciphering cell–cell interactions and communication from gene expression. Nat. Rev. Genet. 2021, 22, 71–88.

81. Bennett, M.L.; Bennett, F.C.; Liddelow, S.A.; Ajami, B.; Zamanian, J.L.; Fernhoff, N.B.; Mulinyawe, S.B.; Bohlen, C.J.; Adil, A.; Tucker, A.; et al. New tools for studying microglia in the mouse and human CNS. Proc. Natl. Acad. Sci. U. S. A. 2016, 113, E1738-46, doi:10.1073/pnas.1525528113.

2.3 RABV modulates intercellular CNS signalling (Article #3)

2.3.1 The amazing complexity of the human CNS

This chapter focusses on understanding the different transcriptome changes that RABV infection is causing in distinct cell populations. Throughout medicine, classifying genotypes and phenotypes between healthy and diseased states remains one of the long-standing challenges, and a powerful method to overcome this challenge offers the analysis of the transcriptome (255). However, and although all cells in our genome share almost identical genomes, it is becoming increasingly clear that every cell type expresses a unique transcriptome reflecting the active subset of the genome (256). To add complexity to this matter, nature decided that transcriptomes are not only different between species, but also between cell types, disease states, and if this was not enough, even in similar cell types (257,258).

According to Pertea *et al.* the human transcriptome is an unfinished story (258): It started with the complete sequencing of the human genome in 2001 (259,260) with the subsequent shock about the small number of genes that gets actively translated into proteins. Out of the 3 billion DNA base pairs of the haploid *Homo sapiens* genome, only 1-2% are protein-coding (261,262). Overall, annotated transcripts cover 3-5% of the human genome, leaving more than 95% transcripts with unknown purpose behind (258). These data visualize well how far we are from understanding the complexity of the human transcriptome. Very recently, Karlsson and colleagues combined information from the HPA Single Cell Type Atlas with genome-wide expression data from sc RNA-seq experiments including the spatial antibody-based bioimaging data (263). The group analysed data from 13 human tissues consisting of 192 cell type clusters. The analysis revealed that only 11% of all protein-coding genes were ubiquitously expressed among all the 192 cell types with most of the protein-coding transcripts being cell type-specific.

Currently, and despite the knowledge about the complex heterogeneity of human tissues, most experiments investigating transcriptome changes are carried out on the assumption that tissues are homogenous missing the important aspect of cell-to-cell variability. Unlike population-level approaches such as bulk RNA-Seq, sc RNA-Seq overcomes these obstacles by quantifying expression levels at the single cell resolution level.

The in the following section presented research article uses sequencing on the single cell level to decipher cell specific antiviral responses caused by CNS cell types, particularly neurons, astrocytes, and microglia upon RABV infection. On top of that, it assesses the

contributions of viral P- and M-proteins to evade cell type-specific immune responses by comparing Tha and Th2P-4M infections.

The article is currently in preparation and the following version presents a draft of the article.

More information about this article can be found here:

https://www.dropbox.com/sh/fuw8pp5a96n7dy7/AAB6sqGjg7lr-cFAxZ5EmU7ma?dl=0

2.3.2 Article #3 *(in preparation)*

Single cell RNA-Seq of human CNS cells reveals that RABV interferes with CNS cell communication

Lena Feige[1], Juan Pablo Cerapio[2-6], Tatsuya Kozaki[7], Lauriane Kergoat[1], Valentina Libri[8], Jean Jacques Fournié[2-6], Florent Ginhoux[7,9,10], Milena Hasan[8], Hervé Bourhy[1,*]

[1] Institut Pasteur, Université de Paris, Lyssavirus Epidemiology and Neuropathology, F75015, Paris, France.

[2] Centre de Recherches en Cancérologie de Toulouse, INSERM UMR1037, Toulouse, France

[3] Toulouse University, Toulouse, France

[4] CNRS UMR 5071, Toulouse, France

[5] Institut Universitaire du Cancer-Oncopole de Toulouse, Toulouse, France

[6] Laboratoire d'Excellence 'TOUCAN-2', Toulouse, France

[7] Singapore Immunology Network, Agency for Science, Technology and Research, Singapore 138648, Singapore

[8] Institut Pasteur, Cytometry and biomarkers platform, F75015, Paris, France.

[9] Shanghai Institute of Immunology, Shanghai JiaoTong University School of Medicine, 280 South Chongqing Road, Shanghai 200025, China

[10] Translational Immunology Institute, SingHealth Duke-NUS Academic Medical Center, 20 College Road, Discovery Tower Level 8, Singapore 169856, Singapore

*Correspondence: herve.bourhy@pasteur.fr

Abbreviations: *BST2* = Bone Marrow Stromal Cell Antigen 2; CCL = C-C Motif Chemokine Ligand; CNS = central nervous system; *C15orf48* = Chromosome 15 Open Reading Frame 48; DENV = dengue virus; *DYNLL* = Dynein Light Chain; EMCV = Encephalomyocardis virus; hiAstrocytes = human induced astrocytes; hiMacs = human induced macrophage-like cells; hiMicors = human induced pluripotent stem cell-derived microglia-like cells; hiNeurons = human induced neurons; hNSC = human neural stem cells; IAV = influenza A virus; *IDO1* = Indoleamine-Pyrrole 2,3 Dioxygenase; IFI35 = Interferon Induced Protein 35; IFIT = IFN-induced protein with tetratricopeptide repeats; IFITM1 = IFN-induced transmembrane protein 1; IFN = interferon; IL32 = Interleukin 32, JAK = Janus Kinase; JEV = Japanese encephalitis virus; LCMV = lymphocytic choriomeningitis virus; iPSCs = induced pluripotent stem cells; *MMP9* = Matrix Metallopeptidase 9; *MX1* = MX Dynamin Like GTPase 1; M-protein = matrix protein; NF-κB = Nuclear Factor Kappa B; *OAS1* = 2'-5'-Oligoadenylate Synthetase 1; P-protein = phosphoprotein; PNS = peripheral nervous system; RABV = rabies virus; *SAMHD1* = SAM And HD Domain Containing Deoxynucleoside; sc RNA-Seq = single cell RNA sequencing; SOD2 = Superoxide Dismutase 2; STAT = Signal Transducer And Activator Of

Transcription Protein; *S100A11* = S100 Calcium Binding Protein A11, *TGFBR2* = Transforming Growth Factor Beta Receptor 2; *TLR4* = Toll Like Receptor 4; UMAP = Uniform manifold approximation and projection; WNV = West Nile virus; ZIKV = Zika virus

Summary

During homeostasis, intercellular communication among CNS cell types ensures neuroprotection whereas dysfunctional communication contributes to disease. Rabies virus (RABV) induces encephalomyelitis in humans, but the underlying cause of this fatal disease is still poorly understood. Here, we performed single cell RNA sequencing (sc RNA-Seq) on a RABV-infected human 2D CNS model, comprising stem cell-derived neurons, astrocytes, stem-like cells, and microglia, to study how RABV interferes with intra- and intercellular signalling pathways. Our results reveal that using a low MOI of canine RABV strain Tha strongly activates whereas a high MOI strongly restricts immune signalling cascades in infected but also bystander neurons and astrocytes. Further, viral immune evasion of glial cells was partly dependent of conserved residues of viral P- and M-proteins. Most importantly, similar transcription profiles were observed in infected and non-infected bystander hiNeurons and hiAstrocytes suggesting that RABV exploits intercellular communication pathways in the virus-infected CNS.

Keywords : Rabies, viral encephalitis, neurons, astrocytes, microglia, single cell RNA-Seq, intercellular communication, viral evasion

Abstract

Rabies is a neglected tropical disease of mammals and still causes major public health concerns worldwide. Although rabies is preventable by vaccination, RABV still contributes to 60.000 human deaths due to fatal encephalomyelitis every year. Comparably little is known about molecular mechanisms of dysfunctional intra- and intercellular signalling cascades mediated by RABV in the infected human CNS. Here, single-cell RNA sequencing (sc RNA-Seq) of 19.374 single-cell RNA transcription profiles of RABV-infected stem cell-derived 2D CNS co-cultures reveals that the canine RABV strain Tha productively infects neurons, astrocytes, precursors, and stem-like cells but fails to infect human microglia *in vitro*. Further, Tha universally inhibited intracellular signalling pathways such as TLR7-8-9-mediated signalling, the MyD88 signalling cascade, the endosomal-vacuolar pathway, and microtubule binding in neurons, astrocytes, and microglia. Strikingly, Tha specifically induced autophagy in neurons, interfered with neurotransmitter release, and transmission and protein interactions at synapses. In astrocytes, Tha inhibited phagosomal-lysosomal fusion, induced PINK1-PRKN-mediated mitophagy, activated the NLRP3 inflammasome, and modified ion transport activities. Although microglia were not susceptible towards Tha infection, Tha induced MAPK1-MAPK3 signalling in microglia and triggered the induction of interferons, *CXCL10*, and *IDO1*. Surprisingly, infected, and non-infected bystander neurons and astrocytes exhibited similar transcription profiles, suggesting that exploitation of intracellular signalling pathways does not necessarily require viral entry. Overall, our results suggest that Tha interferes with intercellular communication pathways in the human CNS. Given the vast differences in RABV-modulation of signalling pathway between CNS cell types, we strongly urge to study cell type-specific pathogen host interactions for neurotropic infections, rather than generalizing the diverse nature of CNS cell types.

Introduction

Rabies is a zoonotic disease caused by viruses belonging to the Lyssavirus genus, including RABV, which is still causing approximately 60.000 human deaths annually (Fooks et al., 2017). Rabies is mostly transmitted to humans upon the bite of a rabid dog: RABV, present in the saliva of the infected animal, enters, and replicates locally in the muscle, and subsequently spreads to the peripheral nervous system (PNS) via the neuromuscular junction. From the infected muscles, centripetal propagation of RABV occurs via retrograde trans-neural transport along the motor route until the virus successfully enters the central nervous system (CNS) (Hemachudha et al., 2013). Despite several defense mechanisms present in the human CNS (Griffin, 2003), RABV evolved several strategies to escape innate and adaptive immune responses of the host (Lafon, 2008, 2011; Roy and Hooper, 2008; Ito, Moseley and Sugiyama, 2016). Those viral evasion mechanisms counteract the host response by ensuring neuronal integrity, limiting apoptosis (Baloul and Lafon, 2003; Baloul, Camelo and Lafon, 2004; Kassis et al., 2004), and restricting neuroinflammation (Lafon, 2005) in the virus-infected CNS ultimately leading to its fatal outcome.

Recently, the strict neuron-specific tropism of RABV has been questioned (Potratz, L. M. Zaeck, et al., 2020; Potratz, L. Zaeck, et al., 2020) and increasing evidence support infection of astrocytes (Potratz, L. Zaeck, et al., 2020) and Schwann cells (Potratz, L. M. Zaeck, et al., 2020) *in vivo*, depending on the viral strain and the infection route used (Potratz, L. Zaeck, et al., 2020). Despite recent advances made in re-defining RABV tropism (Potratz, L. M. Zaeck, et al., 2020; Potratz, L. Zaeck, et al., 2020), mechanistic processes underlying viral susceptibility remain to be elucidated. Overall, the human CNS remains an extremely complex organ with diverse and cell type-specific immune responses including numerous dynamic interactions between different cell populations (Yang and Zhou, 2019). In recent years, advances in high-throughput sequencing technologies, referred to as single cell RNA sequencing (sc RNA-Seq), allow to sequence information from thousands of individual cells independently. For the first time, these technologies allow to gain a deeper and more detailed understanding of multiplex processes, for instance studying intracellular cell type-specific responses and the intercellular crosstalk during homeostasis and disease in complex systems such as the human CNS (Kalisky et al., 2018). Still, sc RNA-Seq data of RABV-infected human CNS models are missing although they might elucidate the roles of glial cells during rabies pathogenesis and, in a wider sense, during neurotropic infections.

To our knowledge, only one sc RNA-Seq experiment was conducted so far to elucidate cell type-specific responses towards RABV infection using the attenuated and glycoprotein-deficient vaccine strain SAD RABV strain (SADΔG) (Huang and Sabatini, 2020). This experiment aimed at elucidating inflammatory responses taking place in the dorsal raphe nucleus of SADΔG-infected mice (Huang and Sabatini, 2020). The authors identified viral mRNA transcripts predominantly in 5-HT neurons, and to lesser extents in microglia, non-resident myeloid cells, and astrocytes. Therefore, Huang and colleagues hypothesised that the detection of RABV transcripts in non-neural cells is due to phagocytosis of mRNA-containing material released from infected neurons. Further, the authors provided evidence that SADΔG downregulates metabolic processes and neurotransmission in neurons and glial cells. Further, microglia and infiltrating $CD4^+$ T cells responded to SADΔG infection with type I and II interferon (IFN)-mediated antiviral responses (Huang and Sabatini, 2020). Nevertheless, the human and murine CNS are relatively different in terms of cell type proportions and gene expression (Hodge et al., 2019) questioning the relevance to extrapolate data directly from SADΔG-infected mice to natural RABV infection in humans.

RABV is known to modulate Janus Kinase (JAK) - Signal Transducer And Activator Of Transcription Protein (STAT) (Wiltzer et al., 2012, 2014; Ben Khalifa et al., 2016; Sonthonnax et al., 2019) and MAPK signalling cascades (Besson et al., 2017, 2019; Liu et al., 2020), two crucial pathways underlying cytokine signalling (Kennedy and Silver, 2016), neuroprotection, and intercellular communication (Hwang and Bergmann, 2019). Even nowadays, our understanding how glial cells and neurons interact with each other to shape the distinctive immune responses of the CNS remains limited. Investigating how RABV infection alters the cellular crosstalk in the virus-infected CNS is crucial to understand how RABV successfully evades glial surveillance in the virus-infected CNS.

Here, we investigate cell type-specific transcriptional profiles of stem cell-derived CNS cultures upon infection with the canine RABV strain Tha and the less virulent Th2P-4M. The latter is unable to evade Nuclear Factor Kappa B (NF-κB) and JAK-STAT signalling pathways due to mutations inserted in viral P- and M-proteins (Sonthonnax et al., 2019). Using two different multiplicities of infection (MOI 0.5 and 5) and two different viral strains (Tha and Th2P-4M), we were able to identify cell type-specific signalling pathways that depend on viral load and P- and M-protein controlled processes.

We provide evidence that Tha induces autophagy and modulates neurotransmission in human neurons, whereas the same inhibits autosome-lysosome fusion and induces mitophagy in human astrocytes. Although Tha was not able to productively infect human microglia, Tha-induced expression of interferons (IFNs), *CXCL10*, and *IDO1* in human microglia. Further, we provide evidence that Tha (MOI 0.5) strongly activates whereas Tha (MOI 5) strongly restricts immune signalling cascades in infected but also bystander neurons and astrocytes and that viral immune evasion of glial cells was strongly dependent on viral P- and M-proteins. Strikingly, vast similarities were observed in infected and non-infected bystander neurons and astrocytes, suggesting that Tha exploits intracellular signalling pathways not by viral entry but rather by interference with cell-to-cell communication in the human CNS.

Results

Specific transcriptional profiles across neural cell lineages are not affected by RABV infection

Prior to infection with Tha or Th2P-4M, we co-cultured human NSC derived primary neurons (hiNeurons) and astrocytes (hiAstrocytes) for three consecutive weeks with human induced macrophage-like cells (hiMacs) to obtain human induced pluripotent stem cell-derived microglia-like cells (hiMicros). Forty-eight hours post-infection, dead cells were removed, and single cells were sequenced according to the 10x pipeline (Fig 1A). Total cell counts per biological condition ranged between 3,633 and 6,055 cells (Fig 1B).

The cellular fate of human CNS cell types was investigated by a score and gate approach (details in Materials and Methods) using published gene signatures (Table S1); which revealed the presence of human neurons, astrocytes, microglia, precursors, and stem-like cells (Fig 1C, S1 Fig, S1 Table). These findings were further validated via fluorescence microscopy using cell type-specific antibodies (S2 Fig, S2 Table). The most common cells in the cultures were neurons (60%), followed by similar proportions of astrocytes (17%) and stem-like cells (16%), microglia (4%), and precursors (2%) (Fig 1D).

Further, we performed a pseudotimed trajectory analysis to unveil the cell differentiation state, through cell transcriptomics kinetics, on a path known as the pseudotime (Material and Methods). The pseudotimed trajectory analysis revealed stem-like cells at the root of the

differentiation process (S3 Fig). Next, the path divides into two different cell populations with distinct transcriptome profiles composed of hiAstrocytes and hiNeurons (S3 Fig). As expected, hiMicros clustered far from hNSC-derived cells along the pseudotime, potentially due to their distinct transcriptome profile and different cellular origin compared to the beforehand described cells (S3 Fig). Further, trajectory analysis revealed 15 milestones (T1-T15, S3 Fig) which reflect the differentiation of stem-like cells to mature CNS cell types *in vitro*. Interestingly, different milestones were identified for hiNeurons (T2–T4), hiAstrocytes (T8-T11), and hiMicros (T13-T15), which might present cellular subtypes, different activation, or infection states. Investigating the role of Tha or Th2P-4M in cellular differentiation or transcriptome changes exhibited that neither Tha nor Th2P-4M infection induced a transition in the cellular states among the trajectory analysis path (S3C Fig) compared to non-infected cells (S3A Fig). Hence, we conclude that neither Tha nor Th2P-4M tremendously interfere with cellular differentiation and cellular states (Fig S3).

To distinguish infected from non-infected cells, we established a threshold to identify 'non-infected' cells to correct for low cell counts of viral transcripts. If the sum of viral transcripts (N-, P-, M-, G-, or L-genes) exceeded 17 reads/cell cells were counted as 'infected', if the sum of viral transcripts did not exceed 17 reads/cell cells were referred to as 'non-infected'. Interestingly, no viral mRNAs were found in cells identified as microglia (Fig 1D, S3 Fig). Quantification of infected cells in the different conditions showed that Tha infected around 21.6% of total cells per condition whereas Th2P-4M infected around 41.4% of total cells per condition (MOI 0.5, S3 Table). Infecting cells with the virulent Tha using a ten times higher MOI (MOI 5) resulted in the infection of 34.1% of cells (S3 Table).

In average, most cells infected by Tha (average calculated based on both biological conditions, Tha MOI 0.5 and MOI 5) were hiNeurons (61%), followed by stem-like cells (19%), hiAstrocytes (17%), and precursors (3%). Similarly, Th2P-4M infected mostly hiNeurons (69%), followed by stem-like cells (14%), hiAstrocytes (14%), and precursors (3%, Fig 1E). Further we compare the proportions of infected cell types per biological condition, to assess if a higher MOI or mutations introduced in viral P- or M-proteins significantly change viral tropism. Comparing the proportions of infected cell types between Tha (MOI 0.5) and Tha (MOI 5) revealed no significant difference between the proportions of infected cell types suggesting that viral tropism is independent of viral load (Chi2 test p-value=0.3536, Fig 1E). Next, comparing the proportions of infected cell types between Tha (MOI 0.5) and Th2P-4M (MOI 0.5) infected cultures exhibited that Th2P-4M infected significantly more neurons (69.2 %) compared to Tha (61.9 %, Chi2 test p-value=0.0003, Fig 1E).

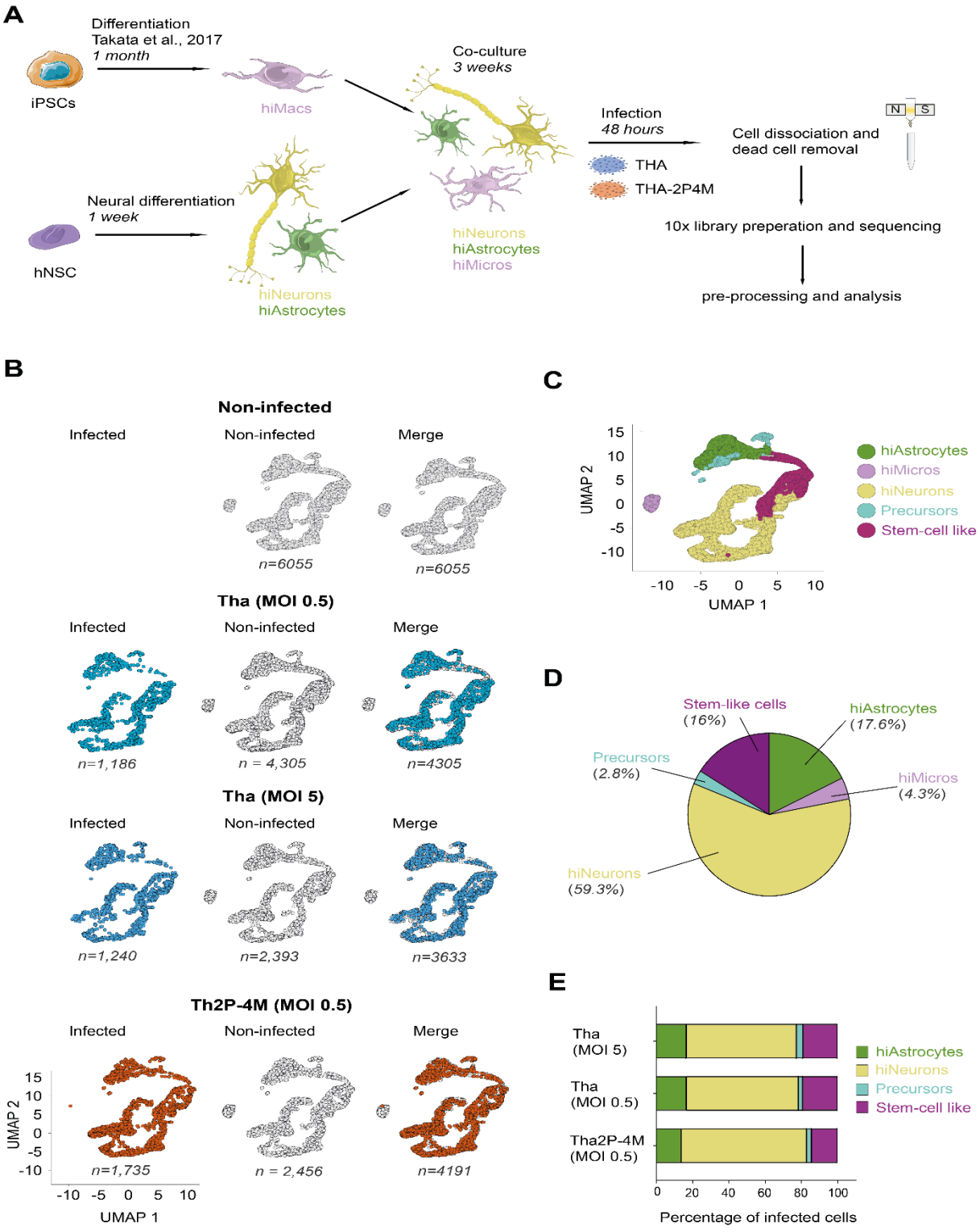

Fig 1. Human stem cell-derived CNS cell types revealed distinct transcriptome profiles and different susceptibilities towards Tha and Th2P-4M infection *in vitro*. (A) Experimental pipeline including differentiation of stem cells, infection experiments, and 10x sc RNA-Seq pipeline. (B) UMAP plots presenting infected and non-infected cells per biological condition. (C) UMAP presenting sc RNA-Seq sequencing data showing presence of hiNeurons, hiAstrocytes, hiMicros, precursors, and stem-like cells. Cellular fate was determined by a score and gate approach using published gene signatures. More information about the used signatures can be found in S1 Fig and S1 Table. (D) Pie chart presenting the proportions of hiNeurons, hiAstrocytes, hiMicros, precursors, and stem-like cells in cultures.

Percentages were calculated by taking the average proportions over the three independent replicates. (E) Histogram showing the proportions of infected cells upon infection by Tha (MOI 0.5), Tha (MOI 5), and Th2P-4M (MOI 0.5). Whereas Tha infected equal proportions of cell populations upon different MOIs (Chi2 test p-value=0.3536), Th2P-4M revealed a significant different viral tropism (Chi2 test p-value=0.0003). (A-E) Single cell sequencing experiments were performed three times (n=3) independently.

Glial cells and in particular microglial cells exhibit a specific transcriptome profile during RABV infection

To further understand how RABV infection modulates the transcriptome profiles of CNS cell populations, a pathway-centric approach was used. In detail, more than 12,000 published pathways (from KEGG, Reactome, Gene Ontology and MsigDB) were evaluated, and pathways which were differentially regulated (adjusted p-value<0.05) in at least one of the cell types were considered. A total of 308 pathways of interest were identified to be implicated in autophagy (n=1), cell communication (n=12), cell cycle (n=5), cell death (n=14), cell growth (n=4), cytoskeleton (n=16), DNA (n=11), endocytosis (n=11), immune response (n=84), intracellular transport (n=10), mitochondria (n=11), neural function (n=39), oxidation (n=2), protein modification (n=17), RABV receptors (n=3), signal transduction (n=8), transcription (n=16), transmembrane transport (n=24), vesicle transport (n=2), virus cycle (n=4), and virus sensing (n=17) (Fig 2, Additional File 1). Results obtained on some of the major pathways of interest in the 3 different neural cell types are reviewed below.

Investigating RABV replication cycle revealed that Tha (MOI 0.5) did not significantly modulate pathways involved in the virus life cycle (R-HSA-9694614, R-HSA-168316, R-HSA-168268). However, by increasing the MOI ten-fold, Tha (MOI 5) significantly upregulated pathways such as Assembly of Viral Components at the Budding Site (R-HSA-168316) and Virus Assembly and Release (R-HSA-168268) in hiAstrocytes and hiNeurons but not in hiMicros.

Pathways related to endocytosis were also investigated to assess if RABV life cycle positively correlates with endosomal pathways. Strikingly, Tha (MOI 0.5) restricted MyD88- (R-HSA-975155) and clathrin-dependent endosomal pathways (R-HSA-8856825) in all three CNS cell types (hiAstrocytes, hiNeurons, and hiMicros). Interestingly, and in contrast to Tha (MOI 0.5), Th2P-4M induced endosomal pathways such as the endosomal-vacuolar pathway (R-HSA-1236977) and the Cross-presentation of soluble exogenous antigens pathway (R-HSA-1236978) among all three CNS cell types. This suggests the importance for conserved residues among P- and M-proteins in the inhibiting antigen presentation pathways in neurons and astrocytes. Nevertheless, infecting cells with a ten-fold higher MOI (Tha MOI 5) also induced the endosomal-vacuolar pathway (R-HSA-1236977) in all three CNS cell types.

In hiAstrocytes, higher viral concentrations (MOI 5) strongly induced endosomal pathways, particularly Clathrin-mediated endocytosis (R-HSA-8856828) and Fc gamma receptor (FCGR) dependent phagocytosis (R-HSA-2029480). Furthermore, Tha (MOI 5) induced Prevention of phagosomal-lysosomal fusion (R-HSA-9636383) in hiAstrocytes suggesting that phago-lysosomal pathway might be defective in efficiently degrading viral particles. In hiMicros, at the opposite, the ER-Phagosome pathway (R-HSA-1236974) and the Cross-presentation of soluble exogenous antigens pathway (R-HSA-1236978) are induced upon high viral concentrations (MOI 5). Thus, hiMicros seem to specially induce phagocytotic pathways leading to the presentation of viral antigens on the microglial cell surface.

Further, pathways implicated in transmembrane transport were mainly induced in hiAstrocytes and hiNeurons upon Tha (MOI 0.5 and 5) and Th2P-4M infection, whereas both viruses

induced only limited pathways associated with intracellular transport in hiMicros. Remarkably, Tha particularly induced ion channel transport (R-HSA-425561, R-HSA-983712), cation channel activity (GO:0008324) and transmembrane transporters (GO:0015075) in hiAstrocytes.

Looking at virus-induced immune responses, Tha (MOI 0.5) induced little immune responses in CNS cell types compared to Th2P-4M. Strikingly, the strongest immune response towards Tha infection (MOI 0.5) was observed in hiMicros suggesting an important role of microglia in mediating antiviral responses during RABV infection: most of the Tha-induced immune pathways in hiMicros were implied in MAPK pathways (R-HSA-5683057, R-HSA-5684996) and IFN signalling (M5911, M5913, R-HSA-913531). Similarly, those pathways were also activated in hiAstrocytes but only upon a higher viral load (MOI 5). Consequently, hiMicros might sense lower concentrations of viral particles compared to hiAstrocytes. Upon a higher MOI, Tha activated interleukin 1 processing and signalling (R-HSA-9020702, R-HSA-446652, R-HSA-449147, GO:0005149, R-HSA-448706), chemokine signalling (R-SSC-380108, GO:0048020, GO:0008009, GO:0042379), and TNF signalling (R-HSA-5676594, R-HSA-5668541, R-HSA-5357786, R-HSA-5669034, M5890) in hiAstrocytes and hiMicros. Interestingly, Tha (MOI 5) restricted most of the immune pathways in hiNeurons. Altogether, low viral concentrations of pathogenic Tha did not induce evident immune responses in hiNeurons and hiAstrocytes whereas hiMicros induced inflammatory signalling cascades upon infection. Increasing the MOI, however, induced astrocyte-mediated immune responses. In contrast to Tha, Th2P-4M specifically activated TNF (R-HSA-5357905, R-HSA-75893), IL17 (R-HSA-448424), IL20 (R-HSA-8854691), and IL21 signalling pathways (R-HSA-9020958) in all three distinct CNS cell types. Comparing Tha- and Th2P-4M-mediated immune responses (MOI 0.5) revealed that Th2P-4M, in contrast to Tha, additionally induced pathways such as Class I MHC-mediated antigen processing (R-HSA-983170, R-HSA-1236975, R-HSA-983169), IFN-γ signalling (R-HSA-877300), NLRP3 inflammasome signalling pathways (R-HSA-844456), and chemokine signalling (GO:0019958, GO:0048020) in all three CNs cell types. This suggests that viral P- and M-proteins of Tha are crucial in evading the beforementioned pathways.

Surprisingly, low viral concentrations of pathogenic Tha (MOI 0.5) induced little cytoskeletal changes in all three cell types. The least modifications were observed in hiAstrocytes and hiNeurons, in which Tha (MOI 0.5) only induced RHO GTPase Effectors. In contrast, Tha (MOI 0.5) induced pathways implied in microtubule minus-end binding (GO:0051011), cytoskeletal protein binding (GO:0008092), and the regulation of the actin cytoskeleton (M18306) in hiMicros. Higher viral titers specifically induced changes in the astrocyte actin cytoskeleton (GO:0051015, GO:0008092, M18306, GO:0003779), whereas the same caused changes in the microtubule organization including its interactions with dyneins (GO:0051010, GO:0070840, GO:0045504) in hiMicros.

Th2P-4M differentially regulated less pathways involved in the re-organization of the actin and microtubule cytoskeleton in hiAstrocytes and hiMicros compared to Tha infection leading to the hypothesis that viral M- and P-proteins are involved in cytoskeletal organization.

Overall, pathways associated to mitochondria biogenesis or signalling were poorly modulated upon either Tha or Th2P-4M infection (MOI 0.5) in contrast to infection with Tha at a ten-fold higher MOI. Indeed, increasing the MOI by ten-fold strongly modulated mitochondria-driven pathways. In detail, Tha strongly restricted pathways involved in mitochondria functions in hiMicros and hiNeurons, whereas the same pathways in hiAstrocytes were activated. More specifically, pathways implied in mitochondrial protein import (R-HSA-1268020), mitochondrial

translation (R-HSA-5368287), and PINK1-PRKN-mediated mitophagy (R-HSA-5205685) were strongly induced in hiAstrocytes, contrasting observations made in hiNeurons and hiMicros.

We next investigated pathways implied in neural function. These pathways were less modulated by Tha and Th2P-4M at MOI 0.5 than by challenging cells with more viral particles of pathogenic Tha (MOI 5). More specifically, Tha universally dampened pathways involved in the release of serotonin (R-HSA-181429), norepinephrine (R-HSA-181430), glutamate (R-HSA-210500), and dopamine (R-HSA-212676). Upon a higher MOI, Tha induced pathways related to dopamine receptors (R-HSA-390651), neurotransmitter clearance (R-HSA-112311), and axon growth stimulation (R-HSA-209563). Interestingly, Tha (MOI 5) induced Neurotransmitter uptake and metabolism in glial cells (R-HSA-112313) pathway in hiMicros. Further, Th2P-4M infection specifically modulated pathways involved in the structure of the post-synapse (GO:0099186, GO:0098973, GO:0098918), suggesting roles for viral P and M proteins in regulating post-synaptic structure and potentially its activity.

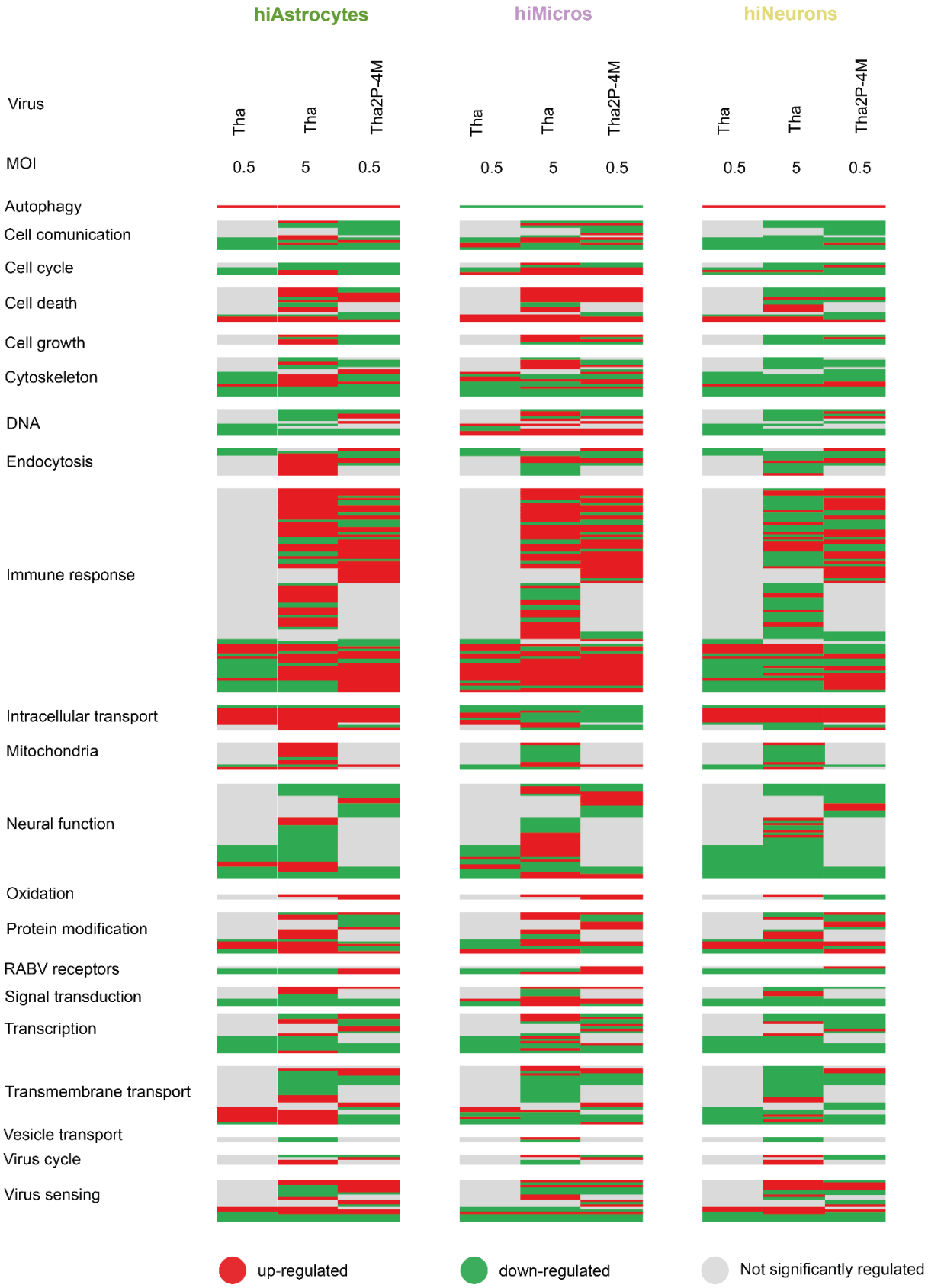

Fig 2 | Tha differentially regulates immune responses, intracellular and transmembrane transport, and mitochondrial functions in distinct CNS cell types *in vitro*. Heatmap showing differentially regulated pathways upon Tha and Tha2P-4M infection. Up- or down-regulated pathways present pathways significantly up- (coloured in red, adjusted p-value<0.05) or down-regulated (coloured

in green, adjusted p-value<0.05) in contrast to pathways which are not significantly regulated (coloured in grey, adjusted p-value>0.05). The indicated biological conditions (indicated by different viral strains and MOIs used) corresponds to infected cells (cells containing viral transcripts above threshold) in the respective condition. A detailed list of investigated pathways can be found in additional file 1. Colour scaling was performed by comparing expression fold changes of gene signatures upon infection to the respective non-infected cell type. Cells are color-coded by cellular fate, following the colour scheme used in Fig 1. MOI = multiplicity of infection.

Tha equally modulates transcription profiles of infected and non-infected bystander cells

In a next step, we took a closer look at gene expression of various genes involved in the differentially modulated pathways described beforehand (Fig 2). In detail, we investigated gene expression of 100 DEGs in hiNeurons, being involved in cytoskeletal arrangement (n=29), immune functions (n=61), and neural function (n=8, Fig 3).

Overall, non-infected hiNeurons robustly expressed immune genes coding for IFIT (*IFIT1, IFIT2, IFIT3*) and IFITM (*IFITM1, IFITM3*) genes, *SOC2*, *FOXO1*, and *JUN* (Fig 3A). Non-infected hiAstrocytes showed specifically a high expression of immune genes coding for *CLSPN*, *IFIT2*, *IFITM1*, *CXCL10*, *LAG3*, and *LIFR* (Fig 3B) whereas non-infected hiMicros strongly expressed. *EGR1*, *FOXO1*, *HLA-A*, *TGFBR2*, *ITPRY*, *IFI6*, *MMP9*, *S100A11*, *SOCS2*, *IL32* (Fig 3C).

Altogether, the different MOIs used during this study induced tremendous differences in the transcriptome profiles: whereas Tha (MOI 0.5) strongly induced genes implicated in cytoskeletal re-arrangement and immune responses in hiNeurons and hiAstrocytes, a higher viral load of Tha (MOI 5) downregulated the same (Fig 3A-B). Further, RABV infection of hiNeurons and hiAstrocytes, revealed overall a strong similarity between transcription profiles of infected and non-infected bystander cells, suggesting viral interference with intercellular signalling pathways.

As mentioned before, genes involved in cytoskeletal processes were mostly induced in Tha (MOI 0.5) infected hiNeurons (*CRYAB*, *ECT2*, *EPB41L3*, *DYNLL1*, *DYNLL2*, *KCNMA1*, Fig 3A) and hiAstrocytes (*CRYAB*, *ECT2*, *EPB41L3*, *SGO2*, *DYNLL1*, *NCALD*, Fig 3B). In contrast, a higher viral load strongly downregulated expression of genes involved in the cytoskeletal organization of hiNeurons (*PLK1*, *TPM2*, *TAGLN*, *NCALD*, Fig 3B) and hiAstrocytes (*PLK1*, *KCNMA1*, Fig 3B). Further, Tha and Th2P-4M (MOI 0.5) both specifically induced expression of Dynein Light Chain 1 (*DYNLL1*) and 2 (*DYNLL2*) in hiNeurons (Fig 3A). Interestingly, hiNeurons which were challenged with virus, but which did not get productively infected (hereafter referred to as 'bystander cells') downregulated *DYNLL1* and *DYNLL2* after Tha and Th2P-4M infection in contrast to virus-infected hiNeurons. The same discrepancy between *DYNLL1* and *DYNLL2* expression was observed between infected and bystander hiAstrocytes upon Tha infection (MOI 0.5, Fig 3B). Thus, *DYNLL1* and *DYNLL2* expression seems to be directly induced by RABV upon viral entry and intracytoplasmic replication rather than via secondary signalling cascades resulting from the infection of neighbouring cells. Surprisingly, infecting cultures with a high viral load of Tha (MOI 5), however, modulated *DYNLL1* and *DYNLL2* expression in hiNeurons less compared to infection with a lower viral load (MOI 0.5).

Tha activated immune pathways in hiNeurons and hiAstrocytes at a low MOI (Fig3A-B). More specifically, Tha (MOI 0.5) induced expression of several immune genes such as Interferon Induced Protein With Tetratricopeptide Repeats 1-3 (*IFIT1, IFIT2, IFIT3*), Interferon Induced

Transmembrane Protein 1 (*IFITM1, IFITM3*), C-C Motif Chemokine Ligand 2 (*CCL2*) and 3 (*CCL3*), Inositol 1,4,5-Trisphosphate Receptor Type 2 (ITPR2), and IFN-γ receptors (*IFNGR1* and *IFNGR2*) in hiNeurons (Fig 3A). Gene expression of the same genes was strongly restricted in infected and bystander hiNeurons upon infection with Tha at a higher MOI. Similar effects were observed in hiAstrocytes, where Tha (MOI 0.5) increased expression of *CCL2*, *CCL3*, *ITPR2*, Lymphocyte Antigen 96 (*LY96*), Interferon Alpha Inducible Protein 27 (*IFI27*) and 6 (IFI6), C-X-C Motif Chemokine Ligand 10 (*CXCL10*), and Complement C3a Receptor 1 (*C3AR1*). Likewise, Tha dampened gene expression of the same at a higher MOI (Fig 3B). In contrast to hiNeurons and hiAstrocytes, comparing transcription profiles of hiMicros infected with a low and a high MOI revealed less profound differences. Upon a low MOI, Tha revealed a widely heterogenous expression of immune genes. Although genes coding for Toll Like Receptor 4 (*TLR4*), Bone Morphogenetic Protein 2 (*BMP2*), and Human Leucocyte Antigen DRB1 (HLA-DRB1) were strongly induced upon Tha (MOI 0.5) infection, gene expression of Heat Shock Protein 90 Alpha Family Class A Member 1 (*HSP90AA1*), *CXC10*, *IDO1*, and NFKB Inhibitor Alpha (*NFKBIA*) was strongly restricted (Fig 3C). Overall, Tha (MOI 5) exhibited a stronger downregulation of immune genes compared to Tha (MOI 0.5). Nevertheless, some genes showed a different tendency, namely a strong induction upon infection at a higher MOI, such as IFIT genes (*IFIT1-3*), *IDO1*, *CXCL10*, *TGFB3*, and *AGER*.

Strikingly, Th2P-4M strongly mounted immune gene expression in hiAstrocytes and hiMicros compared to the respective non-infected cells (Fig 3B-C), whereas immune gene expression was only modestly modulated in Th2P-4M-infected hiNeurons (Fig 3A). This suggests that viral P – and M-proteins are crucial to evade glial immune responses, potentially by interfering with cell-to-cell communication.

Investigating neural function revealed that Tha (0.5) induced expression of GABA Gamma-Aminobutyric Acid Type A Receptor Subunit Beta2 (*GABRB2*) and Cholinergic Receptor Nicotinic Alpha 5 Subunit (*CHRNA5*) in hiNeurons. Further, Tha (MOI 0.5) downregulated expression of Chromosome 15 Open Reading Frame 48 (*C15orf48*) in non-infected and bystander hiNeurons and Astrocytes, whereas a higher MOI resulted in induction of C15orf48 expression.

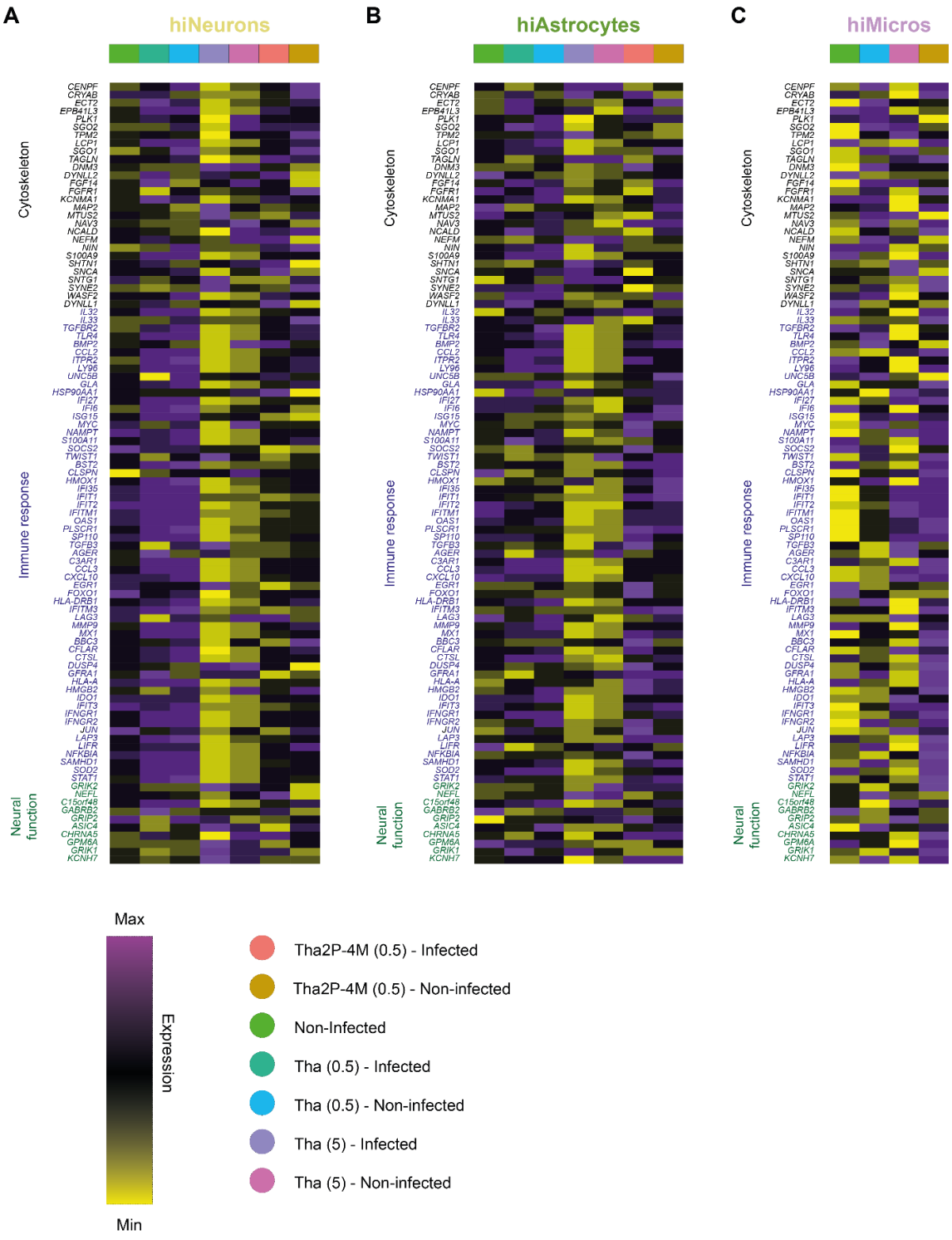

Fig 3 | Tha similarly modulates the cytoskeleton, immune responses, and pathways implicated in neural function of infected and non-infected bystander hiNeurons and hiAstrocytes. (A) Differential gene expression of hiNeurons upon Tha and Th2P-4M infection. (B) Differential gene expression of hiAstrocytes upon Tha and Th2P-4M infection. (C) Differential gene expression of hiMicros upon Tha and Th2P-4M infection. (A-C) Stem-cell derived co-cultures consisting of hiNeurons, hiAstrocytes, and hiMicros were infected with Tha (MOI 0.5 and 5) or Th2P-4M (MOI 0.5). Gene expression was investigated in the distinct cell populations via sc RNA-Seq at 48 hours post-infection following the pipeline indicated in Fig 1A. Cells are color-coded by cellular fate, following the colour scheme used in Fig 1.

Discussion

Here, we present a 2D *in vitro* model of the human brain to study molecular mechanisms underlying CNS cell communication in RABV infection. We investigated 19.374 single cell transcription profiles from mainly neurons (60%), astrocytes (17%), stem-like cells (16%) and microglia (4%) during RABV infection. Here, we reveal profound differences in intra- and intercellular signalling pathways of CNS cell types during Tha infection. Whereas Tha induces autophagy and alters neurotransmission of hiNeurons, Tha inhibits phagosomal-lysosomal fusion in hiAstrocytes and drastically impairs mitochondrial functions of hiAstrocytes. Further, and although we show that hiMicros are not susceptible towards Tha infection *in vitro*, hiMicros induce gene expression of *CXCL10*, *IDO1*, and IFIT genes upon infection with Tha (MOI 5). Surprisingly, we show that RABV infection interferes with intercellular communication in the CNS, altering immune responses of infected and bystanding hiNeurons and hiAstrocytes to similar extents. Therefore, we claim that RABV drastically impairs intra- and intercellular signalling cascades underlying immune responses in the virus-infected human CNS.

Investigation of cell type-specific intracellular signalling cascades linked to cytoskeletal rearrangements revealed that Tha (MOI 5) modulates the actin cytoskeleton of hiAstrocytes whereas Tha induced dynein-dependent microtubule reorganization of hiMicros. More specifically, Tha (MOI 0.5) induced expression of *DYNLL1* and *DYNLL2* in hiNeurons. This downregulation was independent of conserved residues of P- and M-proteins implied in STAT antagonism but dependent on viral entry and replication. This is in line with previous findings which showed that viral P- and L-proteins contain cytoplasmic DYNLL1 binding motifs, mediating the interaction with transcription enhancer DYNLL1, subsequently resulting in modulated cytoskeletal organization and primary viral transcription (Jacob et al., 2000; Raux, Flamand and Blondel, 2000; Bauer et al., 2015). Taken together, we hypothesise that viral proteins exploit the cytoskeleton not only of hiNeurons but also of hiAstrocytes to enable efficient transport of viral proteins via interference with DYNLL1 and DYNLL2 proteins, a crucial step to ensure productive infection and dissemination in the brain using the neurons and astrocytes networks.

Apart from cytoskeletal rearrangements, Tha (MOI 5) strongly modifies mitochondrial functions in hiAstrocytes in contrast to hiNeurons and hiMicros. In detail, Tha (MOI 5) interfered with mitochondrial protein import and translation, induced the release of apoptotic factors from mitochondria, and activated PINK1-PRKN-mediated mitophagy. Similarly, recent results provide evidence that Zika virus (ZIKV) infection induces oxidative stress and mitochondrial failure in iPSC-derived human astrocytes (Ledur et al., 2020). Additionally, our results provide evidence that Tha (MOI 5) dampens *C15orf48* expression, a small protein which expression correlated to genes involved in the regulation of cytokine activity, interferon signalling, and leukocyte chemotaxis (Lee et al., 2021). Very recently, ZIKV and dengue virus (DENV) infection was shown to lower mitochondrial membrane potential and ROS production via Modulator of cytochrome C oxidase during Inflammation (MOCCI, also referred to as *C15orf48*). Reduced ROS production, in turn, supresses pro-inflammatory cytokine and IFN responses, although this process is mitigated by the robust antiviral activity of miR-147b which is induced via MOCCI upon viral infection (Lee et al., 2021). Altogether, complementary roles of MOCCI and miR-147b are believed to mediate maximal host protection by inhibiting inflammation and viral replication (Lee et al., 2021). Consequently, we suggest that Tha might dampen MOCCI expression to reduce antiviral activities via miR-147b. Although we do not completely understand how Tha interferes with mitochondrial functions in astrocytes, a growing consensus states that integer and functional mitochondria are crucial for inflammatory activation (Sugimoto et al., 2016). Hence, we urge further research to investigate the molecular

mechanisms shaping RABV interference with mitochondrial functions in astrocytes and its potential role in viral-mediated immune evasion.

Additionally, Tha induced IL-1, TNF, the NLRP3 inflammasome, the IL-6-JAK-STAT3 signalling pathway, *CXCL10* and *IDO1* expression in hiMicros. This underlines the importance of microglia in sensing the CNS environment and rapidly reacting to changes during viral CNS infections (Chhatbar and Prinz, 2021), even if they are not infected. Nevertheless, we suggest that the capability of Tha (MOI 5) to dampen inflammatory responses in hiNeurons and hiAstrocytes (Fig 3) limits the extent of microglial activation compared to other neurotropic infections which present widespread microglial activation such as during herpes simplex viruses 1 (HSV) encephalitis (Esiri, Drummond and Morris, 1995).

Despite the heterogenous cellular diversity presented by the model, we need to admit that cellular abundances differ strongly from cellular abundances found in the human brain: it is believed that the grey matter of the human cerebral cortex contains a two-fold larger number of glia cells (20 – 40 billion) compared to neurons (10 - 20 billion). In the white matter of the cerebral cortex, it is believed that glial cells are three times more abundant than neurons (von Bartheld, Bahney and Herculano-Houzel, 2016). Further, it is believed that glial cells of the human neocortex are composed of 75% oligodendrocytes, 17-20% astrocytes, and 5-20% microglia (Pelvig et al., 2003, 2008; Lyck et al., 2009), whereas oligodendrocytes present a missing factor in our *in vitro* model.

Despite the limitations of our model of neither mirroring the exact proportions of the human brain nor ensuring the same genetic background of CNS cell types used, we provide novel insights into RABV-mediated CNS cell type-specific modulation of signalling pathways *in vitro*. Using sc RNA-Seq we show that a low MOI used for infection experiments with virulent Tha, induces immune responses in hiNeurons and hiAstrocytes, whereas a ten-fold higher MOI restricts immune responses in the same. Secondly, no vast differences were observed between infected and bystander hiNeurons or hiAstrocytes, suggesting that Tha interferes with intercellular CNS communication pathways to indirectly supress immune responses of non-infected cells. Thus, Th2P-4M exhibited a stronger induction of immune genes in hiAstrocytes and hiMicroglia suggesting that viral P- and M-genes are necessary to inhibit activation of surrounding glial cells. Overall, our study gives a detailed overview on the importance of viral load and accessory functions of viral P- and M-proteins in regulating immune responses in 3 different cell types composing the CNS.

Acknowledgements

Image acquisition with the Opera Phenix® Plus High Content Screening System (Perkin Elmer) and data analysis via the Columbus software (Perkin Elmer) were conducted with the help of Anne Danckaert and Nathalie Aulner of UTechS Photonic BioImaging (PBI) core at Institut Pasteur Paris. PBI, a member of the national infrastructure France-BioImaging supported by the French National Research Agency (ANR-10-INBS-04), kindly acknowledges the financial support of the Région Ile-de France (program DIM1Health) and the Institut Pasteur.

Author contributions

LF and HB conceived the experimental hypothesis and interpreted the data. LF, VL and HB designed the experiments. LF, TK, and LK performed the experiments. LF and JP analysed the data. HB, FG, VL, MH and JJF provided intellectual guidance. All authors read and approved the final manuscript.

Declaration of interests

The authors declare no competing interests.

STAR Methods

Viruses

Thailand virus, referred to as 8764THA (GenBank No. EU293111) is a field strain of RABV isolated from the brain of a Thai patient who died of rabies after being bitten by a rabid dog (Delmas et al., 2008). This field isolate was further adapted to cell culture on BSR cells (a BHK-21 clone, kindly provided by Monique Lafon, Institute Pasteur, Paris) (Sato et al., 1977), consequently called 8743THA (GenBank No. EU293121) (Delmas et al., 2008) and in this manuscript referred to as Tha. Sequence comparison between the cell culture-adapted RABV strain 8743THA (GenBank No. EU293121) and the original field isolate 8764THA (GenBank No. EU293111) demonstrated 98.56% identity (52 mutations) and 99.36% similarity between concatenated protein sequences. The recombinant Th2P-4M (Ref-SKU: 017N-04350) virus harbours the same genetic background as Tha apart from bearing two mutations in the viral P-protein (W265G, M287V) and four mutations in the viral M-protein (R77K, D100A, A104S, M110L) which were previously described (Wiltzer et al., 2014; Ben Khalifa et al., 2016; Sonthonnax et al., 2019). To validate viral infection, recombinant viral Tha-eGFP and Th2P-4M-eGFP constructs were used which were generated by cloning sequences of eGFP (recovered from pEGFP-C1 plasmid, Promega) into the genetic sequence of Tha (Besson et al., 2019) and Th2P-4M, respectively. Viral strains were sequenced before used for infection experiments. Viral titers were determined by virus titration on BSR cells via staining of the viral nucleoprotein (5100, Sigma-Aldrich).

Human neural stem cell culture and differentiation

Human neuronal stem cells (hNSC, EnStem-A™ SCC003, Millipore) were amplified on plates previously cultured with geltrex (A1413201, Invitrogen) in complete neural stem cell (CNSC) medium containing Knock-out D-MEM/F-12 (A1370801, Thermo Fisher), 2 mM Glutamax (35050038, Thermo Fisher), 2% StemPro Neural Supplement (A1050801, ThermoFisher), 20 ng/ml human FGF (PHG0026, Thermo Fisher), and 20 ng/mL human EGF (PHG0311, Thermo Fisher) at 37°C and 5% CO2. For differentiation, hNSC cells were seeded at a density of 1.5x105 cells/cm2 on plates previously coated with poly-ornithine (P4957, Sigma-Aldrich) and laminin (L2020, Sigma-Aldrich). One day after seeding, the medium was changed to differentiation medium containing neurobasal medium (10888022, Thermo Fisher), 2 mM Glutamax (35050038, Thermo Fisher), 2% B-27 serum free supplement (17504044, Thermo Fisher), 200 μM Ascorbid Acid (A4403, Sigma-Aldrich) and 1x Penicillin/Streptomycin (15140148, Thermo Fisher). Human NSC were differentiated for one week before hiMacs were added to the culture. Half of the medium was changed every third day.

Differentiation of hiPSCs to hiMacs

Human induced macrophage-like cells (hiMacs) were generated from iPSCs according to a published method described by Takata et al (Takata et al., 2017). In short, 5 ng/mL BMP-4 (314-BP-050, R&D Systems), 50 ng/mL VEGF (293-VE-500, R&D Systems), 2 μM CHIR99021 (4423, TOCRIS) induced mesoderm specification of human iPSC colonies (XCL-1) and hemangioblast-like cell formation (Kanke et al., 2014). Replacement of CHIR99021 by 20 ng/mL FGF-2 (223-FB-500, R&D Systems), followed by maintenance in 15 ng/mL VEGF and 5 ng/mL FGF-2 induced differentiation into the hematopoietic lineage according to a modified protocol from Grigoriadis et al. (Grigoriadis et al., 2010). Wnt signalling was inhibited and hematopoietic stem cells were matured by incubation with 50 ng/ml SCF (255-SC-01M), 10

ng/mL FGF-2, 20 ng/mL IL-3 (203-IL-050, R&D Systems), 10 ng/mL IL-6 (206-IL-050, R&D Systems), 10 ng/mL VEGF and 30 ng/mL DKK-1(5439-DK-500) for 6 days and with 50 ng/mL SCF, 10 ng/mL FGF-2, 20 ng/mL IL-3 and 10 ng/mL IL-6 for 4 days. To promote terminal differentiation of hiMacs, cells were cultured with 50 ng/mL CSF-1 (216-MC-01M, R&D Systems) for 14 days (Chomarat et al., 2000; Sturgeon et al., 2014; Ackermann et al., 2015).

Differentiation of hiMacs to hiMicros

After hiMacs generation, hiMacs were co-cultured with 70 – 80% confluent one weeks old (day 0 = induction of neural induction) hiNeurons and hiAstrocytes for three consecutive weeks. In detail, 7 days after the induction of neural differentiation, $1x10^4$ cells/cm^2 hiMacs were added to the $1.5x10^5$ cells/cm^2 hiNneurons and hiAstrocytes. Half of the culture medium was changed every third day supplemented with 50 ng/mL recombinant human CSF-1 (216-MC-010, R & D Systems) and 50 ng/mL human IL-34 (5265-IL-010, R & D Systems). Cells were co-cultured for three consecutive weeks before infection experiments were started.

Single cell RNA sequencing

After four weeks of differentiation, cells were infected with Tha or Th2P-4M (MOI of 0.5 or MOI of 5 respectively) for two hours at 37°C and 5% CO2. In short, 500 μl of medium was removed and 500 μl of differentiation medium or virus diluted in differentiation medium was added respectively. Forty-eight hours after infection, cells were dissociated using StemPro Accutase (A1110501, Thermo Scientific) supplemented with 50 U/mL papain (P4762, Sigma Aldrich). In detail, cells were incubated in 400 μl dissociation solution for 10 minutes at 37°C. After 10 minutes, cells were resuspended in neurobasal medium (10888022, Thermo Fisher) supplemented with 2% heat-inactivated fetal bovine serum (S182H-500, Eurobio) and 10 μM ROCK inhibitor Y-27632 (ACS-3030, Stemcell Technologies). Cells were centrifuged at 1000 rpm for 5 minutes at 4°C. Viability was increased by removing dead cells via the Dead Cell Removal Kit (130-090-101, Miltenyi Biotec). In short, cells were resuspended in 100 μl of dead cell removal beads. After 15 minutes of incubation, 400 μl of binding buffer was added to each sample. Samples were added to the freshly washed LS columns (130-042-401, Miltenyi Biotec). Columns were washed with 4.5 mL binding buffer (Miltenyi Biotec) and the flow-through was collected. After the collection of viable cells, cells were centrifuged at 1000 rpm for 5 minutes at 4°C. Meanwhile, viable cells were counted and diluted to a final concentration of 1000 cells/μl. 10.000 cells were loaded per condition using the Chromium Next GEM Single Cell 3' Reagent Kit v3.1 (PN-1000128, 10x Genomics). The 10x libraries were sequenced at a depth of 40.000 reads per cell using the Illumina NovaSeq technology (Novogene).

scRNA-seq data processing

The sequencing output bcl2 files of each sample were converted to FASTQ format by using cellranger-mkfastq algorithm (10x Genomics). A custom reference genome was constructed by using cellranger-mkref algorithm. The complete viral sequence (fasta files in supplementary material) was added to the human genome sequence (GRCh38). To build the (cell, UMI) expression matrix, FASTQ files were align to the custom GRCh38 reference transcriptome applying cellranger-count. Preprocessing, UMI normalization, and QC were assessed using Seurat pipeline (R package) (Hao et al., 2021). Quality control was performed based on mitochondrial genes rates and number of detected genes per cell.

Single cell signatures and scores

Integrated and normalized scRNAseq data was scored for multigene signatures (Table S1) downloaded from the MSigDB (https://www.gsea-msigdb.org/gsea/msigdb/collections.jsp), (Subramanian et al., 2005; Liberzon et al., 2011, 2015) unless described otherwise. Single cell score for each signature was computed as described before (Pont, Tosolini and Fournié, 2019). Briefly, Single-Cell Signature Scorer computes cell score "Cj" for a gene set "GSx" as the sum of all UMI for all the "GSx" genes expressed by "Cj" divided by the sum of all UMI expressed by Cj:

$$\text{Score of cell Cj for geneset GSx} = (\Sigma(\text{UMI})\text{GSx})/(\Sigma(\text{UMI})\text{Cj})1;$$

where "Cj" is a cell, "GSx" is a gene set.

Identification of cellular fate and infection

Single-cell signature scores allows a digital identification of any subset of cells, as previously demostrated (Cerapio et al., 2021). Single cell signature scores were obtained for specific gene signatures (Table S1), as described above, and scores were visualized in function of clusters, obtained by the FindClusters function (R package Seurat) on scatterplots by Single-Cell Virtual Cytometer (Pont et al., 2020). The scores were sequentially visualized as follows:

1. Selection of cluster with higher scores [= hiMicros (n=795)] from scatterplot 'Brain_Darmani_microglia' and 'Seurat_clusters'.

2. Remaining non-hiMicros [=hiAstrocytes+hiNeurons+Stem-like cells(n=18,579)] were plotted on scatterplot 'BrainBrain_CellMarkerDB_Cancer_stem_cell' and 'Seurat_clusters' and the clusters with higher scores [= Stem-like cells (n=3,109)] were selected.

3. From scatterplot 'Brain_Darmani_astrocytes' and 'Seurat_clusters' of non-Stem-like cells, the clusters with higher score [= hiAstrocytes (n=3,350)] were extracted.

4. Finally, from non-hiAstrocytes (n=12,120) hiNeurons (n=11,575) were extracted by using scatterplot 'Brain_Darmani_neuron' and 'Seurat_clusters'; Lastly, non-selected cells were classed as 'Precursors' (n=545).

Trajectory inference

Integrated and normalized scRNAseq data, by 'SCTransform' (Seurat, R package), was used for differentiation trajectory inference. The trajectory inference (TI) was performed using dynverse an R packages collection, which provides more than 45 different TI methods. The TI was obtained by following the recommended workflow (Saelens et al., 2019). Briefly, the normalized (log2) raw expression data was used as an input. The most suitable method to infer the differentiation trajectories of our data after applying 'guidelines' function (dynverse on R) was Minimum Spanning Tree (MST; 'ti_mst' function of dynverse on R). Scored signatures (Table S1), as described above, together with the obtained MST dimension reduction coordinates 1 and 2 (MST1 and MST2), and pseudotime were used to define the trajectory root ('add_root' on R).

Pseudotimed trajectory, the MST attributes (i.e. MST1, MST2, psudotime) allow multiple visualizations, so the data were visualized through pseudotimed trajectories, which is a bidimensional (x, y') representation of the trajectory inferred for any single cell (p) in which (x,y,z) are pseudotime, MST1, and MST2, respectively. The dim_proj method projects this 3-dimension space (X: pseudotime, Y: MST1, Z: MST2) in a 2-dimensional plane. Of note, between the three orthonormal dimensions (XYZ) and the projection plane (XoY'), there is a

rotation angle (ZoY') called β, which is independent of the trajectory and which selection optimize the visulization of the trajectory possible branches (Cerapio et al., 2021).

Data visualization

Single-cell Multilayer Viewer, a serverless software that allows to visualize up to 5 layers of information simultaneously (Cerapio et al., 2021) was used for data visualization. All single cells information, more specifically UMAP and trajectory coordinates, cell signatures scores, and gene expression were merged for analysis and visualization by using Single-Cell Signature Merger (Pont, Tosolini and Fournié, 2019).

Immunofluorescence

Cells were differentiated and co-cultured as mentioned before. After differentiation of co-cultures, cells were infected with Tha-eGFP and Th2P-4M-eGFP at a MOI of 0.5. Fourty-eight hours post-infection, cells were fixed using 4% PFA for 15 minutes at room temperature. After fixation, cells were washed with PBS (10010023, Thermo Scientific) and permeabilized using 0.5% triton X-100 (648463, Millipore) for 10 minutes. Cells were stained with primary and secondary antibodies (S1 Table) and imaged using the Opera PhenixTM High Content Screening System (Perkin Elmer).

Statistical analysis

Means and adjusted p-values were calculated with R (version 4.0.1). All experiments were performed independently at three times. Graphical illustrations were generated via R (version 4.0.1) or the Single-Cell Multilayer Viewer (V.0.20201015). Figures were generated using Illustrator cc 2019.

References

Ackermann, M., Liebhaber, S., Klusmann, J.-H. and Lachmann, N. (2015) 'Lost in translation: pluripotent stem cell-derived hematopoiesis.', EMBO molecular medicine, 7(11), pp. 1388–1402. doi: 10.15252/emmm.201505301.

Baloul, L., Camelo, S. and Lafon, M. (2004) 'Up-regulation of Fas ligand (FasL) in the central nervous system: A mechanism of immune evasion by rabies virus', Journal of NeuroVirology, 10(6), pp. 372–382. doi: 10.1080/13550280490521122.

Baloul, L. and Lafon, M. (2003) 'Apoptosis and rabies virus neuroinvasion', Biochimie, 85(8), pp. 777–788. doi: 10.1016/S0300-9084(03)00137-8.

von Bartheld, C. S., Bahney, J. and Herculano-Houzel, S. (2016) 'The search for true numbers of neurons and glial cells in the human brain: A review of 150 years of cell counting', Journal of Comparative Neurology. Wiley-Liss Inc., pp. 3865–3895. doi: 10.1002/cne.24040.

Bauer, A., Nolden, T., Nemitz, S., Perlson, E. and Finke, S. (2015) 'A Dynein Light Chain 1 Binding Motif in Rabies Virus Polymerase L Protein Plays a Role in Microtubule Reorganization and Viral Primary Transcription.', Journal of virology, 89(18), pp. 9591–9600. doi: 10.1128/JVI.01298-15.

Besson, B., Kim, S., Kim, T., Ko, Y., Lee, S., Larrous, F., Song, J., Shum, D., Grailhe, R. and Bourhy, H. (2019) 'Kinome-Wide RNA Interference Screening Identifies Mitogen-Activated Protein Kinases and Phosphatidylinositol Metabolism as Key Factors for Rabies Virus Infection.', mSphere, 4(3). doi: 10.1128/mSphere.00047-19.

Besson, B., Sonthonnax, F., Duchateau, M., Ben Khalifa, Y., Larrous, F., Eun, H., Hourdel, V., Matondo, M., Chamot-Rooke, J., Grailhe, R. and Bourhy, H. (2017) 'Regulation of NF-κB by the p105-ABIN2-TPL2 complex and RelAp43 during rabies virus infection', PLoS Pathogens. Edited by M. J. Schnell, 13(10), p. e1006697. doi: 10.1371/journal.ppat.1006697.

Cerapio, J.-P., Perrier, M., Balança, C.-C., Gravelle, P., Pont, F., Devaud, C., Franchini, D.-M., Féliu, V., Tosolini, M., Valle, C., Lopez, F., Quillet-Mary, A., Ysebaert, L., Martinez, A., Delord, J. P., Ayyoub, M., Laurent, C. and Fournie, J.-J. (2021) 'Phased differentiation of γδ T and T CD8 tumor-infiltrating lymphocytes revealed by single-cell transcriptomics of human cancers', OncoImmunology. Taylor & Francis, 10(1), p. 1939518. doi: 10.1080/2162402X.2021.1939518.

Chhatbar, C. and Prinz, M. (2021) 'The roles of microglia in viral encephalitis: from sensome to therapeutic targeting', Cellular and Molecular Immunology. Springer Nature, pp. 250–258. doi: 10.1038/s41423-020-00620-5.

Chomarat, P., Banchereau, J., Davoust, J. and Palucka, A. K. (2000) 'IL-6 switches the differentiation of monocytes from dendritic cells to macrophages.', Nature immunology. United States, 1(6), pp. 510–514. doi: 10.1038/82763.

Darmanis, S., Sloan, S. A., Croote, D., Mignardi, M., Chernikova, S., Samghababi, P., Zhang, Y., Neff, N., Kowarsky, M., Caneda, C., Li, G., Chang, S. D., Connolly, I. D., Li, Y., Barres, B. A., Gephart, M. H. and Quake, S. R. (2017) 'Single-Cell RNA-Seq Analysis of Infiltrating Neoplastic Cells at the Migrating Front of Human Glioblastoma', Cell Reports, 21(5), pp. 1399–1410. doi: https://doi.org/10.1016/j.celrep.2017.10.030.

Delmas, O., Holmes, E. C., Talbi, C., Larrous, F., Dacheux, L., Bouchier, C. and Bourhy, H. (2008) 'Genomic diversity and evolution of the lyssaviruses', PLoS ONE, 3(4), pp. 1–6. doi: 10.1371/journal.pone.0002057.

Esiri, M. M., Drummond, C. W. E. and Morris, C. S. (1995) 'Macrophages and microglia in HSV-1 infected mouse brain', Journal of Neuroimmunology, 62(2), pp. 201–205. doi: https://doi.org/10.1016/0165-5728(95)00123-8.

Fooks, A. R., Cliquet, F., Finke, S., Freuling, C., Hemachudha, T., Mani, R. S., Müller, T., Nadin-Davis, S., Picard-Meyer, E., Wilde, H. and Banyard, A. C. (2017) 'Rabies', Nature Reviews Disease Primers. England, 3, p. 17091. doi: 10.1038/nrdp.2017.91.

Griffin, D. E. (2003) 'Immune responses to RNA-virus infections of the CNS', Nature Reviews Immunology, 3(6), pp. 493–502. doi: 10.1038/nri1105.

Grigoriadis, A. E., Kennedy, M., Bozec, A., Brunton, F., Stenbeck, G., Park, I.-H., Wagner, E. F. and Keller, G. M. (2010) 'Directed differentiation of hematopoietic precursors and functional osteoclasts from human ES and iPS cells.', Blood, 115(14), pp. 2769–2776. doi: 10.1182/blood-2009-07-234690.

Hao, Y., Hao, S., Andersen-Nissen, E., Mauck, W. M. 3rd, Zheng, S., Butler, A., Lee, M. J., Wilk, A. J., Darby, C., Zager, M., Hoffman, P., Stoeckius, M., Papalexi, E., Mimitou, E. P., Jain, J., Srivastava, A., Stuart, T., Fleming, L. M., Yeung, B., Rogers, A. J., McElrath, J. M., Blish, C. A., Gottardo, R., Smibert, P. and Satija, R. (2021) 'Integrated analysis of multimodal single-cell data.', Cell, 184(13), pp. 3573-3587.e29. doi: 10.1016/j.cell.2021.04.048.

Hemachudha, T., Ugolini, G., Wacharapluesadee, S., Sungkarat, W., Shuangshoti, S. and Laothamatas, J. (2013) 'Human rabies: neuropathogenesis, diagnosis, and management', The Lancet Neurology, 12(5), pp. 498–513. doi: 10.1016/S1474-4422(13)70038-3.

Hodge, R. D., Bakken, T. E., Miller, J. A., Smith, K. A., Barkan, E. R., Graybuck, L. T., Close, J. L., Long, B., Johansen, N., Penn, O., Yao, Z., Eggermont, J., Höllt, T., Levi, B. P., Shehata, S. I., Aevermann, B., Beller, A., Bertagnolli, D., Brouner, K., Casper, T., Cobbs, C., Dalley, R., Dee, N., Ding, S. L., Ellenbogen, R. G., Fong, O., Garren, E., Goldy, J., Gwinn, R. P., Hirschstein, D., Keene, C. D., Keshk, M., Ko, A. L., Lathia, K., Mahfouz, A., Maltzer, Z., McGraw, M., Nguyen, T. N., Nyhus, J., Ojemann, J. G., Oldre, A., Parry, S., Reynolds, S., Rimorin, C., Shapovalova, N. V., Somasundaram, S., Szafer, A., Thomsen, E. R., Tieu, M., Quon, G., Scheuermann, R. H., Yuste, R., Sunkin, S. M., Lelieveldt, B., Feng, D., Ng, L., Bernard, A., Hawrylycz, M., Phillips, J. W., Tasic, B., Zeng, H., Jones, A. R., Koch, C. and Lein, E. S. (2019) 'Conserved cell types with divergent features in human versus mouse cortex', Nature. Springer US, 573(7772), pp. 61–68. doi: 10.1038/s41586-019-1506-7.

Huang, K. W. and Sabatini, B. L. (2020) 'Single-Cell Analysis of Neuroinflammatory Responses Following Intracranial Injection of G-Deleted Rabies Viruses', Frontiers in Cellular Neuroscience. Frontiers Media S.A., 14. doi: 10.3389/fncel.2020.00065.

Hwang, M. and Bergmann, C. C. (2019) 'Intercellular Communication Is Key for Protective IFNα/β Signaling During Viral Central Nervous System Infection', Viral immunology. 2018/09/15. Mary Ann Liebert, Inc., publishers, 32(1), pp. 1–6. doi: 10.1089/vim.2018.0101.

Ito, N., Moseley, G. W. and Sugiyama, M. (2016) 'The importance of immune evasion in the pathogenesis of rabies virus', Vet. Med. Sci., 7(116), pp. 1089–1098. doi: 10.1292/jvms.16-0092.

Jacob, Y., Badrane, H., Ceccaldi, P. E. and Tordo, N. (2000) 'Cytoplasmic dynein LC8 interacts with lyssavirus phosphoprotein.', Journal of virology, 74(21), pp. 10217–10222. doi: 10.1128/jvi.74.21.10217-10222.2000.

Kalisky, T., Oriel, S., Bar-Lev, T. H., Ben-Haim, N., Trink, A., Wineberg, Y., Kanter, I., Gilad, S. and Pyne, S. (2018) 'A brief review of single-cell transcriptomic technologies', Briefings in Functional Genomics. Oxford University Press, 17(1), pp. 64–76. doi: 10.1093/bfgp/elx019.

Kanke, K., Masaki, H., Saito, T., Komiyama, Y., Hojo, H., Nakauchi, H., Lichtler, A. C., Takato, T., Chung, U.-I. and Ohba, S. (2014) 'Stepwise differentiation of pluripotent stem cells into osteoblasts using four small molecules under serum-free and feeder-free conditions.', Stem cell reports, 2(6), pp. 751–760. doi: 10.1016/j.stemcr.2014.04.016.

Kassis, R., Larrous, F., Estaquier, J. and Bourhy, H. (2004) 'Lyssavirus Matrix Protein Induces Apoptosis by a TRAIL-Dependent Mechanism Involving Caspase-8 Activation', Journal of Virology, 78(12), pp. 6543–6555. doi: 10.1128/jvi.78.12.6543-6555.2004.

Kennedy, R. H. and Silver, R. (2016) 'Neuroimmune Signaling: Cytokines and the CNS', in Pfaff, D. W. and Volkow, N. D. (eds) Neuroscience in the 21st Century. New York, NY: Springer New York, pp. 1–41. doi: 10.1007/978-1-4614-6434-1_174-1.

Ben Khalifa, Y., Luco, S., Besson, B., Sonthonnax, F., Archambaud, M., Grimes, J. M., Larrous, F. and Bourhy, H. (2016) 'The matrix protein of rabies virus binds to RelAp43 to modulate NF-κB-dependent gene expression related to innate immunity', Scientific Reports. Nature Publishing Group, 6(September), p. 39420. doi: 10.1038/srep39420.

Lafon, M. (2005) 'Modulation of the immune response in the nervous system by rabies virus.', Current topics in microbiology and immunology. Germany, 289, pp. 239–58. doi: 10.1007/3-540-27320-4.

Lafon, M. (2008) ‘Immune evasion, a critical strategy for rabies virus.’, Developments in biologicals. Switzerland, 131, pp. 413–419.

Lafon, M. (2011) Evasive Strategies in Rabies Virus Infection. 1st edn, Advances in Virus Research. 1st edn. Elsevier Inc. doi: 10.1016/B978-0-12-387040-7.00003-2.

Ledur, P. F., Karmirian, K., Pedrosa, C. da S. G., Souza, L. R. Q., Assis-de-Lemos, G., Martins, T. M., Ferreira, J. de C. C. G., de Azevedo Reis, G. F., Silva, E. S., Silva, D., Salerno, J. A., Ornelas, I. M., Devalle, S., Madeiro da Costa, R. F., Goto-Silva, L., Higa, L. M., Melo, A., Tanuri, A., Chimelli, L., Murata, M. M., Garcez, P. P., Filippi-Chiela, E. C., Galina, A., Borges, H. L. and Rehen, S. K. (2020) ‘Zika virus infection leads to mitochondrial failure, oxidative stress and DNA damage in human iPSC-derived astrocytes’, Scientific Reports, 10(1), p. 1218. doi: 10.1038/s41598-020-57914-x.

Lee, C. Q. E., Kerouanton, B., Chothani, S., Zhang, S., Chen, Y., Mantri, C. K., Hock, D. H., Lim, R., Nadkarni, R., Huynh, V. T., Lim, D., Chew, W. L., Zhong, F. L., Stroud, D. A., Schafer, S., Tergaonkar, V., St John, A. L., Rackham, O. J. L. and Ho, L. (2021) ‘Coding and non-coding roles of MOCCI (C15ORF48) coordinate to regulate host inflammation and immunity’, Nature Communications, 12(1), p. 2130. doi: 10.1038/s41467-021-22397-5.

Liberzon, A., Birger, C., Thorvaldsdóttir, H., Ghandi, M., Mesirov, J. P. and Tamayo, P. (2015) ‘The Molecular Signatures Database (MSigDB) hallmark gene set collection’, Cell systems, 1(6), pp. 417–425. doi: 10.1016/j.cels.2015.12.004.

Liberzon, A., Subramanian, A., Pinchback, R., Thorvaldsdóttir, H., Tamayo, P. and Mesirov, J. P. (2011) ‘Molecular signatures database (MSigDB) 3.0’, Bioinformatics, 27(12), pp. 1739–1740. doi: 10.1093/bioinformatics/btr260.

Liu, S. Q., Xie, Y., Gao, X., Wang, Q. and Zhu, W. Y. (2020) ‘Inflammatory response and MAPK and NF-κB pathway activation induced by natural street rabies virus infection in the brain tissues of dogs and humans.’, Virology journal. BioMed Central Ltd, 17(1), p. 157. doi: 10.1186/s12985-020-01429-4.

Lyck, L., Santamaria, I. D., Pakkenberg, B., Chemnitz, J., Schrøder, H. D., Finsen, B. and Gundersen, H. J. G. (2009) ‘An empirical analysis of the precision of estimating the numbers of neurons and glia in human neocortex using a fractionator-design with sub-sampling’, Journal of Neuroscience Methods. J Neurosci Methods, 182(2), pp. 143–156. doi: 10.1016/j.jneumeth.2009.06.003.

Pelvig, D. P., Pakkenberg, H., Regeur, L., Oster, S. and Pakkenberg, B. (2003) ‘Neocortical glial cell numbers in Alzheimer’s disease: A stereological study’, Dementia and Geriatric Cognitive Disorders. Dement Geriatr Cogn Disord, 16(4), pp. 212–219. doi: 10.1159/000072805.

Pelvig, D. P., Pakkenberg, H., Stark, A. K. and Pakkenberg, B. (2008) ‘Neocortical glial cell numbers in human brains’, Neurobiology of Aging. Neurobiol Aging, 29(11), pp. 1754–1762. doi: 10.1016/j.neurobiolaging.2007.04.013.

Pont, F., Tosolini, M. and Fournié, J. J. (2019) ‘Single-Cell Signature Explorer for comprehensive visualization of single cell signatures across scRNA-seq datasets.’, Nucleic acids research, 47(21), p. e133. doi: 10.1093/nar/gkz601.

Pont, F., Tosolini, M., Gao, Q., Perrier, M., Madrid-Mencía, M., Huang, T. S., Neuvial, P., Ayyoub, M., Nazor, K. and Fournié, J.-J. (2020) ‘Single-Cell Virtual Cytometer allows user-

friendly and versatile analysis and visualization of multimodal single cell RNAseq datasets', NAR Genomics and Bioinformatics, 2(2). doi: 10.1093/nargab/lqaa025.

Potratz, M., Zaeck, L., Christen, M., Kamp, V., Klein, A., Freuling, C. M., Müller, T. and Finke, S. (2020) 'Astrocyte Infection during Rabies Encephalitis Depends on the Virus Strain and Infection Route as Demonstrated by Novel Quantitative 3D Analysis of Cell Tropism', Cells, 9(January), pp. 1–25. doi: 10.20944/preprints202001.0160.v1.

Potratz, M., Zaeck, L. M., Weigel, C., Klein, A., Freuling, C. M., Müller, T. and Finke, S. (2020) 'Neuroglia infection by rabies virus after anterograde virus spread in peripheral neurons.', Acta neuropathologica communications. England, 8(1), p. 199. doi: 10.1186/s40478-020-01074-6.

Raux, H., Flamand, A. and Blondel, D. (2000) 'Interaction of the Rabies Virus P Protein with the LC8 Dynein Light Chain', Journal of Virology, 74(21), pp. 10212–10216. doi: 10.1128/jvi.74.21.10212-10216.2000.

Roy, A. and Hooper, D. C. (2008) 'Immune evasion by rabies viruses through the maintenance of blood-brain barrier integrity', Journal of NeuroVirology, 14(5), pp. 401–411. doi: 10.1080/13550280802235924.

Saelens, W., Cannoodt, R., Todorov, H. and Saeys, Y. (2019) 'A comparison of single-cell trajectory inference methods', Nature Biotechnology, 37(5), pp. 547–554. doi: 10.1038/s41587-019-0071-9.

Sato, M., Maeda, N., Yoshida, H., Urade, M., Saito, S., Miyazaki, T., Shibata, T. and Watanabe, M. (1977) 'Plaque formation of herpes virus hominis type 2 and rubella virus in variants isolated from the colonies of BHK21/WI-2 cells formed in soft agar', Archives of Virology. Springer-Verlag, 53(3), pp. 269–273. doi: 10.1007/BF01314672.

Sonthonnax, F., Besson, B. B., Bonnaud, E., Jouvion, G., Merino, D., Larrous, F. and Bourhy, H. (2019) 'Lyssavirus matrix protein cooperates with phosphoprotein to modulate the Jak-Stat pathway', Scientific Reports, 9(1), pp. 1–13. doi: 10.1038/s41598-019-48507-4.

Sturgeon, C. M., Ditadi, A., Awong, G., Kennedy, M. and Keller, G. (2014) 'Wnt signaling controls the specification of definitive and primitive hematopoiesis from human pluripotent stem cells.', Nature biotechnology, 32(6), pp. 554–561. doi: 10.1038/nbt.2915.

Subramanian, A., Tamayo, P., Mootha, V. K., Mukherjee, S., Ebert, B. L., Gillette, M. A., Paulovich, A., Pomeroy, S. L., Golub, T. R., Lander, E. S. and Mesirov, J. P. (2005) 'Gene set enrichment analysis: A knowledge-based approach for interpreting genome-wide expression profiles', Proceedings of the National Academy of Sciences, 102(43), pp. 15545 LP – 15550. doi: 10.1073/pnas.0506580102.

Sugimoto, M. A., Sousa, L. P., Pinho, V., Perretti, M. and Teixeira, M. M. (2016) 'Resolution of Inflammation: What Controls Its Onset?', Frontiers in immunology, 7, p. 160. doi: 10.3389/fimmu.2016.00160.

Takata, K., Kozaki, T., Lee, C. Z. W., Thion, M. S., Otsuka, M., Lim, S., Utami, K. H., Fidan, K., Park, D. S., Malleret, B., Chakarov, S., See, P., Low, D., Low, G., Garcia-Miralles, M., Zeng, R., Zhang, J., Goh, C. C., Gul, A., Hubert, S., Lee, B., Chen, J., Low, I., Shadan, N. B., Lum, J., Wei, T. S., Mok, E., Kawanishi, S., Kitamura, Y., Larbi, A., Poidinger, M., Renia, L., Ng, L. G., Wolf, Y., Jung, S., Önder, T., Newell, E., Huber, T., Ashihara, E., Garel, S., Pouladi, M. A. and Ginhoux, F. (2017) 'Induced-Pluripotent-Stem-Cell-Derived Primitive Macrophages Provide a Platform for Modeling Tissue-Resident Macrophage Differentiation and Function.', Immunity. United States, 47(1), pp. 183-198.e6. doi: 10.1016/j.immuni.2017.06.017.

Wiltzer, L., Larrous, F., Oksayan, S., Ito, N., Marsh, G. a., Wang, L. F., Blondel, D., Bourhy, H., Jans, D. a. and Moseley, G. W. (2012) 'Conservation of a Unique Mechanism of Immune Evasion across the Lyssavirus Genus', Journal of Virology, 86(18), pp. 10194–10199. doi: 10.1128/JVI.01249-12.

Wiltzer, L., Okada, K., Yamaoka, S., Larrous, F., Kuusisto, H. V., Sugiyama, M., Blondel, D., Bourhy, H., Jans, D. A., Ito, N. and Moseley, G. W. (2014) 'Interaction of Rabies Virus P-Protein With STAT Proteins is Critical to Lethal Rabies Disease', The Journal Of Infectious Diseases. Oxford University Press, 209(11), pp. 1744–53. doi: 10.1093/infdis/jit829.

Yang, Q. qiao and Zhou, J. wei (2019) 'Neuroinflammation in the central nervous system: Symphony of glial cells', GLIA. John Wiley and Sons Inc., pp. 1017–1035. doi: 10.1002/glia.23571.

Zhang, X., Lan, Y., Xu, J., Quan, F., Zhao, E., Deng, C., Luo, T., Xu, L., Liao, G., Yan, M., Ping, Y., Li, F., Shi, A., Bai, J., Zhao, T., Li, X. and Xiao, Y. (2019) 'CellMarker: a manually curated resource of cell markers in human and mouse', Nucleic Acids Research, 47(D1), pp. D721–D728. doi: 10.1093/nar/gky900.

2.4 Identification of CXCL16 as a new viral target (Article #4)

2.4.1 A closer look at natural RABV infection in humans

This chapter deals with the molecular pathogenesis of naturally RABV-infected humans. As mentioned above, transcriptome analysis enables us partly to deceiver healthy and disease states. Rabies is known to limit inflammation and apoptosis in the CNS (133,264), contrasting the fatality of the disease if left untreated. Although electrophysiological (105), histological (108,265), and physiological changes (96,266) were already studied in naturally infected brains of rabid patients, numerous transcriptome studies have so far only been performed in cell culture models (140,141) and mice (134–136,138,267,268).

Investigating the transcriptome profile of human CNS cell types upon RABV infection has the advantage of having the same genetic background but the disadvantage of lacking complexity compared to the human CNS. In contrast, investigating the RABV-infected murine brain bears approximately the same complexity as the human brain but bears the disadvantage of investigating another genetic background. So can we simply extrapolate murine data to humans?

In recent years, increasing evidence emphasizes the potential limitations of extrapolating data including transcriptome analysis from animal models to humans (269–271). To assess immunological states, mice remain the experimental tool of choice for most immunologists for a reason. Studying the murine immune system provided a tremendous insight of how the human immune system in working (269). Generally, mice mirror the human physiology remarkably well (272), and yet, increasing evidence points out significant discrepancies in innate and adaptive immunity. A few of them imply TLRs, chemokine and chemokine receptor expression, Ig subsets, B and T cell pathway components, Ag presenting functions, Th1/Th2 differentiation but there are many more to mention (269). Given that, we cannot conclude how far we can extrapolate transcriptome data coming from RABV-infected mice to humans.

In the research paper '*Transcriptome profile during RABV infection: Identification of CXCL16 as a new viral target*' we compare the expression of a panel of inflammatory genes in RABV-infected mice with inflammatory gene expression in naturally RABV infected patients from Cambodia. The research article is accepted for publication in the journal *Frontiers in Cellular and Infection Microbiology*.

More information about the research article can be found here:

https://www.dropbox.com/sh/xx4th9ohwigvj58/AAAM-y0Eg8CvXTwSrdCCQCHha?dl=0

2.4.2 Article #4 *(accepted for publication)*

frontiers

Transcriptome profile during rabies virus infection: identification of human CXCL16 as a potential new viral target

Lena Feige[1], Ines Saenz de Santa Maria[1], Beatrice Regnault[1], Rachel Lavenir[1], Anthony Lepelletier[1], Ala Halacu[2], Randrianasolo Rajerison[3], Sylvie Diop[4], Chhor Nareth[5], Jean-Marc Reynes[1], Philippe Buchy[6], Hervé Bourhy[1], Laurent Dacheux[1*]

[1]Institut Pasteur, France, [2]National Agency for Public Health, Moldova, [3]University Hospital Center of Befelatanana, Madagascar, [4]Infectious Diseases Department, National and University Hospital Center of Fann-Dakar, Senegal, [5]Calmette Hospital, Cambodia, [6]GSK Vaccines R&D, Singapore

Submitted to Journal:
Frontiers in Cellular and Infection Microbiology

Specialty Section:
Clinical Microbiology

Article type:
Original Research Article

Manuscript ID:
761074

Received on:
19 Aug 2021

Journal website link:
www.frontiersin.org

In review

Conflict of interest statement

The authors declare that the research was conducted in the absence of any commercial or financial relationships that could be construed as a potential conflict of interest

Author contribution statement

AH, RR, SD, CN performed or organized the collection of brain biopsies in human patients in Moldavia, Madagascar, Senegal, and Cambodia, respectively, LF, HB and LD designed the study. JMR, PB and LD supervised the study in Madagascar, Cambodia and in France (overall study), respectively. LF, RL, AL and LD performed the experiments. LF, LD, BR and ISM analysed the data. LF and LD interpreted the data and wrote the manuscript. All authors read and approved the final manuscript.

Keywords

Rabies, Transcriptome, Neuroinflamación, human, Mouse, Brain, immune response, CXCL16

In review

Abstract

Word count: 279

Rabies virus (RABV), the causative agent for rabies disease is still presenting a major public health concern causing approximately 60,000 deaths annually. This neurotropic virus (genus Lyssavirus, family Rhabdoviridae) induces an acute and almost always fatal form of encephalomyelitis in humans. Despite the lethal consequences associated with clinical symptoms of rabies, RABV limits neuro-inflammation without causing major histopathological lesions in humans. Nevertheless, information about the mechanisms of infection and cellular response in the central nervous system (CNS) remain scarce. Here, we investigated the expression of inflammatory genes involved in immune response to RABV (dog-adapted strain Tha) in mice, the most common animal model used to study rabies. To better elucidate the pathophysiological mechanisms during natural RABV infection, we compared the inflammatory transcriptome profile observed at the late stage of infection in the mouse brain (cortex and brain stem/cerebellum) with the ortholog gene expression in post-mortem brain biopsies of rabid patients. Our data indicate that the inflammatory response associated with rabies is more pronounced in the murine brain compared to the human brain. In contrast to murine transcription profiles, we identified CXC motif chemokine ligand 16 (CXCL16) as the only significant differentially expressed gene in post-mortem brains of rabid patients. This result was confirmed in vitro, in which Tha suppressed interferon alpha (IFN-α)-induced CXCL16 expression in human CNS cell lines but induced CXCL16 expression in IFN-α-stimulated murine astrocytes. We hypothesize that RABV-induced modulation of the CXCL16 pathway in the brain possibly affects neurotransmission, natural killer (NK) and T cell recruitment and activation. Overall, we show species-specific differences in the inflammatory response of the brain, highlighted the importance of understanding the potential limitations of extrapolating data from animal models to human.

Contribution to the field

Despite being one of the oldest known infectious diseases, rabies still resulting in 60.000 human deaths worldwide. Up to date, no efficient treatment exists against this fatal encephalomyelitis and information about the mechanisms of rabies virus (RABV) infection in the brain remain scarce. Here, we report the first transcriptional analysis investigating the expression of inflammatory genes in human brain, based on a cohort including 15 rabid and 12 non-rabid patients. We compare the human transcription profile to RABV infection in mice, the most common in vivo model. Our study reveals that RABV specifically downregulates CXCL16 in human brains in contrast to the murine brain. While the murine brain shows a profound inflammatory response, the human brain shows little inflammation upon natural RABV infection. Overall, our study contributes to improve the knowledge on the pathophysiology of rabies, using on unique biocollection of brain samples collected from rabid patients. Based on our results, we hypothesize that RABV-induced modulation of the CXCL16 pathway in the brain possibly affects neurotransmission and the recruitment of inflammatory cells. Overall, we show species-specific differences in the brain inflammatory response, highlighted the importance of understanding the potential limitations of extrapolating data from animal models.

Funding statement

Lena Feige was supported by the Pasteur - Paris University (PPU) International PhD Program. This work was partially funded by Institut Pasteur International Network Actions Concertees InterPasteuriennes (2003/687). We are also grateful to Santé publique France for the financial support of the National Reference Centre for Rabies.

Ethics statements

Studies involving animal subjects

Generated Statement: The animal study was reviewed and approved by Animal Experimentation Ethics Committee (CETEA no. 089, 25/04/2018 and A75-15-25, 30/07/2002) .

Studies involving human subjects

Generated Statement: The studies involving human participants were reviewed and approved by the national ethical committees (N° 102-SANPF/CAB from the Ministry of Health and Family Planning of Madagascar, N°008/03 NECHR and N° 054NECHR from the Ministry of Health of Cambodia, N°00116 MSPM/DS/DER from the Ministry of Health and Medical Prevention of Senegal). Written informed consent to participate in this study was provided by the participants' legal guardian/next of kin.

Inclusion of identifiable human data

Generated Statement: No potentially identifiable human images or data is presented in this study.

In review

Data availability statement

Generated Statement: The authors acknowledge that the data presented in this study must be deposited and made publicly available in an acceptable repository, prior to publication. Frontiers cannot accept a manuscript that does not adhere to our open data policies.

In review

Transcriptome profile during rabies virus infection: identification of human CXCL16 as a potential new viral target

Lena Feige[1,2]*, Ines Saenz de Santa Maria[3], Beatrice Regnault[4], Rachel Lavenir[1], Anthony Lepelletier[1], Ala Halacu[5], Randrianasolo Rajerison[6], Sylvie Diop[7], Chhor Nareth[8], Jean-Marc Reynes[9], Philippe Buchy[10], Hervé Bourhy[1], Laurent Dacheux[1]*

[1] Institut Pasteur, Lyssavirus Epidemiology and Neuropathology unit, National Reference Center for Rabies, WHO Collaborating Center for Reference and Research on Rabies, Paris, France.

[2] University Paris Diderot, Sorbonne Paris Cité (SPCBio), Université de Paris, Sorbonne Paris Cité, Paris, France.

[3] Institut Pasteur, Membrane Traffic and Pathogenesis Unit, Paris, France.

[4] Institut Pasteur, Genopole, Paris, France (current affiliation: Pathogen Discovery Laboratory, Institut Pasteur, Paris, France).

[5] National Agency for Public Health, Moldova.

[6] University Hospital Center of Befelatanana, Antananarivo, Madagascar.

[7] Infectious Diseases Department, National and University Hospital Center of Fann-Dakar, Dakar, Senegal.

[8] Calmette Hospital, Phnom Penh, Cambodia.

[9] Institut Pasteur de Madagascar, Virology unit, Tananarive, Madagascar (current affiliation : Environment and Infectious Risks, Institut Pasteur, Paris, France).

[10] Institut Pasteur in Cambodia, Virology unit, Phnom Penh, Cambodia (current affiliation: GSK Vaccines R&D, 23 Rochester Park, Singapore 139234).

*Corresponding authors: lena.feige@pasteur.fr, laurent.dacheux@pasteur.fr

Keywords: Rabies, transcriptome, neuroinflammation, human, mouse, brain, immune response, *CXCL16*

In review

Abstract

Rabies virus (RABV), the causative agent for rabies disease is still presenting a major public health concern causing approximately 60,000 deaths annually. This neurotropic virus (genus *Lyssavirus*, family *Rhabdoviridae*) induces an acute and almost always fatal form of encephalomyelitis in humans. Despite the lethal consequences associated with clinical symptoms of rabies, RABV limits neuro-inflammation without causing major histopathological lesions in humans. Nevertheless, information about the mechanisms of infection and cellular response in the central nervous system (CNS) remain scarce. Here, we investigated the expression of inflammatory genes involved in immune response to RABV (dog-adapted strain Tha) in mice, the most common animal model used to study rabies. To better elucidate the pathophysiological mechanisms during natural RABV infection, we compared the inflammatory transcriptome profile observed at the late stage of infection in the mouse brain (cortex and brain stem/cerebellum) with the ortholog gene expression in *post-mortem* brain biopsies of rabid patients. Our data indicate that the inflammatory response associated with rabies is more pronounced in the murine brain compared to the human brain. In contrast to murine transcription profiles, we identified CXC motif chemokine ligand 16 (*CXCL16*) as the only significant differentially expressed gene in *post-mortem* brains of rabid patients. This result was confirmed *in vitro*, in which Tha suppressed interferon alpha (IFN-α)-induced *CXCL16* expression in human CNS cell lines but induced *CXCL16* expression in IFN-α-stimulated murine astrocytes. We hypothesize that RABV-induced modulation of the CXCL16

pathway in the brain possibly affects neurotransmission, natural killer (NK) and T cell recruitment and activation. Overall, we show species-specific differences in the inflammatory response of the brain, highlighted the importance of understanding the potential limitations of extrapolating data from animal models to human.

Introduction

Rabies virus (RABV) is the etiological agent of rabies, an acute and always fatal form of encephalomyelitis which can potentially affect all mammals, including humans. Even though rabies has been known and described for millennia (Baer, 1975), the physio-pathological mechanisms inducing this pathology and ultimately leading to the death of the infected individual remain unknown (T Hemachudha et al., 2013). A breakthrough in eliminating rabies has been made with the introduction of rabies vaccination by Louis Pasteur in the late 1880s (Baer, 1975), opening the way to effective pre- and post-exposure prophylaxis protocols which are nowadays available (O'Brien et al., 2019; WHO, 2018). However, once symptoms appear, no effective human treatment exists so far, resulting in a global burden of estimated 60,000 human deaths per year, more particularly in low-and-middle income countries in Asia and Africa (Fooks et al., 2017; Hampson et al., 2015).

Human rabies is a zoonosis, mainly transmitted after exposure to saliva of infected dogs through bites, scratches, or licking of wounds, or mucosa (Fooks et al., 2014). Upon the bite, it is assumed that RABV replicates locally in the wound, before spreading from the neuromuscular junction to motor neurons to reach the peripheral nervous system (PNS) (Murphy et al., 1974; Watson et al., 1981; Davis et al., 2015). Subsequently, RABV is transported retrogradely from the PNS to the central nervous system (CNS) via trans-synaptic spread between connected neurons (Ugolini, 2011; Ceccaldi et al., 1989). At this stage, the infection will lead to rabies, an acute and always fatal form of encephalomyelitis with two major clinical forms: encephalitic (or furious) rabies associated with phobic (hydrophobia or aerophobia) or inspiratory spasms, autonomic stimulation signs and fluctuating consciousness, or paralytic (or dumb) rabies characterized by an ascending paralysis which can be mistaken with Guillain-Barré syndrome (T Hemachudha et al., 2013; Thiravat Hemachudha et al., 2002). The virus then disseminates to innerved organs or tissues as well as salivary glands through centrifugal (anterograde) propagation via sensory innervations (A C Jackson et al., 1999).

Neurotropic RABV presents a unique pathogen which is particularly well adapted to infect the CNS by preventing neuronal apoptosis and inhibiting the host immune response, two important factors that shape RABV immune evasion (M Lafon, 2008; Davis et al., 2015). Although IFN-antagonistic functions of RABV genes are well studied *in vitro* and *in vivo* (Ito et al., 2016), data on RABV-mediated modulation of signalling pathways in the human CNS are still lacking. Further, increasing evidence points out major discrepancies between human and murine immune systems such as different inflammatory cell subsets, toll-like receptors (TLRs), cytokines and cytokine receptors, chemokines and chemokine receptors and costimulatory molecule expression and function (Mestas et al., 2004). Although animal models are informative to study virus immunopathology (Louz et al., 2013), species-specific features reveal extensive differences between proportions of neuronal cell type populations, laminar distributions, gene expression and cell morphologies between the human and murine cortex (CX) (Hodge et al., 2019) questioning if data acquired from studying neurotropic infections in murine models can be entirely extrapolated to humans.

In mice, infection with wildtype (wt) RABV isolates induces only limited inflammatory responses after intracerebral (ic) or intramuscular (im) inoculation compared to attenuated strains (Zhi W Wang et al., 2005). Still, recent mRNA transcription profiling provides evidence that virulent RABV or other lyssaviruses induce an antiviral immune response in mice, through the differentially modulation of gene expression of several pattern recognition receptors (*Tlr2*, *Tlr3*, *Ddx58*, *Ifih1*), genes of the complement pathway (*C1qa*, *C1qb*, *C1qc*, *C3*, *C4*), IFN regulatory genes (*Myd88*, *Irf1*, *Irf3*, *Irf7*, *Irf8*), chemokines (*Ccl5*, *Cxcl10*, *Ccl12*), and pro-inflammatory cytokines (*Il1β*, *Il6*, *Il12*) (Koraka et al., 2018; Pingsen Zhao et al., 2011). RABV or related lyssaviruses upregulate genes involved in pyroptosis (Koraka et al., 2018), cell adhesion, blood vessel morphogenesis and coagulation (Daiting Zhang et al., 2016), proteolysis, the complement cascade (Pingsen Zhao et al., 2011), whereas genes involved in synaptic

transmission and ion transport were significantly down-regulated in the murine CNS (Daiting Zhang et al., 2016). In detail, the JAK-STAT (Pingsen Zhao et al., 2011; Jamalkandi et al., 2016; Sonthonnax et al., 2019), RAS, PI3/AKT, TLR, and NOTCH (Jamalkandi et al., 2016) signalling pathways were identified as the underlying differentially regulated pathways responsible for immuno-regulation, cell survival or apoptosis, and synapse growth proteins. Additionally, RABV modulates the expression of long non-coding RNAs in mice which are supposedly implied in the host response against RABV infection (Pingsen Zhao et al., 2018). Using subtraction hybridization of RABV CVS-N2c lab isolate infected mice revealed that about 90% of the genes were downregulated at day 6 of infection whereas only 1.4% were upregulated, suggesting that profound suppression of host gene synthesis might trigger neuronal dysfunction in mice (Prosniak et al., 2001; Fu et al., 2005).

In humans, morphological findings are relatively mild (Fu et al., 2005) apart from characteristic neural inclusion bodies, so-called Negri bodies (NBs) (A C Jackson et al., 2001; Jogai et al., 2000), suggesting that RABV preserves neuronal integrity to support its propagation (Alan C Jackson et al., 2008; T Hemachudha et al., 2013). Although controversially discussed (Juntrakul et al., 2005), neuronal apoptosis seems not to play a major role in human rabies (Alan C Jackson et al., 2008; Fernandes et al., 2011) whereas inflammatory cells might undergo apoptosis (Suja et al., 2011). Yet, the role of apoptosis in natural RABV infection has not been elucidated, although virus-dependent and cell-dependent mechanisms may account for it (Fu et al., 2005). It has been suggested that RABV evades the innate immune response of the human CNS (T Hemachudha et al., 2013; Monique Lafon, 2011), however, transcriptome data of human rabies patients are still lacking. Despite the expression of TLR3 in human neurons (Alan C. Jackson et al., 2006), RABV implies TLR3 in the spatial arrangement of RABV-induced NBs (Ménager et al., 2009) possibly inhibiting the downstream induction of IFNs (Monique Lafon, 2011). Further, immunostaining on histopathological sections of 25 brains from patients presenting the two main form of rabies (furious and paralytic rabies) showed no correlation between viral antigen distribution and IL-1β or TNF-α protein expression levels in microglia, macrophages, and lymphocytes (Solanki et al., 2009). Taken together, little is known about the inflammatory response induced in the CNS of rabid patients.

Here, we investigated the expression of a panel of selected inflammatory genes upon infection with the virulent canine RABV strain Tha in the murine cortex (CX) and brain stem/cerebellum (BSC) via quantitative polymerase chain reaction (qPCR). To investigate if similar signalling pathways were differentially modulated in human rabies, we compared the transcriptome profiles of mice to the transcriptome profile of *post-mortem* brain samples from RABV-infected patients. Whereas the murine CNS displayed a strong inflammatory response upon pathogenic RABV infection, expression of inflammatory genes was less modulated in human brain samples. In contrast to the murine model, we identified *CXCL16* as the only slightly differentially downregulated gene in *post-mortem* brain samples from rabid patients. Correspondingly, human and murine CNS cell types *in vitro* revealed the same discrepancy suggesting that virulent canine RABV targets the CXCL16/CXCR6 axis in a species-specific manner.

Materials and Methods

Patients and brain samples

Brain biopsies analysed in this study were obtained from two groups of patients (1 sample per patient). The first one originated from Cambodia and included 10 rabid patients infected with RABV canine strains circulating in this country and 4 non-rabid (control) patients (Table S1). The second group encompassed additional rabid patients from Madagascar (n=1, 1 sample), Senegal (n=1, 1 sample), Moldavia (n=1, 3 samples), as well as one additional control patient from Cambodia (n=1, 1 sample per patient) and France (n=4, 1-3 samples per patient) infected with RABV from carnivores (mainly dog) (Table S2). Biopsies which originated from patients in Cambodia, Madagascar, and Senegal were part of a cohort already described in previous publications (Dacheux et al., 2008; Dacheux et al., 2016), which was approved by the national ethical committees. Brain biopsies which originated from French patients were received at the National Reference Centre for Rabies for diagnostic purpose and included in this study as secondary used. Similarly, the Moldavian patient's brain biopsy was received at the World Health Organization Collaboration Centre for Reference and Research on Rabies for diagnostic

purpose and included in this study as secondary used. In both cases, informed consent was obtained directly from patients or their relatives. A molecular diagnosis of rabies was performed (*ante-mortem* or *post-mortem*) for all patients included in this study by RT-PCR (Table S1 and S2) (Dacheux et al., 2008).

Mice and infection experiments

Six-week-old female BALB/c mice (Charles River Laboratories, France) were im infected with 200 μL (2 x 50 μL in each of hind leg) of a RABV virus suspension of $9.8x10^6$ focus forming units (FFU) per mL (approximately $2x10^6$ FFU per animal). The RABV field strain Tha (isolate 8743THA, EVAg collection Ref-SKU: 014V-02106) (Delmas et al., 2008) was used for infection experiments. This virus, closely related to the ones circulating in Cambodia, was initially isolated from the brain of a Thai patient who died after being infected by a rabid dog. This virus was further adapted to cell culture on BSR cells (a BHK-21 clone) (Sato et al., 1977), and passage 21 was used for this study. Food and water were given *at libitum* and mice were daily observed after infection. Animals were euthanized by dislocation of the cervical vertebrae at the paralysis stage (day 8 post-infection), then CX and BSC were collected after autopsy and used for RNA extraction. Non-infected six-week-old female BALB/c mice were used as negative controls.

All animal experiments were performed according to the French legislation and in compliance with the European Communities Council Directives (N°86/609/CEE, 24-11-1986). The animal experimentation was approved (agreement A75-15-25, 30-07-2002) before experiments were initiate.

Cells and virus infection

The human neuroblastoma cell line SK-N-SH (ATCC HTB-11), human astrocytic cell line SVGp12 (ATCC CRL8621), human microglial cell line HMC3 (ATCC CRL-3304) and murine neuroblastoma cell line Neuro-2a (N2A, ATCC CCL-131) were cultured in Dulbecco's Modified Eagle Medium (DMEM) (10566016, Thermo Scientific) supplemented with 10% heat-inactivated fetal bovine serum (S182H-500, Eurobio) at 37°C and 5% CO_2.

Murine cortical astrocytes (mAstrocytes) prepared from C57BL/6 wild type mice (in-house colony, Institut Pasteur, Paris, France) were used at P0 to P3 (1-3 days after birth), as described previously (Schildge et al., 2013). Briefly, after decapitating the pups, the meninges were stripped off the brain, and cortices were pooled prior to homogenization. Dissociated cortical cells (neocortex) were grown in 75 cm^2 flasks coated with poly-D-lysine (A3890401, Thermo Scientific, working concentration 5 μg/mL) in complete astrocyte medium composed of DMEM supplemented with 10% heat-inactivated fetal bovine serum (S182H-500, Eurobio) and penicillin/streptomycin (15140148, Thermo Scientific). Cultures were kept at 37°C and 5% CO_2 until they reached confluency (within 7–10 days of culture). Culture medium was refreshed every three days. To reduce the proliferation of other glial cells, 10 μg/mL 5-fluoro-2′-deoxyuridine (F0503, Sigma-Aldrich) and 10 μg/mL uridine (U3003, Sigma-Aldrich) were added to the culture for one week. Experiments were performed on cells plated at a density of $2.5x10^4$ cells/cm^2 on 12-well-plates previously coated with poly-D-lysine (A3890401, Thermo Scientific). mAstrocytes were used until passage 5 for experiments, as late passages induce astrocyte phenotype changes (Bang et al., 2021). All animal experiments were performed according to the French legislation and in compliance with the European Communities Council Directives (2010/63/UE, French Law 2013–118, February 6, 2013) and according to the regulations of Institut Pasteur Animal Care Committees. The Animal Experimentation Ethics Committee (CETEA no. 089) of the Institut Pasteur approved this study (25-04-2018) before experiments were initiated.

Cells were infected with the field RABV strain Tha at a multiplicity of infection (MOI) of 5. After 24 hours, cells were stimulated using 2500 U/mL of universal IFN-α active on human and murine cells (I4401, Sigma-Aldrich). Cells were lysed 48 hours post-infection by using the RNeasy Mini Kit (74104, Qiagen).

In review

RNA preparation and cDNA synthesis

Human brain biopsies (size approximatively between 0.25 and 1 cm^3) were washed at least two times in sterile PBS (10010023, Thermo Scientific), then total RNA was extracted using Tri-Reagent (TR118, Molecular Research Center) according to manufacturer recommendations. RNA was purified using RNeasy Micro Kit (74004, Qiagen) with a DNA depletion step using DNase I together with the RNase-Free DNase set (79254, Qiagen), and following the recommendations of the manufacturer. The concentration of RNA was measured by photometric quantification using Nanodrop (Version 2000/2000c, Thermo Scientific) and the RNA integrity was evaluated using 2100 Bioanalyzer system (Agilent) which provides an RNA integrity number (RIN). To have sufficient RNA concentrations for the transcriptomic analysis of samples listed in Tables 1 and 2, an *in vitro* amplification step of RNA was performed using the GeneChip Two-Cycle cDNA Synthesis Kit (Agilent) in combination with the MEGAscript T7 Kit (Ambion), both according to the manufacturer's recommendations, and starting from 10 ng or 100 ng of purified RNA. For additional human samples (Table S2) and for mouse samples, RNA was isolated from tissues using Tri-Reagent as previously described. Quality and quantity of total extracted RNA were controlled by photometric quantification using Nanodrop, and reverse transcription was then performed using SuperScript II Reverse Transcriptase (18064022, Invitrogen) according to the manufacturer's instructions. Generally, 100 ng - 1 μg of purified RNA was converted into cDNA. For qPCR experiments, cDNA was diluted 1:10 – 1:100 depending on the initial RNA concentration that was used for reverse transcription, and the preparation method used.

Quantitative PCR

Quantitative PCR based on the detection of the SYBR Green dye was performed by using 5 μl of the synthesized and diluted cDNA in presence of 10 μl QuantiTect SYBR Green (204143, Qiagen) and 1 mM specific primers (in a final volume of 20 μl, 33 targeted genes), or in the presence of 3.1 μl of Power SYBR Green PCR Master Mix (Applied Biosystems, 4367659) and 0.9 mM specific primers (in a final volume of 25 μl) (Table S3). Oligonucleotides were used for PCR at a concentration of 10 pmol/μl. All the samples were measured in triplicates. Gene expression levels were normalized to the endogenous expression of the geomean of two housekeeping genes, 18S ribosomal RNA (*18S*) and glyceraldehyde-3-phosphate dehydrogenase (*GAPDH*) for human samples and actin beta (*Actb*) and *Gapdh* for murine samples (Figure S1). The ΔCT was calculated by subtracting the geomean of the above-mentioned housekeeping genes from the CT values (Vandesompele et al., 2002). Variations in gene expression were calculated as the n-fold change in expression in the tissues from the infected samples compared with the non-infected samples using the $2^{-\Delta\Delta Ct}$ method (Pfaffl, 2001). The ΔΔCT was calculated by normalizing the ΔCT values to the corresponding non-infected samples. The two best suitable housekeeping genes were selected based on the housekeeping genes showing the least variation between samples (Figure S1). Conditions used for qPCR were the following: initial denaturation step (1x repetition, 10 min, 95°C), amplification step (40x repetitions, 15 sec 95°C, 1 min 60°C) and melting curve determination step (1x repetition, 15 sec, 95°C, 1 min 60°C, 15 sec 95°C, 15 sec 60°C).

Immunofluorescence

Murine Astrocytes were isolated as described before: A total of $1x10^4$ cells/well was seeded into 96-well-plates (655086, Greiner Bio) previously coated with 5 μg/mL Poly-D-Lysine (A3890401, Thermo Scientific). After infection, cells were fixed using 4% paraformaldehyde fixative solution (J61984, Alfa Aesar) for 15 minutes at room temperature. Cells were washed once with PBS (10010023, Thermo Scientific) and permeabilized using 0.5% (v/v) Triton-X (648463, Millipore) for 10 minutes. After permeabilization, cells were stained overnight with GFAP (AB5804, Millipore) at 4°C. Cells were washed with PBS (10010023, Thermo Scientific) and incubated with Rabies DFA agent (5100, Chemicon) and the secondary antibody AlexaFluor 546 (A11035, Thermo Scientific) for 1 hour at 4°C. Cells were stained for 5 minutes with Hoechst (H1399, Thermo Scientific) and imaged using the Opera Phenix™ High Content Screening System (Perkin Elmer).

For Review Only

Statistical analysis

Percentages and means ± SD (standard deviation) were calculated with GraphPad Prism 9 and R (version 3.4.4). Statistical deviation and statistical significance were calculated when at least three independent experiments were conducted. Figureures were generated by R (version 3.4.4), Prism 9, and Adobe Illustrator CC 2019.

Results

RABV strain Tha targets IFN-signalling pathways in the murine CX and BSC

To understand how RABV successfully invades the CNS, we investigated the innate immune gene expression in CX and BSC of mice infected with the RABV strain Tha (Figure 1). Mice were intramuscularly infected, and RNA was extracted from CX and BSC at day 8 post-infection. At this time point, genes encoding viral nucleoprotein (N-protein), matrix protein (M-protein), and phosphoprotein (P-protein) were present in murine CX and BSC (Figure S2), confirming RABV infection. Overall, transcription profiles revealed a strong inflammatory response in CX and BSC of Tha-infected mice compared to non-infected animals (Figure 1). Further, we defined the number of differentially expressed genes (DEGs) as a significant difference in gene expression (adjusted p-value < 0.05) between infected and non-infected animals (Table S4). Among the 33 inflammatory genes investigated, we found 20 genes in the murine CX (20 up-regulated genes) and 30 genes in the murine BSC (26 up-regulated genes, 4 down-regulated genes, Table S4) to be differentially expressed upon Tha infection. In detail, the 20 DEGs observed in the murine CX were also observed in the BSC, presenting a strong universal signature of RABV-induced inflammation in the murine brain (Figure S3). Similarly, Tha infection strongly induced expression of C-X-C motif chemokine ligand 10 (*Cxcl10*), C-C motif chemokine ligand 5 (*Ccl5*), C-C motif chemokine ligand 3 (*Ccl3*), interleukin 6 (*Il6*), 2'-5' oligoadenylate synthetase-like 1 (*Oasl1*), interferon regulatory factor (*Irf7*), guanylate binding protein 1 (*Gbp2b*), and interferon induced protein with tetratricopeptide repeats 2 (*Ifit2*) genes in the murine CX and BSC (average fold change > 100). Expression of Interferon-stimulated gene factor 3 (*Isfg3*), complement C3a receptor 1 (*C3ar1*), Jun proto-oncogene (*Jun*), adenosine deaminase RNA specific (*Adar*), ribonuclease L (*Rnasel*) and Janus kinase 2 (*Jak2*) genes was moderately induced in murine CX and BSC average fold change < 20), but their gene expression was only significantly regulated in the murine BSC. Apart from Tha-induced downregulation of *Cxcl12* and *Cxcl14* in the murine CX and BSC, Tha additionally downregulated expression of nuclear factor kappa B kinase subunit beta (*Ikbkb*), interferon alpha and beta receptor subunit 1 (*Ifnar1*), interferon gamma receptor 2 (*Ifngr2*), *and* C-X3-C Motif Chemokine Receptor 1 (*Cx3cr1*) genes in the murine BSC. When comparing gene expression between the two tissues, *Isfg3* and suppressor of cytokine signalling 3 (*Socs3*) were significantly upregulated in the murine BSC compared to the CX (Figure 1, Table S5).

Preprint

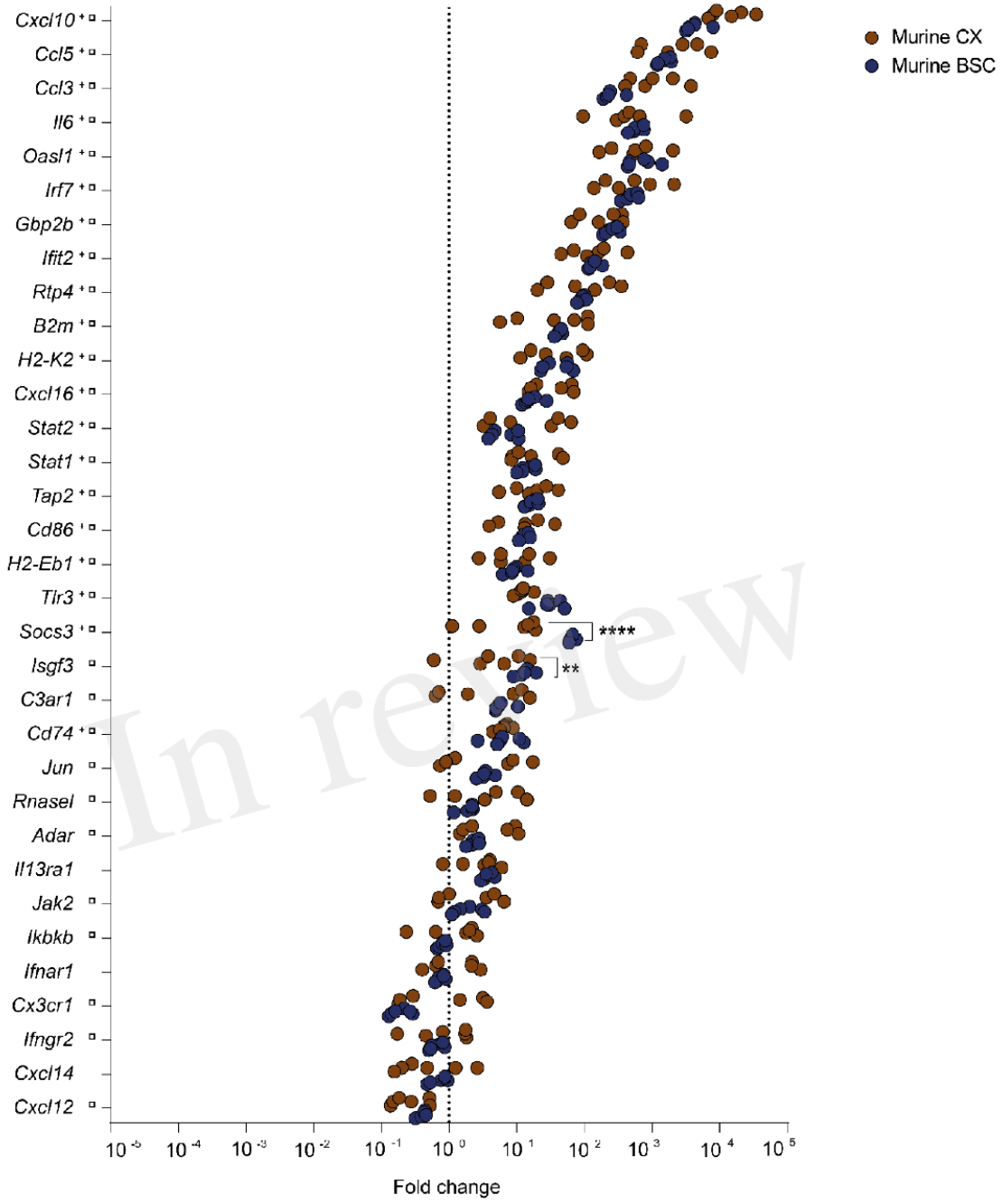

In review

Figure 1. Inflammatory transcription profile of murine CX and BSC upon RABV strain Tha infection at day 8 post-infection. Scatter plot shows gene expression fold changes in murine CX (n=6) and BSC (n=6) upon Tha infection. Fold changes were calculated based on normalization with the geomean of housekeeping genes *Actb* and *Gapdh* (Figure S1) as well as non-infected murine CX (n=6) and non-infected BSC (n=6) respectively. Differential expression was calculated by comparing the gene expression (ΔΔCT values) between murine CX and BSC with the Šídák's multiple comparisons test (adjusted p-value ****: < 0.0001, ***: < 0.001, **: <0.01, *: < 0.05). Gene expression in the murine CX (⁺) or murine BSC (□) that differed significantly from non-infected controls is marked accordingly. A detailed overview of the differential gene expression analysis can be found in Table S4.

The transcriptome profile of natural RABV infection revealed only limited inflammatory responses in the human BSC compared to Tha-infected murine CX and BSC

To understand if RABV infection in mice presents a relevant model to study human RABV infection, we compared the obtained results from RABV Tha strain-infected mice to the orthologous gene expression on a cohort of rabid patients from Cambodia (group 1). Group 1 included 10 rabid patients (4 females and 6 males), all infected with a canine RABV isolate closely genetically related to the RABV Tha strain used in the mouse model (Table S1). These patients were between 8 – 50 years of age (mean= 20.8 years; median= 17 years), and all displayed abnormal behaviour and dysphagia among other symptoms at the time of medical examination (Figure 2A, Table S1). Almost all patients had a history of a rabies exposure after dog bite, ranging back between one year and one month before admission to the hospital. All patients died within 2 – 8 days (mean = 3.7 days, median = 3 days) after the onset of rabies-related symptoms. The time of brain sample collection corresponds to the time of death (Figure 2B, Table S1). The subset of rabid patients was compared to a subset of 4 non-rabid (control) patients from Cambodia, including 2 females and 2 males, ranging from 41 – 65 years of age (mean= 55 years; median= 57 years) (Table S1).

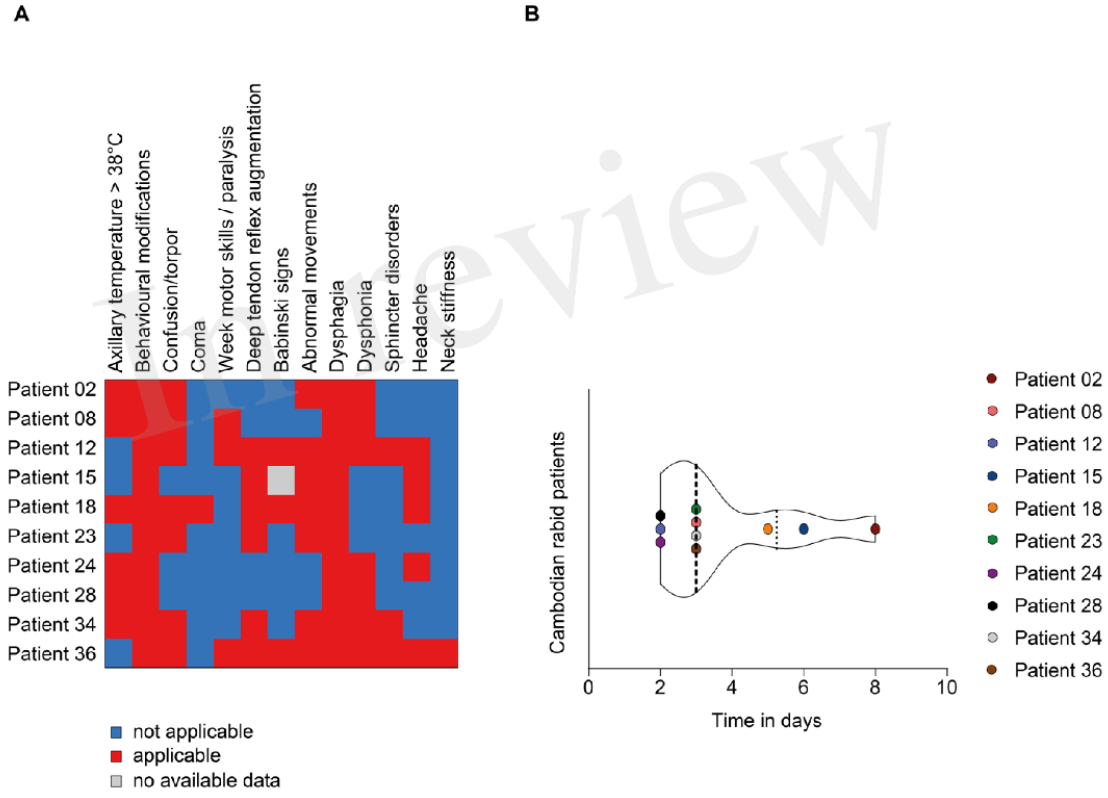

Figure 2. Clinical presentation of Cambodian rabid patients from group 1 (n=10). (A) Description of the clinical signs and symptoms of Cambodian rabid patients. **(B)** Time between the onset of symptoms in and death in days in Cambodian rabid patients. **(A-B)** A detailed overview of the clinical presentation of Cambodian rabid patients belonging to group 1 can be found in Table S1.

Using qPCR, we investigated gene expression in the human BSC of rabid patients targeting ortholog inflammatory genes (Figure 3) which we previously studied in the murine CX and BSC (Figure 1). Unlike the strong innate immune response activation observed in the mouse model upon RABV Tha strain infection (Figure 1), the human inflammatory transcriptome profile of natural RABV infection revealed no clear inflammatory response (Figure 3A, Table S4). Investigating gene expression in naturally infected human brains, only genes coding for IL6, CXCL10, SOCS3, guanylate binding protein 2 (GBP2), and TLR3 showed a modest (average fold change > 10) but not significant upregulation in

Preview

expression. Further, *CCL3* and *CXCL16* represented the only slightly downregulated genes in the brain of rabid patients compared to non-rabid control patients, with *CXCL16* presenting the only DEG in human rabid patients (average fold change = 0.68, Figure 3A and B, Table S4). However, we need to mention that CXCL16 expression levels varied drastically between rabid patients with three rabid patients showing a particularly strong reduction in CXCL16 expression (IPC28, IPC34 and IPC36). Overall, modestly downregulated genes in the human BSC were genes involved in chemotaxis and recruitment of infiltrating leukocytes (*CCL3*, *CXCL16*) suggesting that RABV suppresses recruitment of infiltrating immune cells to the site of infection (Figure 3A and B). Similar results were observed in the mouse model, where downregulated genes in the murine CX and BSC are implied in chemotaxis (*Cxcl12*, *Cxcl14*). In contrast, downregulated pathways implied in IFN signalling (*Ifnar1*, *Ifngr2*, *Ikbkb*) in the murine BSC were not observed in the human BSC of rabid patients (Figure 1, Figure 3B). Apart from *CXCL16* expression, gene expression of other ortholog genes investigated revealed only modest and non-significative modulation in the RABV-infected human BSC (Figure 3B and C): strikingly, and despite the strong similarity of the murine CX and BSC transcriptome profile during RABV Tha strain infection, no gene was found to be differentially up- or downregulated in both, the murine model (murine CX or BSC) and naturally infected rabid patients (Figure 3C, Table S4).

In review

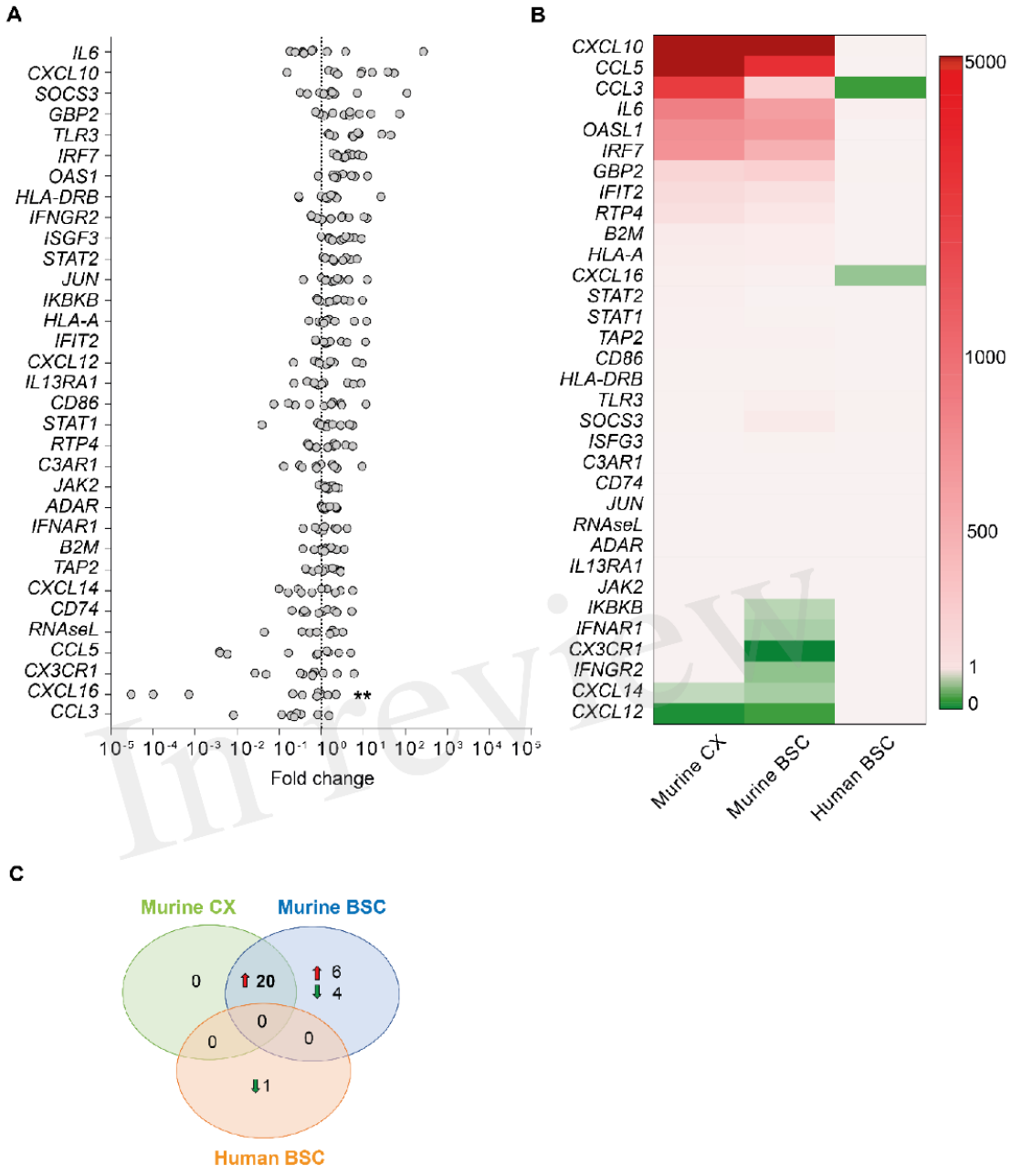

Figure 3. Human transcription profile upon RABV infection. (A) Gene expression fold changes in *post-mortem* brain biopsies of the BSC of rabid patients (n=10) normalized to non-rabid patients (n=4). Differential expression was calculated by comparing the gene expression (ΔCT values) between rabid patients (n=10) and non-rabid (control) patients (n=4) by using the Šídák's multiple comparisons test (** adjusted p-value < 0.01). A detailed overview of the differential gene expression analysis can be found in Table S4. **(B) Heatmap comparing the expression of inflammatory genes between RABV Tha strain-infected murine CX (n=6) and BSC (n=6), and RABV-infected human BSC (n=10).** Heatmap presents gene expression fold changes calculated from normalized gene expression values (ΔΔCT) of infected animals and humans to the respective non-infected controls (murine CX [n=6]; murine BSC [n=6]; human BSC [n=4]). Gene names are indicated in the human gene name nomenclature although expression indicates quantification of human or murine genes depending on the tissue investigated. **(C) Number of differentially expressed genes showing the same tendency (up-**

In review

or downregulation) in the RABV Tha strain-infected murine CX (n=6) or BSC (n=6), and RABV-infected human BSC (n=10). Differential gene expression was calculated to non-infected mice (n=6) or human controls (n=4), respectively. A detailed overview of the differential gene expression analysis can be found in Table S4.

Regulation of *CXCL16* expression in the human and mouse brain during RABV infection

To further investigate the potential downregulation of *CXCL16* by RABV in the human brain, we extended our analysis to an additional group of patients (group 2), which included rabid patients from Moldavia (n=1, 3 samples), Madagascar (n=1, 1 sample) and Senegal (n=1, 1 sample), as well as non-infected control patients from Cambodia (n=2, 2 samples) and France (n=4, 7 samples) (Table S2). Thus, this panel included rabid patients from different geographical origins, all being infected with different RABV strain or phylogenetic clades (Table S2). As presented in Figure 4A, we confirmed the tendency of *CXCL16* downregulation during natural RABV infection in the infected human brain (Figure 4A) although this downregulation was not found to be significant. To evaluate if the nature of the brain biopsies (i.e. CX or BSC) might be a confounding factor in quantifying *CXCL16* expression observed between infected and control patients, we compared *CXCL16* gene expression between the CX and BSC of non-rabid patients. Based on the results of this comparison, *CXCL16* expression levels were slightly but not significantly higher in the human BSC (n=7) compared to the human CX (n=4), although samples did not originate from the same donors (Figure 4B). However, and since most of the human brain samples of rabid patients originated from BSC (n=11) rather than CX (n=4), we can exclude the influence of sampling for the differences of *CXCL16* expression observed in infected RABV patients (Figure 4B). At worst, this difference would be minimised, due to the slightly higher expression level of *CXCL16* in the BSC of non-rabid patients (Figure 4B). Similarly, *CXCL16* was slightly but not significantly higher expressed in the non-infected murine BSC compared to paired samples taken from the murine CX (Figure 4C).

To understand if the difference of *CXCL16* regulation in the murine brain appears due to differences of RABV strain or rather differences in the human versus murine model, we infected different human and murine CNS cell lines with the same RABV Tha isolate previously used for animal infections and evaluated the expression level of *CXCL16* at 48 hours post-infection. For this evaluation, human and murine CNS cell types were infected with Tha (MOI 5) and stimulated at 24 hours post-infection with a hybrid IFN-α which crosses the species barrier to induce *CXCL16* expression. All IFN-α-treated human CNS cell lines, comprising human neuroblastoma cells (SK-N-SH), human microglia-like cells (HMC3), and human astrocyte-like cells (SVGp12), showed a downregulation of *CXCL16* gene expression upon RABV Tha strain infection in contrast to the IFN-α-treated mock (Figure 4D). Conversely, *CXCL16* gene expression of murine neuroblastoma N2A cells and cortical astrocytes treated with universal IFN-α remained unchanged (Figure 4E). Surprisingly, and in contrast to murine N2A cells, cortical murine astrocytes strongly increased *CXCL16* gene expression upon Tha infection (Figure 4E). Thus, activated murine astrocytes might be the source for CXCL16 production in the Tha-infected murine brain.

In review

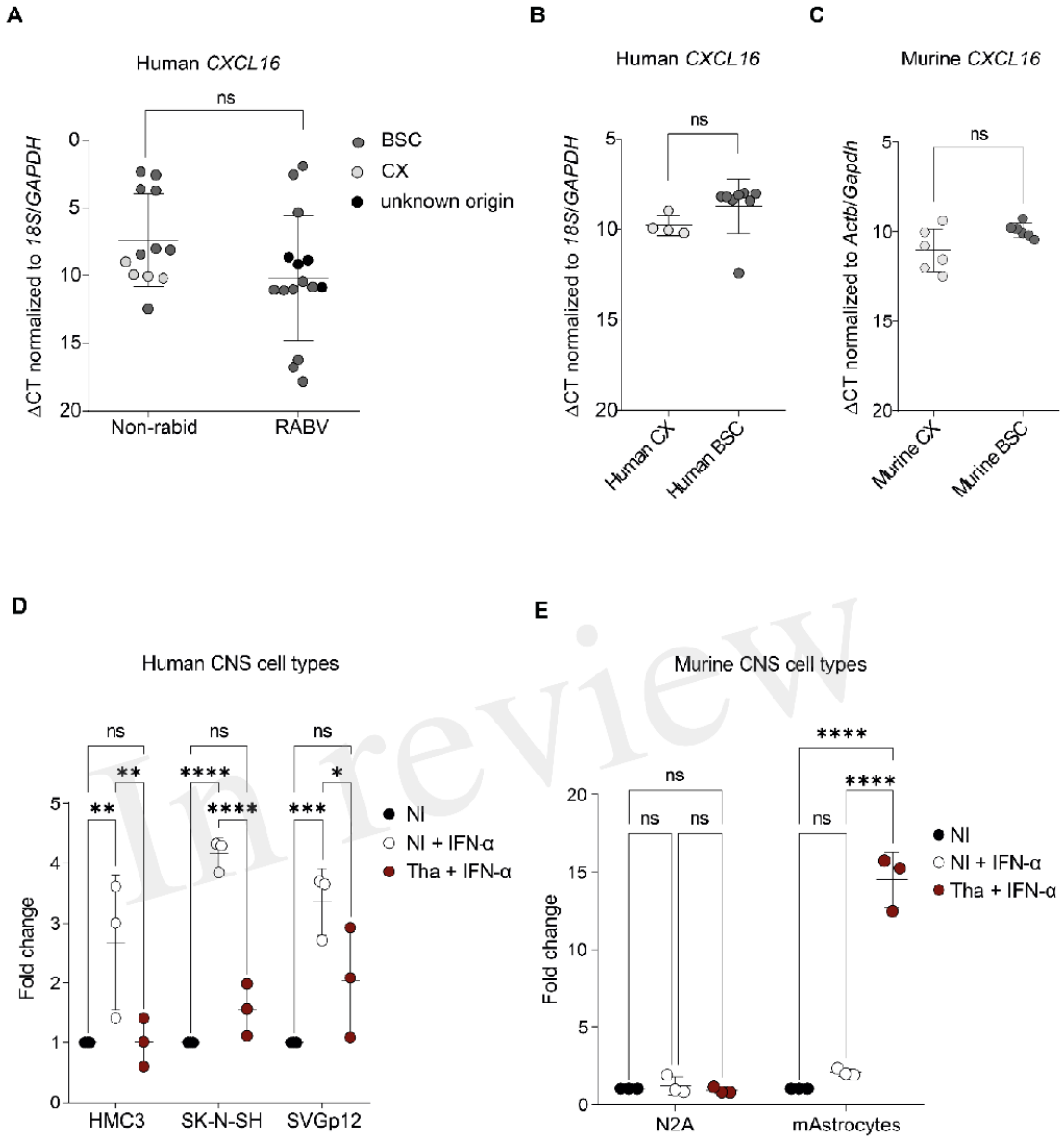

Figure 4. *CXCL16* gene expression in human and murine brains and CNS cell types during RABV infection. (A) *CXCL16* gene expression in brain from non-rabid patients and rabid patients (from group 1 and 2). Comparison of *CXCL16* expression in brains from non-rabid (control) patients (n = 12; 12 samples) from Cambodia (IPC38, IPC39, IPC40, IPC41, IPC42) and France (P448, P447, P465, P521, P552, P523, P524) and from rabid patients (n=12; 15 samples) from Cambodia (IPC02, IPC08, IPC12, IPC15, IPC18, IPC23, IPC24, IPC28, IPC34, IPC36), Senegal (IPS01), Moldavia (1900105, 1900106, 1900107), and Madagascar (IPM01). A detailed overview of the additional included human samples can be found in Table S5. *CXCL16* expression values (ΔCT) were compared by using an unpaired t-test. **(B) *CXCL16* expression in non-infected control human CX (n=4) and BSC (n=8) samples.** *CXCL16* expression values (ΔCT) between CX (P447, P465, P523, P524) and BSC (IPC38, IPC39, IPC40, IPC41, IPC42, P448, P521, P552) were compared by using an unpaired t-test (p=0.072). **(C) CXCL16 expression in the CX (n=6) and BSC (n=6) of non-infected mice.** CXCL16 expression values (ΔCT) between CX and BSC were compared by using a paired t-test (p=0.122). **(D) CXCL16 expression in human CNS cell types (n = 3) infected with RABV Tha (48 hours post-infection).** Human CNS cell types (SK-N-SH, HMC3, SVGp12) were infected with Tha (MOI 5) and treated with IFN-α at 24 hours post-infection. **(E) CXCL16 expression in murine neuroblastoma cells and**

In review

cortical murine astrocytes (n=3) upon RABV Tha strain infection (48 hours post-infection). Murine CNS cell types were infected with Tha (MOI 5) and treated with IFN-α at 24 hours post-infection. Murine astrocytes were extracted from C57BL/6 wild type mice and their phenotype was validated by immunofluorescence and qPCR (Figure S7). **(D - E)** All cell culture experiments were performed in three independently replicates. Bars show average fold changed ± SD with a Tukey's multiple comparison test (adjusted p-value ****: < 0.0001, ***: < 0.001, **: <0.01, *: < 0.05). BSC = brainstem /cerebellum, CX = cortex; HMC3 = human microglial cell line; mAstrocytes = cortical murine astrocytes; NI = non-infected; N2A = murine neuroblastoma cells; SK-N-SH = human neuroblastoma cell line; SVGp12 = human astroglia cell line.

RABV possibly modifies neurotransmission and inflammatory immune cell recruitment in the human brain via modulation of *CXCL16* expression

Lastly, we investigated the modulated pathways in the brain of rabid patients, based on the transcriptomic analysis. First, using the functional enrichment analysis based on gene expression ranks (STRING software), we identified interleukin-10 receptor activity (GO:0004920), of C-C chemokine receptor type 5 (CCR5), interferon receptor activity (GO:0004904), CCR1 chemokine receptor binding (GO:0031726), and TAP binding (GO:0046977) as the most upregulated molecular functions found in gene ontology (GO) in human brains which were naturally infected with RABV strains (Figure S8).

Secondly, we focused on the only significantly differentially expressed gene, *CXCL16*, during RABV infection, and we modelled physical and full protein interaction networks via STRING. The physical interaction network revealed that CXCL16 interacts with the beta and gamma subunits of a range of guanine nucleotide-binding proteins (*GNG/GNB*) which modulate or transduce various transmembrane signalling systems (Figure 5A). Beta and gamma chains are necessary for GTPase activity, to the replacement of GDP by GTP, as well as to the G protein-effector function which mainly conducts the information from G-protein-coupled receptors (GPCRs). Most of the GPCR signalling pathways in the brain are involved in synaptic functions: the five most upregulated KEGG pathways of the physical interaction network were involved in signalling pathways of the GABAergic synapse (hsa04727), serotonergic synapse (hsa04726), the cholinergic synapse (hsa04725), and the glutamatergic synapse (hsa04724), and the dopaminergic synapse (hsa04728). In short, this analysis suggests that RABV could potentially influence neurotransmission and synaptic plasticity by modulating *CXCL16* gene expression. Apart from physical interaction partners, the full interaction network of *CXCL16* revealed the enrichment of T cell, monocyte, and macrophage chemotactic processes (Figure 5B). Consequently, downregulation of *CXCL16* during RABV infection might influence chemotaxis resulting in reduced migration and adhesion of infiltrating immune cells to the infected site.

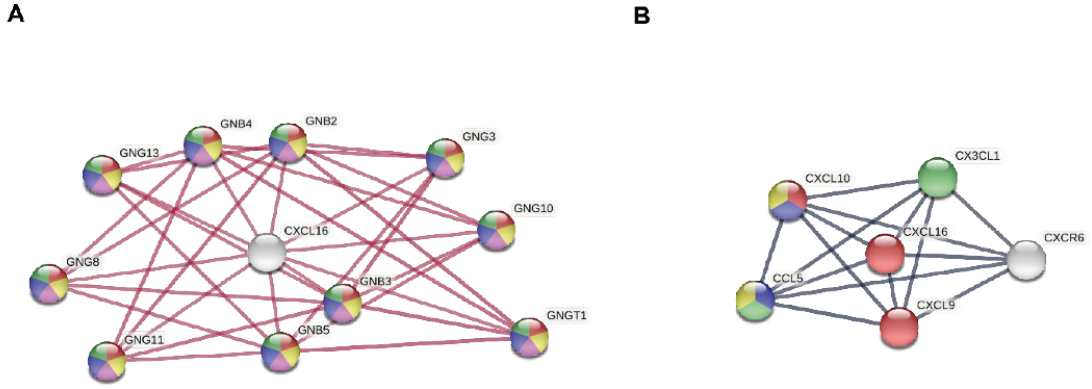

Figure 5. CXCL16 interaction network. (A) Physical network of CXCL16 indicating physical protein associations. Colours present five of the most upregulated KEGG pathways (strength > 2, FDR < 5.94e-21): Red = GABAergic synapse (hsa04727), yellow = serotonergic synapse (hsa04726), purple

= cholinergic synapse (hsa04725), blue = glutamatergic synapse (hsa04724), green = dopaminergic synapse (hsa04728) **(B) Full network of CXCL16 indicating functional and physical protein associations.** Colours present four of the most upregulated biological processes from gene ontology (strength > 2, FDR < 0.00021): Red = T cell chemotaxis (GO:0010818), blue = regulation of T cell chemotaxis (GO:0010819), green = macrophage chemotaxis (GO:0048246), yellow = positive regulation of monocyte chemotaxis (GO:0090026). Networks were generated by using the String version 11.0. GNB = beta unit of guanine nucleotide-binding proteins; GNG = gamma unit of guanine nucleotide-binding proteins.

Discussion

In this study, we compared for the first time the transcriptome profiles during RABV infection at the brain level in a mouse model and in human cases. Analysis of the transcription profiles obtained in mice revealed a strong induction of inflammatory genes upon pathogenic RABV Tha strain infection (canine rabies isolate). Further, transcription profiles of murine CX and BSC showed a universal gene signature presenting 20 out of 33 genes which were differentially upregulated in Tha-infected mice compared to non-infected controls (Figure S3). Between the murine CX and BSC, *Isgf3* and *Socs3* were significantly higher expressed in the murine BSC compared to the CX. Generally, type I and III IFNs induce the formation of transcription factor complex containing Stat2, Stat1, and Irf7, known as Isgf3, which translocates to the nucleus and initiates the transcription of IFN-stimulated genes (ISGs) (Fink et al., 2013). In contrast to the induction of ISGs by Isgf3, Socs proteins initiate a negative feedback regulation of the JAK-STAT pathway to ensure the appropriate activation of innate immune pathways (Shanzhi Huang et al., 2020). Higher expression of *Isgf3* and *Socs3* in the murine BSC suggest that RABV strongly activates canonical and non-canonical IFN signaling pathways in the murine BSC resulting in the transcription of ISGs. Further, IFN signaling pathways induce negative feedback regulation pathways via Socs proteins. Possible explanations for regional differences in innate immune gene expression within the murine brain may rely on the different capabilities of the CX and BSC in mounting antiviral responses (Fitting et al., 2010; Cho et al., 2013) and/or on the different time spans for viral persistence. Indeed, after im infection, RABV is transported via retrograde axonal transport from motor neurons to the CNS (Davis et al., 2015), suggesting that RABV reaches the BSC before reaching the CX. Additionally, viral load in the BSC was slightly higher compared to the murine CX (Figure 2). Thus, we suggest that the murine BSC mounts a stronger inflammatory response towards virulent RABV Tha strain compared to the murine CX, possibly because of longer viral persistence and the natural capacity of the CX to mount enhanced antiviral responses (Cho et al., 2013; Fitting et al., 2010).

Investigating the expression of inflammatory genes in the brain of rabid patients at the late stage of RABV infection revealed profound differences compared to the mouse model (CX and BSC). Compared to the universal gene signature of 20 DEGs observed in the murine brain (CX and BSC), only *CXCL16* (fold change = 0.68) was significantly but slightly downregulated in the human BSC of rabid patients from Cambodia (Figure 3C). Overall, five genes were also modestly but not significantly upregulated upon natural RABV infection (*IL6*, *CXCL10*, *SOCS3*, *GBP2*, *TLR3*) whereas two genes were modestly downregulated: *CCL3*, *CXCL16*, the latter being significantly but slightly downregulated. Interestingly, TLR3 was previously shown to be involved in the spatial arrangement of RABV-induced NBs (Ménager et al., 2009) presenting important sites for viral replication (Ni et al., 1996). Although we show only a modest and not significant increase in TLR3 expression in human rabid patients compared to control patients, RABV might exploit TLR3 functions for viral replication as already shown previously (Ménager et al., 2008; Ménager et al., 2009).

Strikingly, *CCL3* was modestly but not significantly downregulated in the BSC of rabid patients from Cambodia (Figure 3), whereas *Ccl3* was among the most upregulated genes in the murine brain (Figure 1) pointing out profound differences between RABV Tha strain-infected mice and natural RABV infection occurring in humans. *CCL3* bears inflammatory and chemokinetic properties including cellular recruitment and trafficking, immune regulation, and host inflammatory responses (Fitzgerald et al., 2001). Interestingly, it is suggested that *CCL3* plays an important role in macrophage recruitment, T-cell differentiation (Trifilo et al., 2003) and regulation of the BBB permeability (Chui et al., 2010). Zhao and colleagues showed that immunizing mice infected with an attenuated RABV with CCL3 at the

inoculation site, reduced viral pathogenicity and enhanced recruitment of DCs and B cells to the site of immunization (L. Zhao et al., 2010). Thus, targeted downregulation of *CCL3* by wildtype RABV might possibly restrict BBB opening and recruitment of inflammatory cells, ultimately hindering the clearance of RABV from the infected brain. Nevertheless, further studies are needed to elucidate the function of CCL3 in human rabies.

Although RABV induced overall little modulation of gene expression of innate immunity genes in human brains, we identified CCR5 chemokine receptor binding, CCR1 chemokine receptor binding, interleukin-10 receptor activity, interferon receptor activity, and TAP binding as major signalling pathways implied in the modulation of the investigated genes (Figure S8). Nevertheless, we need to admit that identification of these pathways was based on modest changes in gene expression levels, which revealed in most of the cases no significant difference to non-infected controls (Table S4), as well as the prior selection of inflammatory genes investigated. However, and despite these limitations of our study, most of the identified pathways were already described to be involved in RABV infection elsewhere: firstly, the CCL5/CCR5 axis was already shown to be essential to mediate immune cell infiltration in the CNS (Ying Huang et al., 2014). Besides rabies, CCL5 plays a major role in leukocyte recruitment during herpes virus- and West Nile virus-induced encephalomyelitis (Hussmann et al., 2014; Vilela et al., 2009). Recent sequencing data of purified human CNS cells revealed that CCR5 and CCR1 are strongly expressed on infiltrating macrophages and microglia compared to other CNS cell types (Ye Zhang et al., 2014). Further, the transcription factors STAT1 and STAT3 are strongly implied in the regulation of ligand expression for CCR1/CCR5 signalling. In the past, the interaction between STATs and RABV were well studied, and numerous publications reported modulation of STAT activity by virulent RABV via its P-protein (Linda Wiltzer et al., 2014; Lieu et al., 2013; L. Wiltzer et al., 2012; Sonthonnax et al., 2019). Overall, RABV-mediated modulation of the CCR1/CCR5 axis via STAT proteins might hinder macrophage infiltration and microglial activation in the human CNS. Additional modulated pathways imply IFN receptor activity pointing at RABV-modulation of the IFN system. Over the time it has become increasingly clear that the host innate immune system, particularly the IFN system, and RABV-mediated counteractions via accessory protein functions profoundly shape the virus-host relationship (Rieder et al., 2011). Apart from its STAT interactions, the RABV P-protein of pathogenic RABV strains 1088 and HCM-9 have already been shown to interact with the I-kappa B kinase *in vitro* thereby inhibiting the induction of IFN signalling and the establishment of an antiviral response (Masatani et al., 2016).

Despite some differences inherent to the human versus the mouse infection models in our study design (RABV strains, variability in terms of type/origin of samples and quality of RNA, etc.) when comparing human and murine RABV transcription profiles at the brain level, we provide evidence that human rabies patients show only limited expression of inflammatory genes, whereas the mouse model strongly increased the expression of inflammatory genes (*Cxcl10*, *Ccl5*, *Ccl3*, *Il6*, *Irf7*, *Gbp2b*, *Ifit2*) upon RABV Tha strain infection.

Apart from numerous differences between the human and murine immune system in terms of TLRs, leukocyte subsets, antibody subsets, and defensins (Tao et al., 2017), single-nucleus sequencing of human and murine brains have shown marked alterations in cell type proportions and morphologies, laminar distributions and gene expression (Hodge et al., 2019). Hence, differences in human and murine brains, immune systems and viral adaptation mechanisms (Tao et al., 2017; Hodge et al., 2019) as well as differences in viral strains used (natural RABV versus cell adapted RABV) might account for the large difference observed in the establishment of the innate immune response between the RABV-infected human and the murine brain.

Further, we provide for the first time evidence that pathogenic RABV specifically downregulates *CXCL16* expression in the brain of rabid patients, contrasting induction of *CXCL16* expression observed in the murine model. Similarly, RABV Tha strain inhibited IFN-α-mediated induction of *CXCL16* expression in neural, astrocytic, and microglial cell types of human origin but not in murine astrocytes *in vitro*. Although we suggest that activated astrocytes might be the source for *CXCL16* production in the RABV Tha strain-infected murine brain, we cannot exclude that other cells, such as murine microglia, are another important source of CXCL16 upon RABV infection.

CXCL16 is a transmembrane chemokine which can be released in a soluble form from microglia and astrocytes (Ludwig et al., 2005) upon cleavage by metalloproteases ADAM10 and ADAM17 (Trettel et al., 2020). Soluble CXCL16 acts as a chemoattractant for CXCR6/Bonzo-expressing cells such as T cells, NK cells, or glial precursors (Hattermann et al., 2008). Interaction of CXCL16 with CXCR6/Bonzo induces calcium influx, T and NK cell migration and activation via the Akt/mammalian target of rapamycin (*mTOR*) pathways (Matloubian et al., 2000; Jianhua Wang et al., 2008; Günther et al., 2012). Generally, CXCL16 concentrations are increased in inflammatory brain diseases (Ludwig et al., 2005; Le Blanc et al., 2006). Apart from its role in mediating neuro-inflammatory and neurotoxic events in the brain, a role of CXCL16 in mediating crosstalk between astrocytes and neurons has been proposed recently (Trettel et al., 2020; Rosito et al., 2012). Further, CXCL16 induced neuroprotection against excitotoxic damage mediated by excessive glutamate exposure or oxygen glucose deprivation *in vitro* (Rosito et al., 2012). In detail, CXCL16 induces the expression of astrocyte-derived CCL2, which is partly mediating neuroprotection (Rosito et al., 2012). In addition to neuroprotection, CXCL16 exerts a modulatory activity on inhibitory and excitatory synaptic transmission of the murine hippocampus *in vivo* (Di Castro et al., 2016). More specifically, CXCL16 modulates GABA and glutamate release, impacting inhibitory and exhibitory synaptic currents *in vitro* (Di Castro et al., 2016).

Since CXCL16 signaling is implied in neuro-inflammatory as well as neuro-protective and synaptic transmission mechanisms, we can only hypothesize at this stage the effect of RABV-modulated downregulation of *CXCL16* expression in the brain of rabid patients. While chemokines are crucial for the elimination of many different viruses (Alfano et al., 2005; Christensen et al., 2006; Cook et al., 2004; Nansen et al., 2000), the viral modulation of chemokine expression can also result in an inappropriate antiviral response and viral persistence in the infected tissue (Melchjorsen et al., 2003), which might be the case in human rabies pathogenesis. We hypothesize that RABV-mediated downregulation of *CXCL16* expression inhibits T cell, NK cell, and glial precursor recruitment and activation enabling RABV to replicate undetected in the human CNS. Although RABV infection seems not to result in excitotoxicity *in vitro* (Weli et al., 2006), CXCL16 might modulate neurotransmission during viral infection. Undoubtedly, investigating the role of *CXCL16* in modulating neuroprotection and synaptic function remains a significant question of interest to better understand how RABV modulates synaptic function.

Overall, species-specific immune responses highlighted the difference of the transcriptomic profile observed for rabies at the brain level between the mouse model and human cases, thus emphasize the importance of the choice of the most relevant models/samples to study the mechanisms of rabies pathogenesis in human. This study points out vast differences in the expression of innate immunity genes upon pathogenic RABV infection in mice and in humans: whereas intramuscular infection of mice with a virulent canine RABV results in the upregulation of inflammatory genes in murine CX and BSC, transcriptome analysis of *post-mortem* human brains revealed only little inflammatory responses upon infection with closely related canine RABV isolates. Interestingly, RABV specifically downregulates *CXCL16* in the human brain, a mechanism that was not observed in the mouse model. Since *CXCL16* is crucial for the induction of T, NK and glia cell migration to the infected brain area, we hypothesize that RABV-mediated downregulation of *CXCL16* expression hinders the successful virus clearance from the brain. Although animal models have different advantages, especially to study RABV pathogenesis, our results emphasize species-specific differences in CXCL16 signaling during RABV infection to show potential limitations of extrapolating transcriptome data from mice to human.

List of abbreviations

Actb = actin beta; BSC = brain stem/cerebellum; CD = cluster of differentiation; cDNA = complementary DNA, CNS = central nervous system; *Ccl* = CC-chemokine ligand; CCR = C-C chemokine receptor, CX = cortex; *Cxcl* = C-X-C Motif Chemokine Ligand; *Cxcr* = C-X-C Motif Chemokine Receptor; DEGs = differentially expressed genes, *GAPDH* = glyceraldehyde-3-phosphate dehydrogenase; G protein = glycoprotein; GNB = beta unit of guanine nucleotide-binding proteins; GNG = gamma unit of guanine nucleotide-binding proteins; ic = intracerebral; IFN = interferon; *Ifnar* = interferon-α/β receptor; *Ifngr2* = interferon gamma receptor 2, *Ikbkb* = Inhibitor Of Nuclear Factor Kappa B Kinase Subunit Beta; IL = interleukin; im = intramuscular; ISG = interferon stimulated genes;

Isgf3 = interferon Stimulated Gene Factor 3; *Jak* = Janus kinase; mAstrocytes = murine cortical astrocytes; M-protein = matrix protein; MOI = multiplicity of infection; NBs = Negri bodies; NK cells = natural killer cells; N2a = Neuro-2a cells; NBs = Negri bodies; N-protein = nucleoprotein; *Oasl1* = 5'-oligoadenylate synthetase-like protein; PNS = Peripheral nervous system; P-protein = phosphoprotein; qPCR = quantitative PCR; RABV = rabies virus; SD = standard deviation; *Stat* = signal transducer and activator of transcription 1; TLRs = toll-like receptors; wt = wildtype

Declarations

Ethics approval and consent to participate

Brain samples collected from Cambodian, Malagasy and Senegalese patients (patients from group 1 and part of patients from group 2) were obtained in the framework of a previous study already described (Dacheux et al., 2008), which was approved by the national ethical committees (N° 102-SANPF/CAB from the Ministry of Health and Family Planning of Madagascar, N°008/03 NECHR and N° 054NECHR from the Ministry of Health of Cambodia, N°00116 MSPM/DS/DER from the Ministry of Health and Medical Prevention of Senegal). For the other samples collected from French patients, they were received at the National Reference Center for Rabies for diagnostic purpose and were associated to an informed consent obtained directly from them or their relatives by the physicians in charge of this patient, for the secondary use of these samples. For the samples collected from the Moldavian patient, they were received at the World Health Organization Collaboration Centre for Reference and Research on Rabies for diagnostic purpose and were associated to an informed consent obtained directly from him by the physicians in charge of this patient.

Consent for publication

Samples and data collected from Cambodian, Malagasy and Senegalese patients were obtained in the framework of a previous study already described (Dacheux et al., 2008). For the other patients, the secondary use of their samples and their anonymized data were associated to an informed consent obtained directly from them or their relatives by the physicians in charge of these patients. However, this *post-mortem* study relies on the use of samples and anonymized data collected over several years, which does not make it possible to obtain specific consent for the publication of this study.

Availability of data and materials

The datasets supporting the conclusions of this article are included within the article and its additional file (Additional_file_1). The additional file contains the following gene expression data measured by qPCR:

- AF1: Gene expression fold changes of *CXCL16* quantified in human (SVGp12, HMC3, SK-N-SH) and murine cells (N2A, mAstrocytes) *in vitro*.
- AF2: Expression of *CXCL16* (ΔCT) quantified in murine cells (N2A, mAstrocytes) *in vitro*.
- AF3: Gene expression fold changes of *CXCL16* quantified in non-infected human (CX and BSC) and murine brains (CX and BSC).
- AF4: Gene expression of *CXCL16* (ΔCT) quantified in non-infected human brains and naturally RABV-infected human brains.
- AF5: Gene expression fold changes of inflammatory genes quantified in naturally RABV-infected brains from Cambodian patients.
- AF6: Gene expression fold changes of inflammatory genes quantified in the Tha-infected murine CX.
- AF7: Gene expression fold changes of inflammatory genes quantified in the Tha-infected murine BSC.
- AF8: Viral load (N-protein, M-protein, P-protein) quantified in Tha-infected murine brains (CX and BSC).

In review

781 **References**

782

783 Alfano, M., and Poli, G., (2005). Role of Cytokines and Chemokines in the Regulation of Innate
784 Immunity and HIV Infection, *Molecular Immunology*, 42(2):161-82. doi:
785 10.1016/j.molimm.2004.06.016.

786 Baer, G. M., *The Natural History of Rabies*, *CRC Press*, New York: Academic Press, pp. 640,
787 1975.

788 Bang, M., Gonzales, E. L., Shin, C. Y. and Kwon, K. J., (2021). Late Passage Cultivation Inducs
789 Aged Astrocyte Phenotypes in Rat Primary Cultured Cells, *Biomolecules and*
790 *Therapeutics*, 29(2):144-153. doi: 10.4062/biomolther.2020.175.

791 Blanc, L. M. P. Le, Lieshout, A. W. T. Van, Adema, G. J., Riel, P. L. C. M. Van, Verbeek, M.
792 M. and Radstake, T. R. D. J., (2006). CXCL16 Is Elevated in the Cerebrospinal Fluid
793 versus Serum and in Inflammatory Conditions with Suspected and Proved Central
794 Nervous ystem Involvement, *Neuroscience Letters*, 397(1-2):145-8. doi:
795 10.1016/j.neulet.2005.12.029.

796 Brahmachari, S., Fung, Y. K. and Pahan, K., (2006). Induction of Glial Fibrillary Acidic rotein
797 Expression in Astrocytes by Nitric Oxide, *Journal of Neuroscience*, 26(18):4930-9. doi:
798 10.1523/JNEUROSCI.5480-05.2006.

799 Castro, M. A. Di, Trettel, F., Milior, G., Maggi, L., Ragozzino, D. and Limatola, C., (2016). The
800 Chemokine CXCL16 Modulates Neurotransmitter Release in Hippocampal CA1 area,
801 *Scientific Reports*, 6:34633. doi: 10.1038/srep34633.

802 Ceccaldi, P. E., Gillet, J. P. and Tsiang, H., (1989). Inhibition of the Transport of Rabies Virus
803 in the Central Nervous System., *Journal of Neuropathology and Experimental Neurology*,
804 48(6):620-30. doi: 10.1097/00005072-198911000-00004.

805

In review

Cho, H., Proll, S. C., Szretter, K. J., Katze, M. G., Gale, M. and Diamond, M. S., (2013). Differential Innate Immune Response Programs in Neuronal Subtypes Determine Susceptibiliy to Infection in the Brain by Positive-Stranded RNA Viruses, *Nature Medicine*, 19(4):458-64. doi: 10.1038/nm.3108.

Christensen, J. E., Lemos, C. de, Moos, T., Christensen, J. P. and Thomsen, A. R., (2006). CXCL10 Is the Key Ligand for CXCR3 on CD8 + Effector T Cells Involved in Immune Surveillance of the Lymphocytic Choriomeningitis Virus-Infected Central Nervous System , *The Journal of Immunology*, 176(7):4235-43. doi: 10.4049/jimmunol.176.7.4235.

Chui, R. and Dorovini-Zis, K., (2010). Regulation of CCL2 and CCL3 Expression in Human Brain Endothelial Cells by Cytokines and Lipopolysaccharide, *Journal of Neuroinflammation. 7:1. doi: 10.1186/1742-2094-7-1.*

Cook, W. J., Kramer, M. F., Walker, R. M., Burwell, T. J., Holman, H. A., Coen, D. M. and Knipe, D. M., (2004). Persistent Expression of Chemokine and Chemokine Receptor RNA at Primary and Latent Sites of Herpes Simplex Virus 1 Infection, *Virology Journal*, 1:5. doi: 10.1186/1743-422X-1-5.

Dacheux, L., Larrous, F., Lavenir, R., Lepelletier, A., Faouzi, A., Troupin, C., Nourlil, J., Buchy, P. and Bourhy, H., (2016). Dual Combined Real-Time Reverse Transcription Polymerase Chain Reaction Assay for the Diagnosis of Lyssavirus Infection, *PLoS Neglected Tropical Diseases*, 10(7):e0004812. doi: 10.1371/journal.pntd.0004812.

Dacheux, L., Reynes, J., Buchy, P., Sivuth, O., Diop, B. M., Rousset, D., Rathat, C., et al., (2008). A Reliable Diagnosis of Human Rabies Based on Analysis of Skin Biopsy Specimens, *Clinical Infectious Diseases*, 47(11):1410-7. doi: 10.1086/592969.

Davis, B. M., Rall, G. F. and Schnell, M. J., Everything You Always Wanted to Know About Rabies Virus (But Were Afraid to Ask). (2015). *Annual Review of Virology*, 2(1):451-71. doi: 10.1146/annurev-virology-100114-055157.

In review

831

832 Delmas, O., Holmes, E. C., Talbi, C., Larrous, F., Dacheux, L., Bouchier, C. and Bourhy, H.,
833 (2008). Genomic Diversity and Evolution of the Lyssaviruses, *PLoS ONE*, 3(4):e2057.
834 doi: 10.1371/journal.pone.0002057.

835 Fernandes, E. R., Andrade, H. F. de, Lancellotti, C. L. P., Quaresma, J. A. S., Demachki, S.,
836 Costa Vasconcelos, P. F. da and Duarte, M. I. S., (2011). In Situ Apoptosis of Adaptive
837 Immune Cells and the Cellular Escape of Rabies Virus in CNS from Patients with Human
838 Rabies Transmitted by Desmodus Rotundus, *Virus Research*, 156(1-2):121-6. doi:
839 10.1016/j.virusres.2011.01.006.

840 Fink, K. and Grandvaux, N., (2013). STAT2 and IRF9: Beyond ISGF3., *JAK-STAT*,
841 2(4):e27521. doi: 10.4161/jkst.27521.

842 Fitting, S., Zou, S., Chen, W., Vo, P., Hauser, K. F. and Knapp, P. E., (2010). Regional
843 Heterogeneity and Diversity in Cytokine and Chemokine Production by Astroglia:
844 Differential Responses to HIV-1 Tat, Gp120, and Morphine Revealed by Multiplex
845 Analysis, *Journal of Proteome Research*, 9(4):1795-804. doi: 10.1021/pr900926n.

846 Fitzgerald, K. A., O'Neill, L. A. J., Gearing, A. J. H. and Callard, R. E., (2001). MIP-1α, *The*
847 *Cytokine*. In: The Cytokine FactsBook and Webfacts (Second Edition) Academic Press.

848 Fooks, A. R., Banyard, A. C., Horton, D. L., Johnson, N., Mcelhinney, L. M. and Jackson, A.
849 C., (2014). Current Status of Rabies and Prospects for Elimination, *The Lancet*,
850 384(9951):1389-99. doi: 10.1016/S0140-6736(13)62707-5.

851 Fooks, A. R., Cliquet, F., Finke, S., Freuling, C., Hemachudha, T., Mani, R. S., Müller, T., et
852 al., (2017). Rabies, *Nature Reviews Disease Primers*, 3:17091. doi:
853 10.1038/nrdp.2017.91.

854 Fu, Z. F. and Jackson, A. C., (2008). Neuronal Dysfunction and Death in Rabies Virus Infection,
855 *Journal of NeuroVirology*, 14(5):368-75. doi: 10.1080/13550280802216502.

In review

Günther, C., Carballido-Perrig, N., Kaesler, S., Carballido, J. M. and Biedermann, T., (2012). CXCL16 and CXCR6 Are Upregulated in Psoriasis and Mediate Cutaneous Recruitment of Human CD8+ T Cells, *Journal of Investigative Dermatology*, 132(3 Pt 1):626-34. doi: 10.1038/jid.2011.371.

Hampson, K., Coudeville, L., Lembo, T., Sambo, M., Kieffer, A., Attlan, M., Barrat, J., et al., (2015). Estimating the Global Burden of Endemic Canine Rabies, *PLoS Neglected Tropical Diseases*, 9(4):e0003709. doi: 10.1371/journal.pntd.0003709.

Hattermann, K., Ludwig, A., Gieselmann, V., Held-Feindt, J. and Mentlein, R., (2008). The Chemokine CXCL16 Induces Migration and Invasion of Glial Precursor Cells via Its Receptor CXCR6, *Molecular and Cellular Neuroscience*, 39(1):133-41. doi: 10.1016/j.mcn.2008.03.009.

Hemachudha, T, Ugolini, G., Wacharapluesadee, S., Sungkarat, W., Shuangshoti, S. and Laothamatas, J., (2013). Human Rabies: Neuropathogenesis, Diagnosis, and Management, *The Lancet Neurology*, 12(5):498-513. doi: 10.1016/S1474-4422(13)70038-3.

Hemachudha, Thiravat, Laothamatas, J. and Rupprecht, C. E., (2002). Human Rabies: A Disease of Complex Neuropathogenetic Mechanisms and Diagnostic Challenges, *Lancet Neurology*, 1(2):101-9. doi: 10.1016/s1474-4422(02)00041-8.

Hodge, R. D., Bakken, T. E., Miller, J. A., Smith, K. A., Barkan, E. R., Graybuck, L. T., Close, J. L., et al., (2019). Conserved Cell Types with Divergent Features in Human versus Mouse Cortex, *Nature*, 573(7772):61-68. doi: 10.1038/s41586-019-1506-7.

Huang, S., Liu, K., Cheng, A., Wang, M., Cui, M., Huang, J., Zhu, D., et al., (2020). SOCS Proteins Participate in the Regulation of Innate Immune Response Caused by Viruses, *Frontiers in Immunology*, 11:558341. doi: 10.3389/fimmu.2020.558341.

In review

881 Huang, Y., Jiao, S., Tao, X., Tang, Q., Jiao, W., Xiao, J., Xu, X., Zhang, Y., Liang, G. and
882 Wang, H., (2014). Met-CCL5 Represents an Immunotherapy Strategy to Ameliorate
883 Rabies Virus Infection, *Journal of Neuroinflammation*, 11:146. doi: 10.1186/s12974-014-
884 0146-y.

885 Hussmann, K. L. and Fredericksen, B. L., (2014). Differential Induction of CCL5 by Pathogenic
886 and Non-Pathogenic Strains of West Nile Virus in Brain Endothelial Cells and Astrocytes.,
887 *The Journal of General Virology*, 95(Pt 4):862-867. doi: 10.1099/vir.0.060558-0.

888 Ito, N., Moseley, G. W. and Sugiyama, M., (2016). The Importance of Immune Evasion in the
889 Pathogenesis of Rabies Virus, *Vet. Med. Sci.*, 78(7):1089-98. doi: 10.1292/jvms.16-0092.

890 Jackson, A C, Ye, H., Phelan, C. C., Ridaura-Sanz, C., Zheng, Q., Li, Z., Wan, X. and Lopez-
891 Corella, E., (1999). Extraneural Organ Involvement in Human Rabies., *Laboratory*
892 *Investigation; a Journal of Technical Methods and Pathology*, 79(8):945-51.

893 Jackson, A C, Ye, H., Ridaura-Sanz, C. and Lopez-Corella, E., (2001). Quantitative Study ofthe
894 Infection in Brain Neurons in Human Rabies., *Journal of Medical Virology*, 65(3):614-8.

895 Jackson, Alan C., Rossiter, J. P. and Lafon, M., (2006). Expression of Toll-like Receptor 3 in
896 the Human Cerebellar Cortex in Rabies, Herpes Simplex Encephalitis, and Other
897 Neurological Diseases, *Journal of NeuroVirology*, 12(3):229-34. doi:
898 10.1080/13550280600848399.

899 Jackson, Alan C, Randle, E., Lawrance, G. and Rossiter, J. P., (2008). Neuronal Apoptosis
900 Does Not Play an Important Role in Human Rabies Encephalitis, *Journal of*
901 *Neurovirology*, 14(5):368-75. doi: 10.1080/13550280802216502.

902 Jamalkandi, S. A., Mozhgani, S. H., Pourbadie, H. G., Mirzaie, M., Noorbakhsh, F., Vaziri, B.,
903 Gholami, A., Ansari-Pour, N. and Jafari, M., (2016). Systems Biomedicine of Rabies
904 Delineates the Affected Signaling Pathways, *Frontiers in Microbiology*, 7:1688. doi:
905 10.3389/fmicb.2016.01688.

In review

Jogai, S., Radotra, B. D. and Banerjee, A. K., (2000). Immunohistochemical Study of Human Rabies, *Neuropathology*, 20(3):197-203. doi: 10.1046/j.1440-1789.2000.00332.x.

Juntrakul, S., Ruangvejvorachai, P., Shuangshoti, S., Wacharapluesadee, S. and Hemachudha, T., (2005). Mechanisms of Escape Phenomenon of Spinal Cord and Brainstem in Human Rabies, *BMC Infectious Diseases*, 5:104. doi: 10.1186/1471-2334-5-104.

Koraka, P., Martina, B. E. E., Ham, H. J. van den, Zaaraoui-Boutahar, F., IJcken, W. van, Roose, J., Amerongen, G. van, Andeweg, A. and Osterhaus, A. D. M. E., (2018). Analysis of Mouse Brain Transcriptome after Experimental Duvenhage Virus Infection Shows Activation of Innate Immune Response and Pyroptotic Cell Death Pathway, *Frontiers in Microbiology*, 9:397. doi: 10.3389/fmicb.2018.00397.

Lafon, M, (2008). Immune Evasion, a Critical Strategy for Rabies Virus., *Developments in Biologicals*, 2008;131:413-9.

Lafon, Monique, (2011). Evasive Strategies in Rabies Virus Infection, *Advances in Virus Research*, 79:33-53. doi: 10.1016/B978-0-12-387040-7.00003-2.

Lieu, K. G., Brice, A., Wiltzer, L., Hirst, B., Jans, D. A., Blondel, D. and Moseley, G. W., (2013). The Rabies Virus Interferon Antagonist P Protein Interacts with Activated STAT3 and Inhibits Gp130 Receptor Signaling., *Journal of Virology*, 87(14):8261-5. doi: 10.1128/JVI.00989-13.

Louz, D., Bergmans, H. E., Loos, B. P., and Hoeben, R. C., (2013). Animal Models in Virus Research: Their Utility and Limitations., *Critical Reviews in Microbiology*, 39(4):325-61. doi: 10.3109/1040841X.2012.711740.

Ludwig, A., Schulte, A., Schnack, C., Hundhausen, C., Reiss, K., Brodway, N., Held-Feindt, J. and Mentlein, R., (2005). Enhanced Expression and Shedding of the Transmembrane

In review

931 Chemokine CXCL16 by Reactive Astrocytes and Glioma Cells, *Journal of*
932 *Neurochemistry*, 93(5):1293-303. doi: 10.1111/j.1471-4159.2005.03123.x.

933 Masatani, T., Horie, M., Yamada, K., Ozawa, M., Okuya, K., Tsukiyama-Kohara, K., Nishizono,
934 A., Ito, N., Sugiyama, M. and Matsuu, A., (2016). Contribution of the Interaction between
935 the Rabies Virus P Protein and I-Kappa B Kinase ϵ to the Inhibition of Type I IFN Induction
936 Signalling, *Journal of General Virology*, 97(2):316-326. doi: 10.1099/jgv.0.000362.

937 Matloubian, M., David, A., Engel, S., Ryan, J. E. and Cyster, J. G., A (2000). Transmembrane
938 CXC Chemokine Is a Ligand for HIV-Coreceptor Bonzo., *Nature Immunology*, 1(4):298-
939 304. doi: 10.1038/79738.

940 Melchjorsen, J., Sørensen, L. N. and Paludan, S. R., (2003). Expression and Function of
941 Chemokines during Viral Infections: From Molecular Mechanisms to in Vivo Function,
942 *Journal of Leukocyte Biology*, 74(3):331-43. doi: 10.1189/jlb.1102577.

943 Ménager, P., Roux, P., Mégret, F., Bourgeois, J.-P., Sourd, A.-M. Le, Danckaert, A., Lafage,
944 M., Préhaud, C. and Lafon, M., (2009). Toll-like Receptor 3 (TLR3) Plays a Major Role in
945 the Formation of Rabies Virus Negri Bodies., *PLoS Pathogens*, 5(2):e1000315. doi:
946 10.1371/journal.ppat.1000315.

947 Ménager, P., Roux, P., Mégret, F., Préhaud, C., Bourgeois, J.-P., Sourd, A.-M. Le, Lafage, M.
948 and Lafon, M., (2008). TLR3 Is a Key Component of Rabies Virus Induced Negri Bodies,
949 *BMC Proceedings*, 2(Suppl 1):P41

950 Mestas, J. and Hughes, C. C. W., (2004) Of Mice and Not Men: Differences between Mouse
951 and Human Immunology, *The Journal of Immunology*, 172(5):2731-8. doi:
952 10.4049/jimmunol.172.5.2731.

953 Murphy, F. A. and Bauer, S. P., (1974). Early Street Rabies Virus Infection in Striated Muscle
954 and Later Progression to the Central Nervous System., *Intervirology*, 3(4):256-68. doi:
955 10.1159/000149762.

In review

956 Nansen, A., Marker, O., Bartholdy, C. and Thomsen, A. R., (2000). CCR2+ and CCR5+ CD8+
957 T Cells Increase during Viral Infection and Migrate to Sites of Infection, *European Journal*
958 *of Immunology*, 30(7):1797-806. doi: 10.1002/1521-4141(200007)30:7<1797::AID-
959 IMMU1797>3.0.CO;2-B.

960 Ni, Y., Iwatani, Y., Morimoto, K. and Kawai, A., (1996). Studies on Unusual Cytoplasmic
961 Structures Which Contain Rabies Virus Envelope Proteins., *The Journal of General*
962 *Virology*, 77 (Pt 9):2137-47. doi: 10.1099/0022-1317-77-9-2137.

963 O'Brien, K. L., and Nolan, T., (2019) The WHO Position on Rabies Immunization – 2018
964 Updates, *Vaccine*.

965 Pfaffl, M. W., (2001). A New Mathematical Model for Relative Quantification in Real-Time RT-
966 PCR., *Nucleic Acids Research*, 29(9):e45. doi: 10.1093/nar/29.9.e45.

967 Prosniak, M., Hooper, D. C., Dietzschold, B. and Koprowski, H., (2001). Effect of Rabies Virus
968 Infection on Gene Expression in Mouse Brain, 98(5):2758-63. doi:
969 10.1073/pnas.051630298.

970 Rieder, M. and Conzelmann, KK., (2011). Interferon in Rabies Virus Infection, in *Advances in*
971 *Virus Research*, 79:91-114. doi: 10.1016/B978-0-12-387040-7.00006-8.

972 Rosito, M., Deflorio, C., Limatola, C. and Trettel, F., (2012). CXCL16 Orchestrates Adenosine
973 A 3 Receptor and MCP-1/CCL2 Activity to Protect Neurons from Excitotoxic Cell Death in
974 the CNS, *Journal of Neuroscience*, 32(9):3154-63. doi: 10.1523/JNEUROSCI.4046-
975 11.2012.

976 Sato, M., Maeda, N., Yoshida, H., Urade, M., Saito, S., Miyazaki, T., Shibata, T. and Watanabe,
977 M., (1977). Plaque Formation of Herpes Virus Hominis Type 2 and Rubella Virus in
978 Variants Isolated from the Colonies of BHK21/WI-2 Cells Formed in Soft Agar, *Archives*
979 *of Virology*, 53(3):269-73. doi: 10.1007/BF01314672.

980

In review

981 Schildge, S., Bohrer, C., Beck, K. and Schachtrup, C., (2013). Isolation and Culture of Mouse
982 Cortical Astrocytes., *Journal of Visualized Experiments : JoVE*, (71):50079. doi:
983 10.3791/50079.

984 Solanki, A., Radotra, B. D. and Vasishta, R. K., (2009). Correlation of Cytokine Expression
985 with Rabies Virus Distribution in Rabies Encephalitis, *Journal of Neuroimmunology*,
986 217(1-2):85-9. doi: 10.1016/j.jneuroim.2009.09.019.

987 Sonthonnax, F., Besson, B. B., Bonnaud, E., Jouvion, G., Merino, D., Larrous, F. and Bourhy,
988 H., (2019). Lyssavirus Matrix Protein Cooperates with Phosphoprotein to Modulate the
989 Jak-Stat Pathway, *Scientific Reports*, 9(1):12171. doi: 10.1038/s41598-019-48507-4.

990 Suja, M. S., Mahadevan, A., Madhusudana, S. N. and Shankar, S. K., (2011). Role of
991 Apoptosis in Rabies Viral Encephalitis: A Comparative Study in Mice, Canine, and Human
992 Brain with a Review of Literature, *Pathology Research International*, 2011:374286. doi:
993 10.4061/2011/374286.

994 Tao, L. and Reese, T. A., (2017). Making Mouse Models That Reflect Human Immune
995 Responses, *Trends in Immunology*, 38(3):181-193. doi: 10.1016/j.it.2016.12.007.

996 Trettel, F., Castro, M. A. Di, and Limatola, C., (2020). Chemokines: Key Molecules That
997 Orchestrate Communication among Neurons, Microglia and Astrocytes to Preserve Brain
998 Function, *Neuroscience*, 439:230-240. doi: 10.1016/j.neuroscience.2019.07.035.

999 Trifilo, M. J., Bergmann, C. C., Kuziel, W. A. and Lane, T. E., (2003). CC Chemokine Ligand
1000 3 (CCL3) Regulates CD8 + -T-Cell Effector Function and Migration Following Viral
1001 Infection , *Journal of Virology*, 77(7):4004-14. doi: 10.1128/jvi.77.7.4004-4014.2003.

1002 Troupin, C., Dacheux, L., Tanguy, M., Sabeta, C., Blanc, H., Bouchier, C., Vignuzzi, M.,
1003 Duchene, S., Holmes, E. and H, B., (2016). Large-Scale Phylogenomic Analysis Reveals
1004 the Complex Evolutionary History of Rabies Virus in Multiple Carnivore Hosts, *PLoS*
1005 *Pathogens*, 12(12):e1006041. doi: 10.1371/journal.ppat.1006041.

In review

1006 Ugolini, G., (2011). Rabies Virus as a Transneuronal Tracer of Neuronal Connections.,
1007 *Advances in Virus Research*, 79:165-202. doi: 10.1016/B978-0-12-387040-7.00010-X.

1008 Vandesompele, J., Preter, K. De, Pattyn, F., Poppe, B., Roy, N. Van, Paepe, A. De and
1009 Speleman, F., (2002). Accurate Normalization of Real-Time Quantitative RT-PCR Data
1010 by Geometric Averaging of Multiple Internal Control Genes, *Genome Biology*,
1011 3(7):RESEARCH0034. doi: 10.1186/gb-2002-3-7-research0034.

1012 Vilela, M. C., Mansur, D. S., Lacerda-Queiroz, N., Rodrigues, D. H., Lima, G. K., Arantes, R.
1013 M. E., Kroon, E. G., Silva Campos, M. A. Da, Teixeira, M. M. and Teixeira, A. L., (2009).
1014 The Chemokine CCL5 Is Essential for Leukocyte Recruitment in a Model of Severe Hepes
1015 Simplex Encephalitis, *Annals of the New York Academy of Sciences*, 1153:256-63. doi:
1016 10.1111/j.1749-6632.2008.03959.x.

1017 Wang, J., Lu, Y., Wang, J., Koch, A. E., Zhang, J. and Taichman, R. S., (2008). CXCR6
1018 Induces Prostate Cancer Progression by the AKT/Mammalian Target of Rapamycin
1019 Signaling Pathway., *Cancer Research*, 68(24):10367-76. doi: 10.1158/0008-5472.CAN-
1020 08-2780.

1021 Wang, Z. W., Sarmento, L., Wang, Y., Li, X., Dhingra, V., Tseggai, T., Jiang, B., Zhen, F. and
1022 Fu, Z. F., (2005). Attenuated Rabies Virus Activates, While Pathogenic Rabies Virus
1023 Evades, the Host Innate Immune Responses in the Central Nervous System, *Virology*
1024 *Journal*, 79(19):12554-65. doi: 10.1128/JVI.79.19.12554-12565.2005.

1025 Watson, H. D., Tignor, G. H. and Smith, A. L., (1981). Entry of Rabies Virus into the Peripheral
1026 Nerves of Mice., *The Journal of General Virology*, 56(Pt 2):372-82. doi: 10.1099/0022-
1027 1317-56-2-371.

1028 Weli, S. C., Scott, C. A., Ward, C. A. and Jackson, A. C., (2006). Rabies Virus Infection of
1029 Primary Neuronal Cultures and Adult Mice: Failure To Demonstrate Evidence of
1030 Excitotoxicity, *Journal of Virology*, 80(20):10270-3. doi: 10.1128/JVI.01272-06.

In review

1031 WHO, (2008). Weekly Epidemiological Record, Vol 93

1032 Wiltzer, L., Larrous, F., Oksayan, S., Ito, N., Marsh, G. a., Wang, L. F., Blondel, D., Bourhy,
1033 H., Jans, D. a. and Moseley, G. W., (2012). Conservation of a Unique Mechanism of
1034 Immune Evasion across the Lyssavirus Genus, *Journal of Virology*, 86(18):10194-9. doi:
1035 10.1128/JVI.01249-12.

1036 Wiltzer, Linda, Okada, K., Yamaoka, S., Larrous, F., Kuusisto, H. V., Sugiyama, M., Blondel,
1037 D., et al., (2014). Interaction of Rabies Virus P-Protein With STAT Proteins Is Critical to
1038 Lethal Rabies Disease, *The Journal Of Infectious Diseases*, 209(11):1744-53. doi:
1039 10.1093/infdis/jit829.

1040 Zhang, D., He, F., Bi, S., Guo, H., Zhang, B., Wu, F., Liang, J., et al., (2016). Genome-Wide
1041 Transcriptional Profiling Reveals Two Distinct Outcomes in Central Nervous System
1042 Infections of Rabies Virus, *Frontiers in Microbiology*, 7:751. doi:
1043 10.3389/fmicb.2016.00751.

1044 Zhang, Y., Chen, K., Sloan, S. A., Bennett, M. L., Scholze, A. R., O'Keeffe, S., Phatnani, H.
1045 P., et al., (2014). An RNA-Sequencing Transcriptome and Splicing Database of Glia,
1046 Neurons, and Vascular Cells of the Cerebral Cortex, *Journal of Neuroscience*,
1047 34(36):11929-47. doi: 10.1523/JNEUROSCI.1860-14.2014.

1048 Zhao, L., Toriumi, H., Wang, H., Kuang, Y., Guo, X., Morimoto, K. and Fu, Z. F., (2010).
1049 Expression of MIP-1 (CCL3) by a Recombinant Rabies Virus Enhances Its
1050 Immunogenicity by Inducing Innate Immunity and Recruiting Dendritic Cells and B Cells,
1051 *Journal of Virology*, 84(18):9642-8. doi: 10.1128/JVI.00326-10.

1052 Zhao, P., Liu, S., Zhong, Z., Jiang, T., Weng, R., Xie, M., Yang, S. and Xia, X., (2018). Analysis
1053 of Expression Profiles of Long Noncoding RNAs and MRNAs in Brains of Mice Infected
1054 by Rabies Virus by RNA Sequencing, *Scientific Reports*, 8(1):11858. doi:
1055 10.1038/s41598-018-30359-z.

In review

1056 Zhao, P., Zhao, L., Zhang, T., Qi, Y., Wang, T., Liu, K., Wang, H., et al., (2011). Innate Immune
1057 Response Gene Expression Profiles in Central Nervous System of Mice Infected with
1058 Rabies Virus, *Comparative Immunology, Microbiology and Infectious Diseases*,
1059 34(6):503-12. doi: 10.1016/j.cimid.2011.09.003.

1060

1061

In review

3. Discussion

When starting my PhD thesis, I was addressing two objectives, both involved in the cellular susceptibilities of human CNS cell types to RABV infection and the impact of innate immune responses in defining rabies virus tropism.

The main objective aimed to understand if there is a link between cellular immune responses and RABV tropism. Therefore, RABV tropism and -mediated immune responses were investigated in the distinct human CNS cell types *in vitro* (chapter 3.1). As mentioned beforehand, RABV tropism has been extensively studied by other authors beforehand (191,193,194,199,209). Nevertheless, previous research focused on investigating RABV tropism in *in vitro* cell models derived from primary tissues or directly *in vivo*. *In vitro* cultures derived from primary tissues in the past have the disadvantage that purification methods were still inefficient resulting in possible impurities of cultures. Those impurities might lead to false conclusions. *In vivo* cultures present the susceptibilities within the complexity of the animal model, however, viruses might not have the same susceptibilities between species. Additionally, some imaging techniques have technical limitations. While addressing my first objective, I went from a simple monoculture set-up to more sophisticated co-culture models, trying to mirror the complexity of the CNS. Additionally, I used stem cell-derived cultures: those cultures always face the problem of immaturity after differentiation, nevertheless, once the transcriptome shows that cells are mature and fully differentiated, mirror human CNS physiology better compared to cell line-derived models (273). Apart from differences in CNS models, I studied the transcriptome of different CNS cell types upon RABV infection to understand their distinct and complementary roles in the viral-infected CNS. Therefore, I went from bulk approaches such as RT-qPCR (Article #2) and RNA-Seq (Article #6) to more sophisticated models such as sc RNA-Seq (Article #3) to investigate RABV infection at the single cell resolution level.

Another objective was to investigate the inflammatory transcriptome profile of naturally infected human brains in comparison to RABV-infected mice (chapter 3.2). Today, there are large datasets available investigating the transcriptome of RABV-infected mice (134–139).

However, no single study investigated the inflammatory transcriptome profile in *post-mortem* human brains yet. Thus, this objective aimed at assessing if we can extrapolate transcriptomic data from RABV-infected mice to naturally RABV-infected humans.

3.1. Studying the role of glial cells during RABV infection *in vitro*

To answer the first question, namely RABV tropism in the CNS, I assessed RABV tropism conventional cell lines and in stem-cell derived CNS cells. The microscopic analysis revealed that neurons and astrocytes are highly susceptible to the pathogenic dog RABV Tha, whereas iPSC-derived microglia did not support a productive infection *in vitro* (Article #2). These results were further confirmed by sc RNA-Seq (Article #3).

Previous publications already gave evidence that primary murine astrocytes can get infected with lab-attenuated RABV *in vitro* (at early stages of infection) and *in vivo* (141,207,209). In contrast to wt RABV, Tian *et al.* showed that lab-attenuated RABV causes abortive infection of murine astrocytes (208). Tian and colleagues hypothesise that abortion of RABV infection is due to the fact that lab-attenuated RABV produces more ds RNA compared to wt RABV, resulting in the activation of RIG-I and MDA5, ultimately leading to the expression of ISGs and abortion of RABV infection (208). It is assumed that highly virulent filed RABV are able to evade the host immune response (159), whereas attenuated viruses have limited immune-evasive capacities rendering those viruses susceptible to the host immune response (133) which might result in abortion of astrocyte infection (207). Recently, comparative immunofluorescence analysis revealed that all field RABV investigated showed a tropism for astrocytes *in vivo* (8-27%) whereas only one lab-attenuated RABV, when administered intracerebrally, showed infection of astrocytes (13%) (194). Thus, evidence is accumulating that wt RABV, in contrast to lab-attenuated RABV, productively infects murine astrocytes *in vivo*.

Human data on RABV infection of astrocytes are scarce. Suja and colleagues showed that oligodendrocytes and fibrous astrocytes from *post-mortem* human tissues and infected dogs stained positive for RABV antigens, whereas significantly less glial cells stained positive in mice infected with two different RABV strains (street virus and lab-attenuated strain) and two infection routes used (264). Therefore, they suggested variable permissiveness of glial cells between species (264). Considering their study, we need to think about re-defining RABV tropism: previous data provide evidence that RABV field strains demonstrate a strong astrocyte tropism (8-27%) in mice, however, infection of astrocytes might potentially be even more profound in humans (264). Hence, our picture of RABV as a predominantly neuron-specific

virus might simply be wrong. It is true that RABV has a strong tropism for neurons but especially viruses which are used for transneural tracing are based on attenuated or genetically modified viruses (199,274). During my thesis, I investigated RABV tropism in co-cultures consisting of stem cell-derived neurons, astrocytes, and microglia. Immunofluorescence results revealed that the cell culture-adapted RABV field virus Tha infects stem cell-derived human astrocytes (21-32%) and neurons (21-33%) to similar extents (Article #2), whereas sc RNA-Seq suggested a more neuron-specific tropism (61% hiNeurons, 17% hiAstrocytes, Article #3). Despite the discrepancies between data obtained by imaging or sequencing, human CNS *in vitro* models provide evidence that astrocyte infection does not occur occasionally as originally believed but rather because field RABV strains are able to productively infect human astrocytes. Thus, one could hypothesise that there might be a link between RABV immune evasive capabilities and RABV tropism.

Strikingly, I showed that the RABV field virus Tha is not able to infect stem cell-derived microglia *in vitro* (Article #2 and #3). Infection of microglia during RABV infection has been controversially discussed in the past: Ray and colleagues suggested that RABV productively infects primary human microglia *in vitro* (209). However, it is important to mention that their results are based on virus titration and antigen staining. Virus titration of infected cells that have previously been isolated and purified presents a difficult task. Since we cannot be entirely sure that cultures are completely pure or that cells might not de-differentiate during cultivation, it does not present a reliable way to validate viral tropism. Although staining for RABV antigens is specific, it does not prove productive astrocyte infection. Staining positive for RABV antigens might simply be the result of microglial-mediated phagocytosis of infected cells. If infected or not, there are numerous reports providing evidence that human microglia get activated upon RABV infection. Despite activation of human microglia (108,275–278), however, none of these publications gave evidence for productive infection of human microglia. Taken together, microglia are suggested to be susceptible towards RABV infection based on a study which was performed more than 20 years ago with methods that comprise technical limitations. Nowadays, we are able to study RABV tropism *ex-vivo* using more sophisticated CNS models (279). Using stem human cell-derived models to investigate susceptibility of microglia towards RABV infection, I question permissiveness of human microglia to RABV infection *in vitro* (Article #2 and #3).

Apart from elucidating RABV tropism, I investigated in a next step the immune responses of CNS cell types towards RABV infection, trying to link cellular susceptibilities to their respective immune responses. Viral tropism is mainly determined by two factors i) the expression of virus entry receptors and ii) cell type-specific immune responses (280). Strikingly, the broad and rather unspecific expression of p75NTR, mGluR2, NAchR, and NCAM

in the human brain (195,196,281) does not fully explain cellular suscebilities towards RABV infections in the human brain. Apart from varying expression of entry receptors between CNS cell types (135,195) which might partly but not completely explain RABV tropism, we know for a long time that cellular responses are not universal, and that especially cell type-specific transcriptome profiles in the CNS vary tremendously among cell types (282). Genome-wide transcriptome analysis of 16 human tissues classed the mammalian brain among the three tissues with the highest level of alternative splicing (283). Consequently, alternative splicing is partly responsible for profound differences in gene expression between distinct CNS cell types and differentiation states, supporting the formation of complex neuronal networks and the plasticity of delicate synapses. By these means, the distinct cell types in the CNS are able to perform multiple different roles and functions during homeostasis and pathology (195,284,285), potentially influencing their perimissiveness towards virus infection.

Although our model pledges strong cellular diversities regarding host pathogen interactions in the virus-infected CNS (Article #2 and #3), we need to admit that our model does not completely mirror the abundances found in the human brain (286). In detail, the human cerebral cortex consists of two times more glial cells (20 – 40 billion) compared to neurons (10 – 20 billion) (286) whereas our model consisted of more neurons compared to glial cells (Article #2 and #3). More specifically, the main part of the human neocortex consists of oligodendrocytes (approx. 75%) (287–289), a building block which is completely missing in our model (Article #2 and #3). Another limitation presents the different genetical background between hNSC-derived neuronal (female karyotype) and iPSC-derived microglial (male karyotype) cell types (Article #2 and #3). Nowadays, we know that many genetic loci, especially sex-associated loci (290), control host pathogen interactions, especially innate immune responses (291). Despite these limitations, our stem cell-derived human 2D CNS model provides novel insights about cell type-specific immune responses in the RABV-infected CNS supporting the idea that immune responses partly explain RABV tropism. Even nowadays, cancer cell lines are routinely used in molecular biology since cell lines are inexpensive and easy to grow. Still, many cancer cell lines differ significantly from the primary cancer source rendering them inappropriate to study the specific research question (292,293). Given that, discrepancies between cancer cell lines and primary healthy tissues might even provide more profound than the beforehand limitations mentioned about our model. During my PhD project, I demonstrated more profound differences in innate immune responses upon RABV infection between distinct CNS cell types of stem cell-derived cultures compared to cell line models (Article #2). Consequently, cell line models might be inappropriate to study the complex cellular interactions in the virus-infected CNS. Taken together, we developed a stem cell-derived human *ex vivo* CNS model which does not mirror the complexity of the CNS, but which is

appropriate to study host pathogen interactions in a more physiological context compared to classical cell line models. In the following sections, I summarize cell type-specific transcriptome profiles of stem cell-derived CNS cell types upon Tha infection (Figure 1).

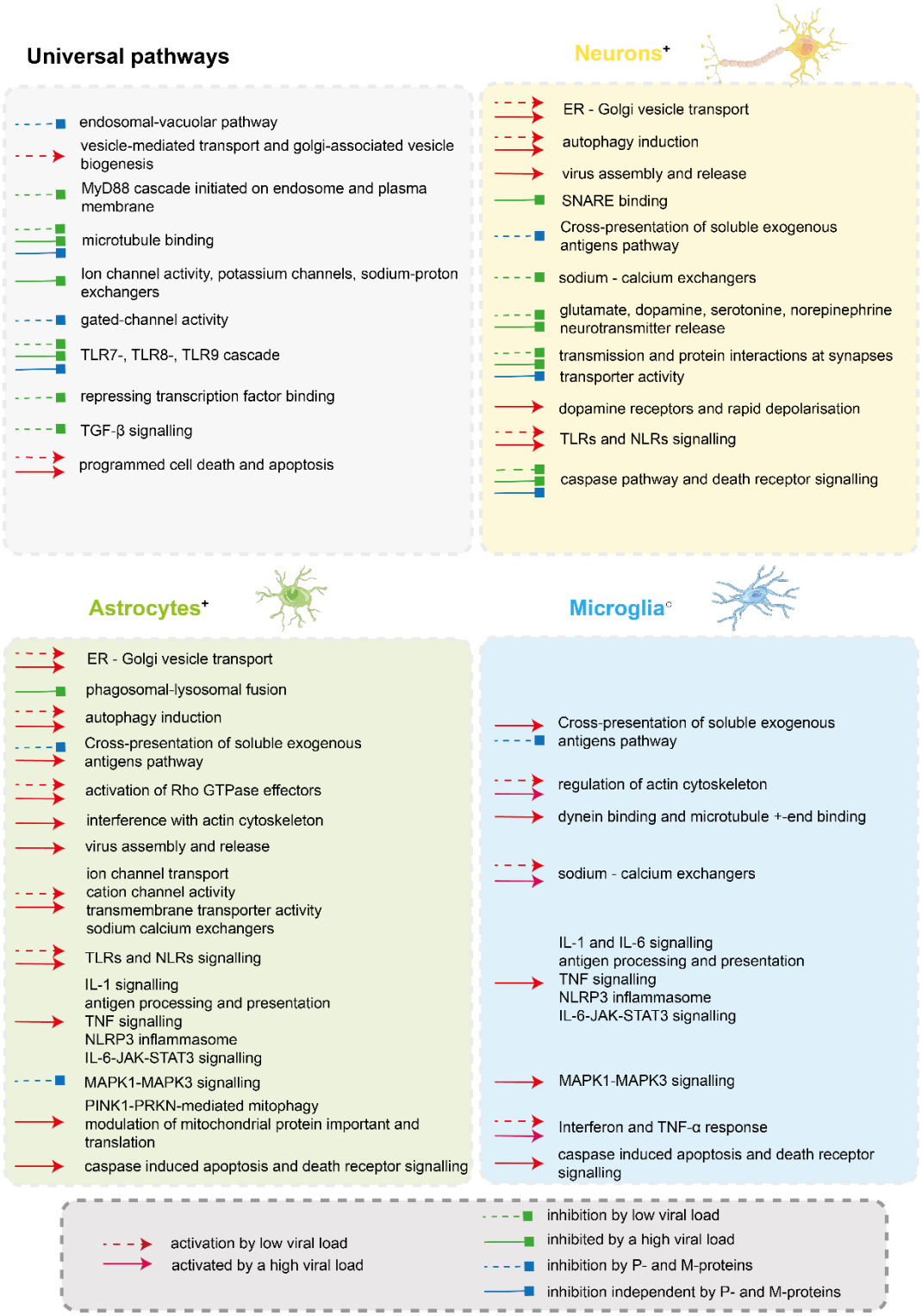

Figure 7 | Cell type-specific signalling pathways modulated during Tha infection. Symbols indicate if cells are susceptible (+) or resistant (○) towards Tha infection. Figures summarizes findings from Article #2 and Article #3 about susceptibilities and modulated signalling pathways in stem cell-derived CNS cell types *in vitro*. Indicated signalling pathways are based on gene expression studies (sc RNA-

Seq and qPCR studies). A more detailed description about the signalling pathways investigated can be found in the supplementary information of Article #3.

3.1.1. Neurons

To begin, neurons are the main target in the CNS for various viruses, such as RABV, HSV, Japanese encephalitis virus (JEV), West Nile Virus (WNV) and many more (213,294). Consequently, we expect neurons to respond first to viral infections, eventually activating surrounding glial cells. This has indeed been shown for several neurotropic infections (295–298), however, there is evidence pointing out that neurons show restricted immune responses compared to glial cells (204). Transcriptome results from Tha-infected stem cell-derived human neurons revealed that neurons, similar to HSV-infected neurons (204), initiated little immune responses compared to glial cells (Article #2 and #3). Similarly, we demonstrated that IFN-regulated pathways and the induction of ISGs were less profound in neurons compared to glial cells. Lastly, and similar to Yordy *et al.* (204), we observed that neurons rather induce autophagy upon Tha infection compared to IFN-induced pathways (Article #3). Induction of autophagy has already been described for human neurons infected by other neurotropic viruses, such as HSV-1 (204). We assume that IFN-regulated pathways are restricted in neurons compared to glial cells since those pathways induce toxic by-products which might potentially cause harm to non-renewable populations such as neurons (204). Autophagy is a highly conserved catabolic pathway essential for maintaining the turnover of cellular compartments (299) as well as mediating viral containment (300). Given that neurons are post-mitotic cells which cannot dilute cellular waste via cell division, autophagy is crucial for neurons to ensure long-term viability (301). Autophagy has been previously reported in RABV infection, although the exact mechanisms underlying RABV-mediated autophagy remain unresolved (205,302–304). Wildtype RABV has been shown to induce autophagy in murine and human neuroblastoma cells *in vitro* (205). Interestingly, induction of autophagy decreased apoptosis *in vitro* (205). Further, Peng and colleagues propose that the M-protein of wt RABV induces autophagy (205). Although we know that autophagy plays a central role in RABV infection (205,302–304), we do not fully understand its role during rabies pathogenesis. Since RABV induces fatal encephalomyelitis in humans (11), autophagy remains an inefficient pathway to control RABV infection since it does not result in virus clearance. Yet, the autophagy pathway might be specifically targeted by RABV to inhibit premature neuronal death. Cell death is linked to autophagy, although its connection is still controversially discussed (305). It has been assumed that basal autophagy at a low level is cytoprotective, whereas excessive autophagy triggers cell death (305). However, more data is required to prove this hypothesis. Given that

RABV is highly adapted to evade the host innate immune system (206), one can just assume that RABV exploits the neuronal autophagy pathway for its own benefits.

Apart from autophagy, Tha induces vesicle transport from the endoplasmic reticulum (ER) to the Golgi apparatus, inhibits SNARE binding, and interferes with transmembrane transport (Article #3), possibly interfering with synapse functions. Remarkably, Tha inhibits glutamate, dopamine, serotonin, and norepinephrine neurotransmitter release independent of the viral load (Article #3). Upon a high viral load, Tha induces the transcription of genes related to neurotransmitter clearance and dopamine receptors (Article #3). Defective neurotransmission, particularly regarding acetylcholine, GABA, and serotonin release during RABV infection has been studied previously: Ceccaldi and colleagues suggested that RABV infection specifically affects 5-HT_{1D} receptor subtypes in the murine cerebral cortex at early stages of viral infection via a potential indirect effect which is not yet known (306). Consequently, impaired release and binding of serotonin (306) might partly account for neuronal dysfunction observed during rabies pathogenesis (123). In the hippocampus of CVS-24-infected rats, norepinephrine, serotonin, and dopamine increased until day 3 post-infection and subsequently declined steadily. At day 7 post-infection, neurotransmitter concentrations were at or below neurotransmitter concentrations observed before infection (123).

Additionally, we showed that Tha interfered with neurotransmission, particularly inhibiting sodium – calcium exchangers which potentially affects the membrane potential (Article #3). Iwata *et al.* previously provided evidence that neuroblastoma cells exhibited a significantly decreased amplitude of the voltage-dependent sodium current channels and inward rectifier potassium current at 3 days post-infection (307). Additionally, the cellular resting potential was reduced suggesting RABV-induced depolarisation (307). Here, we show that Tha inhibits rapid depolarisation in hiNeurons which was independent of viral load but supposedly depends on accessory functions of M- and/or P-proteins (Article #3).

Further, gene expression of *DYNLL1* and *DYNLL2* were strongly induced in Tha and Th2P-4M infected hiNeurons (MOI 0.5, Article #3) in contrast to non-infected bystander hiNeurons. This leads to the suggestion that Tha exploits the dynein-dependent transport in neurons upon viral entry for its own benefits. Likewise, previous data indicate that viral P- and L-proteins manipulate the microtubule network through interaction with dynein motors, enabling efficient viral transport and primary viral transcription (308–310).

3.1.2. Astrocytes

Apart from neurons, hNSC-derived astrocytes are permissive to RABV infection *in vitro* (Article #2 and #3). Despite these similarities, Tha induced TLRs and NLRs signalling cascades, the vesicle transport between ER and Golgi apparatus, as well as autophagy in hiAstrocytes (Article #3). Additionally, Tha interfered with the regulation of the actin cytoskeleton and activated RHO GTPase effector proteins which are known to regulate the organization of the cytoskeleton and intracellular trafficking (311). Further, we provide evidence that Tha specifically modulates ion channel activity and transmembrane transporter activity in hiAstrocytes, particularly inducing sodium calcium exchangers. Increasing evidence states the importance of viral interference with intracellular Ca^{2+} levels to favour virus entry, viral replication, and the release of virions (312). More specifically, several voltage-gated calcium channel (VGCC) blockers inhibited influenza A virus (IAV) infection in multiple cell lines *in vitro*. Additionally, the VGCC blocker diltiazem, was demonstrated to prolong survival of IAV-infected mice (313). A high-throughput screening of FDA-approved drugs identified three VGCCs blockers, manidipine, cilnidipine, and benidipine hydrochloride, for potential treatment of JEV, Zika virus, dengue virus, and WNV infection (314). Although more research is needed to understand the interference of RABV with intracellular Ca^{2+} levels, calcium levels could possibly serve as novel treatment targets for rabies, given the success of VGCCs blockers for other neurotropic infections.

Further, a high viral load of Tha (MOI 5) modulated the actin cytoskeleton, induced autophagy, and PTEN-induced kinase 1 (PINK1)- Parkin RBR E3 Ubiquitin Protein Ligase (PRKN)-mediated mitophagy and inhibited phagosomal-lysosomal fusion (Article #3). Mitophagy presents a homeostatic process, more specifically the selective degradation of mitochondria by autophagy, which limits the detrimental outcome of mitochondrial damage ultimately avoiding inflammasome activation (315,316). More specifically, the loss of mitochondrial membrane potential mediates accumulation of PINK1 at the outer mitochondrial membrane and recruitment of PRKN to damaged mitochondria. Subsequently, PRKN promotes the engulfment of mitochondria by phagophores followed by the fusion of autophagosomes with lysosomes (316). Here, Tha inhibits phagosomal-lysosomal fusion, potentially inducing selective degradation of mitochondria via PINK1-PRKN-mediated mitophagy. We hypothesise that Tha might exploit mitochondrial processes in hiAstrocytes for its own benefits given the profound changes observed in RABV-infected hiAstrocytes (Article #3). Still, more research is needed to understand how exactly RABV interferes with mitochondrial function in human astrocytes. Further, Tha-mediated inhibition of phagosomal-lysosomal fusion might potentially explain why astrocytes are unable to clear viral particles from infected astrocytes. Similarly, previous results already showed that human astrocytes

serve as a reservoir for other neurotropic viruses, such as human immunodeficiency virus (HIV) (317). Interaction between the HIV-associated protein Negative Regulatory Factor and the autophagosome (318) potentially explain how HIV successfully interferes with astrocyte-mediated autophagy and viral clearance (319). In a similar manner, Tha might block the autophagosome formation in astrocytes. A recent study performed by Ojeda and colleagues showed that HIV-1 productively infects human astrocytes *in vitro*, inducing mitochondrial injury (320). The latter, however, is counteracted by mitochondrial fission and elimination of damaged mitochondria via mitophagy resulting in cell survival (320). Nevertheless, astrocytes exhibiting cell-to-cell contacts with primarily infected astrocytes succumb to a bystander effect: bystander cells do not get productively but abortively infected with HIV-1 since viral replication induces mitochondrial-associated oxidative stress and the activation of the NLRP3 inflammasome ultimately leading to cell death and pyroptosis (320). Unlike HIV, sc RNA-Seq data exhibited similar transcriptome profiles of infected and non-infected bystander hiAstrocytes during Tha infection (Article #3) suggesting modulation of similar signalling pathways in both astrocyte subsets. Nevertheless, we would need to investigate genes implicated in cell death and mitochondrial functions more in depth to be confident enough to claim that infected and non-infected bystander hiAstrocytes exhibit similar mitochondrial functions. In detail, we show that Tha (MOI 5) activates inflammatory pathways such as IL-1, TNF-α, IL-6-JAK-STAT3 signalling, as well as caspase-mediated apoptosis (Article #2 and #3). Consequently, we hypothesise that Tha induces mitochondrial injury inducing PINK1-PRKN-mediated mitophagy in hiAstrocytes resulting in NLRP3 activation and IL-1 processing, eventually leading to caspase-induced apoptosis. Nevertheless, given that astrocytes represent approximately one sixth of Tha-infected cells in our *in vitro* CNS model (17%, Article #3), it is hard to believe that induction of either mitophagy or apoptosis result in abortion of Tha infection. In contrast to a low MOI, infection with a high MOI of virulent Tha dampened expression of immune genes in hiAstrocytes. This suggests that the balance between activation and repression of immune genes during RABV infection is highly dependent of the initial level of infection, in our case the MOI used for infection experiments. Hence, further research is needed to understand the consequences of Tha-mediated induction of mitophagy and inhibition of phagosomal-lysosomal fusion in hiAstrocytes.

Analysis of differential gene expression identified that a high viral load of Tha dampened gene expression of *TGFBR2*, *TLR4*, IFN-induced protein with tetratricopeptide repeats (IFIT) family genes (*IFIT1*, *IFIT2*, *IFIT3),* and IFN-induced transmembrane protein 1 (*IFITM1*) in infected and bystander hiAstrocytes compared to mock-infected astrocytes (Article #3). Although TLR3 (216,238) and TLR7 (321) are classically known to be involved in RABV pathogenesis, several publications already reported a possible regulatory role for TLR4 in

RABV infection (108,322). Although TLR4 is classically known to bind LPS, G-proteins of various viruses such as VSV, Ebola virus, and dengue virus were already shown to activate TLR4 by a yet unknown mechanism (323). Further, the TLR4 signalling cascade initiates recruitment of MyD88 (323) which presented a universally induced pathway in Tha-infected hiNeurons, hiAstrocytes, and hiMicros (Article #3).

Further, genes belonging to the IFIT and IFITM family are known to exhibit broad-spectrum antiviral activity targeting the replication and spread of a variety of human viruses (324). Like hiNeurons, Tha (MOI 0.5) induces gene expression of IFIT and IFITM genes in infected and bystander hiAstrocytes whereas a higher MOI (MOI 5) dampens gene expression of the beforementioned genes. Further, we provide evidence that IFIT and IFITM gene regulation in hiAstrocytes strongly depends on accessory functions of viral P- and M-proteins (Article #3). The induction of IFIT family genes has been reported for various RNA viruses, such as JEV (325,326), lymphocytic choriomeningitis virus (327), and the RABV strain CVS (326). More specifically, IFIT2 and IFIT3 have been shown to restrict RABV replication (328,329). Thus, we suggest that Tha antagonizes activation of hiAsrocytes, particularly the induction of glial IFIT and IFITM genes, via secondary effects mediated by viral P- and M-proteins and that this effect is dependent of the viral load. Surprisingly, hiAstrocytes were unable to abort Tha and Th2P-4M infection upon a low MOI (MOI 0.5) despite the induction of IFIT and IFITM genes.

3.1.3. Microglia

Although microglia remain the only mature CNS cell type investigated which did not support productive RABV infection (Article #2 and #3), microglia exhibit transcriptome changes upon challenge with either Tha or Th2P-4M: independent of viral load, Tha challenge resulted in the regulation of the actin cytoskeleton. Generally, microglia are highly motile cells which rapidly migrate towards chemoattractant via lamellipodia and filopodia structures, two structures primarily driven by actin polymerization (330) emphasizing the importance of the actin cytoskeleton in microglia motility. Further, infction with a high viral load (MOI 5) induced additional pathways implicated in dynein binding and microtubule plus-end binding. The microtubule system is involved in generating protrusive activity for cellular motility, actin rearrangements, and dynamics (331). More specifically, polar microtubule filaments grow via extension of their plus ends (331), a process which was also shown to be induced upon Tha infection. Consequently, we suggest that microglia possibly respond to Tha infection via actin- and microtubule-dependent motility towards infected cells. Still, the underlying triggers inducing microglial motility remain to be identified.

Unlike hiNeurons and hiAstrocytes, we show that Tha restricts the autophagy pathway in hiMicros, a pathway that seemed to be independent of accessory functions of viral M- and P-

proteins (Article #3). However, a very recent publication investigating autophagy in the microglial cell line BV2 provided evidence that autophagy induction mainly depends on the multiplicity of infection rather than the pathogenicity of the virus (vaccine vs virulent RABV strain) (304). More specifically, Wang and colleagues demonstrated that the production of RABV progeny particles was strongly impaired in BV2 cells. Further, RABV infection lead to the accumulation of autophagosomes in BV2 cells, probably due to RABV-mediated inhibition of the fusion between autophagosomes and lysosomes (304). Although Wang *et al.* showed a positive correlation between viral load and autophagy induction in BV2 cells (304), we did not observe the induction of autophagy upon either a low or a high viral MOI used (Article #3). Thus, we conclude that cell line and stem cell-derived models of microglia show profound discrepancies, suggesting using rather primary microglia for mechanistic studies despite their limited availability.

Apart from cytoskeletal changes, microglia mounted immune responses upon Tha infection: Apart from induction of the NOD-, LRR- and pyrin domain-containing protein 3 (NLRP3) inflammasome, IL-1-, TNF-, and IL-6-JAK-STAT3 signalling which were also observed in hiAstrocytes, hiMicros additionally increased expression of type I and II IFNs and IL-6 pathways upon Tha infection (Article #3). A previous study provided evidence that astrocytes and not microglia are the main source of IFN-β in the RABV-infected murine brain, however, they used the lab-attenuated SAD strain for infection experiments (207). In contrast, Reinert and colleagues showed that microglia are the main source of type I IFNs during neurotropic HSV-1 infection *in vivo* (247). Although interferon expression in neurotropic infections remains a controversial topic which might depend on multiple factors such as the virus strain and the time point of investigation, our *in vitro* results provide evidence that Tha strongly induces IFN signalling pathways in hiMicros at 48 hours post-infection. Apart from controlling CNS invasion, type I IFNs tremendously shape cellular permissiveness (332). Thus, microglia-mediated expression of type I and II IFNs compared to hiNeurons and hiAstrocytes might potentially explain their resistance towards productive Tha infection. Apart from type I and II IFNs, challenge with a high viral load of Tha induced MAPK1-MAPK3 signalling in hiMicros, possibly activating the expression of pro-inflammatory cytokines (333), particularly IL-1β (334) and CXCL10 (335) production (Article #3).

Taking a closer look at the differentially expressed genes (DEGs), indicated a clear induction in Indoleamine 2,3-Dioxygenase 1 (*IDO1*) and *CXCL10* gene expression upon both Tha (MOI 5) and Th2P-4M infection compared to mock-infected hiMicros. Several publications already described microglial-mediated induction of CXCL-10 upon RABV infection (140,335,336) whereas data on RABV-mediated induction of IDO-1 remain scarce. The tryptophan-catabolizing enzyme IDO-1 was reported to be upregulated in a model of acute

viral encephalitis, more specifically by activated murine microglia in the cerebellum of mice infected with Encephalomyocardis virus (337). Whereas IFN-γ-inducible IDO-1 was shown to have a protective effect in cytomegalovirus infection (338), HSV-1, and HSV-2 infection (339,340), inhibition of IDO-1 decreased HIV-1-infected monocyte-derived macrophages compared to controls (341). At the same time, IDO-1 inhibition enhanced cytotoxic T lymphocytes-mediated clearance of HIV-infected macrophages in the murine brain (341). Hence, IDO-1-mediated activities present a double-edged sword in the context of CNS infections: whereas IDO-1 limits the growth of the infectious agent and primes secondary immune responses to limit the spread of the pathogen, IDO-1 at the same time mediates the destruction of non-renewable cell populations. Although immunosuppressive and neurotoxic properties of IDO-1 remain to be elucidated (342), IDO-1 might serve as a potential target for antiviral therapies of CNS infections including rabies.

3.2. And what is happening in naturally infected humans?

For my second objective, I compared the transcriptome profile of RABV infection in artificially infected mice with naturally infected humans. In contrast to the murine brain, naturally infected human brains showed little inflammation upon RABV infection. More specifically, out of the 33 genes investigated 20 were differentially expressed in the human cortex and brainstem/cerebellum, whereas only 1 gene was differentially expressed in the human brainstem/cerebellum of rabid Cambodian patients, namely Chemokine (C-X-C Motif) Ligand 16 (*CXCL16*, fold change = 0.68). More specifically, we showed significant upregulation of *CXCL16* in the murine brain and significant downregulation of *CXCL16* in *post-mortem* brains from Cambodian rabid patients (Article #4). Investigating *CXCL16* expression *in vitro* revealed that the field RABV strain Tha downregulated *CXCL16* expression in IFN-α-stimulated human neuronal, astrocytic, and microglial cell lines whereas *CXCL16* was induced in IFN-α-stimulated murine astrocytes. Overall, our data provide evidence of species-specific expression of *CXCL16* during RABV infection. How can we interpret these species-specific differences?

First, all scientific data obtained strongly depend on the experimental set-up underlying data acquisition. Meaning that every generated dataset presents only limited reliability and accuracy. Changing one parameter in the experimental set-up strongly impacts the obtained results. Thus, we need to think in advance about potential benefits or limitations of selected study models to exclude that wrong conclusion are drawn. Throughout history, mice have always been the preferential model organism to study rabies pathogenesis (343). Innate and

adaptive systems of mammals are closely linked, nevertheless, a variety of factors influence the host immune response. Apart from the choice of the model organism, other biological factors shape tremendously the outcome of the triggered immune response including age, timing, sex, temperature, genetic background and polymorphisms, diet, circadian rhythms, and microbiota (to name only a few of them) (343). Consequently, and although the need for human brain biopsies to study rabies pathogenesis remains undeniable, obtaining samples from encephalitic patients presents a difficult task. Between human brains biopsies collected, there might be profound differences in time points of collection, brain region targeted, biopsy sizes, as well as differences in transport and storage of biological samples. Apart from these technical difficulties increasing the technical variation, the above-mentioned biological factors account for the biological variation among study participants. Due to the insufficient assessment of all technical and biological factors, it is impossible to separate technical from biological variation (a phenomenon known as confounding) in such a complex study design. In a nutshell, various technical and biological factors influence gene expression, making Omics studies on human biopsies in a complex environment especially prone to errors and limiting the overall reliability of their results.

Still, considering the profound differences to RABV infection in the expression of various inflammatory genes between the human and murine system (Article #4), it is highly unlikely that this is simply a result based on technical and biological confounding. More likely, species-specific differences or differences in RABV strains shape the immune responses to RABV infection. Therefore, we should keep in mind the problems arising when extrapolating data from mice to humans, as it is commonly done in research (269,344). Although mice mirror human biology remarkably well and that there are only as little as 300 genes which appear specific to one species or the other (345), there are large differences in body sizes and lifespans, not to forget the fact that humans and mice diverged between 65 - 75 million years ago (269). Until today, we have lived in different ecological niches where we encountered different pathogenic challenges that profoundly shaped our immune system (269). Clearly, I do not want to state that mice are an invalid model to study RABV biology because they have given us tremendous insights into rabies pathogenesis in the past (134–136,138,267,268). Nevertheless, we should be careful in making universal statements since research papers are mostly constructed on a precise biological question which is – in most cases - assessed in a purely artificial environment.

Secondly, Jamalkandi *et al.* recently integrated nine high-throughput transcriptome datasets (mainly composed of murine brain tissues infected with the CVS-11 strain) to identify consensus differentially expressed genes (138). In conclusion, this systems biomedicine approach revealed that the IFN circumvent, proliferation and survival pathways, as well as

neuropathological clues explained the molecular neuropathology of rabies in the analysed datasets. Interestingly, *CXCL16* was identified as a main source node in the rabies-modulated signalling network (138). In contrast to our results obtained in Tha-infected mice (Article #4), *CXCL16* was downregulated in mice in the brain or spinal cord of mice or murine microglia infected with CVS-11, ERA, FJDRV, or RABV-Cre strains (138). Thus, even within the murine brain *CXCL16* expression strongly depends on the RABV strain used for infection experiments. Another study conducted by Zhao and colleagues investigated the microRNA profile of murine brains upon infection with a street RABV strain (Fujian strain) (224). They showed that street RABV modulated miRNA expression in murine brains, among them miRNA *mmu-miR-190* which is implicated in the KEGG pathway cytokine-cytokine receptor interaction (*mmu04060*). The target genes of this pathway involve *FASL*, *HGF*, *IL6*, and *CXCL16*. Taken together, several other publications already confirmed or suggested RABV-mediated modulation of *CXCL16* expression in the murine brain (138,224). Nevertheless, no previous publication revealed that *CXCL16* – and maybe other immunity genes – might be modulated differentially in RABV-infected human brains compared to murine brains.

Lastly, identification of RABV-specific modulation of *CXCL16* expression in the human brain increases our knowledge of rabies pathogenesis – and in a wider sense – might elucidate pathways implied in chemotaxis and neurotransmission. As elaborated earlier, CXCL16 is a transmembrane chemokine that is cleaved by metalloproteases (346) and released from microglia or astrocytes (347), consequently acting as a chemoattractant for T cells, NK cells, or glial precursors (348). Although this mechanism is usually initiated in inflammatory brain diseases (347,349), RABV-induced encephalomyelitis apparently presents the contrasting picture (Article #4), namely downregulation of *CXCL16* expression at the final stage of disease. Therefore, we hypothesise that lowered *CXCL16* expression inhibits recruitment of CXCR6/Bonzo-expressing cells to the CNS (348), ultimately enabling RABV to replicate uninhibited. This fits to the overall picture of rabies pathogenesis, namely limited inflammation and apoptosis in human brains following RABV infection despite the fatality of the disease (11,100,264). Taken together, RABV-mediated inhibition of *CXCL16* expression might directly limit immune cell recruitment and thereby inhibit viral clearance from the CNS. Apart from interaction with CXCR6/Bonzo-expressing (348), CXCL16 is known to modulate neurotransmission: in the murine hippocampus, CXCL16 was shown to exert modulatory activity on both excitatory and inhibitory synapses. Further, CXCL16 modulates GABA and glutamate release *in vitro*, indirectly modulating exhibitory and inhibitory currents (350). Previously, various studies already reported abnormalities in neurotransmission during RABV infection (123). GABA uptake and release was shown to be impaired in primary rat cortical neuronal cultures infected with the CVS strain (351). Ladogana and colleagues observed a

reduction of GABA uptake, whereas GABA release was increased. Further, kinetic analysis revealed no significant changes in K_m, meaning the concentration of GABA which permit the enzyme to achieve half of V_{max}. Consequently, they suggested an unchanged and constant affinity of the GABA transport system for its substrate during RABV infection. Nevertheless, V_{max} (maximal rate of reaction) was significantly reduced suggesting a reduction of active GABA transport sites. Taken together, their data provide evidence that RABV modifies GABA uptake and release in primary cortical neurons (351). Similarly, we demonstrated that Tha (0.5) induced expression of *GABRB2* in hiNeurons (Article #3). Generally, rabies is characterized by episodes of emotional disturbances, aggressive behaviour, alternating phases of hyperexcitation and relapses, and generalized convulsions. This abnormal behaviour suggests a role of the GABAergic system during RABV infection since changes in the GABAergic system are associated with aggressive behaviour and epileptic disorders (352–354). Although the importance of RABV-modulated GABA release has not yet been studied *in vivo*, clinical data of human patients strongly suggest that RABV modifies neurotransmitter release (355). The exact mechanism, however, how field RABV specifically downregulates *CXCL16* expression and *CXCL16* expression could potentially affect neurotransmission, remains a significant question of interest.

4. Concluding remarks

4.1. Challenges and perspectives

The need for an effective rabies treatment is undeniable. Nevertheless, treatment options will be unavailable before we do not fully understand the molecular pathogenesis of rabies pathogenesis. Large datasets have been generated and examined on rabies pathogenesis in the past (138,141,356) leading to increasing knowledge of RABV-induced encephalomyelitis and vaccination strategies. However, the fatality of the disease (11,12) and the restricted accessibility of human infected nervous tissue render this disease particularly difficult to study. Thus, research is limited to classical *in vitro* models and animal models to develop future treatment strategies (357). Studies investigating molecular aspects of RABV pathogenesis are predominantly performed in animal models and neuronal monocultures (279). These models greatly improved our molecular understanding of rabies pathogenesis. However, ethical, and biological constraints limit universal validity of the results. Murine data cannot be directly translated to humans due to species-specific differences, as discussed earlier (269). Similarly, results obtained from neuronal monocultures cannot be directly translated to a functional human brain, since monoculture models are limited in terms of complexity (358).

Despite these limitations, new advances have been made in recent years in molecular biology, opening new venues to study rabies disease: with vast speed stem cell-derived cultures (151,279,359,360), new reverse genetics systems (361,362), and new sequencing technologies such as sc RNA-Seq (141,363) evolved, rendering it possible to study brain pathology, more specifically rabies-virus induced encephalomyelitis in more complex experimental set-ups. All these technologies came along with pitfalls, such as immaturity or lack of complexity of *in vitro* cultures as well as the technical limitations of sc RNA-Seq data (364,365). Despite these pitfalls, however, modern *ex-vivo* CNS technologies overcome many of the limitations of traditional culture systems and sequencing techniques used in the past providing researchers with additional information that would have been unimaginable 50 years ago. However, and personally speaking the biggest pitfall these modern methods imply is the

limitation of these advanced *in vitro* CNS technologies to a very limited research community, especially due to the need of a particular *know-how* and high costs implied. Nevertheless, as research is advancing at an enormous speed, fabrication costs are decreasing making these technologies available to bigger research communities.

Through the enormous scientific advances made in recent years, knowledge about RABV pathogenesis will most probably improve throughout the next years. Especially in a time we understand more and more the underlying mechanisms at a cellular level, I am optimistic about elucidating the role of glial cells during RABV pathogenesis and even more - the role of glial cells in CNS homeostasis and pathology. Understanding glial reactions during RABV infection, will open new treatment strategies for rabies but also potentially for various other neurotropic infections. Thus, understanding the complexity of glial biology during RABV and other neurotropic infections may open new horizons for promising therapeutics.

4.2. Closing remarks

The work performed in this thesis has provided a useful insight of glial biology during RABV infection. Although innate immune mechanisms during RABV pathogenesis are commonly studied in neuronal cultures, vast technological advances in recent years have enabled us to study pathogens in more complex *ex vivo* systems. The culture and sequencing pipeline I set up during my thesis can be used to study complex neurological diseases *in vitro*, without needing to sacrifice animals for infection experiments. Although the established pipeline is time-, labour- and cost-intensive, sc RNA-Seq experiments on *ex-vivo* human CNS cultures lead to the generation of gigantic datasets that will help to elucidate various distinct research questions. Especially in a global collaborative world, these datasets can be used among collaborations to fill remaining knowledge gaps. Despite the challenges faced while setting up such a pipeline, the corresponding datasets could potentially be used to assess i) the role of distinct CNS cell types during homeostasis, ii) the role of distinct CNS cell types during disease, and iii) the potential crosstalk taking place between the different cell types.

In a nutshell, elucidating how cell type-specific signalling pathways in the CNS are affected during viral pathogenesis is a clue to develop new therapeutic targets, not only for rabies but for various neurotropic infections.

Acknowledgements

‘Expect for the best, plan for the worst, and prepare to be surprised.’

~ Denis Waitley

I guess there are many ways to describe a PhD project but the above mentioned one described it the best for me. Especially lab work positively correlates with failure making emotional support essential. So where should I start?

Ein riesengroßer Dank an meine Familie die eventuell immer noch nicht genau verstanden hat was ich hier tagtäglich gemacht habe, mich aber dennoch jederzeit unterstützt hat (inklusiver statistischer Tests von Oli). An Flo – der mit mir einen Lockdown auf 15 qm durchgestanden hat und es trotzdem noch geschafft hat mich zu jeder Zeit aufzumuntern.

Thanks to my Pasteur crew without whom I would have never reached the end of this project. A gigantic thanks to Fabi, Gaëlle, Mara, and Lucia. *En la union está la fuerza.*

A special thanks to my lab which supported me during good and bad times. Especially Hervé who made this project possible. Thanks for all the time and support, the endless coffees, sweets, and beers. A big, big hug to Wahiba, Malika, and Laurent for emotional support!

Un grand merci à mes colocataires qui était vraiment des bons colocataires – Eric, Sylvie, Nina et Gaëlle – pour un confinement agréable, les repas innombrables, les soirées (films), les dragons, et surtout pour m’expliquer la structure de l’acétone.

A huge thanks to all my friends – inside and outside of Pasteur – particularly Nora, Rodrigo, Jonas, Juan-Pablo, Nathan, Kyrie, Lewis and to you – the reader – for being interested about the topic!

Appendices

4.3. Lessons from Sars-Cov-2 (Article #5)

More information about the research article can be found here:

https://www.embopress.org/doi/full/10.15252/emmm.202114122

This article was published on the 12th of July in the *EMBO Molecular Medicine* journal as following:

de Melo GD, Lazarini F, Larrous F, **Feige L**, Kornobis E, Levallois S, Marchio A, Kergoat L, Hardy D, Cokelaer T, Pineau P, Lecuit M, Lledo PM, Changeux JP, Bourhy H. **Attenuation of clinical and immunological outcomes during SARS-CoV-2 infection by ivermectin.** EMBO Mol Med. 2021 Jun 25:e14122. doi: 10.15252/emmm.202114122. Epub ahead of print. PMID: 34170074.

Article

SOURCE DATA | TRANSPARENT PROCESS | OPEN ACCESS

EMBO Molecular Medicine

Attenuation of clinical and immunological outcomes during SARS-CoV-2 infection by ivermectin

Guilherme Dias de Melo[1], Françoise Lazarini[2], Florence Larrous[1], Lena Feige[1], Etienne Kornobis[3,4], Sylvain Levallois[5], Agnès Marchio[6], Lauriane Kergoat[1], David Hardy[7], Thomas Cokelaer[3,4], Pascal Pineau[6], Marc Lecuit[5,8], Pierre-Marie Lledo[2], Jean-Pierre Changeux[9] & Hervé Bourhy[1,*]

Abstract

The devastating pandemic due to SARS-CoV-2 and the emergence of antigenic variants that jeopardize the efficacy of current vaccines create an urgent need for a comprehensive understanding of the pathophysiology of COVID-19, including the contribution of inflammation to disease. It also warrants for the search of immunomodulatory drugs that could improve disease outcome. Here, we show that standard doses of ivermectin (IVM), an anti-parasitic drug with potential immunomodulatory activities through the cholinergic anti-inflammatory pathway, prevent clinical deterioration, reduce olfactory deficit, and limit the inflammation of the upper and lower respiratory tracts in SARS-CoV-2-infected hamsters. Whereas it has no effect on viral load in the airways of infected animals, transcriptomic analyses of infected lungs reveal that IVM dampens type I interferon responses and modulates several other inflammatory pathways. In particular, IVM dramatically reduces the *Il-6/Il-10* ratio in lung tissue and promotes macrophage M2 polarization, which might account for the more favorable clinical presentation of IVM-treated animals. Altogether, this study supports the use of immunomodulatory drugs such as IVM, to improve the clinical condition of SARS-CoV-2-infected patients.

Keywords coronavirus; inflammation; ivermectin; SARS-CoV-2; viral infections
Subject Categories Immunology; Microbiology, Virology & Host Pathogen Interaction
DOI 10.15252/emmm.202114122 | Received 11 February 2021 | Revised 22 June 2021 | Accepted 23 June 2021
EMBO Mol Med (2021) e14122

Introduction

Coronaviruses cause respiratory disease in a wide variety of hosts. During the ongoing pandemic of SARS-CoV-2 causing coronavirus disease 19 (COVID-19), clinical signs other than respiratory symptoms have been linked to infection, frequently associated with neurological symptoms such as anosmia and ageusia. These features have been related to an over-responsiveness of patients' immune system to SARS-CoV-2 (Bhaskar *et al*, 2020; Han *et al*, 2020; Qiu *et al*, 2020). Consequently, there is an urgent need to understand the hallmarks of this over-responsiveness and to find novel therapeutics or repurpose drugs to improve the clinical condition of COVID-19 patients (Batalha *et al*, 2021).

Ivermectin (IVM), a macrocyclic lactone, is a commercially available anti-parasitic drug which prevents infection by a wide range of endo- and ectoparasites (Sajid *et al*, 2006; Heidary & Gharebaghi, 2020). IVM is an efficient positive allosteric modulator of the α-7 nicotinic acetylcholine receptor (nAChR) (Krause *et al*, 1998) and of several ligand-gated ion channels, including the muscle receptor for glutamate (GluCl) in worms (Hibbs & Gouaux, 2011). Furthermore, IVM has been shown to exert an immunomodulatory effect in humans and animals (Sajid *et al*, 2006; Heidary & Gharebaghi, 2020) under conditions that are known to involve the α-7 nAChR (Pavlov & Tracey, 2012), even though its underlying mechanisms are yet to be established (Laing *et al*, 2017). A direct or indirect interaction of SARS-CoV-2 with nAChR has also been hypothesized, in particular because of sequence homologies between SARS-CoV-2 spike proteins and nAChR ligands such as snake venom toxins (Changeux *et al*, 2020). IVM has been shown to be active beyond its anti-parasitic activity in a wide variety of pathologies, including cancer, allergy, and viral infections (Laing *et al*, 2017). Recently, IVM has been

1 Lyssavirus Epidemiology and Neuropathology Unit, Institut Pasteur, Paris, France
2 Perception and Memory Unit, Institut Pasteur, CNRS UMR 3571, Paris, France
3 Biomics Technological Platform, Center for Technological Resources and Research (C2RT), Institut Pasteur, Paris, France
4 Bioinformatics and Biostatistics Hub, Computational Biology Department, Institut Pasteur, Paris, France
5 Biology of Infection Unit, Institut Pasteur, Inserm U1117, Paris, France
6 Nuclear Organization and Oncogenesis Unit, Institut Pasteur, Paris, France
7 Experimental Neuropathology Unit, Institut Pasteur, Paris, France
8 Division of Infectious Diseases and Tropical Medicine, Institut Imagine, Université de Paris, Necker-Enfants Malades University Hospital, AP-HP, Paris, France
9 Neuroscience Department, Institut Pasteur, Collège de France, Paris, France
*Corresponding author. Tel: +33 1 45 68 87 85; E-mail: herve.bourhy@pasteur.fr

© 2021 The Authors. Published under the terms of the CC BY 4.0 license

reported to reduce viral load and improve the clinical status of mice infected by an animal coronavirus, the mouse hepatitis virus (MHV) (Arévalo *et al*, 2021). *In vitro* inhibition of SARS-CoV-2 replication by IVM in Vero/hSLAM cells has also been reported (Caly *et al*, 2020), albeit at much higher concentrations (50- to 100-fold) than those clinically attainable in humans (150–400 μg/kg) (Guzzo *et al*, 2002; Bray *et al*, 2020; Chaccour *et al*, 2020).

The aim of this study is to investigate the impact of IVM on the pathogenesis of COVID-19, in a SARS-CoV-2 infection model, the golden Syrian hamster. This species is naturally permissive to this virus and the most reliable and affordable animal model for COVID-19 (Chan *et al*, 2020; Muñoz-Fontela *et al*, 2020). Moreover, it was recently used to demonstrate the importance of lowering the inflammation with intranasal administration of type I IFN to prevent

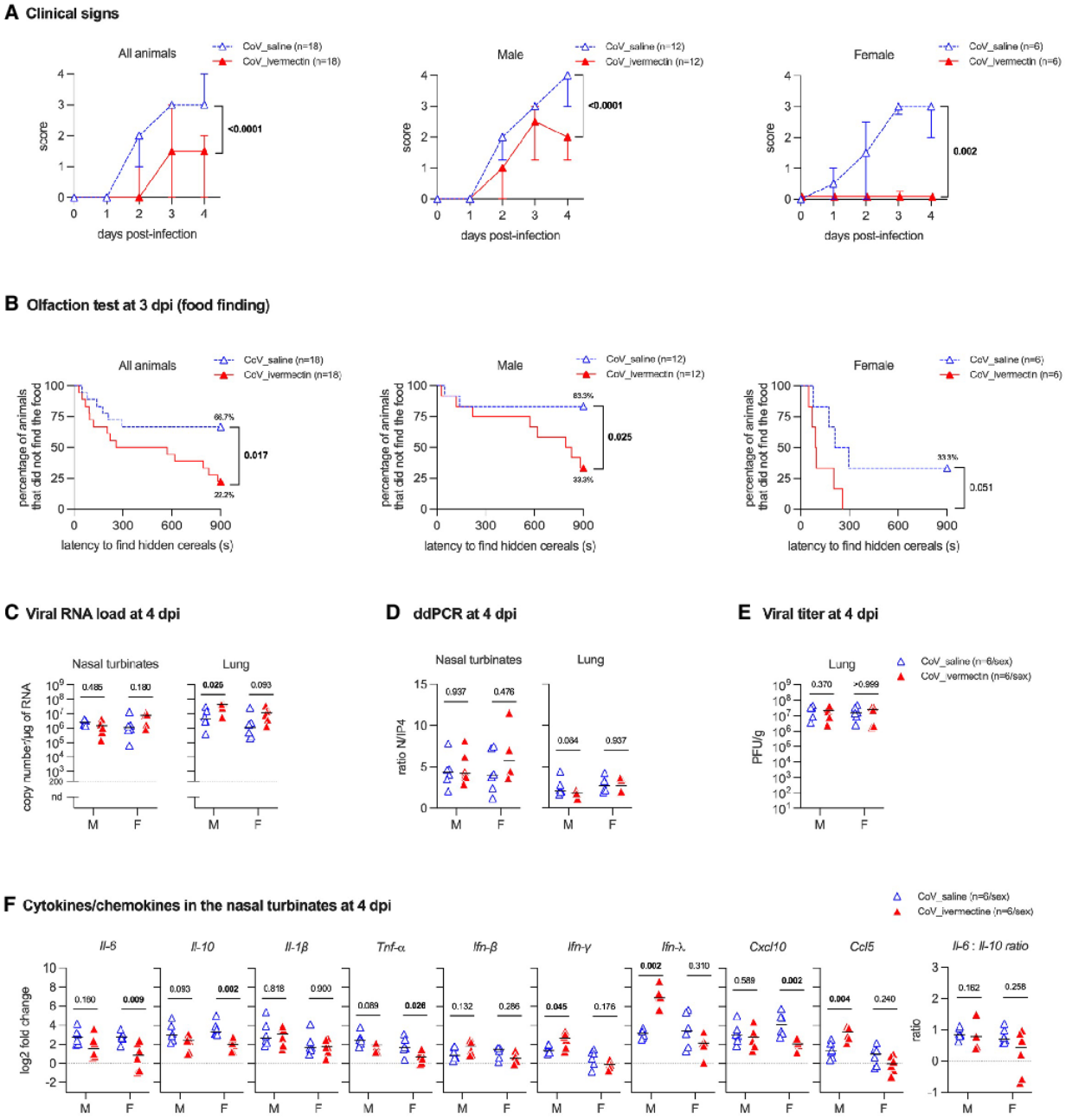

Figure 1.

© 2021 The Authors

Figure 1. Clinical presentation, olfaction test, viral load and immune profile in the nasal turbinates of SARS-CoV-2-infected hamsters with and without ivermectin treatment.

A Clinical signs in infected hamsters. The clinical score is based on a cumulative 0–4 scale: ruffled fur; slow movements; apathy; and absence of exploration activity. Symbols indicate the median ± interquartile range.

B Olfactory performance in infected hamsters. The olfaction test is based on the hidden (buried) food finding test. Curves represent the percentage of animals that did not find the buried food. Food finding assays were performed at 3 days post-infection (dpi). Data were obtained from three independent experiments for males and two independent experiments for females.

C Viral load in the nasal turbinates and in the lungs at 4 dpi.

D Ratio between the CPD (copy per droplets, normalized to *γ-actin* and *Hprt* reference gene relative expression) of structural [N, nucleocapsid] and non-structural [IP4: RdRp, RNA-dependent RNA polymerase] viral gene expression determined by digital droplet PCR (ddPCR) in the nasal turbinates and in the lungs at 4 dpi.

E Infectious viral titer in the lung at 4 dpi expressed as plaque-forming units (PFU)/g of tissue.

F Cytokine and chemokine transcripts in the nasal turbinates at 4 dpi in male and female SARS-CoV-2-infected hamsters, treated with saline or with 400 µg/kg ivermectin.

Data information: Horizontal lines indicate medians. The *P* value is indicated in bold when significant at a 0.05 threshold. Mann–Whitney test (A, C–F) and log-rank (Mantel–Cox) test (B). M: male hamsters and F: female hamsters. Data were obtained from two independent experiments for each sex. See Figs EV1 and EV2 and Appendix Fig S1.
Source data are available online for this figure.

disease progression (Hoagland *et al*, 2020). Male and female adult golden Syrian hamsters were intranasally inoculated with 6×10^4 PFU of SARS-CoV-2 [BetaCoV/France/IDF00372/2020]. This inoculum size was selected as it invariably causes symptomatic infection in golden Syrian hamster, with a high incidence of anosmia and high viral loads in the upper and lower respiratory tracts within 4 days post-inoculation (dpi) (de Melo *et al*, 2021). At the time of infection, animals received a single subcutaneous injection of IVM at the anti-parasitic dose of 400 µg/kg, commonly used in human clinical setting, and were monitored over 4 days.

Here, we show that the modulation of the host's inflammatory response using IVM as a repurposed drug strongly diminished the clinical score and severity of the disease (including anosmia) observed in these animals, although it has no impact on viral load. IVM-treated animals presented a strong modulation in several signaling pathways, including a significant reduction of the type I and III interferon response and of the *Il-6/Il-10* ratio, along with the presence of M2 macrophages in the lung. These effects were mostly compartmentalized and sex-dependent, and treated infected females exhibited better clinical outcomes.

Results and Discussion

COVID-19 clinical outcome is attenuated by ivermectin

In order to study the effects of IVM chemical therapy on clinical outcome, we assessed body weight, clinical score, and olfactory performance daily for 4 days post-infection. The golden hamster model reproduces a moderate-to-severe COVID-19 in humans, with a clinical phase lasting 5–6 days post-infection followed by a complete recovery by 2 weeks post-infection, with no death occurring. The viral titers and viral RNA loads in the airways of infected animals are elevated after 2–4 days post-infection, but they drastically drop by 7 days post-infection (Chan *et al*, 2020; Sia *et al*, 2020; de Melo *et al*, 2021).

The IVM-treated infected animals, of both sexes, showed a decrease in body weight similar to that observed in saline-treated infected hamsters (Fig EV1A). However, IVM-treated infected animals exhibited a significant reduction in the severity of the clinical score, in a sex-dependent manner: Infected males presented a significantly reduced clinical score, and it fully returned to normal in infected females (Fig 1A). Remarkably, IVM treatment reduced the olfactory deficit in infected animals (Figs 1B and EV1B–D): 66.7% (12/18) of the saline-treated infected hamsters presented with hyposmia/anosmia, whereas only 22.2% (4/18) of IVM-treated infected hamsters presented with signs of olfactory dysfunction (Figs 1B and EV1B–D). The olfactory performance was also influenced by sex: 83.3% (10/12) of the saline-treated infected males presented with hyposmia/anosmia, against only 33.3% (4/12) of IVM-treated infected males (Figs 1B and EV1B–D). In females, while 33.3% (2/6) of saline-treated infected animals presented with hyposmia/anosmia, no olfactory deficit was observed in IVM-treated infected females (0/6; Figs 1B and EV1B–D).

Since males presented a higher incidence of anosmia/hyposmia, we subsequently performed a dose-response curve to test the effect of IVM on the clinical presentation and olfactory functions of infected males: Lower doses of IVM (100 or 200 µg/kg) elicited similar clinical outcomes as the anti-parasitic dose of 400 µg/kg (Fig EV2). As expected, no signs of olfactory deficit were observed in mock-infected hamsters (Fig EV1B–D).

Ivermectin treatment does not influence SARS-CoV-2 load in the respiratory tract of infected hamsters

To evaluate the effect of IVM treatment on the viral load in the respiratory tract, we tested the nasal turbinates and lungs of infected hamsters using both classical RT–qPCR (Fig 1C) and the highly sensitive technique of digital droplet PCR (Suo *et al*, 2020; Fig 1D, Appendix Fig S1). Surprisingly, the viral RNA load in the respiratory tract remained unaffected by IVM treatment in both samples in both sexes. Furthermore, IVM treatment did not influence viral replication rate, as evaluated by the ratio between structural and non-structural gene transcription (Fig 1D, Appendix Fig S1). Finally, IVM treatment did not alter infectious viral titers in the lungs (Fig 1E). These results illustrate that no antiviral activity of IVM is detected *in vivo* at the standard anti-parasitic dose of 400 µg/kg, in contrast to a previous report suggesting that IVM inhibits the replication of SARS-CoV-2 *in vitro*, albeit used at far higher concentrations (Caly *et al*, 2020). Therefore, the action of IVM on COVID-19 clinical signs of infected golden hamsters does not result from a decrease in viral replication.

© 2021 The Authors

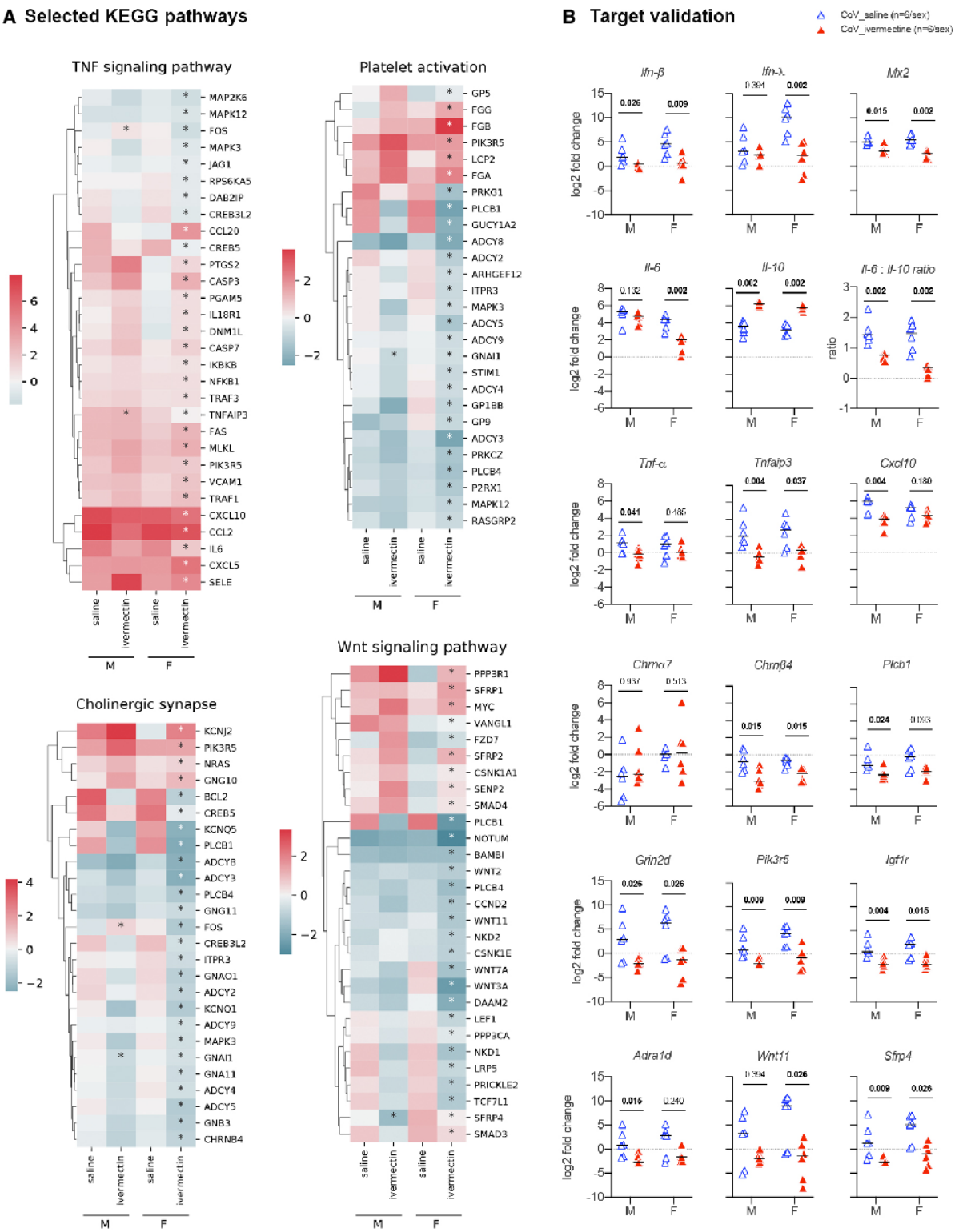

Figure 2.

© 2021 The Authors

Figure 2. Transcriptomic profile in the lung of SARS-CoV-2-infected hamsters with and without ivermectin treatment at 4 days post-infection.

A Heatmaps showing the differentially expressed genes according to the selected KEGG pathways calculated in comparison with mock-infected hamsters. * indicates Benjamini–Hochberg-adjusted *P*-value < 0.05 in the comparison between saline and ivermectin within the same sex. Color gradient represents the transcription $\log_2$ fold change comparing infected and mock-infected. Complete analyses are listed in Dataset EV1.

B Validation targets in the lung at 4 dpi. Horizontal lines indicate medians. The *P* value is indicated in bold when significant at a 0.05 threshold. Mann–Whitney test.

Data information: M: male hamsters and F: female hamsters. Data were obtained from two independent experiments for each sex. See Figs EV3–EV5.
Source data are available online for this figure.

Ivermectin therapy modulates local immune responses in infected hamsters' nasal turbinates

Anosmia is a typical symptom of COVID-19 in humans, with some sex-dependent differences (Han *et al*, 2020; Qiu *et al*, 2020; Xydakis *et al*, 2020). Inflammation in the nasal cavity, following olfactory sensory neurons infection and deciliation, has been shown to be an underlying factor for smell loss during SARS-CoV-2 infection (de Melo *et al*, 2021), and the chemokine *Cxcl10* could be directly implicated due to its neurotoxic potential (Oliviero *et al*, 2020). We therefore tested a possible modulation by IVM of the local inflammatory response in hamsters and in particularly in the nasal turbinates, the primary target tissue of SARS-CoV-2 infection (de Melo *et al*, 2021), that could correlate its effect on the olfactory score. To this aim, a panel of cytokines (*Il-6, Il-10, Il-1β, Tnf-α*, *Ifn-β, Ifn-γ*, and *Ifn-λ*) and chemokines (*Cxcl10* and *Ccl5*) were used to assess the impact of IVM treatment on immune responses in the nasal turbinates of SARS-CoV-2-infected hamsters at 4 dpi. Upon treatment with IVM, females presented a significant downregulation of *Il-6, Il-10, and Tnf-α*, which are key inflammatory mediators of prognostic value in COVID-19 patients (McElvaney *et al*, 2020a), and of *Cxcl10* (Fig 1F), in line with their better olfactory performance observed in the food finding tests (Fig 1B). The differences between sex groups are illustrated by the increase in three pro-inflammatory mediators (*Ifn-γ*, *Ifn-λ*, and *Ccl5*) only in males (Fig 1F). No difference for the *Il-6/Il-10* ratio was observed in the nasal turbinates.

Lung immunometabolism is affected by SARS-CoV-2 infection and modulated by ivermectin

IVM attenuates lung pathology and inflammation pathways, including cholinergic synapse-related genes

In order to further study the mode of action of IVM on clinical signs, we performed at 4 dpi a comparative agnostic transcriptomic approach using RNA-seq in the lower respiratory tract in hamsters treated or not with IVM. In SARS-CoV-2-infected lungs, male and female hamsters exhibited an overall similar pattern, although there were slightly more KEGG pathways modulated by infection in males (Fig 2A). A high number of common dysregulated inflammatory and metabolic pathways in SARS-CoV-2-infected males and females (Fig EV3) were similar to those observed in lung cells from human COVID-19 patients, such as "cytokine-cytokine receptor interaction", "TNF signaling pathway", and "insulin resistance" (Dey *et al*, 2020; Islam *et al*, 2020) including many genes of the IFN response. The transcriptomic profiles observed in the lungs from IVM-treated hamsters compared to non-treated infected hamsters presented a striking sex difference: Lungs of IVM-treated females presented 1,206 downregulated genes and 1,428 upregulated genes, whereas only 36 downregulated and 51 upregulated genes were detected in the lungs of IVM-treated males. This sex difference is also illustrated by KEGG and GO enrichments representations (Fig EV4).

Several KEGG pathways were significantly regulated in IVM-treated females: "TNF signaling pathway" and "cholinergic synapse", in line with the activation of vagus nerve cholinergic anti-inflammatory pathway (CAP) (Pavlov & Tracey, 2012; De Virgiliis & Di Giovanni, 2020), and "platelet activation", related to prevention of thrombosis (Zhang *et al*, 2020b; Chen & Pan, 2021) (Figs 2A and EV4A). We also observed a modulation of the "Wnt signaling pathway" KEGG pathway in the IVM treatment group, which has been shown to correlate with lung homeostasis and regeneration (Raslan & Yoon, 2020), obesity, type-2 diabetes, and cancer (Melotti *et al*, 2014; Aamir *et al*, 2020) (Figs 2A and EV4A). Further modulated pathways in IVM-treated female hamsters were "renin secretion", "vascular smooth muscle contraction", and "adrenergic signaling in cardiomyocytes" which could be related to the prevention of vaso-constriction and therefore attenuation of lung pathology (Fig EV4A) (Potus *et al*, 2020; Vaduganathan *et al*, 2020). Moreover, carbohydrate metabolism and insulin resistance were frequent terms observed in RNA-seq analyses of the lung of female hamsters during SARS-CoV-2 infection, linked to hyperglycemia, metabolic syndrome, and impairments in the immune system, similarly to what is observed in COVID-19 in humans (Pavlov & Tracey, 2012; Gianchandani *et al*, 2020). In IVM-treated hamsters, specifically in females, the term "insulin resistance" was no longer observed in the KEGG enrichment, and the insulin secretion pathway was downregulated. Several other related pathways linking hyperglycemia, inflammation, and lung pathology were downregulated, such as Rap1, AGE-RAGE, and cGMP-PKG signaling pathways (Figs EV4 and EV5) (Oczypok *et al*, 2017; Pei *et al*, 2020; Isidori *et al*, 2021). In IVM-treated males, significant modulated pathways determined by KEGG and GO enrichments were related to tight junctions, muscular and epithelial cells (Fig EV4).

Additionally, the GO enrichment in IVM-treated females revealed important modulated pathways including "regulation of neurotransmitter secretion" (Fig EV4B). Several important neurotransmitter receptors were indeed downregulated in both IVM-treated males and females, including cholinergic nicotinic (*Chrnb4*), adrenergic (*Adra1d*), GABAergic (*Gabbr1*), and glutamatergic (*Grin2d/Nmdar2d, Grid1*), the latter possibly related to a protection of glutamate-induced lung injury (Said, 1999; Zhe *et al*, 2018).

IVM exerts a strong regulation of type I and III IFN-related genes and lowers down the Il-6/Il-10 ratio in the lungs of SARS-CoV-2-infected hamsters

To analyze in more details the modulated genes in IVM-treated animals, we selected representative target genes from these relevant

© 2021 The Authors

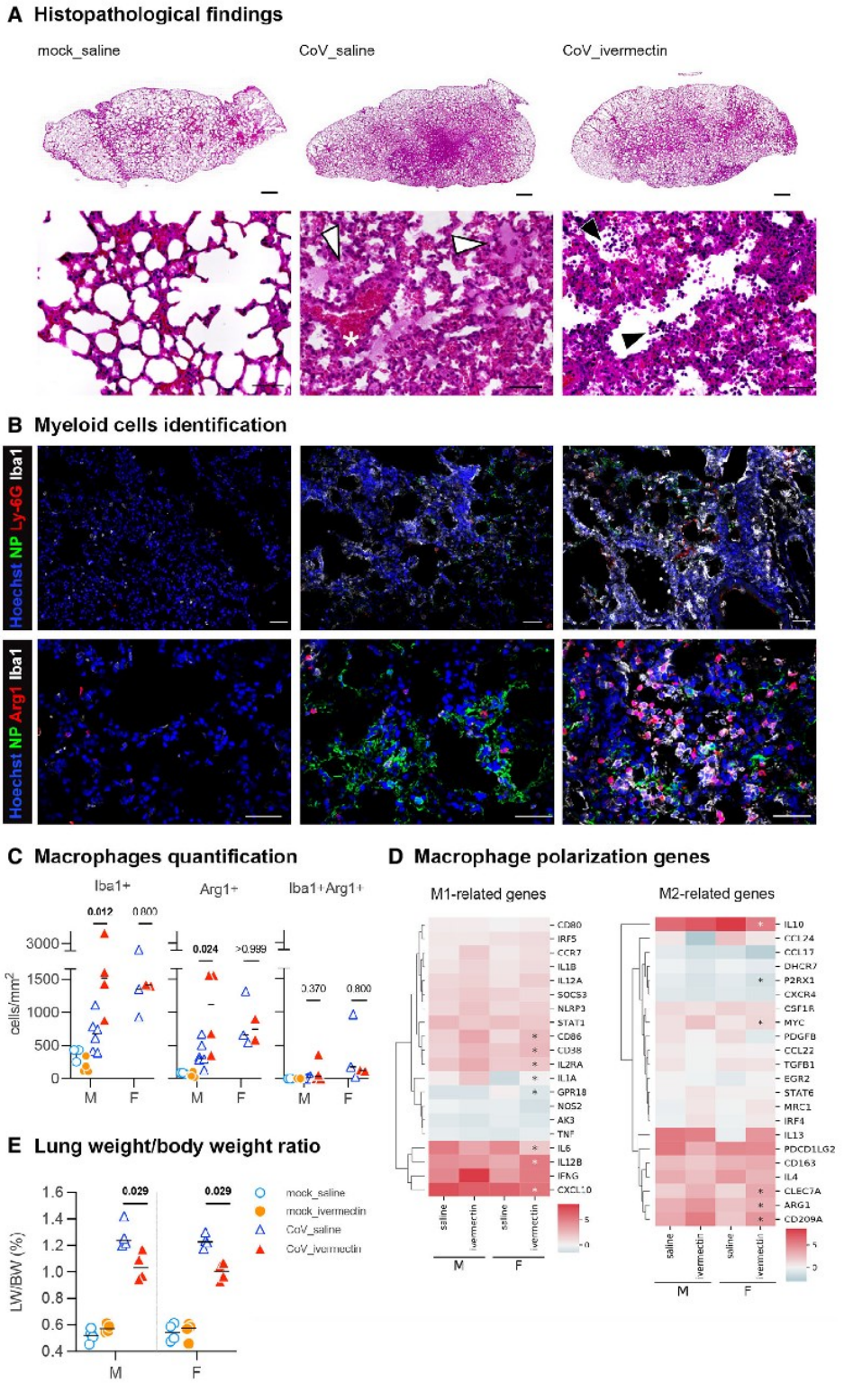

Figure 3.

© 2021 The Authors

Figure 3. Identification of macrophages in the lung of SARS-CoV-2-infected hamsters with and without ivermectin treatment and characterization of their transcriptomic profile related to M1/M2 polarization.

A Representative histopathology photomicrographies of lungs according to the different groups: mock_saline, CoV_saline, and CoV_ivermectin. Top panels: whole lung sections. Bottom panels: high magnification. CoV_saline section exhibits important congestion (*), edema associated with few mononuclear cells (white arrowheads). Note the thickening of the alveolar walls. CoV_ivermectin section exhibits important amounts of mononuclear cells (black arrowheads) and less marked signs of congestion or edema. Hematoxylin and eosin. Scale bars = 1 mm (top panels) and 20 μm (bottom panels).

B Representative immunofluorescence photomicrographies of neutrophils (Ly-6G), monocytes/macrophages (Iba1), M2 macrophages (Arg1), and SARS-CoV-2 (NP) in the lung. Scale bars = 50 μm.

C Quantification of $Iba1^+$ cells, $Arg1^+$ cells, and $Iba1^+Arg1^+$ cells in the lungs. mock_saline $n = 3$ (males), mock_ivermectin $n = 4$ (males), CoV_saline $n = 9$ (6 males and 3 females), and CoV_ivermectin $n = 6$ (4 males and 2 females).

D Heatmaps showing the differentially expressed genes related to the M1/M2 polarization in comparison with mock-infected hamsters. *indicates Benjamini–Hochberg-adjusted *P*-value < 0.05 in the comparison between saline and ivermectin within the same sex. Color gradient represents the transcription $\log_2$ fold change comparing infected and mock-infected. Complete analyses are listed in Dataset EV1.

E Lung weight-to-body weight ratio in the different groups ($n = 4$/sex/group).

Data information: M: male hamsters and F: female hamsters. Horizontal lines indicate medians. The *P* value is indicated in bold when significant at a 0.05 threshold. Mann–Whitney test (C, E).
Source data are available online for this figure.

pathways that were highly regulated in IVM-treated females and we compared by RT–qPCR their respective transcription levels in the lungs of the different groups of animals. Among these genes, several were also significantly modulated between IVM- and saline-treated infected males including *Tnfaip3*, *Sfrp4*, *Epha2*, *Gnai1*, *Hgf*, and *Fos*. Others presented a similar regulation in males compared to females (from KEGG and GO enrichments) although their modulation was not invariably significant: *Casp3, Plcb1, Chrna7, Chrnb4, Adra1d, Grin2d/Nmdar2d, Grid1, Gabrr1, Pik3r5, Igf1r, Wnt11, Wnt3a, Il-2, Il-2ra, Prkg1, Krt4, Creb5, and Ager*. The modulation of these targets, together with other genes from relevant inflammatory mediators taken from the literature (Boudewijns *et al*, 2020; Hoagland *et al*, 2020) (*Il-6, Il-10, Il-1β, Tnf-α, Ifn-β, Ifn-λ, Ifn-γ, Tgf-β, Cxcl10, Ccl5*, and *Mx2)*, was confirmed by RT–qPCR (Figs 2B and EV5).

IVM limited the expression of *Ifn-β* (males and females), *Ifn-λ* (females), and IFN-stimulated gene *Mx2* (males and females) in the lung of infected and IVM-treated hamsters compared to infected and saline-treated hamsters. In contrast, saline-treated hamsters presented an increased expression of *Ifn-β*, *Ifn-λ*, and *Mx2* compared to non-infected hamsters (males and females). This is expected as type I and III IFN signaling pathways have already been shown to correlate with lung pathology severity in SARS-CoV-2-infected hamsters, possibly resulting from a STAT2-dependent response (Boudewijns *et al*, 2020). In contrast, type I and III IFNs are differently expressed in the nasal turbinates, where *Ifn-λ* is upregulated in treated males (Fig 1F). This difference between upper and lower airways may be explained by two factors: (i) the specificity of *Ifn-λ* in the nasal cavity's antiviral response (Okabayashi *et al*, 2011; Klinkhammer *et al*, 2018), whereas type I and III IFNs perform redundant actions in the lung (Stanifer *et al*, 2020), and (ii), following studies with influenza A virus, type I and III IFNs have a sequential activation, where *Ifn-λ* comes at first to fight infection, and type I IFNs come later, with pro-inflammatory and reinforced antiviral effects (Galani *et al*, 2017; Stanifer *et al*, 2020).

Interestingly, some of these genes are not only involved in the previously mentioned pathways but also play a major role in other molecular functions that may be critical in the pathogenesis of SARS-CoV-2 infection and the efficacy of the IVM treatment in hamsters. Among them, the significant overexpression of *Il-10* was a common feature of IVM-treated males and females (Fig 2B). This effect may be related to a modulation of the inflammatory response in the lung (downregulation of *Tnf-α* in males, *Tnfaip3* in both sexes, and *Il-6* in females) associated with reduced clinical signs. *Tnf-α* reduction and better clinical presentation are common features caused by the IVM treatment in another model of coronavirus infection, where mice were infected with MHV (Arévalo *et al*, 2021). Additionally, differently from the nasal turbinates, the *Il-6/Il-10* ratio in the lung of IVM-treated hamsters was significantly lower than in non-treated animals (Fig 2B), which may relate to their comparatively better clinical presentation. Of note, lower plasmatic *Il-6/Il-10* ratios were detected in hospitalized COVID-19 patients who did not require intensive care (McElvaney *et al*, 2020a; McElvaney *et al*, 2020b).

IVM increases the infiltration of monocytes/macrophages and promote M2 polarization in the lung of SARS-CoV-2-infected hamsters

To assess directly lung pathology in infected animals, we performed histopathological analyses. The lungs of SARS-CoV-2-infected and saline-treated hamsters exhibited substantial lesions with focal areas of edema, congestion, microhemorrhages, associated with mononuclear cells, hyaline membranes, alveolar walls thickening (Fig 3A), in line with previous reports (Chan *et al*, 2020; Sia *et al*, 2020). In contrast, the lungs of SARS-CoV-2-infected and IVM-treated hamsters exhibited with reduced degrees of edema and congestion, yet with greater amounts of mononuclear cells in the alveolar spaces (Fig 3A). SARS-CoV-2 infection caused an increase in the lung weight/body weight ratio; however, this increase was lowered in IVM-treated as compared to saline-treated infected animals (Fig 3E).

The better clinical presentation observed in IVM-treated animals could be correlated with the activation of the cholinergic anti-inflammatory pathway (CAP) under vagus nerve control (Pavlov & Tracey, 2012). Indeed, the interaction of IVM with the α-7 nAChR in macrophages may account for the immune response modulation in IVM-treated hamsters (Gahring *et al*, 2017; Zhao *et al*, 2019), eliciting *Il-10* production, promoting M2 polarization (dampening inflammation and triggering tissue-repair), and counterbalancing M1 action (pro-inflammatory, associated with tissue damages and microbicidal activity) (Sang *et al*, 2015). This interpretation is supported by the upregulation of *Il-10* observed in the lung of IVM-

© 2021 The Authors

treated animals, along with the reduction of key M1 pro-inflammatory mediators, such as *Il-6*, *Tnf-α*, and *Cxcl10* (Fig 2B), in similar ways as observed in other viral infections (Sang *et al*, 2015).

Whereas few Iba1$^+$ cells were observed in mock-infected animals, most likely resident interstitial and alveolar macrophages, we observed a large number of Iba1$^+$ myeloid cells in the lungs of IVM-treated animals (Fig 3B). No distinguishable differences were observed in neutrophils population (Ly-6G$^+$) between saline-treated and IVM-treated animals (Fig 3B). Part of these Iba1$^+$ cells were also Arg1$^+$ cells (Fig 3B), a marker of M2-polarized macrophages. IVM treatment was associated with an increase of both Iba1$^+$ and Arg1$^+$ cells in the lungs of SARS-CoV-2-infected male hamsters (Fig 3C). In contrast, in females, while infection promoted an increase of both Iba1$^+$ and Arg1$^+$ cells (Fig 3C), IVM had no impact on the recruitment of these cells. Additionally, RNA-seq analyses in the lung identified the upregulation of key M2-related genes (*Arg1, Cd209a/DC-SIGN, Clec7a/Dectin-1,* and *Myc/c-Myc*) along with classical M1 markers (*Cd86* and *Cd38*; Fig 3D), giving additional support to the M2 polarization tendency caused by the IVM treatment.

Conclusions

Our results demonstrate that IVM improves clinical outcome in SARS-CoV-2-infected animals and is associated with a reduced inflammatory status, but with no impact of SARS-CoV-2 loads in the upper and lower respiratory tracts. Thus, in hamsters, as in humans (preprint: Cereda *et al*, 2020; Hasanoglu *et al*, 2021), symptomatology and therefore the severity of SARS-CoV-2 infection is not strictly correlated with viral load. The main effect of IVM in the lungs is on type I and III IFN responses and other related signaling pathways including phospholipases, kinases, and adenylate cyclases, which are important therapeutic targets (Melotti *et al*, 2014; Raker *et al*, 2016; Hu *et al*, 2020; Li *et al*, 2020; preprint: Masood *et al*, 2020; Isidori *et al*, 2021), and this translates clinically into an improved clinical score.

The results presented herein are consistent with a role of type I and III IFN responses in the pathogenesis of SARS-CoV-2-associated lung disease in hamsters. They show that IVM administration limits IFN response and lung inflammation, even though defects in the type I IFN pathways have been associated with severe COVID-19 (Bastard *et al*, 2020; Zhang *et al*, 2020a). This result may suggest that while IFN signaling is crucial to control viral replication and prevent severe disease, in infected hamsters, which only develop a moderate disease, IFN signaling may actually increase tissue damage and associated signs such as anosmia. This is consistent with previous reports in animal models where inhibition of IFN pathways was shown to increase viral replication but with lower lung pathology (Boudewijns *et al*, 2020; Sun *et al*, 2020).

Even if the effects observed may, to some extent, share similarities with the impact of dexamethasone (Horby *et al*, 2020) and tocilizumab (anti-IL-6) (Rossotti *et al*, 2020) on COVID-19, IVM action is steady and strong in the golden hamsters and is not expected to block the effectors of inflammation but rather to dampen its initiation. Interestingly, the activation of nuclear factor erythroid 2-related transcription factor (Nrf2) via low-dose radiotherapy (LDRT) treatment has been proposed to cause a shift from M1 to M2 macrophages and a blockade of NLRP3 inflammasomes (Calabrese *et al*, 2021) and to be potentially beneficial on the lungs of COVID-19 patients. Along the same line, we noticed via our RNA-seq analyses that IVM treatment increased the gene expression of Nrf2 (or Nfe2l2) in the lungs of female hamsters and slightly in males (Dataset EV1), which gives additional evidence of the broad and upstream activity of IVM during SARS-CoV-2 infection. Further, our data show that these effects are compartmentalized and that the upper and lower respiratory tracts of hamsters respond differently to IVM treatment.

Considerable sex differences are observed in terms of clinical presentation, inflammatory profile, and transcriptomic signatures in the lungs of hamsters, as seen in COVID-19 human patients, where men tend to develop more severe disease than women (Jin *et al*, 2020; Takahashi *et al*, 2020), possibly in relation with androgen signaling (vom Steeg & Klein, 2019; Samuel *et al*, 2020; Scully *et al*, 2020). Interestingly, sex steroids, here female hormones, might also influence both the course of COVID-19 in hamsters and the effects of IVM, possibly due to the potentiation of cell receptors signaling in females, such as nAChRs (Krause *et al*, 1998; Cross *et al*, 2017) and GlyRs (Van Den Eynden *et al*, 2009; Cerdan *et al*, 2020), of which IVM is a positive allosteric modulator.

Moreover, the data presented herein are consistent with those reported in human clinical trials with IVM (Kory *et al*, 2021). In humans, IVM is widely used as anti-helminthic and anti-scabies at therapeutic doses (150–400 μg/kg) (Guzzo *et al*, 2002) that are in the range of those used in our hamster experiments. Further, several clinical trials on COVID-19 using IVM have been declared, where IVM has been associated with reduction of inflammatory markers and disease severity (preprint: Hill *et al*, 2021; Kaur *et al*, 2021). Interestingly, in a long-term care facility where the residents received IVM to control a scabies outbreak, no death or severe COVID-19 was observed (Bernigaud *et al*, 2021). IVM has already been administered to hospitalized COVID-19 patients, with contrasting outcomes: one study related no efficacy of late IVM administration (8–18 days after symptom onset) in severe COVID-19 patients treated in combination with other drugs (hydroxychloroquine, azithromycin, tocilizumab, steroids) (Camprubí *et al*, 2020), whereas another study reported lower mortality, especially in severe COVID-19 patients treated with IVM in addition to other treatments (hydroxychloroquine, azithromycin, or both) (Rajter *et al*, 2020). Importantly, in a study that administered IVM alone within 72 h of symptom onset, the authors noticed an important diminution of anosmia/hyposmia in the IVM group without differences in PCR positivity between IVM and placebo groups (Chaccour *et al*, 2021).

The presently available data support the view that IVM pharmacokinetics is quite stable across species, generally with slow absorption, broad distribution, low metabolism, and slow excretion, even if some conditions, such as route of administration, formulation, and body condition, may modify these features. In humans, the oral route is the only approved, and the administration of a single dose of 30 mg of IVM (corresponding to 347–594 μg/kg) leads to a C_{max} (maximum concentration) of 84.8 ng/ml, a t_{max} (time to reach the C_{max}) of 4.3 h and a half-life of 20.1 h (Guzzo *et al*, 2002). In animal models, the subcutaneous route is most often used, and comparatively, golden hamsters that received a subcutaneous injection of 400 μg/kg of IVM (as in the present study) showed comparable results with a C_{max} of 80.2 ng/ml and a t_{max} of ~4 h (Hanafi *et al*, 2011). Further, based on veterinary data

 © 2021 The Authors

(Lifschitz *et al*, 2000), simulations using a minimal physiologically based pharmacokinetic (mPBPK) model revealed that the lungs would be exposed to IVM concentrations 2.7× greater than those found in the plasma (Jermain *et al*, 2020). Yet, this dose did not suffice to achieve the range of antiviral concentrations reported *in vitro* (Caly *et al*, 2020).

Consequently, considering the results observed in the golden hamster model, IVM may be considered as a therapeutic agent against COVID-19, which would not strongly affect SARS-CoV-2 replication but limit the pathophysiological consequences of the infection *in vivo,* potentially mediated by type I and III IFN responses and several other related signaling pathways, and a favorable M1/M2 myeloid cells ratio in the lungs. A characteristic modulation of the immune response in the lower airways was observed in IVM-treated hamsters characterized by a transcriptomic profile similar to that observed in humans exhibiting less severe symptoms and a better prognosis (preprint: Masood *et al*, 2020; McElvaney *et al*, 2020b). Our data are consistent with the hypothesis that this effect is mediated by the cholinergic anti-inflammatory action of IVM on the vagus nerve reflex (Changeux *et al*, 2020; Tizabi *et al*, 2020), that should be addressed experimentally. In particular, the precise contribution of the nAChR in IVM action should be elucidated in comparison with that of other possible IVM targets (Zemkova *et al*, 2014). Altogether, this study brings the proof of concept that an IVM-based immunomodulatory therapy improves the clinical condition of SARS-CoV-2-infected hamsters, and in clinical trials, it alleviates symptoms of COVID-19 in humans and possibly limits post-COVID-19 syndrome (also known as long COVID) via an anti-inflammatory action.

Materials and Methods

Ethics

All animal experiments were performed according to the French legislation and in compliance with the European Communities Council Directives (2010/63/UE, French Law 2013–118, February 6, 2013) and according to the regulations of Pasteur Institute Animal Care Committees. The Animal Experimentation Ethics Committee (CETEA 89) of the Institut Pasteur approved this study (200023; APAFIS#25326-2020050617114340 v2) before experiments were initiated. Hamsters were housed by groups of 4 animals in isolators and manipulated in class III safety cabinets in the Pasteur Institute animal facilities accredited by the French Ministry of Agriculture for performing experiments on live rodents. All animals were handled in strict accordance with good animal practice.

Production and titration of SARS-CoV-2 virus

The isolate BetaCoV/France/IDF00372/2020 (EVAg collection, Ref-SKU: 014V-03890) was kindly provided by Sylvie Van der Werf. Viral stocks were produced on Vero-E6 cells infected at a multiplicity of infection of 1×10^{-4} plaque-forming units (PFU). The virus was harvested 3 days post-infection, clarified, and then aliquoted before storage at −80°C. Viral stocks were titrated on Vero-E6 cells by classical plaque assays using semisolid overlays (Avicel, RC581-NFDR080I, DuPont) (Baer & Kehn-Hall, 2014).

SARS-CoV-2 model and ivermectin treatment of hamsters

Male and female Syrian hamsters (*Mesocricetus auratus;* RjHan: AURA) of 5–6 weeks of age (average weight 60–80 g) were purchased from Janvier Laboratories and handled under specific pathogen-free conditions. The animals were housed and manipulated in isolators in a Biosafety level-3 facility, with *ad libitum* access to water and food. Before manipulation, animals underwent an acclimation period of 1 week.

Animals were anesthetized with an intraperitoneal injection of 200 mg/kg ketamine (Imalgène 1000, Merial) and 10 mg/kg xylazine (Rompun, Bayer) and received one single subcutaneous injection of 200 µl of freshly diluted ivermectin (I8898, Sigma-Aldrich) at the classical anti-parasitic dose of 400 µg/kg (Beco *et al*, 2001) (or at 100–200 µg/kg for the dose–response experiment). Non-treated animals received one single subcutaneous injection of 200 µl of physiological solution. 100 µl of physiological solution containing 6×10^4 PFU of SARS-CoV-2 was then administered intranasally to each animal (50 µl/nostril). Mock-infected animals received the physiological solution only.

Infected and mock-infected animals were housed in separate isolators, and all hamsters were followed up daily during 4 days at which the body weight and the clinical score were noted. The clinical score was based on a cumulative 0–4 scale: ruffled fur, slow movements, apathy, and absence of exploration activity.

At day 3 post-infection (dpi), animals underwent a food finding test to assess olfaction as previously described (Lazarini *et al*, 2012; de Melo *et al*, 2021). Briefly, 24 h before testing, hamsters were fasted and then individually placed into a fresh cage ($37 \times 29 \times 18$ cm) with clean standard bedding for 10 min. Subsequently, hamsters were placed in another similar cage for 2 min when about five pieces of cereals were hidden in 1.5 cm bedding in a corner of the test cage. The tested hamsters were then placed in the opposite corner, and the latency to find the food (defined as the time to locate cereals and start digging) was recorded using a chronometer. The test was carried out during a 15-min period. As soon as food was uncovered, hamsters were removed from the cage. One minute later, hamsters performed the same test but with visible chocolate cereals, positioned upon the bedding. The tests were realized in isolators in a Biosafety level-3 facility that were specially equipped for that.

At 4 dpi, animals were euthanized with an excess of anesthetics (ketamine and xylazine) and exsanguination (AVMA, 2020), and samples of nasal turbinates and lungs were collected and immediately frozen at −80°C. Fragments of lungs were also collected and fixed in 10% neutral buffered formalin.

RNA isolation and transcriptional analyses by quantitative PCR from golden hamsters' tissues

Frozen tissues were homogenized with TRIzol (15596026, Invitrogen) in Lysing Matrix D 2-ml tubes (116913100, MP Biomedicals) using the FastPrep-24™ system (MP Biomedicals) at the speed of 6.5 m/s during 1 min. Total RNA was extracted using the Direct-zol RNA MicroPrep Kit (R2062, Zymo Research: nasal turbinates) or MiniPrep Kit (R2052, Zymo Research: lung) and reverse-transcribed to first-strand cDNA using the SuperScript™ IV VILO™ Master Mix (11766050, Invitrogen). qPCR was performed in a final volume of 10 µl per reaction in 384-well PCR plates using a thermocycler

© 2021 The Authors

(QuantStudio 6 Flex, Applied Biosystems). Briefly, 2.5 µl of cDNA (12.5 ng) was added to 7.5 µl of a master mix containing 5 µl of Power SYBR Green Mix (4367659, Applied Biosystems) and 2.5 µl of nuclease-free water with nCoV_IP2 primers (nCoV_IP2-12669Fw: 5′-ATGAGCTTAGTCCTGTTG-3′; nCoV_IP2-12759Rv: 5′-CTCCCTTTGT TGTGTTGT-3′) at a final concentration of 1 µM (WHO, 2020). The amplification conditions were as follows: 95°C for 10 min, 45 cycles of 95°C for 15 s and 60°C for 1 min; followed by a melt curve, from 60 to 95°C. Viral load quantification of hamster tissues was assessed by linear regression using a standard curve of eight known quantities of plasmids containing the *RdRp* sequence (ranging from 10^7 to 10^0 copies). The threshold of detection was established as 200 viral copies/µg of RNA. The Golden hamster gene targets were selected for quantifying host inflammatory mediator transcripts in the tissues using the *Hprt* (hypoxanthine phosphoribosyltransferase), the *γ-actin,* and/or the actinB genes as reference (Appendix Table S1). Variations in gene expression were calculated as the *n*-fold change in expression in the tissues from the infected hamsters compared with the tissues of the uninfected ones using the $2^{-\Delta\Delta C_t}$ method (Pfaffl, 2001).

Droplet digital PCR (ddPCR)

Reverse transcription

200 ng of RNA was reverse-transcribed using iScript Advanced cDNA Synthesis kit for RT–qPCR (1702537, Bio-Rad) according to the manufacturer's specifications.

Quantitative PCR for γ-actin and Hprt reference genes

Real-time PCR was performed in a CFX96 qPCR machine (Bio-Rad). All samples were measured in duplicate. The 10 µl PCR included 0.8 ng of cDNA, 1× PowerUp PCR master mix (A25742, Applied Biosystems), and 0.5 µM of each primer (Appendix Table S1). The reactions were incubated in a 96-well optical plate at 95°C for 2 min, followed by 40 cycles of 95°C for 15 s and 60°C for 1 min.

Droplet digital PCR

ddPCRs were performed on the QX200 Droplet Digital PCR system according to the manufacturer's instructions (Bio-Rad). Briefly, reaction mixture consisted in 10 µl ddPCR Supermix for probe no dUTP (1863023, Bio-Rad), 0.25-1 ng of cDNA, primers and probes for E/IP4 and N/nsp13 duplex reactions used at concentration listed in Appendix Table S2 in a final volume of 20 µl. PCR amplification was conducted in a iCycler PCR instrument (Bio-Rad) with the following condition: 95°C for 10 min, 40 cycles of 94°C for 30 s with a ramping of 2°/s, 59°C for 1 min with a ramping of 2°/s, followed by 98°C for 5 min with a ramping of 2°/s and a hold at 4°C. After amplification, the 96-well plate was loaded onto the QX200 droplet reader (Bio-Rad) that measures automatically the fluorescence intensity in individual droplets. Generated data were subsequently analyzed with QuantaSoft™ software (Bio-Rad) based on positive and negative droplet populations. Data are expressed as CPD (copy per droplets) normalized to *γ-actin* and *Hprt* reference gene relative expression.

Viral titration in golden hamsters' lung

Frozen lung fragments were weighted and homogenized with 1 ml of ice-cold DMEM supplemented with 1% penicillin/streptomycin (15140148, Thermo Fisher) in Lysing Matrix M 2-ml tubes (116923050-CF, MP Biomedicals) using the FastPrep-24™ system (MP Biomedicals) and the following scheme: homogenization at 4.0 m/s during 20 s, incubation at 4°C during 2 min, and new homogenization at 4.0 m/s during 20 s. The tubes were centrifuged at 10,000 *g* during 1 min at 4°C, and the supernatants were titrated on Vero-E6 cells by classical plaque assays using semisolid overlays (Avicel, RC581-NFDR080I, DuPont) (Baer & Kehn-Hall, 2014).

Transcriptomics analysis in golden hamsters' lung

RNA preparation was used to construct strand-specific single-end cDNA libraries according to the manufacturers' instructions (TruSeq Stranded mRNA sample prep kit, Illumina). Illumina NextSeq 500 sequencer was used to sequence libraries. The RNA-seq analysis was performed with the Sequana framework (Cokelaer *et al*, 2017). We used the RNA-seq pipeline (v0.9.16), which is available online (https://github.com/sequana/sequana_rnaseq). It is built on top of Snakemake 5.8.1 (Köster & Rahmann, 2012). Reads were trimmed from adapters using Cutadapt 2.10 (Martin, 2011) and then mapped to the golden hamster MesAur1.0 genome assembly from Ensembl using STAR 2.7.3a (Dobin *et al*, 2012). FeatureCounts 2.0.0 (Liao *et al*, 2014) was used to produce the count matrix, assigning reads to features using annotation MesAur1.0.100 with strand-specificity information. Quality control statistics were summarized using MultiQC 1.8 (Ewels *et al*, 2016). Statistical analysis on the count matrix was performed to identify differentially regulated genes, comparing infected versus non-infected samples considering all samples and separating by sex. Clustering of transcriptomic profiles was assessed using a principal component analysis (PCA). Differential expression testing was conducted using DESeq2 library 1.24.0 (Love *et al*, 2014) scripts based on SARTools 1.7.0 (Varet *et al*, 2016) indicating the significance (Benjamini–Hochberg-adjusted *P*-values, false discovery rate FDR < 0.05) and the effect size (fold change) for each comparison. Finally, enrichment analysis was performed using modules from Sequana, first by converting golden hamster ensembl ids to gene names and then using human annotations for GO terms and KEGG pathways. The GO enrichment module uses PantherDB (Mi *et al*, 2019) and QuickGO (Huntley *et al*, 2014) services; the KEGG pathways enrichment uses gseapy (https://github.com/zqfang/GSEApy/), EnrichR (Chen *et al*, 2013), KEGG (Kanehisa & Goto, 2000), and BioMart services. All programmatic accesses to the online web services were performed via BioServices (Cokelaer *et al*, 2013).

Histopathology

Lung fragments fixed in 10% neutral buffered formalin were embedded in paraffin. Four-µm-thick sections were cut and stained with hematoxylin and eosin staining. The slides were then scanned using Axioscan Z1 Zeiss slide scanner, using the Zen 2 blue edition software.

Immunofluorescence

Lung fragments fixed in 10% neutral buffered formalin were washed in PBS and then embedded in O.C.T compound (4583, Tissue-Tek), frozen on dry ice, and cryostat-sectioned into 20-µm-thick sections. Sections were rinsed in PBS, and epitope retrieval was performed by

 © 2021 The Authors

incubating sections for 20min in citrate buffer pH 6.0 (C-9999, Sigma-Aldrich) at 96°C for 20 min. Sections were then blocked in PBS supplemented with 10% goat serum, 4% fetal calf serum, and 0.4% Triton X-100 for 2 h at room temperature, followed by overnight incubation at 4°C with primary antibodies: rat anti-Ly6G (1/100, 551459, BD-Biosciences), chicken anti-Iba1 (1/500, 234006, Synaptic Systems), rabbit anti-Arg1 (1/250, PA5-29645, Invitrogen), and rabbit anti-SARS-CoV nucleoprotein (1/500, provided by Dr Nicolas Escriou, Institut Pasteur, Paris). After rinsing, slides were incubated with the appropriate secondary antibodies (1/500: goat anti-rat Alexa Fluor 546, A11081, Invitrogen; goat anti-rabbit Alexa Fluor 488, A11034, Invitrogen; goat anti-chicken Alexa Fluor 647, A32933, Invitrogen) for 2 h at room temperature. All sections were then counterstained with Hoechst (H3570, Invitrogen), rinsed thoroughly in PBS, and mounted in Fluoromount-G (15586276, Invitrogen) before observation with a Zeiss LM 710 inverted confocal microscope through a Plan Apochromat 20x/0.8 Ph2 M27 lens. Cell quantification was performed in an automated manner using ImageJ. Single-channel images were extracted, thresholded, and converted to binary images. Cells were then counted using the *Particles Analyzer* ImageJ plug-in.

Statistics

Statistical analysis was performed using Prism software (GraphPad, version 9.0.0, San Diego, USA), with $P < 0.05$ considered significant. Quantitative data were compared across groups using log-rank test or two-tailed Mann–Whitney test. Randomization and blinding were not possible due to pre-defined housing conditions (separated isolators between infected and non-infected animals). *Ex vivo* analysis was blinded (coded samples). All animals were included, and data were provided from 2 replications, except food finding in males, that were replicated 3 times.

Data availability

The datasets produced in this study are available in the following databases: RNA-seq: ArrayExpress E-MTAB-10128 (https://www.ebi.ac.uk/arrayexpress/experiments/E-MTAB-10128/).

Expanded View for this article is available online.

Acknowledgements
The SARS-CoV-2 strain was supplied by the National Reference Centre for Respiratory Viruses hosted by Institut Pasteur (Paris, France) and headed by Dr. Sylvie van der Werf. The human sample from which strain 2019-nCoV/IDF0372/2020 was isolated has been provided by Dr. X. Lescure and Pr. Y. Yazdanpanah from the Bichat Hospital (Paris, France). This work was supported by Institut Pasteur TASK FORCE SARS COV2 (NicoSARS, NeuroCovid, and Cov-DROP projects) and received help from the European Union's Horizon 2020 Framework Programme for Research and Innovation under Specific Grant Agreement No. 945539 (Human Brain Project SGA3). We thank Elodie Turc and Laure Lemée, Biomics Platform, C2RT, Institut Pasteur, Paris, France, supported by France Génomique (ANR-10-INBS-09-09), IBISA and the Illumina COVID-19 Projects' offer. We would like to thank Marion Berard, Laetitia Breton, Rachid Chennouf, Hamidou Diakhate, and Eddie Maranghi for their help in implementing experiments in the Institut Pasteur animal facilities and Nicolas Escriou Innovation laboratory: Vaccines, Institut Pasteur, Paris, for providing the anti-SARS-CoV-2 nucleoprotein antibody. We thank Magali Tichit and Johan Bedel for the help with histopathology. We thank Gerard Orth, Arnaud Tarantola, and Andrew Holtz for critical reading of the manuscript. The synopsis illustration was created with BioRender.com.

The paper explained

Problem
The current pandemic of COVID-19 has caused more than 3.5 million deaths and more than 150 million laboratory-confirmed cases worldwide since December 2019 (as of May 2021). COVID-19, caused by SARS-CoV-2, commonly brings about upper airways and pulmonary symptoms and in severe cases can lead to respiratory distress and death. Different therapeutic approaches have been proposed to fight this disease but comprehensive therapeutic studies are still lacking.

Results
We report that ivermectin, used at the standard anti-parasitic dose of 400 µg/kg, protects infected hamsters from developing clinical signs and from losing the sense of smell during SARS-CoV-2 infection. The treated animals exhibited a specific inflammatory response, presenting a reduced type I/III interferon stimulation and a modulation in several intracellular signaling pathways, with an important reduction of the *Il-6/Il-10* ratio and promoting M2 polarization of myeloid cells recruited to the lung. These effects are strongly influenced by sex, with treated females exhibiting the best outcome. Surprisingly, ivermectin treatment did not limit viral replication, as treated and non-treated animals presented similar amounts of SARS-CoV-2 in the nasal cavity and in the lungs.

Impact
The results of this study establish that irrespective of viral load, the symptoms and severity of COVID-19 highlight the critical role played by host inflammatory response in COVID-19 severity and highlight that reduced type I/III interferon and *Il-6/Il-10* and the presence of M2 macrophages might account for a more favorable clinical presentation, contributing to a better understanding of COVID-19 pathophysiology. Ivermectin might then be considered as promising therapeutic agent against COVID-19 with no impact on SARS-CoV-2 replication but alleviating inflammation and ensuing symptoms.

Author contributions
JPC and HB conceived the experimental hypothesis. GDM, FLaz, FLar, and HB designed the experiments. GDM, FLaz, FLar, LF, LK, SL, AM, and DH performed the experiments. GDM, FLaz, FLar, LF, EK, SL, AM, TC, PP, ML, and P-ML analyzed the data. GDM, J-PC, and HB wrote the manuscript, and all authors edited it.

Conflict of interests
The authors declare that they have no conflict of interest.

For more information
- COVID-19 section of the WHO website: https://covid19.who.int/
- COVID-19 section of the Institut Pasteur website: https://www.pasteur.fr/en/news-covid-19

References

Aamir K, Khan HU, Sethi G, Hossain MA, Arya A (2020) Wnt signaling mediates TLR pathway and promote unrestrained adipogenesis and

© 2021 The Authors

metaflammation: therapeutic targets for obesity and type 2 diabetes. *Pharmacol Res* 152: 104602

Arévalo AP, Pagotto R, Pórfido JI, Daghero H, Segovia M, Yamasaki K, Varela B, Hill M, Verdes JM, Duhalde Vega M *et al* (2021) Ivermectin reduces *in vivo* coronavirus infection in a mouse experimental model. *Sci Rep* 11: 7132

AVMA (2020) *AVMA guidelines for the euthanasia of animals: 2020 edition**. Schaumburg, IL: American Veterinary Medical Association

Baer A, Kehn-Hall K (2014) Viral concentration determination through plaque assays: using traditional and novel overlay systems. *J Vis Exp* e52065

Bastard P, Rosen LB, Zhang Q, Michailidis E, Hoffmann HH, Zhang Y, Dorgham K, Philippot Q, Rosain J, Béziat V *et al* (2020) Autoantibodies against type I IFNs in patients with life-threatening COVID-19. *Science* 370: eabd4585

Batalha PN, Forezi LSM, Lima CGS, Pauli FP, Boechat FCS, de Souza MCBV, Cunha AC, Ferreira VF, da Silva FdC (2021) Drug repurposing for the treatment of COVID-19: Pharmacological aspects and synthetic approaches. *Bioorg Chem* 106: 104488

Beco L, Petite A, Olivry T (2001) Comparison of subcutaneous ivermectin and oral moxidectin for the treatment of notoedric acariasis in hamsters. *Veterinary Record* 149: 324–327

Bernigaud C, Guillemot D, Ahmed-Belkacem A, Grimaldi-Bensouda L, Lespine A, Berry F, Softic L, Chenost C, Do-Pham G, Giraudeau B *et al* (2021) Oral ivermectin for a scabies outbreak in a long-term–care facility: potential value in preventing COVID-19 and associated mortality? *Br J Dermatol* 184: 1207–1209

Bhaskar S, Sinha A, Banach M, Mittoo S, Weissert R, Kass JS, Rajagopal S, Pai AR, Kutty S (2020) Cytokine storm in COVID-19—immunopathological mechanisms. Clinical considerations, and therapeutic approaches: the REPROGRAM consortium position paper. *Front Immunol* 11: 1648

Boudewijns R, Thibaut HJ, Kaptein SJF, Li R, Vergote V, Seldeslachts L, Van Weyenbergh J, De Keyzer C, Bervoets L, Sharma S *et al* (2020) STAT2 signaling restricts viral dissemination but drives severe pneumonia in SARS-CoV-2 infected hamsters. *Nat Commun* 11: 5838

Bray M, Rayner C, Noël F, Jans D, Wagstaff K (2020) Ivermectin and COVID-19: a report in antiviral research, widespread interest, an FDA warning, two letters to the editor and the authors' responses. *Antiviral Res* 178: 104805

Calabrese EJ, Kozumbo WJ, Kapoor R, Dhawan G, Jimenez PCL, Giordano J (2021) NRF2 activation putatively mediates clinical benefits of low-dose radiotherapy in COVID-19 pneumonia and acute respiratory distress syndrome (ards): novel mechanistic considerations. *Radiother Oncol* 160: 125–131

Caly L, Druce JD, Catton MG, Jans DA, Wagstaff KM (2020) The FDA-approved drug ivermectin inhibits the replication of SARS-CoV-2 *in vitro*. *Antiviral Res* 178: 104787

Camprubí D, Almuedo-Riera A, Martí-Soler H, Soriano A, Hurtado JC, Subirà C, Grau-Pujol B, Krolewiecki A, Muñoz J (2020) Lack of efficacy of standard doses of ivermectin in severe COVID-19 patients. *PLoS One* 15: e0242184

Cerdan AH, Sisquellas M, Pereira G, Barreto Gomes DE, Changeux JP, Cecchini M (2020) The glycine receptor allosteric ligands library (GRALL). *Bioinformatics* 36: 3379–3384

Cereda D, Tirani M, Rovida F, Demicheli V, Ajelli M, Poletti P, Trentini F, Guzzetta G, Marziano V, Barone A *et al* (2020) The early phase of the COVID-19 outbreak in Lombardy, Italy. *arXiv* https://arxiv.org/abs/2003.09320 [PREPRINT]

Chaccour C, Hammann F, Ramón-García S, Rabinovich NR (2020) Ivermectin and COVID-19: keeping rigor in times of urgency. *Am J Trop Med Hyg* 102: 1156–1157

Chaccour C, Casellas A, Blanco-Di Matteo A, Pineda I, Fernandez-Montero A, Ruiz-Castillo P, Richardson M-A, Rodríguez-Mateos M, Jordán-Iborra C, Brew J *et al* (2021) The effect of early treatment with ivermectin on viral load, symptoms and humoral response in patients with non-severe COVID-19: a pilot, double-blind, placebo-controlled, randomized clinical trial. *EClinicalMedicine* 32: 100720

Chan JF, Zhang AJ, Yuan S, Poon VK, Chan CC, Lee AC, Chan WM, Fan Z, Tsoi HW, Wen L *et al* (2020) Simulation of the clinical and pathological manifestations of Coronavirus Disease 2019 (COVID-19) in golden Syrian hamster model: implications for disease pathogenesis and transmissibility. *Clin Infect Dis* 9: 2428–2446

Changeux J-P, Amoura Z, Rey FA, Miyara M (2020) A nicotinic hypothesis for Covid-19 with preventive and therapeutic implications. *CR Biol* 343: 33–39

Chen EY, Tan CM, Kou Y, Duan Q, Wang Z, Meirelles GV, Clark NR, Ma'ayan A (2013) Enrichr: interactive and collaborative HTML5 gene list enrichment analysis tool. *BMC Bioinformatics* 14: 128

Chen W, Pan JY (2021) Anatomical and pathological observation and analysis of SARS and COVID-19: microthrombosis is the main cause of death. *Biol Proced Online* 23: 4

Cokelaer T, Pultz D, Harder LM, Serra-Musach J, Saez-Rodriguez J (2013) BioServices: a common Python package to access biological Web Services programmatically. *Bioinformatics* 29: 3241–3242

Cokelaer T, Desvillechabrol D, Legendre R, Cardon M (2017) Sequana': a set of snakemake NGS pipelines. *J Open Source Softw* 2: 352

Cross SJ, Linker KE, Leslie FM (2017) Sex-dependent effects of nicotine on the developing brain. *J Neurosci Res* 95: 422–436

De Virgiliis F, Di Giovanni S (2020) Lung innervation in the eye of a cytokine storm: neuroimmune interactions and COVID-19. *Nat Rev Neurol* 16: 645–652

Dey A, Sen S, Maulik U (2020) Unveiling COVID-19-associated organ-specific cell types and cell-specific pathway cascade. *Brief Bioinform* 22: 914–923

Dobin A, Davis CA, Schlesinger F, Drenkow J, Zaleski C, Jha S, Batut P, Chaisson M, Gingeras TR (2012) STAR: ultrafast universal RNA-seq aligner. *Bioinformatics* 29: 15–21

Ewels P, Magnusson M, Lundin S, Käller M (2016) MultiQC: summarize analysis results for multiple tools and samples in a single report. *Bioinformatics* 32: 3047–3048

Gahring LC, Myers EJ, Dunn DM, Weiss RB, Rogers SW (2017) Nicotinic alpha 7 receptor expression and modulation of the lung epithelial response to lipopolysaccharide. *PLoS One* 12: e0175367

Galani IE, Triantafyllia V, Eleminiadou E-E, Koltsida O, Stavropoulos A, Manioudaki M, Thanos D, Doyle SE, Kotenko SV, Thanopoulou K *et al* (2017) Interferon-λ mediates non-redundant front-line antiviral protection against influenza virus infection without compromising host fitness. *Immunity* 46: 875–890.e6

Gianchandani R, Esfandiari NH, Ang L, Iyengar J, Knotts S, Choksi P, Pop-Busui R (2020) Managing hyperglycemia in the COVID-19 inflammatory storm. *Diabetes* 69: 2048–2053

Guzzo CA, Furtek CI, Porras AG, Chen C, Tipping R, Clineschmidt CM, Sciberras DG, Hsieh JY, Lasseter KC (2002) Safety, tolerability, and pharmacokinetics of escalating high doses of ivermectin in healthy adult subjects. *J Clin Pharmacol* 42: 1122–1133

Han AY, Mukdad L, Long JL, Lopez IA (2020) Anosmia in COVID-19: mechanisms and significance. *Chem Senses* 45: 423–428

Hanafi HA, Szumlas DE, Fryauff DJ, El-Hossary SS, Singer GA, Osman SG, Watany N, Furman BD, Hoel DF (2011) Effects of ivermectin on blood-feeding *Phlebotomus papatasi*, and the promastigote stage of *Leishmania major*. *Vector Borne Zoonotic Dis (Larchmont, NY)* 11: 43–52

 © 2021 The Authors

Hasanoglu I, Korukluoglu G, Asilturk D, Cosgun Y, Kalem AK, Altas AB, Kayaaslan B, Eser F, Kuzucu EA, Guner R (2021) Higher viral loads in asymptomatic COVID-19 patients might be the invisible part of the iceberg. *Infection* 49: 117 – 126

Heidary F, Gharebaghi R (2020) Ivermectin: a systematic review from antiviral effects to COVID-19 complementary regimen. *J Antibiot* 73: 593 – 602

Hibbs RE, Gouaux E (2011) Principles of activation and permeation in an anion-selective Cys-loop receptor. *Nature* 474: 54 – 60

Hill A, Abdulamir A, Ahmed S, Asghar A, Babalola OE, Basri R, Chaccour C, Chachar AZK, Chowdhury ATM, Elgazzar A *et al* (2021) Meta-analysis of randomized trials of ivermectin to treat SARS-CoV-2 infection. *Res Squ* https://doi.org/10.21203/rs.3.rs-148845/v1 [PREPRINT]

Hoagland DA, Møller R, Uhl SA, Oishi K, Frere J, Golynker I, Horiuchi S, Panis M, Blanco-Melo D, Sachs D *et al* (2020) Leveraging the antiviral type-I interferon system as a first line defense against SARS-CoV-2 pathogenicity. *Immunity* 54: 557 – 570

Horby P, Lim WS, Emberson JR, Mafham M, Bell JL, Linsell L, Staplin N, Brightling C, Ustianowski A, Elmahi E *et al* (2020) Dexamethasone in hospitalized patients with Covid-19 - preliminary report. *N Engl J Med* 384: 693 – 704

Hu X, Cai X, Song X, Li C, Zhao J, Luo W, Zhang Q, Ekumi IO, He Z (2020) Possible SARS-coronavirus 2 inhibitor revealed by simulated molecular docking to viral main protease and host toll-like receptor. *Future Virol* 15: 359 – 368

Huntley RP, Sawford T, Mutowo-Meullenet P, Shypitsyna A, Bonilla C, Martin MJ, O'Donovan C (2014) The GOA database: gene ontology annotation updates for 2015. *Nucleic Acids Res* 43: D1057 – D1063

Isidori AM, Giannetta E, Pofi R, Venneri MA, Gianfrilli D, Campolo F, Mastroianni CM, Lenzi A, d'Ettorre G (2021) Targeting the NO-cGMP-PDE5 pathway in COVID-19 infection. The DEDALO project. *Andrology* 9: 33 – 38

Islam T, Rahman MR, Aydin B, Beklen H, Arga KY, Shahjaman M (2020) Integrative transcriptomics analysis of lung epithelial cells and identification of repurposable drug candidates for COVID-19. *Eur J Pharmacol* 887: 173594

Jermain B, Hanafin PO, Cao Y, Lifschitz A, Lanusse C, Rao GG (2020) Development of a minimal physiologically-based pharmacokinetic model to simulate lung exposure in humans following oral administration of ivermectin for COVID-19 drug repurposing. *J Pharm Sci* 109: 3574 – 3578

Jin J-M, Bai P, He W, Wu F, Liu X-F, Han D-M, Liu S, Yang J-K (2020) Gender differences in patients with COVID-19: focus on severity and mortality. *Frontiers in Public Health* 8: 152

Kanehisa M, Goto S (2000) KEGG: kyoto encyclopedia of genes and genomes. *Nucleic Acids Res* 28: 27 – 30

Kaur H, Shekhar N, Sharma S, Sarma P, Prakash A, Medhi B (2021) Ivermectin as a potential drug for treatment of COVID-19: an in-sync review with clinical and computational attributes. *Pharmacol Rep* 73: 736 – 749

Klinkhammer J, Schnepf D, Ye L, Schwaderlapp M, Gad HH, Hartmann R, Garcin D, Mahlakõiv T, Staeheli P (2018) IFN-λ prevents influenza virus spread from the upper airways to the lungs and limits virus transmission. *eLife* 7: e33354

Kory P, Meduri GU, Varon J, Iglesias J, Marik PE (2021) Review of the emerging evidence demonstrating the efficacy of ivermectin in the prophylaxis and treatment of COVID-19. *Am J Ther* 28: e299 – e318

Köster J, Rahmann S (2012) Snakemake—a scalable bioinformatics workflow engine. *Bioinformatics* 28: 2520 – 2522

Krause RM, Buisson B, Bertrand S, Corringer PJ, Galzi JL, Changeux JP, Bertrand D (1998) Ivermectin: a positive allosteric effector of the alpha7 neuronal nicotinic acetylcholine receptor. *Mol Pharmacol* 53: 283 – 294

Laing R, Gillan V, Devaney E (2017) Ivermectin – old drug, new tricks? *Trends Parasitol* 33: 463 – 472

Lazarini F, Gabellec M-M, Torquet N, Lledo P-M (2012) Early activation of microglia triggers long-lasting impairment of adult neurogenesis in the olfactory bulb. *The Journal of Neuroscience* 32: 3652 – 3664

Li N, Zhao L, Zhan X (2021) Quantitative proteomics reveals a broad-spectrum antiviral property of ivermectin, benefiting for COVID-19 treatment. *J Cell Physiol* 236: 2959 – 2975

Liao Y, Smyth GK, Shi W (2014) featureCounts: an efficient general purpose program for assigning sequence reads to genomic features. *Bioinformatics* 30: 923 – 930

Lifschitz A, Virkel G, Sallovitz J, Sutra JF, Galtier P, Alvinerie M, Lanusse C (2000) Comparative distribution of ivermectin and doramectin to parasite location tissues in cattle. *Vet Parasitol* 87: 327 – 338

Love MI, Huber W, Anders S (2014) Moderated estimation of fold change and dispersion for RNA-seq data with DESeq2. *Genome Biol* 15: 550

Martin M (2011) Cutadapt removes adapter sequences from high-throughput sequencing reads. *EMBnet J* 17: 10

Masood KI, Mahmood SF, Shahid S, Nasir N, Ghanchi N, Nasir A, Jamil B, Khanum I, Razzak S, Kanji A *et al* (2020) Transcriptomic profiling of disease severity in patients with COVID-19 reveals role of blood clotting and vasculature related genes. *medRxiv* https://doi.org/10.1101/2020.06.18.20132571 [PREPRINT]

McElvaney OJ, Hobbs BD, Qiao D, McElvaney OF, Moll M, McEvoy NL, Clarke J, O'Connor E, Walsh S, Cho MH *et al* (2020a) A linear prognostic score based on the ratio of interleukin-6 to interleukin-10 predicts outcomes in COVID-19. *EBioMedicine* 61: 103026

McElvaney OJ, McEvoy NL, McElvaney OF, Carroll TP, Murphy MP, Dunlea DM, Ní Choileáin O, Clarke J, O'Connor E, Hogan G *et al* (2020b) Characterization of the inflammatory response to severe COVID-19 illness. *Am J Respir Crit Care Med* 202: 812 – 821

de Melo GD, Lazarini F, Levallois S, Hautefort C, Michel V, Larrous F, Verillaud B, Aparicio C, Wagner S, Gheusi G *et al* (2021) COVID-19-related anosmia is associated with viral persistence and inflammation in human olfactory epithelium and brain infection in hamsters. *Sci Transl Med* 13: eabf8396

Melotti A, Mas C, Kuciak M, Lorente-Trigos A, Borges I, Ruiz i Altaba A (2014) The river blindness drug Ivermectin and related macrocyclic lactones inhibit WNT-TCF pathway responses in human cancer. *EMBO Mol Med* 6: 1263 – 1278

Mi H, Muruganujan A, Ebert D, Huang X, Thomas PD (2019) PANTHER version 14: more genomes, a new PANTHER GO-slim and improvements in enrichment analysis tools. *Nucleic Acids Res* 47: D419 – D426

Muñoz-Fontela C, Dowling WE, Funnell SGP, Gsell P-S, Riveros-Balta AX, Albrecht RA, Andersen H, Baric RS, Carroll MW, Cavaleri M *et al* (2020) Animal models for COVID-19. *Nature* 586: 509 – 515

Oczypok EA, Perkins TN, Oury TD (2017) All the "RAGE" in lung disease: The receptor for advanced glycation endproducts (RAGE) is a major mediator of pulmonary inflammatory responses. *Paediatr Respir Rev* 23: 40 – 49

Okabayashi T, Kojima T, Masaki T, Yokota S-I, Imaizumi T, Tsutsumi H, Himi T, Fujii N, Sawada N (2011) Type-III interferon, not type-I, is the predominant interferon induced by respiratory viruses in nasal epithelial cells. *Virus Res* 160: 360 – 366

Oliviero A, de Castro F, Coperchini F, Chiovato L, Rotondi M (2020) COVID-19 pulmonary and olfactory dysfunctions: is the chemokine CXCL10 the common denominator? *The Neuroscientist* 27: 214 – 221

Pavlov VA, Tracey KJ (2012) The vagus nerve and the inflammatory reflex—linking immunity and metabolism. *Nat Rev Endocrinol* 8: 743 – 754

© 2021 The Authors

Pei J, Xiao Z, Guo Z, Pei Y, Wei S, Wu H, Wang D (2020) Sustained stimulation of β(2)AR inhibits insulin signaling in H9C2 cardiomyoblast cells through the PKA-dependent signaling pathway. *Diabetes Metab Syndr Obes* 13: 3887–3898

Pfaffl MW (2001) A new mathematical model for relative quantification in real-time RT-PCR. *Nucleic Acids Res* 29: e45

Potus F, Mai V, Lebret M, Malenfant S, Breton-Gagnon E, Lajoie AC, Boucherat O, Bonnet S, Provencher S (2020) Novel insights on the pulmonary vascular consequences of COVID-19. *Am J Physiol Lung Cell Mol Physiol* 319: L277–L288

Qiu C, Cui C, Hautefort C, Haehner A, Zhao J, Yao Qi, Zeng H, Nisenbaum EJ, Liu Li, Zhao Yu *et al* (2020) Olfactory and gustatory dysfunction as an early identifier of COVID-19 in adults and children: an international multicenter study. *Otolaryngol Head Neck Surg* 163: 714–721

Rajter JC, Sherman MS, Fatteh N, Vogel F, Sacks J, Rajter J-J (2020) Use of ivermectin is associated with lower mortality in hospitalized patients with COVID-19 (ICON study). *Chest* 159: 85–92

Raker VK, Becker C, Steinbrink K (2016) The cAMP pathway as therapeutic target in autoimmune and inflammatory diseases. *Front Immunol* 7: 123

Raslan AA, Yoon JK (2020) WNT signaling in lung repair and regeneration. *Mol Cells* 43: 774–783

Rossotti R, Travi G, Ughi N, Corradin M, Baiguera C, Fumagalli R, Bottiroli M, Mondino M, Merli M, Bellone A *et al* (2020) Safety and efficacy of anti-il6-receptor tocilizumab use in severe and critical patients affected by coronavirus disease 2019: A comparative analysis. *J Infect* 81: e11–e17

Said SI (1999) Glutamate receptors and asthmatic airway disease. *Trends Pharmacol Sci* 20: 132–135

Sajid MS, Iqbal Z, Muhammad G, Iqbal MU (2006) Immunomodulatory effect of various anti-parasitics: a review. *Parasitology* 132: 301–313

Samuel RM, Majd H, Richter MN, Ghazizadeh Z, Zekavat SM, Navickas A, Ramirez JT, Asgharian H, Simoneau CR, Bonser LR *et al* (2020) Androgen signaling regulates SARS-CoV-2 receptor levels and is associated with severe COVID-19 symptoms in men. *Cell Stem Cell* 27: 876–889.e12

Sang Y, Miller LC, Blecha F (2015) Macrophage polarization in virus-host interactions. *J Clin Cell Immunol* 6: 311

Scully EP, Haverfield J, Ursin RL, Tannenbaum C, Klein SL (2020) Considering how biological sex impacts immune responses and COVID-19 outcomes. *Nat Rev Immunol* 20: 442–447

Sia SF, Yan L-M, Chin AWH, Fung K, Choy K-T, Wong AYL, Kaewpreedee P, Perera RAPM, Poon LLM, Nicholls JM *et al* (2020) Pathogenesis and transmission of SARS-CoV-2 in golden hamsters. *Nature* 583: 834–838

Stanifer ML, Guo C, Doldan P, Boulant S (2020) Importance of type I and III interferons at respiratory and intestinal barrier surfaces. *Front Immunol* 11: 608645

vom Steeg LG, Klein SL (2019) Sex and sex steroids impact influenza pathogenesis across the life course. *Semin Immunopathol* 41: 189–194

Sun J, Zhuang Z, Zheng J, Li K, Wong R-Y, Liu D, Huang J, He J, Zhu A, Zhao J *et al* (2020) Generation of a broadly useful model for COVID-19 pathogenesis, vaccination, and treatment. *Cell* 182: 734–743.e5

Suo T, Liu X, Feng J, Guo M, Hu W, Guo D, Ullah H, Yang Y, Zhang Q, Wang X *et al* (2020) ddPCR: a more accurate tool for SARS-CoV-2 detection in low viral load specimens. *Emerg Microbes Infect* 9: 1259–1268

Takahashi T, Ellingson MK, Wong P, Israelow B, Lucas C, Klein J, Silva J, Mao T, Oh JE, Tokuyama M *et al* (2020) Sex differences in immune responses that underlie COVID-19 disease outcomes. *Nature* 588: 315–320

Tizabi Y, Getachew B, Copeland RL, Aschner M (2020) Nicotine and the nicotinic cholinergic system in COVID-19. *FEBS J* 287: 3656–3663

Vaduganathan M, Vardeny O, Michel T, McMurray JJV, Pfeffer MA, Solomon SD (2020) Renin–angiotensin–aldosterone system inhibitors in patients with covid-19. *N Engl J Med* 382: 1653–1659

Van Den Eynden J, SahebAli S, Horwood N, Carmans S, Brône B, Hellings N, Steels P, Harvey R, Rigo J-M (2009) Glycine and glycine receptor signalling in non-neuronal cells. *Front Mol Neurosci* 2: 9

Varet H, Brillet-Guéguen L, Coppée JY, Dillies MA (2016) SARTools: A DESeq2- and EdgeR-based R pipeline for comprehensive differential analysis of RNA-Seq data. *PLoS One* 11: e0157022

WHO (2020) *Protocol: real-time RT-PCR assays for the detection of SARS-CoV-2*, Paris: Institut Pasteur. https://www.who.int/docs/default-source/coronaviruse/real-time-rt-pcr-assays-for-the-detection-of-sars-cov-2-institut-pasteur-paris.pdf?sfvrsn=3662fcb6_2

Xydakis MS, Dehgani-Mobaraki P, Holbrook EH, Geisthoff UW, Bauer C, Hautefort C, Herman P, Manley GT, Lyon DM, Hopkins C (2020) Smell and taste dysfunction in patients with COVID-19. *Lancet Infect Dis* 20: 1015–1016

Zemkova H, Tvrdonova V, Bhattacharya A, Jindrichova M (2014) Allosteric modulation of ligand gated ion channels by ivermectin. *Physiol Res* 63 (Suppl 1): S215–S224

Zhang Q, Bastard P, Liu Z, Le Pen J, Moncada-Velez M, Chen J, Ogishi M, Sabli IKD, Hodeib S, Korol C *et al* (2020a) Inborn errors of type I IFN immunity in patients with life-threatening COVID-19. *Science* 370: eabd4570

Zhang SI, Liu Y, Wang X, Yang LI, Li H, Wang Y, Liu M, Zhao X, Xie Y, Yang Y *et al* (2020b) SARS-CoV-2 binds platelet ACE2 to enhance thrombosis in COVID-19. *J Hematol Oncol* 13: 120

Zhao X, Yu Z, Lv Z, Meng L, Xu J, Yuan S, Fu Z (2019) Activation of alpha-7 nicotinic acetylcholine receptors (α7nAchR) promotes the protective autophagy in LPS-induced acute lung injury (ALI) *in vitro* and *in vivo*. *Inflammation* 42: 2236–2245

Zhe Z, Hongyuan B, Wenjuan Q, Peng W, Xiaowei L, Yan G (2018) Blockade of glutamate receptor ameliorates lipopolysaccharide-induced sepsis through regulation of neuropeptides. *Biosci Rep* 38: BSR20171629

License: This is an open access article under the terms of the Creative Commons Attribution License, which permits use, distribution and reproduction in any medium, provided the original work is properly cited.

4.4. RABomics (Article #6)

This article is currently in review in the *Frontiers in Microbiology* journal as:

Kim S, Larrous F, Varet H, Legendre H, **Feige L**, Dumas G, Matsas R, Kouroupi G, Grailhe R, Bourhy H. **Early transcriptional changes in rabies virus-infected human neurons and extended effect on neuronal function**. Frontiers in Microbiology, 2021

frontiers

Early transcriptional changes in rabies virus-infected human neurons and extended effect on neuronal function

Seonhee Kim[1, 2, 3], Florence Larrous[1], Hugo Varet[1], Rachel Legendre[1], Lena Feige[1, 2], Guillaume Dumas[4], Rebecca Matsas[5], GEORGIA KOUROUPI[5], Regis Grailhe[3], Hervé Bourhy[1*]

[1]Institut Pasteur, France, [2]Université de Paris, France, [3]Korea Pasteur Institute, South Korea, [4]Université de Montréal, Canada, [5]Pasteur Hellenic Institute, Greece

Submitted to Journal:
Frontiers in Microbiology

Specialty Section:
Virology

Article type:
Original Research Article

Manuscript ID:
730892

Received on:
25 Jun 2021

Journal website link:
www.frontiersin.org

In review

frontiers

Conflict of interest statement

The authors declare that the research was conducted in the absence of any commercial or financial relationships that could be construed as a potential conflict of interest

Author contribution statement

SK, FL, RG and HB contributed to the design of the study. HV, RL and GD established analysis pipelines. SK, FL and LF performed experiments. SK, FL, HV and RL analyzed data. RM and GK provided materials. SK, FL and HB wrote the manuscript. All authors contributed to the revision of the manuscript and approved the submitted version.

Keywords

Rabies virus, Transcriptome, Early post-infection, matrix protein, Neuronal dysfunction, calcium imaging

Abstract

Word count: 259

Rabies is a zoonotic disease caused by a neurotropic virus, rabies virus (RABV). Successful invasion of central nervous system by the virus only induces nonspecific symptoms at the initial stage, but as the disease progresses, patients develop an array of severe neurological symptoms that invariably lead to coma and death. Surprisingly, Post-mortem analysis of human brains suggests no significant inflammation or structural damages on neurons in spite of the dramatic clinical symptomology. As the probable cause of neurological symptoms, the nature of neuronal dysfunctions has not been explored systematically to this date. In the current study, we have characterized the transcriptomic changes in infected human neurons, at the early time-points of RABV infection. Using a street strain RABV and its mutant virus, we have found that the RABV matrix protein plays an important role in early suppression of host gene expression, especially for those involved in neuronal functions. The scale of differential gene expression was controlled by RABV up to 24hrs post-infection, and the presence of intact viral matrix protein was imperative. The signaling pathways previously studied in relation to the innate immune response and RABV were modulated in our study, and contributed to the changes in neuronal function-associated processes. We have verified a set of regulated genes that could impact neuronal functions collectively, and demonstrated in calcium imaging that indeed the spontaneous activity of neurons are influenced by RABV infection. Overall, our findings suggest that the neuronal function-associated genes are modulated by RABV from early on, potentially through the viral matrix protein-interacting signaling molecules and their downstream pathways.

Contribution to the field

Rabies encephalitis is an acute viral infection of the central nervous system. Patients in advanced stage of the disease develop severe neurological symptoms, but postmortem examinations suggest no significant inflammation or structural damages on neurons, which implies neuronal dysfunction as the potential cause of the fatal outcome. Furthermore, efforts to understand the virulence of the virus using animal models have been ineffective because of the complexity of the approach. Here in “Early transcriptional changes in Rabies virus-infected human neurons and extended effect on neuronal function,” we use stem cell-derived human neurons and two different rabies viruses to identify the underlying state of the infected neurons and discern potential mechanisms for the neuronal dysfunction. The comparative transcriptome analysis of infected neurons by pathogenic or attenuated rabies virus show differential expression profiles at early hours of infection, highlighting the role of viral matrix protein in host gene modulation associated with neuronal functions. Through this study, we also emphasize the importance of immune response-related pathways in neuronal functions, and show that host genes modulated by rabies virus infection collectively influence the spontaneous activity of neurons.

Funding statement

This work was supported by grants from Partenariat Hubert Curien (No. 41432ZB), Ministry of Science and ICT of Korea (No. 2017M3A9G6068257 and 2018K1A3A1A21041166), and internal fundings of Institut Pasteur.

In review

Ethics statements

Studies involving animal subjects
Generated Statement: No animal studies are presented in this manuscript.

Studies involving human subjects
Generated Statement: No human studies are presented in this manuscript.

Inclusion of identifiable human data
Generated Statement: No potentially identifiable human images or data is presented in this study.

In review

Data availability statement

Generated Statement: The datasets presented in this study can be found in online repositories. The names of the repository/repositories and accession number(s) can be found in the article/supplementary material.

In review

Early transcriptional changes in rabies virus-infected human neurons and extended effect on neuronal function

Seonhee Kim[1, 2, 3], Florence Larrous[2], Hugo Varet[4, 5], Rachel Legendre[4, 5], Lena Feige[1, 2, 3], Guillaume Dumas[6, 7], Georgia Kouroupi[8], Rebecca Matsas[8], Regis Grailhe[1], Hervé Bourhy[2*]

[1] Tech Development Platform, Institut Pasteur Korea, Seongnam, Republic of Korea

[2] Lyssavirus Epidemiology and Neuropathology Unit, Institut Pasteur, Paris, France

[3] Université de Paris, Doctoral School Bio Sorbonne Paris Cité, Paris, France

[4] Hub de Bioinformatique et Biostatistique, Département Biologie Computationnelle, Institut Pasteur, Paris, France

[5] Plate-forme Technologique Biomics, Centre de Ressources et Recherches Technologiques (C2RT), Institut Pasteur, Paris, France

[6] CHU Sainte-Justine Research Center, Department of Psychiatry, University of Montreal, Quebec, Canada

[7] Mila, Quebec Artificial Intelligence Institute, University of Montreal, Quebec, Canada

[8] Laboratory of Cellular and Molecular Neurobiology-Stem Cells, Department of Neurobiology, Hellenic Pasteur Institute, Athens, Greece

* **Correspondence:**
Hervé Bourhy
herve.bourhy@pasteur.fr

Keywords: rabies virus, transcriptome, early post-infection, matrix protein, neuronal dysfunction, calcium imaging

Number of words from main body: 8,059

Number of main figures: 5

In review

ABSTRACT

Rabies is a zoonotic disease caused by a neurotropic virus, rabies virus (RABV). Successful invasion of central nervous system by the virus only induces nonspecific symptoms at the initial stage, but as the disease progresses, patients develop an array of severe neurological symptoms that invariably lead to coma and death. Surprisingly, *Post-mortem* analysis of human brains suggests no significant inflammation or structural damages on neurons in spite of the dramatic clinical symptomology. As the probable cause of neurological symptoms, the nature of neuronal dysfunctions has not been explored systematically to this date. In the current study, we have characterized the transcriptomic changes in infected human neurons, at the early time-points of RABV infection. Using a street strain RABV and its mutant virus, we have found that the RABV matrix protein plays an important role in early suppression of host gene expression, especially for those involved in neuronal functions. The scale of differential gene expression was controlled by RABV up to 24hrs post-infection, and the presence of intact viral matrix protein was imperative. The signaling pathways previously studied in relation to the innate immune response and RABV were modulated in our study, and contributed to the changes in neuronal function-associated processes. We have verified a set of regulated genes that could impact neuronal functions collectively, and demonstrated in calcium imaging that indeed the spontaneous activity of neurons are influenced by RABV infection. Overall, our findings suggest that the neuronal function-associated genes are modulated by RABV from early on, potentially through the viral matrix protein-interacting signaling molecules and their downstream pathways.

In review

This is a provisional file, not the final typeset article

INTRODUCTION

Rabies is a fatal disease that occurs through the transmission of lyssavirus, mainly by one of the species called rabies virus (RABV) (Fooks et al., 2014, 2017; Hampson et al., 2015). The virus is transmitted from infected animals to humans, through broken skin caused by bites or scratches, or on rarer occasions, licking on the mucosa. RABV transmission from dog-mediated exposures is responsible for more than 98% of human rabies cases, leading to approximately 59,000 deaths every year. Rabies is hard to diagnose without a history of exposure since at the initiation stage the symptoms are very similar to that of many other illnesses (Hemachudha et al., 2013), however as the disease progresses, more specific symptoms appear which may include insomnia, anxiety, confusion, paralysis, excitation, hallucinations, agitation and difficulty in swallowing, hydrophobia and aerophobia (Jackson, 2014). The fatality rate is close to 100% once these neurological symptoms have manifested, and as to this date, there are no known cures or treatments that can effectively block the advance of RABV (Dacheux, Delmas, & Bourhy, 2011; Rogée et al., 2019).

Human rabies cases do not show prominent pathological features such as neuron degeneration, infiltration of adaptive immune cells, aggravated inflammation or apoptosis by routine histopathological analysis (Adle-Biassette et al., 1996; Davis, Rall, & Schnell, 2015; Fisher, Streicker, & Schnell, 2018; Jackson, 2014). This is due to the fact that RABV is capable of evading or delaying immune responses and cell death for the duration of replication and spread in the infected body. RABV encodes five viral proteins in its genome, Nucleoprotein (N), Phosphoprotein (P), Matrix protein (M), Glycoprotein (G) and Large RNA polymerase protein (L), and all of them are actively mediating signaling pathways to subvert innate immune responses. Three of the viral proteins (P, M and G) have been more extensively studied. The C-terminal domain of P protein binds to STAT1/2 therefore blocking the translocation of the STAT protein complex (Vidy, Chelbi-Alix, & Blondel, 2005; Wiltzer et al., 2014), which suppresses the consequential expression of antiviral effectors. Further, M protein has been demonstrated to interact with RelA43, a splicing analog of RelA (Besson et al., 2017; Khalifa et al., 2016; Luco et al., 2012) and intervenes with the activation of IFN-β and TNF-α. Conversely, a field isolate of RABV, in which four critical residues have been mutated on M protein to hinder the interaction with RelA43, showed a stronger inflammatory cytokine response and a lower pathogenesis *in vivo* (Sonthonnax et al., 2019). Finally, G protein also contributes to the replication of the virus by associating with MAST2 and PTPN4, which alters the balance of PI3K-AKT pathway and enables the infected neuron to evade apoptosis (Caillet-Saguy et al., 2015; Préhaud et al., 2010). The two other viral proteins, N (Masatani et al., 2013) and L (Tian et al., 2016) proteins have been shown to be involved in the modulation of the host immune response but their mechanisms of action have been less studied. Even though these transcriptional modulations induced by RABV proteins would explain the lack of major inflammation or neuronal death and how the physical network of neurons, their axons and dendrites, is relatively well preserved up until the demise of the host, the mechanism of neuronal dysfunction, which is the probable cause of neurological symptoms, remains elusive.

There is different evidence showing that virus or virus infection-associated changes in host gene expression could affect the neuronal activity. Inflammatory cytokines, such as TNF-α, IFN-γ or IL-1β resulting from the activation of pattern recognition receptors during acute viral encephalitis (Denizot, Neal, & Gasque, 2012), have been demonstrated to desensitize neurons to GABA stimulation and subsequently cause network hyperexcitability (Clarkson, Kahoud, McCarthy, & Howe, 2017), of which could result in cognitive impairment and seizure as demonstrated in animal models (Habbas et al., 2015; Nimmervoll et al., 2013). Phosphoprotein of Borna disease virus competes with substrate proteins of PKC and decreases the phosphorylation level of PKC

downstream proteins, such as SNAP25 and MARCKS. This action directly affects the synaptic vesicle recycling and structural integrity of synapse, and therefore disrupting synaptic plasticity (Bétourné et al., 2018). The mechanisms involved in the regulation of the interferon production observed during RABV infection could also influence the expression of other genes such as those involved in brain development, neuron specification, myelination, synaptic plasticity and cell survival (Harrison et al., 2020; Ji, He, Regev, & Struhl, 2019; Kesanakurti, Chetty, Rajasekhar Maddirela, Gujrati, & Rao, 2013; Lehmann, Lehmann, & Erfle, 2019; Miyamoto, Torii, Tanoue, & Yamauchi, 2016; Xiong, Zhang, Xiong, & Williams-Villalobo, 2020; D. Zhang et al., 2016; Zhao et al., 2011). In addition, there are studies showing hyperpolarization and disturbance of neuronal network synchronicity as results of RABV infection (Ceccaldi, Fillion, Ermine, Tsiang, & Fillion, 1993; Fu & Jackson, 2005; Gourmelon, Briet, Clarençon, Court, & Tsiang, 1991; Iwata, Komori, Unno, Minamoto, & Ohashi, 1999); This was shown to be partly due to the lower membrane conductance of Na+ and possibly reduced expression of the corresponding ion channels. However, the changes in membrane potential and the associated neuronal dysfunction could originate from multiple other mechanisms that remain unexplored, and more importantly, their connections to the RABV infection and the altered signaling pathways by the infection in neurons have not been properly studied as yet.

RNA sequencing has been a crucial tool to understand gene expression kinetics in comparative studies. Here, we analyze the RNA transcriptome of RABV-infected human neurons at the early hours of infection and attempt to identify the origin of RABV-induced neuronal dysfunction, tracking the signaling pathways that are directly affected by the viral modulation.

In review

This is a provisional file, not the final typeset article

MATERIALS AND METHODS

Viruses and reverse genetics

Two recombinant rabies viruses were generated from the rabies strain 8743THA (EVAg collection, Ref-SKU: 014V-02106), an isolate collected from the brain of a man who died of rabies after a dog bite in Thailand. In both viruses, E2-Crimson fluorescence gene (Clontech, 632556) was inserted between M and G protein genes of RABV (Besson et al., 2019) to obtain, the wild-type virus, Tha-E2-Crimson (Tha) and an M protein mutant virus, Th4M-E2-Crimson, (Th4M). The Matrix protein of Th4M virus differs from Tha's at 4 amino acid positions: R77K, D100A, A104S and M110L. Both viruses were constructed and rescued as already described (Besson et al., 2019; Khalifa et al., 2016). Full-length viral cDNA (2.5 μg) and plasmids N-pTIT (2.5 μg), P-pTIT (1.25 μg), and L-pTIT (1.25 μg) were transfected in 106 BSR T7/5 cells (Buchholz, Finke, & Conzelmann, 1999) in 6-well plates. Cells were then passaged every 3 days until 100% of the cells were infected. The supernatant was harvested and titrated on BSR cells to determine the multiplicity of infection (MOI).

Cells

BSR cells (Sato, Tanaka, Yanada, & Yamamoto, 1977) are part of the collection of our laboratory and were cultured at 37 °C, 5% CO2 in Dulbecco's minimal essential medium (DMEM) supplemented with 10% calf serum. BSR-T7 cells, kindly provided by K.K. Conzelmann (Max von Pettenkofer Institute and Gene Center, Munnich) (Buchholz et al., 1999) were cultured in Glasgow medium supplemented with 10% calf serum, tryptose phosphate, nonessential amino acids and geneticin. Neurons used in this study were differentiated either from neural progenitor cells (NPCs) derived from human induced pluripotent stem cells (hiPSCs) generated from a healthy subject (Kouroupi et al., 2017) or H9-NSC (H9 human ESC-derived neural stem cell, Invitrogen, Cat. No. N7800-100).

Differentiation and infection of neurons

hiPSC-derived NPCs were maintained only up to passage number 10 for the usage of neuronal differentiation, in DMEM/F12 medium (DMEM/F12/Glutamax (Gibco 10565-018), supplemented with N-2 1X (Gibco 17502-048), B27 1X (without vitamin A, Gibco 12587010), Penicillin/Streptomycin 1% (Gibco, 15140-122), HEPES 20mM (Gibco, 15630080), MEM Non-essential amino acid 1X (Gibco, 11140050), bFGF 20 ng/ml (CHAMEDITECH) to the final concentration) and on Poly-L-Ornithine (Sigma P4957) and Laminin (Sigma L2020)-coated T25 flasks. Medium for maintenance was refreshed every second day. On day 0 of differentiation, the NPCs were dissociated by incubation with Accutase (StemPro, A1110501) for 30 minutes at 37°C, counted and seeded onto PLO/Laminin-coated 96-well plates or 24-well plates for RNA-Seq and RT-qPCR, or 384-well plates for calcium imaging with 10μM ROCK inhibitor (Y27632; Tocris 1254). The ROCK inhibitor was withdrawn within 2 hours after seeding, and fresh Neurobasal medium for differentiation (Neurobasal (Gibco 21103-049), supplemented with B27 2%, and Glutamax 1X to the final concentration) was added onto the cells. The differentiation medium was 50% refreshed every 2~3 days for two weeks. On day 14 of differentiation, the hiPSC-derived neurons were subjected to

In review

RABV infection with a MOI 3 and media was changed after 2 hours. Two days post-infection hiPSC-derived neurons were subjected to RNA preparation for RNA-Seq or RT-qPCR, and 5 days post-infection were fixed with 4% paraformaldehyde (ThermoFisher, AAJ19943K2) and analyzed by immunocytochemistry or were processed for calcium imaging. H9-NSCs were maintained and differentiated in N2B27 medium on PLO/Laminin-coated flasks. N2B27 medium was 1:1 mixture of N2 and B27 media: N2 medium was composed of DMEM/F12/Glutamax, N-2 1X, MEM Non-essential amino acids 1X, Insulin 5µg/ml (Sigma I9278-5ML), 2-Mercapoethanol (Sigma M7522) and Pen/Strep 1% to the final concentration. B27 medium was composed of Neurobasal, B27 1X, Glutamax 1X, Pen/Strep 1% to the final concentration. EGF 20 ng/ml (Millipore GF144) and bFGF 20 ng/ml were added to N2B27 medium to complete NSC maintenance medium. For differentiation medium, B27 with vitamin A (Gibco, 17504044) was used instead and the growth factors were withdrawn. BDNF (Peprotech, 450-02) and GDNF (Peprotech, 450-10) were added to the differentiation medium to aid neuron survival, at a final concentration of 10ng/ml each. On day 0 of H9-NSC differentiation, cells were detached with Accutase and seeded in T25 flasks in 20% confluence. Within 2 hours after seeding, the medium was replaced by N2B27 differentiation medium and once more the next day. The medium was refreshed every second day until day 12. On day 12, the post-mitotic H9 neurons were gently dissociated from T25 flasks and seeded onto 24-well plates for RT-qPCR or 384-well plates for calcium imaging with ROCK inhibitor. The inhibitor was withdrawn within 2 hours, and the differentiation medium was 50% refreshed every 2~3 days up until day 27. The neurons were subjected to RABV infection as above and subsequently used for calcium imaging and RT-qPCR at 2 days post-infection.

RNA preparation, RNA-Seq and data processing

Total RNAs from collected cell pellets were prepared using Trizol (Invitrogen, Cat. No. 15596026) and ethanol precipitation. For RNA-Seq, non-infected / infected neurons were collected at 0, 8, 24 and 40 hours post-infection using Accutase and kept as pellets at -80°C until the RNA extraction. All samples were collected in biological triplicates. RNA preparation followed the Trizol manufacturer's protocol, with addition of Glycogen 10µg per sample to increase RNA yield. After that, RNAs were treated with DNase I (Promega, Cat. No. M6101) for 30 minutes at 37°C followed by second Trizol extraction. The acquired RNAs were mixed with 3 volumes of ethanol and 0.1 volumes of 3M sodium acetate, and kept at -20°C for overnight. Next day, the samples were centrifuged and washed with 75% ethanol twice to achieve RNAs in high purity. Sequencing libraries were constructed from the polyA RNA fraction using Illumina TruSeq Stranded mRNA library kit and were sequenced on the Illumina NovaSeq 6000 targeting 12 giga-base reads per sample. After that, raw data was subjected to data cleaning to remove adapter sequences and low-quality sequences using cutadapt version 1.11 (Martin, 2011). Only the sequences greater than 25 ucleotides (nt) in length were considered for further analysis. Mapping to reference genome was conducted using STAR version 2.5.0a (Dobin et al., 2013) (reference genome: Human (GRCh38) from ENSEMBL version 98) and Bowtie version 1.2.2 (Langmead, Trapnell, Pop, & Salzberg, 2009) for short DNAs (reference genome: rabies virus genome from NCBI) with default parameters. Following this, genes were counted using featureCounts version 1.4.6-p3 (Liao, Smyth, & Shi, 2014) from the Subreads package (parameters: -t gene -g gene_id -s 2 -p). This resulted an estimated expression level (or read count) for each annotated gene, and statistical analyses followed using R and BioConductor packages, including DESeq2 (Love, Huber, & Anders, 2014) and the PF2tools package (version 1.6.3) developed at PF2 (Institut Pasteur). The statistical analysis process includes data normalization, graphical exploration of raw and normalized data, test for differential expression for each feature

In review

This is a provisional file, not the final typeset article

between the conditions, raw P value adjustment and export of lists of features with significant differential expression between the conditions. The genes with adjusted P value less than 0.05 were considered as differentially expressed compared to non-infected condition. The datasets generated and analyzed for this study can be found in NCBI's Gene Expression Omnibus (accession number GSE178583).

Geneset enrichment analysis with Gene Ontology (GO) and Kyoto Encyclopedia of Genes and Genomes (KEGG) databases, keywords filtering, and upstream analysis

Over-Representation Analysis was performed to generate lists of comparisons between non-infection / infection conditions and time-points, to show the details of how differentially expressed genes (DEGs) are distributed over the genesets. Enrichment scores for genesets in this study were calculated based on $\log_2$ fold-change rankings of DEGs. Adjusted P value was used to calculate false discovery rate (FDR) in given geneset, the probability of a geneset with an enrichment score to be falsely overpresented. Odds-ratio was calculated as a ratio of DEGs in a particular geneset divided by the ratio of all DEGs in all genesets. In order to highlight the relevant ontologies and pathways to the study, subsets of Biological Process (GO) or KEGG Pathways were created by the same set of keyword detection (stringr package, R Studio). For instance, the keywords we used to produce "GO_interest" or "KEGG_interest" included "signal", "cascade", "cytokine", "receptor", "transport", "neuron" and 24 more, and the resulting list of subsets were provided on Supplementary Table 1. For GO, 767 terms were selected out of 2681, and 72 KEGG terms out of 323 from this filtering. Relevant filters were applied on Figure 1E-H as well and the produced results were provided on Supplementary Table 2. For upstream analysis and DEG grouping per pathway, KEGG pathway database, TRANSFEC (geneXpression), GeneCards (GeneHancer Regulatory Elements), STRING, and bibliography search were used as references.

RT-qPCR

For the selected and grouped DEGs, we confirmed the gene regulation at 40hrs post-infection (hiPSC-derived neurons) or 48hrs post-infection (H9-NSC neurons) by RT-qPCR. Total RNAs were prepared from Trizol extraction and ethanol precipitation, and RT-qPCRs were carried out using SuperScript IV VILO master mix with ezDNase (Invitrogen, Cat. No. 11766050) and QuantiTect SYBR Green PCR kit (Qiagen, Cat. No. 204143) following manufacturer's protocols. Specific primers for each DEG were selected from QuantiTect Primer Assay (Qiagen, Cat. No. 249900), and listed in Supplementary Table 3. Viral RNA level was assessed by N protein-specific primers (N1130: 5'-CTGACGTAGCACTGGCAGAC-3'; N1247: 5'-AGTCGACCTCCGTTCATCAT-3'), and human GAPDH (forward 5'-GAAGGTGAAGGTCGGAGT-3'; reverse 5'-GGTCATGAGTCTTCCACGAT-3') was measured as a control gene for each sample. One-way ANOVA was used to validate the significant differences between conditions.

Spontaneous activity recording with calcium imaging

At the end-point of RABV infection, human neurons were incubated with 3μM Fluo-4 AM (Invitrogen, Cat. No. F14201) at 37°C for 40 minutes in 50% BrainPhys Neuronal Medium

(STEMCELL, Cat. No. 05790) and 50% of differentiation medium. BrainPhys medium (Bardy & Gage, 2015) was supplemented with 2% B27, and used as loading and reading medium in this study. Subsequently, the cells were gently washed by 70% medium change for 4 times to remove excessive Fluo-4 probe and subjected to recording at 1.72 Hz for 4.5 minutes with 10X Air objective lens and temperature control at 37°C (Operetta system, PerkinElmer). From the collected TIFF images, information on frequency of calcium oscillations and the magnitude on each detected soma was extracted, using FIJI macro and CalBlitz-incorporated Python scripts (open source: https://github.com/agiovann/CalBlitz): first, global background intensity was calculated and subtracted from each frame using FIJI macro, and then the modified images were subjected to motion correction and source extraction workflow (Giovannucci et al., 2019; Pnevmatikakis, 2019). Template for motion correction was generated from aligning all image frames to register common area of field as reference and correct the shift of each image from the template. This removes motional artifacts from the time-course dataset. Based on the corrected information, segregation of region of interest (ROI; soma) was performed using Independent Component Analysis (matrix factorization) and watershed algorithm, filtered by an assigned size of soma. The relative intensity variation $\Delta F/F$ was calculated from comparison of the intensity of ROI to the average intensity of each reading frame. After deconvolution of $\Delta F/F$ trace with estimated impulse response of neuron, we set the threshold for calcium oscillation peak to at least 2% decrease from maxima by the following frame. The extracted number of calcium peaks was presented in box graphs (Prism 9) or in Raster plot (R studio), along with exemplary traces of calcium oscillation of individual soma.

Immunocytochemistry and image analysis

Non-infected or infected human neurons were fixed with 4% paraformaldehyde for 30 minutes at room temperature, and washed with PBS 3 times. Neurons were subsequently incubated with a primary antibody against TUBB3 (1:1000; BioLegend, Cat. No. MMS-435P), diluted in PBS with 5% normal goat serum (Gibco, PCN5000) for 2 h at 37°C, followed by incubation with the appropriate secondary antibody conjugated to AlexaFluor 488 (ThermoFisher, Cat. No. A28175) for at least 1 h at room temperature. Nuclei were counterstained with Hoechst (1:1000). For RABV N protein detection, Anti-Rabies Nucleocapsid Conjugate (Bio-Rad, Cat. No. 3572112) was used according to the manufacturer's protocol. Following the staining, images were obtained from Operetta or Opera Phenix (PerkinElmer) with 20X Air objective lens and analyzed in Columbus Image Data Management System (PerkinElmer).

In review

This is a provisional file, not the final typeset article

RESULTS

Temporal dynamic expression of significantly selected genes in wild-type RABV-infected neurons

To understand the transcriptional changes at early time points of RABV infection on neurons and distinguish the modulated processes or pathways that are potentially involved in neuronal dysfunction, we have infected NPC-derived 2 weeks-differentiated neurons with wild-type RABV (Tha virus) and performed RNA-Seq analysis at early time-points: 8, 24, 40 hours post-infection (Figure 1 and Supplementary Figure 1A-B) in biological triplicates. At each time-point, infected samples were compared to the non-infected one, to select the differentially expressed genes (DEGs).

Overall the datasets showed strong correlations between experimental conditions and gene expression as described in Supplementary Figure 1C. The replicates are clustered according to non-infection / infection conditions and to the time-points, which demonstrates the genuine effects of RABV infection on the transcriptome. As the post-infection time-point-dependent changes in gene expression was an intriguing aspect of the datasets, we ran the DEG dataset of wild-type RABV through Gene Set Enrichment Analysis (GSEA) pipeline. In total, 610 genes were significantly modulated in Tha dataset (Figure 1A), with 101 and 96 genes at 8hrs and 24hrs respectively, and then a larger group of 516 genes at 40hrs post-infection (Table 1). These genes are involved in diverse range of biological compartments and functions, as Gene Ontology (GO) analysis laid out on Figure 1B-D and Supplementary Table 4. The involvement of DEGs in GO genesets exponentially increases over time, for particular genesets standing out more on 24hrs post-infection than on 40hrs. At 8hrs and 24hrs post-infection, DEGs were more concentrated on relatively smaller numbers of GO terms, 672 and 596 terms in Biological Process, respectively. The types of GO terms involved are also varying according to the time post-infection. Between 8hrs and 24hrs GO terms, there are only 237 terms in common, in contrast to 24hrs and 40hrs comparison which shows 585 common terms in Biological Process (Supplementary Table 4). The fact that only 7 DEGs are detected as common between 8hrs and 24hrs datasets and that 81% of 8hrs DEGs are down-regulated, strongly supports that wild-type RABV impacts the RNA transcription of the infected neurons differently at the earlier stage of infection than at the later ones.

Neuronal function-related processes are regulated before immune response processes

To understand which processes are regulated early on during the RABV infection and how they evolve over time, further analysis focusing on GO terms in Biological Process has been performed. We filtered the GO terms using keyword detection in R dplyr package, and assembled 4 groups of GO terms that are associated with Cell Cycle (cell division, DNA damage and repair, apoptosis), Gene Expression (RNA transcription, protein translation and folding, vesicle transportation), Immune Response (cytokines and interferon, innate immune-response-related pathways), and Neuronal Function (neuron projection and synapse formation, extracellular matrix, ion balance, membrane potential) (Figure 1E-H). Up- and down-regulated genes were distributed differently in each group, for instance in the group of Cell Cycle (Figure 1E) the down-regulated genes take up to three-fourth of gene regulation and together with up-regulated genes, are connected to 120 GO terms (Supplementary Table 2 and 4). Further, the Odds-ratio of Cell Cycle GO terms gradually increased over time until 40hrs post-infection, more than the GO terms of other groups, and most of these Cell Cycle GO terms have FDR smaller than 0.05 at the last time-point. Illustrating these points, Cell

Cycle GO terms with the most significant Odds-ratio such as G1/S transition of mitotic cell cycle (27 out of 30 DEGs down-regulated), mitotic spindle organization (16 out of 17) and mitotic cytokinesis (16 out of 16) showed a higher ratio of down-regulated DEGs at 40hrs. In comparison, the group Gene Expression (Figure 1F) presented a higher Odds-ratio at 24hrs compared to 40hrs post-infection, implicating relatively more significant regulation exerted by RABV on host cells at 24hrs. It showed 198 DEG involved in 87 GO terms (Supplementary Table 2 and 4), related to mRNA stabilization, protein folding, or sequestering transcription factor with significant Odds-ratio. Similar kinetics have been observed on the group Immune Response (Figure 1G). Innate immune response-associated 133 genes were involved in GO terms related to cytokine production, regulation of NF-kB signaling, or response to TNF among others. Close to 70% of DEGs are up-regulated in this group, including *NFKB1, NFKB2, RELB* and *NFKBIA*, all detected from 24hrs to 40hrs. This could indicate that the modulation of host immune response by RABV starts to become more efficient from 24hrs post-infection. On the other hand, the genes involved in the group Neuronal Function (Figure 1F) are detected from earlier on, among 212 GO terms 87 of them (41%) contain DEGs that were regulated at 8hrs post-infection. Many of genes in this group such as *CCL2, TNFAIP3, NFKB2, MEF2C* and others were implicated in both major signaling pathways involved in immune response and also in important processes for neuronal functions, which include dendritic morphology, synaptic membrane adhesion, neuronal differentiation, neurotransmitter secretion and more (Supplementary Table 4).

Mutated M protein delays the suppression of gene expression-associated processes but does not impact the RABV's control over host immune response

Since the failure of autonomic nerve system is postulated as the main cause of RABV-associated death, we took a mutant RABV (Th4M virus; four point mutations on M protein at amino acid positions 77, 100, 104 and 110) that showed better longevities and delays of neurological symptoms in infected mice (Khalifa et al., 2016; Sonthonnax et al., 2019) and performed a RNA-Seq analysis on infected neurons. As we mentioned above, M protein from Th4M virus lacks the affinity for the NF-κB signaling protein RelAp43 and therefore allows the induction of IFN-β, TNF-α and other pro-inflammation cytokines upon infection (Besson et al., 2017; Khalifa et al., 2016), resulting in a reduced pathogenesis of the virus *in vivo* (Sonthonnax et al., 2019). We then undertook a comparative ontology analysis on RNA-Seq datasets obtained from neurons infected with Tha- and the attenuated mutant Th4M (Figure 2, Supplementary Figure 2). As expected, DEGs are regulated differently by two viruses at early time-points post-infection. As described on Table 1, Figures 2A and 2B, both datasets show eventual increase of the number of DEGs at 40hrs post-infection, but the progression of DEGs at earlier time-points greatly differs between the two datasets.

At 8hrs post-infection, Tha dataset shows a modulation of 101 genes, while Th4M shows only 18 DEG at the same time-point (Table 1). Among these 18 DEG, 14 of them are also observed in Tha dataset at the same time-point, and only 4 genes (*ACSBG1, SFRP4, HPCAL4* and *GLRA1*) are unique to Th4M dataset. The DEGs in Tha dataset at 8hrs were associated with 672 Biological Process GO terms compared to 162 terms of Th4M (Figure 2B), but 85% of the Th4M GO terms (137 terms) were shared with Tha dataset at this time-point. Among the 87 DEGs uniquely detected on Tha dataset at 8hr post-infection, 73 DEGs are down-regulated genes associated with DNA replication and repair, kinetochore assembly, response to redox state (447 GO terms; Odds-ratio > 20) and 14 DEGS are up-regulated genes detected in GO terms such as phospholipid homeostasis, mRNA catabolic process, cation ion homeostasis among others (79 GO terms; Odds-ratio > 20).

In review

This is a provisional file, not the final typeset article

On 24hrs post-infection, Tha dataset maintained a similar number of DEGs (n=95) as observed at 8hrs post-infection, with 55 up-regulated and 41 down-regulated genes (Table 1). In contrast, Th4M dataset showed a dramatic increase of the number of DEGs compared to 8hrs, 419 genes with 117 up-regulated and 302 down-regulated. To investigate the potential delays in the transcriptional modulation by Th4M virus, we analyzed the distribution of DEGs and GO terms at different time-points of two datasets. We found that only 4 DEGs were common between Tha 8hrs and Th4M 24hrs datasets, and 19 DEGs between Tha 8hrs and Th4M 40hrs datasets. However, the overview of GO term distribution was different from that of DEGs. Sixty-seven percent of Tha 8hrs GO terms appeared on Th4M dataset at 24hrs, and 80% of Tha 8hrs GO terms on Th4M 40hrs dataset. This could mean that even though the transcriptome profiles of Tha and Th4M datasets are distinct, the DEGs of both datasets are involved in similar biological processes, at earlier time-points in the case of Tha compared to Th4M.

At 24 hrs post-infection, 596 GO terms were associated with Tha dataset and 1413 terms with Th4M (Figure 2B), which is 2.4 times more than that of Tha dataset at the same time-point. We also found that amongst the terms recorded with Th4M at 24hrs post-infection, 507 terms were shared with Tha 24hrs and then an even higher number of terms, 1006, with Tha 40hrs dataset. To conclude with this comparison, Th4M induced a more dramatic modification of the transcriptional profile than Tha at 24 hrs post-infection. This involves GO terms such as regulation of NF-kappaB signaling (GO:1901222), intrinsic apoptotic signaling pathway in response to ER stress (GO:0070059), cytokine-mediated signaling pathway (GO:0019221), and KEGG terms including TNF signaling (hsa04668), JAK-STAT signaling (hsa04630), MAPK signaling (hsa04010) and PI3K-AKT signaling (hsa04151), as further detailed on Figure 2C and D. Further, most of immune response-related processes from Th4M dataset overlap with that of Tha dataset, since the numbers of DEGs that are involved in the relevant pathways are very close between the two datasets. At 24hr post-infection, Tha and Th4M datasets show 24 and 18 DEGs associated with Immune response, respectively. Commonly, 15 DEGs including *NFKB1, NFKB2, NFKBIA, RELB* and *TNFAIP3* are detected on both datasets at this time-point, and are associated with pathways that are known to be modulated by RABV: NF-kB, TNF, MAPK, JAK-STAT, PI3K-AKT, IL-17, TLR, NLR, RLR or chemokine pathways (Besson et al., 2019; Caillet-Saguy et al., 2015; Fooks et al., 2017; Gerlier & Lyles, 2011; Wiltzer et al., 2014).

On 40hrs post-infection, the two datasets show a relatively similar contribution to the biological processes, as 1,335 GO terms (87% of Tha and 79% of Th4M terms) (Figure 2B) are commonly detected in both datasets and 372 genes are shared between them (Table 1).

To conclude, Tha and Th4M datasets display different dynamics of gene regulation in neurons especially at early time-points, but they become similar at 40hrs post-infection at a time when the feedback response from host cells becomes more prominent. Overall, Tha virus secures more control over the gene modulation than Th4M at the early hours of infection, which emphasizes the role of M protein in the regulation of host gene expression at that time.

RABV-associated pathways are involved in neuronal differentiation, synaptic activity and morphological changes in Tha and Th4M datasets

In order to understand which genes in the aforementioned RABV-associated pathways could directly impact neuronal functions or related processes, we investigated relevant DEGs identified in the

KEGG pathways. At 24h post-infection, TNF, IL-17 and NF-kB pathways scored relatively high Odds-Ratios compared to other genesets (Figure 3A). The DEGs detected in these pathways are mainly up-regulated in both Tha and Th4M datasets (Figure 3B, C, D), and many of these genes are induced at 24hrs post-infection and maintained a high expression level until 40hrs post-infection. These pathways are associated through their component genes to biological processes such as extracellular matrix organization (GO:0030198), calcium-mediated signaling (GO:0019722), cytoskeleton organization (GO:0007010), and negative regulation of neuronal apoptosis (GO: 0043524). In comparison, MAPK signaling pathway on Figure 3E shows more down-regulated DEGs than the previously mentioned pathways, notably *IL1RAP* (8hrs on Tha; involved in inflammatory response, regulation of pre-/post-synaptic density assembly, positive regulation of NF-kB activity), *CACNB3* (24hrs on Th4M; involved in membrane depolarization), *TEK* (40hrs on Tha and Th4M; involved in negative regulation of apoptotic process, negative regulation of inflammatory response, positive regulation of PI3K activity) as indicated on Supplementary Table 4 and 5. MAPK pathway is also associated through the subset genes to neuronal function-related biological processes such as synapse assembly (GO:007416), neuron differentiation (GO:0045664), and Wnt calcium modulating pathway (GO:0007223). As presented in heatmaps, the overall DEG expression ranges from -1.2 to 3 $\log_2$-fold changes compared to non-infection conditions at each time point. This highlights the stealthy nature of RABV-induced modulation over gene expression in neurons and relatively mild feedback from the host defense mechanism during the first replication cycle of RABV, in absence of glial cells.

The up- or down-regulated DEGs of RABV-associated pathways impact neuronal function-related processes through signaling transduction network. We have identified several direct and indirect connections from the signaling transduction-related DEGs to the neuronal function-associated DEGs through upstream search using KEGG pathway database, TRANSFEC (geneXpression), GeneCards (GeneHancer Regulatory Elements), STRING and bibliography search. The examples of MAPK, NF-kB, and JAK-STAT pathway DEGs that are associated with neuronal functions are validated with RT-qPCR and assembled on Figure 4. *DUSP5* on Figure 4A was previously studied for its contribution to the RABV replication (Besson et al., 2019), and plays important role in de-phosphorylation of active ERK and controlling neurite outgrowth and postsynaptic density (Hardingham, Pruunsild, Greenberg, & Bading, 2017; Kidger et al., 2017; Kim et al., 2015; Lacar et al., 2016), along with other DUSP proteins. In our results, *DUSP5* increased by 0.996 2-fold-change in Tha dataset and 0.787 in Th4M from RNA-Seq, and at least 0.3 2-fold-change or higher in both Tha and Th4M RT-qPCR validations. Other MAPK pathway downstream elements *FOS, FOSB* and *JUNB* are up-regulated to varying degrees under Tha and T4M infection, which then directly act as transcription factors for GDF15 (increases Glutamate release through up-regulation of voltage-gated calcium channel (Liu, Lu, Zhao, Hu, & Mei, 2016)), SLC3A2 (forms cystine/glutamate transporter with SLC7A11 and regulates glutamate uptake (Bhutia & Ganapathy, 2016)), NR4A1 (NGF nuclear receptor, associated with dendritic spine attrition and cognitive impairment (Jeanneteau et al., 2018)) and GABRQ (extrasynaptic GABA receptor subunit theta (Fatemi, Folsom, Rooney, & Thuras, 2013)). As part of GABAA receptor, GABRQ localizes on extrasynaptic membrane of neuron and contributes to GABA-mediated chloride ion fluxes and inhibitory regulation of action potential. All these DEGs have been confirmed to increase under Tha and Th4M infections in both RNA-Seq and RT-qPCR validation. WNT mediates neuronal circuit formation and could be up-regulated by MAPK pathway modulation through the upstream transcription factor CDX2 (De, 2011), which is validated by RT-qPCR. DYNLL1 (LC8) is an important protein involved in the translocation of RABV particles but also involved in DNA damage response pathway and anti-apoptotic activity by interacting with TP53BP1, BIM and BMF (Fooks et al., 2017; He et al., 2018; West et al., 2019), and it is up-regulated through ATMIN / PAK1 interaction (He et al., 2018), from p.i. 24hrs to 40hrs by

This is a provisional file, not the final typeset article

more than 2 log_2-fold changes in RNA-Seq and close to 10 log_2-fold changes in RT-qPCR, in both datasets. On Figure 4B, selected DEGs from canonical and non-canonical NF-kB pathways and the possible downstream genes that are up-regulated under Tha and Th4M infection are presented. NFKB1, NFKB2, RELB, NFKBIA are involved in host immunity and oncogenesis, as well as in synaptic plasticity, communication from synapse to nucleus, response to membrane potential changes and neurite outgrowth through downstream regulation (Dresselhaus & Meffert, 2019; Engelmann & Haenold, 2016; Kaltschmidt & Kaltschmidt, 2009). ICAM1 and VCAM1 could receive signals from both MAPK and NF-kB pathways for expression (Taniguchi & Karin, 2018), and contribute to neuron adhesion, stability of extracellular matrix, and permeability of brain barriers. TNFAIP3 (A20) is involved in negative regulation of inflammatory response and apoptosis, and heterozygosity of this gene causes exacerbated cognitive impairment under inflammatory condition (Daems et al., 2020; Martín-Vicente et al., 2020). The primary function of CCL2 and CXCL10 is chemokines for monocytes macrophages, but also could cause neuronal dysfunction indirectly through the recruited immune cells (Lehmann et al., 2019), or increase intracellular calcium level within neurons leading towards hyperpolarization and excitotoxicity (Kodangattil, Möddel, Müller, Weber, & Gorji, 2012). As already mentioned, the RABV P-protein interferes with JAK-STAT pathway resulting in the downstream modification of the transcriptional pattern (Fooks et al., 2017; Wiltzer et al., 2014). On Figure 4C, STAT3 increases under Tha and Th4M infection, and so do the downstream effectors SLC7A11 and HSP90AA1. As mentioned above, SLC7A11 forms Xc- cystine/glutamate anti-transporter, and HSP90AA1 as scaffold protein maintains the integrity of cytoskeletal proteins in neurons and induces clearance of abnormally aggregated proteins (Ou, Tan, Xie, Yu, & Tan, 2014). The validation of several DEGs was confirmed again in H9-NSC-derived neuron cultures, as displayed in Supplementary Figure 3.

RABV infection hinders spontaneous activity of neurons

To understand the impact of RABV infection on neuronal activity, we performed calcium imaging on the NPC-derived neuron cultures. Calcium imaging with Ca2+ probes reflects the genuine neuronal activity, number of action potential and the amplitude correlating to the observed calcium traces (Kirwan et al., 2015). After two weeks of differentiation, neurons expressed the neuronal marker TUBB3 and formed complex network over the desirable size of field of view (Supplementary Figure 4; over 500 somas detectable under 10X lens). Such neurons were infected with Tha or Th4M virus at the same MOI as used in RNA-Seq experiment and then the calcium oscillations that originate from spontaneous activity of neurons were measured, using Fluo-4 AM calcium indicator at 5 days post-infection. Upon imaging, Tha- and Th4M-infected neurons exhibited lower neuronal activities compared to the non-infected samples (Figure 5A-C). The number of active neurons that had more than one calcium peak over the course of reading was significantly higher on non-infected samples than on the Tha-infected ones, as well as the rate of detected calcium peaks displaying similar pattern. This is independent of the virus used, as the comparison between Tha- and Th4M-infected neurons was not statistically significant on either activity ratio or the peak rate (Figure 5B). Average of amplitude of calcium peaks showed similar heights between non-infected and infected neurons, as exemplified by the extracted calcium traces from somas with higher peak rate (Figure 5D). The Tha-infected neurons exhibit a reduced frequency of calcium peak, hence of the presumptive action potential firings, but has not been affected on the amplitude of spontaneous activities. As summarized in graphs on Supplementary Figure 4, the results of calcium imaging did not originate from visible structural damages such as axonal / dendrite degeneration (neurite count / length) or apoptosis (bleb count). Interestingly, when we reduced the duration of infection to two days to observe the effect of

In review

Tha virus infection in similar timeline as the RNA-Seq experiment (Figure 5E-F), the difference of peak rate was less significant between non-infected and infected neurons in comparison to 5 days post-infection, but the Tha-infected neurons exhibited higher sensitivity to the presence of GABA, which corresponds to the regulation of neurotransmitter uptake-associated genes and the increased expression of GABA receptor subunit that we have observed in the RNA-Seq datasets.

In review

This is a provisional file, not the final typeset article

DISCUSSION

As rabies advances, signs of autonomic and cognitive neuronal dysfunction become more prominent (Fooks et al., 2017). Many viral encephalitis studies attributed similar neurological symptoms to the strong immune response from the macrophage / monocytes, neutrophils and adaptive immune cells, infiltrating CNS or recruited through disrupted blood-brain / CSF barriers (Carod-Artal, 2018; Denizot et al., 2012; Ludlow et al., 2016). Excessive immune response against virus in CNS results in neurodegenerative pathologies, such as neuronal death, axon degeneration or demyelination (Kennedy, 2015; Ramesh, MacLean, & Philipp, 2013; Tsunoda, 2008). In contrast, rabies virus has developed strategies to evade immune responses at the site of initial entry and infect motor neurons to swiftly move into CNS, maybe even before the onset of symptoms (Hemachudha et al., 2013; Jackson, 2006). Our study aimed to understand the early event of RABV infection in neurons, and identify neuronal function-associated genes that could directly be affected by RABV modulation of signaling pathways. Spontaneous activity of neuron and its alteration represents the overall outcome of RABV infection. In this study, we analyzed the dynamic transcriptome changes during the first hours following the infection of neurons, especially around the first cycle of virus replication (less than 24 hours post-infection) in absence of secondary inputs from glial cells, to provide a clear perspective of neuronal modification induced by RABV infection. The originality of this work lies on the fact that the transcriptome kinetic analysis has been performed for the first time from very early time-point of RABV infection up to 40hrs post-infection, and that the role of M protein in transcriptome modulation and neuronal dysfunction has been investigated in human neurons.

M protein regulates neuronal function-associated genes from early time-points of infection

At 8hrs post-infection, Tha dataset showed faster regulation of host gene expression than Th4M dataset, with the majority of these DEGs are being down-regulated (81%). We have shown that in Tha dataset, the group Neuronal Function particularly stood out at 8hrs compared to the group Cell Cycle, Gene Expression or Immune response, since 44% of DEGs at 8hrs post-infection is associated with neuronal functions. Some of the high Odds-ratios we observe might occur due to the slightly smaller size of genesets in Neuronal Function, or also because the specific gene ontologies are highly influenced by Tha virus infection at 8hrs compared to the others. Also, the virus infection may have direct contribution onto this regulation, through immediate early genes (IEGs). IEGs regulation in host cells can be triggered by early event of virus infection – attachment, internalization, intracellular trafficking and uncoating – and activate series of transcription factors and DNA-binding proteins that are best-characterized in Ras/Erk/MAPK-associated signaling pathways (Gallo, Katche, Morici, Medina, & Weisstaub, 2018; Tullai et al., 2007). These genes are induced to maximum level within 1-4 hours after stimulation and activate or suppress secondary transcription within few hours. Many of Neuronal Function-associated DEGs observed at 8hrs (*GRHL3, PDPN, TNFRSF11B, SPP1, COL11A1, PTX3, CRISPLD2, CDH2, EZR, NT5E, SMAD7, MEF2C, CLDN1, RGS4, ANXA1, CEMIP, ARNTL, LEF1, HBEGF, TGFA, WEE1*) have transcription factor binding sites associated with Ras/Erk/MAPK or related pathways (identified by TRANSFEC search) on upstream, so it is possible that M protein of RABV may interact with Ras/Erk/MAPK signaling pathway proteins and affects the downstream transcription. Another point being addressed regarding the regulation of neuronal function in early time-points is the proportion of down-regulated genes in DEGs. There are 86 processes in the group Neuronal Function at 8hrs post-infection, and 64 of them are influenced by down-regulated genes. Compared to the 26 processes of Th4M dataset in the same criteria and the sudden expansion of DEGs at 24hrs, the results show how important the role of M protein is in the

In review

early repression of host gene expression. Vesicular stomatitis virus (VSV), another rhabdovirus belonging to the Vesiculovirus genus (a genus closely related to that of the lyssavirus genus), also globally suppresses the transcription and translation of the host cells by 4 to 6 hours post-infection, and the M protein of VSV is primarily responsible for this inhibition (Lyles, Kuzmin, & Rupprecht, 2013). The scale of host gene expression inhibition induced by RABV M protein seems to be much smaller than that of VSV, as demonstrated in this study. However, if our results suggest that RABV is a milder inducer of host gene expression than VSV, RABV has developed more specific ways to control signaling pathways than general inhibition. This is in line with previous studies showing the crucial role of RABV M protein *in vitro* and *in vivo* (Besson et al., 2017; Khalifa et al., 2016; Luco et al., 2012).

Size of differential expression during the first round of virus replication is controlled by M protein

In Tha dataset, we have observed that the control of M protein over the host gene expression was maintained at 24hrs post-infection, in contrast to the delayed but drastically increasing number of DEGs on Th4M dataset. It seems that during the first round of virus life cycle (~24hrs post-infection), RABV has the competition between host response and virus replication under its control due to the presence of functional M protein, which implies that the suppression of host gene expression by M protein at early time-points of virus replication maybe significant for keeping the host cells relatively "quiet". Modulating host gene expression by the virus is not necessarily bound to immune responses here, since Tha and Th4M datasets display similar number of DEGs detected directly in immune response-associated pathways at 24hrs (according to KEGG pathway definition) and also similar number of GO terms related to innate immune responses at that time-point (Tha 92 terms, Th4M 105 terms by keyword filtering in Biological Process). This is to a certain degree a discrepancy from the previously reported studies showing stronger immune responses elicited by attenuated RABV (Koraka et al., 2018; Wang et al., 2005). Considering the genetic differences between the virulent RABV strain Tha and its mutant virus Th4M are 4 amino acids, the results we obtained only highlight the specific characters of M protein regulation. Additionally in our datasets, Th4M dataset has more DEGs that are directly or indirectly involved in gene expression, metabolism, or immune response processes from 24hrs post-infection onwards, which may affect the kinetics of virus replication as presented in Supplementary Figure 1 and partly cause the delayed neurological symptoms in Th4M-infected mice (Sonthonnax et al., 2019). In this study, we were able to provide clearer perspectives on the kinetics of the progression of neuronal dysfunction in RABV infection since we used neuron culture and shorter incubation time. In comparison, Zhang et al. used intranasally inoculated mice model to study CVS-11 and HEP-Flury transcriptome modification in the brain, but the earliest time point for RNA harvest was 10 days post-infection and the CVS-11 dataset showed over 2,800 DEGs ranging from –2 to 11 $\log_2$ fold-changes (D. Zhang et al., 2016). The analysis showed immune responses and cell death-oriented gene ontology distribution for the CVS-11 dataset, which most likely comes from combination of cell types in the brain and therefore difficult to interpret for the neuronal dysfunction. A study published in 2016 (Jamalkandi et al., 2016) took a systemic approach by meta-analyzing the existing datasets and extracted 7 relevant signaling pathways to RABV pathogenesis (WNT, MAPK, RAS, PI3K/AKT, TLR, JAK-STAT, and NOTCH), which are similar to the KEGG pathways filtered on p.i. 24hrs based on higher Odd-Ratios in Figure 3. However, the datasets in this study as well were produced from mouse brain, spinal cord, and microglial cells with varying microarray systems and virus strains, and the time points for the sample collection were unclear. As the primary target for RABV replication, neurons are expressing receptor molecules such as nicotinic acetylcholine receptor (nAChR), neuronal cell adhesion molecule

This is a provisional file, not the final typeset article

(NCAM), p75 neurotrophin receptor (p75NTR) or metabotropic glutamate receptor subtype 2 (mGluR2) (Guo et al., 2019; Y. Zhang et al., 2014). Neurons are therefore exposed to host transcriptome modulation of RABV earlier than the other types of cells present in the nervous system, astrocyte, microglia or oligodendrocyte. From our study, the changes in neurons at early hours of infection seem crucial to maintain the control of RABV on preexisting host defense system and in particular on neuronal function regulation, as 137 out of a total 610 DEGs in Tha dataset are involved in neuronal function regulation, and 316 genes out of 969 DEGs for Th4M. Thus, this study provides an important insight on the sceneries of RABV's first replication cycle in its target domain and how the temporal regulation shifts to eventually affect neuronal functions.

Immune response-associated pathways that interact with rabies virus impact neuronal functions

Regulation of many neuronal function-associated genes roots from the signaling pathways that are directly affected by RABV infection. One of such pathways is NF-kB signaling pathway. NF-kB pathway is intensively studied for its involvement in host immune responses, but also in relation to neuronal functions as it is localized in synapse for fast signaling transmission. NF-kB is constitutively activated in glutamatergic neurons (e.g. granule cells and pyramidial neurons in hippocampus CA1 and CA3) and responds to the increase of calcium level at the post-synaptic dendritic spine and translocate to nucleus (Engelmann & Haenold, 2016; Kaltschmidt & Kaltschmidt, 2009). Matrix protein of RABV interacts with RelA and more specifically its splicing variant RelAp43. Consequently, this interaction hinders the translocation and re-balances the downstream transcription by NF-kB pathway, including of IFN and TNF (Besson et al., 2017; Khalifa et al., 2016; Luco et al., 2012). RelA mainly partners with NF-kB p50, but also can interacts with p52 and translocate to nucleus to act as transcription factor. With external stimulation such as TNF-α, IL1-β, CXCL10 or TGF-β1, or internal stimulation like viral RNA detection by RIG-I or TLRs, the RelA-p50 dimer transcribes inflammatory cytokines and inducible nitric oxide synthases (iNOS) and hinders the virus replication. With RelA stalled by M protein interaction, the downstream of NF-kB pathway weighs more on other transcription factors / co-activators / repressors, such as RelB, c-Rel, p50 and p52, frequently STATs, AP-1, p53 and IRFs in combinations (Taniguchi & Karin, 2018). The shifted transcription spectrum affects wide range of biological processes including neuronal functions, as exemplified by TNFAIP3, ICAM1 or VCAM1. Also, the TPL2 (MAP3K8) -dependent interaction of M protein to p105 would prevent the positive regulation of MEK1/2 by TPL2 (Besson et al., 2017) and subsequently ERK1/2 or p38 signaling path, which suppresses the expression of inflammatory receptors (Xu, Matsumoto, McKenzie, & Zarrin, 2018). This may lead to increasing the survival of neurons but also alters the signaling pathways that interact with TPL2, such as release and destabilization of A20 binding inhibitor of NF-kB (ABIN2), which subsequently influence A20 (TNFAIP3) -mediated ubiquitination / de-ubiquitiantion of NF-kB signaling proteins (Martín-vicente et al., 2020; Webb, Ventura, & Ley, 2019). As mentioned before, modification of ERK / MAPK signaling plays important roles in both inflammation- and neuronal function-associated transcriptions. In our study, we have confirmed that several DEGs related to neurotransmitter uptake (SLC3A11, SLC2A11) and postsynaptic activity (GABRQ) are indeed regulated by RABV infection and this could result from the direct interaction between RABV proteins and MAPK pathway components. Of note, host genes of MAPK pathway that are important for virus replication are not necessarily modulated during the RABV infection, since the virus replication-assisting / inhibiting MAPK pathway genes from previous study (Besson et al., 2019) do not appear on Tha dataset. JAK-STAT pathway could also be significantly modified by RABV infection, as STAT1/2 is efficiently sequestered by interaction with P protein. To lesser degree in human neurons, P protein also binds to

637 STAT3 (Harrison et al., 2020) and interferes with Gp130 receptor-dependent signaling that are
638 involved in neuroprotection, neurite outgrowth and synapse formation (Chen et al., 2016; Lieu et al.,
639 2013).

640 In conclusion, our study shows that the gene expression in neurons is significantly regulated by
641 RABV infection from the initiation point of virus replication cycle, and M protein of RABV plays
642 important roles in keeping the host gene expressions at bay during this time. RABV infection in
643 neurons especially alters the expression of genes associated with neurotransmitter-gated ion channels
644 / neurotransmitter uptake / morphology and extracellular matrix through RABV-interacting pathways
645 at early hours of infection, which contribute to the eventual decrease of spontaneous activity in the
646 infected neurons.

In review

This is a provisional file, not the final typeset article

Funding

This work was supported by grants from Partenariat Hubert Curien (No. 41432ZB), Ministry of Science and ICT of Korea (No. 2017M3A9G6068257 and 2018K1A3A1A21041166), and internal fundings of Institut Pasteur.

Acknowledgements

We would like to thank Odile Sismeiro and Jean-Yves Coppée for their help in library preparation and helpful discussions on the RNA-Seq protocol, Andrew Holtz for the constructive comments, as well as to the members of Tech Development Platform and Lyssavirus Epidemiology and Neuropathology laboratories for their assistance.

In review

657 **Reference**

658 Adle-Biassette, H., Bourhy, H., Gisselbrecht, M., Chrétien, F., Wingertsmann, L., Baudrimont, M.,
659 … Gray, F. (1996). Rabies encephalitis in a patient with AIDS: A clinicopathological study. Acta
660 Neuropathologica, 92(4), 415–420. https://doi.org/10.1007/s004010050538

661 Bardy, C., & Gage, F. H. (2015). Neuronal medium that supports basic synaptic functions and
662 activity of human neurons *in vitro*. Proceedings of the National Academy of Sciences, 112(20),
663 E2725–E2734. https://doi.org/10.1073/pnas.1504393112

664 Besson, B., Kim, S., Kim, T., Ko, Y., Lee, S., Shum, D., … Bourhy, H. (2019). Kinome-Wide RNA
665 Interference Screening Identifies Mitogen-Activated Protein Kinases and Phosphatidylinositol
666 Metabolism as Key Factors for Rabies Virus Infection. MSphere, 4(3), in press. https://doi.org/c

667 Besson, B., Sonthonnax, F., Duchatea, M., Khalifa, Y. Ben, Larrous, F., Eun, H., … Bourhy, H.
668 (2017). Regulation of NF-kB by the p105-ABIN2-TPL2 complex and RelAp43 during rabies virus
669 infection. PLoS Pathogens, 1–24.

670 Bétourné, A., Szelechowski, M., Thouard, A., Abrial, E., Jean, A., Zaidi, F., … Gonzalez-Dunia, D.
671 (2018). Hippocampal expression of a virus-derived protein impairs memory in mice. Proceedings of
672 the National Academy of Sciences, 115(7), 201711977. https://doi.org/10.1073/pnas.1711977115

673 Bhutia, Y. D., & Ganapathy, V. (2016). Glutamine transporters in mammalian cells and their
674 functions in physiology and cancer. Biochimica et Biophysica Acta - Molecular Cell Research,
675 1863(10), 2531–2539. https://doi.org/10.1016/j.bbamcr.2015.12.017

676 Buchholz, U. J., Finke, S., & Conzelmann, K.-K. (1999). Generation of Bovine Respiratory Syncytial
677 Virus (BRSV) from cDNA: BRSV NS2 Is Not Essential for Virus Replication in Tissue Culture, and
678 the Human RSV Leader Region Acts as a Functional BRSV Genome Promoter. Journal of Virology,
679 73(1), 251–259. https://doi.org/10.1128/jvi.73.1.251-259.1999

680 Caillet-Saguy, C. C., Maisonneuve, P., Delhommel, F., Terrien, E., Babault, N., Lafon, M., … Wolff,
681 N. (2015). Strategies to interfere with PDZ-mediated interactions in neurons: What we can learn from
682 the rabies virus. Progress in Biophysics and Molecular Biology, 119(1), 53–59.
683 https://doi.org/10.1016/j.pbiomolbio.2015.02.007

684 Carod-Artal, F. J. (2018). Infectious diseases causing autonomic dysfunction. Clinical Autonomic
685 Research, 28(1), 67–81. https://doi.org/10.1007/s10286-017-0452-4

686 Ceccaldi, P. E., Fillion, M. P., Ermine, A., Tsiang, H., & Fillion, G. (1993). Rabies virus selectively
687 alters 5-HT1 receptors subtypes in rat brain. European Journal of Pharmacology: Molecular
688 Pharmacology, 245(2), 129–138. https://doi.org/10.1016/0922-4106(93)90120-X

689 Chen, H., Lin, W., Zhang, Y., Lin, L., Chen, J., Zeng, Y., … Liu, N. (2016). IL-10 Promotes Neurite
690 Outgrowth and Synapse Formation in Cultured Cortical Neurons after the Oxygen-Glucose
691 Deprivation via JAK1/STAT3 Pathway. Scientific Reports, 6(July), 1–16.
692 https://doi.org/10.1038/srep30459

693 Clarkson, B. D. S., Kahoud, R. J., McCarthy, C. B., & Howe, C. L. (2017). Inflammatory cytokine-
694 induced changes in neural network activity measured by waveform analysis of high-content calcium

This is a provisional file, not the final typeset article

695 imaging in murine cortical neurons. Scientific Reports, 7(1), 1–13. https://doi.org/10.1038/s41598-
696 017-09182-5

697 Dacheux, L., Delmas, O., & Bourhy, H. (2011). Human rabies encephalitis prevention and treatment :
698 progress since Pasteur's discovery. Infect Disord Drug Targets, 11(2), 251–299. https://doi.org/doi:
699 10.2174/187152611795768079

700 Daems, C., Sékulic, M., Vulsteke, V., van Loo, G., D'Hooge, R., Callaerts-Végh, Z., & Callaerts, P.
701 (2020). A20/TNFAIP3 heterozygosity predisposes to behavioral symptoms in a mouse model for
702 neuropsychiatric lupus. Brain, Behavior, & Immunity - Health, 2(October 2019), 100018.
703 https://doi.org/10.1016/j.bbih.2019.100018

704 Davis, B. M., Rall, G. F., & Schnell, M. J. (2015). Everything You Always Wanted to Know about
705 Rabies Virus (But Were Afraid to Ask). Annual Review of Virology, 2, 451–471.
706 https://doi.org/10.1146/annurev-virology-100114-055157

707 De, A. (2011). Wnt/Ca2+ signaling pathway: a brief overview. Acta Biochimica et Biophysica
708 Sinica, 43(10), 745–756. Retrieved from https://doi.org/10.1093/abbs/gmr079

709 Denizot, M., Neal, J. W., & Gasque, P. (2012). Encephalitis due to emerging viruses: CNS innate
710 immunity and potential therapeutic targets. Journal of Infection, 65(1), 1–16.
711 https://doi.org/10.1016/j.jinf.2012.03.019

712 Dobin, A., Davis, C. A., Schlesinger, F., Drenkow, J., Zaleski, C., Jha, S., … Gingeras, T. R. (2013).
713 STAR: Ultrafast universal RNA-seq aligner. Bioinformatics, 29(1), 15–21.
714 https://doi.org/10.1093/bioinformatics/bts635

715 Dresselhaus, E. C., & Meffert, M. K. (2019). Cellular specificity of NF-κB function in the nervous
716 system. Frontiers in Immunology, 10(MAY). https://doi.org/10.3389/fimmu.2019.01043

717 Engelmann, C., & Haenold, R. (2016). Transcriptional Control of Synaptic Plasticity by
718 Transcription Factor NF-κB. Neural Plasticity, 2016. https://doi.org/10.1155/2016/7027949

719 Fatemi, S. H., Folsom, T. D., Rooney, R. J., & Thuras, P. D. (2013). MRNA and protein expression
720 for novel GABA A receptors θ and ρ2 are altered in schizophrenia and mood disorders; Relevance to
721 FMRP-mGluR5 signaling pathway. Translational Psychiatry, 3(April).
722 https://doi.org/10.1038/tp.2013.46

723 Fisher, C. R., Streicker, D. G., & Schnell, M. J. (2018). The spread and evolution of rabies virus:
724 Conquering new frontiers. Nature Reviews Microbiology, 16(4), 241–255.
725 https://doi.org/10.1038/nrmicro.2018.11

726 Fooks, A. R., Banyard, A. C., Horton, D. L., Johnson, N., McElhinney, L. M., & Jackson, A. C.
727 (2014). Current status of rabies and prospects for elimination. The Lancet, 384(9951), 1389–1399.
728 https://doi.org/10.1016/S0140-6736(13)62707-5

729 Fooks, A. R., Cliquet, F., Finke, S., Freuling, C., Hemachudha, T., Mani, R. S., … Banyard, A. C.
730 (2017). Rabies. Nature Reviews Disease Primers, 3. https://doi.org/10.1038/nrdp.2017.91

In review

731 Fu, Z. F., & Jackson, A. C. (2005). Neuronal dysfunction and death in rabies virus infection. Journal
732 of NeuroVirology, 11(1), 101–106. https://doi.org/10.1080/13550280590900445

733 Gallo, F. T., Katche, C., Morici, J. F., Medina, J. H., & Weisstaub, N. V. (2018). Immediate early
734 genes, memory and psychiatric disorders: Focus on c-Fos, Egr1 and Arc. Frontiers in Behavioral
735 Neuroscience, Vol. 12. https://doi.org/10.3389/fnbeh.2018.00079

736 Gerlier, D., & Lyles, D. S. (2011). Interplay between Innate Immunity and Negative-Strand RNA
737 Viruses: towards a Rational Model. Microbiology and Molecular Biology Reviews, 75(3), 468–490.
738 https://doi.org/10.1128/MMBR.00007-11

739 Giovannucci, A., Friedrich, J., Gunn, P., Kalfon, J., Brown, B. L., Koay, S. A., … Pnevmatikakis, E.
740 A. (2019). CaImAn an open source tool for scalable calcium imaging data analysis. ELife, 8, 1–45.
741 https://doi.org/10.7554/eLife.38173

742 Gourmelon, P., Briet, D., Clarençon, D., Court, L., & Tsiang, H. (1991). Sleep alterations in
743 experimental street rabies virus infection occur in the absence of major EEG abnormalities. Brain
744 Research, 554(1–2), 159–165. https://doi.org/10.1016/0006-8993(91)90184-W

745 Guo, Y., Duan, M., Wang, X., Gao, J., Guan, Z., & Zhang, M. (2019). Early events in rabies virus
746 infection—Attachment, entry, and intracellular trafficking. Virus Research, 263(September 2018),
747 217–225. https://doi.org/10.1016/j.virusres.2019.02.006

748 Habbas, S., Santello, M., Becker, D., Stubbe, H., Zappia, G., Liaudet, N., … Volterra, A. (2015).
749 Neuroinflammatory TNFα Impairs Memory via Astrocyte Signaling. Cell, 163(7), 1730–1741.
750 https://doi.org/10.1016/j.cell.2015.11.023

751 Hampson, K., Coudeville, L., Lembo, T., Sambo, M., Kieffer, A., Attlan, M., … Dushoff, J. (2015).
752 Estimating the Global Burden of Endemic Canine Rabies. PLoS Neglected Tropical Diseases, 9(4),
753 1–20. https://doi.org/10.1371/journal.pntd.0003709

754 Hardingham, G. E., Pruunsild, P., Greenberg, M. E., & Bading, H. (2017). Lineage divergence of
755 activity-driven transcription and evolution of cognitive ability. Nature Reviews Neuroscience.
756 https://doi.org/10.1038/nrn.2017.138

757 Harrison, A. R., Lieu, K. G., Larrous, F., Ito, N., Bourhy, H., & Moseley, G. W. (2020). Lyssavirus
758 P-protein selectively targets STAT3-STAT1 heterodimers to modulate cytokine signalling. PLoS
759 Pathogens, 16(9), 1–23. https://doi.org/10.1371/JOURNAL.PPAT.1008767

760 He, Y. J., Meghani, K., Caron, M. C., Yang, C., Ronato, D. A., Bian, J., … Chowdhury, D. (2018).
761 DYNLL1 binds to MRE11 to limit DNA end resection in BRCA1-deficient cells. Nature, 563(7732),
762 522–526. https://doi.org/10.1038/s41586-018-0670-5

763 Hemachudha, T., Ugolini, G., Wacharapluesadee, S., Sungkarat, W., Shuangshoti, S., &
764 Laothamatas, J. (2013). Human rabies: Neuropathogenesis, diagnosis, and management. The Lancet
765 Neurology, 12(5), 498–513. https://doi.org/10.1016/S1474-4422(13)70038-3

766 Iwata, M., Komori, S., Unno, T., Minamoto, N., & Ohashi, H. (1999). Modification of membrane
767 currents in mouse neuroblastoma cells following infection with rabies virus. British Journal of
768 Pharmacology, 1691–1698.

This is a provisional file, not the final typeset article

In review

769 Jackson, A. C. (2006). Rabies Virus Infection. In Current Therapy in Neurologic Disease (pp. 142–
770 144). https://doi.org/10.1016/b978-0-323-03432-6.50036-2

771 Jackson, A. C. (2014). Rabies. Handbook of Clinical Neurology, 123, 601–618.
772 https://doi.org/10.1016/B978-0-444-53488-0.00029-8

773 Jamalkandi, S. A., Mozhgani, S. H., Pourbadie, H. G., Mirzaie, M., Noorbakhsh, F., Vaziri, B., …
774 Jafari, M. (2016). Systems biomedicine of rabies delineates the affected signaling pathways.
775 Frontiers in Microbiology, 7, 1–22. https://doi.org/10.3389/fmicb.2016.01688

776 Jeanneteau, F., Barrére, C., Vos, M., De Vries, C. J. M., Rouillard, C., Levesque, D., … Arango-
777 Lievano, M. (2018). The stress-induced transcription factor NR4a1 adjusts mitochondrial function
778 and synapse number in prefrontal cortex. Journal of Neuroscience, 38(6), 1335–1350.
779 https://doi.org/10.1523/JNEUROSCI.2793-17.2017

780 Ji, Z., He, L., Regev, A., & Struhl, K. (2019). Inflammatory regulatory network mediated by the joint
781 action of NF-kB, STAT3, and AP-1 factors is involved in many human cancers. Proceedings of the
782 National Academy of Sciences of the United States of America, 116(19), 9453–9462.
783 https://doi.org/10.1073/pnas.1821068116

784 Kaltschmidt, B., & Kaltschmidt, C. (2009). NF-kB in the Nervous System. Cold Spring Harbor
785 Perspectives in Biology, 1(3), a001271–a001271. https://doi.org/10.1101/cshperspect.a001271

786 Kennedy, P. G. E. (2015). Viruses, apoptosis, and neuroinflammation--a double-edged sword.
787 Journal of Neurovirology, 21(1), 1–7. https://doi.org/10.1007/s13365-014-0306-y

788 Kesanakurti, D., Chetty, C., Rajasekhar Maddirela, D., Gujrati, M., & Rao, J. S. (2013). Essential
789 role of cooperative NF-κB and Stat3 recruitment to ICAM-1 intronic consensus elements in the
790 regulation of radiation-induced invasion and migration in glioma. Oncogene, 32(43), 5144–5155.
791 https://doi.org/10.1038/onc.2012.546

792 Khalifa, Y. B., Luco, S., Besson, B., Sonthonnax, F., Archambaud, M., Grimes, J. M., … Bourhy, H.
793 (2016). The matrix protein of rabies virus binds to RelAp43 to modulate NF-κB-dependent gene
794 expression related to innate immunity. Scientific Reports, 6(September), 1–13.
795 https://doi.org/10.1038/srep39420

796 Kidger, A. M., Rushworth, L. K., Stellzig, J., Davidson, J., Bryant, C. J., Bayley, C., … Caunt, C. J.
797 (2017). Dual-specificity phosphatase 5 controls the localized inhibition, propagation, and
798 transforming potential of ERK signaling. Proceedings of the National Academy of Sciences of the
799 United States of America, 114(3), E317–E326. https://doi.org/10.1073/pnas.1614684114

800 Kim, S. Y., Han, Y. M., Oh, M., Kim, W. K., Oh, K. J., Lee, S. C., … Han, B. S. (2015). DUSP4
801 regulates neuronal differentiation and calcium homeostasis by modulating ERK1/2 phosphorylation.
802 Stem Cells and Development, 24(6), 686–700. https://doi.org/10.1089/scd.2014.0434

803 Kirwan, P., Turner-Bridger, B., Peter, M., Momoh, A., Arambepola, D., Robinson, H. P. C., &
804 Livesey, F. J. (2015). Development and function of human cerebral cortex neural networks from
805 pluripotent stem cells *in vitro*. Development, 142(18), 3178–3187.
806 https://doi.org/10.1242/dev.123851

In review

807 Kodangattil, J. N., Möddel, G., Müller, M., Weber, W., & Gorji, A. (2012). The inflammatory
808 chemokine CXCL10 modulates synaptic plasticity and neuronal activity in the hippocampus.
809 European Journal of Inflammation, 10(3), 311–328. https://doi.org/10.1177/1721727X1201000307

810 Koraka, P., Martina, B. E. E., Van Den Ham, H.-J., Zaaraoui-Boutahar, F., Van Ijcken, W., Roose, J.,
811 … Osterhaus, A. D. M. E. (2018). Analysis of Mouse Brain Transcriptome After Experimental
812 Duvenhage Virus Infection Shows Activation of Innate Immune Response and Pyroptotic Cell Death
813 Pathway. Frontiers in Microbiology, 9. https://doi.org/10.3389/fmicb.2018.00397

814 Kouroupi, G., Taoufik, E., Vlachos, I. S., Tsioras, K., Antoniou, N., Papastefanaki, F., … Matsas, R.
815 (2017). Defective synaptic connectivity and axonal neuropathology in a human iPSC-based model of
816 familial Parkinson's disease. Proceedings of the National Academy of Sciences, E3679–E3688.
817 https://doi.org/10.1073/pnas.1617259114

818 Lacar, B., Linker, S. B., Jaeger, B. N., Krishnaswami, S., Barron, J., Kelder, M., … Gage, F. H.
819 (2016). Nuclear RNA-seq of single neurons reveals molecular signatures of activation. Nature
820 Communications, 7. https://doi.org/10.1038/ncomms11022

821 Langmead, B., Trapnell, C., Pop, M., & Salzberg, S. L. (2009). Ultrafast and memory-efficient
822 alignment of short DNA sequences to the human genome. Genome Biology, 10(3).
823 https://doi.org/10.1186/gb-2009-10-3-r25

824 Lehmann, M. H., Lehmann, J. M., & Erfle, V. (2019). Nef-induced CCL2 Expression Contributes to
825 HIV/SIV Brain Invasion and Neuronal Dysfunction. Frontiers in Immunology, 10(October), 1–10.
826 https://doi.org/10.3389/fimmu.2019.02447

827 Liao, Y., Smyth, G. K., & Shi, W. (2014). FeatureCounts: An efficient general purpose program for
828 assigning sequence reads to genomic features. Bioinformatics, 30(7), 923–930.
829 https://doi.org/10.1093/bioinformatics/btt656

830 Lieu, K. G., Brice, A., Wiltzer, L., Hirst, B., Jans, D. A., Blondel, D., & Moseley, G. W. (2013). The
831 Rabies Virus Interferon Antagonist P Protein Interacts with Activated STAT3 and Inhibits Gp130
832 Receptor Signaling. Journal of Virology, 87(14), 8261–8265. https://doi.org/10.1128/jvi.00989-13

833 Liu, D. D., Lu, J. M., Zhao, Q. R., Hu, C., & Mei, Y. A. (2016). Growth differentiation factor-15
834 promotes glutamate release in medial prefrontal cortex of mice through upregulation of T-Type
835 calcium channels. Scientific Reports, 6(June), 1–13. https://doi.org/10.1038/srep28653

836 Love, M. I., Huber, W., & Anders, S. (2014). Moderated estimation of fold change and dispersion for
837 RNA-seq data with DESeq2. Genome Biology, 15(12), 1–21. https://doi.org/10.1186/s13059-014-
838 0550-8

839 Luco, S., Delmas, O., Vidalain, P.-O., Tangy, F., Weil, R., & Bourhy, H. (2012). RelAp43, a
840 Member of the NF-κB Family Involved in Innate Immune Response against Lyssavirus Infection.
841 PLoS Pathogens, 8(12), e1003060. https://doi.org/10.1371/journal.ppat.1003060

842 Ludlow, M., Kortekaas, J., Herden, C., Hoffmann, B., Tappe, D., Trebst, C., … Osterhaus, A. D. M.
843 E. (2016). Neurotropic virus infections as the cause of immediate and delayed neuropathology. Acta
844 Neuropathologica, 131(2), 159–184. https://doi.org/10.1007/s00401-015-1511-3

In review

This is a provisional file, not the final typeset article

845 Lyles, D. S., Kuzmin, I. V., & Rupprecht, C. E. (2013). Rhabdoviridae. In D. M. Knipe & P. Howley
846 (Eds.), Fields Virology (6th ed.). LIPPINCOTT WILLIAMS & WILKINS.

847 Martín-Vicente, M., González-sanz, R., Cuesta, I., Monzón, S., Resino, S., & Martínez, I. (2020).
848 Downregulation of A20 expression increases the immune response and apoptosis and reduces virus
849 production in cells infected by the human respiratory syncytial virus. Vaccines, 8(1).
850 https://doi.org/10.3390/vaccines8010100

851 Martin, M. (2011). Cutadapt removes adapter sequences from high-throughput sequencing reads.
852 EMBnet.Journal, 17(1). https://doi.org/doi.org/10.14806/ej.17.1.200

853 Masatani, T., Ito, N., Ito, Y., Nakagawa, K., Abe, M., Yamaoka, S., … Sugiyama, M. (2013).
854 Importance of rabies virus nucleoprotein in viral evasion of interferon response in the brain.
855 Microbiology and Immunology, Vol. 57, pp. 511–517. https://doi.org/10.1111/1348-0421.12058

856 Miyamoto, Y., Torii, T., Tanoue, A., & Yamauchi, J. (2016). VCAM1 acts in parallel with CD69 and
857 is required for the initiation of oligodendrocyte myelination. Nature Communications, 7, 1–16.
858 https://doi.org/10.1038/ncomms13478

859 Nimmervoll, B., White, R., Yang, J. W., An, S., Henn, C., Sun, J. J., & Luhmann, H. J. (2013). LPS-
860 induced microglial secretion of TNFα increases activity-dependent neuronal apoptosis in the neonatal
861 cerebral cortex. Cerebral Cortex, 23(7), 1742–1755. https://doi.org/10.1093/cercor/bhs156

862 Ou, J. R., Tan, M. S., Xie, A. M., Yu, J. T., & Tan, L. (2014). Heat shock protein 90 in Alzheimer's
863 disease. BioMed Research International, 2014, 6–8. https://doi.org/10.1155/2014/796869

864 Pnevmatikakis, E. A. (2019). Analysis pipelines for calcium imaging data. Current Opinion in
865 Neurobiology, 55, 15–21. https://doi.org/10.1016/j.conb.2018.11.004

866 Préhaud, C., Wolff, N., Terrien, E., Lafage, M., Mégret, F., Babault, N., … Lafon, M. (2010).
867 Attenuation of rabies virulence: takeover by the cytoplasmic domain of its envelope protein. Science
868 Signaling, 3(August 2016), ra5. https://doi.org/10.1126/scisignal.2000510

869 Ramesh, G., MacLean, A. G., & Philipp, M. T. (2013). Cytokines and Chemokines at the Crossroads
870 of Neuroinflammation, Neurodegeneration, and Neuropathic Pain. Mediators of Inflammation, 2013,
871 1–20. https://doi.org/10.1155/2013/480739

872 Rogée, S., Larrous, F., Jochmans, D., Ben-Khalifa, Y., Neyts, J., & Bourhy, H. (2019).
873 Pyrimethamine inhibits rabies virus replication *in vitro*. Antiviral Research, 161(June 2018), 1–9.
874 https://doi.org/10.1016/j.antiviral.2018.10.016

875 Sato, M., Tanaka, H., Yanada, T., & Yamamoto, N. (1977). Archives of Virology Persistent Infection
876 of BHK 21/WI-2 Cells With Rubella Virus and Characterization of Rubella Variants. In Archives of
877 Virology (Vol. 5).

878 Sonthonnax, F., Besson, B., Bonnaud, E., Jouvion, G., Merino, D., Larrous, F., & Bourhy, H. (2019).
879 Lyssavirus matrix protein cooperates with phosphoprotein to modulate the Jak-Stat pathway.
880 Scientific Reports, 33(0), 1–13. https://doi.org/10.1038/s41598-019-48507-4

In review

881 Taniguchi, K., & Karin, M. (2018). NF-κB, inflammation, immunity and cancer: coming of age.
882 Nature Reviews Immunology. https://doi.org/10.1038/nri.2017.142

883 Tian, D., Luo, Z., Zhou, M., Li, M., Yu, L., Wang, C., … Zhao, L. (2016). Critical Role of K1685
884 and K1829 in the Large Protein of Rabies Virus in Viral Pathogenicity and Immune Evasion. Journal
885 of Virology, 90(1), 232–244. https://doi.org/10.1128/jvi.02050-15

886 Tsunoda, I. (2008). Axonal degeneration as a self-destructive defense mechanism against neurotropic
887 virus infection. Future Virology, 3(6), 579–593. https://doi.org/10.2217/17460794.3.6.579

888 Tullai, J. W., Schaffer, M. E., Mullenbrock, S., Sholder, G., Kasif, S., & Cooper, G. M. (2007).
889 Immediate-early and delayed primary response genes are distinct in function and genomic
890 architecture. Journal of Biological Chemistry, Vol. 282, pp. 23981–23995.
891 https://doi.org/10.1074/jbc.M702044200

892 Vidy, A., Chelbi-Alix, M., & Blondel, D. (2005). Rabies Virus P Protein Interacts with STAT1 and
893 Inhibits Interferon Signal Transduction Pathways. Journal of Virology, 79(22), 14411–14420.
894 https://doi.org/10.1128/jvi.79.22.14411-14420.2005

895 Wang, Z. W., Sarmento, L., Wang, Y., Li, X., Dhingra, V., Tseggai, T., … Fu, Z. F. (2005).
896 Attenuated Rabies Virus Activates , while Pathogenic Rabies Virus Evades , the Host Innate Immune
897 Responses in the Central Nervous System Attenuated Rabies Virus Activates , while Pathogenic
898 Rabies Virus Evades , the Host Innate Immune Responses in the Ce. Society, 79(19), 12554–12565.
899 https://doi.org/10.1128/JVI.79.19.12554

900 Webb, L. V., Ventura, S., & Ley, S. C. (2019). ABIN-2, of the TPL-2 Signaling Complex, Modulates
901 Mammalian Inflammation. Trends in Immunology, 40(9), 799–808.
902 https://doi.org/10.1016/j.it.2019.07.001

903 West, K. L., Kelliher, J. L., Xu, Z., An, L., Reed, M. R., Eoff, R. L., … Leung, J. W. C. (2019).
904 LC8/DYNLL1 is a 53BP1 effector and regulates checkpoint activation. Nucleic Acids Research,
905 47(12), 6236–6249. https://doi.org/10.1093/nar/gkz263

906 Wiltzer, Okada, K., Yamaoka, S., Larrous, F., Kuusisto, H. V., Sugiyama, M., … Moseley, G. W.
907 (2014). Interaction of Rabies Virus P-Protein With STAT Proteins is Critical to Lethal Rabies
908 Disease. Journal of Infectious Diseases, 209(November), 1744–1753.
909 https://doi.org/10.1093/infdis/jit829

910 Xiong, Y., Zhang, Y., Xiong, S., & Williams-Villalobo, A. E. (2020). A glance of p53 functions in
911 brain development, neural stem cells, and brain cancer. Biology, 9(9), 1–13.
912 https://doi.org/10.3390/biology9090285

913 Xu, D., Matsumoto, M. L., McKenzie, B. S., & Zarrin, A. A. (2018). TPL2 kinase action and control
914 of inflammation. Pharmacological Research, 129, 188–193.
915 https://doi.org/10.1016/j.phrs.2017.11.031

916 Zhang, D., He, F., Bi, S., Guo, H., Zhang, B., Wu, F., … Luo, Y. (2016). Genome-wide
917 transcriptional profiling reveals two distinct outcomes in central nervous system infections of rabies
918 virus. Frontiers in Microbiology, 7(MAY), 1–16. https://doi.org/10.3389/fmicb.2016.00751

In review

This is a provisional file, not the final typeset article

919 Zhang, Y., Chen, K., Sloan, S. A., Bennett, M. L., Scholze, A. R., O'Keeffe, S., … Wu, J. Q. (2014).
920 An RNA-Sequencing Transcriptome and Splicing Database of Glia, Neurons, and Vascular Cells of
921 the Cerebral Cortex. Journal of Neuroscience, 34(36), 11929–11947.
922 https://doi.org/10.1523/JNEUROSCI.1860-14.2014

923 Zhao, P., Zhao, L., Zhang, T., Qi, Y., Wang, T., Liu, K., … Xia, X. (2011). Innate immune response
924 gene expression profiles in central nervous system of mice infected with rabies virus. Comparative
925 Immunology, Microbiology and Infectious Diseases, 34, 503–512.
926 https://doi.org/10.1016/j.cimid.2011.09.003

In review

927 **Figure legends**

928

929 Figure 1. Global and specified GO analysis of DEGs upon Tha infection. (A) Venn diagram for the
930 number of genes that were significantly regulated at one time-point or more. (B-D) Subsets of
931 categorized GO terms identified with Tha-induced DEGs were presented in each panel. The GO
932 terms for Molecular Function (B) and Cellular Component (C) were selected by False Discovery
933 Rate (FDR) < 0.01, size of geneset from 20 to 200, or the number of DEGs > 5 for display. Twenty
934 GO terms from Biological Process were selected among the genesets that scored high Odds-ratios on
935 24hr and 40hr time-points, and displayed on (D). Full list of the selected GO terms for each
936 categories is provided in Supplementary Table 4. Biological Process was further filtered into 4
937 groups, Cell Cycle-related GO terms (E), Gene Expression (F), Immune Response (G), Neuronal
938 Function (H) and the number of up or down-regulated genes indicated in pie charts. The GO terms
939 that have Odds-ratios higher than 10, or FDR smaller than 0.05 on at least one time-point are
940 displayed in panels, and the full list the specified GO terms is provided in Supplementary Table 2.
941 The numbers in parentheses indicate the size of geneset for each GO term.

942

943 Figure 2. Comparison of Tha and Th4M dataset. (A) From 0 to 40 hpi, DEGs (in red) were
944 progressively selected more at the later time points. The common DEGs between two datasets were
945 marked with a larger dot in red, and DEGs unique to one dataset with a smaller dot in red. The exact
946 number of DEGs can be referred to Table 1. (B) Th4M dataset shares the majority of associated GO
947 terms (Biological Process) with Tha. As the number of DEGs increases over time, the shared GO
948 terms take the majority of ontology proportion at each dataset. At 8 hpi, Th4M shares 85% of its GO
949 terms with Tha, and at 24 hpi, Tha shares 85% of GO terms with Th4M due to their lower number of
950 DEGs compare to the opponent. At 40 hpi, both datasets share over 79% of GO terms with the other.
951 (C) The list of DEGs from all time-points that are only detected in Th4M dataset was crosschecked
952 with the relevant GO term subset. Both the GO subset and DEG crosscheck are provided in
953 Supplementary Table 6. (D) Crosscheck of unique DEGs in Th4M dataset with the relevant KEGG
954 pathway subset.

955

956 Figure 3. DEG heatmaps of RABV-associated KEGG pathways and the connection to the neuronal
957 function. (A) The relevant KEGG subset was crosschecked with DEGs from 24 hpi Tha dataset,
958 highlighting multiple pathways that are important to cell cycle, differentiation, signal transduction,
959 and immune response among others. (B) DEGs involved in NF-kB signaling (hsa04064) and the
960 expression level indicated in $\log_2$-fold changes. The time-points of significant selection were marked
961 with black dot. Examples of DEGs and their association with neuronal function-GO terms are
962 underlined at the base of figure. (C) DEGs detected in TNF signaling (hsa04668). (D) DEGs in IL-17
963 signaling (hsa04657). (E) DEGs detected in MAPK signaling (hsa04010). DEGs validated in RT-
964 qPCR for their expression at 40 hpi (displayed on Figure 4) are marked in bold font.

965

966 Figure 4. Validation of neuronal function-related DEGs with RT-qPCR at Tha- and Th4M-infected
967 condition and grouping in the associated pathways. (A) DEGs associated with MAPK signaling.
968 DUSP5, FOS, FOSB, JUNB are detected within KEGG MAPK signaling geneset, and the association

This is a provisional file, not the final typeset article

969 of the remaining group was identified using different tools for upstream search (refer to text). (B)
970 DEGs detected directly in KEGG NF-kB signaling geneset are NFKB1, NFKB2, RELB, NFKBIA,
971 TNFAIP3, ICAM1 and VCAM1. (C) STAT3 was directly detected in JAK-STAT KEGG geneset,
972 and the associations of SLC7A11 and HSP90AA1 were identified through upstream search. (D)
973 RABV RNA level was detected in RT-qPCR using N protein primers.

974

975 Figure 5. Decreased spontaneous activity in RABV-infected neurons. The hiPSC-derived NPCs were
976 differentiated into neurons for two weeks and then infected with Tha / Th4M virus for 5 days at MOI
977 3. (A) Examples of calcium imaging with Fluo-4 staining, representing 1.6% of field of view
978 (150X150 pixels out of 1360X1024). The individual soma marked with white arrows shows the
979 changing intensity in different time frames, and the total recording of 470 frames (frequency 1.72Hz,
980 100 frames approximately 1 minute) was compiled in video format and presented as Stack. (B) The
981 active / inactive neurons were counted from four experiments of non-infected / infected conditions
982 each, and presented as ratio in Min-Max box graph on the left. The neurons that has more than one
983 calcium peak above threshold ($\Delta F/F > 2\%$) were considered as active. The midline in the box
984 represents median value, and the box marks from 25% to 75% quantile values of each dataset.
985 Bartlett's test evaluated significant difference (P value < 0.001) between the conditions. On the right,
986 the rate of calcium peak from each soma were collected and presented in Min-Max box graph.
987 Student's t-test was performed to show the statistically significant difference (P value < 0.001)
988 between conditions. (C) From the representative field of view of each condition, individual calcium
989 peak of 200 somas over time were displayed as a dot in Raster plot. Notice the spontaneous activity
990 without global synchronization at all conditions, and also the density differences from one to another.
991 (D) Representative calcium traces from somas that are ranked as upper 5% in calcium peak
992 frequencies on each condition. (E) H9-NSC-derived neurons and the decreased spontaneous activity
993 on 2 days post-infection. The H9-NSCs derived into neurons for four weeks and then infected with
994 Tha virus for 2 days at MOI 1. On the left, the active / inactive neurons were counted from three
995 independent experiments and presented as ratio in Min-Max box graph. On the right, peak rate of
996 calcium oscillations from individual soma were collected and presented in Min-Max box graph. The
997 non-infected and infected samples showed statistical difference in Student's t-test (P value < 0.01),
998 while GABA-treated non-infected and infected samples presented stronger differences (P value <
999 0.0001). (F) Representative calcium traces of Tha-infected neurons with or without GABA treatment.
1000 GABA, Gamma-aminobutric acid; Bic, Bicuculline.

1001

1002 Table 1. DEG regulation in Tha and Th4M datasets. Number of up- and down-regulated genes are
1003 marked in parentheses.

DEGs in dataset	8hrs (up/down)	24hrs (up/down)	40hrs (up/down)
Tha	101 (19/82)	96 (55/41)	523 (210/313)
Th4M	18 (7/11)	419 (117/302)	624 (364/261)
Common genes	14 (5/9)	51 (32/19)	372 (145/227)

1004

In review

This is a provisional file, not the final typeset article

Figure 1.TIF

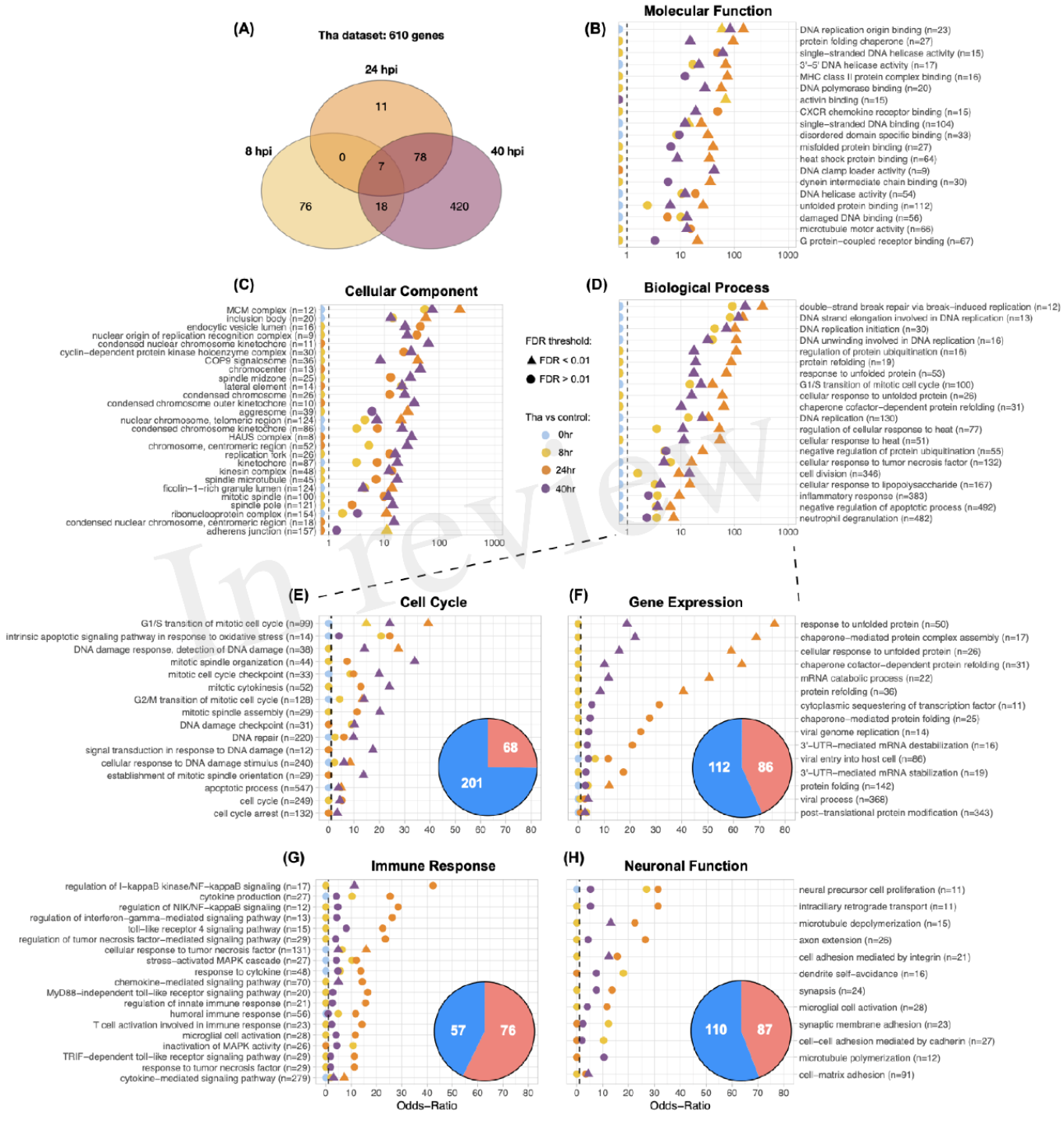

In review

Figure 2.TIF

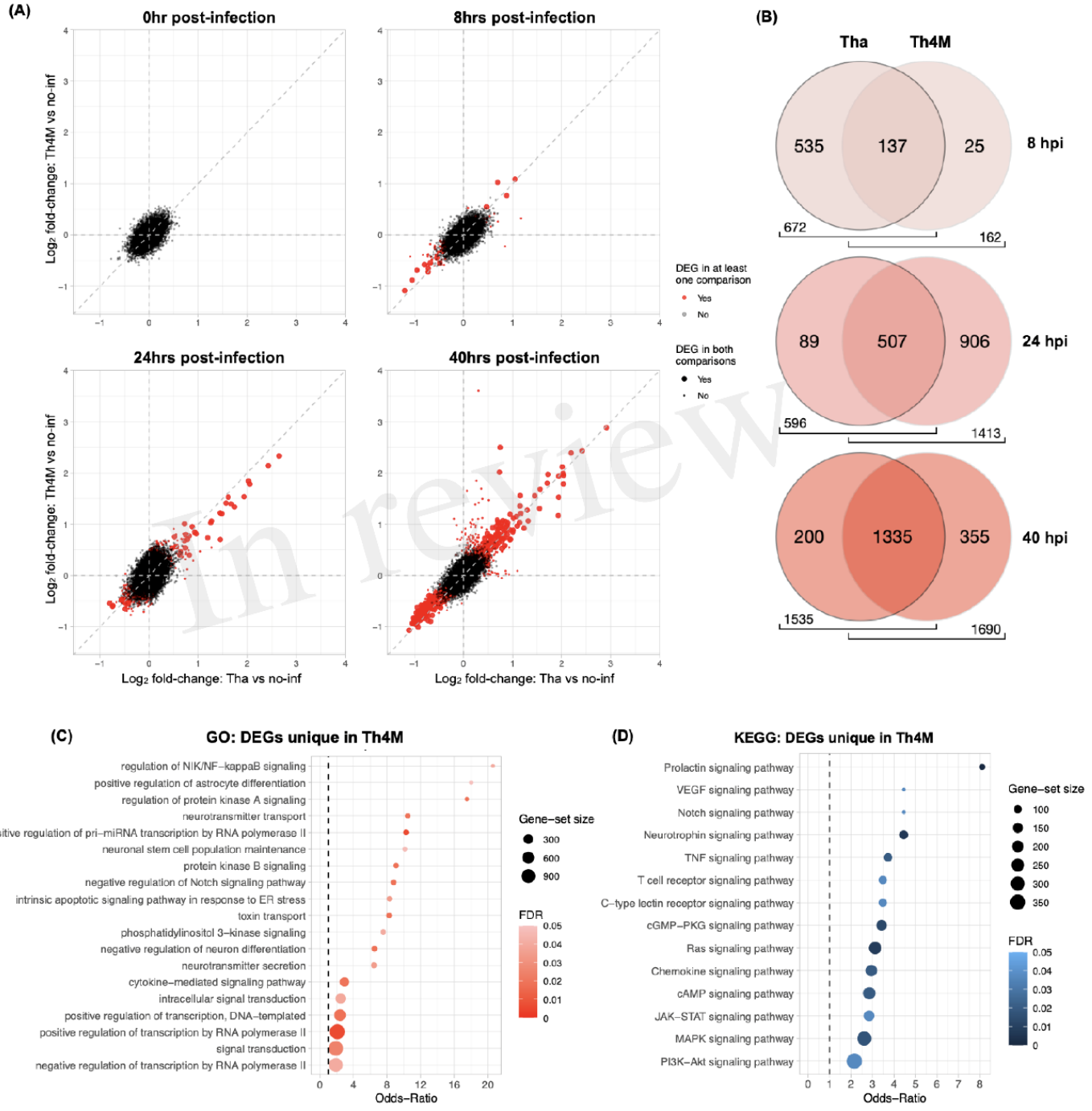

In review

Figure 3.TIF

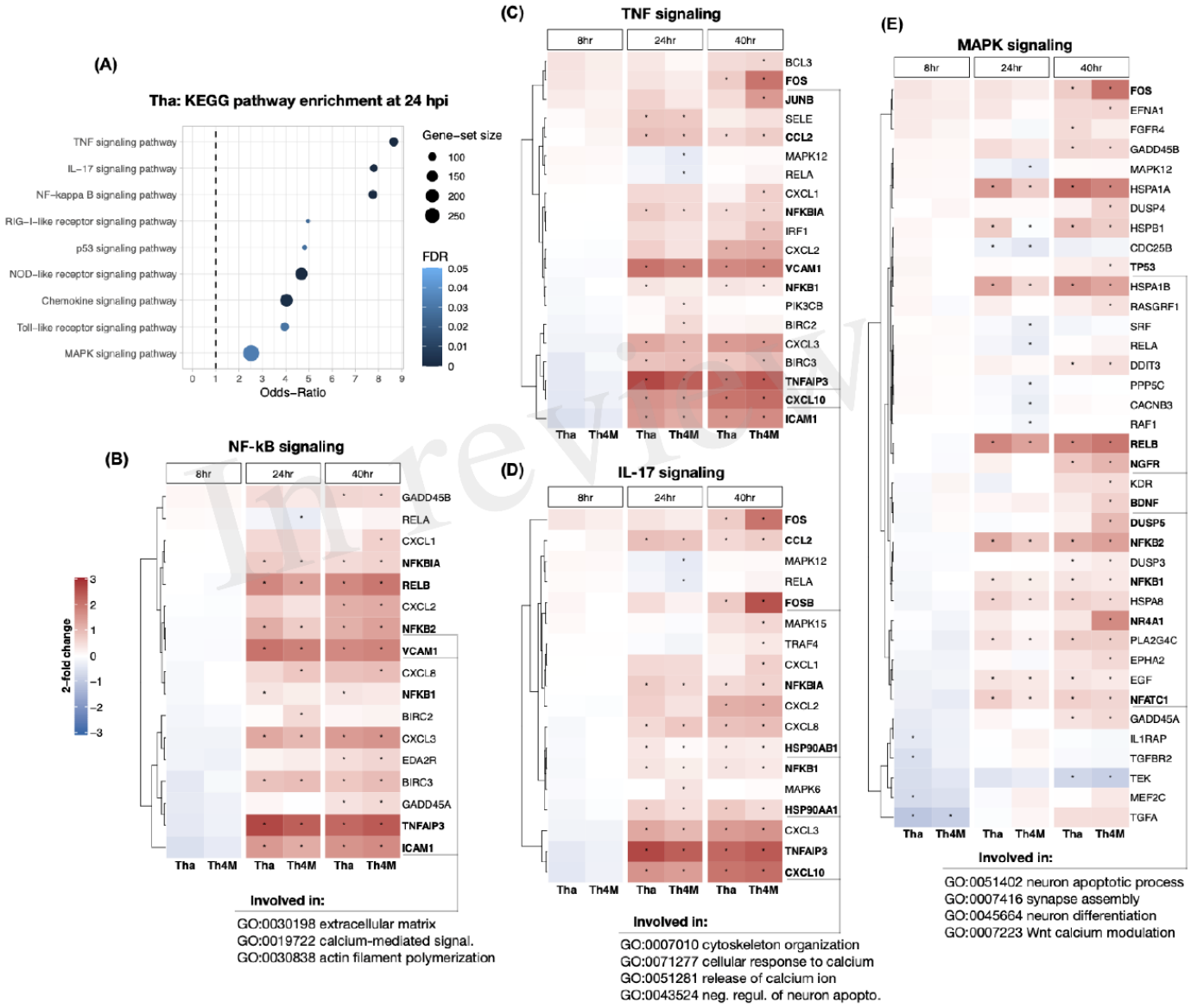
(A)
Tha: KEGG pathway enrichment at 24 hpi
TNF signaling pathway
IL−17 signaling pathway
NF−kappa B signaling pathway
RIG−I−like receptor signaling pathway
p53 signaling pathway
NOD−like receptor signaling pathway
Chemokine signaling pathway
Toll−like receptor signaling pathway
MAPK signaling pathway
Odds−Ratio
Gene−set size
FDR
(B)
NF-kB signaling
2−fold change
Involved in:
GO:0030198 extracellular matrix
GO:0019722 calcium-mediated signal.
GO:0030838 actin filament polymerization
(C)
TNF signaling
(D)
IL-17 signaling
Involved in:
GO:0007010 cytoskeleton organization
GO:0071277 cellular response to calcium
GO:0051281 release of calcium ion
GO:0043524 neg. regul. of neuron apopto.
(E)
MAPK signaling
Involved in:
GO:0051402 neuron apoptotic process
GO:0007416 synapse assembly
GO:0045664 neuron differentiation
GO:0007223 Wnt calcium modulation
8hr
24hr
40hr
Tha
Th4M

Figure 4.TIF

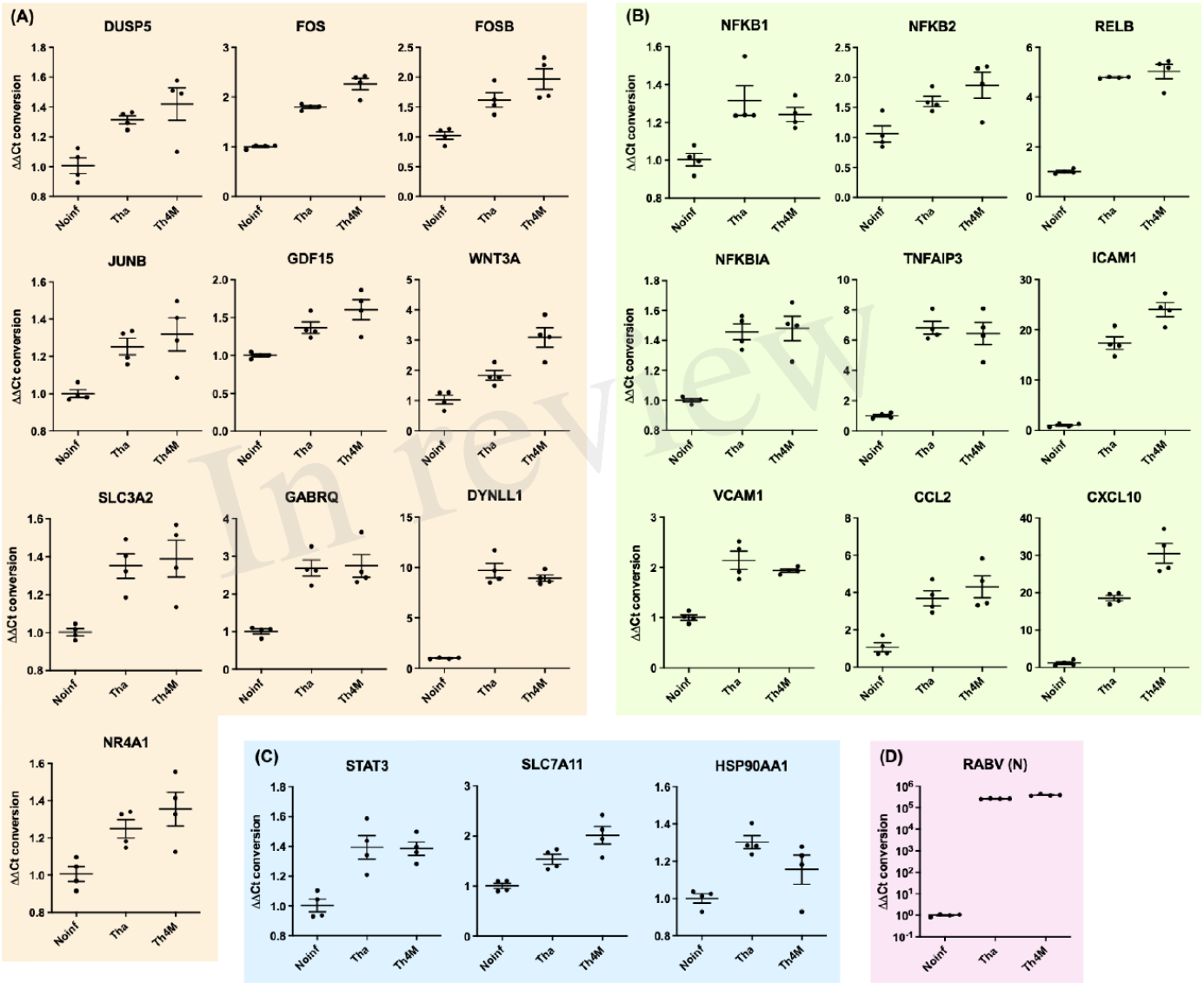

In review

Figure 5.TIF

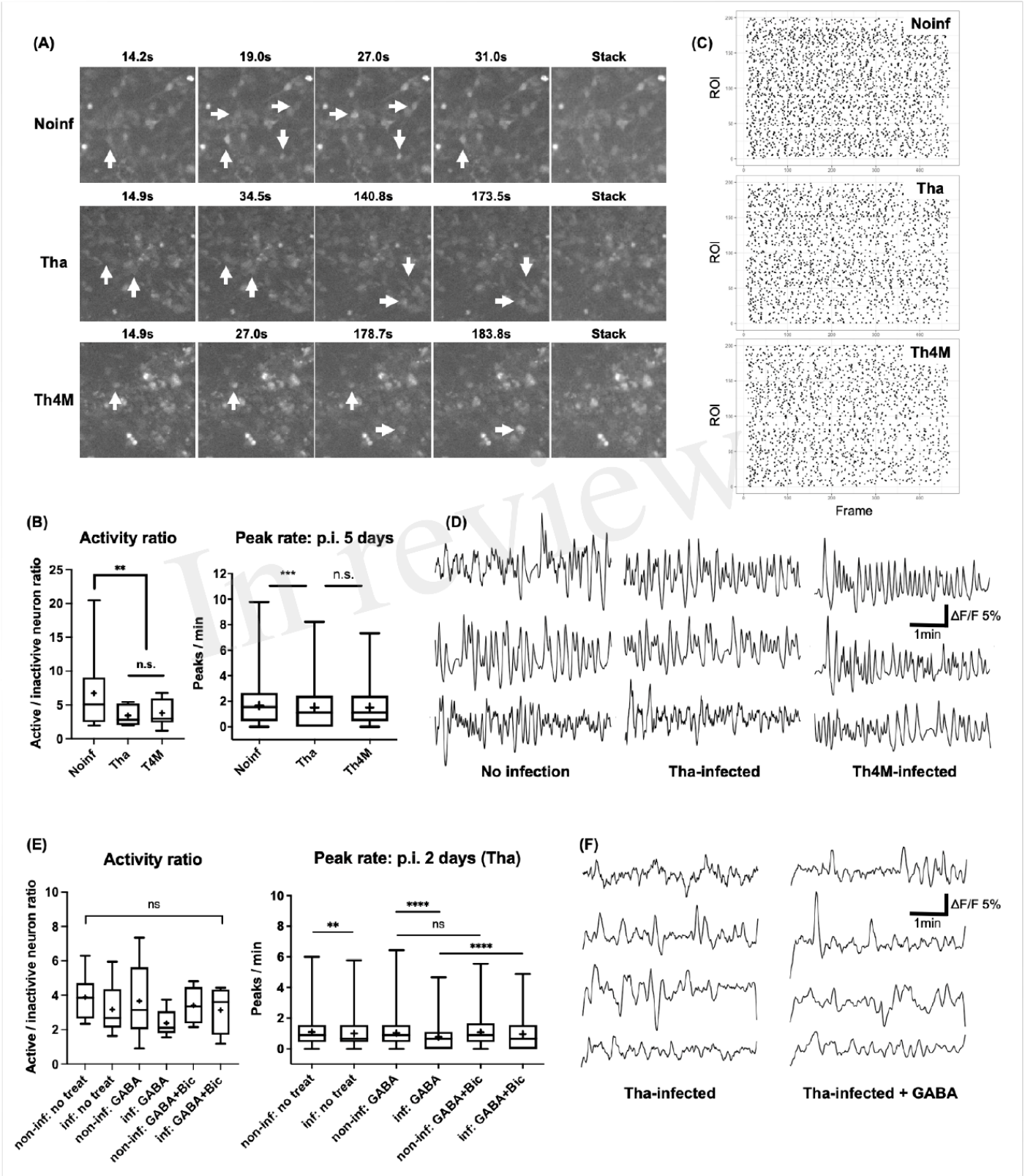

In review

Literature

1. Hampson K, Coudeville L, Lembo T, Sambo M, Kieffer A, Attlan M, et al. Estimating the Global Burden of Endemic Canine Rabies. PLoS Negl Trop Dis. 2015;9(4):1–20.
2. Baer GM. The Natural History of Rabies. Vol. 2nd editio, CRC Press. New York: Academic Press; 1975. 640 p.
3. Tarantola A. Four thousand years of concepts relating to rabies in animals and humans, its prevention and its cure. Trop Med Infect Dis. 2017;2(2).
4. Fooks AR, Banyard AC, Horton DL, Johnson N, Mcelhinney LM, Jackson AC. Current status of rabies and prospects for elimination. Lancet [Internet]. 2014;384(9951):1389–99. Available from: http://dx.doi.org/10.1016/S0140-6736(13)62707-5
5. Cleaveland S, Kaare M, Knobel D, Laurenson MK. Canine vaccination-Providing broader benefits for disease control. Vet Microbiol [Internet]. 2006 Oct 5 [cited 2021 Jun 15];117(1):43–50. Available from: https://pubmed.ncbi.nlm.nih.gov/16701966/
6. Murphy FA, Bauer SP. Early street rabies virus infection in striated muscle and later progression to the central nervous system. Intervirology. 1974;3(4):256–68.
7. Watson HD, Tignor GH, Smith AL. Entry of rabies virus into the peripheral nerves of mice. J Gen Virol. 1981 Oct;56(Pt 2):372–82.
8. Davis BM, Rall GF, Schnell MJ. Everything You Always Wanted to Know About Rabies Virus (But Were Afraid to Ask). Annu Rev Virol. 2015 Nov;2(1):451–71.
9. Ugolini G. Rabies virus as a transneuronal tracer of neuronal connections. Adv Virus Res. 2011;79:165–202.
10. Ceccaldi PE, Gillet JP, Tsiang H. Inhibition of the transport of rabies virus in the central nervous system. J Neuropathol Exp Neurol. 1989 Nov;48(6):620–30.
11. World Health Organization. WHO Expert Consultation on Rabies. Second report. World Health Organization technical report series. 2013.
12. Eke CB, Omotowo IB, Ukoha OM, Ibe BC. Human rabies: Still a neglected preventable disease in Nigeria. Niger J Clin Pract. 2015;18(2):268–72.
13. Organization WH. WHO expert consultation on rabies: third report [Internet]. Geneva PP - Geneva: World Health Organization; 2018. (WHO technical report series;1012).

Available from: https://apps.who.int/iris/handle/10665/272364

14. Knobel DL, Cleaveland S, Coleman PG, Fèvre EM, Meltzer MI, Miranda MEG, et al. Re-evaluating the burden of rabies in Africa and Asia. Bull World Health Organ. 2005 May;83(5):360–8.

15. Mallewa M, Fooks AR, Banda D, Chikungwa P, Mankhambo L, Molyneux E, et al. Rabies encephalitis in malaria-endemic area, Malawi, Africa. Emerg Infect Dis. 2007;13(1):136–9.

16. Zeiler FA, Jackson AC. Critical Appraisal of the Milwaukee Protocol for Rabies: This Failed Approach Should Be Abandoned. Can J Neurol Sci Le J Can des Sci Neurol. 2016 Jan;43(1):44–51.

17. Preiss S, Chanthavanich P, Chen LH, Marano C, Buchy P, van Hoorn R, et al. Post-exposure prophylaxis (PEP) for rabies with purified chick embryo cell vaccine: a systematic literature review and meta-analysis [Internet]. Vol. 17, Expert Review of Vaccines. Taylor and Francis Ltd; 2018 [cited 2021 Jun 15]. p. 525–45. Available from: https://pubmed.ncbi.nlm.nih.gov/29939085/

18. World Health Organization. WHO Expert Consultation on Rabies. Third report. World Health Organization technical report series. 2018.

19. O'Brien KL, Nolan T. The WHO position on rabies immunization – 2018 updates [Internet]. Vol. 37, Vaccine. Elsevier Ltd; 2019 [cited 2021 Jun 4]. p. A85–7. Available from: https://pubmed.ncbi.nlm.nih.gov/30342901/

20. WHO. World Health Organization Expert Consultation on Rabies. Second report: Technical ReportSeries 982. [Internet]. Geneva, Switzerland, Switzerland; 2013. Available from: http://www.pimr.org.in/Barecha.PDF

21. Diallo MK, Diallo AO, Dicko A, Richard V, Espié E. Human rabies post exposure prophylaxis at the Pasteur Institute of Dakar, Senegal: Trends and risk factors. BMC Infect Dis [Internet]. 2019 Apr 11 [cited 2021 Jun 15];19(1):1–9. Available from: https://doi.org/10.1186/s12879-019-3928-0

22. Baxter JM. One in a million, or one in thousand: What is the morbidity of rabies in India? J Glob Health. 2012;2(1):1–4.

23. Hampson K, Dushoff J, Cleaveland S, Haydon DT, Kaare M, Packer C, et al. Transmission dynamics and prospects for the elimination of canine Rabies. PLoS Biol. 2009;7(3):0462–71.

24. Coleman PG, Fèvre EM, Cleaveland S. Estimating the Public Health Impact of Rabies. Emerg Infect Dis. 2004;10(1):140–2.

25. Dale JL, Peters D. Protein Composition of the Virions of Five Plant Rhabdoviruses. Intervirology [Internet]. 1981;16(2):86–94. Available from: https://www.karger.com/DOI/10.1159/000149252

26. Walker PJ, Byrne KA, Riding GA, Cowley JA, Wang Y, McWilliam S. The genome of bovine ephemeral fever rhabdovirus contains two related glycoprotein genes. Virology. 1992;191(1):49–61.

27. Walker PJ, Wang Y, Cowley JA, McWilliam SM, Prehaud CJN. Structural and antigenic analysis of the nucleoprotein of bovine ephemeral fever rhabdovirus. J Gen Virol. 1994;75(8):1889–99.

28. McWilliam SM, Kongsuwan K, Cowley JA, Byrne KA, Walker PJ. Genome organization and transcription strategy in the complex G(NS)-L intergenic region of bovine ephemeral fever rhabdovirus. J Gen Virol. 1997;78(6):1309–17.

29. Wang Y, McWilliam SM, Cowley JA, Walker PJ. Complex Genome Organization in the GNS-L Intergenic Region of Adelaide River Rhabdovirus. Vol. 203, Virology. 1994. p. 63–72.

30. Basurco B, Benmansour A. Distant Strains of the Fish Rhabdovirus VHSV Maintain a Sixth Functional Cistron Which Codes for a Nonstructural Protein of Unknown Function. Virology. 1995;212(2):741–5.

31. Bourhy H, Cowley JA, Larrous F, Holmes EC, Walker PJ. Phylogenetic relationships among rhabdoviruses inferred using the L polymerase gene. J Gen Virol. 2005;86(10):2849–58.

32. Poch O, Sauvaget I, Delarue M, Tordo N. Identification of four conserved motifs among the RNA-dependent polymerase encoding elements. EMBO J. 1989;8(12):3867–74.

33. Xiong Y, Eickbush TH. Origin and evolution of retroelements based upon their reverse transcriptase sequences. EMBO J. 1990;9(10):3353–62.

34. Sleat DE, Banerjee AK. Transcriptional activity and mutational analysis of recombinant vesicular stomatitis virus RNA polymerase. J Virol. 1993;67(3):1334–9.

35. Walker PJ, Firth C, Widen SG, Blasdell KR, Guzman H, Wood TG, et al. Evolution of genome size and complexity in the rhabdoviridae. PLoS Pathog. 2015 Feb;11(2):e1004664.

36. Walker PJ, Blasdell KR, Calisher CH, Dietzgen RG, Kondo H, Kurath G, et al. ICTV virus taxonomy profile: Rhabdoviridae. J Gen Virol. 2018;99(4):447–8.

37. Kuzmin I V., Orciari LA, Arai YT, Smith JS, Hanlon CA, Kameoka Y, et al. Bat lyssaviruses (Aravan and Khujand) from Central Asia: Phylogenetic relationships according to N, P and G gene sequences. Virus Res. 2003;97(2):65–79.

38. Bourhy H, Kissi B, Tordo N. Molecular diversity of the lyssavirus genus. Vol. 194, Virology. 1993. p. 70–81.

39. Hayman DTS, Fooks AR, Marston DA, Garcia-R JC. The Global Phylogeography of Lyssaviruses - Challenging the “Out of Africa” Hypothesis. PLoS Negl Trop Dis. 2016;10(12):1–13.

40. Badrane H, Bahloul C, Perrin P, Tordo N. Evidence of Two Lyssavirus Phylogroups with Distinct Pathogenicity and Immunogenicity. J Virol [Internet]. 2001;75(7):3268–76. Available from: https://www.ncbi.nlm.nih.gov/pubmed/11238853

41. Rupprecht CE, Diretzschold B, Wunner WH, Kaprowski H. Antigenic relationships of lyssaviruses. In: The Natural History of Rabies. 1991. p. 69–100.

42. Fooks AR. The challenge of new and emerging lyssaviruses. Expert Rev Vaccines. 2004;3(4):333–6.

43. Fekadu M, Shaddock JH, Sanderlin DW, Smith JS. Efficacy of rabies vaccines against Duvenhage virus isolated from European house bats (Eptesicus serotinus), classic rabies and rabies-related viruses. Vaccine. 1988;6(6):533–9.

44. Bahloul C, Jacob Y, Tordo N, Perrin P. DNA-based immunization for exploring the enlargement of immunological cross-reactivity against the lyssaviruses. Vaccine. 1998;16(4):417–25.

45. Srinivasan A, Burton EC, Kuehnert MJ, Rupprecht C, Sutker WL, Ksiazek TG, et al. Transmission of Rabies Virus from an Organ Donor to Four Transplant Recipients. N Engl J Med [Internet]. 2005 Mar 17 [cited 2018 Mar 22];352(11):1103–11. Available from: http://www.ncbi.nlm.nih.gov/pubmed/15784663

46. Badrane H. Host Switching in Lyssavirus History from Chiroptera to the Carnivora Orders. J Virol. 2001;75(17):8096–104.

47. Nadin-Davis SA. Molecular Epidemiology [Internet]. Third Edit. Rabies. Elsevier Inc.; 2013. 123–177 p. Available from: http://dx.doi.org/10.1016/B978-0-12-396547-9.00004-3

48. Hanlon CA. Rabies in Terrestrial Animals. Rabies. 2013. 179–213 p.

49. Banyard AC, Hayman DTS, Freuling CM, Müller T, Fooks AR, Johnson N. Bat Rabies. Rabies. 2013. 215–267 p.

50. Finke S, Conzelmann K-K. Replication strategies of rabies virus. Virus Res [Internet]. 2005 Aug;111(2):120–31. Available from: http://www.sciencedirect.com/science/article/pii/S0168170205001188

51. Albertini AAV, Ruigrok RWH, Blondel D. Rabies Virus Transcription and Replication [Internet]. Vol. 79, Advances in Virus Research. 2011 [cited 2021 Jun 2]. 1–22 p. Available from: https://pubmed.ncbi.nlm.nih.gov/21601039/

52. Tordo N, Poch O. Structure of Rabies Virus. In: Campbell JB, Charlton KM, editors. Rabies Developments in Veterinary Virology. Volume 7. Boston, MA: Springer; 1988. p. 25–45.

53. Tordo N, Poch O, Ermine A, Keith G, Rougeon F. Completion of the rabies virus genome sequence determination: Highly conserved domains among the L (polymerase) proteins of unsegmented negative-strand RNA viruses. Virology. 1988;165(2):565–76.

54. Tordo N, Poch O, Ermine A, Keith G. Primary structure of leader RNA and nucleoprotein genes of the rabies genome: Segmented homology with VSV. Nucleic Acids Res. 1986;14(6):2671–83.

55. Tordo N, Poch O. Strong and weak transcription signals within the rabies genome. Virus Res. 1988;Sup.2:30.

56. Morimoto K, Ohkubo A, Kawai A. Structure and transcription of the glycoprotein gene of attenuated HEP-Flury strain of rabies virus. Virology. 1989;173(2):465–77.

57. Sacramento D, Bourhy H, Tordo N. PCR technique as an alternative method for diagnosis and molecular epidemiology of rabies virus. Mol Cell Probes. 1991;5(3):229–40.

58. Dietzgen RG. Morphology, genome organization, transcription and replication of rhabdoviruses. In: Rhabdoviruses: Molecular taxonomy, evolution, genomics, ecology, host-vector interactions, cytopathology and control [Internet]. 2012 [cited 2021 Jun 15]. p. 5–11. Available from: https://espace.library.uq.edu.au/view/UQ:281214

59. Superti F, Derer M, Tsiang H. Mechanism of rabies virus entry into CER cells. J Gen Virol. 1984;65(4):781–9.

60. Gaudin Y. Rabies virus-induced membrane fusion pathway. J Cell Biol. 2000;150(3):601–11.

61. Roche S, Gaudin Y. Evidence that Rabies Virus Forms Different Kinds of Fusion Machines with Different pH Thresholds for Fusion. J Virol. 2004;78(16):8746–52.

62. Piccinotti S, Whelan SPJ. Rabies Internalizes into Primary Peripheral Neurons via Clathrin Coated Pits and Requires Fusion at the Cell Body. Heise MT, editor. PLOS Pathog [Internet]. 2016 Jul 27 [cited 2018 Mar 22];12(7):e1005753. Available from: http://dx.plos.org/10.1371/journal.ppat.1005753

63. Lewis P, Lentz TL. Rabies virus entry into cultured rat hippocampal neurons. J Neurocytol. 1998;27(8):559–73.

64. Piccinotti S, Kirchhausen T, Whelan SPJ. Uptake of Rabies Virus into Epithelial Cells by Clathrin-Mediated Endocytosis Depends upon Actin. J Virol. 2013;87(21):11637–47.

65. Anggono V, Robinson PJ. Dynamin. Encycl Neurosci [Internet]. 2009 Jan 1 [cited 2020 Apr 10];725–35. Available from: https://www.sciencedirect.com/science/article/pii/B9780080450469013632?via%3Dihub

66. Lentz TL, Burrage TG, Smith AL, Crick J, Tignor GH. Is the acetylcholine receptor a rabies virus receptor? Science [Internet]. 1982 Jan 8 [cited 2018 Mar 22];215(4529):182–4. Available from: http://www.ncbi.nlm.nih.gov/pubmed/7053569

67. Thoulouze MI, Lafage M, Schachner M, Hartmann U, Cremer H, Lafon M. The neural cell adhesion molecule is a receptor for rabies virus. J Virol [Internet]. 1998 Sep [cited 2018 Mar 22];72(9):7181–90. Available from: http://www.ncbi.nlm.nih.gov/pubmed/9696812

68. Tuffereau C, Bénéjean J, Blondel D, Kieffer B, Flamand A. Low-affinity nerve-growth factor receptor (P75NTR) can serve as a receptor for rabies virus. EMBO J [Internet]. 1998 Dec 15 [cited 2018 Mar 22];17(24):7250–9. Available from: http://www.ncbi.nlm.nih.gov/pubmed/9857182

69. Wang J, Wang Z, Liu R, Shuai L, Wang X, Luo J, et al. Metabotropic glutamate receptor subtype 2 is a cellular receptor for rabies virus. 2018;2:1–21.

70. Pulmanausahakul R, Li J, Schnell MJ, Dietzschold B. The Glycoprotein and the Matrix Protein of Rabies Virus Affect Pathogenicity by Regulating Viral Replication and Facilitating Cell-to-Cell Spread. J Virol [Internet]. 2008 Mar 1 [cited 2018 Mar

31];82(5):2330–8. Available from: http://www.ncbi.nlm.nih.gov/pubmed/18094173

71. Velandia MLMML, Pérez-Castro R, Hurtado H, Castellanos JJEJ. Ultrastructural description of rabies virus infection in cultured sensory neurons. Mem Inst Oswaldo Cruz [Internet]. 2007 Oct 19 [cited 2018 Jun 13];102(4):441–7. Available from: http://www.scielo.br/scielo.php?script=sci_arttext&pid=S0074-02762007000400003&lng=en&tlng=en

72. Flamand A, Delagneau JF, Bussereau F. An RNA polymerase activity in purified rabies virions. J Gen Virol. 1978;40(1):233–8.

73. Flamand A, Delagneau JF. Transcriptional mapping of rabies virus in vivo. J Virol. 1978;28(2):518–23.

74. Bourhy H, Tordo N, Lafon M, Sureau P. Complete cloning and molecular organization of a rabies-related virus, Mokola virus. J Gen Virol. 1989;70(8):2063–74.

75. Tordo N, Kouknetzoff A. The rabies virus genome: an overview. Onderstepoort J Vet Res. 1993;60(4):263–9.

76. Charlton KM. The pathogenesis of rabies and other lyssaviral infections: recent studies. Curr Top Microbiol Immunol. 1994;187:95–119.

77. Messenger SL, Smith JS, Rupprecht CE. Emerging Epidemiology of Bat-Associated Cryptic Cases of Rabies in Humans in the United States. Clin Infect Dis. 2002;35(6):738–47.

78. Zhang J, Lin J, Tian Y, Ma L, Sun W, Zhang L, et al. Transmission of rabies through solid organ transplantation: A notable problem in China. BMC Infect Dis. 2018;18(1):1–6.

79. Maier T, Schwarting A, Mauer D, Ross RS, Martens A, Kliem V, et al. Management and Outcomes after Multiple Corneal and Solid Organ Transplantations from a Donor Infected with Rabies Virus. Clin Infect Dis [Internet]. 2010 Apr 15 [cited 2018 Mar 22];50(8):1112–9. Available from: http://www.ncbi.nlm.nih.gov/pubmed/20205588

80. Vora NM, Orciari LA, Niezgoda M, Selvaggi G, Stosor V, Lyon GM, et al. Clinical management and humoral immune responses to rabies post-exposure prophylaxis among three patients who received solid organs from a donor with rabies. Transpl Infect Dis [Internet]. 2015 Jun [cited 2018 Mar 22];17(3):389–95. Available from: http://www.ncbi.nlm.nih.gov/pubmed/25851103

81. Chen S, Zhang H, Luo M, Chen J, Yao D, Chen F, et al. Rabies Virus Transmission in

Solid Organ Transplantation, China, 2015–2016. Emerg Infect Dis [Internet]. 2017 Sep [cited 2018 Mar 22];23(9):1600–2. Available from: http://www.ncbi.nlm.nih.gov/pubmed/28820377

82. Johnson N, Phillpotts R, Fooks AR. Airborne transmission of lyssaviruses. J Med Microbiol [Internet]. 2006 Jun 1 [cited 2018 Mar 22];55(6):785–90. Available from: http://www.ncbi.nlm.nih.gov/pubmed/16687600

83. Winkler WG, Baker EF, Hopkins CC. An outbreak of non-bite transmitted rabies in a laboratory animal colony. Am J Epidemiol [Internet]. 1971 Mar [cited 2018 Mar 22];95(8):267–77. Available from: http://www.ncbi.nlm.nih.gov/pubmed/4551654

84. Winkler WG, Fashinell TR, Leffingwell L, Howard P, Conomy P. Airborne rabies transmission in a laboratory worker. JAMA [Internet]. 1973 Dec 3 [cited 2018 Mar 22];226(10):1219–21. Available from: http://www.ncbi.nlm.nih.gov/pubmed/4800498

85. Davis AD, Rudd RJ, Bowen RA. Effects of Aerosolized Rabies Virus Exposure on Bats and Mice. J Infect Dis. 2007;195(8):1144–50.

86. Zhu J, Pan J, Lu Y. A case report on indirect transmission of human rabies. Vol. 16, Journal of Zhejiang University. Science. B. 2015. p. 969–70.

87. Lafon M. Rabies virus receptors. J Neurovirol. 2005 Feb;11(1):82–7.

88. Tsiang H. Evidence for an intraaxonal transport of fixed and street rabies virus. J Neuropathol Exp Neurol [Internet]. 1979 May [cited 2018 Mar 22];38(3):286–99. Available from: http://www.ncbi.nlm.nih.gov/pubmed/86604

89. Lycke E, Tsiang H. Rabies virus infection of cultured rat sensory neurons. J Virol [Internet]. 1987 Sep 1 [cited 2018 Mar 22];61(9):2733–41. Available from: http://www.ncbi.nlm.nih.gov/pubmed/2441076

90. Gillet JP, Derer P, Tsiang H. Axonal transport of rabies virus in the central nervous system of the rat. J Neuropathol Exp Neurol [Internet]. 1986 Nov [cited 2018 Mar 22];45(6):619–34. Available from: http://www.ncbi.nlm.nih.gov/pubmed/2430067

91. Kucera P, Dolivo M, Coulon P, Flamand A. Pathways of the early propagation of virulent and avirulent rabies strains from the eye to the brain. J Virol. 1985;55(1):158–62.

92. Lahaye X, Vidy A, Pomier C, Obiang L, Harper F, Gaudin Y, et al. Functional Characterization of Negri Bodies (NBs) in Rabies Virus-Infected Cells: Evidence that NBs Are Sites of Viral Transcription and Replication. J Virol [Internet]. 2009 Aug 15 [cited 2018 Mar 22];83(16):7948–58. Available from:

http://www.ncbi.nlm.nih.gov/pubmed/19494013

93. Charlton KM, Casey GA, Campbell JB. Experimental rabies in skunks: immune response and salivary gland infection. Comp Immunol Microbiol Infect Dis [Internet]. 1987 [cited 2018 Mar 22];10(3–4):227–35. Available from: http://www.ncbi.nlm.nih.gov/pubmed/3427891

94. Charlton KM, Casey GA, Wandeler AI, Nadin-Davis S. Early events in rabies virus infection of the central nervous system in skunks (Mephitis mephitis). Acta Neuropathol. 1995;91(1):89–98.

95. Tirawatnpong S, Hemachudha T, Manutsathit S, Shuangshoti S, Phanthumchinda K, Phanuphak P. Regional distribution of rabies viral antigen in central nervous system of human encephalitic and paralytic rabies. J Neurol Sci. 1989;92(1):91–9.

96. Laothamatas J, Hemachudha T, Mitrabhakdi E, Wannakrairot P, Tulayadaechanont S. MR imaging in human rabies. AJNR Am J Neuroradiol. 2003;24(6):1102–9.

97. Fishbein D, Bernard K. Rabies Virus. In: Bennett's Principles and Practice of Infectious Diseases. Eighth Edi. 1995. p. 1527–43.

98. Smith JS, Fishbein DB, Rupprecht CE, Clark K. Unexplained rabies in three immigrants in the United States. A virological Investigation. N Engl J Med. 1991;324(4):205–11.

99. Hemachudha T, Phuapradit P. Rabies. Curr Opin Neurol. 1997 Jun;10(3):260–7.

100. Hemachudha T, Laothamatas J, Rupprecht CE. Human rabies: A disease of complex neuropathogenetic mechanisms and diagnostic challenges. Lancet Neurol. 2002;1(2):101–9.

101. Huang CC, Liu CC, Chang YC, Chen CY, Wang ST, Yeh TF. Neurologic complications in children with enterovirus 71 infection. N Engl J Med. 1999;341(13):936–42.

102. Goh KJ, Tan CT, Chew NK, Tan PSK, Kamarulzaman A, Sarji SA, et al. Clinical features of Nipah virus encephalitis among pig farmers in Malaysia. N Engl J Med. 2000;342(17):1229–35.

103. Solomon T, Dung NM, Kneen R, Gainsborough M, Vaughn DW, Khanh VT. Japanese encephalitis. J Neurol Neurosurg Psychiatry. 2000;68(4):405–15.

104. Hemachudha T, Ugolini G, Wacharapluesadee S, Sungkarat W, Shuangshoti S, Laothamatas J. Human rabies: neuropathogenesis, diagnosis, and management. Lancet Neurol [Internet]. 2013 May [cited 2018 Mar 22];12(5):498–513. Available from:

http://www.ncbi.nlm.nih.gov/pubmed/23602163

105. Mitrabhakdi E, Shuangshoti S, Wannakrairot P, Lewis RA, Susuki K, Laothamatas J, et al. Difference in neuropathogenetic mechanisms in human furious and paralytic rabies. J Neurol Sci. 2005 Nov;238(1–2):3–10.

106. Chopra JS, Banerjee AK, Murthy JMKK, Pal SR. Paralytic rabies: A clinico-pathological study. Brain. 1980;103(4):789–802.

107. Jamadagni SB, Singh CK, Sandhu BS. Histopathological alterations in brains of rabies infected buffaloes and cattle. Ital J Anim Sci. 2007;6(SUPPL. 2):872–4.

108. Farahtaj F, Alizadeh L, Gholami A, Tahamtan A, Shirian S, Fazeli M, et al. Natural infection with rabies virus: A histopathological and immunohistochemical study of human brains. Osong Public Heal Res Perspect. 2019;10(1):6–11.

109. Perl D, Good P. The pathology of rabies in the central nervous system. In: The Natural History of Rabies, CRC Press, Boca, Raton. 1991. p. 163–90.

110. Zivadinov R, Bakshi R. Role of MRI in multiple sclerosis I: inflammation and lesions. Front Biosci. 2004 Jan;9:665–83.

111. Tangchai P, Yenbutr D, Vejjajjva A. Central nervous system lesions in human rabies. A study of twenty-four cases. J Med Assoc. 1970;53(7):471–86.

112. Lowenberg K. Rabies in man: Microscopic observations. Arch Neurol Psychiatry [Internet]. 1928 Apr 1;19(4):638–46. Available from: https://doi.org/10.1001/archneurpsyc.1928.02210100067005

113. Rossiter JP, Jackson AC. Pathology. In: Jackson AC, Wunner WHBT-R (Second E, editors. Rabies (Seond edition) [Internet]. Oxford: Academic Press; 2007. p. 383–409. Available from: http://www.sciencedirect.com/science/article/pii/B9780123693662500117

114. Dupont JR, Earle KM. Human rabies encephalitis. A study of forty-nine fatal cases with a review of the literature. Neurology. 1965 Nov;15(11):1023–34.

115. Hurst EW, Pawan JL. A further account of the Trinidad outbreak of acute rabic myelitis: histology of the experimental disease. Caribb Med J. 1959;21:25–45.

116. Babes V. Sur certains caractères des lésions histologiques de la rage. In: Ann Inst Pasteur. 1892. p. 209–23.

117. Love S, Wiley C. Viral diseases. In: Greenfield's Neuropathology (7th edition). 2002. p.

1–105.

118. De Brito T, De Fátima Araujo M, Tiriba A. Ultrastructure of the Negri body in human rabies. J Neurol Sci [Internet]. 1973;20(4):363–72. Available from: http://www.sciencedirect.com/science/article/pii/0022510X73901706

119. Iwasaki Y, Sako K, Tsunoda I, Ohara Y. Phenotypes of mononuclear cell infiltrates in human central nervous system. Acta Neuropathol. 1993;85(6):653–7.

120. Iwasaki Y TM. Pathology. In: Rabies. 2002. p. 283–306.

121. Miyamoto K, Matsumoto S. Comparative studies between pathogenesis of street and fixed rabies infection. J Exp Med [Internet]. 1967 Mar 1 [cited 2018 Apr 5];125(3):447–56. Available from: http://www.pubmedcentral.nih.gov/articlerender.fcgi?artid=2138291&tool=pmcentrez&rendertype=abstract

122. Murphy FA. Rabies pathogenesis. Arch Virol [Internet]. 1977 [cited 2018 Mar 22];54(4):279–97. Available from: http://www.ncbi.nlm.nih.gov/pubmed/907476

123. Fu ZF, Jackson AC. Neuronal dysfunction and death in rabies virus infection. J Neurovirol. 2005 Feb;11(1):101–6.

124. Juntrakul S, Ruangvejvorachai P, Shuangshoti S, Wacharapluesadee S, Hemachudha T. Mechanisms of escape phenomenon of spinal cord and brainstem in human rabies. BMC Infect Dis [Internet]. 2005;5(1):104. Available from: https://doi.org/10.1186/1471-2334-5-104

125. Jackson AC, Park H. Apoptotic cell death in experimental rabies in suckling mice. Acta Neuropathol. 1998 Feb;95(2):159–64.

126. Yan, Mikhail Prosniak, Mark T Curti X, Prosniak M, Curtis MT, Weiss ML, Faber M, Dietzschold B, et al. Silver-haired bat rabies virus variant does not induce apoptosis in the brain of experimentally infected mice. J Neurovirol [Internet]. 2001 Jan [cited 2018 Mar 31];7(6):518–27. Available from: http://www.ncbi.nlm.nih.gov/pubmed/11704884

127. Jackson AC, Rossiter JP. Apoptosis plays an important role in experimental rabies virus infection. J Virol. 1997 Jul;71(7):5603–7.

128. Theerasurakarn S, Ubol S. Apoptosis induction in brain during the fixed strain of rabies virus infection correlates with onset and severity of illness. J Neurovirol. 1998;4(4):407–14.

129. Reid JE, Jackson AC. Experimental rabies virus infection in Artibeus jamaicensis bats with CVS-24 variants. J Neurovirol. 2001;7(6):511–7.

130. Sarmento L, Li X, Howerth E, Jackson AC, Fu ZF. Glycoprotein-mediated induction of apoptosis limits the spread of attenuated rabies viruses in the central nervous system of mice. J Neurovirol. 2005 Dec;11(6):571–81.

131. Ubol S, Kasisith J. Reactivation of Nedd-2, a developmentally down-regulated apoptotic gene, in apoptosis induced by a street strain of rabies virus. J Med Microbiol. 2000 Nov;49(11):1043–6.

132. Baloul L, Lafon M. Apoptosis and rabies virus neuroinvasion. Biochimie. 2003;85(8):777–88.

133. Wang ZW, Sarmento L, Wang Y, Li X, Dhingra V, Tseggai T, et al. Attenuated rabies virus activates, while pathogenic rabies virus evades, the host innate immune responses in the central nervous system. Virol J [Internet]. 2005;79(19):12554–65. Available from: http://jvi.asm.org/content/79/19/12554.long%5Cnfile:///Users/schnelllab3/Documents/Tessa Journal Articles/Wang et al/Wang et al._Attenuated Rabies Virus Activates , while Pathogenic Rabies Virus Evades , the Host Innate Immune Responses in the Central Ner

134. Koraka P, Martina BEE, van den Ham HJ, Zaaraoui-Boutahar F, van IJcken W, Roose J, et al. Analysis of mouse brain transcriptome after experimental Duvenhage virus infection shows activation of innate immune response and pyroptotic cell death pathway. Front Microbiol [Internet]. 2018 Mar 20 [cited 2021 May 11];9(MAR):1–14. Available from: www.frontiersin.org

135. Zhang D, He F, Bi S, Guo H, Zhang B, Wu F, et al. Genome-wide transcriptional profiling reveals two distinct outcomes in central nervous system infections of rabies virus. Front Microbiol. 2016;7(751):1–16.

136. Zhao P, Liu S, Zhong Z, Jiang T, Weng R, Xie M, et al. Analysis of expression profiles of long noncoding RNAs and mRNAs in brains of mice infected by rabies virus by RNA sequencing. Sci Rep [Internet]. 2018 Dec 1 [cited 2021 May 11];8(1). Available from: https://pubmed.ncbi.nlm.nih.gov/30089776/

137. Zhao W, Su J, Wang N, Zhao N, Su S. Expression Profiling and Bioinformatics Analysis of CircRNA in Mice Brain Infected with Rabies Virus. Int J Mol Sci. 2021 Jun;22(12).

138. Jamalkandi SA, Mozhgani SH, Pourbadie HG, Mirzaie M, Noorbakhsh F, Vaziri B, et al. Systems biomedicine of rabies delineates the affected signaling pathways. Front

Microbiol [Internet]. 2016 Nov 7 [cited 2021 May 11];7(NOV):1688. Available from: www.frontiersin.org

139. Sui B, Chen D, Liu W, Tian B, Lv L, Pei J, et al. Comparison of lncRNA and mRNA expression in mouse brains infected by a wild-type and a lab-attenuated Rabies lyssavirus. J Gen Virol [Internet]. 2021 Dec 7 [cited 2021 May 4];102(3). Available from: https://pubmed.ncbi.nlm.nih.gov/33284098/

140. Zhao P, Yang Y, Feng H, Zhao L, Qin J, Zhang T, et al. Global gene expression changes in BV2 microglial cell line during rabies virus infection. Infect Genet Evol [Internet]. 2013 Dec;20:257–69. Available from: http://dx.doi.org/10.1016/j.meegid.2013.09.016

141. Huang KW, Sabatini BL. Single-Cell Analysis of Neuroinflammatory Responses Following Intracranial Injection of G-Deleted Rabies Viruses. Front Cell Neurosci [Internet]. 2020 Mar 20 [cited 2021 May 18];14. Available from: https://pubmed.ncbi.nlm.nih.gov/32265666/

142. Ji S, Zhu M, Zhang J, Cai Y, Zhai X, Wang D, et al. Microarray analysis of lncRNA expression in rabies virus infected human neuroblastoma cells. Infect Genet Evol [Internet]. 2019;67:88–100. Available from: https://www.sciencedirect.com/science/article/pii/S1567134818305458

143. Akira S, Uematsu S, Takeuchi O. Pathogen recognition and innate immunity. Cell. 2006 Feb;124(4):783–801.

144. Bowie AG, Unterholzner L. Viral evasion and subversion of pattern-recognition receptor signalling. Nat Rev Immunol. 2008 Dec;8(12):911–22.

145. Hornung V, Ellegast J, Kim S, Brzózka K, Jung A, Kato H, et al. 5’-Triphosphate RNA is the ligand for RIG-I. Science [Internet]. 2006 Nov 10 [cited 2018 Apr 16];314(5801):994–7. Available from: http://www.ncbi.nlm.nih.gov/pubmed/17038590

146. Zarember KA, Godowski PJ. Tissue expression of human Toll-like receptors and differential regulation of Toll-like receptor mRNAs in leukocytes in response to microbes, their products, and cytokines. J Immunol. 2002 Jan;168(2):554–61.

147. Kawai T, Akira S. The roles of TLRs, RLRs and NLRs in pathogen recognition. Int Immunol. 2009;21(4):317–37.

148. Soung A, Klein RS. Viral Encephalitis and Neurologic Diseases: Focus on Astrocytes. Trends Mol Med. 2018;24(11):950–62.

149. Philips T, Rothstein JD. Oligodendroglia: metabolic supporters of neurons. J Clin Invest

[Internet]. 2017/09/02. 2017;127(9):3271–80. Available from: https://www.ncbi.nlm.nih.gov/pubmed/28862639

150. Kuhn S, Gritti L, Crooks D, Dombrowski Y. Oligodendrocytes in Development, Myelin Generation and Beyond. Cells. 2019 Nov;8(11).

151. Ginhoux F, Greter M, Leboeuf M, Nandi S, See P, Gokhan S, et al. Fate mapping analysis reveals that adult microglia derive from primitive macrophages. Science. 2010 Nov;330(6005):841–5.

152. Chen Z, Zhong D, Li G. The role of microglia in viral encephalitis: a review. J Neuroinflammation [Internet]. 2019/04/11. 2019;16(1):76. Available from: https://www.ncbi.nlm.nih.gov/pubmed/30967139

153. Carty M, Reinert L, Paludan SR, Bowie AG. Innate antiviral signalling in the central nervous system. Trends Immunol [Internet]. 2014 Feb [cited 2018 Mar 22];35(2):79–87. Available from: http://www.ncbi.nlm.nih.gov/pubmed/24316012

154. Broderick C, Hoek RM, Forrester J V, Liversidge J, Sedgwick JD, Dick AD. Constitutive retinal CD200 expression regulates resident microglia and activation state of inflammatory cells during experimental autoimmune uveoretinitis. Am J Pathol. 2002 Nov;161(5):1669–77.

155. Zhang S, Wang XJ, Tian LP, Pan J, Lu GQ, Zhang YJ, et al. CD200-CD200R dysfunction exacerbates microglial activation and dopaminergic neurodegeneration in a rat model of Parkinson's disease. J Neuroinflammation [Internet]. 2011;8(1):154. Available from: http://www.jneuroinflammation.com/content/8/1/154

156. Yi MH, Zhang E, Kang JW, Shin YN, Byun JY, Oh SH, et al. Expression of CD200 in alternative activation of microglia following an excitotoxic lesion in the mouse hippocampus. Brain Res [Internet]. 2012;1481:90–6. Available from: http://dx.doi.org/10.1016/j.brainres.2012.08.053

157. Hoek RM, Ruuls SR, Murphy CA, Wright GJ, Goddard R, Zurawski SM, et al. Down-regulation of the macrophage lineage through interaction with OX2 (CD200). Science. 2000 Dec;290(5497):1768–71.

158. Pabon MM, Bachstetter AD, Hudson CE, Gemma C, Bickford PC. CX3CL1 reduces neurotoxicity and microglial activation in a rat model of Parkinson's disease. J Neuroinflammation. 2011 Jan;8:9.

159. Ito N, Moseley GW, Sugiyama M. The importance of immune evasion in the

pathogenesis of rabies virus. Vet Med Sci. 2016;7(116):1089–98.

160. Gerard FCA, Ribeiro E de AJ, Leyrat C, Ivanov I, Blondel D, Longhi S, et al. Modular organization of rabies virus phosphoprotein. J Mol Biol. 2009 May;388(5):978–96.

161. Fouquet B, Nikolic J, Larrous F, Bourhy H, Wirblich C, Lagaudrière-Gesbert C, et al. Focal Adhesion Kinase Is Involved in Rabies Virus Infection through Its Interaction with Viral Phosphoprotein P. J Virol [Internet]. 2015;89(3):1640–51. Available from: http://jvi.asm.org/lookup/doi/10.1128/JVI.02602-14

162. Li Y, Dong W, Shi Y, Deng F, Chen X, Wan C, et al. Rabies virus phosphoprotein interacts with ribosomal protein L9 and affects rabies virus replication. Virology. 2016 Jan;488:216–24.

163. Oksayan S, Nikolic J, David CT, Blondel D, Jans DA, Moseley GW. Identification of a Role for Nucleolin in Rabies Virus Infection. J Virol. 2015;89(3):1939–43.

164. Wiltzer L, Okada K, Yamaoka S, Larrous F, Kuusisto HV, Sugiyama M, et al. Interaction of Rabies Virus P-Protein With STAT Proteins is Critical to Lethal Rabies Disease. J Infect Dis [Internet]. 2014 Jun 1 [cited 2018 Mar 29];209(11):1744–53. Available from: https://academic.oup.com/jid/article-lookup/doi/10.1093/infdis/jit829

165. Oksayan S, Ito N, Moseley G, Blondel D. Subcellular trafficking in rhabdovirus infection and immune evasion: a novel target for therapeutics. Infect Disord Drug Targets. 2012 Feb;12(1):38–58.

166. Rowe CL, Wagstaff KM, Oksayan S, Glover DJ, Jans DA, Moseley GW. Nuclear Trafficking of the Rabies Virus Interferon Antagonist P-Protein Is Regulated by an Importin-Binding Nuclear Localization Sequence in the C-Terminal Domain. PLoS One. 2016;11(3):e0150477.

167. Leyrat C, Ribeiro EA, Gérard FCA, Ivanov I, Ruigrok RWH, Jamin M. Structure, interactions with host cell and functions of rhabdovirus phosphoprotein. Future Virol. 2011;6(4):465–81.

168. Chelbi-Alix MK, Vidy A, El Bougrini J, Blondel D. Rabies viral mechanisms to escape the IFN system: the viral protein P interferes with IRF-3, Stat1, and PML nuclear bodies. J Interf cytokine Res Off J Int Soc Interf Cytokine Res. 2006 May;26(5):271–80.

169. Brzozka K, Finke S, Conzelmann K-K. Identification of the Rabies Virus Alpha/Beta Interferon Antagonist: Phosphoprotein P Interferes with Phosphorylation of Interferon Regulatory Factor 3. J Virol [Internet]. 2005 Jun 15 [cited 2018 Mar 29];79(12):7673–

81. Available from: http://www.ncbi.nlm.nih.gov/pubmed/15919920

170. Rieder M, Brzozka K, Pfaller CK, Cox JH, Stitz L, Conzelmann K. Genetic Dissection of Interferon-Antagonistic Functions of Rabies Virus Phosphoprotein: Inhibition of Interferon Regulatory Factor 3 Activation Is Important for Pathogenicity. J Virol [Internet]. 2011 Jan 15 [cited 2018 Mar 29];85(2):842–52. Available from: http://www.ncbi.nlm.nih.gov/pubmed/21084487

171. Brzózka K, Finke S, Conzelmann K-KK-KK-K, Brzozka K, Finke S, Conzelmann K-KK-KK-K, et al. Identification of the Rabies Virus Alpha/Beta Interferon Antagonist: Phosphoprotein P Interferes with Phosphorylation of Interferon Regulatory Factor 3. J Virol [Internet]. 2005 Jun 15 [cited 2018 Mar 29];79(12):7673–81. Available from: http://www.ncbi.nlm.nih.gov/pubmed/15919920

172. Vidy A, Chelbi-Alix M, Blondel D. Rabies Virus P Protein Interacts with STAT1 and Inhibits Interferon Signal Transduction Pathways. J Virol [Internet]. 2005 Nov 15 [cited 2018 Mar 29];79(22):14411–20. Available from: http://www.ncbi.nlm.nih.gov/pubmed/16254375

173. Brzózka K, Finke S, Conzelmann K-K. Inhibition of Interferon Signaling by Rabies Virus Phosphoprotein P: Activation-Dependent Binding of STAT1 and STAT2. J Virol [Internet]. 2006 Mar 15 [cited 2018 Mar 29];80(6):2675–83. Available from: http://jvi.asm.org/cgi/doi/10.1128/JVI.80.6.2675-2683.2006

174. Lieu KG, Brice A, Wiltzer L, Hirst B, Jans DA, Blondel D, et al. The rabies virus interferon antagonist P protein interacts with activated STAT3 and inhibits Gp130 receptor signaling. J Virol [Internet]. 2013 Jul [cited 2018 Mar 29];87(14):8261–5. Available from: http://www.ncbi.nlm.nih.gov/pubmed/23698294

175. Harrison AR, Lieu KG, Larrous F, Ito N, Bourhy H, Moseley GW. Lyssavirus P-protein selectively targets STAT3-STAT1 heterodimers to modulate cytokine signalling. PLoS Pathog. 2020;16(9):1–23.

176. Ito N, Moseley GW, Blondel D, Shimizu K, Rowe CL, Ito Y, et al. Role of interferon antagonist activity of rabies virus phosphoprotein in viral pathogenicity. J Virol [Internet]. 2010 Jul 1 [cited 2018 Apr 11];84(13):6699–710. Available from: http://www.ncbi.nlm.nih.gov/pubmed/20427527

177. Pasdeloup D, Poisson N, Raux H, Gaudin Y, Ruigrok RWH, Blondel D. Nucleocytoplasmic shuttling of the rabies virus P protein requires a nuclear localization signal and a CRM1-dependent nuclear export signal. Virology [Internet]. 2005 Apr 10

[cited 2018 Apr 11];334(2):284–93. Available from: http://www.ncbi.nlm.nih.gov/pubmed/15780878

178. Wiltzer L, Larrous F, Oksayan S, Ito N, Marsh G a., Wang LF, et al. Conservation of a Unique Mechanism of Immune Evasion across the Lyssavirus Genus. J Virol. 2012;86(18):10194–9.

179. Vidy A, El Bougrini J, Chelbi-Alix MK, Blondel D. The Nucleocytoplasmic Rabies Virus P Protein Counteracts Interferon Signaling by Inhibiting both Nuclear Accumulation and DNA Binding of STAT1. J Virol [Internet]. 2007 Apr 15 [cited 2018 Apr 12];81(8):4255–63. Available from: http://www.ncbi.nlm.nih.gov/pubmed/17287281

180. Moseley GW, Lahaye X, Roth DM, Oksayan S, Filmer RP, Rowe CL, et al. Dual modes of rabies P-protein association with microtubules: a novel strategy to suppress the antiviral response. J Cell Sci. 2009 Oct;122(Pt 20):3652–62.

181. Ben Khalifa Y, Luco S, Besson B, Sonthonnax F, Archambaud M, Grimes JM, et al. The matrix protein of rabies virus binds to RelAp43 to modulate NF-κB-dependent gene expression related to innate immunity. Sci Rep [Internet]. 2016;6(September):39420. Available from: http://www.nature.com/articles/srep39420

182. Besson B, Sonthonnax F, Duchateau M, Ben Khalifa Y, Larrous F, Eun H, et al. Regulation of NF-κB by the p105-ABIN2-TPL2 complex and RelAp43 during rabies virus infection. Schnell MJ, editor. PLoS Pathog [Internet]. 2017 Oct 30 [cited 2018 Mar 29];13(10):e1006697. Available from: http://www.ncbi.nlm.nih.gov/pubmed/29084252

183. Sonthonnax F, Besson BB, Bonnaud E, Jouvion G, Merino D, Larrous F, et al. Lyssavirus matrix protein cooperates with phosphoprotein to modulate the Jak-Stat pathway. Sci Rep. 2019;9(1):1–13.

184. Masatani T, Ito N, Ito Y, Nakagawa K, Abe M, Yamaoka S, et al. Importance of rabies virus nucleoprotein in viral evasion of interferon response in the brain. Microbiol Immunol. 2013;57(7):511–7.

185. Masatani T, Ito N, Shimizu K, Ito Y, Nakagawa K, Abe M, et al. Amino acids at positions 273 and 394 in rabies virus nucleoprotein are important for both evasion of host RIG-I-mediated antiviral response and pathogenicity. Virus Res. 2011 Jan;155(1):168–74.

186. Masatani T, Ito N, Shimizu K, Ito Y, Nakagawa K, Sawaki Y, et al. Rabies Virus Nucleoprotein Functions To Evade Activation of the RIG-I-Mediated Antiviral Response. J Virol [Internet]. 2010 Apr [cited 2018 Apr 4];84(8):4002–12. Available from: http://www.ncbi.nlm.nih.gov/pubmed/20130065

187. Masatani T, Horie M, Yamada K, Ozawa M, Okuya K, Tsukiyama-Kohara K, et al. Contribution of the interaction between the rabies virus P protein and I-kappa B kinase ϵ to the inhibition of type I IFN induction signalling. J Gen Virol [Internet]. 2016 Feb 1 [cited 2018 Mar 29];97(2):316–26. Available from: http://www.microbiologyresearch.org/content/journal/jgv/10.1099/jgv.0.000362

188. Ogino T, Green TJ. Transcriptional Control and mRNA Capping by the GDP Polyribonucleotidyltransferase Domain of the Rabies Virus Large Protein. Viruses. 2019 Jun;11(6).

189. Decroly E, Ferron F, Lescar J, Canard B. Conventional and unconventional mechanisms for capping viral mRNA. Nat Rev Microbiol [Internet]. 2012;10(1):51–65. Available from: https://doi.org/10.1038/nrmicro2675

190. Ogino M, Ito N, Sugiyama M, Ogino T. The Rabies Virus L Protein Catalyzes mRNA Capping with GDP Polyribonucleotidyltransferase Activity. Viruses. 2016 May;8(5).

191. Tsiang H, Koulakoff A, Bizzini B, Berwald-Netter Y. Neurotropism of rabies virus. An in vitro study. J Neuropathol Exp Neurol [Internet]. 1983 Jul [cited 2018 Apr 6];42(4):439–52. Available from: http://www.ncbi.nlm.nih.gov/pubmed/6864237

192. Sun L, Tang Y, Yan K, Yu J, Zou Y, Xu W, et al. Differences in neurotropism and neurotoxicity among retrograde viral tracers. Mol Neurodegener [Internet]. 2019 [cited 2021 May 10];14(1). Available from: https://doi.org/10.1186/s13024-019-0308-6

193. Potratz M, Zaeck LM, Weigel C, Klein A, Freuling CM, Müller T, et al. Neuroglia infection by rabies virus after anterograde virus spread in peripheral neurons. Acta Neuropathol Commun. 2020 Nov;8(1):199.

194. Potratz M, Zaeck L, Christen M, Kamp V, Klein A, Freuling CM, et al. Astrocyte Infection during Rabies Encephalitis Depends on the Virus Strain and Infection Route as Demonstrated by Novel Quantitative 3D Analysis of Cell Tropism. Cells. 2020;9(January):1–25.

195. Zhang Y, Chen K, Sloan SA, Bennett ML, Scholze AR, O'Keeffe S, et al. An RNA-sequencing transcriptome and splicing database of glia, neurons, and vascular cells of the cerebral cortex. J Neurosci. 2014;34(36):11929–47.

196. Hawrylycz MJ, Lein ES, Guillozet-Bongaarts AL, Shen EH, Ng L, Miller JA, et al. An anatomically comprehensive atlas of the adult human brain transcriptome. Nature. 2012 Sep;489(7416):391–9.

197. Tang Y, Rampin O, Giuliano F, Ugolini G. Spinal and brain circuits to motoneurons of the bulbospongiosus muscle: Retrograde transneuronal tracing with rabies virus. J Comp Neurol [Internet]. 1999 Nov 15 [cited 2021 Apr 29];414(2):167–92. Available from: https://onlinelibrary.wiley.com/doi/10.1002/(SICI)1096-9861(19991115)414:2%3C167::AID-CNE3%3E3.0.CO;2-P

198. Graf W, Gerrits N, Yatim-Dhiba N, Ugolini G. Mapping the oculomotor system: the power of transneuronal labelling with rabies virus. Eur J Neurosci [Internet]. 2002 May [cited 2021 Apr 29];15(9):1557–62. Available from: https://hal.archives-ouvertes.fr/hal-00347822

199. Ugolini G. Advances in viral transneuronal tracing. J Neurosci Methods. 2010 Dec 15;194(1):2–20.

200. Ugolini G, Klam F, Dans MD, Dubayle D, Brandi AM, Büttner-Ennever J, et al. Horizontal eye movement networks in primates as revealed by retrograde transneuronal transfer of rabies virus: Differences in monosynaptic input to “slow” and “fast” abducens motoneurons. J Comp Neurol [Internet]. 2006 Oct 20 [cited 2021 Apr 29];498(6):762–85. Available from: https://pubmed.ncbi.nlm.nih.gov/16927266/

201. Griffin DE. Recovery from viral encephalomyelitis: Immune-mediated noncytolytic virus clearance from neurons [Internet]. Vol. 47, Immunologic Research. Immunol Res; 2010 [cited 2021 Jun 3]. p. 123–33. Available from: https://pubmed.ncbi.nlm.nih.gov/20087684/

202. Levine B. Apoptosis in viral infections of neurons: A protective or pathologic host response? [Internet]. Vol. 265, Current Topics in Microbiology and Immunology. Springer Verlag; 2002 [cited 2021 Jun 3]. p. 95–118. Available from: https://pubmed.ncbi.nlm.nih.gov/12014197/

203. Khanna KM, Lepisto AJ, Hendricks RL. Immunity to latent viral infection: Many skirmishes but few fatalities. Trends Immunol [Internet]. 2004 [cited 2021 Jun 3];25(5):230–4. Available from: https://pubmed.ncbi.nlm.nih.gov/15099562/

204. Yordy B, Iijima N, Huttner A, Leib D, Iwasaki A. A neuron-specific role for autophagy in antiviral defense against herpes simplex virus. Cell Host Microbe. 2012 Sep 13;12(3):334–45.

205. Peng J, Zhu S, Hu L, Ye P, Wang Y, Tian Q, et al. Wild-type rabies virus induces autophagy in human and mouse neuroblastoma cell lines. Autophagy [Internet]. 2016 Oct 2 [cited 2021 May 4];12(10):1704–20. Available from:

https://pubmed.ncbi.nlm.nih.gov/27463027/

206. Lafon M. Immune evasion, a critical strategy for rabies virus. Dev Biol (Basel). 2008;131:413–9.

207. Pfefferkorn C, Kallfass C, Lienenklaus S, Spanier J, Kalinke U, Rieder M, et al. Abortively Infected Astrocytes Appear To Represent the Main Source of Interferon Beta in the Virus-Infected Brain. J Virol [Internet]. 2016;90(4):2031–8. Available from: http://jvi.asm.org/lookup/doi/10.1128/JVI.02979-15

208. Tian B, Zhou M, Yang Y, Yu L, Luo Z, Tian D, et al. Lab-attenuated rabies virus causes abortive infection and induces cytokine expression in astrocytes by activating mitochondrial antiviral-signaling protein signaling pathway. Front Immunol [Internet]. 2018 [cited 2018 Apr 2];8(JAN):1–17. Available from: http://www.ncbi.nlm.nih.gov/pubmed/29403485

209. Ray NB, Power C, Lynch WPP, Ewalt LCC, Lodmell DLL. Rabies viruses infect primary cultures of murine, feline, and human microglia and astrocytes. Arch Virol [Internet]. 1997 [cited 2018 Apr 6];142(5):1011–9. Available from: http://www.ncbi.nlm.nih.gov/pubmed/9191865

210. Balachandran A, Charlton K. Experimental rabies infection of non-nervous tissues in skunks (Mephitis mephitis) and foxes (Vulpes vulpes). Vet Pathol. 1994 Jan;31(1):93–102.

211. Charlton KM, Nadin-Davis S, Casey GA, Wandeler AI. The long incubation period in rabies: delayed progression of infection in muscle at the site of exposure. Acta Neuropathol. 1997 Jul;94(1):73–7.

212. Charlton KM, Casey GA. Experimental rabies in skunks: immunofluorescence light and electron microscopic studies. Lab Invest. 1979 Jul;41(1):36–44.

213. Griffin DE. Immune responses to RNA-virus infections of the CNS. Nat Rev Immunol. 2003 Jun;3(6):493–502.

214. Velandia-Romero ML, Castellanos JE, Martínez-Gutiérrez M. In vivo differential susceptibility of sensory neurons to rabies virus infection. J Neurovirol. 2013 Aug;19:367–75.

215. Prehaud C, Mégret F, Lafage M, Lafon M. Virus infection switches TLR-3-positive human neurons to become strong producers of beta interferon. J Virol [Internet]. 2005 Oct 15 [cited 2018 Mar 22];79(20):12893–904. Available from:

http://jvi.asm.org/cgi/content/abstract/79/20/12893

216. Ménager P, Roux P, Mégret F, Bourgeois J-P, Le Sourd A-M, Danckaert A, et al. Toll-like receptor 3 (TLR3) plays a major role in the formation of rabies virus Negri Bodies. PLoS Pathog [Internet]. 2009 Feb [cited 2018 Mar 22];5(2):e1000315. Available from: http://www.ncbi.nlm.nih.gov/pubmed/19247444

217. Nikolic J, Le Bars R, Lama Z, Scrima N, Lagaudrière-Gesbert C, Gaudin Y, et al. Negri bodies are viral factories with properties of liquid organelles. Nat Commun [Internet]. 2017 Dec 1 [cited 2021 Jun 15];8(1). Available from: /pmc/articles/PMC5498545/

218. Jackson AC, Rossiter JP, Lafon M. Expression of Toll-like receptor 3 in the human cerebellar cortex in rabies, herpes simplex encephalitis, and other neurological diseases. J Neurovirol [Internet]. 2006 Jun [cited 2021 May 3];12(3):229–34. Available from: https://pubmed.ncbi.nlm.nih.gov/16877304/

219. Salaun B, Coste I, Rissoan M-C, Lebecque SJ, Renno T. TLR3 Can Directly Trigger Apoptosis in Human Cancer Cells. J Immunol. 2006;176(8):4894–901.

220. Rieder M, Conzelmann K-KK. Interferon in Rabies Virus Infection. In: Advances in Virus Research [Internet]. 1st ed. United States: Elsevier Inc.; 2011. p. 91–114. Available from: http://dx.doi.org/10.1016/B978-0-12-387040-7.00006-8

221. Lindqvist R, Mundt F, Gilthorpe JD, Wölfel S, Gekara NO, Kröger A, et al. Fast type I interferon response protects astrocytes from flavivirus infection and virus-induced cytopathic effects. J Neuroinflammation [Internet]. 2016;13(1):1–15. Available from: http://dx.doi.org/10.1186/s12974-016-0748-7

222. Kallfass C, Ackerman A, Lienenklaus S, Weiss S, Heimrich B, Staeheli P. Visualizing production of beta interferon by astrocytes and microglia in brain of La Crosse virus-infected mice. J Virol. 2012 Oct;86(20):11223–30.

223. Detje CN, Lienenklaus S, Chhatbar C, Spanier J, Prajeeth CK, Soldner C, et al. Upon intranasal vesicular stomatitis virus infection, astrocytes in the olfactory bulb are important interferon Beta producers that protect from lethal encephalitis. J Virol. 2015 Mar;89(5):2731–8.

224. Zhao P, Zhao L, Zhang K, Feng H, Wang H, Wang T, et al. Infection with street strain rabies virus induces modulation of the microRNA profile of the mouse brain. Virol J [Internet]. 2012;9(1):1. Available from: Virology Journal

225. Ceyzériat K, Abjean L, Carrillo-de Sauvage MA, Ben Haim L, Escartin C. The complex

STATes of astrocyte reactivity: How are they controlled by the JAK-STAT3 pathway? Neuroscience. 2016;330:205–18.

226. Sugamata M, Miyazawa M, Mori S, Spangrude GJ, Ewalt LC, Lodmell DL. Paralysis of street rabies virus-infected mice is dependent on T lymphocytes. J Virol. 1992 Feb;66(2):1252–60.

227. Bertoune M, Nickl B, Krieger T, Wohlers L, Bonaterra GA, Dietzschold B, et al. The phenotype of the RABV glycoprotein determines cellular and global virus load in the brain and is decisive for the pace of the disease. Virology [Internet]. 2017 Nov;511:82–94. Available from: http://www.sciencedirect.com/science/article/pii/S0042682217302829

228. Nakamichi K, Inoue S, Takasaki T, Morimoto K, Kurane I. Rabies Virus Stimulates Nitric Oxide Production and CXC Chemokine Ligand 10 Expression in Macrophages through Activation of Extracellular Signal-Regulated Kinases 1 and 2. J Virol [Internet]. 2004 Sep [cited 2018 Apr 5];78(17):9376–88. Available from: http://www.ncbi.nlm.nih.gov/pubmed/15308732

229. Nakamichi K, Saiki M, Sawada M, Takayama-Ito M, Yamamuro Y, Morimoto K, et al. Rabies Virus-Induced Activation of Mitogen-Activated Protein Kinase and NF- B Signaling Pathways Regulates Expression of CXC and CC Chemokine Ligands in Microglia. J Virol [Internet]. 2005 Sep [cited 2018 Apr 5];79(18):11801–12. Available from: http://www.ncbi.nlm.nih.gov/pubmed/16140757

230. Valério-Gomes B, Guimarães DM, Szczupak D, Lent R. The Absolute Number of Oligodendrocytes in the Adult Mouse Brain. Front Neuroanat. 2018;12:90.

231. Mori T, Morimoto K. Rabies virus glycoprotein variants display different patterns in rabies monosynaptic tracing. Front Neuroanat. 2014;7:47.

232. Osanai Y, Shimizu T, Mori T, Yoshimura Y, Hatanaka N, Nambu A, et al. Rabies virus-mediated oligodendrocyte labeling reveals a single oligodendrocyte myelinates axons from distinct brain regions. Glia [Internet]. 2017 Jan 1 [cited 2018 Apr 6];65(1):93–105. Available from: http://doi.wiley.com/10.1002/glia.23076

233. Fontenas L, Kucenas S. Livin' On The Edge: glia shape nervous system transition zones. Curr Opin Neurobiol. 2017 Dec;47:44–51.

234. Jenson AB, Rabin ER, Bentinck DC, Melnick JL. Rabies virus neuronitis. J Virol. 1969 Feb;3(2):265–9.

235. Murphy FA, Bauer SP, Harrison AK, Winn WCJ. Comparative pathogenesis of rabies and rabies-like viruses. Viral infection and transit from inoculation site to the central nervous system. Lab Invest. 1973 Mar;28(3):361–76.

236. Begeman L, GeurtsvanKessel C, Finke S, Freuling CM, Koopmans M, Müller T, et al. Comparative pathogenesis of rabies in bats and carnivores, and implications for spillover to humans. Lancet Infect Dis. 2017;18(4):e147–59.

237. Zaeck L, Potratz M, Freuling CM, Müller T, Finke S. High-Resolution 3D Imaging of Rabies Virus Infection in Solvent-Cleared Brain Tissue. JoVE [Internet]. 2019 Apr;(146):e59402. Available from: https://www.jove.com/t/59402

238. Ménager P, Roux P, Mégret F, Préhaud C, Bourgeois J-P, Le Sourd A-M, et al. TLR3 is a key component of rabies virus induced Negri bodies. BMC Proc. 2008;2(S1):3.

239. Luco S, Delmas O, Vidalain P-OO, Tangy F, Weil R, Bourhy H. RelAp43, a Member of the NF-κB Family Involved in Innate Immune Response against Lyssavirus Infection. PLoS Pathog. 2012;8(12):e1003060.

240. Niu X, Tang L, Tseggai T, Guo Y, Fu ZF. Wild-type rabies virus phosphoprotein is associated with viral sensitivity to type I interferon treatment. Arch Virol. 2013 Nov;158(11):2297–305.

241. Miao F-M, Zhang S-F, Wang S-C, Liu Y, Zhang F, Hu R-L. Comparison of immune responses to attenuated rabies virus and street virus in mouse brain. Arch Virol. 2017;162(1):247–57.

242. Azevedo FAC, Carvalho LRB, Grinberg LT, Farfel JM, Ferretti REL, Leite REP, et al. Equal numbers of neuronal and nonneuronal cells make the human brain an isometrically scaled-up primate brain. J Comp Neurol. 2009 Apr;513(5):532–41.

243. Herculano-Houzel S. The glia/neuron ratio: how it varies uniformly across brain structures and species and what that means for brain physiology and evolution. Glia. 2014 Sep;62(9):1377–91.

244. Sierra A, de Castro F, Del Río-Hortega J, Rafael Iglesias-Rozas J, Garrosa M, Kettenmann H. The “Big-Bang” for modern glial biology: Translation and comments on Pío del Río-Hortega 1919 series of papers on microglia. Glia. 2016 Nov;64(11):1801–40.

245. Jäkel S, Dimou L. Glial Cells and Their Function in the Adult Brain: A Journey through the History of Their Ablation. Front Cell Neurosci. 2017;11:24.

246. Nayak D, Johnson KR, Heydari S, Roth TL, Zinselmeyer BH, McGavern DB. Type I interferon programs innate myeloid dynamics and gene expression in the virally infected nervous system. PLoS Pathog. 2013;9(5):e1003395.

247. Reinert LS, Lopušná K, Winther H, Sun C, Thomsen MK, Nandakumar R, et al. Sensing of HSV-1 by the cGAS-STING pathway in microglia orchestrates antiviral defence in the CNS. Nat Commun [Internet]. 2016 [cited 2018 Jan 13];7. Available from: https://www.ncbi.nlm.nih.gov/pmc/articles/PMC5109551/pdf/ncomms13348.pdf

248. Del Río Hortega P. Estudios sobre la neuroglía. La microglía y su transformación en células en bastoncito y cuerpos granuloadiposos. Trab Lab Invest Biol. 1920;(18):37–82.

249. Del Río-Hortega P. La glía de escasas radiaciones (oligodendroglía). Bol Real Soc Esp Hist Nat. 1921;(21):63–92.

250. Hirbec H, Déglon N, Foo LC, Goshen I, Grutzendler J, Hangen E, et al. Emerging technologies to study glial cells. Glia. 2020 Sep;68(9):1692–728.

251. Kelly RM, Strick PL. Rabies as a transneuronal tracer of circuits in the central nervous system. J Neurosci Methods. 2000 Nov;103(1):63–71.

252. Morcuende S, Delgado-García JM, Ugolini G, Delgado-Garcia J-M, Ugolini G. Neuronal premotor networks involved in eyelid responses: retrograde transneuronal tracing with rabies virus from the orbicularis oculi muscle in the rat. J Neurosci [Internet]. 2002 Oct 15 [cited 2021 Apr 29];22(20):8808–18. Available from: https://pubmed.ncbi.nlm.nih.gov/12388587/

253. Ugolini G. Specificity of rabies virus as a transneuronal tracer of motor networks: transfer from hypoglossal motoneurons to connected second-order and higher order central nervous system cell groups. J Comp Neurol. 1995 Jun;356(3):457–80.

254. Kelly RM, Strick PL. Macro-architecture of basal ganglia loops with the cerebral cortex: use of rabies virus to reveal multisynaptic circuits. Prog Brain Res. 2004;143:449–59.

255. Yang X, Kui L, Tang M, Li D, Wei K, Chen W, et al. High-Throughput Transcriptome Profiling in Drug and Biomarker Discovery. Front Genet. 2020;11:19.

256. He S, Wang L-H, Liu Y, Li Y-Q, Chen H-T, Xu J-H, et al. Single-cell transcriptome profiling of an adult human cell atlas of 15 major organs. Genome Biol [Internet]. 2020;21(1):294. Available from: https://doi.org/10.1186/s13059-020-02210-0

257. Huang S. Non-genetic heterogeneity of cells in development: more than just noise.

Development. 2009 Dec;136(23):3853–62.

258. Pertea M. The human transcriptome: An unfinished story. Genes (Basel). 2012;3(3):344–60.

259. Chen J, Sun M, Lee S, Zhou G, Rowley JD, Wang SM. Identifying novel transcripts and novel genes in the human genome by using novel SAGE tags. Proc Natl Acad Sci U S A. 2002 Sep;99(19):12257–62.

260. Venter JC, Adams MD, Myers EW, Li PW, Mural RJ, Sutton GG, et al. The sequence of the human genome. Science. 2001 Feb;291(5507):1304–51.

261. Harrow J, Frankish A, Gonzalez JM, Tapanari E, Diekhans M, Kokocinski F, et al. GENCODE: the reference human genome annotation for The ENCODE Project. Genome Res. 2012 Sep;22(9):1760–74.

262. International Human Genome Sequencing Consortium. Finishing the euchromatic sequence of the human genome. Nature. 2004 Oct;431(7011):931–45.

263. Karlsson M, Zhang C, Méar L, Zhong W, Digre A, Katona B, et al. A single–cell type transcriptomics map of human tissues. Sci Adv. 2021;7(31):eabh2169.

264. Suja MS, Mahadevan A, Madhusudana SN, Shankar SK. Role of Apoptosis in Rabies Viral Encephalitis: A Comparative Study in Mice, Canine, and Human Brain with a Review of Literature. Patholog Res Int [Internet]. 2011 Aug 25 [cited 2021 May 12];2011:1–13. Available from: https://pubmed.ncbi.nlm.nih.gov/21876844/

265. Suja MS, Mahadevan A, Sundaram C, Mani J, Sagar BC, Hemachudha T, et al. Rabies encephalitis following fox bite--histological and immunohistochemical evaluation of lesions caused by virus. Clin Neuropathol. 2004;23(6):271–6.

266. Laothamatas J, Sungkarat W, Hemachudha T. Neuroimaging in rabies. Adv Virus Res. 2011;79:309–27.

267. Zhao P, Zhao L, Zhang T, Qi Y, Wang T, Liu K, et al. Innate immune response gene expression profiles in central nervous system of mice infected with rabies virus. Comp Immunol Microbiol Infect Dis [Internet]. 2011 Dec [cited 2021 May 11];34(6):503–12. Available from: https://pubmed.ncbi.nlm.nih.gov/22005334/

268. Prosniak M, Hooper DC, Dietzschold B, Koprowski H. Effect of rabies virus infection on gene expression in mouse brain. 2001 Feb 27 [cited 2018 Mar 31];98(5):2758–63. Available from: http://www.ncbi.nlm.nih.gov/pubmed/11226313

269. Mestas J, Hughes CCW. Of Mice and Not Men: Differences between Mouse and Human Immunology. J Immunol. 2004;172(5):2731–8.

270. Louz D, Bergmans HE, Loos BP, Hoeben RC. Animal models in virus research: their utility and limitations. [Internet]. Vol. 39, Critical reviews in microbiology. Crit Rev Microbiol; 2013 [cited 2021 Jun 30]. p. 325–61. Available from: https://pubmed.ncbi.nlm.nih.gov/22978742/

271. Hodge RD, Bakken TE, Miller JA, Smith KA, Barkan ER, Graybuck LT, et al. Conserved cell types with divergent features in human versus mouse cortex. Nature [Internet]. 2019;573(7772):61–8. Available from: http://dx.doi.org/10.1038/s41586-019-1506-7

272. Haley PJ. Species differences in the structure and function of the immune system. Toxicology. 2003 Jun;188(1):49–71.

273. Gordon J, Amini S, White MK. General overview of neuronal cell culture. Methods Mol Biol [Internet]. 2013;1078:1–8. Available from: https://pubmed.ncbi.nlm.nih.gov/23975816

274. Ugolini G. Viruses in connectomics: Viral transneuronal tracers and genetically modified recombinants as neuroscience research tools. J Neurosci Methods. 2020 Dec;346:108917.

275. Babes V.M. Sur certains caractères des lésions histologiques de la rage. In: Annales de L'Institut Pasteur. 1892. p. 209–23.

276. Guinto G, Felix I, Rivas A. [A case of rabies encephalitis with long survival. Clinical pathological correlations]. Gac Med Mex. 1995;131(2):223–8.

277. Suja MS, Mahadevan A, Madhusudhana SN, Vijayasarathi SK, Shankar SK. Neuroanatomical mapping of rabies nucleocapsid viral antigen distribution and apoptosis in pathogenesis in street dograbies - An immunohistochemical study. Clin Neuropathol. 2009;28(2):113–24.

278. Liu SQ, Xie Y, Gao X, Wang Q, Zhu WY. Inflammatory response and MAPK and NF-κB pathway activation induced by natural street rabies virus infection in the brain tissues of dogs and humans. Virol J [Internet]. 2020 Oct 1 [cited 2021 May 11];17(1):157. Available from: https://doi.org/10.1186/s12985-020-01429-4

279. Sundaramoorthy V, Godde N, Farr RJ, Green D, Haynes JM. Modelling Lyssavirus Infections in Human Stem Cell-Derived Neural Cultures. 2019;1–24.

280. McFadden G, Mohamed MR, Rahman MM, Bartee E. Cytokine determinants of viral

tropism [Internet]. Vol. 9, Nature Reviews Immunology. Nature Publishing Group; 2009 [cited 2021 Apr 13]. p. 645–55. Available from: /pmc/articles/PMC4373421/

281. Zhang Y, Sloan SAA, Clarke LEE, Caneda C, Plaza CAA, Blumenthal PDD, et al. Purification and Characterization of Progenitor and Mature Human Astrocytes Reveals Transcriptional and Functional Differences with Mouse. Neuron [Internet]. 2016 Jan 6;89(1):37–53. Available from: http://dx.doi.org/10.1016/j.neuron.2015.11.013

282. McKenzie AT, Wang M, Hauberg ME, Fullard JF, Kozlenkov A, Keenan A, et al. Brain Cell Type Specific Gene Expression and Co-expression Network Architectures. Sci Rep. 2018 Jun;8(1):8868.

283. Yeo G, Holste D, Kreiman G, Burge CB. Variation in alternative splicing across human tissues. Genome Biol. 2004;5(10):R74.

284. Norris AD, Calarco JA. Emerging Roles of Alternative Pre-mRNA Splicing Regulation in Neuronal Development and Function. Front Neurosci. 2012;6:122.

285. Zheng S, Black DL. Alternative pre-mRNA splicing in neurons: growing up and extending its reach. Trends Genet. 2013 Aug;29(8):442–8.

286. von Bartheld CS, Bahney J, Herculano-Houzel S. The search for true numbers of neurons and glial cells in the human brain: A review of 150 years of cell counting [Internet]. Vol. 524, Journal of Comparative Neurology. Wiley-Liss Inc.; 2016 [cited 2021 Jul 26]. p. 3865–95. Available from: /pmc/articles/PMC5063692/

287. Pelvig DP, Pakkenberg H, Stark AK, Pakkenberg B. Neocortical glial cell numbers in human brains. Neurobiol Aging [Internet]. 2008 Nov [cited 2021 Jul 26];29(11):1754–62. Available from: https://pubmed.ncbi.nlm.nih.gov/17544173/

288. Pelvig DP, Pakkenberg H, Regeur L, Oster S, Pakkenberg B. Neocortical glial cell numbers in Alzheimer's disease: A stereological study. Dement Geriatr Cogn Disord [Internet]. 2003 [cited 2021 Jul 26];16(4):212–9. Available from: https://pubmed.ncbi.nlm.nih.gov/14512716/

289. Lyck L, Santamaria ID, Pakkenberg B, Chemnitz J, Schrøder HD, Finsen B, et al. An empirical analysis of the precision of estimating the numbers of neurons and glia in human neocortex using a fractionator-design with sub-sampling. J Neurosci Methods [Internet]. 2009 Sep 15 [cited 2021 Jul 26];182(2):143–56. Available from: https://pubmed.ncbi.nlm.nih.gov/19520115/

290. Ingersoll MA. Sex differences shape the response to infectious diseases. PLoS Pathog

[Internet]. 2017 Dec 28;13(12):e1006688–e1006688. Available from: https://pubmed.ncbi.nlm.nih.gov/29284060

291. Wells CA, Ravasi T, Faulkner GJ, Carninci P, Okazaki Y, Hayashizaki Y, et al. Genetic control of the innate immune response. BMC Immunol [Internet]. 2003;4(1):5. Available from: https://doi.org/10.1186/1471-2172-4-5

292. Gillet J-P, Calcagno AM, Varma S, Marino M, Green LJ, Vora MI, et al. Redefining the relevance of established cancer cell lines to the study of mechanisms of clinical anti-cancer drug resistance. Proc Natl Acad Sci U S A. 2011 Nov;108(46):18708–13.

293. Yu K, Chen B, Aran D, Charalel J, Yau C, Wolf DM, et al. Comprehensive transcriptomic analysis of cell lines as models of primary tumors across 22 tumor types. Nat Commun [Internet]. 2019;10(1):3574. Available from: https://doi.org/10.1038/s41467-019-11415-2

294. Klein RS, Garber C, Funk KE, Salimi H, Soung A, Kanmogne M, et al. Neuroinflammation During RNA Viral Infections. Annu Rev Immunol [Internet]. 2019 Apr 26;37(1):73–95. Available from: https://doi.org/10.1146/annurev-immunol-042718-041417

295. Zhang B, Chan YK, Lu B, Diamond MS, Klein RS. CXCR3 mediates region-specific antiviral T cell trafficking within the central nervous system during West Nile virus encephalitis. J Immunol. 2008 Feb;180(4):2641–9.

296. Klein RS, Lin E, Zhang B, Luster AD, Tollett J, Samuel MA, et al. Neuronal CXCL10 directs CD8+ T-cell recruitment and control of West Nile virus encephalitis. J Virol. 2005 Sep;79(17):11457–66.

297. Howe CL, LaFrance-Corey RG, Goddery EN, Johnson RK, Mirchia K. Neuronal CCL2 expression drives inflammatory monocyte infiltration into the brain during acute virus infection. J Neuroinflammation. 2017 Dec;14(1):238.

298. Delhaye S, Paul S, Blakqori G, Minet M, Weber F, Staeheli P, et al. Neurons produce type I interferon during viral encephalitis. Proc Natl Acad Sci U S A. 2006 May;103(20):7835–40.

299. Klionsky DJ, Emr SD. Autophagy as a regulated pathway of cellular degradation. Science. 2000 Dec;290(5497):1717–21.

300. Virgin HW, Levine B. Autophagy genes in immunity. Nat Immunol. 2009 May;10(5):461–70.

301. Damme M, Suntio T, Saftig P, Eskelinen E-L. Autophagy in neuronal cells: general principles and physiological and pathological functions. Acta Neuropathol. 2015 Mar;129(3):337–62.

302. Li L, Jin H, Wang H, Cao Z, Feng N, Wang J, et al. Autophagy is highly targeted among host comparative proteomes during infection with different virulent RABV strains. Oncotarget. 2017 Mar;8(13):21336–50.

303. Heydarabadi FH, Abdoli A, Gharibzadeh S, Sayyah M, Bashar R, Sheikholeslami F. Role of autophagy in nerve cell apoptosis in mice infected with street rabies virus. Arch Virol. 2020 Dec;165(12):2857–67.

304. Wang Y, He H, Li J, Chen L, Luo J, Kuang Y, et al. Rabies Virus-Induced Autophagy Is Dependent on Viral Load in BV2 Cells. Front Microbiol. 2021;12:595678.

305. Jung S, Jeong H, Yu S-W. Autophagy as a decisive process for cell death. Exp Mol Med [Internet]. 2020;52(6):921–30. Available from: https://doi.org/10.1038/s12276-020-0455-4

306. Ceccaldi PE, Fillion MP, Ermine A, Tsiang H, Fillion G. Rabies virus selectively alters 5-HT1 receptor subtypes in rat brain. Eur J Pharmacol [Internet]. 1993 Apr 15 [cited 2018 Apr 12];245(2):129–38. Available from: http://www.ncbi.nlm.nih.gov/pubmed/8491253

307. Iwata M, Komori S, Unno T, Minamoto N, Ohashi H. Modification of membrane currents in mouse neuroblastoma cells following infection with rabies virus. Br J Pharmacol [Internet]. 1999 Apr [cited 2018 Apr 12];126(8):1691–8. Available from: http://www.ncbi.nlm.nih.gov/pubmed/10372810

308. Bauer A, Nolden T, Nemitz S, Perlson E, Finke S. A Dynein Light Chain 1 Binding Motif in Rabies Virus Polymerase L Protein Plays a Role in Microtubule Reorganization and Viral Primary Transcription. J Virol. 2015 Sep;89(18):9591–600.

309. Raux H, Flamand A, Blondel D. Interaction of the Rabies Virus P Protein with the LC8 Dynein Light Chain. J Virol. 2000;74(21):10212–6.

310. Jacob Y, Badrane H, Ceccaldi PE, Tordo N. Cytoplasmic dynein LC8 interacts with lyssavirus phosphoprotein. J Virol. 2000 Nov;74(21):10217–22.

311. Sahai E, Marshall CJ. RHO-GTPases and cancer. Nat Rev Cancer. 2002 Feb;2(2):133–42.

312. Chen X, Cao R, Zhong W. Host Calcium Channels and Pumps in Viral Infections. Cells. 2019 Dec;9(1).

313. Fujioka Y, Nishide S, Ose T, Suzuki T, Kato I, Fukuhara H, et al. A Sialylated Voltage-Dependent Ca(2+) Channel Binds Hemagglutinin and Mediates Influenza A Virus Entry into Mammalian Cells. Cell Host Microbe. 2018 Jun;23(6):809-818.e5.

314. Wang S, Liu Y, Guo J, Wang P, Zhang L, Xiao G, et al. Screening of FDA-Approved Drugs for Inhibitors of Japanese Encephalitis Virus Infection. J Virol. 2017 Nov;91(21).

315. Zhong Z, Umemura A, Sanchez-Lopez E, Liang S, Shalapour S, Wong J, et al. NF-κB Restricts Inflammasome Activation via Elimination of Damaged Mitochondria. Cell. 2016 Feb;164(5):896–910.

316. Zhang L, Qin Y, Chen M. Viral strategies for triggering and manipulating mitophagy. Autophagy. 2018;14(10):1665–73.

317. Churchill MJ, Wesselingh SL, Cowley D, Pardo CA, McArthur JC, Brew BJ, et al. Extensive astrocyte infection is prominent in human immunodeficiency virus-associated dementia. Ann Neurol. 2009 Aug;66(2):253–8.

318. Saribas AS, Khalili K, Sariyer IK. Dysregulation of autophagy by HIV-1 Nef in human astrocytes. Cell Cycle. 2015;14(18):2899–904.

319. Zhou D, Spector SA. Human immunodeficiency virus type-1 infection inhibits autophagy. AIDS. 2008 Mar;22(6):695–9.

320. Ojeda DS, Grasso D, Urquiza J, Till A, Vaccaro MI, Quarleri J. Cell Death Is Counteracted by Mitophagy in HIV-Productively Infected Astrocytes but Is Promoted by Inflammasome Activation Among Non-productively Infected Cells. Front Immunol. 2018;9:2633.

321. Luo Z, Lv L, Li Y, Sui B, Wu Q, Zhang Y, et al. Dual Role of Toll-Like Receptor 7 in the Pathogenesis of Rabies Virus in a Mouse Model. J Virol [Internet]. 2020 Feb 26 [cited 2021 May 3];94(9). Available from: https://pubmed.ncbi.nlm.nih.gov/32102880/

322. Tang H-B, Lu Z-L, Wei X-K, Zhong T-Z, Zhong Y-Z, Ouyang L-X, et al. Viperin inhibits rabies virus replication via reduced cholesterol and sphingomyelin and is regulated upstream by TLR4. Sci Rep [Internet]. 2016 Jul 26;6:30529. Available from: https://pubmed.ncbi.nlm.nih.gov/27456665

323. Olejnik J, Hume AJ, Mühlberger E. Toll-like receptor 4 in acute viral infection: Too much of a good thing. PLoS Pathog [Internet]. 2018 Dec 20;14(12):e1007390–e1007390. Available from: https://pubmed.ncbi.nlm.nih.gov/30571771

324. Diamond MS, Farzan M. The broad-spectrum antiviral functions of IFIT and IFITM

proteins. Nat Rev Immunol [Internet]. 2012/12/14. 2013 Jan;13(1):46–57. Available from: https://pubmed.ncbi.nlm.nih.gov/23237964

325. Saha S, Sugumar P, Bhandari P, Rangarajan PN. Identification of Japanese encephalitis virus-inducible genes in mouse brain and characterization of GARG39/IFIT2 as a microtubule-associated protein. J Gen Virol. 2006 Nov;87(Pt 11):3285–9.

326. Saha S, Rangarajan PN. Common host genes are activated in mouse brain by Japanese encephalitis and rabies viruses. J Gen Virol. 2003 Jul;84(Pt 7):1729–35.

327. Wacher C, Müller M, Hofer MJ, Getts DR, Zabaras R, Ousman SS, et al. Coordinated regulation and widespread cellular expression of interferon-stimulated genes (ISG) ISG-49, ISG-54, and ISG-56 in the central nervous system after infection with distinct viruses. J Virol. 2007 Jan;81(2):860–71.

328. Chai B, Tian D, Zhou M, Tian B, Yuan Y, Sui B, et al. Murine Ifit3 restricts the replication of Rabies virus both in vitro and in vivo. J Gen Virol. 2021 Jul;102(7).

329. Davis BM, Fensterl V, Lawrence TM, Hudacek AW, Sen GC, Schnell MJ. Ifit2 Is a Restriction Factor in Rabies Virus Pathogenicity. J Virol [Internet]. 2017 Aug 10;91(17):e00889-17. Available from: https://pubmed.ncbi.nlm.nih.gov/28637751

330. Franco-Bocanegra DK, McAuley C, Nicoll JAR, Boche D. Molecular Mechanisms of Microglial Motility: Changes in Ageing and Alzheimer's Disease. Cells [Internet]. 2019 Jun 25;8(6):639. Available from: https://pubmed.ncbi.nlm.nih.gov/31242692

331. Etienne-Manneville S. Actin and microtubules in cell motility: which one is in control? Traffic. 2004 Jul;5(7):470–7.

332. Welsch JC, Charvet B, Dussurgey S, Allatif O, Aurine N, Horvat B, et al. Type I Interferon Receptor Signaling Drives Selective Permissiveness of Astrocytes and Microglia to Measles Virus during Brain Infection. J Virol. 2019 Jul;93(13).

333. Bachstetter AD, Xing B, de Almeida L, Dimayuga ER, Watterson DM, Van Eldik LJ. Microglial p38α MAPK is a key regulator of proinflammatory cytokine up-regulation induced by toll-like receptor (TLR) ligands or beta-amyloid (Aβ). J Neuroinflammation [Internet]. 2011;8(1):79. Available from: https://doi.org/10.1186/1742-2094-8-79

334. Kim SH, Smith CJ, Van Eldik LJ. Importance of MAPK pathways for microglial pro-inflammatory cytokine IL-1 beta production. Neurobiol Aging. 2004 Apr;25(4):431–9.

335. Nakamichi K, Saiki M, Sawada M, Yamamuro Y, Morimoto K, Kurane I, et al. Rabies

Virus-Induced Activation of Mitogen-Activated Protein Kinase and NF- κ B Signaling Pathways Regulates Expression of CXC and CC Chemokine Ligands in Microglia Rabies Virus-Induced Activation of Mitogen-Activated Protein Kinase and NF- B Signaling . Society. 2005;79(18):11801–12.

336. Chai Q, She R, Huang Y, Fu ZF. Expression of Neuronal CXCL10 Induced by Rabies Virus Infection Initiates Infiltration of Inflammatory Cells, Production of Chemokines and Cytokines, and Enhancement of Blood-Brain Barrier Permeability. J Virol [Internet]. 2015 Jan [cited 2018 Mar 29];89(1):870–6. Available from: http://jvi.asm.org/lookup/doi/10.1128/JVI.02154-14

337. Taguchi A, Niwa M, Hoshi M, Saito K, Masutani T, Hisamatsu K, et al. Indoleamine 2,3-dioxygenase 1 is upregulated in activated microglia in mice cerebellum during acute viral encephalitis. Neurosci Lett. 2014 Apr;564:120–5.

338. Bodaghi B, Goureau O, Zipeto D, Laurent L, Virelizier JL, Michelson S. Role of IFN-gamma-induced indoleamine 2,3 dioxygenase and inducible nitric oxide synthase in the replication of human cytomegalovirus in retinal pigment epithelial cells. J Immunol. 1999 Jan;162(2):957–64.

339. Adams O, Besken K, Oberdörfer C, MacKenzie CR, Takikawa O, Däubener W. Role of indoleamine-2,3-dioxygenase in alpha/beta and gamma interferon-mediated antiviral effects against herpes simplex virus infections. J Virol. 2004 Mar;78(5):2632–6.

340. Adams O, Besken K, Oberdörfer C, MacKenzie CR, Rüssing D, Däubener W. Inhibition of human herpes simplex virus type 2 by interferon gamma and tumor necrosis factor alpha is mediated by indoleamine 2,3-dioxygenase. Microbes Infect. 2004 Jul;6(9):806–12.

341. Potula R, Poluektova L, Knipe B, Chrastil J, Heilman D, Dou H, et al. Inhibition of indoleamine 2,3-dioxygenase (IDO) enhances elimination of virus-infected macrophages in an animal model of HIV-1 encephalitis. Blood. 2005 Oct;106(7):2382–90.

342. Kwidzinski E, Bechmann I. IDO expression in the brain: a double-edged sword. J Mol Med (Berl). 2007 Dec;85(12):1351–9.

343. Scott T, Nel L. Subversion of the Immune Response by Rabies Virus. Viruses [Internet]. 2016 Aug 19 [cited 2018 Apr 8];8(8):231. Available from: http://www.ncbi.nlm.nih.gov/pubmed/27548204

344. Ioannidis JPA. Extrapolating from animals to humans. Sci Transl Med. 2012

Sep;4(151):151ps15.

345. Waterston RH, Lindblad-Toh K, Birney E, Rogers J, Abril JF, Agarwal P, et al. Initial sequencing and comparative analysis of the mouse genome. Nature. 2002 Dec;420(6915):520–62.

346. Trettel F, Di Castro MA, Limatola C. Chemokines: Key Molecules that Orchestrate Communication among Neurons, Microglia and Astrocytes to Preserve Brain Function. Vol. 439, Neuroscience. Elsevier Ltd; 2020. p. 230–40.

347. Ludwig A, Schulte A, Schnack C, Hundhausen C, Reiss K, Brodway N, et al. Enhanced expression and shedding of the transmembrane chemokine CXCL16 by reactive astrocytes and glioma cells. J Neurochem [Internet]. 2005 [cited 2021 Apr 2];93(5):1293–303. Available from: https://pubmed.ncbi.nlm.nih.gov/15934948/

348. Hattermann K, Ludwig A, Gieselmann V, Held-Feindt J, Mentlein R. The chemokine CXCL16 induces migration and invasion of glial precursor cells via its receptor CXCR6. Mol Cell Neurosci. 2008 Sep 1;39(1):133–41.

349. Le Blanc LMP, Van Lieshout AWT, Adema GJ, Van Riel PLCM, Verbeek MM, Radstake TRDJ. CXCL16 is elevated in the cerebrospinal fluid versus serum and in inflammatory conditions with suspected and proved central nervous system involvement. Neurosci Lett [Internet]. 2006 Apr 10 [cited 2021 Apr 2];397(1–2):145–8. Available from: https://pubmed.ncbi.nlm.nih.gov/16406320/

350. Di Castro MA, Trettel F, Milior G, Maggi L, Ragozzino D, Limatola C. The chemokine CXCL16 modulates neurotransmitter release in hippocampal CA1 area. Sci Rep [Internet]. 2016 Oct 10 [cited 2021 May 17];6. Available from: https://pubmed.ncbi.nlm.nih.gov/27721466/

351. Ladogana A, Bouzamondo E, Pocchiari M, Tsiang H. Modification of tritiated γ-amino-η-butyric acid transport in rabies virus-infected primary cortical cultures. J Gen Virol [Internet]. 1994 Mar 1 [cited 2018 Apr 12];75(3):623–7. Available from: http://www.ncbi.nlm.nih.gov/pubmed/8126458

352. L IR. The neural and behavioural mechanism of aggression and their alteration by rabies and other viral infections. In: Progress in Rabies Control. 1989. p. 17–23.

353. Roberts E. Disinhibition as an organizing principle in the nervous system.The role of the GABA system.Application to neurologic and psychiatric disorders. In: GABA in Nervous System Functions. 1976. p. 515–539.

354. Schmidt D, Loscher W. GABA concentrations in cerebrospinal fluid and plasma of patients with epileptic seizures. In: Neurotransmitters, Seizures and Epilepsy. 1981. p. 315–324.

355. Hemachudha T. Human rabies: clinical aspects, pathogenesis, and potential therapy. Curr Top Microbiol Immunol. 1994;187:121–43.

356. Li T, Wang X, Cheng H. Meta-analysis of immunogenicity and safety of human rabies vaccination under Zagreb and Essen regimens. J Comp Eff Res. 2020 May;9(7):459–68.

357. de Melo GD, Sonthonnax F, Lepousez G, Jouvion G, Minola A, Zatta F, et al. A combination of two human monoclonal antibodies cures symptomatic rabies. EMBO Mol Med. 2020;12(11):1–10.

358. Nikolakopoulou P, Rauti R, Voulgaris D, Shlomy I, Maoz BM, Herland A. Recent progress in translational engineered in vitro models of the central nervous system. Brain [Internet]. 2020 Nov 1;143(11):3181–213. Available from: https://doi.org/10.1093/brain/awaa268

359. Lancaster MA, Renner M, Martin C-A, Wenzel D, Bicknell LS, Hurles ME, et al. Cerebral organoids model human brain development and microcephaly. Nature. 2013 Sep;501(7467):373–9.

360. Takata K, Kozaki T, Lee CZW, Thion MS, Otsuka M, Lim S, et al. Induced-Pluripotent-Stem-Cell-Derived Primitive Macrophages Provide a Platform for Modeling Tissue-Resident Macrophage Differentiation and Function. Immunity. 2017 Jul;47(1):183-198.e6.

361. Conzelmann K-K. Reverse Genetics of Mononegavirales: The Rabies Virus Paradigm. Sendai Virus Vector: Advantages and Applications. 2013. p. 1–20.

362. Zhu S, Li H, Wang C, Luo F, Guo C. Reverse genetics of rabies virus: new strategies to attenuate virus virulence for vaccine development. J Neurovirol [Internet]. 2015;21(4):335–45. Available from: https://doi.org/10.1007/s13365-015-0350-2

363. Darmanis S, Sloan SA, Zhang Y, Enge M, Caneda C, Shuer LM, et al. A survey of human brain transcriptome diversity at the single cell level. Proc Natl Acad Sci U S A [Internet]. 2015 Jun 9 [cited 2021 Apr 22];112(23):7285–90. Available from: https://pubmed.ncbi.nlm.nih.gov/26060301/

364. Bacher R, Kendziorski C. Design and computational analysis of single-cell RNA-

sequencing experiments. Genome Biol. 2016 Apr;17:63.

365. Hicks SC, Townes FW, Teng M, Irizarry RA. Missing data and technical variability in single-cell RNA-sequencing experiments. Biostatistics. 2018 Oct;19(4):562–78.